CRANFIELD UNIVERSITY

Tim Oxley

A COMPLEX SYSTEMS APPROACH TO MODELLING ENVIRONMENTAL CATASTROPHE

Innovation and Technology Assessment Unit
(IERC)

PhD Thesis

CRANFIELD UNIVERSITY

INNOVATION AND TECHNOLOGY ASSESSMENT UNIT

(International Ecotechnology Research Centre)

PhD Thesis

Academic Years 1990-93

Tim Oxley

A COMPLEX SYSTEMS APPROACH TO MODELLING ENVIRONMENTAL CATASTROPHE

Supervisor: Professor P M Allen

August 1994

This thesis is submitted in partial submission for the degree of Doctor of Philosophy

ABSTRACT

In recognition of the widespread deterioration of the natural environment, and the continual emergence of sudden catastrophic environmental changes resulting from complex interactions of theretofore apparently disparate phenomena, this research presents a complex systems approach to the modelling of such environmental catastrophes.

Recognizing contemporary views of complexity and evolution, this research presents a dynamic complex systems model which displays emergent characteristics which can be directly related to the modelled phenomena - linking acid rain and eutrophication - and the study region, the Rutland Water catchment.

This is achieved through the definition of a catastrophe indicator which indicates both the proximity and magnitude of catastrophe arising from the non-linear and discontinuous acid-phosphorus relationship within the soil domain which lies at the heart of this Chemical Time Bomb phenomenon. This facilitates assessment of the vulnerability of the Rutland Water catchment to potential propagation of this CTB given continued acidification and phosphate accumulation.

The main contributions of this research may thus be found in the following areas:

* Development of a dynamic complex systems model - transferable to alternative catchments due to the minimal data requirements and its generic representation - which may be used to describe non-point sources of phosphates as part of assessments of potential eutrophication, overcoming such limitations found in existing models.

* Definition of a catastrophe indicator (R_0) - which highlights both the proximity and magnitude of catastrophe - describing a specific Chemical Time Bomb phenomenon whereby the soil suddenly changes from being a sink to a source of phosphates; long-term accumulations of phosphate in the soil being released as a consequence of soil acidification in the short-term.

* Presentation of a complex systems approach - hinged upon this concept of a catastrophe indicator - to the representation of non-linearities and discontinuities between heretofore apparently disparate phenomena which are 'competing' for a common resource.

ACKNOWLEDGEMENTS

I would like to convey my thanks to the following people:

To Peter Allen for his supervisory support and guidance in key technical and philosophical areas of the research.

To Jamie McGlade for his enthusiasm and intuitive understanding of my goals at critical points during the research.

To Martyn Cordey-Hayes for his confidence in me during unexpected difficulties in the early stages.

Special thanks to Rick for both recognizing the initial opportunity and for providing emotional, spiritual and intellectual support throughout.

Finally, to my adopted itinerant family for their unlooked for patience and friendship.

大有

CONTENTS

1. INTRODUCTION 1

1.1 Chemical Time Bombs 2

1.2 Notions of Complexity and Evolution 4

2. REVIEW OF MODELLING 7

2.1 Review of relevant models 8
2.1.1 Acidification models 10
2.1.2 Adsorption models 14
2.1.3 Soil hydrological models 18
2.1.4 Catchment/Eutrophication models 21

2.2 Location of Current Research 23

3. MODEL CONCEPTUALIZATION & STRUCTURE 25

3.1 Model Conceptualization 28
3.1.1 Eutrophication 28
3.1.2 Acid Rain 28
3.1.3 Soil Interactions 30
3.1.3.1 Soil Acidification 30
3.1.3.2 Phosphate Adsorption 30
3.1.4 Summary 31

3.2 Model Specification 32
3.2.1 Scoping the model 32
3.2.2 Scaling the model 32
3.2.3 Process Identification 33
3.2.4 Variable Identification 34
3.2.5 Change Indicator Specification 34
3.2.6 Assumptions and Omissions 35

3.3 Study Region 36
3.3.1 Rutland Water Catchment 36
3.3.2 Data Sources 37

3.4 Model Structure and Procedure 40
3.4.1 Chemical Sub-Module 40
3.4.2 Hydrological Sub-Module 42
3.4.3 Catchment (Control) Module 42
3.4.4 Model Procedure 44
3.4.5 Simulation Strategy 48
3.4.5.1 Catchment Simulation Strategy 49

4. CHEMICAL SUB-MODULE 51

4.1 Description of Sub-Module 53
4.1.1 Phosphate Adsorption 54
4.1.1.1 Model Equations 56
4.1.2 Acid Buffering 59
4.1.2.1 Model Equations 60
4.1.3 State Variable Changes 64
4.1.3.1 Calcium 64
4.1.3.2 Aluminium 66
4.1.3.3 Phosphate 66
4.1.3.4 Acid Level 67
4.1.4 Flushing Potential & Detection 67

4.2 Characteristics of Sub-Module 73
4.2.1 Phosphate Adsorption 73
4.2.1.1 Key Characteristics 74
4.2.1.2 Adsorption Affinity 79
4.2.2 Acid Buffering 83
4.2.2.1 Dissolution Rates 84
4.2.3 R_0 Characteristics 85
4.2.3.1 Remaining Capacity, R_{Ca} 85
4.2.3.2 Theoretical Capacity change, $Rdep_{Ca,Po}$ 88
4.2.4 Summary of characteristics 88

5. HYDROLOGICAL SUB-MODULE 90

5.1 HOST Classification System 90
5.1.1 Modifications to HOST classifications 92

5.2 Description of Sub-Module 95
5.2.1 Flow Equations 96
5.2.2 State Variable Changes 98
5.2.3 Losses to Rivers 99

5.3 Characteristics of Sub-Module 102
5.3.1 Hydrological Flows 103
5.3.1.1 Baseline Characteristics 103
5.3.1.2 Infiltration Rate Changes 104
5.3.1.3 Relative Slope Changes 108
5.3.1.4 Losses to River Systems 108
5.3.2 R_0 Characteristics 115
5.3.2.1 Simulation I 115
5.4 Summary of characteristics 121

6. CATCHMENT SIMULATIONS 122

6.1 Hydrological (Spatial) Constraints 123
6.1.1 Simple, Homogenous Catchments 123
6.1.1.1 Simulation II 124
6.1.1.2 Simulation III 124
6.1.1.3 Simulation IV 126
6.1.1.4 Simulation V 128
6.1.2 Complex, Homogenous Catchments (Rutland) 130
6.1.2.1 Simulation VI 131
6.1.2.2 Simulation VII 131
6.1.2.3 Simulation VIII 135
6.1.2.4 Simulation IX 136
6.1.3 Summary of Hydrological effects 137

6.2 Effects of Chemical Variability 137
6.2.1 Complex, Heterogenous Catchments (Rutland) 138
6.2.1.1 Simulation X 139
6.2.1.2 Simulation XI 142
6.2.2 Surface Vegetation Effects 156
6.2.2.1 Simulation XII 156
6.2.2.2 Simulation XIII 156
6.2.3 Summary of Chemical effects 160

6.3 External Perturbations 162
6.3.1 Variations in Acid Deposition 163
6.3.1.1 Simulation XIV 163
6.3.1.2 Simulation XV 165
6.3.2 Variations in Phosphate Applications 165
6.3.2.1 Simulation XVI 166
6.3.2.2 Simulation XVII 166

6.4 Summary of Observations 166

7. INTERPRETATION OF RESULTS 171

7.1 Inherent Characteristics of R_0 172
7.1.1 Non-Spatial Characteristics 173
7.1.1 Spatial Characteristics 175

7.2 Hydrological Constraints upon R_0 178
7.2.1 Simulations of Simple Catchments 179
7.2.2 Simulations of Complex Catchments 180
7.2.3 Summary 181

7.3 Effects of Chemical Variability upon R_0 182
7.3.1 Baseline Reference Point 183
7.3.2 Land-Use & Vegetation Cover 184
7.3.3 Summary 185

7.4 External Perturbatory Influences 186
7.4.1 Variations in acid & phosphate loading 187

8. CONCLUSIONS 188

8.1 Observations and Interpretations of Change 188

8.2 Potential for Experimentation 191

8.3 Expansion of the Scope 193

8.4 Contribution of Current Research 194

REFERENCES 197

LIST OF FIGURES

Chapter 3

3.1 Schematic representation of acid and phosphate pathways 29
3.2 Acid buffering and phosphate adsorption feedbacks 31
3.3 Map of study region (Rutland Water) 38
3.4 Schematic representation of the overall model structure 41
3.5 Simple and complex flow patterns as defined by the Catchment Module 43
3.6 Alternative output representations 44
3.7 Flowchart showing the operation of the Chemical Sub-Module 46
3.8 Flowchart showing the operation of the integrated model 47

Chapter 4

4.1 Acid buffering and phosphate adsorption interactions 52
4.2 Adsorption affinity and cation dissolution curves 55
4.3 Adsorption affinity surfaces determined by pH and Conc(PO_4) 58
4.4 Adsorption capacity surfaces depending upon pH 59
4.5 Buffering rate surfaces determined by pH and Acid loading 65
4.6 Relationships between concentration, processes and capacities 68
4.7 Indication of peak flushing potential by P_0 69
4.8 Family of R_0 and Conc(PO_4) trajectories with varying Q_{Ca} content 72
4.9 3-Dimensional trajectories of current 'state' of the system 75
4.10 Relationships between cation composition, soil pH & resource availability 76
4.11 Variations in flushing given different proportions of adsorbed phosphate 77
4.12 Changes in characteristic trajectories given modified adsorption affinity functions 80
4.13 Acid buffering rates in relation to varying pH 84
4.14 The effects of liming upon characteristic R_0 trajectories 85
4.15 The effects of 'set-aside' on R_0 87
4.16 Comparison of R_0 trajectories with varying affinity functions 89

Chapter 5

5.1 Schematic representation of spatial hydrological flows 91
5.2 River input flows 101
5.3 Schematic representation of the influences determining the Catastrophe Indicator, R_0 102
5.4 Hydrological Flows (Baseline characteristics) 105
5.5 Hydrological Flows (Infiltration rate changes) 106
5.6 Hydrological Flows (Relative slope changes) 109
5.7 Hydrological Flows (Catchment feeders) 111
5.8 Hydrological Flows (Catchment rivers) 112
5.9 Hydrological Flows (All river categories) 113
5.10 Hydrological Flows (Specimen rainfall pattern) 114
5.11 R_0 and Phosphate concentration landscapes 116
5.12 Temporal snapshots of spatial R_0 landscape (Simulation I) 118

Chapter 6

6.1 Simulation II (R_0 landscapes) 125
6.2 Simulation II (Phosphate concentration landscapes) 126
6.3 Simulation III (R_0 landscapes) 127
6.4 Simulation III (Phosphate concentration landscapes) 128
6.5 Simulation IV (R_0 landscapes) 129
6.6 Simulation V (R_0 landscapes) 130
6.7 Rutland Water hydrology R_0 landscapes at T=100000 132
6.8 Comparison of Rutland Water R_0 landscapes at T=100000 133
6.9 Bands of Equipotential in the Rutland Water catchment 134
6.10 Simulation VII (Phosphate concentration landscape) 136
6.11 Variations between calculated and measured pH values 139
6.12 Simulation X (R_0 landscapes) 143
6.13 Simulation XI (R_0 landscapes) 146
6.14 Comparison of Simulations X and XI 149
6.15 Relative change in flushing times for Simulations X and XI 154
6.16 Effect of woodland and urban areas on Simulations X and XI 155
6.17 Comparison of temporal changes in flushing due to OS141 data 155
6.18 Effects upon flushing times of arable or livestock/woodland land usage 159
6.19 R_0 differences between Simulations XIII and XI for four illustrative cells 160
6.20 Effects upon flushing times given changes in acid loading 164
6.21 Effects upon flushing times given changes in phosphate loading 165

LIST OF TABLES

Chapter 2

2.1 Summary of models reviewed 9

Chapter 5

5.1 HOST Classifications (Reproduced from Boorman & Hollis (1992)) 93

Chapter 6

6.1 NSI data used for the definition of initial conditions 140
6.2 Selected snapshots of differences between Simulations X and XI 152
6.3 Comparison of the effects of urban cover in Simulations IX to XI 157
6.4 Variations in flushing time (T) experienced due to arable (XII) and woodland (XIII) vegetation 161
6.5 Differences in flushing times due to changes in acid and phosphate loads (Simulations XIV to XVII) 167

LIST OF NOTATIONS USED

α	parameter related to R_{Al}
Γ	Leaching inhibition term
ε	Inhibition term required in determining lateral flow
Θ	Definition of adsorption affinity curve (Calcium)
Θ_A	Definition of calcium dissolution curve
μ	Percentage infiltration
ϕ	Definition of adsorption affinity curve (Aluminium)
Φ	Controlling term defining Lat_{soil}
ϕ_Γ	coefficient required by Γ
ϕ_A	Definition of Aluminium dissolution curve
A	Affinity term (Langmuir 'isotherm')
A_1, A_2	Affinity terms (2-term Langmuir)
A_{Al}	Adsorption affinity (Aluminium)
A_{Ca}	Adsorption affinity (Calcium)
Ads_{Al}	Adsorption by Aluminium
$Ads_{Al,Po}$	Adsorption by Aluminium wrt P_0
Ads_{Ca}	Adsorption by Calcium
$Ads_{Ca,Po}$	Adsorption by Calcium wrt P_0
Ads_{tot}	Total adsorption
Al	Aluminium
Al_{diss}	Dissolution rate of Aluminium
BC_{Al}	Buffer Capacity of Aluminium
BC_{Ca}	Buffer Capacity of Calcium
BR_{Al}	Buffer Rate of Aluminium
BR_{Ca}	Buffer Rate of Calcium
BR_{si}	Rate of Silicate Buffering
$Buff_{Al}$	Acid buffering by Aluminium
$Buff_{Ca}$	Acid buffering by Calcium
$Buff_{Ca,Po}$	Buffering by Calcium wrt P_0
$Buff_{tot}$	Total acid buffering
C	Concentration of phosphate in solution
Ca	Calcium
Ca_{diss}	Dissolution rate of Calcium
CEC	Cation Exchange Capacity
H	Acid in solution
HOST	Hydrology Of Soil Types
H_{si}	Acid remaining in solution after Silicate Buffering
Inf	Infiltration rate
k	Inhibition constant for spatial flows
K_1, K_2	Constants used by Ca_{diss}
k_{al}	Constant related to adsorption by Aluminium
k_{Al}	Constant used by BC_{Al}
k_{Ca}	Constant used by BC_{Ca}

k_{cp}	Constant related to adsorption by Calcium
K_{lat}	Constant used by ε
K_{spr}	Constant used to modify SPR
k_t	Constant to convert from yearly to daily rates
Lat	Sub-surface lateral flow
Lat_{soil}	Lateral flow resulting from soil water
Lat_{surf}	Lateral flow resulting from surface water
Lea	Leaching rate
Lime	Calcium Oxide
M_{Al}	Adsorption maximum (Aluminium)
M_{Ca}	Adsorption maximum (Calcium)
M_{spr}	Modified value of SPR
P	Phosporus/Phosphate
P_0	Catastrophe Potential (peak concentration of P)
P_{flush}	Phosphate flushed as a result acid buffering by Calcium
Q_{Al}, Q_a	Reserves of phosphate adsorbed by Aluminium
Q_{Ca}, Q_c	Reserves of phosphate adsorbed by Calcium
R_0	Catastrophe Indicator
R_{Al}	Adsorptive capacity of Aluminium
R_{Ca}	Adsorptive capacity of Calcium
$Rdep_{Ca}$	Depletion rate of Calcium reserves (actual)
$Rdep_{Ca,Po}$	Depletion rate of Calcium reserves wrt P_0 (theoretical)
Run	Surface Runoff
ß	parameter related to R_{Ca}
SPR	Standard Percentage Runoff
$ß_{sat}$	Base Saturation
VMC	Volumetric Moisture Content
W_{soil}	Soil Water reserves
W_{surf}	Surface Water reserves
X_m	Adsorption maximum (Langmuir 'isotherm')
X_{m1}, X_{m2}	Adsorption maxima (2-term Langmuir)

CHAPTER 1. INTRODUCTION

> "An understanding of the threat of disaster is as important to the comprehension of disaster as the disaster event itself"
>
> [Susman et al. 1983].

The motivation for this research is based upon a recognition of the widespread deterioration of the natural environment, and the continual emergence of sudden catastrophic environmental changes resulting from complex interactions of theretofore apparently disparate phenomena. Further discussions of complexity and chemical time bomb phenomena are presented below.

Measures have been taken which attempt to assess and counteract the environmental effects of industrial development, such as Environmental Impact Assessment (EIA) [EEC 1985], but these tend to fall short of identifying potentially catastrophic indirect effects of polluting developments. It is often the indirect effects of these developments which indicate the complexity of environmental change and represent significant elements of potential chemical time bomb phenomena (see below).

Furthermore, although the IRES study [Beanlands et al. 1983] strongly advocates the use of conceptual and quantitative modelling wherever possible in impact assessments - in preference to purely descriptive studies - it also observed that a "limited and sporadic" use of either was apparent in practice. The workshop participants displayed difficulties in conceptualizing a hypothetical development scenario because of the "general difficulty that most discipline-oriented professionals have in thinking in a conceptual, inter-disciplinary mode.".

It is not the intention of this research to investigate further the practical implementation of EIA or its effectiveness, but instead to address the manner in which the complex inter-relationships of industrial pollution (the direct effects of development) and environmental disasters can be modelled and comprehended.

Thus, perceiving such a relationship between acid rain and eutrophication - specifically through soil acidification and soil phosphate retention - the purpose of this research is to observe and interpret the interactions and discontinuities emerging from the acid-phosphorus relationships within the soil domain. To this end, a complex systems model will be developed which addresses both chemical interactions and spatial hydrological flows in the context of the Rutland Water catchment.

The complexity and speed of change, and its disparity with Darwinian world-views has resulted in the validity of Darwinian and Newtonian views of change being contested. The growing dissatisfaction with these 'incomplete' views of the world has coincided with the increasing strength of the environmental debate and ideas of sustainable futures and socio-natural development [Clark & Munn 1986]. New theories of complexity have emerged from this debate which acknowledge the human influences upon environmental evolution, identifying a fundamental change in perceptions of evolutionary change, where "the fulcrum of evolution passes from *genetics* to *perception-judgement-behaviour*" [Allen 1990].

These post-Darwinian views of complexity contest 'scientific' paradigms based upon unique causality and the predictability of change, taking instead a more holistic view which accommodates multiple causalities and the interdependencies and non-linearities inherent in socio-natural change. Such views of multiple causality are reflected in current research into land degradation acknowledging the complex confluence of natural and anthropogenic causes of change, taking long-term perspectives addressing the delays and non-linearities in socio-natural change [CEC 1993a, 1993b].

Mannermaa (1991) observed that the scientific (modelling) and decision making communities - economists and politicians - have experienced different paradigm shifts concerning their views of development or progress. The paradigms may be broadly categorized as descriptive (or mechanistic), systemic or evolutionary. Such differences in paradigms suggest possible reasons for some of the difficulties experienced by the 'scientific' community in incorporating contemporary views of complexity and evolution - as expressed by Prigogine, Allen, Boulding, Checkland and others - into decision making frameworks.

Recognizing the contemporary views of complexity and evolution discussed below, this research presents a dynamic complex systems model (which would fall into the systemic category) which displays emergent characteristics which can be directly related to the modelled phenomena and the study region.

The objectives of the research are thus threefold:

1. To develop a dynamic complex systems model linking, both spatially and temporally, the heretofore apparently disparate phenomena of acid rain and eutrophication.

2. To define a catastrophe indicator which will indicate both the proximity and magnitude of catastrophe arising from the non-linear and discontinuous acid-phosphorus relationship in the soil domain which lies at the heart of this CTB phenomenon.

3. To assess the vulnerability of the Rutland Water catchment to potential propagation of this CTB given continued acidification and phosphate accumulation.

1.1 CHEMICAL TIME BOMBS

Of particular importance with regard to industrial development or commercialized agriculture is the question of chemical contamination and accumulation and its long-term effect on the quality of the natural environment [Bonazountas 1987].

This contamination and accumulation has occurred partly due to the ability of the natural environment (particularly soils and sediments) to adsorb and immobilize chemicals in what are termed as *chemical sinks* and which are traditionally perceived as limitless, and partly due to the short-term socio-economic benefits of industrial developments prevailing over long-term environmental disbenefits; contemporary

economic analyses tend to overlook the problems caused by the legacy of chemicals accumulated in the environment over time [Stigliani 1991].

It is because of the limited capacity of these sinks that Chemical Time Bomb (CTB) phenomena emerge; once a sink reaches its capacity, or the capacity is reduced through other influences (eg. acidification), a sudden release of previously inert chemicals may occur. This suggests how a change in the environmental conditions may suddenly transform a sink into a *chemical source*.

> "A Chemical Time Bomb is a concept that refers to a chain of events resulting in the delayed and sudden occurrence of harmful effects due to the mobilization of chemicals stored in soils and sediments in response to slow alterations of the environment."
>
> [Stigliani 1991]

Such non-linear and discontinuous behaviour depends upon two time scales. One is slow (or long-term), relating to the gradual accumulation of chemicals (adsorption of phosphates, for example) giving the impression of a chemical sink, whereas the fast time scale relates to the non-linear response of this chemical sink to short-term perturbations such as acidification. Such non-linearities and disparate temporal characteristics of inter-related environmental phenomena highlight the complexity inherent in chemical time bombs. Notions of complexity are discussed below.

In analysis of CTB phenomena, therefore, the complex interactions of human chemical inputs, natural chemical stores, the various factors influencing the mobilization and immobilization of chemicals, and the adsorptive capacity of soils and sediments must all be addressed. The complexity of these interactions is discussed in detail by Bonazountas (1987).

Some examples of potential CTB's are summarized below:

- Forest dieback in the early 1980's, due in part to soil acidification caused by acid rain, is a recent example of a sudden, unanticipated environmental problem resulting from delayed responses to pollutants and possibly the leaching of Aluminium from soils [Stigliani 1991].

- A simple example relates to this leaching from the soil of toxic Aluminium compounds - Aluminium existing in abundance in most soils - when the soil pH drops below 4.2, potentially provoked by acid rain [Stigliani 1988, 1991].

  The potential timescales of such changes can be related to the continual acidification of soils over 200 years since the Industrial Revolution, where the natural rates of replenishment of neutralizing ions in the soil has persistently been exceeded.

- The rate of phosphate application for agriculture in The Netherlands is such that the storage capacities of soils may be exceeded, with consequential leaching into, and contamination of water supplies, resulting in an increased potential for eutrophication [Stigliani 1988; Borggaard & Moberg 1991].

In examining the extent of phosphate saturation in soils, Breeuwsma and Reijerink (1992) also noted the delays apparent between the applications and effects of phosphates.

Further examples of CTB phenomena may be found in the sediments of both the Rotterdam estuary and New York harbour, where aeration of the sediments will lead to the mobilization of heavy metals, and various examples of microbially induced or biological time bombs discussed by Stigliani (1991).

Given the complexity, and often counterintuitive nature of CTB phenomena, there is the problem of attempting to predict the unpredictable. Stigliani (1991) suggests that two approaches may be taken towards this end. Firstly, identification of potentially vulnerable regions may be useful given that, for example, prolonged exposure to pollutants is likely to affect the capacity of the environment to absorb them. This does not, however, necessarily indicate what the consequence may be apart from the obvious wider dispersal of the given pollutant.

Secondly, a 'bottom-up' approach is suggested, involving four main steps. It is this approach which has been followed by the current research:

i) Identify the key factors influencing the mobility of 'pollutants', and their relationship to the soil/sediment properties.

ii) Determine the environmental conditions that cause the soils/sediments to possess these properties.

iii) Construct scenarios by which these environmental conditions could change.

iv) Assess the effects of changing environmental conditions on the storage capacities.

1.2 NOTIONS OF COMPLEXITY AND EVOLUTION

"The complexity of a system is in the eye of the beholder. It concerns both the system observed and the observer who seeks to understand causes, to expect behaviour and, in acting, to achieve some defined purpose. Complexity is perceived and surprises occur when causes turn out to be sharply different than was conceived, when behaviours are profoundly unexpected and when action achieves a purpose opposite from that intended - in short, when perceived reality departs *qualitatively* from expectation. ...Complexity is relative to a frame of reference that gives order to understanding, expectation and action."

[Holling 1987]

Central to this research is the recognition of complexity and persistent evolutionary change as suitable concepts for understanding 'reality', in preference to mechanistic perceptions of change implying tendencies towards homeostasis. Allen (1988) asserts that it is precisely this ability to evolve which has been removed in order to arrive at mechanistic models of 'reality'.

Allen identifies key elements of complexity and evolution as being non-average behaviour, diversity, interconnectivity, uncertainty and surprise; the latter, when related to anthropogenic development, emerging from the coupling of human spatial and temporal scales with smaller and larger ones in nature [Holling 1987]. It is proposed by Allen that it is the *evolutionary potential*, qualitatively determined by these key characteristics, that results in "the whole [being] greater than the sum of its parts", whereas in a mechanistic representation, the whole is necessarily equal to the sum of its parts.

Representation of such qualitative change is possible through conceptualizations of dynamic landscapes [Allen 1990] whereby spatial characteristics of observed phenomena, such as relative sensitivity or resilience to perturbations, may be represented by the landscape, and temporal characteristics by the qualitative changes in the landscape over time. Thus, a number of significant ideas of complexity and evolution emerge, often suggesting contrary perceptions to those resulting from mechanistic views:

- Diversity and non-average behaviour;
- Bifurcations and mutations;
- Sensitivity and resilience;
- Dis-equilibria and non-linearities;
- Feedbacks and feedforwards;
- Interdependencies;
- Qualitative change;
- Uncertainty and surprise;
- Adaptability;
- Evolutionary pathways and landscapes.

All of these issues of complexity and evolutionary change are variously addressed by Prigogine, Boulding, Holling, Allen & McGlade, and others in discussions of modelling complex systems [Allen et al. 1987].

The importance of addressing issues of sensitivity and resilience to perturbation - emergent as a result of qualitative changes to the observed phenomena - has been highlighted by Holling (1987) when related to policy decisions displaying short-term objectives. In areas as diverse as spruce budworm suppression in Canada, forest-fire suppression in the USA, cattle stocking and range management in Africa, the USA, India and Australia, salmon protection in the Pacific and malaria control in Brazil and The Mediterranean, successfully implemented short-term policies have resulted in the environments evolving to display qualitatively different properties, more vulnerable to collapse in the face of perturbation. In the case of forest-fires, his

comments were vindicated in 1988 by the loss of 50% of Yellowstone National Park through fire [Jeffery 1989].

A perfect illustration of complexity may be found in the consequences of the British Army 'solving' the problem of malaria in Burma by widespread spraying of DDT [Allen 1994 (personal communication)]. It initially appeared successful. However, the DDT bio-accumulated through the mosquitoes being eaten by lizards, themselves eaten by cats; both the lizards and the cats died. The result was rats infesting the village from the surrounding forest because there were no cats, and an explosion of termites, no longer controlled by the lizards. Thus, instead of dying of malaria, the population died of plague while their houses collapsed around their ears.

What this illustration shows is that there may be immense complexity inherent in what is perceived as a simple relationship; mosquitoes spread malaria, therefore get rid of them. It also shows that, in addressing such problems, a broader perspective of change is essential. No thought of rats was likely to occur when observing the village in isolation, but, with a perspective showing the village surrounded by forest, it would become apparent that where there were cats, there were no rats.

Given the complexity and evolutionary nature of 'reality', and the need to understand the spatial and temporal environmental consequences of pollution, this thesis presents a complex systems approach to modelling environmental catastrophe by examining the complex inter-relationships, within the soil domain, which represent a link between acid rain and eutrophication.

In Chapter 2, a review is presented of existing models which are potentially relevant and may provide useful representations of the significant processes involved in this CTB phenomenon being examined by this research.

Specification of the model developed for this research is presented in Chapter 3, with the definition and analysis of the chemical and hydrological sub-modules in Chapters 4 and 5, respectively. Chapter 6 presents a series of spatial catchment simulations, commencing with a simple (hypothetical), homogenous catchment and culminating in complex simulations of external perturbations on the Rutland Water catchment. An interpretation of the observations is provided in Chapter 7.

Finally, Chapter 8 summarizes and interprets the findings of the research and identifies the contributions of the research regarding modelling and chemical time bomb phenomena.

CHAPTER 2. REVIEW OF MODELLING

In Chapter 1, the area of concern addressed by this research - the relationship between acid rain and eutrophication in the soil domain, and potential discontinuities in this relationship - has already been introduced. The linkages between these two phenomena are reiterated during the conceptualization of the model in Chapter 3.

The current chapter addresses approaches taken to modelling the movement of 'pollutants' through the environment, and examines a selection of models potentially relevant to this research where the 'pollutants' are taken to be acid and phosphorus. Finally, the elements of these models selected for use in the model presented by this research are identified, clarifying the objectives of this research model in understanding the discontinuous interactions defining this Chemical Time Bomb (CTB) phenomenon.

A useful introduction to modelling the movement of chemical pollutants through the environment is provided by Bonazountas (1987), where he identifies three distinct environments for this movement and the three principle types of model applied. The three environments traditionally modelled are the land surface (watershed), the saturated soil zone (groundwater) and the unsaturated soil zone (soil). Modelling soil processes tends to be highly complex due to the physical and chemical dynamics being governed by extraneous forces such as rainfall, air temperature and solar radiation, whereas water and soil models are generally simpler, being governed by 'in-compartmental' forces [Bonazountas 1987].

The three principle types of models involve the modelling of dissolved pollutants, non-aqueous phase liquids and speciation. The model developed in this research addresses the complex soil 'compartment' and the interaction of two dissolved pollutants (acid and phosphorus).

Bonazountas (1987) also identifies the principle processes which need to be addressed in chemical fate modelling by highlighting four different, but often inter-related, types of model: adsorption, surface complexation, capacitance and ion-exchange models. The current research addresses both adsorption (phosphates) and ion-exchange, the latter addressing the buffering of acid by the soil; although ion-exchange models tend to address the movement of inorganic metals, ion-exchange is also evident in the 'buffering' of acid by Calcium:

$$2\,H^{+} + [\text{clay}] \times Ca \longleftrightarrow Ca^{2+} + [\text{clay}] \times 2H$$

Finally, Bonazountas (1987) suggests that the purpose of such modelling is for the assessment of environmental quality, the assessment of human exposure, or for decision-making through examination of control strategies. This research addresses environmental quality, but specifically examining potential catastrophic qualitative environmental change resulting from discontinuities relating to the interaction of two 'competing' pollutants.

These discontinuities are central to the current research in order to model this CTB phenomenon potentially affecting eutrophication. It will be seen that, under continued acidification and phosphate applications, the modelled discontinuities are 'one-way'. However, as Scheffer (1991) noted, two-way discontinuities emerge in fish-zooplankton-phytoplankton interactions under eutrophic conditions in the aquatic continuum. Stigliani (1991) presented the simplest such non-linearities involved un CTB phenomena with a step function, H:

$$C = H(Y - 1/V)$$

where C is the *effect* (eg. release of Aluminium in soil),
Y is a function of *stress* (eg. additional acid inputs), and
V is the *vulnerability* (eg. buffering capacity)

The current research presents a mechanism by which both the magnitude of catastrophe, P_0 (see Equation 22), and the timing of catastrophe may be observed graphically with reference to a complex, but determinable, qualitative indicator, R_θ (see Equation 27).

Finally, observation of the vulnerability of a region to such discontinuities, particularly when the range of influences stretch across many disciplines, needs to be presented as simply as possible. This research draws upon output formats employed by Costanza (1990) and Costanza and others (1988) for interpretations of the CELSS (Coastal Ecological Landscape Spatial Simulation) model.

The CELSS model provides a highly complex spatial representation of part of the Mississippi delta involving 2479 interconnected $1km^2$ cells - each dealing with salts, nitrogen and suspended sediments - simulating plant community succession across the region. Presentation of the output of different scenarios involved the provision of a 'baseline' case against which any *differences* emerging from alternative scenarios may be interpreted. Presentation of the differences only would be meaningless, but in conjunction with the context-providing baseline, the effect of differences in the scenarios may be examined. Similarly, but presenting the catastrophe indicator, R_θ, across the spatial grid as a 3-dimensional surface, this research provides related graphical outputs highlighting the differences with preceding baseline cases. This approach is elaborated upon in Chapter 3 and detailed definition of each simulation is provided in Chapter 6.

2.1 REVIEW OF RELEVANT MODELS

A number of models are examined below which each address one or more phenomena of potential relevance to modelling the influence of acidification upon the propagation of eutrophication. The phenomena addressed by each of the models have been summarized in Table 2.1, with brief comments regarding their applicability to the current research. Each is examined more closely in the following pages. For ease of discussion, these models have been loosely categorized into acidification, phosphate adsorption, soil hydrological, and catchment or eutrophication models.

Table 2.1 - Summary of models reviewed

	Alcamo et al. (1990)	Mein & Larsen (1971)	Chen & Waganet (1992)	Workman & Skaggs (1990)	Barrow (1978)	Enfield et al. (1976)	Jones et al. (1984)	Bonazountas & Wagner (1984)	Whitehead (1990)	Costanza et al. (1990)	Scheffer (1991)	Billen (1992)	Sanglier & Allen (1988)	Svirejeva (1993)	Current Research
Socio-Economic	X												X	X	
Emissions	X														
Atmos. Trans.	X														
Buffering	X							X	X						X
Adsorption	X				X	X	X	X							X
Soil Hydrology		X	X	X				X							X
Runoff		X							X						X
Aquifers									X						
Rivers									X	X		X		X	
Estuaries										X		X		X	
Eutrophication											X	X			
Acidification equations															
Micro level															
Micro level (macropores)															
Micro level (Preferential flow)															
Adsorption 'isotherms'															
Adsorption 'isotherms'															
8 pools of phosphates															
Limited to one 'pollutant'															
Limited soil types															
Complex spatial grid															
Eutrophication discontinuities															
Omission of soil adsorption															
Demographic															
Integration of above															
Soil acid-phosphate interaction															

Discussion of acidification revolves primarily around the RAINS (Regional Acidification INformation Simulation) model [Alcamo et al. 1990], developed by IIASA and used widely in Europe for the definition of SO_2 emissions protocols [Clark 1990]. The RAINS model addresses sources, transportation, deposition and the effects of acidification. Whitehead (1990) and Bonazountas & Wagner (1984) also present models addressing the buffering of acid by the soil.

Regarding phosphate adsorption, most models are based upon one of a small number of adsorption equations and variants thereof. Three of these - the Freundlich, Langmuir and Tempkin equations - are reviewed by Barrow (1978). Enfield and others (1976) compare five alternative kinetic models for adsorption, including variants of the above, whereas Jones and others (1984) present a model involving eight different 'pools' of phosphorus within the soil. Again, Bonazountas & Wagner (1984) provide a model capable of representing adsorption.

The hydrological models have been split into two categories - soil and catchment - with the latter including dynamics of eutrophication. The soil hydrological models primarily address detailed dynamics of infiltration [Mein & Larsen 1971; Chen & Waganet 1992; Workman & Skaggs 1990], the latter concerned with water management practices. Catchment models include a model of the Thames [Whitehead 1990] concerned with nitrate levels in public water supplies, and a model of the Scheldt in Belgium [Billen 1992]. Billen tracks nutrients and oxygen affected by agricultural and human inputs, ultimately addressing the eutrophic potential of the river. Scheffer (1991), as discussed above, examines dynamics of eutrophication but not the hydrological dynamics.

Finally, models by Sanglier & Allen (1989) and Svirejeva (1993) have been included since the latter has integrated the socio-economic model of Sanglier & Allen with the river system model of Billen (1992). These are only discussed within that context.

2.1.1 ACIDIFICATION MODELS

Negotiations among 20 European countries on SO_2 emissions protocols placed extraordinary reliance upon a single model (Clark 1990) - the Regional Acidification INformation Simulation (RAINS) model developed by IIASA [Alcamo et al. 1990]. The RAINS model addresses the entire sequence of air pollution events: pollution generation (emissions) and costs in 27 countries; atmospheric processes affecting the transportation and wet and dry deposition (acid rain); and the environmental impacts of acidification, including soil acidity, lake acidity and SO_2 forest impacts.

Recognizing that both emissions and atmospheric transportation are non-uniform across Europe and that some regions are more sensitive (often as a result of prior acidification), with others more tolerant to acidification, the model has been developed for use by non-technical people, allowing questions to be asked of it, such as: *"What would happen to Norway's lakes and forests if the UK were to cut SO_2 emissions from power plants by 30% ?" ... "How much would it cost ?".* However, since this research is concerned with the indirect effects of such questions, and the

potential propagation of CTB phenomena, only the deposition and soil acidification modules are examined further. As such, the fundamental concepts of *Acid Loading* and *Acid Buffering* are discussed below.

Acid Loading

The initial version of the RAINS model assumed that sulphate deposition is the only source of acid loading; nitrates may influence acid loading and are to be included, and ammonium (NH_4^+) may both increase acidification or neutralize it as a base cation [Kauppi & Alcamo 1990].

Calculation of the acid load assumes that all sulphur comes into contact with water in the atmosphere or the soil forming sulphuric acid (H_2SO_4). The implication is that for each mole of sulphur deposition, an acid load equivalent to two moles of protons (H^+) is produced.

Acid loading is not, in practice, so simple to estimate. This calculated acid load is modified by neutralization effects of base cation (Ca^{2+}, Mg^{2+}) deposition, and further modified by the vegetation; experimental evidence suggests that deposition to forests is greater than to adjacent open land [Kauppi & Alcamo 1990].

The extent of neutralization by base cations presents problems since neither models nor emissions estimates are available; the sources are mainly from soil and road dusts, agricultural fertilizer, quarry dust, and other non point sources not directly rèlated to sulphur emissions. However, it has been suggested that combined Ca^{2+} and Mg^{2+} deposition will neutralize approximately 33% of sulphur deposition with a range of 12% to 44% [Kamari 1986]. The RAINS model also utilizes a *forest filtering factor* (τ), estimated at an average of 1.8, varying depending upon the percentage of forest cover in the grid.

The equations to determine the acid load, modified by base cation deposition and forest filtering, used in the RAINS model are of the form:

$$d_f = \tau d_o$$

$$d_{tot} = f d_f + (1 - f) d_o$$

where,
- f = fraction of forests within the grid,
- d_{tot} = total sulphur deposition,
- d_f = deposition on forests,
- d_o = deposition on open land,
- τ = forest filtering factor.

Substitution yields:

$$d_o = d_{tot} / [1 - (\tau + 1)f]$$

$$d_f = d_{tot}\tau / [1 + (\tau - 1)f]$$

thus, the net acid load of sulphur, A_o, can be estimated by:

$$A_o = d_x - d_{bc}$$

where, d_{bc} = Base Cation load,
d_x = Forest or Open Land deposition, as appropriate

The soil acidification processes implemented in the RAINS model are based upon these two fundamental concepts of *Acid Loading* and *Acid Buffering*, where the acid loading is driven by the wet and dry deposition rates of sulphur. Acid buffering is dependent upon the soil type and the soil pH, and indirectly determines the effect of additional acid loading on the soil through a change in soil pH.

Acid Buffering

As explained by Kauppi and others (1990), acid buffering is determined by two variables, *Buffer Capacity* (the gross potential for buffering by the reservoir of base cations and acid cations) and *Buffer Rate* (the dissolution rate of base and acid cations under the influence of additional H^+ ions), where the dominant buffering reactions in soil solution vary with soil pH and may be classified into five *Buffer Ranges* [Ulrich 1983]. These buffer ranges are summarized below:

- *Carbonate Buffer Range*: Calcareous soils (pH≥6.2), where the dissolution rate of $CaCO_3$ is high enough to buffer reasonable levels of acid deposition;

- *Silicate Buffer Range*: Silicate weathering produces base cations in all soils, with the effect of neutralizing a proportion of the acid load;

- *Cation Exchange Range*: (4.2<pH<6 approx.) When the acid load is not completely neutralized by silicate weathering, the soils' base cation reserves are depleted. The buffer capacity of the cation exchange range is defined as the product of the *Cation Exchange Capacity* (CEC_{tot}) and the *Base Saturation* (β_{sat}). As the base cation reserves are depleted, β_{sat} and pH reduce until the soil enters the Aluminium buffer range;

- *Aluminium Buffer Range*: (3.8<pH<4.2) Base saturation declines to approximately 5%. Aluminium is released from oxides and hydroxides and reacts with H^+. Acid cations (Al^{3+}) are mobilized in the soil. Since aluminium compounds are abundant in soils, buffer capacity is rarely depleted;

- *Iron Buffer Range*: (pH<3.8) Iron oxides become soluble, but aluminium may still act as the dominant buffer compound. However, soils with pH as low as 3.8 cannot support fauna and flora because they leach toxic heavy metals and nutrients.

The buffer range of primary interest to this research, since most agricultural soils have a pH in the range 4 to 6.5 (approx.), is the Cation Exchange Range. The form of the equations used to model these buffering processes in the RAINS model is as follows:

$$A = A_o - BR_{si}$$

$$BC_{ce,t} = BC_{ce,t-1} - A$$

$$pH = 4 + 1.6 * (BC_{ce,t} / CEC_{tot})^{3/4}$$

where,
A_o = Acid load,
A = Acid load after silicate buffering,
BR_{si} = Buffer rate of silicate weathering,
BC_{ce} = Buffer capacity of Cation Exchange Range,
CEC_{tot} = Total cation exchange capacity.

In this way, the sub-model will calculate the change in soil acidity (pH) as affected by the soil type and the additional acid loading on the soil caused by deposition of atmospheric sulphur compounds.

Finally, the model omits the effects of organic matter, since it is not describable Europe-wide, assumes that the buffer rate of silicates is independent of soil pH, and concentrates upon the effects on forest soils. It is also suggested that the model may be best suited to non-calcareous soils with high levels of deposition. However, it describes clearly the process of acid buffering and provides a simple representation of changes to the soil pH; of critical importance since a changing pH is central to the CTB phenomenon addressed by this research.

Two further models addressing soil acidification should also be mentioned, but it rapidly becomes evident that they are not suitable for use in this research. Whitehead (1990) makes use of the Model of Acidification of Groundwaters In Catchments (MAGIC) [Cosby et al. 1985] which addresses anion retention in the soil (buffering), adsorption and exchange of base and acid cations by soils, and alkalinity generation by Carbonic Acid, with Aluminium (Al^{3+}) concentrations assumed to be in equilibrium with $Al(OH)_3$. However, the model is a lumped aggregate representation - using equilibrium and mass balance equations - of a catchment, and is limited to simulating up to 2 soil types only, thus making it unsuitable for this research.

Finally, Bonazountas & Wagner (1984) have developed SESOIL, a soil compartmental model which can be tailored both spatially and temporally to the users needs. The hydrological 'compartment' is based upon estimates from available data, and the pollutant 'compartment' addresses organics, inorganics (including acid), metals and gases. A high degree of chemistry is involved, but only a single pollutant may be addressed at a time, precluding its use in this research since the latter's interest is in the discontinuities emerging from the inter-relationships of two pollutants - acid and phosphorus.

Detailed definition of acid buffering and changes to the soil pH which are used in this research - based upon the representations employed by RAINS - may be found in Chapter 4 (Equations (6) through (14)).

2.1.2 ADSORPTION MODELS

The complexity of the processes of phosphate adsorption have resulted in a number of empirical and mechanistic equations to represent adsorption depending upon the precision or generality required [Enfield et al. 1976; Barrow 1978]. These each attempt to account for influences on adsorption such as increases in negative charges at or near adsorption sites due to adsorption, concentrations of phosphate in the soil solution, maximum adsorptive capacity and various affinity constants addressing the relative rates of adsorption and desorption.

Jones and others (1984) present a more complex model involving complex flows of phosphorus between eight different 'pools' of phosphorus in the soil. This model, and the equations employed by Barrow (1978) and Enfield and others (1976) are discussed below.

Prior to examining the more commonly used adsorption equations, Barrow (1978) noted that Bowden and others (1973) attempted also to account for pH changes by addressing the electrostatic effects involved in adsorption. However, the model developed requires seven parameters: three are to describe the charge characteristics of the surfaces as determined from titration curves, one is an electrical capacitance term, and three are specific for phosphate adsorption (the adsorption maximum and two affinity constants for the two ionic species usually present). Furthermore, the model required fitting to measured data and is difficult to use. The more commonly use adsorption 'isotherms' examined by Barrow (1978) were the Freundlich, the Tempkin and the Langmuir equations.

The Freundlich equation was first used by Russell & Prescott in 1916 and is of the form:

$$X = k\,C^{b}$$

where: X is the amount of phosphate adsorbed per unit of soil,
C is the phosphate concentration in solution, and
k and b are affinity constants.

This equation was commonly used before the Langmuir equation (below) emerged, with the change in rate of adsorption over time regarded as exponentially decreasing. However, recognition that previously adsorbed phosphates may also influence the adsorption rate, this equation has been modified to account for this previously adsorbed phosphate, giving an equation of the form:

$$X + Q = k\,C^{b}$$

where Q is the phosphate already adsorbed.

This equation reflects an exponentially decreasing adsorption affinity as adsorption increases, but is also now influenced by previously adsorbed phosphates. However, it has been argued that it doesn't invoke any physical model [Gunary 1970], and that it is empirical and thus only of value for interpolation [Glasstone 1959].

The Tempkin equation is derived from one where the affinity term decreases linearly as adsorption increases [Hayward and Trapnell 1964], and, ignoring very high and low phosphate concentrations, has been reduced to:

$$X = k_1 \ln(k_2 C)$$

where k_1 and k_2 are coefficients.

The perceived advantage of this equation lies in the ability to graphically present the relationship between the phosphate concentration and the amount adsorbed as a straight line when X is plotted against the log of the concentration. Barrow (1978) suggests that this form of adsorption equation is of limited value for describing adsorption.

The Langmuir equation was first used by Olsen & Watanabe (1957) and has often superseded the use of the Freundlich equation. The simple Langmuir equation is given by:

$$X = A\, X_m\, C / (1 + A\, C)$$

where: A is an affinity term describing the relative rates of adsorption and desorption, and

X_m is the adsorption maximum.

The appeal of this equation is that it can be transformed into a linear form in order to use linear regression analysis to determine the coefficients. It also has the advantage that the adsorption maximum can be determined. However, it has the disadvantage of being able to deal with a limited range of concentrations, and in this form, is often a poor fit to the data.

Barrow (1978) identifies problems with this simple Langmuir form being that the affinity term is constant and the effect of negative charge changes is not accounted for, arguing that the simple Langmuir form seldom applies in practice. Gunary (1970) attempted to overcome this by modifying the equation through the form $C/X=1/(AX_m) + C/X_m$ to the following:

$$C / X = a + bC + d\sqrt{C}$$

Barrow suggests that the rate of decrease in affinity may not in practice correspond to this modification. in essence only reflecting a square root term forced into the equation.

A further modification to the simple Langmuir is to address the possibility of multiple surfaces for adsorption, and it is this modification which has been used by the model presented in the following chapters, accounting for two discrete surfaces, and may be written thus:

$$X = A_1X_{m1}C/(1+A_1C) + A_2X_{m2}C/(1+A_2C)$$

Enfield and others (1976) examined five different kinetic models for phosphate adsorption, relating the simulations to detailed data representing 25 different soils. Regression analysis was used to fit the data to each of the five models. The models were:

- *A linearized 1st-order sorption equation*, used by Lapidus & Amundson (1952), with

$$\delta S/\delta t = \alpha (K C - S)$$

where S is the sorbed phosphate,
$\delta S/\delta t$ is the rate of sorption, and
α and K are constants.

This equation assumes that the driving force is related to the difference between the concentration and what has already been adsorbed. It also assumes a linear relationship with the diffusion coefficient (α) constant.

- *A 1st-order Freundlich equation*, used by Hornsby & Davidson (1975), with

$$\delta S/\delta t = ß (m C^n - S)$$

where ß, m and n are constants to describe pesticides kinetics in soils.

This equation assumes that there is a maximum that can be adsorbed, as in the variant of the Freundlich equation discussed by Barrow (1978) above.

- *An empirical equation*, used by Enfield (1974), with

$$\delta S/\delta t = a C^b S^d$$

where a, b and d are constants.

An obvious limitation with this equation is that the function becomes undefined as t approaches infinity.

- *A diffusion-limited Freundlich equation*, following an approach similar to Skopp & Warwick (1974), where

$$S_{avg} = F(C) - \text{Diffusion term}$$

where S_{avg} is average sorbed phosphate per soil particle, and
F(C) is a sorption function.

Thus, the diffusion-limited Freundlich equation uses the relationship:

$$F(C) = j\ C^k$$

where j and k are constants.

- *A diffusion-limited Langmuir equation*, employing the relationship:

$$F(C) = S_{max}\ b_l\ C\ /\ (1 + b_l\ C)$$

where S_{max} is the maximum phosphate that can be sorbed, and
b_l is a constant.

Fitting each equation to the experimental data resulted in varying degrees of correlation, with the linearized 1st-order sorption equation showing the worst fit and the diffusion-limited Freundlich and Langmuir equations showing the closest fit. Attempts to correlate the physical and chemical properties of the 25 soils with the regression coefficients of the kinetic models were unsuccessful, confirming the highly complex relationship between phosphate adsorption and soil composition [Enfield et al. 1976]

The model described by Jones and others (1984), a soil and plant phosphorus model used as part of the Erosion-Productivity Impact Calculator (EPIC) agricultural management model, takes an alternative approach. Encompassing 10 soil layers, the model maintains 'pools' of stable, active and labile inorganic phosphorus, fresh and stable organic phosphorus, and grain, stover and root phosphorus.

This model operates on a daily timestep and is sensitive to soil chemical and physical properties, crop phosphate requirements, tillage practices, the rate of fertilizer application, soil temperatures and soil water content.

Of interest to this research is the movement from the active inorganic phosphorus 'pool' to the stable inorganic pool, simulating the slow adsorption of inorganic phosphorus from the soil solution. However, the equation used to simulate this adsorption is of the form:

$$R_{as} = K_{as}\ (4\ P_{ia} - P_{is})$$

where R_{as} is the rate of movement between the pools (ie. adsorption),
K_{as} is constant, and
P_{ia} and P_{is} represent the active and stable inorganic pools.

This equation reflects the linearized 1st-order sorption equation examined by Enfield and others (1976) which showed the worst fit with the experimental data, and is

forced towards an equilibrium where the pool of stable inorganic phosphorus cannot exceed 4 times the active inorganic pool.

Detailed definition of the phosphate adsorption equations used in this research, based upon a modification to the 2-term Langmuir equation, may be found in Chapter 4 (Equations (1) through (5)).

2.1.3 SOIL HYDROLOGICAL MODELS

As with the chemical dynamics in the soil, modelling of water movement through the soil is highly complex, involving the effects of surface water levels, infiltration, leaching and lateral flow and runoff. Three models are described below, with Mein & Larsen (1973) also identifying a number of empirical and theoretically derived algebraic equations for infiltration.

Mein & Larsen (1973) developed a model to address the relationship of infiltration to rainfall and runoff. Prior to selecting the Richards (or diffusion) equation for use in their model, a summary was provided of existing infiltration equations, reiterated here.

- *The Kostyakov equation* - put forward in 1932 - is the simplest and is of the form:

$$F = a\,t^b$$

where F is the total infiltration volume,
t is the time, and
a and b are constants.

However, the constants a and b cannot be predicted in advance and there is no provision for predicting when runoff will begin following a rainfall event.

- *The Horton equation* - proposed in 1940 - is possibly the best known infiltration equation, and is of the form:

$$f_p = f_c + (f_o - f_c)\,e^{-kt}$$

where f_p is the infiltration capacity at time t,
f_o is the initial infiltration capacity,
f_c is the equilibrium infiltration capacity, and
k is a constant depending upon the soil type and initial soil moisture content.

It is suggested that the good fit with experimental data is due to the three parameters - f_o , f_c and k - rather than its representation of the infiltration process.

- *The Holtan equation*, more recently, has been developed from a substantial volume of field data, and is of the form:

$$f_p = f_c + a\, F_p^{\,n}$$

where f_p and f_c are the same as in the Horton equation,
F_p is the potential infiltration volume,
a is a constant between 0.25 and 0.8, and
n is a constant depending upon soil type.

This equation is well suited to watershed models, linking infiltration to soil moisture levels, and is not directly time dependent.

- *The Green-Ampt equation*, theoretically derived from applying Darcy's Law to the wetted zone in the soil, is given by

$$f_p = K_s \frac{(L + S)}{L}$$

where K_s is the hydraulic conductivity of the wetted zone,
L is the distance of the wetting front below the surface, and
S is the capillary suction at the wetted front.

Laboratory tests for layered soils have shown excellent agreement, but none, however, addressed the effect of rainfall.

- *The Philip equation*, for a homogenous soil with uniform initial moisture content and excess surface water, is given by

$$F = s\, t^{1/2} + A\, t$$

where F is the infiltration to time t, and
s and A are constants depending upon the soil type and initial moisture content.

This form of equation is convenient - s and A are predictable in advance - but predicting these constants is complex and beyond the scope of a simple watershed model. Again, the rainfall effect is not addressed.

Thus, Mein & Larsen (1973) selected the 2nd-order, non-linear, partial differential Richards equation, given by

$$\frac{\delta\Theta}{\delta t} = -\frac{\delta}{\delta z}\left(K(\Theta)\frac{\delta S(\Theta)}{\delta z}\right) - \frac{\delta K(\Theta)}{\delta z}$$

where Θ is the volumetric moisture content,
t is time,
z is the distance below the surface,
$S(\Theta)$ is the capillary suction, and
$K(\Theta)$ is the unsaturated hydraulic conductivity.

This equation was shown by Mein & Larsen (1973) to provide a good representation of soil moisture flow under a variety of input conditions. However, with detailed knowledge of capillary suction and hydraulic conductivity necessary, it is not suitable for use in the current research.

The above models also reflect assumptions of soil homogeneity, a limitation addressed by Chen & Waganet (1992) and Workman & Skaggs (1990) through the recognition of macropores and preferential flow, respectively. Both of these models, however, make use of the Richards equation (above) where there are no macropores present.

Chen & Waganet (1992) model the influence of macropores upon infiltration by maintaining three 'control' situations - macropore, matrix and application - and three flow regions (matrix, macropore and transfers between them). For flow in the matrix region (assumed to be homogenous), the Richards equation has been used, and for flow in the macropores, the Hagen-Poiseuille equation for average velocity, U, is used, where

$$U = \frac{g\, r^2}{8\, v_k} \cdot \frac{\delta h}{\delta z}$$

where g is the acceleration due to gravity,
r is the radius of the tube (macropore),
v_k is the kinematic viscosity of water, and
$\delta h/\delta z$ is the gradient of the hydraulic head (h is the hydraulic head, z is the length of the tube).

The model requires detailed knowledge of hydraulic conductivity (both matrix and macropore), the soil bulk density or saturated water content, and the maximum and minimum macropore sizes.

Finally, Workman & Skaggs (1990) present a water management model (PREFLO) capable of simulating preferential flow; a similar recognition of the existence of macropores in the soil. For the homogenous region, the Richards equation is again used, with the macropore flow computed for vertical flow in a capillary tube.

Although PREFLO addresses rainfall (on an hourly basis), evaporation, evapo-transpiration and plant uptake (on a daily basis), detailed knowledge is also required of the rooting depth, the leaf area index, hydraulic conductivity, pressure heads and the number of pores present.

It has become clear, therefore, that all of the models above address the movement of the soil water at the micro-level, and are thus not suitable for use in this research given both the scale of the proposed model and the limited availability of data in the proposed study region. It will also become clear that the river system and catchment models discussed below are unsuitable; they have been included for the sake of completion.

Thus an alternative approach to modelling the hydrological flows was required. The approach selected represents an aggregated definition of flows depending upon the physical characteristics of soils and watertables, as opposed to specific soil types and hydraulic conductivities. The categorization of soils and related flow characteristics are provided by the HOST (Hydrology Of Soil Types) classification system [Boorman & Hollis 1992]; this classification system is described in detail at the beginning of Chapter 5 (Hydrological Sub-Module). Detailed definition of the hydrological flows implemented in the model are also to be found in Chapter 5 (Equations (28) through (42)).

2.1.4 CATCHMENT/EUTROPHICATION MODELS

Two catchment models are examined below. Firstly, a nitrate model of the Thames [Whitehead 1991], and secondly Billen's (1992) PHISON river system model - initially developed for studying the Scheldt river system in Belgium [Billen et al. 1990] - examining nutrient transformations in the aquatic continuum. Finally, Scheffer's (1991) zooplankton-phytoplankton model is discussed, although this model addresses eutrophic phenomena as opposed to the hydrology of a river system.

Whitehead (1990) employs a semi-distributed approach to modelling the effects of agricultural nitrates on public water supplies. Chemical transformations are addressed by the acidification model (MAGIC) discussed above. For the hydrology, three models have been used:

i) A daily hydrological model, specific to the Thames catchment, addresses flows from tributaries, sub-catchments and aquifers;

ii) A soil zone / aquifer model accounts for nitrate movement, given land usage and fertilizer application levels; and

iii) An integrated flow model is used for the main river, with non-point sources being derived from the preceding models - i) and ii) above.

This model, however, is antithetical to the ideas of complexity discussed in Chapter 1. Through its use of a time-series approach to modelling it assumes that the 'Law of Large Systems' applies. In other words, it assumes that all complex non-linearities and distributed elements will result in aggregated system behaviour which is relatively simple in dynamic terms [Whitehead 1990].

From the point of view of the current research, this model is unsuitable for three further reasons. Firstly, it addresses the relationship between nitrates and public water supplies, and not phosphates and eutrophication. Secondly, the model is specific to the Thames catchment and underlying aquifers, and thirdly, as discussed above, the MAGIC model used for acidification effects is only able to address two soil types.

Billen's (1992) PHISON model - the generic form of his Scheldt model - is a complex representation of the hydrochemical dynamics of an entire river system, based upon an integration of the RIVERSTRAHLER river model and three biological models, HSB, AQUAPHY and VENICE [cited by Billen 1992].

The RIVERSTRAHLER model is based upon the concept of 'stream order', where the geomorphologic characteristics of each stream order may be used to calculate hydrological discharges in response to rainfall events. Thus, for each stream order, values may be provided relating to baseflow and hypodermic runoff.

The biological sub-models address the effects or organic matter degradation and bacterial processes (HSB), phytoplankton development (AQUAPHY), and the dynamics of benthic microbial activity (VENICE). In addition, a physio-chemical model addresses the dynamics of oxygen, nitrogen, manganese and iron, with adsorption/desorption of orthophosphates on suspended ferric oxides using a Langmuir isotherm as described above. However, this adsorption is addressed within the aquatic continuum as opposed to the soil domain, although possible saturation levels are discussed in a hypothetical future.

The PHISON model represents a useful tool for predicting major trends of the role of river systems in terrigenous Carbon, Nitrogen and Phosphorus transfer to the sea, in response to land use and human perturbations [Billen 1992]. It is in this context that, more recently [Svirejeva 1993], the Scheldt model [Billen et al 1990] has been integrated with a socio-economic model of the Belgian provinces [Sanglier & Allen 1989] with the aim of examining the dynamic effects of socio-economic development upon this nutrient transfer.

However, a major omission from these PHISON-based models is their lack of a sub-model addressing the hydro-chemical dynamics within the soil domain. It is the soil which may act as both a sink and a source of chemicals and nutrients, and in so doing may effect delays in the modelled nutrient transfer or may release unforeseen levels of nutrients into the aquatic continuum in the form of a chemical time bomb. It is this 'hole' in the PHISON model which the current research addresses, as suggested in Table 2.1. This research presents a model, the output of which could be adapted to provide input for non-point sources of phosphates for a PHISON-based river system model.

Finally, Scheffer's (1991) zooplankton-phytoplankton interaction model introduces a further dynamic: the effects of fish. Scheffer thus accounts for the complex interactions of three trophic levels, which, under eutrophic conditions, display discontinuities and often counterintuitive responses; these discontinuities becoming more pronounced under high nutrient loads.

Scheffer uses minimal modelling techniques - in order to examine the generic behaviour of the system - with manipulation of both fish and nutrient levels possible, and observation of the zooplankton-phytoplankton responses. The method of analysis was by means of zero-isocline representations of the zooplankton-phytoplankton interactions; lines in the phase space on which the derivative of either of the two state variables is zero. The zooplankton-phytoplankton isoclines were observed to shift in the phase space in response to fish and nutrient levels respectively.

It is towards the intersection of the two isoclines that the system attempts to achieve equilibrium. However, the resultant changing densities of fish and nutrients affect the isoclines, thus shifting the intersect. With the non-linear response of the isoclines to fish and nutrient densities, states are achieved where three intersects emerge, two of which are stable and the third unstable. It is at this point that system discontinuities become pronounced.

2.2 LOCATION OF CURRENT RESEARCH

As suggested in Table 2.1 - and discussed above - this research is centred around the interactions and flows of acid and phosphorus within and through the soil domain, with acid deposition and phosphorus applications (fertilizer) being treated as manipulable inputs, and output flows of phosphates perceived as contributory influences to eutrophic phenomena in the watercourses. Three areas of interest thus require inclusion in the model: acid buffering and phosphate adsorption within the soil domain, and hydrological flows through the soil.

Regarding acid buffering, the model will be based upon the representations employed in the RAINS model of regional acidification in Europe [Alcamo et al 1990]. These representations incorporate definitions of the changing pH (central to the acid-phosphorus interactions) and the alternatives display limitations in the context of the present work; Bonazountas & Wagner (1984) can only address acid and phosphorus individually, and the MAGIC model used by Whitehead (1990) is limited to addressing two soil types.

The complexity of phosphate adsorption has traditionally been simulated using adsorption 'isotherms', the most common of which are the Freundlich and Langmuir equations discussed above. The Freundlich equation - or a variant - may have been suitable for use in the present research, but, in preference, a variant of the 2-surface Langmuir has been employed (see Chapter 4) since it can address an adsorption maximum and is more easily integrated with the processes of acid buffering. Finally, Jones and others (1984) employ 8 pools of phosphorus, of which 6 would be treated as extraneous by the current model, and Bonazountas & Wagner (1984) encounter the same problem as with acidification; only a single pollutant can be examined.

Thirdly, the models of soil water movement are primarily focused at the micro-level involving infiltration [Mein & Larsen 1971; Chen & Waganet 1992; Workman & Skaggs 1990] and require detailed definitions of hydraulic conductivity, capillary suction, pore sizes and numbers, and other information in detail that exceeds the

scope of this research. The river system/catchment models [Whitehead 1990; Billen 1992] tend to the other extreme and describe soil water dynamics through reference to aggregated runoff figures and baseflow data in response to rainfall events. The current research, therefore, proposes an intermediate perspective of soil water flows based upon the geophysical HOST classification system for defining the hydrological characteristics of a region [Boorman & Hollis 1992]. The HOST classification system is described in detail in Chapter 5.

The model described in the following chapters will thus be structured in a modular form with sub-modules addressing the acid-phosphorus chemical dynamics and the soil hydrological flows. These sub-modules interact and are coordinated and constrained by a third 'catchment' module. The catchment is represented by an 8 x 8 square grid of 5 km square (25km^2) cells. This structure is elaborated upon in the following chapter.

Thus, with the purpose of this model to observe the interactions and discontinuities emerging from the acid-phosphorus relationships within the soil domain, rainfall events, acid deposition and phosphorus loading will be treated as manipulable inputs, and leaching and river outflows as measurable outputs. An understanding of the effects of the non-linear dynamics will emerge through observation and interpretation of 3-dimensional 'sensitivity' landscapes.

In this way it will be demonstrated that the relative sensitivity or resilience of a region to this specific phosphorus-related Chemical Time Bomb phenomenon can be gauged, with reference to landscapes generated by a catastrophe indicator, R_θ, in both hypothetical and real situations; in this instance, Rutland Water. The model addresses dynamics occurring in the soil domain which are influenced by human development (pollution) and have a potentially significant influence upon non-point sources of phosphorus entering the aquatic continuum.

CHAPTER 3. MODEL CONCEPTUALIZATION AND STRUCTURE

In the preceding chapters, the phenomena to be modelled in the current research have been clearly described; namely, the discontinuous inter-relationship of soil acidification and phosphate adsorption. However, for the purposes of conceptualizing and specifying the model, it is appropriate to restate these discussions, but in the context of the model specification as opposed to the phenomena themselves.

The current chapter, therefore, presents three key activities involved in the model development: model conceptualization, model specification, and definition of the structure and procedural aspects of the model. In addition, the study region is identified and a summary of the simulation strategy is provided. Firstly, however, some comment is needed concerning multiple causality, the balance between generality, realism and precision, and the use of hierarchical structures, since these issues have a direct bearing, respectively, on the key activities noted above.

The nature of a proposed development - which may be subject to Environmental Impact Assessment - will immediately identify some of the potential direct impacts of the development, such as quantifications of toxic discharges, carbon dioxide and sulphur emissions, noise levels etc. However, it is the qualitative nature of the *indirect effects* of such quantified influences on the wider environment which provokes concern. The consequences of indirect effects may become apparent in the form of unexpected catastrophe on a spatio-temporal scale out of all obvious proportion with the initial causal influence; such is the nature of Chemical Time Bomb phenomena [Stigliani 1991].

Mapping 'reality' onto an abstract model therefore requires a clear perception of the multiplicity of potential changes influenced by the direct effects of the development, such as sulphur emissions, and conversely the multiplicity of causal influences contributing to qualitative change in the wider environment. The regions where such phenomena - relating to causal influences and potential effects - interact in a common domain, may highlight inter-relationships which act as a trigger for a CTB.

Thus, to perceive indirect effects, and ultimately identify the points of conflict and the key mechanisms of change, the multiplicity of causes and effects requires close examination. For example, sulphur dioxide (SO_2) emissions represent a *contributory* cause of many environmental changes (effects). Thus, if impact assessment starts from a contributory cause, a rapid spatial and temporal divergence of inter-related effects will demand examination; immediately, the complexity of the exercise may become prohibitive either economically, technologically, or both.

However, if the starting point becomes an effect rather than a cause, there may be multiple contributory causes influencing a single effect, as found with eutrophication - for example, by fertilizers, detergents, sewerage treatment, hydrology and soil characteristics [Harper 1992]. Thus, a balance must be sought between the identification of contributory causes and potential effects, in order to determine the key inter-relationships.

Having conceptualized the phenomena and the key inter-relationships, a model may begin to be specified. A dynamic computer model, is, in the words of Levins (1966), "... essential for understanding reality, *[but]* should not be confused with reality itself.". It must reflect an appropriate balance between generality, realism and precision in its representation of 'reality', thus maximizing the clarity of observable changes significant for enhanced understanding of that 'reality'.

To use Levins's geographical analogy, the precision and realism of a map in abstractly representing a spatial 'reality' provides ample understanding of the location of hills, valleys and the more general topological information describing that 'reality'. However, if areas represented as woodland or urban on the map are minutely examined, only fibres on the paper can be observed, not individual trees or houses. The generic characteristics of the map are not found in the representation itself but in the approach used in creating that representation.

Similarly, the current model is intended to provide a graphical representation of specific qualitative characteristics of a catchment without the need to provide detailed information relating to the diversity of chemical states of the soil which are evident within the catchment.

The fundamental nature of the phenomena - for example whether it involves potentially damaging additions to the wider environment, the loss or degradation of natural resources, or competition between two opposing processes for limited resources - will determine the approach to representation of the phenomena and thus necessarily the generality displayed by the model. The current research uses generic equations for the representation of acidification dynamics and phosphate adsorption processes within the soil, the generic form of the adsorption equation being:

$$\text{Adsorption} = A\,M\,C\,/\,(1 + A\,C)$$

where C is the phosphate concentration in the soil solution,
M is the adsorption maximum, and
A is an affinity term describing the rates of adsorption and desorption.

However, the characteristics displayed by these generic equations will emerge as a direct consequence of the specific spatial location to which they are applied since both the adsorption maximum and the affinity term are directly dependent upon the chemical characteristics of the soil and the soil pH. Further details of the adsorption equation and its application may be found in the following chapter.

The correlation of the model with 'reality' must necessarily reflect the spatio-temporal perspective of the phenomena, giving an understanding of 'reality' through observation and interpretation of simulated changes. The current research demands observation of spatial patterns emerging across an entire river catchment; the spatial resolution of the model and thus the perspective of observations must therefore clearly highlight these patterns in order to provide interpretable simulations which are representative of the observable 'reality'.

The precision of the model need only reflect the perspective necessary to represent 'reality' and provide an appropriate heuristic. Conceptualizing 'reality' in a hierarchical framework allows models to accommodate multiple levels of resolution.

For examination of phenomena across a catchment - specifically the relative resilience or sensitivity to eutrophic change - the degree of resolution employed must relate to the constraints imposed by the spatial and temporal characteristics of the catchment. If the resolution is too great, then mechanisms of change defined within this discrete hierarchy may not be appropriate for the definition of communication pathways through a fundamentally continuous hierarchical perception of the real world; the detail of the representations may become too far removed from the observational perspective for meaningful examination.

Given that 'reality' will necessarily be abstracted through various conceptual representations into a dynamic computer model, precise quantification of elements of that 'reality' becomes progressively more meaningless and precludes logical validation [Mankin et al. 1975]. Qualitative representations of spatio-temporal patterns of change may thus provide a better heuristic of inherent sensitivity or resilience to perturbations. Accordingly, the current research reflects a perspective whereby observations of patterns of change at the catchment level are possible without the need to address micro-level dynamics of microbial activity or soil structuring dynamics.

Although the current model is structured hierarchically - described in detail in the following sections - notions of hierarchies have been employed in far broader fields. As observed by Allen and Starr (1982), hierarchical arrangements are central to biology and even have an Aristotelian origin. They also highlight the complementary relationship of notions of hierarchies and computers, where computers are based upon hierarchical structures but also provide tools assisting further development of theories of hierarchies.

However, it is essential to recognize that 'reality' is not discretely hierarchical, but rather it reflects continuities across arbitrarily defined spatial and temporal boundaries, and displays considerable heterogeneity amongst mechanisms of change [Simon 1962]. Representations of 'reality' based upon discrete hierarchies may therefore result in some patterns of change remaining unobserved. The notion of hierarchies is thus a consequence of human intrusion resulting from a desire to make sense of observations of change. The heuristic value of hierarchies becomes apparent when attempts are made to achieve a convergence between observations and understanding of change [Allen & Starr 1982].

This line of thought could be elaborated upon with an examination of the rigour of Systems ideas and hierarchies and the ability to unambiguously represent continuous 'realities' using inherently discrete structures. This discussion has been continued by Checkland (1991; 1992), examining such concepts as holons [Koestler 1967], but is beyond the scope of the current research.

3.1 MODEL CONCEPTUALIZATION

Owing to the complexity of the phenomena to be modelled and the non-linear and discontinuous inter-relationships of the phenomena, it is useful to employ the concept of a notional indicator of change focusing upon these inter-relationships. It is already clear that this focus involves the influence of Acid Rain upon the characteristics of the soil affecting the potential for retention or release of phosphates.

This notional indicator will become formalized (see Section 3.2.5) as a specification for the catastrophe indicator (see Chapter 4, Equation 27). The following sections clarify this focus by addressing the 'contributory cause' *(Acid Rain)*, the 'potential effect' *(Eutrophication)*, and the region of potential conflict between these phenomena *(Soil Dynamics)*.

3.1.1 EUTROPHICATION

Eutrophication is a naturally occurring phenomenon whereby high nutrient loads in watercourses result in excessive growth of aquatic plants and algae, reducing the oxygen content of the water and potentially killing the resident animal life. However, under 'normal' conditions, eutrophication is controlled by one or more limiting nutrients, and it is only when such limiting nutrients become abundant that eutrophic algal growth represents a potential problem.

In the case of Rutland Water, widespread eutrophication appeared in 1989 in the form of 'Blue-Green Algae' - or *Microcystis aeruginosa* - which is phosphate-limited [Trow 1990]. In this instance the problem was compounded by the extraction of water for human consumption from depths showing the smallest concentrations of phosphates.

Ignoring the potentially exacerbative effects of water abstraction practices, some potential linkages between the sources of phosphates and ultimate eutrophication are shown in Figure 3.1(a). Sources of phosphates may be from agriculture or sewerage outfalls, estimated in approximately equal quantities in the case of Rutland Water [Ball 1990], suggesting multiple point and dispersed sources. These phosphates may then accumulate and become concentrated in rivers and lakes, potentially reaching eutrophic concentrations.

Where eutrophication is perceived as a problem, the problem must be addressed at the source of the phosphates if continual 'fire-fighting', through mitigation of the observed eutrophic effects, is to be avoided.

3.1.2 ACID RAIN

Acid Rain encompasses both wet and dry deposition of airborne acidic materials, in particular airborne sulphates, nitrates and ammonia. The sources of these acidic substances are many and diverse, but the major sources can be identified as from fossil fuel combustion arising from power stations [Gillham et al. 1992].

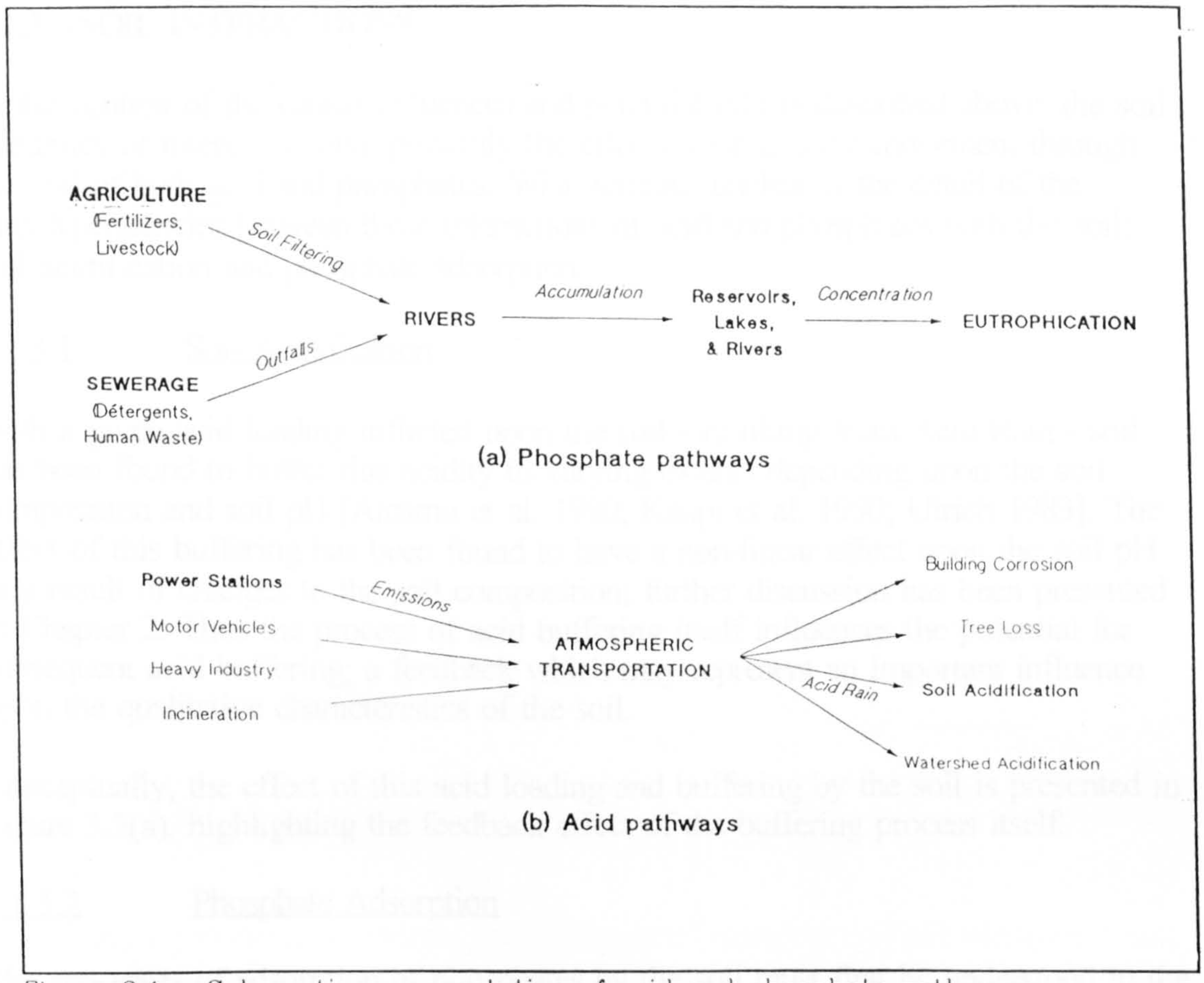

Figure 3.1 – Schematic representation of acid and phosphate pathways

Irrespective of the specific source, all such airborne acidic emissions will be dispersed spatially through atmospheric transportation, and, depending upon the climatic conditions, will be deposited over a wide area. The regional sources, atmospheric transportation and eventual deposition have been estimated and modelled across Europe by the RAINS model of acidification [Alcamo et al. 1990], discussed in Chapter 2.

Figure 3.1(b) identifies a number of the potential effects of acid rain and highlights a potential linkage with the acid source, namely atmospheric transportation. These effects may be as diverse as building corrosion, watershed acidification, tree loss, soil acidification, and others.

A possible linkage between a source of acid emissions and the potential indirect propagation of eutrophication has therefore been identified; the common element involving soil acidification and its effect upon the ability of the soil to act as a source or a sink for phosphates determining, in part, the rate of release of agricultural phosphates into the river systems. This suggests that the point of conflict between the contributory cause and potential effect lies in the interactions of the soil with acidity and phosphates.

3.1.3 SOIL INTERACTIONS

In the context of the causal influences and potential effects described above, the soil dynamics of interest involve primarily the effects upon and the movement through the soil of both acid and phosphates. What remains unclear is the detail of the interdependencies between these interactions of acid and phosphates with the soil; soil acidification and phosphate adsorption.

3.1.3.1 Soil Acidification

With a given acid loading inflicted upon the soil - resulting from Acid Rain - soil has been found to buffer this acidity to varying extents depending upon the soil composition and soil pH [Alcamo et al. 1990; Kaupi et al. 1990; Ulrich 1983]. The effect of this buffering has been found to have a non-linear effect upon the soil pH as a result of changes to the soil composition; further discussion has been presented in Chapter 2. Thus the process of acid buffering itself influences the potential for subsequent acid buffering; a feedback which may represent an important influence upon the qualitative characteristics of the soil.

Conceptually, the effect of this acid loading and buffering by the soil is presented in Figure 3.2(a), highlighting the feedback effect of the buffering process itself.

3.1.3.2 Phosphate Adsorption

The processes of adsorption of phosphates by the soil must first be understood in the context of their underlying characteristics:

- the adsorption process itself is highly complex, resulting in diverse rates and permanence of adsorption involving the emergence of many similar and dissimilar phosphate compounds of varying chemical stability within the soil [Cosgrove 1977; Barrow 1978; Jones et al. 1984]; see Chapter 2 for details.

- these processes represent an inherent part of a specific Chemical Time-Bomb phenomenon, triggered upon reaching the adsorptive capacity of the soil [Breeuwsma & Reijerink 1992].

The complexity of adsorption is addressed, and abstracted to an appropriate degree for modelling, in the following sections. The chemical time-bomb characteristics displayed suggest these adsorptive processes are potentially highly significant regarding future unexpected eutrophic releases of phosphate.

Adsorption is dependent upon the soil composition, rates varying significantly between calcareous and acidic, or sandy, soils [Barrow 1980a, 1980b], and adsorption also affects the soil composition itself through effective removal of potential adsorption sites. However, although most of these studies identify the rates of adsorption - determined experimentally or through simulations - as being affected by the soil pH, the studies do not address the effect upon these rates of a changing pH. These studies have been discussed in detail in Chapter 2.

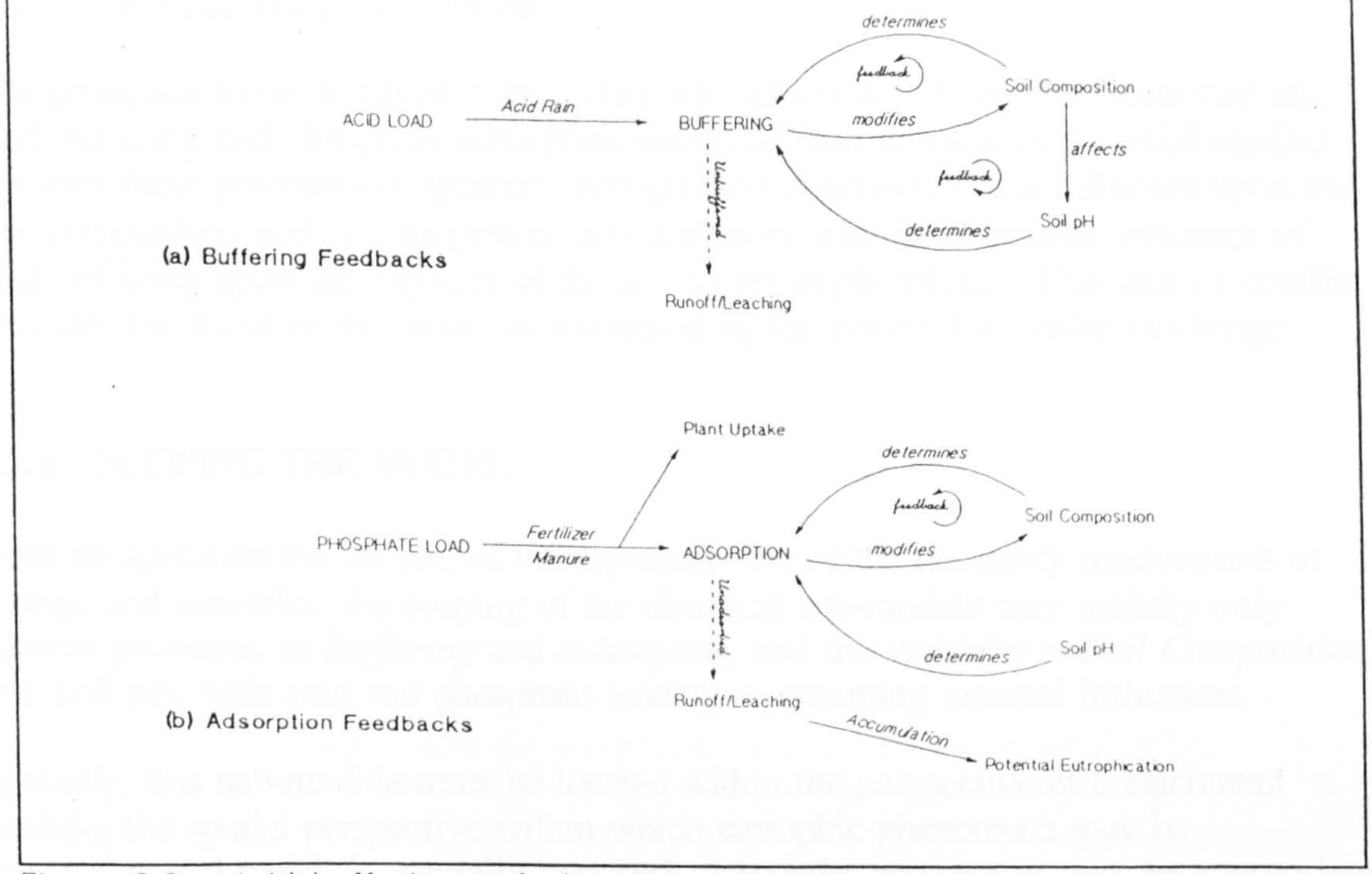

Figure 3.2 – Acid buffering and phosphate adsorption feedbacks

It is therefore essential to address this influence of changing soil pH when the focus of the model also involves the effects of acid deposition. Stevenson (1986) identifies the varying affinity for adsorption depending upon the soil pH, and thus provides a basis upon which these conflicting processes of acid buffering and phosphate adsorption may be related.

The feedbacks associated with adsorption are presented in Figure 3.2(b). Immediately, it becomes apparent where the area of conflict between these processes of adsorption and buffering may appear, namely in the manner in which they are affected by and affect the soil composition and the soil pH.

3.1.4 SUMMARY

Acid emissions from a proposed power station may be dispersed through atmospheric transportation and deposited as acid rain. This acidity will be completely or partially buffered through chemical reactions within the soil, affecting both the soil composition and the soil pH. These changes to the composition and pH of the soil have a consequent non-linear and discontinuous effect upon the adsorptive affinity of the soil in relation to applied fertilizer phosphates and manure, potentially providing a trigger for a phosphate related chemical time-bomb resulting in eutrophication.

The point of conflict between these processes - the focus maintained by the notional indicator conceptualized earlier - may therefore be identified where the feedbacks inherent in adsorption and buffering overlap to act as this trigger.

3.2 MODEL SPECIFICATION

The processes to be represented by a chemical sub-module have been identified as acid buffering and phosphate adsorption within the soil domain. A potential conflict between these processes is apparent through their dependency and influence upon the soil composition and pH, suggesting a perturbatory and discontinuous influence of acid buffering upon the capacity of the soil to retain phosphates. This area of conflict provides the focus of the model as suggested by the notional indicator of change.

3.2.1 SCOPING THE MODEL

With no specification, as yet, of the representation of the necessary mechanisms of change and variables, the scoping of the chemical sub-module may initially only address processes as *Buffering* and *Adsorption*, and the variables as *Soil Composition* and *Soil pH*, with acid and phosphate loading representing external influences.

Spatially, this sub-module must be located within the perspective of a catchment module; the spatial perspective within which eutrophic phenomena may be observable and which is naturally bounded. A broader perspective may be appropriate if groundwater flows were to be addressed in addition to surface flows.

Since acidic emissions are subject to atmospheric transportation over a wider area (effectively many catchments), this model can only address acid rain as an external perturbatory influence upon the catchment module. Thus, the model addresses the causal influences, shown schematically in Figure 3.1(b), only from the point of acid deposition, modelling its influence upon soil acidification.

The focus of the model requires similar demarcation with regards to the effectual processes shown in Figure 3.1(a). Since the focus involves the capacity of the soil to retain phosphates, once phosphates have been lost from the soil and entered the river system, they are assumed to have no further influence upon the capacity reflected by the model. The hydrological dynamics of the catchment require implementation in a hydrological sub-module controlled by the catchment module, recognizing that meaningful observation of accumulations of phosphate within the river system may be different to that required for observation of capacity variations within the soil.

Finally, the functional scoping of the model assumes that buffering and adsorption processes represent the only influence upon the soil composition and soil pH.

3.2.2 SCALING THE MODEL

With the scope of the model clearly bounded functionally, and spatially by the definition of a catchment, the spatial scale of the individual cells - each containing chemical and hydrological sub-modules - within the catchment requires definition. The spatial representation is based upon an 8 x 8 spatial grid, as discussed in section 3.4.

Spatial demarcation of the cells should ideally reflect a scale compatible with definitions of the buffering and adsorption processes, and where spatial data is available to define the soil composition and soil pH. However, this may not always be feasible, and in the present case the data necessary for appropriate definition of soil composition and pH is available from a single source and reflects measurements at 5km intervals across England and Wales [Loveland 1990].

Therefore, with the currently available data (see Section 3.3), the individual cells will necessarily reflect a 5km square space of the catchment. If a greater degree of resolution is needed then further data collection would be required.

Finally, temporal scaling will be dependent upon the representations of the processes themselves, but may require modification in order to ensure that modelled rates within both the individual cells and the catchment module are compatible.

3.2.3 PROCESS IDENTIFICATION

The mechanisms of acid buffering, as defined by Alcamo and others (1990), represent an abstraction of the actual chemical processes - based upon the cation composition of the soil - which is compatible with the spatial scaling of this model due to the broad spatial perspective required of RAINS. This representation of buffering also provides a non-linear definition of the soil pH as a consequence of acidification.

Definition of phosphate adsorption, however, requires additional spatial abstraction since, although many perceptions of this mechanism of change have been described [Olsen & Watanabe 1957; Russell & Prescott 1916; Hayward & Trapnell 1964; Barrow 1978; Jones et al. 1984], they tend to describe the changes at the 'micro' scale, incompatible spatio-temporally with the perspective required of this model. Such descriptions address the complexity of phosphate compounds and the diversity of compounds' stability and reaction rates [Enfield et al. 1976], the specific dynamics of phosphate adsorption in calcareous or acidic soils [Barrow 1980a, 1980b], the influence of microbial activity and organic matter levels upon adsorption [Cosgrove 1977], and the effects of temperature, plant uptake and diffusion of phosphates through the soil solution [Barrow 1974; Barrow & Shaw 1975a, 1975b].

The current research, for the reasons discussed in Chapter 2, employs a variant of the multi-term Langmuir 'isotherm'. This will result in the omission of some of these micro-level influences to the benefit of a representation which can accommodate the key inter-relationships with acid buffering.

The hydrological processes requiring representation are primarily related to the spatial flows through the catchment; flow directions being controlled at the catchment level. These hydrological representations will define the boundary conditions relating to the spatial flow of acid and phosphates between individual cells. The HOST classification provides the basis for definition of these hydrological dynamics [Boorman & Hollis 1992] and is described in Chapter 5.

3.2.4 VARIABLE IDENTIFICATION

Since the fundamental difference in this model to existing representations of phosphate adsorption is the changing pH resulting from acidification, it is necessary to define the soil composition to reflect the definition of acidification. Thus, by abstracting the representation of adsorption to a degree compatible with this definition of soil composition, the major variables required of the model become apparent:

- *Soil Composition*, for acidification purposes, may be represented by two variables, **Base Cations** and **Acid Cations**. As will be shown in Chapter 4, the processes of adsorption may be abstracted to reflect a similar cation split, but aggregates the base and acid cations to be represented by **Calcium** and **Aluminium** respectively;

- *Soil pH*, determined by the base/acid cation levels and the soil pH itself in a similar fashion as employed by RAINS [Alcamo et al. 1990] and discussed in Chapter 2.

- *Acid Loading*, representing a manipulatable input affecting the degree of acid buffering;

- *Phosphate Loading*, representing a manipulatable input affecting phosphate adsorption rates.

Finally, variables in the hydrological sub-module will be required to define the volumes of water maintained both on the surface and within the soil, reflecting saturation levels for each of the individual cells.

3.2.5 CATASTROPHE INDICATOR SPECIFICATION

A notional indicator of change has already been conceptualized to locate a focus reflecting the remaining adsorptive capacity of the soil in the face of continued acidification and phosphate application. However, a quantification of such a state will inherently be temporally static and will not reflect the potential for change in this capacity.

As shown in Figure 3.2, this capacity will be determined by the soil composition and the soil pH. However, since these are continually changing due to buffering and adsorption, a meaningful indicator of change must also reflect these influences, thus suggesting both the remaining capacity and the rate of change in the capacity.

Ambiguity is, however, still inherent in such an indicator of change since it only suggests *continuous* characteristics of change. The theoretical point at which the adsorptive processes show discontinuities, with potential sudden releases of phosphates, must be identified and incorporated into the indicator of change. A determinable indicator of change - or catastrophe indicator - will thus reflect:

- the soil composition and pH (Adsorptive Capacity);
- the rate of change in capacity due to phosphate adsorption;
- the rate of change in capacity due to acid buffering; and
- the proximity of potential discontinuities resulting in the sudden release, as opposed to retention, of phosphates from the soil.

3.2.6 ASSUMPTIONS AND OMISSIONS

Within this brief conceptualization, a number of assumptions have been made along with potentially significant omissions. In order to enhance the clarity of interpretations of observed simulated change, it is important to highlight the assumptions in, and omissions from the model.

The major assumptions may be summarized as:

- Only the buffering of acid and the adsorption of phosphates has any influence upon the soil composition and soil pH.
- The 'active' soil composition is assumed to be only base and acid cation reserves represented by Calcium and Aluminium, respectively.
- The soil pH is determinable from this soil composition and the soil pH itself [Alcamo et al 1990; Kaupi at el. 1990; Ulrich 1983].
- The significant hydrological characteristics of the soil are adequately represented by the HOST classification system and related Standard Percentage Runoff (SPR) and Volumetric Moisture Content (VMC). For the estimation of catchment response, HOST shows a correlation with more than 80% and 60% of measured variations in the Base Flow Index (BFI) and SPR, respectively (see Chapter 5).
- Acid rain and phosphate loadings may be treated as external influences, and phosphates lost to watercourses are taken to have no further influence since the focus of the model lies in the retention or release of phosphates by the soil, and not subsequent potentially eutrophic accumulations of phosphate in the river systems.
- A 5km square spatial definition - imposed due to the format of available data - will provide change observable from the catchment perspective.

The major omissions may be summarized as:

- The effects of alternative cation sites for both buffering and adsorption.

- The variability and complexity of phosphate compounds and their solubility or permanence.

- The influence of organic matter and microbial activity on the processes of buffering and adsorption, and of these and weathering on the soil composition. The additional complexity surrounding such influences is reflected in the model presented by Jones and others (1984) and is discussed in Chapter 2.

- The effects of groundwater flows since these, as are rivers, are external to the soil region acting as a sink or source of phosphates.

- The effects of temperature.

3.3 STUDY REGION

This research is not concerned with a specific proposed development, but has identified a possible linkage between the direct impacts of a particular type of development (Acid Emissions) and an ecological phenomenon perceived as an environmental problem (Eutrophication).

An appropriate study region for representation by a dynamic spatio-temporal model should therefore ideally represent a region where eutrophication has either already been observed or is perceived as a potential problem.

In a European context, an ideal such location may be found in The Netherlands or Belgium since these are already clearly identified as being intensive agricultural regions with high levels of phosphorus inputs and the soils being near to their adsorptive capacity [Breeuwsma & Reijerink 1992]. These regions are also subjected to high levels of acid deposition [Alcamo et al 1990]. Furthermore, in a Belgian context, development of a soil acidification/adsorption model may be complemented by the availability of hydro-chemical models of river basins [Billen 1992] and models of anthropogenic development [Sanglier & Allen 1989] in addition to the regional acidification model, RAINS. The location of the current research in relation to such models has been discussed in Chapter 2.

However, due to practical limitations imposed on this research, a study region in the United Kingdom has been identified.

3.3.1 RUTLAND WATER CATCHMENT

Rutland Water in Leicestershire presents an interesting example. Rutland Water is the largest man-made lake in Europe, completed in 1975, but by 1989 had already been subject to eutrophication in the form of toxic 'Blue-Green Algae', or *Microcystis æruginosa*, at critical levels resulting in the death of livestock drinking from the reservoir [Trow 1990; Phillips 1990]. With the abstraction of water for human consumption being made from the most phosphate free depths, this problem of eutrophication remains a concern.

Measures such as dumping iron filings in the reservoir in order to precipitate phosphates into the sediments have been carried out resulting in a degree of control over the quality of the water. However, these measures do not remove the phosphates and potentially create an environment supportive of CTB phenomena in the instance of sediment disturbance; this potential is not addressed by this research.

The region of interest is the catchment which supplies Rutland Water, namely the catchments of the River Welland and the River Nene; pumping stations at Tinwell and Elton Lock, Wansford on the Welland and Nene, respectively, provide the majority of water held in the reservoir. These catchments are subjected to acid rain through their proximity to heavily industrialized regions and power stations [DoE 1990; Gillham et al. 1992; Rose 1988], but, unlike the continental examples the region is not low lying, sandy and near to its phosphate capacity.

Using the Rutland catchments as a study region, therefore, may assist understanding of whether the catchment itself is potentially sensitive to eutrophic phenomena, which is not as immediately apparent as in The Netherlands, or whether the problem is confined to Rutland Water and contemporary water abstraction practices.

The study region used as a focus for this work may therefore be described spatially by the boundaries of the Nene and Welland catchments, as shown in Figure 3.3. These boundaries provide the spatial definition of the catchment module described in Section 3.4. For the purposes of mapping this study region onto a spatial form in the model, use is made of a spatial grid with the flow pattern defined as in Figure 3.5(b).

3.3.2 DATA SOURCES

With the spatial boundaries of the 'reality' to be observed clearly defined by the natural boundaries of the Rutland Water catchment - encompassing the Rivers Nene and Welland - the necessary data for model development could be obtained.

Initial examination of The Soil Geochemical Atlas of England and Wales [McGrath & Loveland 1992] identified both the enforced scaling of 5km cells in the model and the necessary sources of soil composition data. For each 5km cell, the following data was obtained from the National Soil Inventory (NSI) held at the Soil Survey and Land Research Centre (SSLRC) at Silsoe College [Loveland 1990]:

- Soil pH.
- Phosphorus content (total conc. mg/kg Soil), interpreted in the model as previously adsorbed phosphate.
- Phosphorus content (extractable conc. mg/litre), interpreted in the model as the concentration of phosphate in the soil water.
- Aluminium content (mg/kg Soil).
- Calcium content (mg/kg Soil).

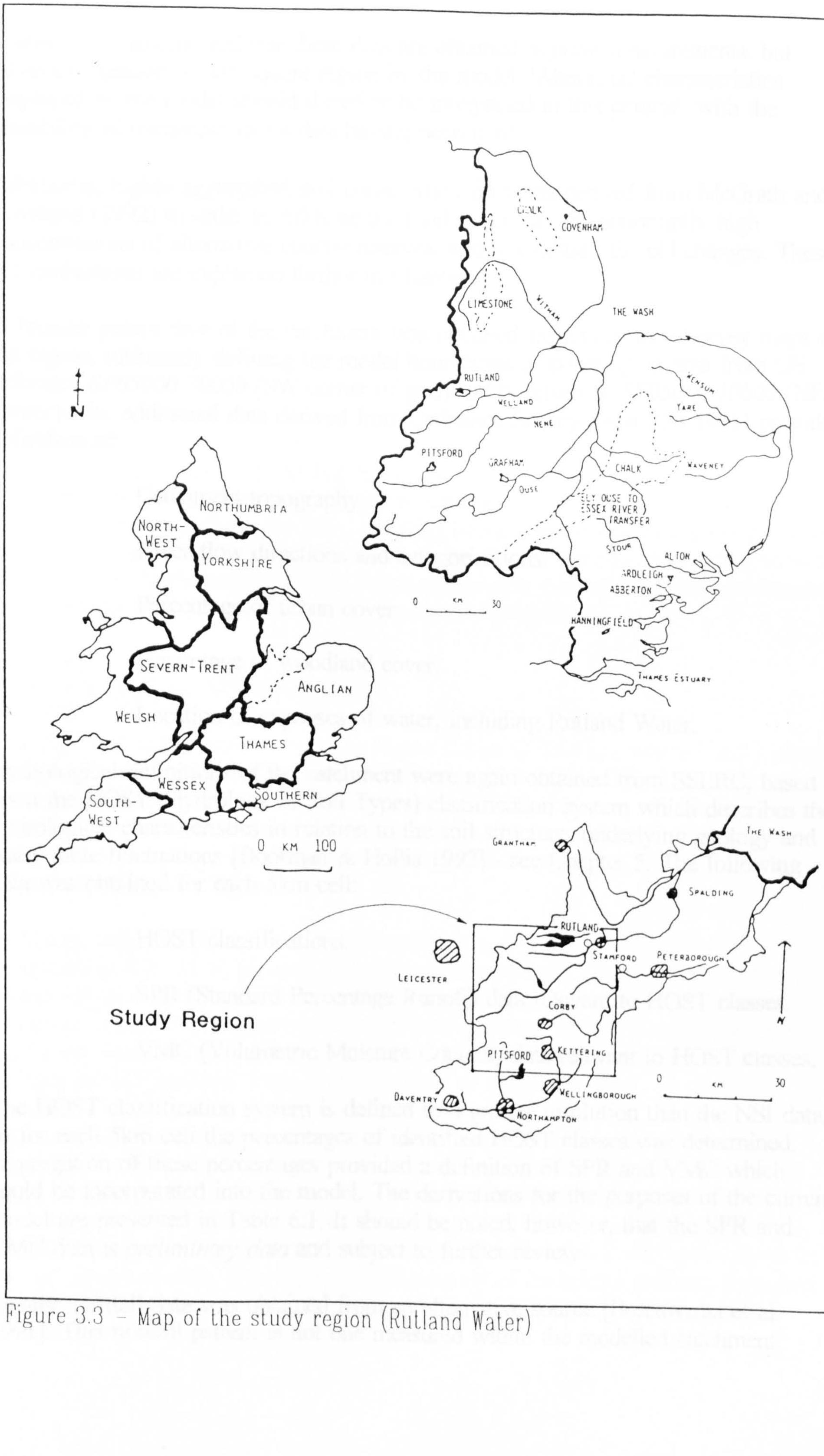

Figure 3.3 – Map of the study region (Rutland Water)

It should be remembered that these data are obtained as *point* measurements, but taken to represent a 5km square region by the model. 'Abnormal' characteristics displayed by the model should therefore be interpreted in this context, with the possibility of unrepresentative data having been used.

Additional, highly aggregated, soil composition data was derived from McGrath and Loveland (1992) in order to calibrate the model, account for abnormally high concentrations of alternative cations reserves, and to calibrate the pH changes. These pH calibrations are explained further in Chapter 6.

A broader perspective of the catchment was obtained from Ordnance Survey maps of the region, ultimately defining the model boundaries as covering an area from OS reference *SP65000 70000* (SW corner of grid) to OS reference *TF05000 10000* (NE corner). The additional data derived from Ordnance Survey maps [OS 1991] provided definition of:

- Catchment topography.
- River flow directions and categorizations.
- Percentage of urban cover.
- Percentage of woodland cover.
- Location of expanses of water, including Rutland Water.

Hydrological definitions of the catchment were again obtained from SSLRC, based upon the HOST (Hydrology of Soil Types) classification system which describes the hydrological characteristics in relation to the soil structure, underlying geology and water table fluctuations [Boorman & Hollis 1992] - see Chapter 5. The following data was obtained for each 5km cell:

- HOST classifications.
- SPR (Standard Percentage Runoff) data relevant to HOST classes.
- VMC (Volumetric Moisture Content) data relevant to HOST classes.

The HOST classification system is defined to a greater resolution than the NSI data, so for each 5km cell the percentages of identified HOST classes was determined. Aggregation of these percentages provided a definition of SPR and VMC which could be incorporated into the model. The derivations for the purposes of the current model are presented in Table 6.1. It should be noted, however, that the SPR and VMC data is *preliminary data* and subject to further reviews.

Finally, rainfall data was obtained from an alternative source [Breeuwsma et al. 1991]. This rainfall pattern is not one measured within the modelled catchment.

However, since this model is defining acid and phosphate inputs as homogenous and continuous, and unrelated to rainfall events, the daily variations in rainfall are unimportant; any 'realistic' annual rainfall pattern is therefore assumed to be adequate, repeating the pattern for each simulated year. The potential for experimentation in this area is discussed in later chapters.

An average, continuous input of 10 kM ha^{-1} $year^{-1}$ of acid rain, and 31 kg ha^{-1} $year^{-1}$ of phosphate is imposed on the model until the latter simulations, reflecting aggregate annual deposition levels [Ulrich 1983] and average fertilizer application levels [MAFF 1983], respectively.

3.4 MODEL STRUCTURE AND PROCEDURE

The preceding discussions have referred to the use of hierarchical structures, and to sub-modules addressing the chemical dynamics and the hydrological characteristics, with a catchment module providing the overall control. In order to provide a clear understanding of the computational and procedural requirements of the model, the interactions between these modules, and their hierarchical relationships are discussed below, with reference to the schematic representation of the model structure provided in Figure 3.4. In the context of this structure, the operation of the model is discussed and the logic of the simulation strategy adopted in clarified.

3.4.1 CHEMICAL SUB-MODULE

The chemical sub-module - shown in Figure 3.4 as CHEM(i,j), where i and j identify the spatial cell - addresses the chemical phenomena being modelled, maintains a set of state variables defining the soil composition, and operates on a daily basis with a timestep, dt, of 0.1. The chemical phenomena modelled are Acid Buffering and Phosphate Adsorption, and the state variables are Calcium (Ca), Aluminium (Al), Phosphorus (P), acid (H) and the soil pH.

Buffering and adsorption, as discussed earlier, are dependent upon the soil composition (Ca, Al, P, H) and, internally, by the soil pH. Each timestep the rate of change of these state variables are calculated and the state variables updated. However, inputs of phosphorus, acid and lime (Calcium Oxide) - controlled by the catchment module - will affect the current state, thus also affecting the rates of change, as will 'in-flows' from, and 'out-flows' to adjacent cells.

Outputs from the chemical sub-module are twofold: spatial flows of acid and phosphorus, determined by the hydrological sub-module discussed below, and the value of the catastrophe indicator (R_0). This catastrophe indicator (see Chapter 4, Equations 21-27) is calculated from the current state and the catastrophe potential, P_0, which is determined by the relative influences of buffering and adsorption upon the rate of change of state. It is through interpretation of the spatial surfaces generated using R_0 that the sensitivity of the catchment to the CTB phenomenon being modelled may be assessed.

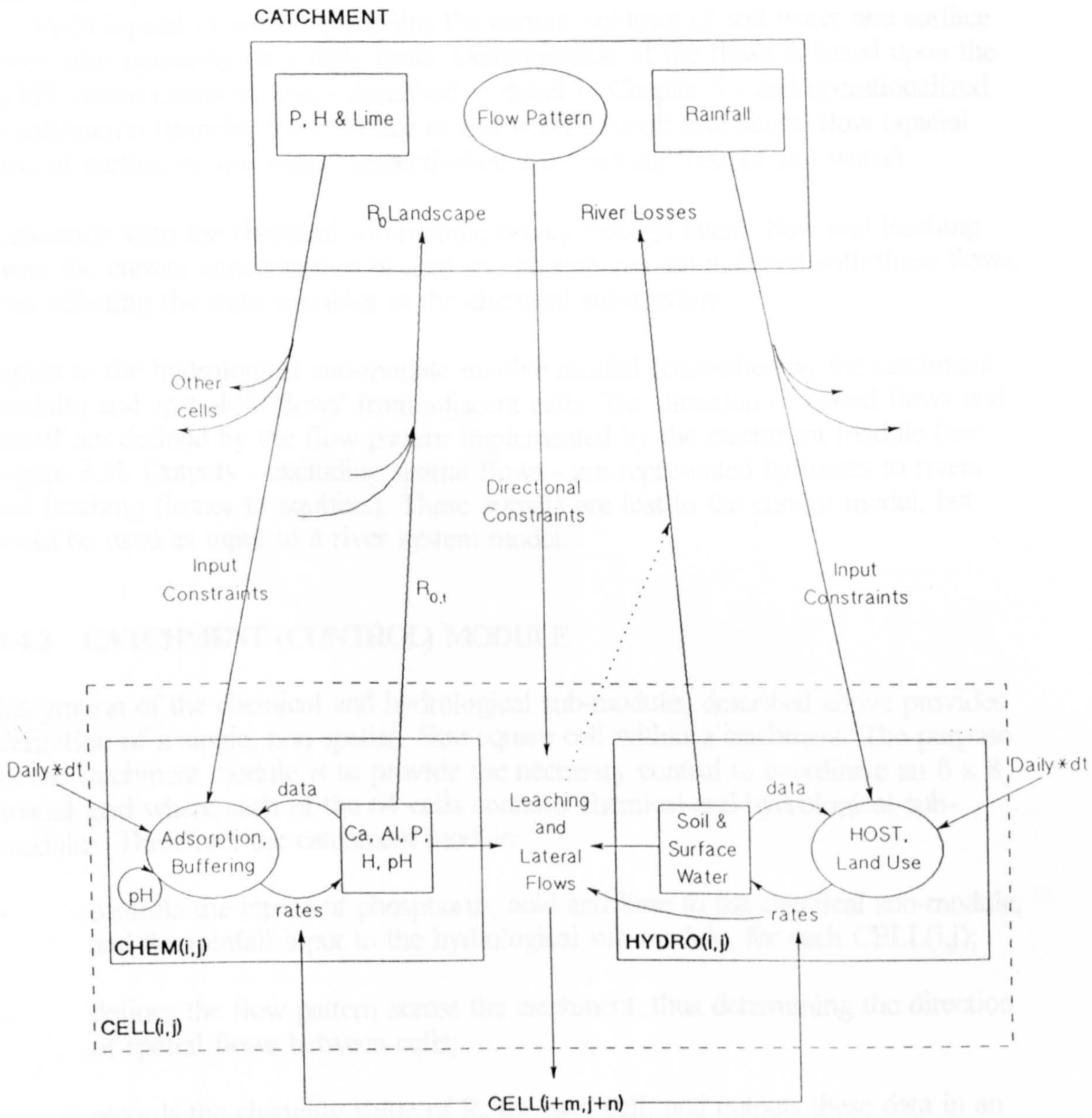

Figure 3.4 - Schematic representation of the overall model structure

3.4.2 HYDROLOGICAL SUB-MODULE

The hydrological sub-module - shown in Figure 3.4 as HYDRO(i,j) - addresses the soil hydrological flows and maintains the current volumes of soil water and surface water, also operating on a daily basis. Determination of the flows is based upon the HOST classification system - described in detail in Chapter 5 - and operationalized as infiltration (transfer from surface to soil water), runoff and lateral flow (spatial flow of surface or soil water, respectively), and leaching (loss of soil water).

Interaction with the chemical sub-module occurs through lateral flow and leaching rates; the current concentration of acid and phosphorus are included with these flows, thus affecting the state variables in the chemical sub-module.

Inputs to the hydrological sub-module involve rainfall (controlled by the catchment module) and spatial 'in-flows' from adjacent cells. The direction of lateral flows and runoff are defined by the flow pattern implemented by the catchment module (see Figure 3.5). Outputs - excluding spatial flows - are represented by losses to rivers and leaching (losses to aquifers). These outputs are lost to the current model, but could be used as input to a river system model.

3.4.3 CATCHMENT (CONTROL) MODULE

Integration of the chemical and hydrological sub-modules described above provides definition of a single, non-spatial, 5km square cell within a catchment. The purpose of the catchment module is to provide the necessary control to coordinate an 8 x 8 spatial grid where each of the 64 cells contains chemical and hydrological sub-modules. Therefore, the catchment module:

- controls the inputs of phosphorus, acid and lime to the chemical sub-module, and the rainfall input to the hydrological sub-module, for each CELL(i,j);

- defines the flow pattern across the catchment, thus determining the direction of spatial flows between cells;

- records the changing value of R_0 for each cell, and outputs these data in an appropriate format for the generation of spatial surfaces; and

- records the losses to rivers and the leaching flows from each cell.

Two flow patterns have been used, as described in Figures 3.5(a) and 3.5(b). The former defines a simple, hypothetical catchment used for examination of the characteristic patterns emerging from simulations. The latter provides an abstract definition of a complex catchment used for the examination of the study region, Rutland Water.

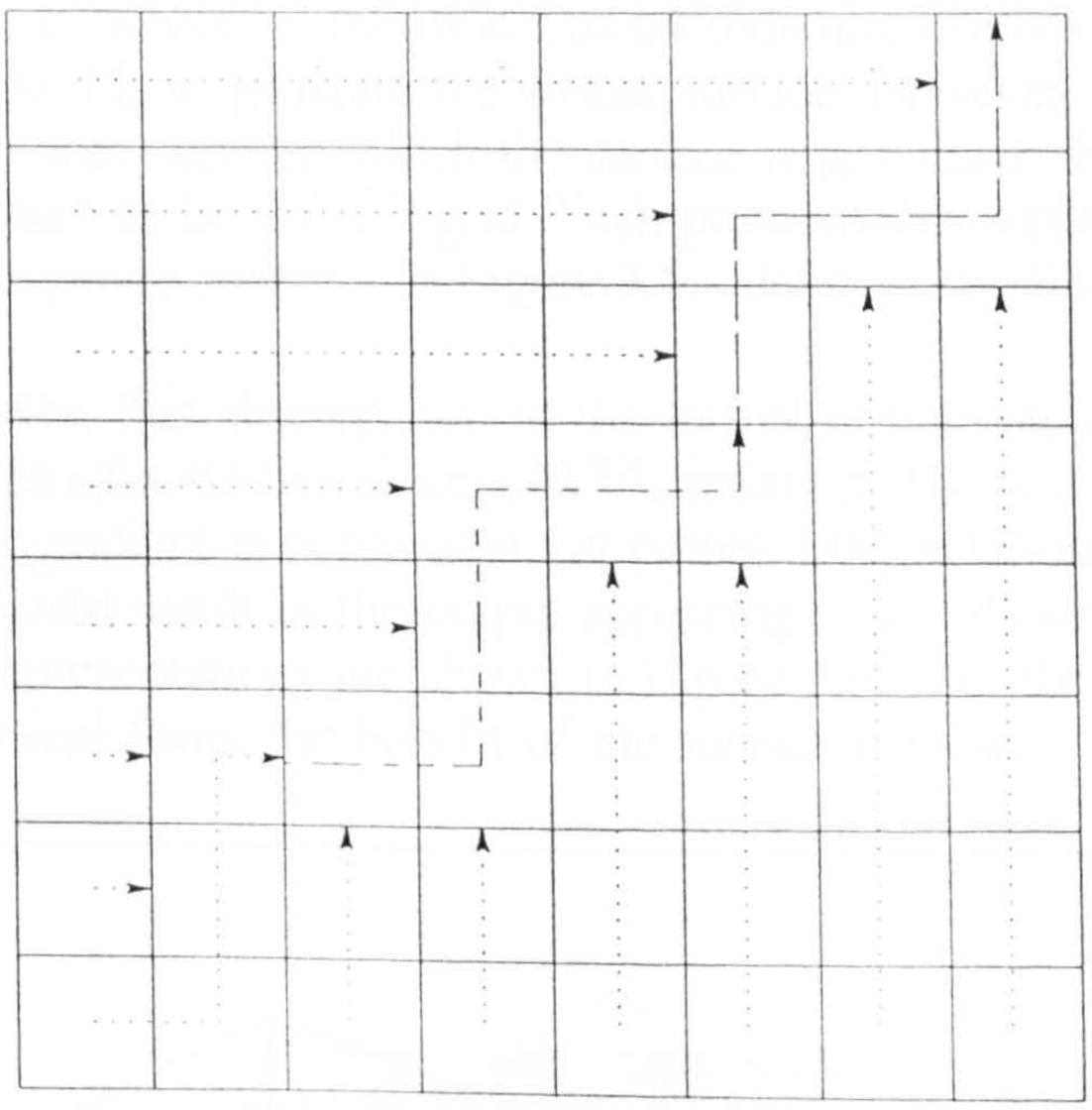

(a)
Simple Catchment Flows

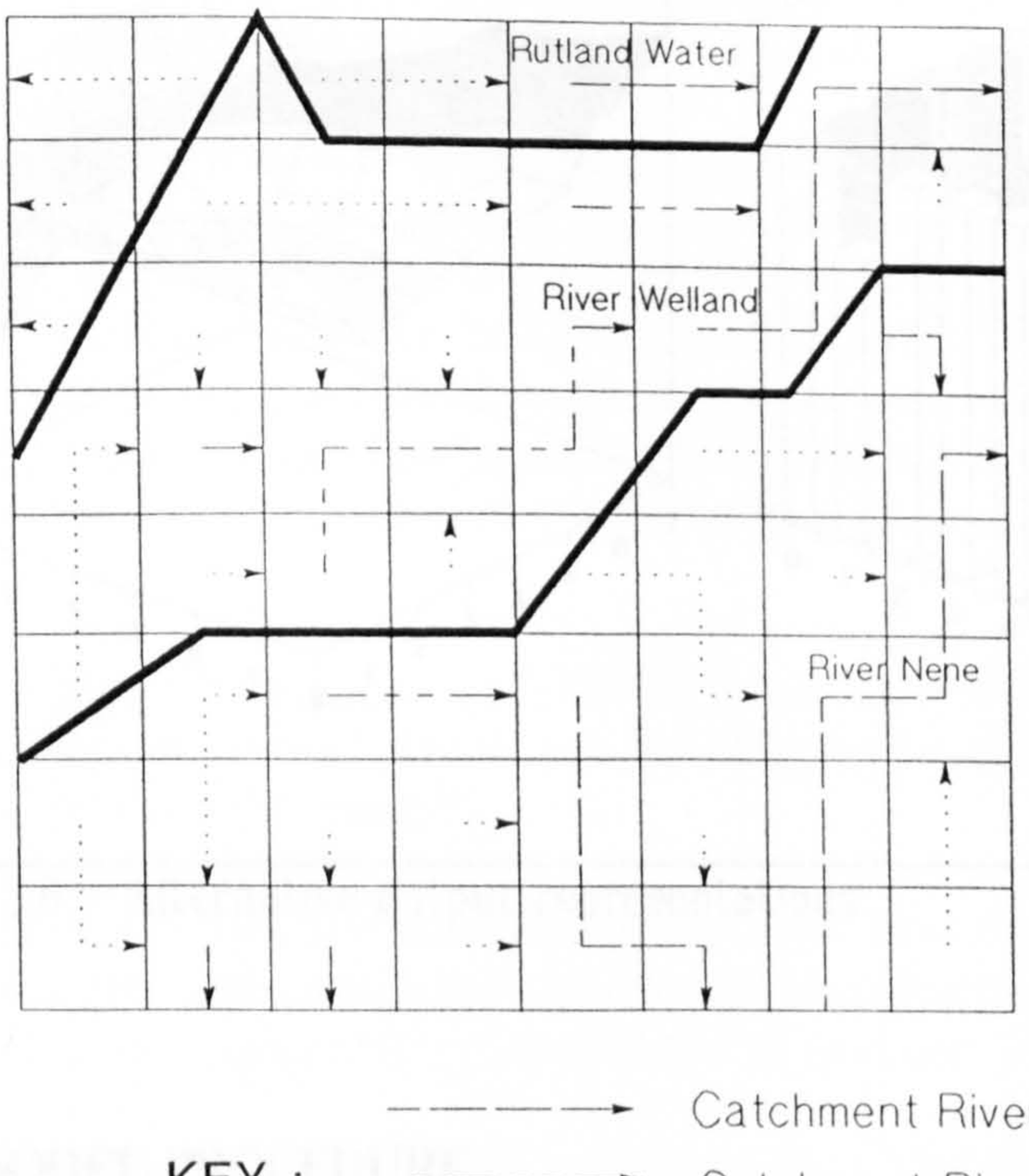

(b)
Rutland Water Catchment Flows

KEY :
- ——— → Catchment River flows
- — - - → Catchment River Feeder flows
- ..... → Flow Direction (No River)

Figure 3.5 - Simple and complex flow patterns as defined by the Catchment Module

For the interpretation of the spatial surfaces, it should be noted that the data defining the surface is output by the model as 64 individual values. These values are then used by EXCEL to generate the spatial surface. However, EXCEL treats these values as single points between which the surface is generated, thus providing an output which appears to be a 7 x 7 grid. Each point on this surface must therefore be related to the appropriate square - in Figure 3.5 - defining the flow pattern.

Paradoxically, this 'discrepancy' in the format of the output results in generation of a more meaningful surface since EXCEL interprets the data as a point and can thus generate a gradient between adjacent points. Interpretation as a 25km^2 area - as in the model - would result in the output appearing as a 3-dimensional bar graph. These possible representations are shown in Figure 3.6, with the same data used to generate each graphical form; the benefit of the surface is clear.

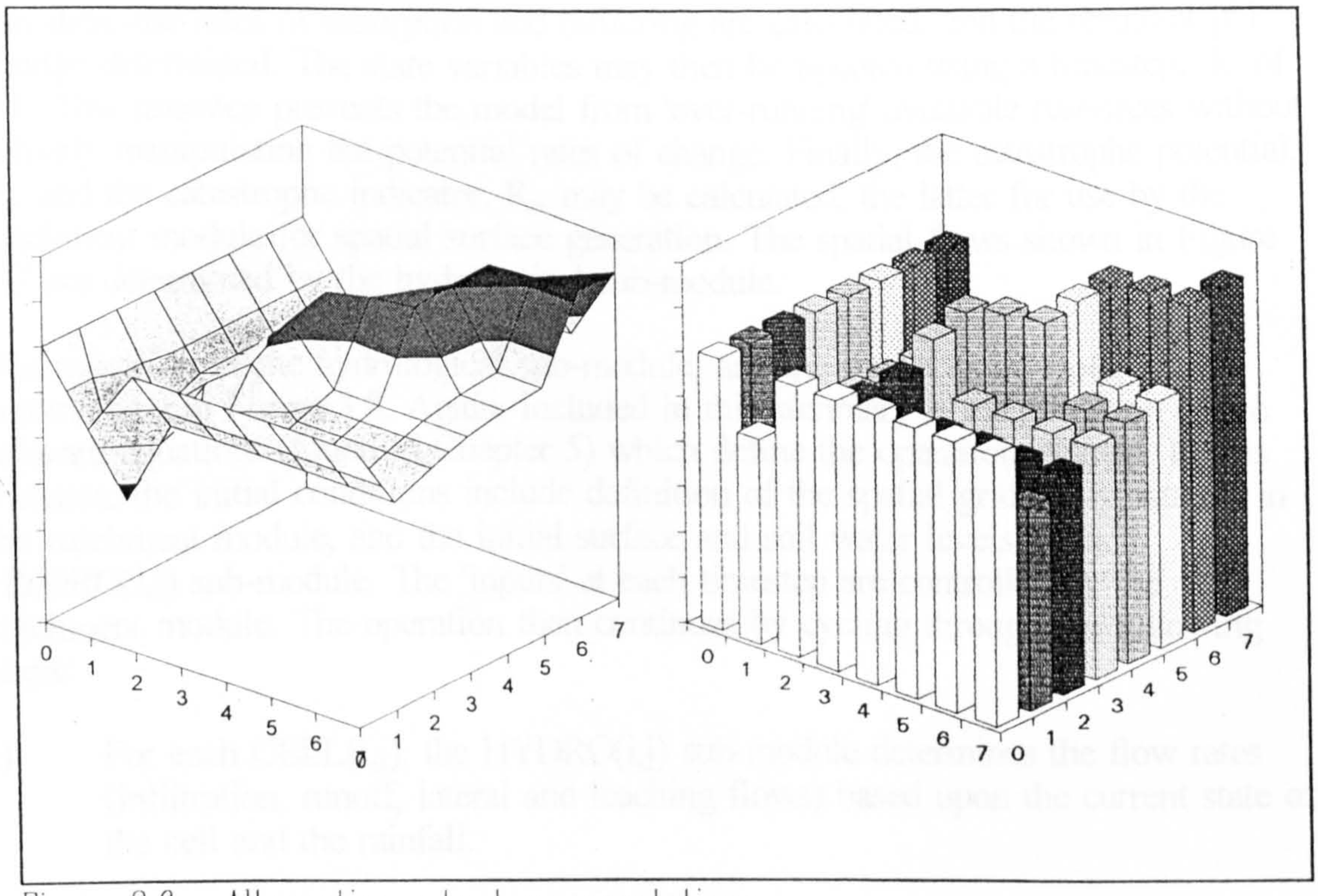

Figure 3.6 – Alternative output representations

3.4.4 MODEL PROCEDURE

The model has been developed and implemented on an Intel 80386 based personal computer. The operation of the model is thus necessarily sequential and requires further explanation; had parallel technology been available, the sub-modules described above could be implemented quasi-independently with interrupt based communications and coordination of the modules.

The following discussion of the model procedure shows that the chemical sub-module can indeed be implemented as a separate module (see Figure 3.7), whereas the implementation of the hydrological and the catchment (control) modules involves interleaving the operation of all the sub-modules in order to overcome the limitations of a sequentially based computational environment (see Figure 3.8).

The operation of the chemical sub-module is summarized in Figure 3.7. Included in this summary is the identification of the relevant equations (found in Chapter 4) which define the operations shown. A call to the chemical sub-module will result in equivalent operation except at time zero (ie. t=0) when the initial conditions of the state variables are input.

The first operation is to recall the current state (stored internally) and to input phosphorus, acid and lime as constrained by the catchment (control) module. With this data, the rates of adsorption and buffering are calculated, and the resultant pH change determined. The state variables may then be updated using a timestep, dt, of 0.1. This timestep prevents the model from 'over-running' available resources without actively manipulating the potential rates of change. Finally, the catastrophe potential, P_0, and the catastrophe indicator, R_0, may be calculated, the latter for use by the catchment module for spatial surface generation. The spatial flows shown in Figure 3.7 are determined by the hydrological sub-module.

The operation of the hydrological sub-module, and the model as a whole, is summarized in Figure 3.8. Again, included in this summary is identification of the relevant equations (found in Chapter 5) which define the operations shown. In this instance, the initial conditions include definition of the spatial grid (flow pattern) in the catchment module, and the initial surface and soil water levels in each HYDRO(i,j) sub-module. The 'inputs' at each timestep are controlled by the catchment module. The operation then continues by cycling through the following steps:

i) For each CELL(i,j), the HYDRO(i,j) sub-module determines the flow rates (infiltration, runoff, lateral and leaching flows) based upon the current state of the cell and the rainfall.

ii) The CATCHMENT module calculates the boundary flows between cells based upon the flow pattern and the lateral flows determined in (i); included in these flows are appropriate concentrations of acid and phosphorus.

iii) For each CELL(i,j), a call is made to the CHEM(i,j) sub-modules (see Figure 3.7) which use these flow rates to modify the chemical state of the cell.

iv) With all flow rates determined across the grid, the HYDRO(i,j) state variables are updated for each CELL(i,j), again utilizing a timestep, dt, of 0.1.

v) The CATCHMENT module outputs the spatial data necessary for surface generation, updates t and specifies the inputs for the next timestep.

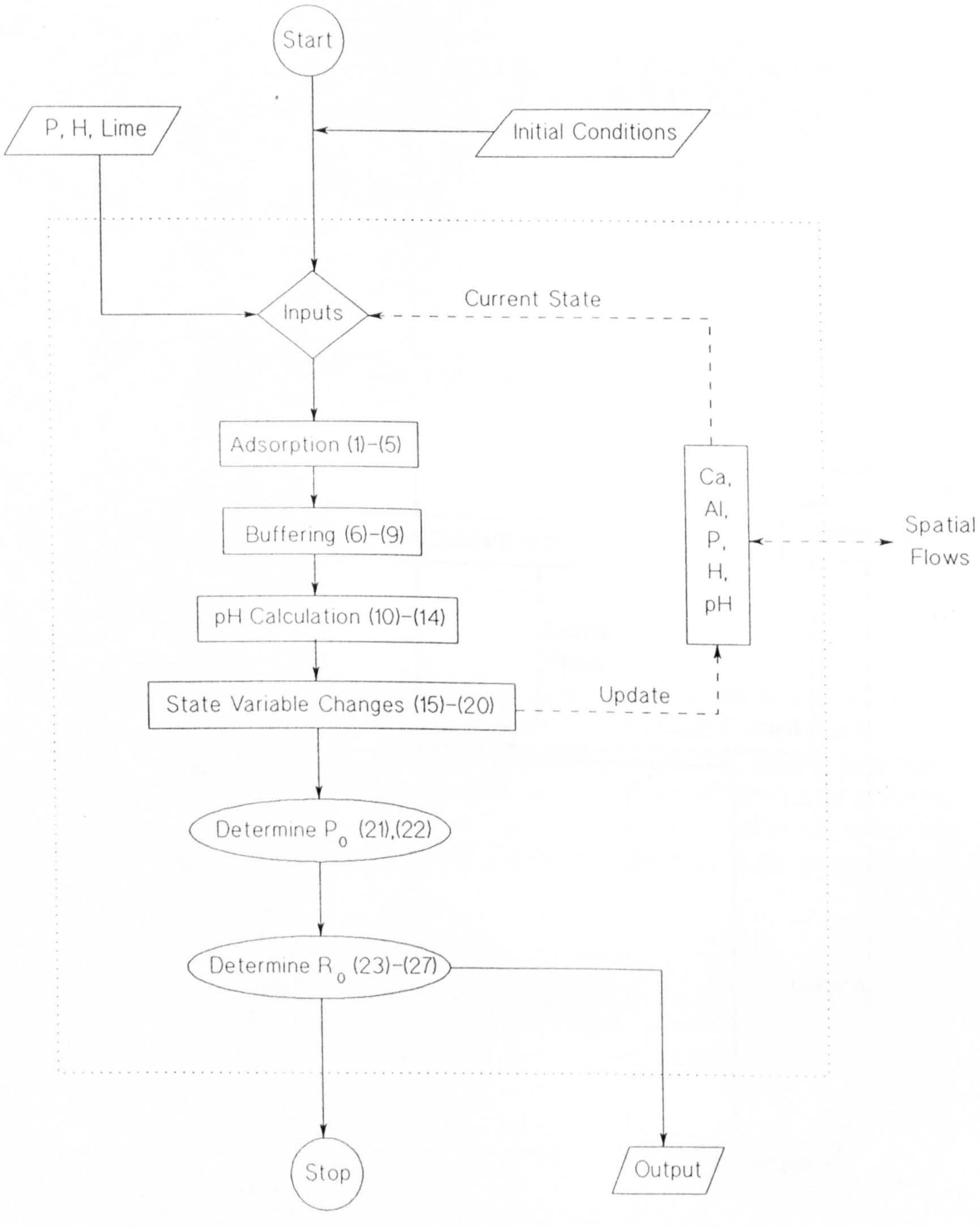

Figure 3.7 - Flowchart showing the operation of the Chemical Sub-Module

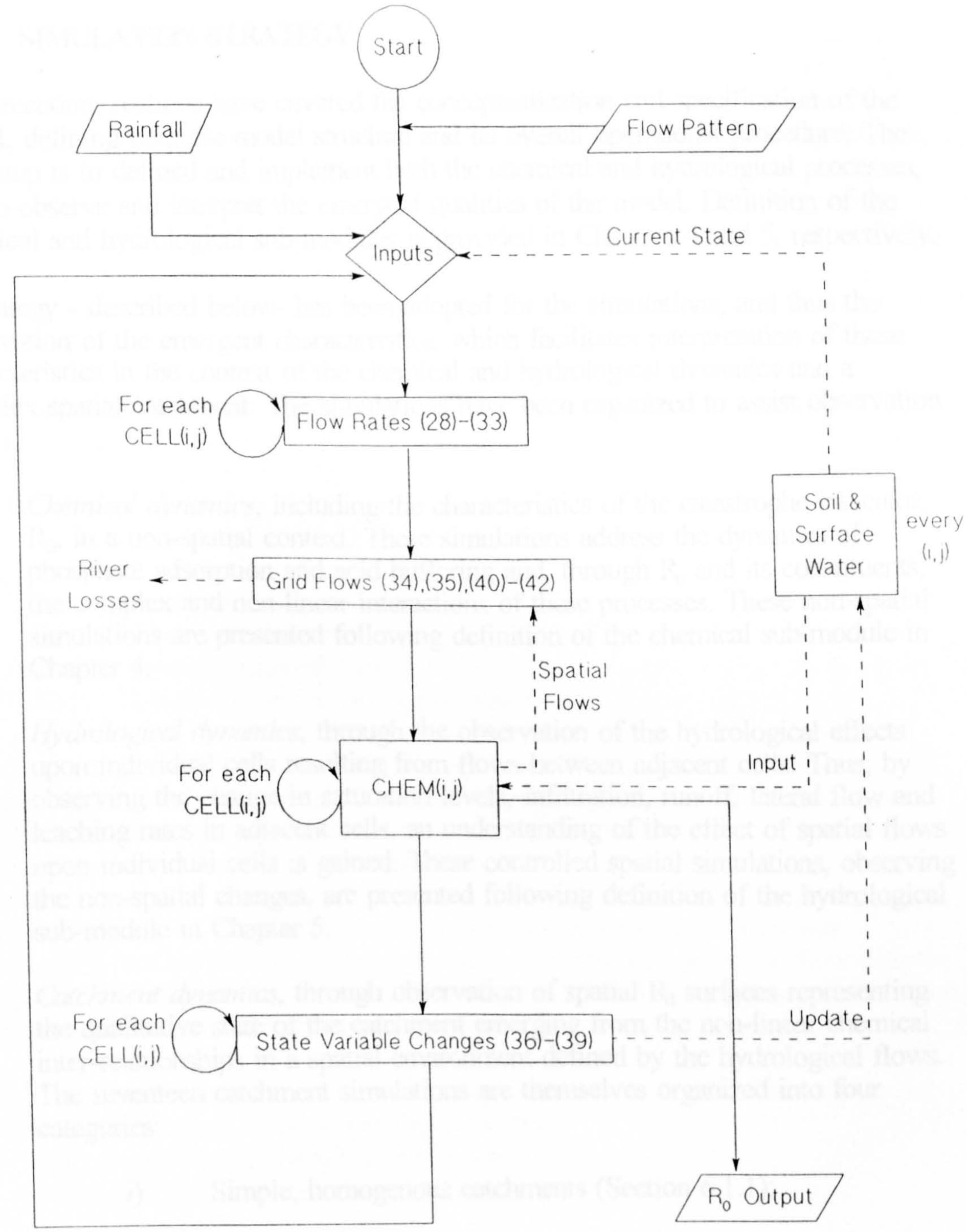

Figure 3.8 - Flowchart showing the operation of the integrated model

3.4.5 SIMULATION STRATEGY

The preceding sections have covered the conceptualization and specification of the model, defining both the model structure and its overall operational procedure. The next step is to defined and implement both the chemical and hydrological processes, and to observe and interpret the emergent qualities of the model. Definition of the chemical and hydrological sub-modules is provided in Chapters 4 and 5, respectively.

A strategy - described below- has been adopted for the simulations, and thus the observation of the emergent characteristics, which facilitates interpretation of these characteristics in the context of the chemical and hydrological dynamics and a complex spatial catchment. The simulations have been organized to assist observation of:

- *Chemical dynamics*, including the characteristics of the catastrophe indicator, R_0, in a non-spatial context. These simulations address the dynamics of phosphate adsorption and acid buffering and, through R_0 and its constituents, the complex and non-linear interactions of these processes. These non-spatial simulations are presented following definition of the chemical sub-module in Chapter 4.

- *Hydrological dynamics*, through the observation of the hydrological effects upon individual cells resulting from flows between adjacent cells. Thus, by observing the change in saturation levels, infiltration, runoff, lateral flow and leaching rates in adjacent cells, an understanding of the effect of spatial flows upon individual cells is gained. These controlled spatial simulations, observing the non-spatial changes, are presented following definition of the hydrological sub-module in Chapter 5.

- *Catchment dynamics*, through observation of spatial R_0 surfaces representing the qualitative state of the catchment emerging from the non-linear chemical inter-relationships in a spatial environment defined by the hydrological flows. The seventeen catchment simulations are themselves organized into four categories:

  i) Simple, homogenous catchments (Section 6.1.1);

  ii) Complex, homogenous catchments (Section 6.1.2);

  iii) Complex, heterogenous catchments (Section 6.2); and

  iv) Manipulation of external inputs to complex, heterogenous catchments (Section 6.3).

The logic of the progression through these simulations is clarified below. The simulations are presented in Chapter 6.

3.4.5.1 Catchment Simulation Strategy

Owing to the complexity of the phenomena being modelled and the observation of the emergent characteristics through the catastrophe indicator, R_0, defined by the non-linear inter-relationships, the simulations logically progress from the most simple to the most complex scenario. Thus, the simulations progress from simple to complex catchments, and from chemical and hydrological homogeneity to heterogeneity within the catchments. In this way a comprehensive picture of the dynamics is built up which assists interpretation of the effects of external perturbations imposed upon the most complex scenario.

Simulations I to V address a simple, chemically and hydrologically homogenous catchment with the direction of spatial flows defined by the flow pattern in Figure 3.5(a), but varying the river categorizations. Based upon this flow pattern, the five simulations may be distinguished as follows:

I	No rivers
II	All catchment feeder rivers
III	All catchment rivers
IV	A combination of I and II
V	Categorizations as per Figure 3.5(a)

Although simulations II and III, and possibly I and IV, represent unrealistic catchments, by using simulation I as a baseline reference, these simulations assist interpretation of the characteristics of the model as opposed to the effects of diversity and heterogeneity within the catchment.

Simulations VI to IX address a complex, chemically homogenous catchment (representing Rutland Water) with the direction of flows defined by the flow pattern of Figure 3.5(b). Simulations VI and VII are hydrologically homogenous. Based upon this flow pattern, the four simulations may be distinguished as:

VI	No rivers
VII	Categorizations as per Figure 3.5(b)
VIII	Inclusion of HOST classifications
IX	Inclusion of variations in slope

Simulation VI provides a baseline reference for the Rutland Water catchment, the characteristics of which may be compared with those of Simulation I (simple catchment) since chemical and hydrological homogeneity has been maintained. The characteristics displayed by simulation VII can, similarly, be interpreted in the light of the dynamics displayed by simulations II to V. Simulations VIII and IX present the inclusion of hydrological heterogeneity within the catchment, comparable only with Simulation VII.

Simulations I to V will, therefore, have highlighted the effect of spatial flows upon R_0 since, due to homogenous initial conditions, the only factors causing variations in

R_0 across the grid are the definitions in the model of the hydrological flows. Simulations VI and VII will have highlighted the nature of these variations within the Rutland Water catchment, with simulations VIII and IX incorporating a degree of hydrological variability across the catchment so that influences on the emergent characteristics are no longer solely the model definitions.

Having highlighted the relative sensitivity to sudden releases of phosphates - shown by the variation of R_0 across the grid - occurring as a result of the hydrological dynamics alone, a spatial context has been provided within which the effects of chemical variability may be examined.

Simulations X to XIII, therefore, address a complex, chemically heterogenous catchment with the hydrological definitions retained from simulation IX. Based upon this hydrological representation, the four simulations may be distinguished as:

X Inclusion of NSI data
XI Inclusion of Ordnance Survey data
XII Imposition of arable vegetation
XIII Imposition of woodland or pasture

Simulation X provides a further baseline reference point since the simulation outputs will no longer be directly comparable with preceding simulations due to the incorporation of chemical heterogeneity across the catchment; the initial conditions for each cell are now unique. Thus, variations in the individual R_0 values is no longer the result solely of spatial hydrological flows. However, given the variations emerging in simulations I to IX, the influence of the diverse chemical states across the catchment may be assessed within the context of these flows. Simulations XI to XII incorporate further definitions of the topography and land usage evident in the catchment.

Finally, in the context of this complex and chemically and hydrologically heterogenous representation of the Rutland Water catchment, simulations XIV to XVII may be used to examine the overall effect of external perturbations, through manipulation of the key inputs - acid loading and phosphate applications. These four simulations are distinguished as:

XIV Acid loading doubled
XV Acid loading trebled
XVI Phosphate applications doubled
XVII Phosphate applications trebled.

CHAPTER 4. CHEMICAL SUB-MODULE

Two main processes have been identified which can be used to address the ability of the soil to act as a sink or a source of phosphates with respect to the acid loading inflicted upon the soil. These processes represent the ability of the soil to buffer additional acid (*Acid Buffering*) and its ability to retain phosphates available in the soil solution (*Phosphate (PO_4) Adsorption*).

A schematic representation of the inter-relationships of these processes is provided in Figure 4.1(a). Each of the components comprising Figure 4.1(a) may be related to the processes, variables and inputs identified in the model specification and the definition of its structure presented in the preceding chapter. A distinction is made between cation reserves which are free of phosphates and thus available for subsequent adsorption (Ca, Al) and the reserves accounting for previously adsorbed phosphates (Q_{Ca}, Q_{Al}).

The *inputs* of acid rain, phosphates and lime (Calcium Oxide) have a positive influence upon the pools of acid (H), phosphate (P) and 'free' calcium (Ca), respectively, maintained by the chemical sub-module.

The *variables* define the current state of the sub-module and are necessary inputs to the buffering and adsorption processes. The pools of acid and phosphate represent the loadings applied to the buffering and adsorption processes, respectively. The pools of 'free' calcium and aluminium define the remaining adsorptive capacity - depending upon the soil pH - by base (R_{Ca}) and acid (R_{Al}) reserves, respectively. The soil pH, determined by itself and the ratio of base and acid cations reserves, influences both acid buffering and phosphate adsorption rates.

The *processes* of acid buffering and phosphate adsorption directly affect the pools of acid, phosphate, calcium and aluminium, but only indirectly affect the soil pH. Acid buffering has a negative influence on the pool of acid, and upon the pools of calcium and aluminium (depending upon the pH). Phosphate adsorption has a negative effect upon the pool of phosphate. However, it also has the effect of reducing the pools of 'free' cations (Ca, Al) and increasing proportionately the pools of adsorbed phosphates (Q_{Ca}, Q_{Al}).

The time bomb phenomenon, whereby an sudden release of phosphates may occur due to changing conditions in the soil, becomes evident when the 'free' base cation reserves (Ca) are depleted and acid buffering is still predominately by base cations; since there are no remaining reserves of 'free' base cations, further acid buffering by base cations leads to the release of the phosphates associated with these sites; Sulphuric Acid, H_2SO_4, has been shown to increase the solubility of Calcium Phosphate, $Ca_3(PO_4)_2$, in water [Linke 1958; Ghani & Aleem 1943]. This change is shown schematically in Figure 4.1(b). Acid buffering now has a negative effect upon the remaining base cation pool (Q_{Ca}) which in consequence increases the phosphate pool (P) proportionately, and phosphate adsorption can only occur using the 'free' acid cation reserves.

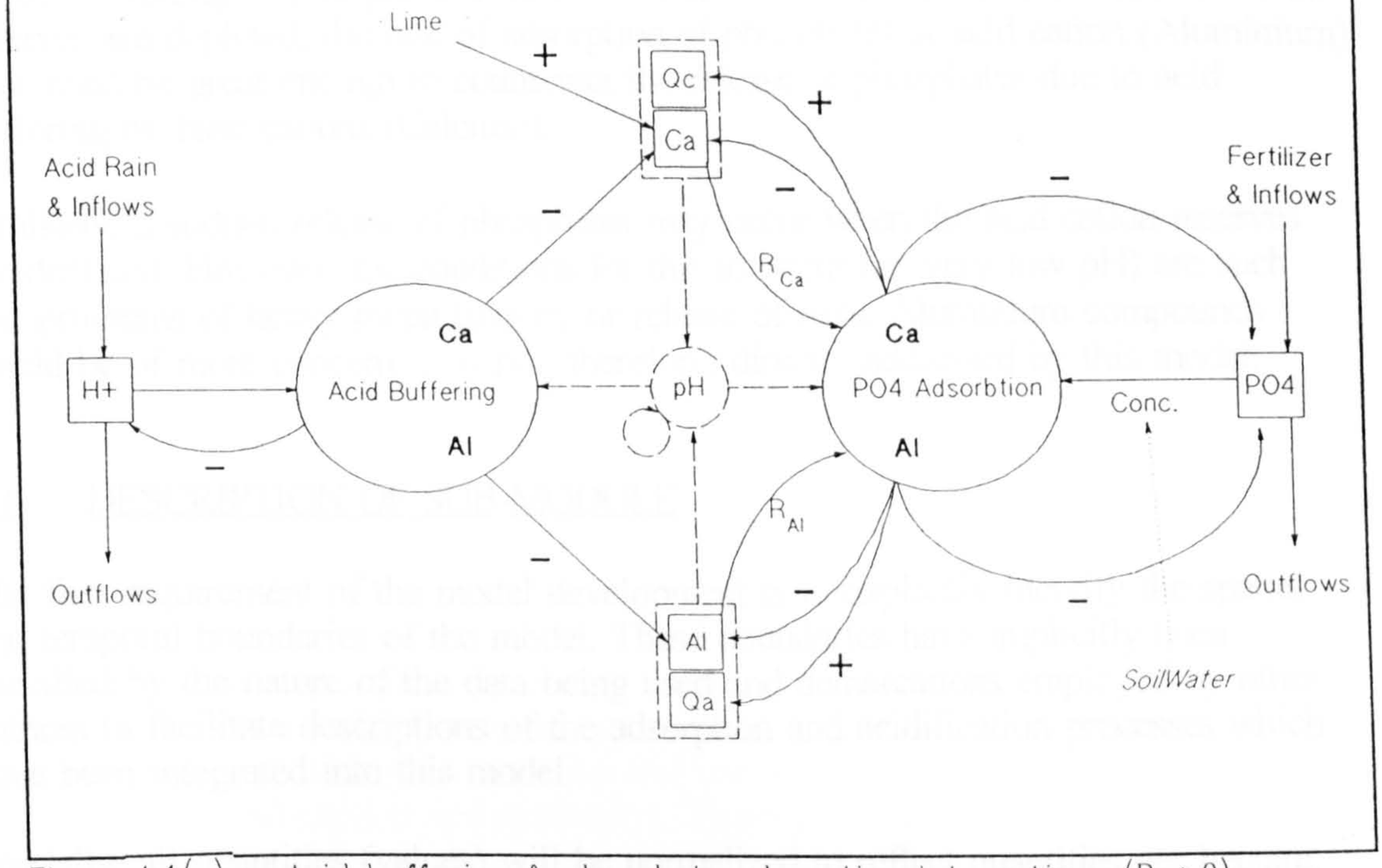

Figure 4.1(a) - Acid buffering & phosphate adsorption interactions ($R_{Ca}>0$)

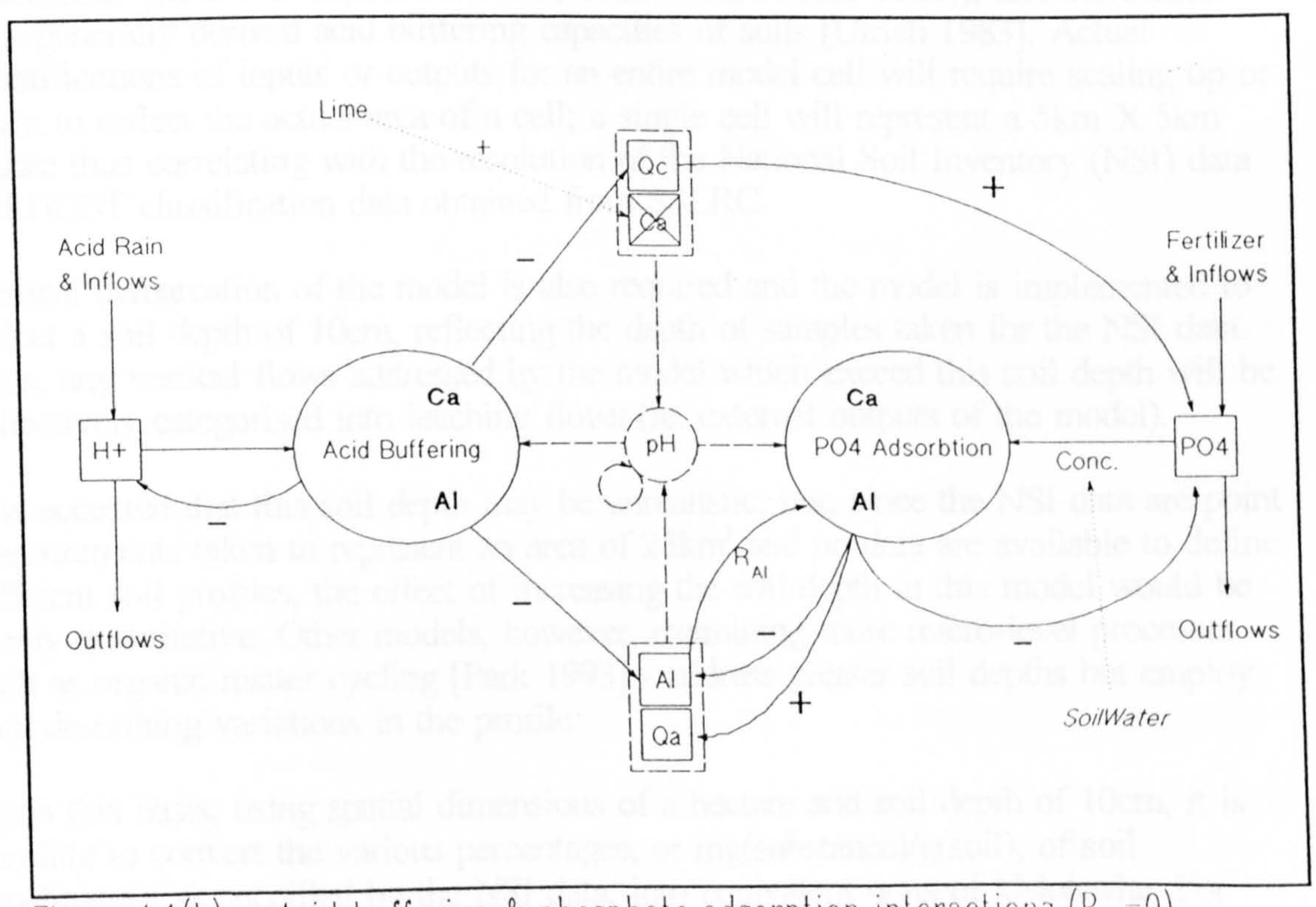

Figure 4.1(b) - Acid buffering & phosphate adsorption interactions ($R_{Ca}=0$)

Thus, if flushing of phosphate from the soil is to be avoided when the 'free' calcium reserves are depleted, the rate of adsorption of phosphates at acid cation (Aluminium) sites must be great enough to counteract the release of phosphates due to acid buffering by base cations (Calcium).

Similarly, a sudden release of phosphates may occur when the acid cation reserves are depleted. However, the conditions for this to occur (ie. very low pH) are such that problems of heavy metal toxicity or release of toxic Aluminium compounds would be of more concern; it is not, therefore, directly addressed by this model.

4.1 DESCRIPTION OF SUB-MODULE

The first requirement of the model development is to explicitly identify the spatial and temporal boundaries of the model. These boundaries have implicitly been specified by the nature of the data being used and demarcations employed by other authors to facilitate descriptions of the adsorption and acidification processes which have been integrated into this model.

Spatially, all quantities (values) will be normalized to reflect quantities per hectare. Thus, all input and output must reflect the spatial unit of a hectare; this enables easy use of input data such as Phosphorus inputs (on average in the region of $31kgha^{-1}yr^{-1}$ in fertilizer [MAFF 1983; ADAS 1982; CAS 1978; Archer 1988]), and correlation with generally derived acid buffering capacities of soils [Ulrich 1983]. Actual quantifications of inputs or outputs for an entire model cell will require scaling up or down to reflect the actual area of a cell; a single cell will represent a 5km X 5km square thus correlating with the resolution of the National Soil Inventory (NSI) data and HOST classification data obtained from SSLRC.

Vertical demarcation of the model is also required and the model is implemented to reflect a soil depth of 10cm, reflecting the depth of samples taken for the NSI data. Thus, any vertical flows addressed by the model which exceed this soil depth will be collectively categorised into leaching flows (ie. external outputs of the model).

It is accepted that this soil depth may be unrealistic, but, since the NSI data are point measurements taken to represent an area of $25km^2$ and no data are available to define different soil profiles, the effect of increasing the soil depth in this model would be purely quantitative. Other models, however, examining more micro-level processes - such as organic matter cycling [Park 1993] - address greater soil depths but employ data describing variations in the profile.

Upon this basis, using spatial dimensions of a hectare and soil depth of 10cm, it is possible to convert the various percentages, or mg(substance)/g(soil), of soil constituents, as specified by the NSI data, into equivalent units of kMoles/ha. For many of the processes (such as acid buffering) it is appropriate to further modify these figures to reflect kEquivalence(H^+)/ha, thus avoiding the potential confusion of dealing with the varying ionic charges (Al^{3+}, Ca^{2+}, H^+, PO_4^{3-}).

Finally, temporal rates of change will be addressed on a daily basis, thus reflecting the definition of Standard Percentage Runoff (SPR) which is a daily runoff rate, the daily rainfall data, and the phosphate adsorption rates identified by Olsen & Watanabe (1957). The acid buffering rates identified in the RAINS model reflect a yearly rate, so these have been modified to provide an average (continuous) daily rate. This continuous rate could ultimately be replaced by linking the model to an atmospheric transport model such as used by RAINS. With processes normalized to daily rates, the model utilizes a further timestep, *dt*, of 0.1, as discussed in Chapter 3; The model thus implements partial changes to key state variables 10 times a day.

4.1.1 PHOSPHATE ADSORPTION PROCESSES

The complexity of the processes of phosphate adsorption have resulted in a number of empirical and mechanistic equations to represent adsorption depending upon the precision or generality required [Barrow 1978; Enfield et al. 1976]. These each attempt to account for influences on adsorption such as increases in negative charges at or near adsorption sites due to adsorption, concentrations of phosphate in the soil solution, maximum adsorptive capacity and various affinity constants addressing the relative rates of adsorption and desorption. These adsorption equations have been discussed in Chapter 2.

It was concluded in Chapter 2 that a multiple surface Langmuir form of adsorption equation would be the most suitable for use in the current research since it facilitates integration with the processes of acid buffering through the common elements of calcium, aluminium and soil pH. Accounting for two discrete surfaces, the generic adsorption equation may be written thus:

$$X = A_1X_{m1}C/(1+A_1C) + A_2X_{m2}C/(1+A_2C) \qquad ...(1)$$

where: A_1 and A_2 are affinity terms describing the relative rates of adsorption and desorption by the two surfaces, and X_{m1} and X_{m2} are the adsorption maxima.

Using this 2-surface form of the Langmuir equation, the model will deal with the changing affinity for adsorption in the following ways:

1. The 'surfaces' will be distinct and will address adsorption by Base Cation (Ca) sites separately to Acid Cation (Al) sites. Thus X_{m1} and X_{m2} will change with the base and acid cation composition of the soil at any one time;

2. The affinity terms, A_1 and A_2, will be dependent upon the pH of the soil at any one time, thus addressing the solubility of Calcium and Aluminium phosphates at a given pH and consequently the ability to adsorb phosphate at these sites.

The affinity terms controlling adsorption at either base or acid cation sites will thus reflect the changing total capacity for adsorption due to both changes in pH (affected by additional acid loading) and through previous adsorption of phosphates.

The affinity terms, A_1 and A_2, are derived (see below) to reflect the relative ability of the soil to adsorb phosphates as identified by Stevenson (1986) where adsorption tends to be at a minimum at around pH 6.5, and increases both above pH 6.5, due to base cation reserves, and below, due to acid cation reserves. Stevenson's graphical representation of these adsorption affinities is reproduced in Figure 4.2(a).

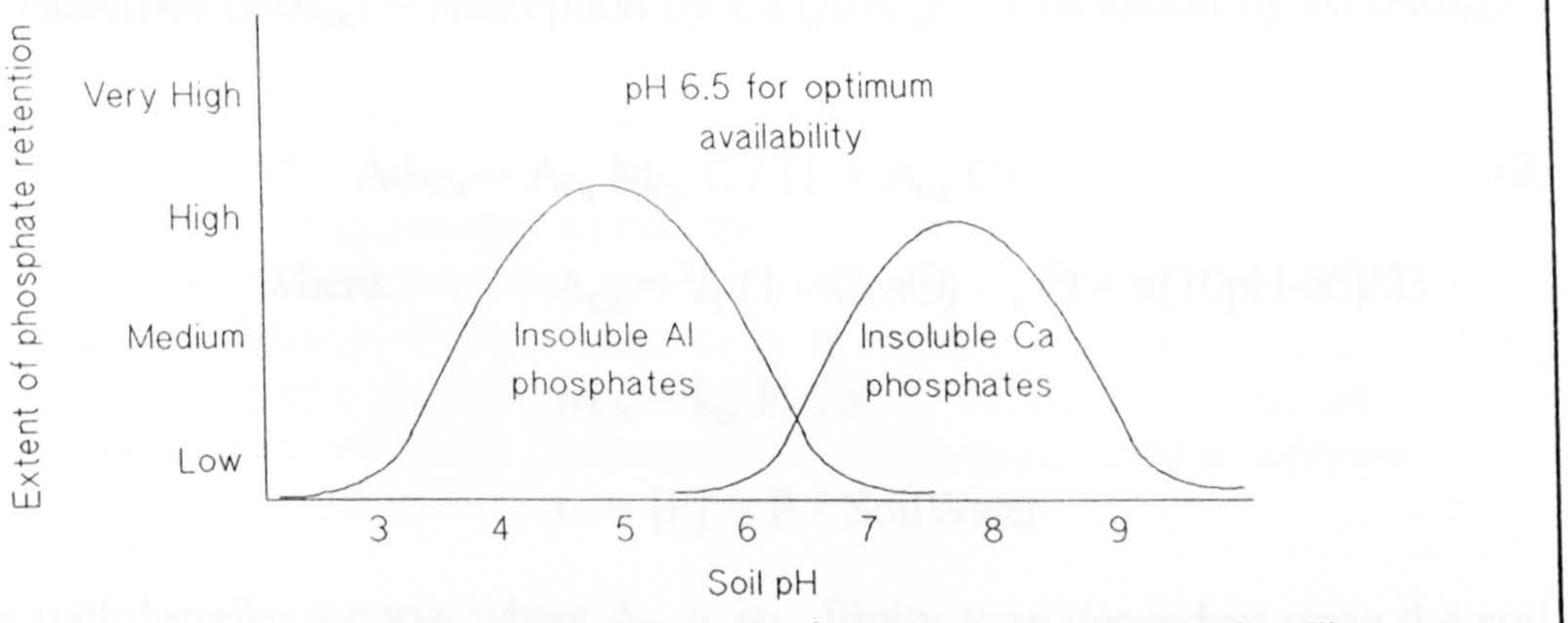

(a) Effect of pH on phosphate adsorption (Adapted from Stevenson (1986))

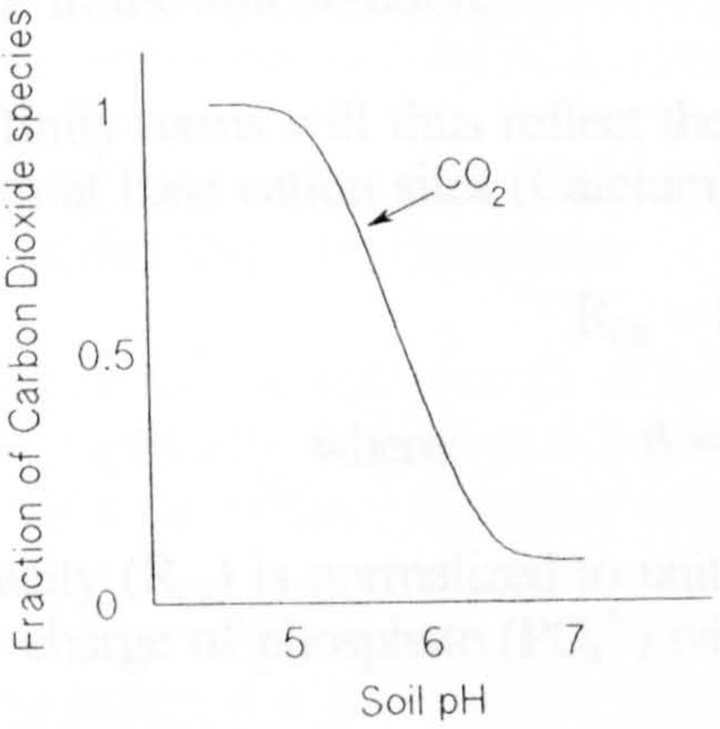

(b) Calcium dissolution curve in response to soil CO_2 (Adapted from Manahan (1991))

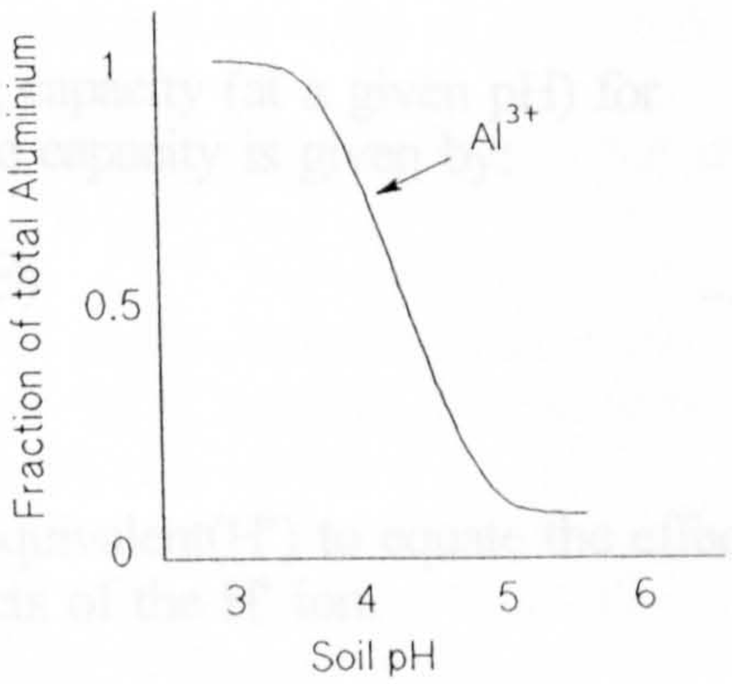

(c) Aluminium dissolution curve (Adapted from Dalal (1975))

Figure 4.2 – Adsorption affinity and cation dissolution curves

4.1.1.1 Adsorption Equations

In order to incorporate these varying adsorption affinities identified by Stevenson (1986), use is made of cosine functions to describe the curves with reference to the soil pH. Hence the derivations of Θ and ϕ used in the following equations to convert a pH value varying between 4 and 8 (approx) to appropriate values between 0 and 1 to describe the adsorption affinity of Calcium and Aluminium, respectively. A factor of $^4/_5$ is used to modify A_{Ca}, reflecting the reduced peak suggested by Stevenson (1986).

Thus, using the 2-Surface Langmuir equation as a basis - details of the units and constants are provided overleaf - we have:

Total P Adsorbed (Ads_{tot}) = Adsorption by Ca (Ads_{Ca}) + Adsorption by Al (Ads_{Al})

where:
$$Ads_{Ca} = A_{Ca}\, M_{Ca}\, C / (1 + A_{Ca}\, C) \qquad ...(2)$$

where:
$$A_{Ca} = {}^2/_5\,(1 - \cos\Theta) \quad , \Theta = \pi(10pH-56)/23$$

$$M_{Ca} = k_{cp}\, k_t\, Ca$$

$$C = [P] = P / SoilWater$$

This term will describe a curve where A_{Ca} is an affinity term dependent upon the soil pH, M_{Ca} is a maximum rate dependent upon the available reserves of base cations (Ca), with k_t and k_{cp} constants (described below) and C is the concentration of phosphate in the soil solution.

These affinity terms will thus reflect the remaining capacity (at a given pH) for adsorption at base cation sites (Calcium), where the capacity is given by:

$$R_{Ca} = \beta\,(1 - \cos\Theta) \qquad ...(3)$$

where:
$$\beta = {}^6/_5\, k_{cp}\, Ca$$

The capacity (R_{Ca}) is normalized to units of Kilo-equivalent(H^+) to equate the effects of the 3^- charge of phosphate (PO_4^{3-}) with the effects of the H^+ ion.

Similarly, the term describing adsorption by Aluminium (acid cation sites) is given by:

$$Ads_{Al} = A_{Al}\, M_{Al}\, C / (1 + A_{Al}\, C) \qquad ...(4)$$

where:
$$A_{Al} = {}^1/_2\,(1 - \cos\phi) \quad , \phi = \pi(2pH-6)/5$$

$$M_{Al} = k_{ap}\, k_t\, Al$$

with the remaining capacity given by:

$$R_{Al} = \alpha (1 - Cos\phi) \qquad ...(5)$$

where: $\alpha = {}^3/_2\ k_{ap}\ Al$

Using equations (2) and (4), the units and constants required to reflect phosphate adsorption are as follows:

- The concentration of phosphate in solution, C=P/SoilWater, has units of kMole/kLitre.

- The affinity terms, A_{Ca} and A_{Al}, vary between 0 and 1, depending upon pH, and have units the inverse of the concentration, C [Olsen and Watanabe 1957]; these affinity curves are varied during sensitivity analysis to determine their qualitative effect upon adsorption.

- The constant, $k_t = {}^1/_{365}$, is used to coordinate the effects of adsorption and buffering. Since both processes use the same cation reserves and buffering requires modification of these reserves from a yearly to a daily capacity, this modification is also applied to adsorption. Thus, the interaction of the processes should reflect the processes themselves rather than a different treatment by the model of the reserves used.

- The maximum adsorption rates, M_{Ca} and M_{Al}, have units of $kMha^{-1}day^{-1}$; the constants, k_{cp} and k_{ap}, equate the ionic charges of Ca and Al with that of PO_4. A further factor of 3 has been included in k_{cp} and k_{ap} to provide correlation with the adsorption maxima calculated by Olsen & Watanabe (1957), suggesting that the use of k_t indeed achieves the correct order of magnitude.

- Thus, the rate of adsorption determined by equations (2) and (3) also has units of $kMha^{-1}day^{-1}$ of Phosphate.

The influences of the components of these adsorption and capacity equations are presented graphically in Figures 4.3 (Adsorption) and 4.4 (Capacity), below. Both figures reflect the affinity functions derived from Stevenson (1986).

Figures 4.3(a) and (b), surfaces generated by varying the phosphate concentration and pH and maintaining a static supply of cations, show the influence of pH and Phosphate concentration on adsorption at base cation and acid cation sites respectively. Figure 4.3(c), similarly generated, shows the combined influences of each term on the total adsorption of phosphate. These surfaces are unrealistic in the sense that adsorption will reduce the cation reserves. However, they provide a temporally static representation of the qualitative characteristics of the adsorption equations. The inclusion of a time element is discussed in section 4.2.

Figures 4.4(a) and (b) show the influence of pH and total cation reserves (acid and base), on the adsorptive capacity provided by acid and base cation sites respectively.

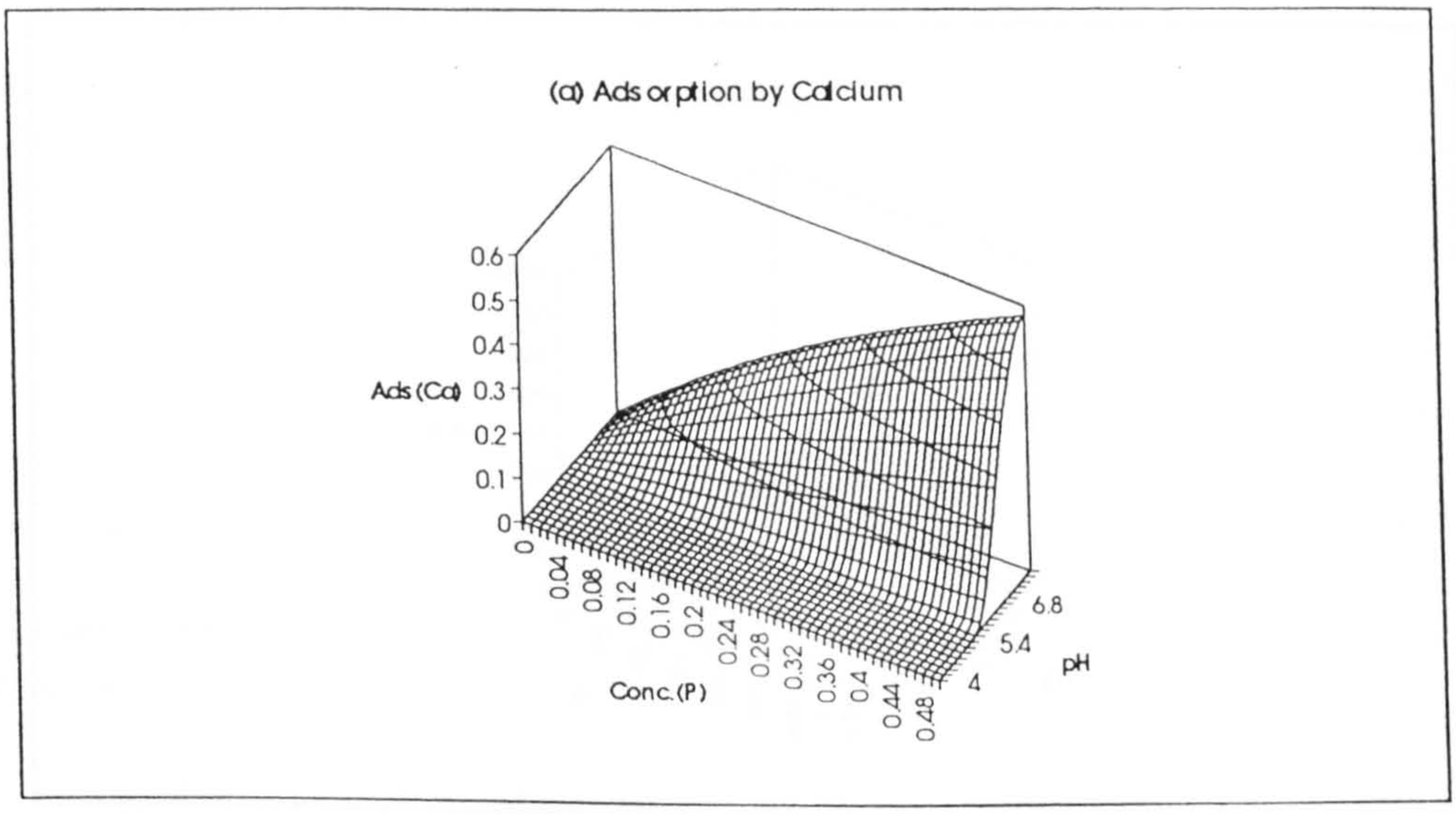

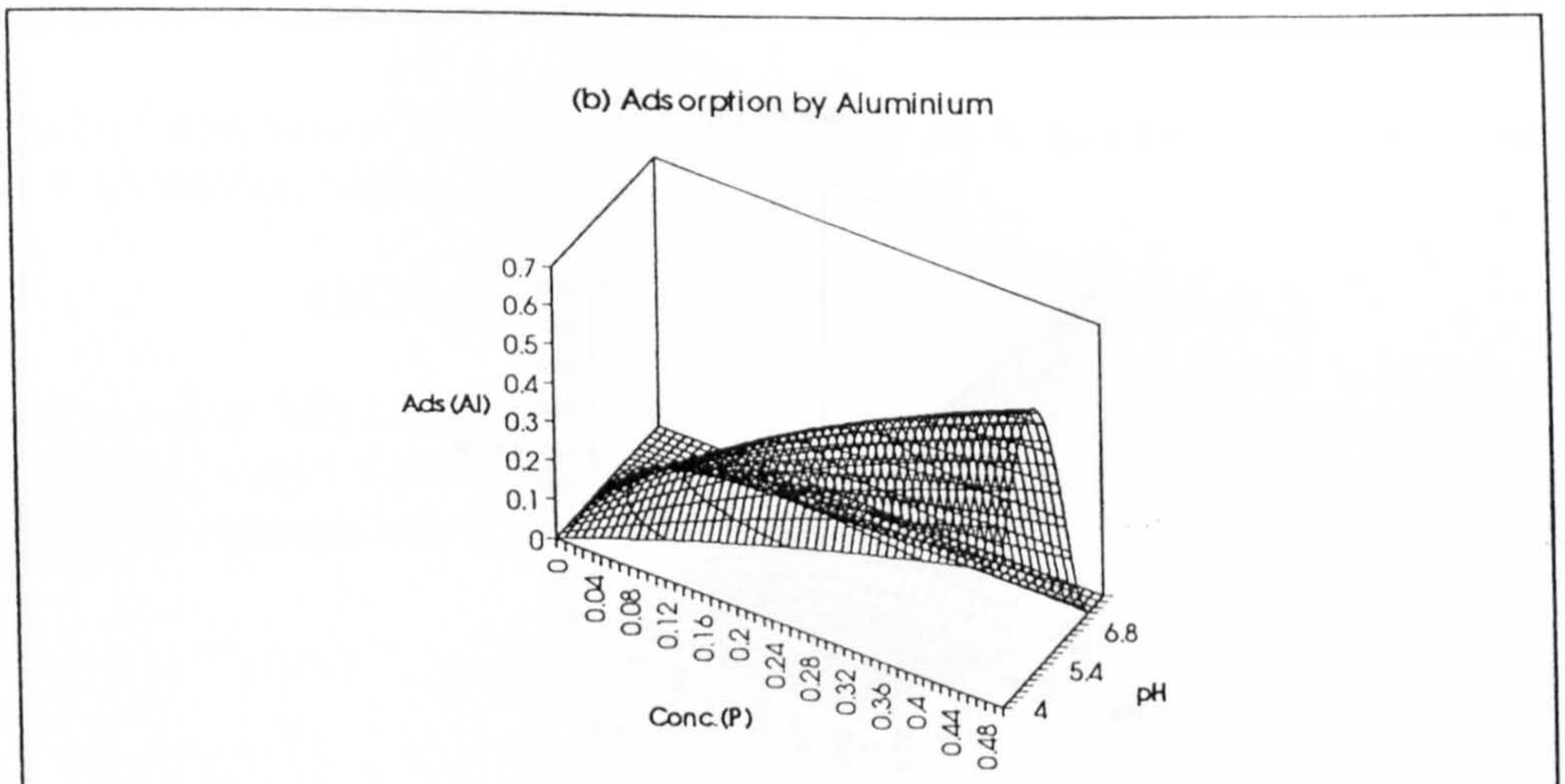

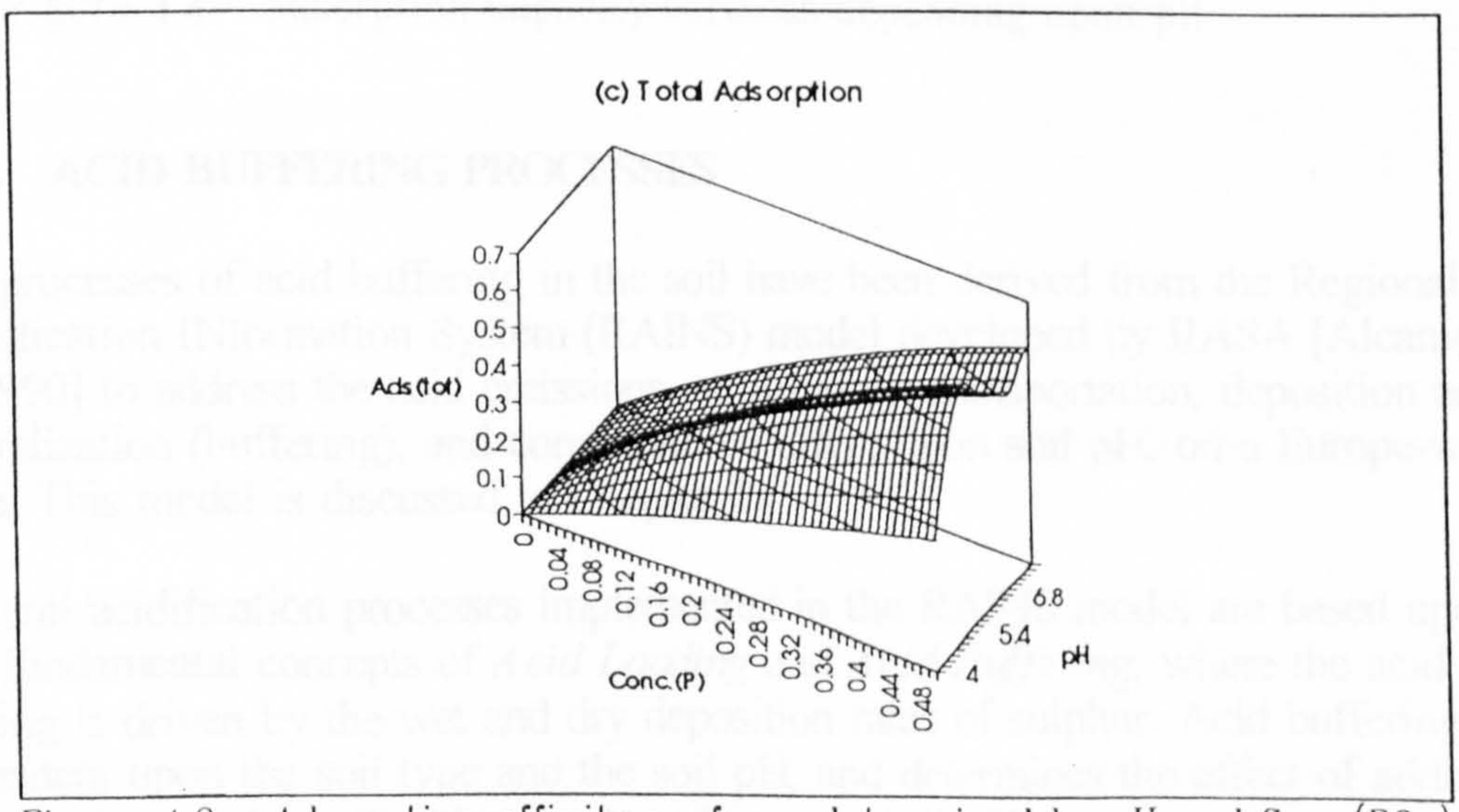

Figure 4.3 – Adsorption affinity surfaces determined by pH and Conc(PO_4)

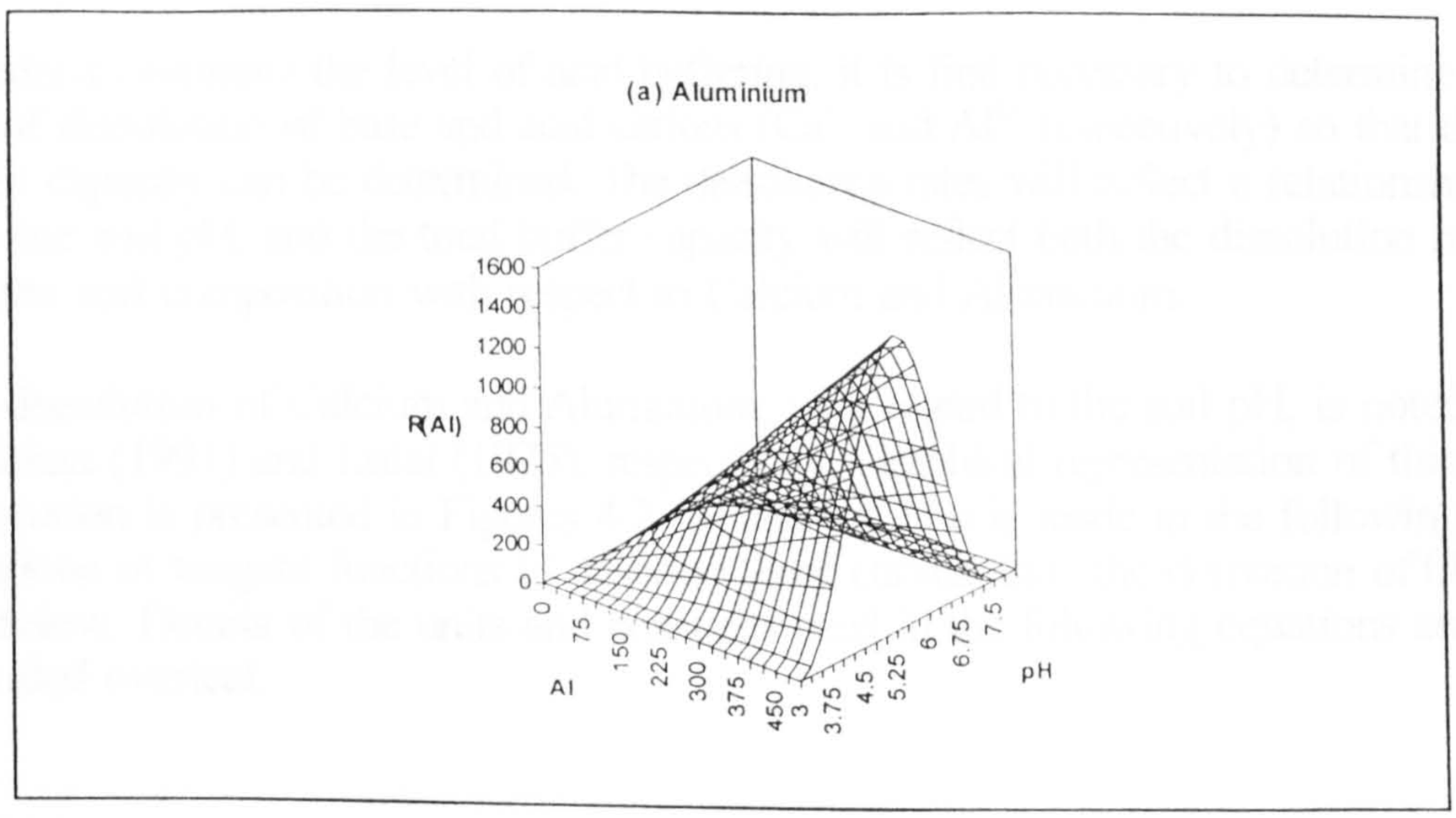

Figure 4.4 – Adsorption Capacity surfaces depending upon pH

4.1.2 ACID BUFFERING PROCESSES

The processes of acid buffering in the soil have been derived from the Regional Acidification INformation System (RAINS) model developed by IIASA [Alcamo et al. 1990] to address the acid emissions, atmospheric transportation, deposition and neutralization (buffering), and consequential effect upon soil pH, on a Europe-wide scale. This model is discussed in Chapter 2.

The soil acidification processes implemented in the RAINS model are based upon the two fundamental concepts of *Acid Loading* and *Acid Buffering*, where the acid loading is driven by the wet and dry deposition rates of sulphur. Acid buffering is dependent upon the soil type and the soil pH, and determines the effect of additional acid loading on the soil with regards a change in soil pH.

4.1.2.1 Buffering Equations

In order to estimate the level of acid buffering, it is first necessary to determine the rate of dissolution of base and acid cations (Ca^{2+} and Al^{3+} respectively) so that the buffer capacity can be determined. The dissolution rates will reflect a relationship with the soil pH, and the total buffer capacity will reflect both the dissolution rates and the soil composition with respect to Calcium and Aluminium.

The dissolution of Calcium and Aluminium, with regard to the soil pH, is noted by Manahan (1991) and Dalal (1975), respectively. Graphical representation of this dissolution is presented in Figures 4.2 (b) and (c). Use is made in the following equations of tangent functions to describe these curves; thus the derivation of Θ_A and ϕ_A, below. Details of the units and constants used in the following equations are provided overleaf.

Calcium

The rate of dissolution of Calcium is related to the level of CO_2 present in the soil solution [Manahan 1991], and follows the reaction:

$$CaCO_3(s) + CO_2(aq) + H_2O \longleftrightarrow Ca^{2+} + 2HCO_3^-$$

As described by Manahan, the fraction of Carbon Dioxide species present in solution (CO_2 , HCO_3^-, and CO_3^{2-}) changes with changing pH, and thus the dissolution rate of Ca^{2+} may be represented by:

$$Ca_{diss} = K_1 + K_2 (\tfrac{1}{2} - {}^1/_{\pi}\, Tan^{-1}\Theta_A) \qquad ...(6)$$

where: $\Theta_A = (17pH-115)/3$

and K_1 , K_2 are constants.

Thus, the Buffer Rate with respect to Calcium, BR_{Ca}, can be given by:

$$BR_{Ca} = BC_{Ca}\, Ca_{diss}\, k_t \qquad ...(7)$$

where: $BC_{Ca} = 2\, k_{Ca}\, (Ca + Q_{Ca})$

and Q_{Ca} is calcium bound to adsorbed phosphate
k_t and k_{Ca} are constants

Aluminium

Dalal (1975) identified the fraction of Aluminium species present in solution due to hydrolysis in relation to the pH, from which the dissolution rate of $A\beta^+$ may be represented as:

$$Al_{diss} = \frac{1}{2} - \frac{1}{\pi} \text{Tan}^{-1}\phi_A \qquad ...(8)$$

where: $\phi_A = (17pH-71)/2$

which gives the Buffer Rate with respect to Aluminium (BR_{Al}) as:

$$BR_{Al} = BC_{Al}\ Al_{diss}\ k_t \qquad ...(9)$$

where: $BC_{Al} = 3\ k_{Al}\ (Al + Q_{Al})$

and Q_{Al} is aluminium bound to adsorbed phosphate
k_t and k_{Al} are constants

In order to calculate the level of acid buffering and to determine the change in soil pH in the Cation Exchange Range (see Equation 13), two further relationships are required - the total Cation Exchange Capacity (CEC) and the Base Saturation ($ß_{sat}$). These can be represented by:

$$CEC = BR_{Ca} + BR_{Al} \qquad ...(10)$$

and

$$ß_{sat} = BR_{Ca} / CEC \qquad ...(11)$$

Using equations (6) through (11), the units and appropriate normalizing constants required to reflect acid buffering capabilities are as follows:

- The dissolution rate controlling equations, Ca_{diss} and Al_{diss}, are unitless and vary between 0 and 1 depending upon pH. The constants K_1 and K_2 are both set to 0.5; the effect of varying these constants is shown whilst examining the model characteristics.

- The buffer capacities, in units of $kEq(H^+)ha^{-1}$, include constants, k_{Ca} and k_{Al}, which are both set to 0.25 so that the annual capacities correlate with the findings of Ulrich (1983). This results in buffer rate units of $kEqha^{-1}day^{-1}$ through the incorporation of k_t.

- The Cation Exchange Capacity (CEC) thus also has units of $kEqha^{-1}day^{-1}$, and the Base Saturation, $ß_{sat}$, is unitless, representing the percentage of base cations making up the CEC.

- The changes in Calcium and Aluminium reserves due to acid buffering (see following equations) are given in units of $kMha^{-1}day^{-1}$.

As discussed in Chapter 2, the predominate buffering mechanisms depend upon the soil pH and the base saturation level, which together identify the appropriate Buffer Range in the following way:

Calcium Carbonate Buffer Range	-	pH>6.2 and $ß_{sat}$>85%
Silicate Buffer Range		
Cation Exchange Buffer Range	-	pH>4.2 and $ß_{sat}$>5%
Aluminium Buffer Range	-	pH<4.2 and $ß_{sat}$<5%

Acid buffering for each of these ranges, plus the re-calculation of the soil pH subsequent to buffering, are each described separately below.

Calcium Carbonate Range

When the soil pH exceeds 6.2 and the base saturation exceeds 85%, the depletion of Calcium and Aluminium reserves may be given by:

$$Buff_{Ca} = H / 2 \qquad (\text{if } BR_{Ca} \geq H)$$

$$Buff_{Ca} = BR_{Ca} / 2 \qquad (\text{if } BR_{Ca} < H)$$

$$Buff_{Al} = 0$$

where: $Buff_{Ca}$ is the change in Calcium reserves due to buffering,
$Buff_{Al}$ is the change in Aluminium reserves due to buffering, &
H is the remaining unbuffered acid (H^+) in solution.

In the Calcium Carbonate range there is no significant buffering by acid cations (Aluminium). The resultant pH has been determined using a linear relationship between remaining Calcium and pH, where:

$$pH = 6 + 2\,(CaQ - k_3)/CaQ \qquad ...(12)$$

where: $CaQ = Ca + Q_{Ca}$, and k_3=95

Since there is no indication of an alternative pH calculation in the literature, equation (12) was derived experimentally within the context of this model. The abundance of calcium at high pH's ensures that any change will be gradual, and the value of the constant, k_3, ensures that a relatively smooth switch is made between the use of this pH calculation and equation (13). However, some discontinuities may be observed in the outputs (see Figure 4.8 after approx 40 years simulation) resulting from this switch between pH calculations.

Cation Exchange Range

When the soil pH exceeds 4.2 and the base saturation exceeds 5% but is not as great as 85%, the depletion of Calcium and Aluminium reserves may be given by:

$$Buff_{Ca} = ß_{sat}\, H_{si} / 2 \qquad (\text{if } CEC \geq H_{si})$$

$$Buff_{Ca} = BR_{Ca} / 2 \qquad \text{(if CEC} < H_{si})$$

$$Buff_{Al} = (1-ß_{sat})\ H_{si} / 3 \qquad \text{(if CEC} \geq H_{si})$$

$$Buff_{Al} = BR_{Al} / 3 \qquad \text{(if CEC} < H_{si})$$

where: $H_{si} = 0$, if $BR_{si} \geq H$, or
$H_{si} = H - BR_{si}$, if $BR_{si} < H$, and
BR_{si} is the silicate buffer rate (fixed)

In the Cation Exchange range, the buffering by either base or acid cation reserves is controlled by the relative dissolution rates and total capacities as reflected by the base saturation, $ß_{sat}$. The resultant pH is determined based upon the equations from the RAINS model, but extending the range to coincide with the lowest pH (6.2) responding to the Calcium Carbonate range. The non-linear relationship between pH and base saturation, adopted in the RAINS model and based upon results of an equilibrium model by Reuss (1983), has been retained. The new pH is given by:

$$pH = 4 + 2.2\ ß_{sat}^{3/4} \qquad ...(13)$$

Aluminium Buffer Range

When the soil has entered the Aluminium buffer range (pH<4.2 and $ß_{sat}$<5%), there is minimal buffering by Calcium since available reserves has been depleted and the base saturation level implies a higher propensity for buffering by Aluminium. Buffering by Aluminium is determined, as in the RAINS model, by calculating the equilibrium state with Gibbsite. Thus, the depletion of Calcium and Aluminium reserves are given by:

$$Buff_{Ca} = ß_{sat}\ H / 2 \qquad \text{(if CEC} \geq H)$$

$$Buff_{Ca} = BR_{Ca} / 2 \qquad \text{(if CEC} < H)$$

$$Buff_{Al} = \text{Gibbsite Equilibrium (see pH calculation)}$$

The resultant pH is calculated by using Cardan's solution to the equation $z^3+3Hz+G=0$ to determine Gibbsite Equilibrium, whereby Aluminium is dissolved or precipitated until the equilibrium state is reached:

$$Al^{3+}(aq) / [H^{+}(aq)]^3 = K_{gibb}\ , \quad K_{gibb} = 10^{2.5} \qquad ...(14)$$

The influences of the components of these acid buffering equations are presented graphically in Figure 4.5 below. Figures (a) and (b) show the effect of varying the pH and Acid loading, with no change in cation reserves, on buffering by acid and base cations respectively. Figure (c) shows the combined influence of each term on the total buffering. As with Figure 4.3, these surfaces have no temporal dimension and thus only present the qualitative characteristics of the buffering equations.

4.1.3 STATE VARIABLE CHANGES

With the processes for phosphate adsorption and acid buffering, and the re-calculation of soil pH described, the effect of these processes upon the state variables in the model needs to be identified. There are four main state variables affected by these processes, namely Calcium (including Q_{Ca}), Aluminium (including Q_{Al}), and Phosphates and Protons (H^+) in solution.

It is helpful at this point to clarify the ionic relationships between the state variables and the rates of change due to adsorption and buffering. The state variables maintain ionic charges of Ca^{2+}, Al^{3+}, PO_4^{3-} and H^+. Thus, Q_{Ca} and Lime (Calcium Oxide input) also reflect 2+ charges, and Q_{Al} reflects a 3+ charge. The buffering rates, $Buff_{Ca}$ and $Buff_{Al}$, have been calculated to reflect charges of 2+ and 3+, respectively; note the need to include factors of 2 and 3 in Equation (20). However, the adsorption rates, Ads_{Ca} and Ads_{Al}, refer to the adsorption of phosphate (3-), thus requiring modification by a factor of $^3/_2$ when accounting for calcium depletion (Equation (15)); 1½ Moles of calcium are required to adsorb 1 Mole of phosphate.

4.1.3.1 Calcium

In the pre-flushing state, as shown in Figure 4.1(a), the amount of 'free' Calcium (ie. available for adsorption of phosphates) and the amount of 'phosphate adsorbed' Calcium (Q_{Ca}), at time *t+1* can be given by:

$$Ca_{t+1} = Ca_t + (Lime - {}^3/_2 Ads_{Ca} - Buff_{Ca})\ dt \qquad ...(15)$$

$$Q_{Ca,t+1} = Q_{Ca,t} + {}^3/_2 Ads_{Ca}\ dt$$

whereas, in the post-flushing state, as shown in Figure 4.1(b), where $Ads_{Ca}=0$ since the reserves have been depleted (ie. Ca=0), Ca_{t+1} and $Q_{Ca,t+1}$ can be given by:

$$Ca_{t+1} = Lime\ dt \qquad ...(16)$$

$$Q_{Ca,t+1} = Q_{Ca,t} - Buff_{Ca}\ dt$$

where: Lime reflects additions of Calcium Oxide

Total Calcium reserves, for the purposes of determination of soil pH and acid buffering rates is thus given by:

$$CaQ_{t+1} = Ca_{t+1} + Q_{Ca,t+1}$$

Calcium inputs are assumed to occur only through liming by farmers. The liming rates used will maintain units of $kM(Ca)ha^{-1}day^{-1}$. It is assumed that no explicit outputs of Calcium occur, and that Calcium is lost only through the effects of acid buffering and phosphate adsorption.

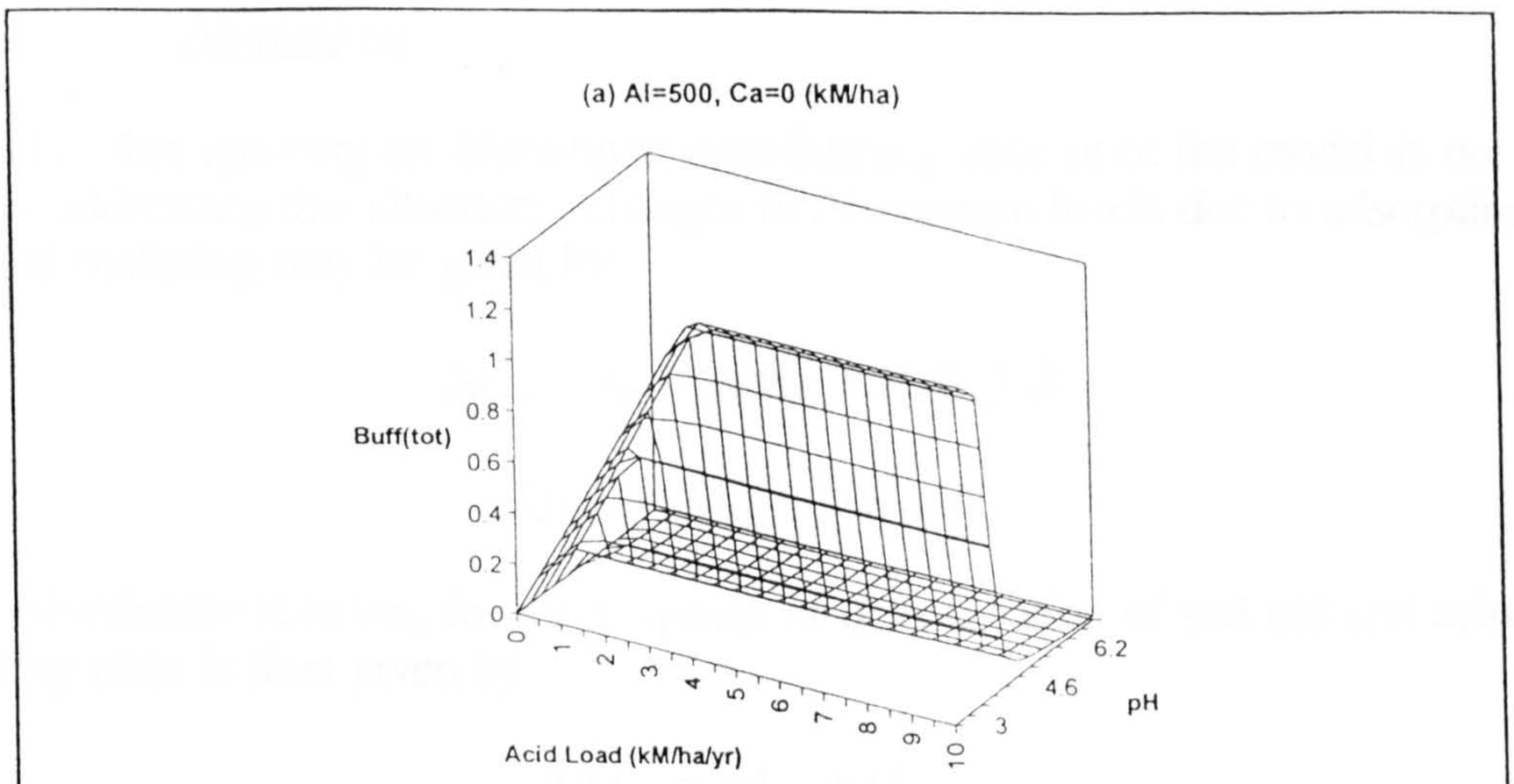

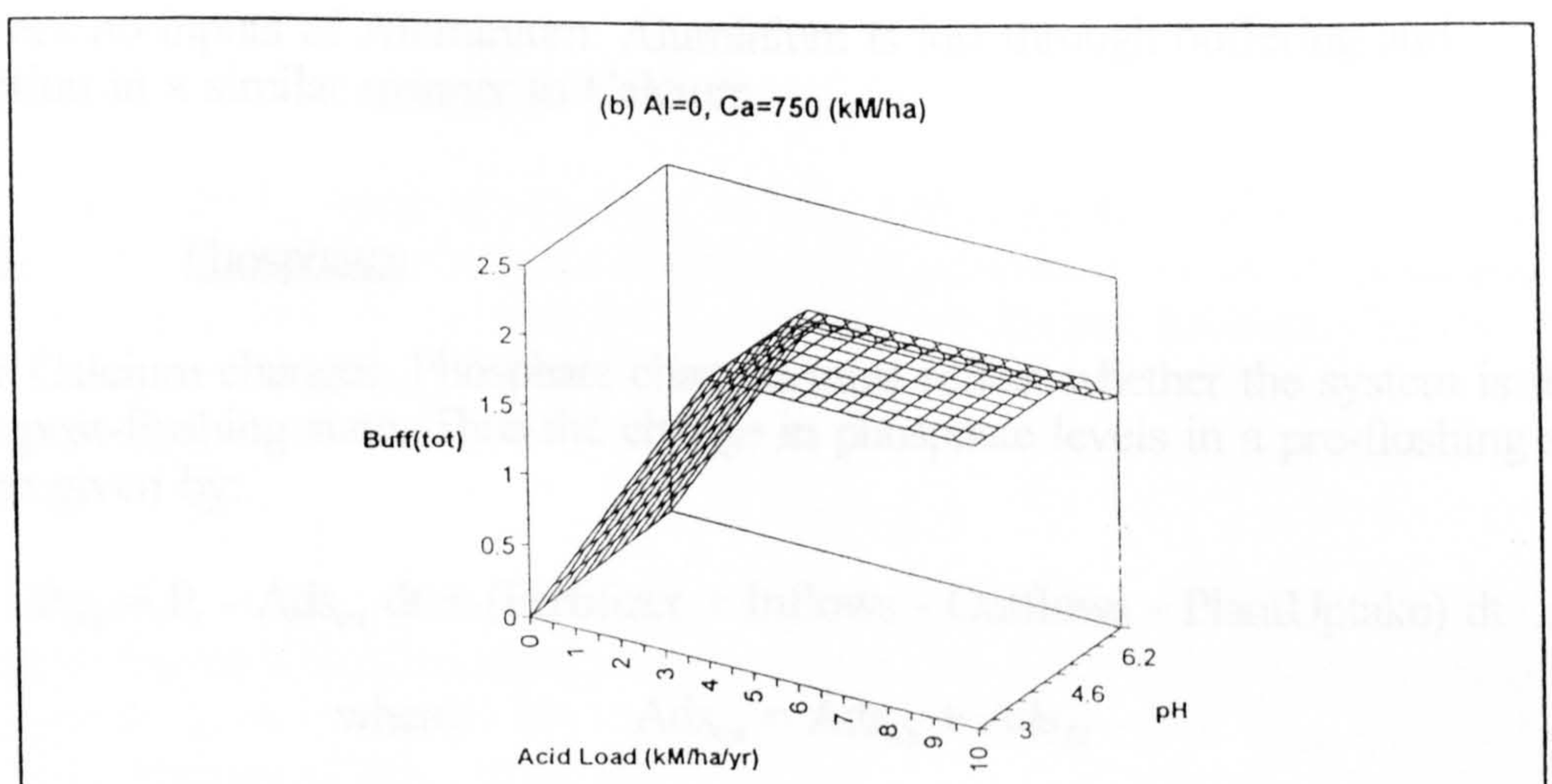

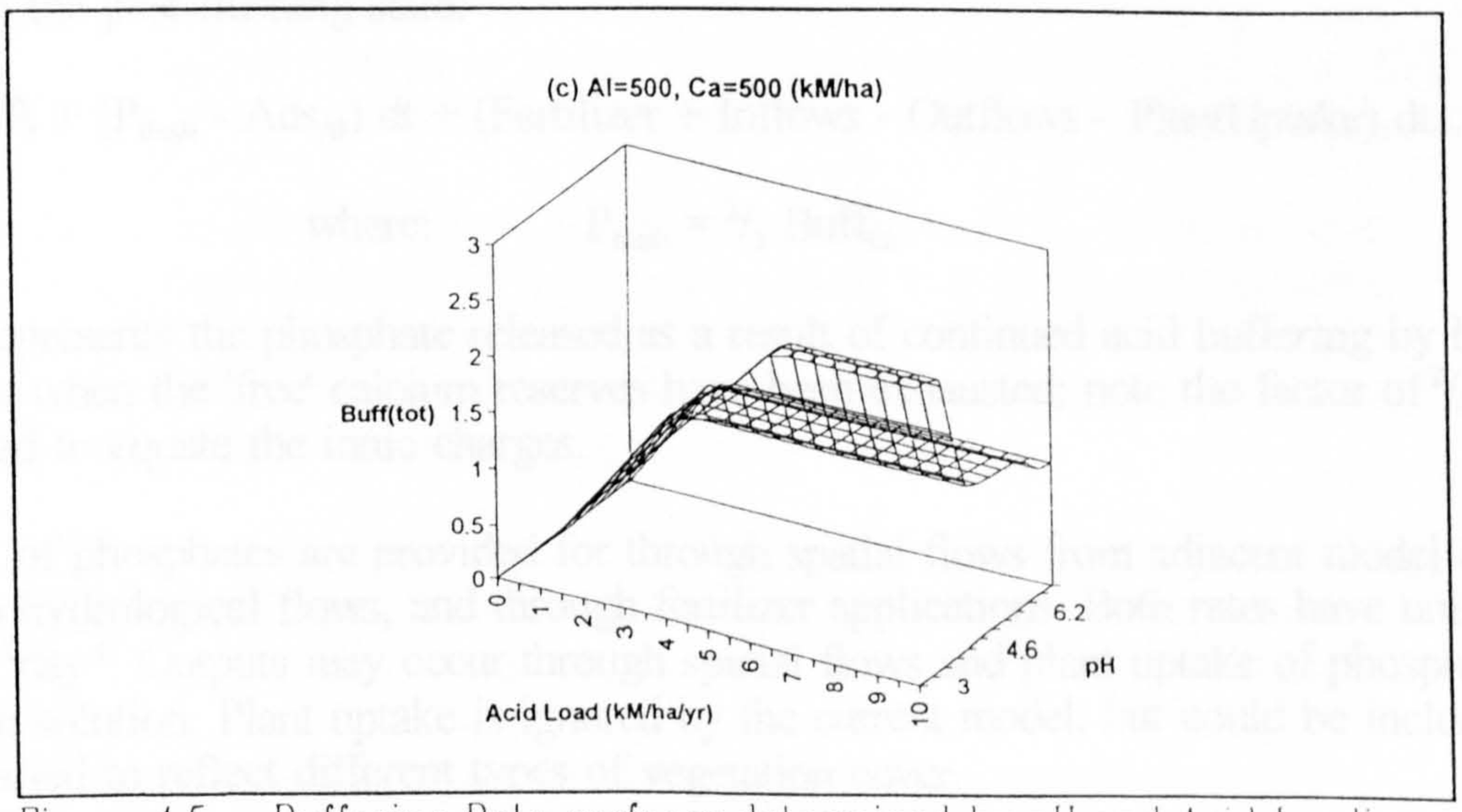

Figure 4.5 – Buffering Rate surfaces determined by pH and Acid Loading

4.1.3.2 Aluminium

Similarly - but ignoring an Aluminium post-flushing state since the model is not directly addressing this situation - changes in Aluminium levels due to adsorption and acid buffering may be given by:

$$Al_{t+1} = Al_t - (Ads_{Al} + Buff_{Al})\ dt \qquad ...(17)$$

$$Q_{Al,t+1} = Q_{Al,t} + Ads_{Al}\ dt$$

Total Aluminium reserves, for the purposes of determination of soil pH and acid buffering rates is thus given by:

$$AlQ_{t+1} = Al_{t+1} + Q_{Al,t+1}$$

There are no inputs of Aluminium. Aluminium is lost through buffering and adsorption in a similar manner to Calcium.

4.1.3.3 Phosphates

As for Calcium changes, Phosphate changes must reflect whether the system is in a pre or post-flushing state. Thus the change in phosphate levels in a pre-flushing state may be given by:

$$P_{t+1} = P_t - Ads_{tot}\ dt + (Fertilizer + Inflows - Outflows - PlantUptake)\ dt \qquad ...(18)$$

where: $Ads_{tot} = Ads_{Ca} + Ads_{Al}$

and, in the post-flushing state:

$$P_{t+1} = P_t + (P_{flush} - Ads_{Al})\ dt + (Fertilizer + Inflows - Outflows - PlantUptake)\ dt \qquad ...(19)$$

where: $P_{flush} = {}^2/_3\ Buff_{Ca}$

P_{flush} represents the phosphate released as a result of continued acid buffering by base cations when the 'free' calcium reserves have been exhausted; note the factor of $^2/_3$ required to equate the ionic charges.

Inputs of phosphates are provided for through spatial flows from adjacent model cells due to hydrological flows, and through fertilizer applications. Both rates have units of $kMha^{-1}day^{-1}$. Outputs may occur through spatial flows and plant uptake of phosphate held in solution. Plant uptake is ignored by the current model, but could be included and varied to reflect different types of vegetation cover.

4.1.3.4 Acid Level

Finally, the amount of unbuffered acid (H) remaining in solution, which is independent of the effects of phosphate adsorption, may be given by:

$$H_{t+1} = H_t - Buff_{tot}\, dt + (A_{load} + Inflows - Outflows)\, dt \qquad ...(20)$$

where: $Buff_{tot} = 2\, Buff_{Ca} + 3\, Buff_{Al} + Buff_{si}$

$Buff_{si}$ is the change due to silicate buffering,
A_{load} is the acid loading from Acid Rain

Acid inputs are provided for through spatial flows, as for phosphate, and the level of acid loading, A_{load}. Losses, excluding through buffering, are due to further spatial hydrological flows.

4.1.4 CATASTROPHE POTENTIAL & DETECTION

As discussed above, when the reserves of 'free' Calcium (base cations) have been depleted, the effect of further acid buffering is to provoke a release of phosphate. If, in this situation, there is no increase of phosphate in the soil solution, then the rate at which phosphate is being adsorbed by Aluminium (acid cations) would have to be greater than or equal to the rate of additional release through acid buffering by Calcium.

The simulation output presented in Figure 4.6 highlights the relationship between acid buffering by Calcium, adsorption by Aluminium (both in kEq), the concentration of phosphate in solution, and the remaining adsorptive capacities (R_{Ca}, R_{Al}, R_{tot}). The noticeable features of this output are threefold:

i) The overall adsorptive capacity, R_{tot}, drops to a minimum after approximately 15 years. This characteristic is discussed more fully in section 4.2 (Liming Paradox).

ii) A sharp decline in buffering by calcium, $Buff_{Ca}$, is observed at approximately 37 years. This reflects a switch in the buffering calculations from the Carbonate buffer range to the Cation Exchange buffer range where buffering by aluminium accounts for an increasing proportion of buffering as the pH drops.

iii) A sudden increase in phosphate concentration, followed by a rapid increase in adsorption by aluminium (Ads_{Al}), is experienced at 47 years. This represents the switch from a pre to a post-flushing state.

After flushing has begun, shown by this rapid increase in concentration, the adsorption rate by aluminium can be seen to be less than the buffering rate by calcium. This is evident until the phosphate concentration peaks (*Flushing Peak*), at

which point it can be seen that the rate of adsorption exceeds the rate of buffering and the phosphate concentration begins to drop. The units of Ads_{Al} and $Buff_{Ca}$ in Figure 4.6 are in kEq; note therefore the need to again include a factor of $^2/_3$ in equation (21).

The turning point, or flushing peak, thus represents the point where no further increase in concentration is produced by additional flushing. The point at which the system passes through this turning point is of key interest in identifying the flushing potential, with the following relationship holding:

$$Ads_{Al} = {}^2/_3\ Buff_{Ca} \qquad ...(21)$$

Equation (21) may be viewed in relation to P_{flush} in equation (19). However, it should be noted that, in a post-flushing state, P_{flush} is always valid, changing in response to $Buff_{Ca}$, whereas the relationship described by equation (21) holds *only* at the point where the phosphate concentration has peaked.

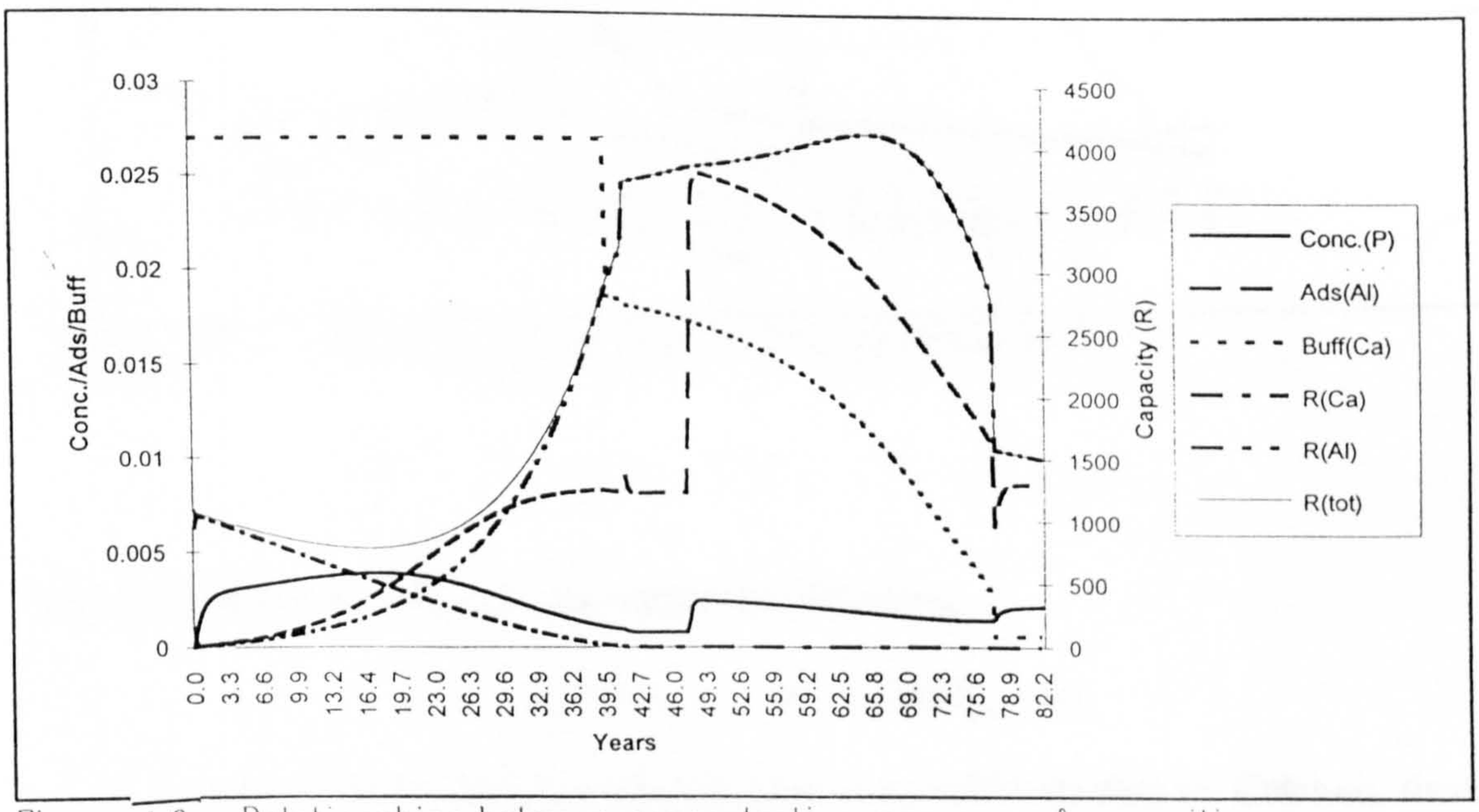

Figure 4.6 – Relationships between concentration, processes & capacities

Having identified the point at which the flushing of phosphate reaches a peak, and by substituting Equation (4), defining Ads_{Al}, the concentration of phosphate in solution (*Catastrophe Potential (P_0)*) is given by:

$$P_0 = 4Buff_{Ca} \,/\, 3(1 - Cos\phi)(M_{Al} - {}^2/_3 Buff_{Ca}) \qquad ...(22)$$

The change in P_0 over time is shown in the simulation output presented in Figure 4.7, and reflects primarily the relative changes of $Buff_{Ca}$ and $Cos\phi$, the affinity curve - dependent upon pH - defining acid cation adsorption. The outputs for Ads_{Al}, $Buff_{Ca}$ and phosphate concentration are repeated from Figure 4.6. Of note in Figure 4.7 is indication of the point at which equation (21) holds, and the trajectory of P_0 through the simulation; if flushing had occurred earlier in the simulation this peak would therefore have been greater.

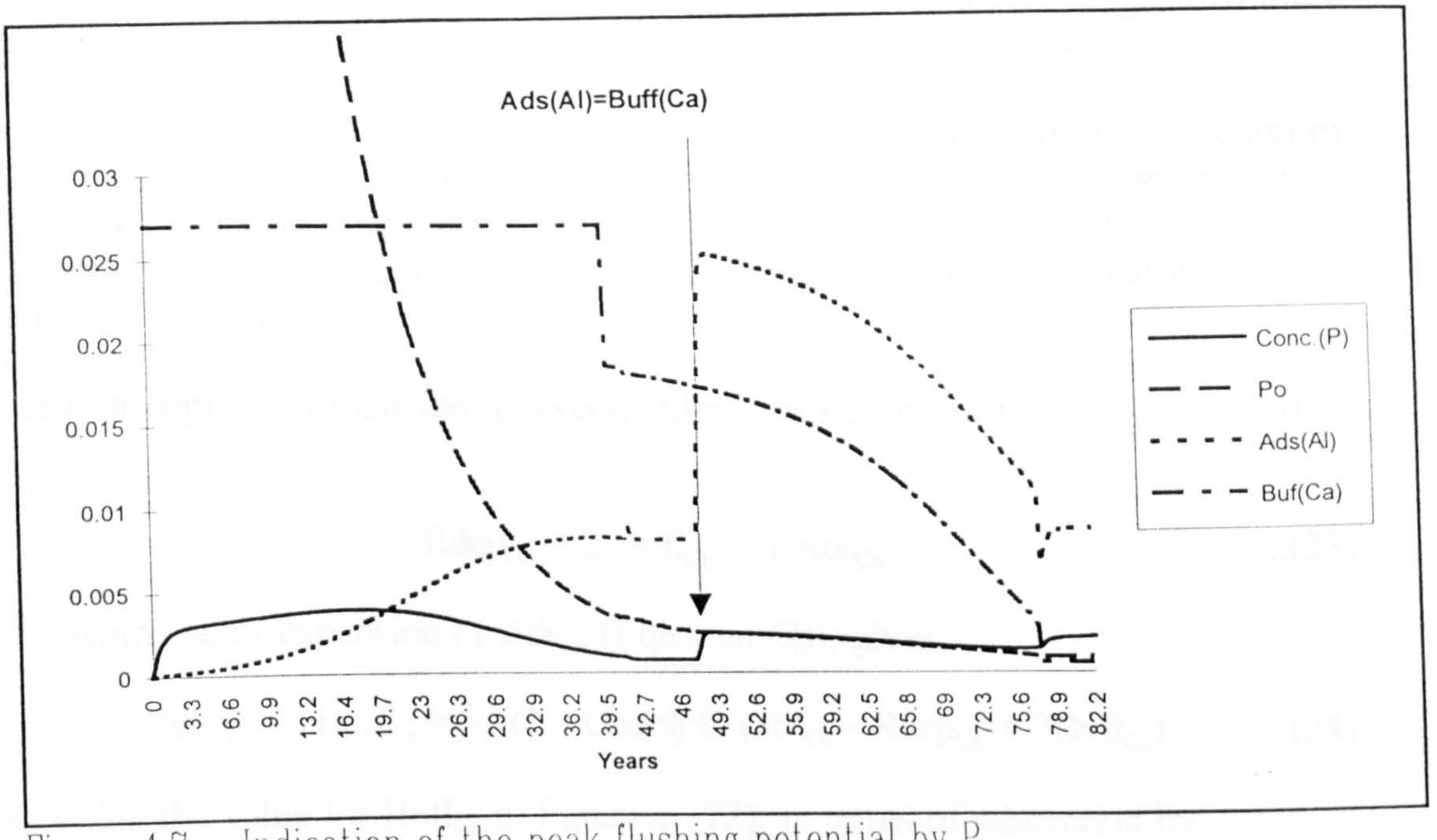

Figure 4.7 – Indication of the peak flushing potential by P_0

The characteristics of P_0 will thus reflect the following:

$$P_0 \rightarrow 0 \qquad \text{as} \qquad Buff_{Ca} \rightarrow 0$$

which would be expected since if there is no acid buffering by Calcium, there will be no consequential release of phosphate, and

$$P_0 \rightarrow \infty \qquad \text{as} \qquad Cos\phi \rightarrow 1$$
$$\text{or} \qquad M_{Al} \rightarrow {}^2/_3 Buff_{Ca}$$

where $Cos\phi=1$ indicates that no adsorption by Aluminium is possible since pH>8 and thus the adsorption affinity, A_{Al}, is zero. The term $(M_{Al}-{}^2/_3 Buff_{Ca})$ in equation (22) may be approximated to M_{Al} since Aluminium reserves for adsorption, in $kMha^{-1}$, far exceeds any rate of acid buffering by Calcium reserves that are addressed by this model with the consistent result that $M_{Al} >> Buff_{Ca}$.

Thus, at a high pH, P_0 will appear to increase exponentially as $Cos\phi \rightarrow 1$ and at a lower pH, where $Buff_{Ca}$ is small due to depleted calcium reserves, P_0 will tend slowly towards zero.

Detection of Catastrophe

Having determined the flushing peak (or catastrophe potential) where the reserves of Calcium have been depleted, attention is now turned towards detection of when these reserves become depleted (ie. the point at which flushing will commence).

The remaining adsorptive capacity by Calcium is given by Equation (3). Detection of the flushing point requires an understanding of the rate of depletion of the reserves ($Rdep_{Ca}$) with regard to the remaining capacity, but must also account for the catastrophe potential in order to gauge the magnitude of flushing, reached when equation (21) is valid.

The rate of depletion of calcium reserves, $Rdep_{Ca}$, in kilo-Equivalents(H^+), is given by:

$$Rdep_{Ca} = 2\ Buff_{Ca} + 3\ Ads_{Ca} \qquad ...(23)$$

which, after expansion of Ads_{Ca} (Equation (2)), gives:

$$Rdep_{Ca} - 2Buff_{Ca} = {}^{2}/_{5}\ (1 - Cos\Theta)\ C\ (3M_{Ca} - Rdep_{Ca} + 2Buff_{Ca}) \qquad ...(24)$$

Substituting the value for $Buff_{Ca}$ in Equation (22), in terms of adsorption by Aluminium when flushing has peaked to a concentration given by P_0, where:

$$Buff_{Ca,Po} = 3M_{Al}(1-Cos\phi)P_0 \,/\, 4(1+{}^{1}/_{2}(1-Cos\phi)P_0) \qquad ...(25)$$

gives:

$$Rdep_{Ca,Po} = 3\left\{ {}^{2}/_{5}M_{Ca}(1-Cos\Theta)C \,/\, 1+{}^{2}/_{5}(1-Cos\Theta)C \right\} + 3\left\{ {}^{1}/_{2}M_{Al}(1-Cos\phi)P_0 \,/\, 1+{}^{1}/_{2}(1-Cos\phi)P_0 \right\}$$

which reduces to, given the above substitution whereby $C=P_0$:

$$Rdep_{Ca,Po} = 3\ Ads_{Ca,Po} + 3\ Ads_{Al,Po} \qquad ...(26)$$

where $Ads_{Al,Po}$ and $Ads_{Ca,Po}$ represent the adsorption by acid and base cation reserves respectively, given a theoretical phosphate concentration in solution equal to the peak potential flushing concentration (P_0).

From the above equations, there are now two potential mathematical representations of the change in adsorptive capacity over time (in units of $kEqha^{-1}$):

(i) $$R_{Ca,t+1} = R_{Ca,t} - (3\ Ads_{Ca} + 2\ Buff_{Ca})\ dt$$

(ii) $$R_{Ca,t+1} = R_{Ca,t} - (3\ Ads_{Ca,Po} + 3\ Ads_{Al,Po})\ dt$$

The former describes the actual change in capacity, and will provide no additional understanding of the potential flushing scenario than if R_{Ca} were to be tracked over time. However, the theoretical capacity change described by the latter will track the change in capacity given a depletion rate dependent upon P_0.

Thus, by tracking the theoretical capacity change, $Rdep_{Ca,Po}$, over time, a family of curves will be described, dependent upon R_{Ca} and P_0 which will indicate the potential timing and magnitude of catastrophe. R_{Ca} will vary in accordance with the actual capacity change, $Rdep_{Ca}$ (Equation (23)), and the phosphate concentration, C. If the effects upon R_{Ca} were linear, then the timing of catastrophe could be determined by dividing R_{Ca} by $Rdep_{Ca}$ (the gradient). However, the effects are non-linear and the magnitude of potential catastrophe is continually changing. Thus by dividing R_{Ca} by the theoretical change, $Rdep_{Ca,Po}$, an alternative indication of the timing of catastrophe is provided which accounts for P_0.

However, since R_{Ca} becomes very large at a high pH, indication of the timing and magnitude of catastrophe will still require examination of both R_{Ca} and the depletion rate $Rdep_{Ca,Po}$. Since an appropriate indicator should inherently describe both the timing and magnitude of catastrophe, it was found that one further modification was useful. By tracking the logarithm of this ratio, it is possible to detect the point and extent of flushing without unnecessary reference to the current *actual* level of resource remaining.

Thus, the equation required to track this potential against time is given by:

$$R_{0,t+1} = LOG_{10}\left(R_{Ca,t+1} / Rdep_{Ca,Po,t} \right) \qquad ...(27)$$

Given that the units of R_{Ca} are in $kEqha^{-1}$, and those of $Rdep_{Ca,Po}$ are in $kEqha^{-1}day^{-1}$, the units of R_0 are derived as LOG_{10}(days) - equivalent to days, but interpreted against a logarithmic scale.

Thus, R_0 could be described as a *Leading Indicator* (timing of flushing) of the *Catastrophe Potential* (magnitude of flushing) since the curve described by this equation will follow a relatively constant trajectory, owing to the employment a logarithmic function, until the remaining resource, $R_{Ca,t+1}$, becomes depleted relative to the rate of change in the resource determined by the theoretical conditions necessary to avoid the catastrophe, $Rdep_{Ca,Po,t}$.

As shown in Figure 4.8, detection of the proximity of flushing is provided by the trajectory falling increasingly rapidly and the magnitude is indicated by the height from which the trajectory falls.

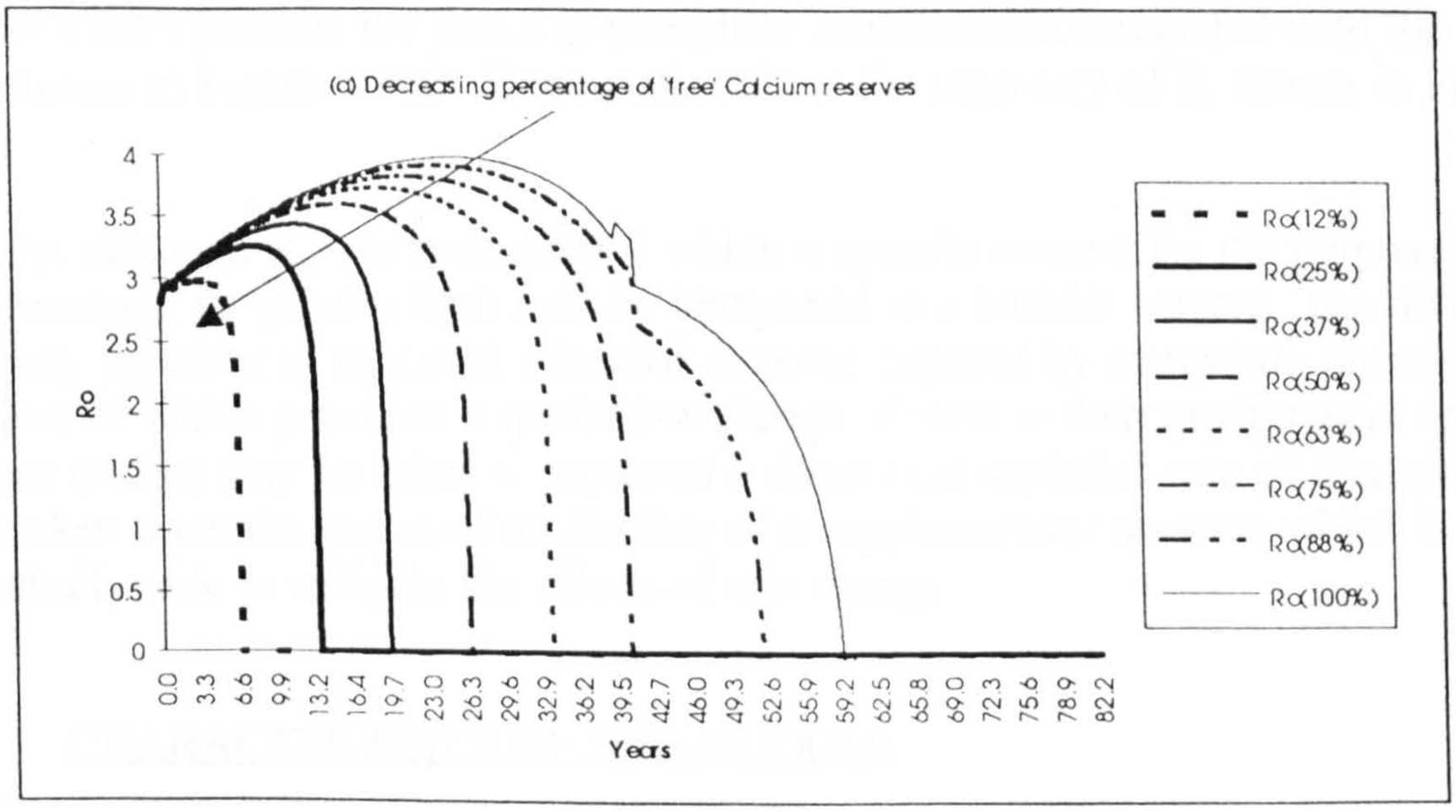

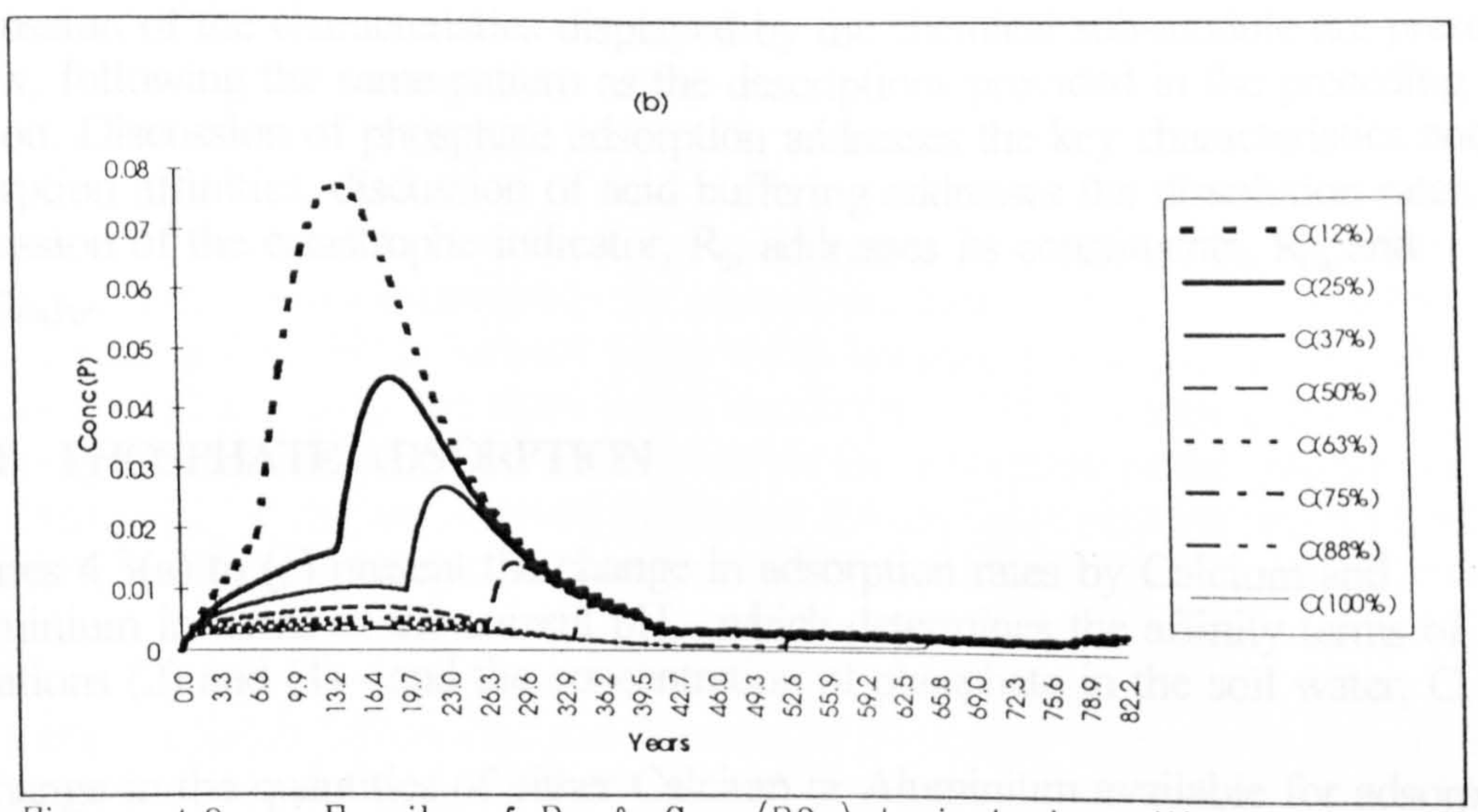

Figure 4.8 - Family of R_0 & Conc(PO_4) trajectories with varying Q_{Ca} content

The family of curves described by R_0, given variations in the proportion of free Calcium to total Calcium in the soil, will describe different trajectories over time, reflecting the remaining capacity, R_{Ca}, and the flushing potential, P_0. The lower the trajectory, the sooner potential flushing may occur and greater the flushing peak will be.

A subset of this family of curves and the associated flushing peaks is shown in Figure 4.8. Figure 4.8(a) presents R_0 trajectories where the free calcium content varies from 12% (Q_{Ca}=88%) to 100% (Q_{Ca}=0%) of the total reserves. The lower the percentage, the smaller the available reserves (R_{Ca}) and thus the sooner that catastrophe is indicated, given equivalent initial conditions except for the Ca:Q_{Ca} ratio.

Note also the discontinuities at approximately 40 years where the model switches between alternative pH calculations.

Figure 4.8(b) presents the peaks in phosphate concentration associated with the trajectories in Figure 4.8(a). These peaks mirror the trajectory of P_0 shown in Figure 4.7.

Finally, although R_0 has been defined within a specific context for the purposes of this research, its generic form may be interpreted in a broader context. The dividend (R) may be taken to represent a limited resource required by competing phenomena, the loss of which provokes a qualitative change of state in their environment and the divisor (Rdep) may be taken to represent a theoretical depletion rate of this resource dependent upon the extent of availability of a supplementary resource which is potentially able to mitigate the effects of this change.

4.2 CHARACTERISTICS OF SUB-MODULE

Discussion of the characteristics displayed by the chemical sub-module are presented below, following the same pattern as the descriptions provided in the preceding section. Discussion of phosphate adsorption addresses the key characteristics and adsorption affinities, discussion of acid buffering addresses the dissolution rates, and discussion of the catastrophe indicator, R_0, addresses its constituents, R_{Ca} and $Rdep_{Ca,Po}$.

4.2.1 PHOSPHATE ADSORPTION

Figures 4.3(a) to (c) present the change in adsorption rates by Calcium and Aluminium in terms of the current pH - which determines the affinity terms of Equations (2) and (4) - and the concentration of phosphate in the soil water, C.

A change in the quantities of either Calcium or Aluminium available for adsorption, whether due to reduced overall quantities or indirectly through previously adsorbed phosphates, will have a linear effect upon the current rates of adsorption. For example, using Equation (2), adsorption due to Calcium reserves may be shown as:

$$Ads_{Ca} = K_{phos}\, k_{cp}\, k_t\, Ca$$

where k_{cp} and k_t are constants already described above, and

$$K_{phos} = A_{Ca}\, C / (1 + A_{Ca}\, C)$$

which is independent of the Calcium content, Ca.

A similar relationship may be found with the Aluminium reserves.

These non-spatial dynamic characteristics are, however, only static representations of the adsorption rates, with a single point on the surface of Figure 4.3(c) representing the current 'state' of the model. By tracking this current 'state' of the system against time, this single point would appear to move around this 3-dimensional space on a

highly non-linear trajectory. Examples of such trajectories are shown in Figures 4.9(a) and (b) below. Any selected point of these trajectories will lie on a static surface similar to those shown in Figures 4.3(a) or (b), respectively. However, due to changing levels of Calcium and Aluminium reserves over time, the surfaces of Figure 4.3 will appear to move, and thus render meaningful analysis of the trajectory almost impossible.

Since these outputs implicitly involve a highly non-linear, dynamic scale for time (it would require 4 dimensions to represent a static, linear scale for time), values of the pH, phosphate concentration (C), and adsorption rates (Ads_{Ca} , Ads_{Al} and Ads_{tot}) have been plotted against time in Figure 4.11, to be described below.

Using initial conditions of 1½% Calcium content and 1½% Aluminium content of the soil, the relationships between Calcium and R_{Ca} , and between Aluminium and R_{Al} , with regards to soil pH and time, is shown in Figure 4.10. The trough observed in Section 4.1.4, where R_{tot} is at a minimum, may now be seen in relation to the changing pH. It is assumed for this simulation output that there is no previously adsorbed phosphate in the soil (ie. $Q_{Ca}=Q_{Al}=0$).

Slightly different adsorption dynamics will be displayed if a proportion of the Calcium reserves are unavailable for adsorption, there already being adsorbed phosphate in the soil; a different relationship between pH and available Calcium will be observed. By using the same initial conditions of 1½% Calcium content, but varying the percentage of Calcium available for adsorption in the manner presented in Figure 4.8, it can be observed that when the available reserves are depleted, a flushing of phosphates occurs due to the continued effects of acid neutralization by Calcium.

Figures 4.11(a)-(h) show that this flushing of phosphate increases as the pH at which it occurs increases. As would be expected, the lower the percentage of available Calcium, the greater the flushing of phosphate and the higher the pH at which this will occur. In general terms, the flushing point will be reached sooner. The change in flushing peaks in relation to the $Ca:Q_{Ca}$ ratio can be clearly observed throughout these outputs.

4.2.1.1 Key Characteristics

The trajectories described in Figure 4.11 identify two key characteristics of this dynamic, non-spatial system:

1. *The Flushing Point*

   The point at which the sudden flushing of phosphate from the soil occurs - observed where the concentration (C) suddenly increases as R_{Ca} reaches zero - identifies the point at which the qualitative nature of the system switches from a pre-flushing to a post-flushing state. This point represents the discontinuity giving rise to potential catastrophic release of phosphates for which the catastrophe indicator, R_0, has been developed to detect.

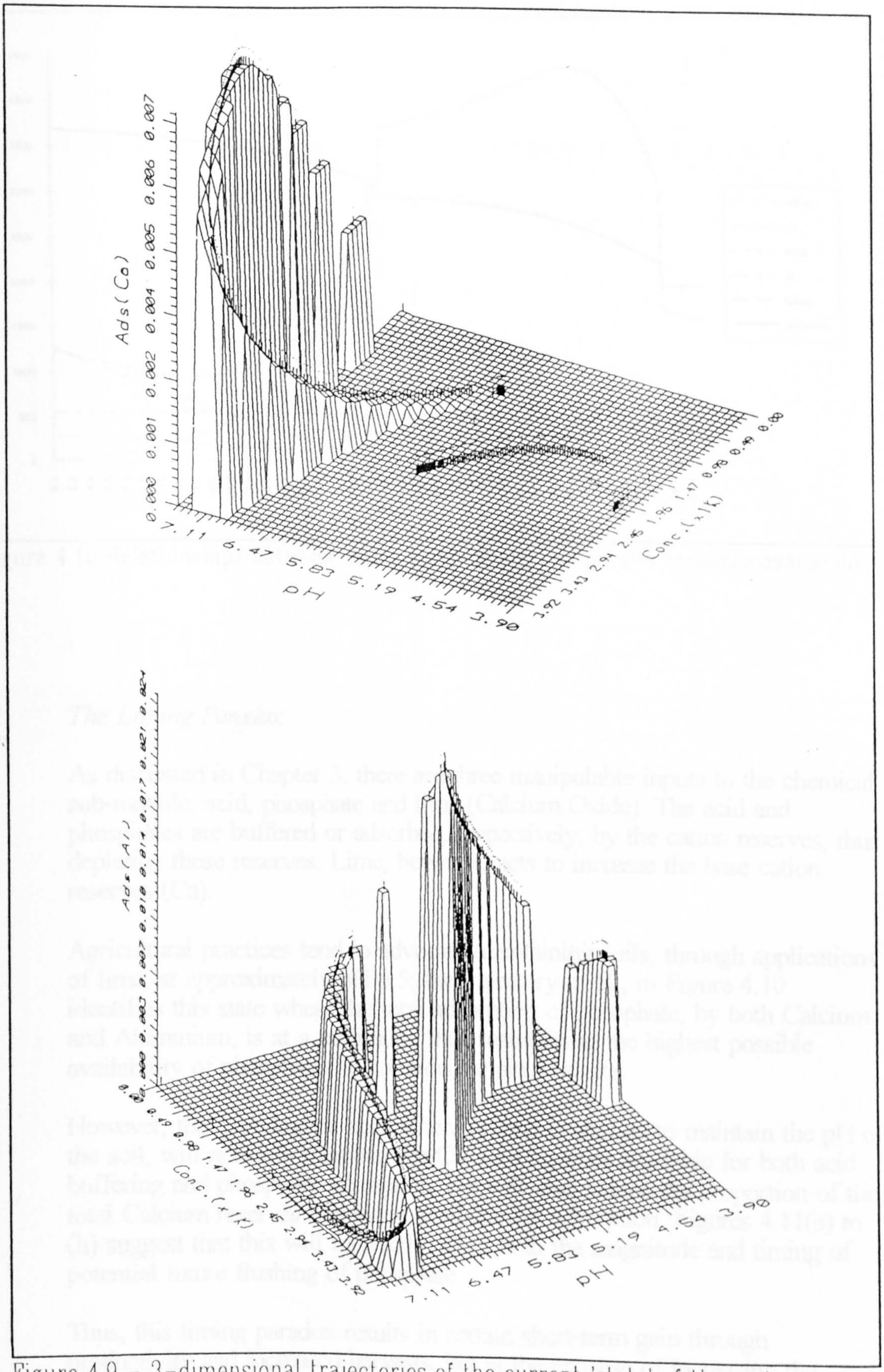

Figure 4.9 - 3-dimensional trajectories of the current 'state' of the system

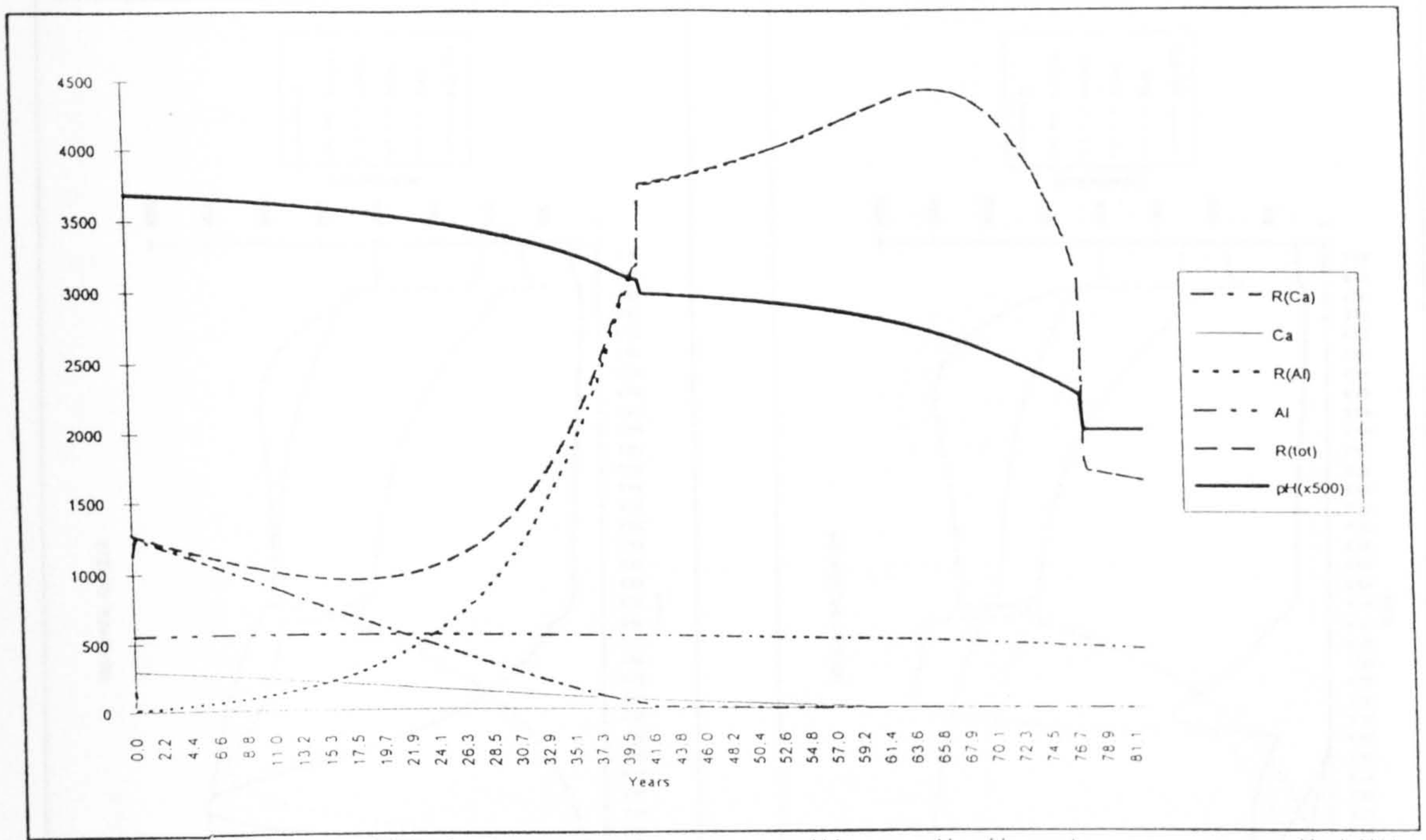

Figure 4.10 Relationships between cation composition, soil pH and resource availability

2. *The Liming Paradox*

As discussed in Chapter 3, there are three manipulable inputs to the chemical sub-module: acid, phosphate and lime (Calcium Oxide). The acid and phosphates are buffered or adsorbed, respectively, by the cation reserves, thus depleting these reserves. Lime, however, acts to increase the base cation reserves (Ca).

Agricultural practices tend to advocate maintaining soils, through applications of lime, at approximately pH 6.5; the trajectory of R_{tot} in Figure 4.10 identifies this state where the total adsorption of phosphate, by both Calcium and Aluminium, is at a minimum, thus maintaining the highest possible availability of phosphates in solution for plant uptake.

However, this paradoxical state whereby lime is applied to maintain the pH of the soil, will not only maintain the Calcium reserves available for both acid buffering and phosphate adsorption, but will also reduce the proportion of the total Calcium reserves which are available for adsorption. Figures 4.11(a) to (h) suggest that this will indirectly affect both the magnitude and timing of potential future flushing of phosphate.

Thus, this liming paradox results in certain short-term gain through productivity and increased harvests, but at the expense of increasing the catastrophe potential in the long-term. The potential catastrophic effects of

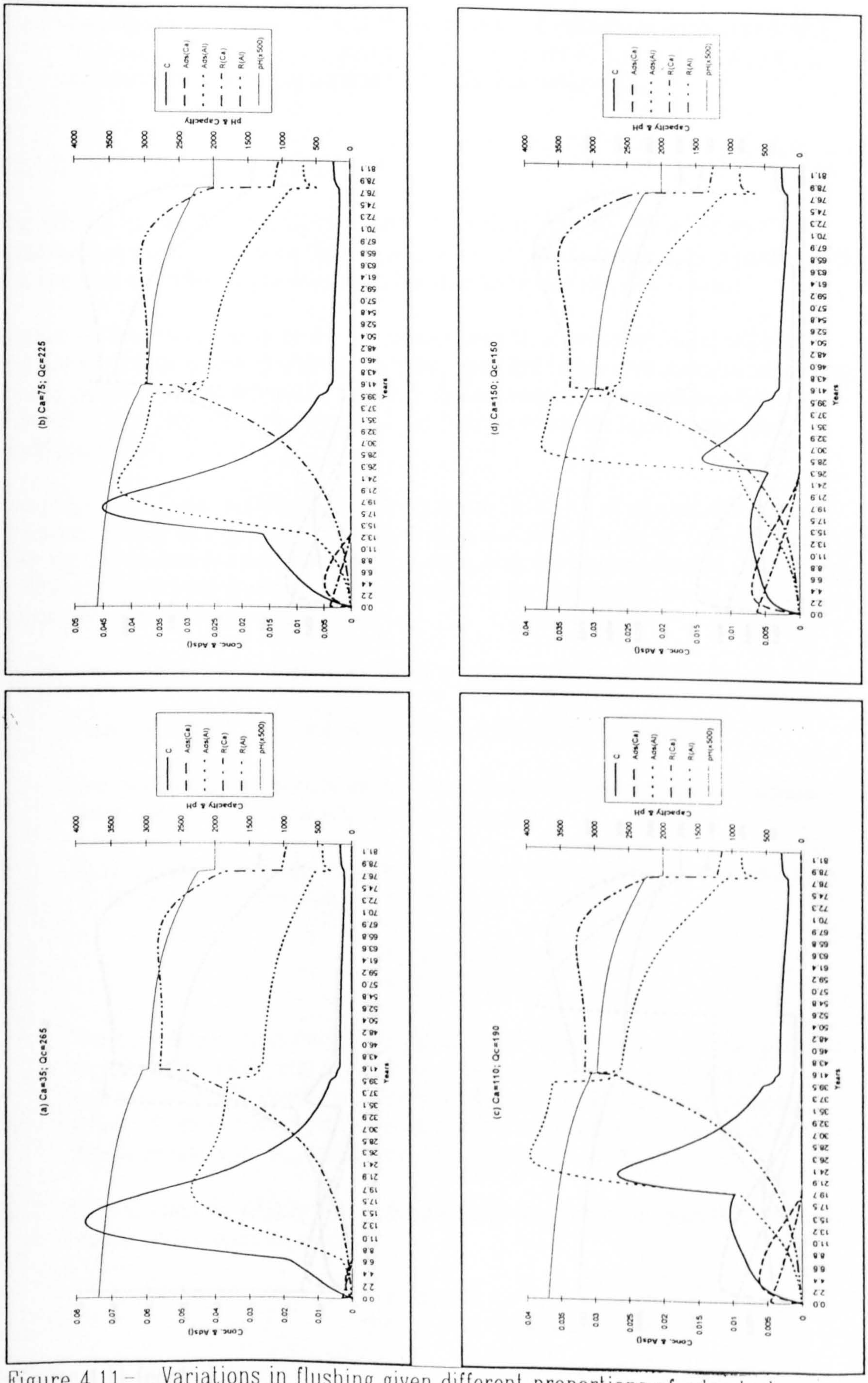

Figure 4.11– Variations in flushing given different proportions of adsorbed phosphate

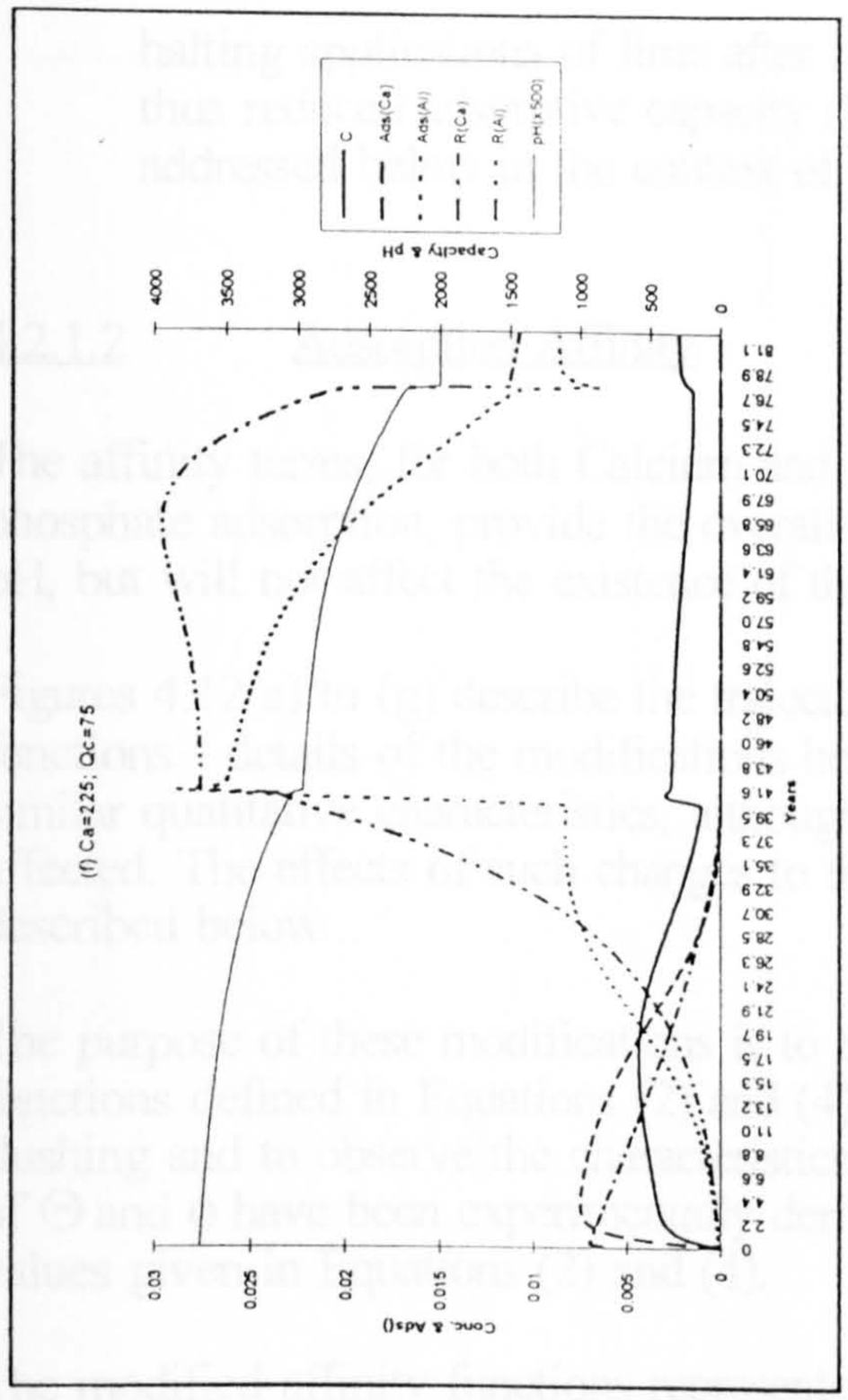

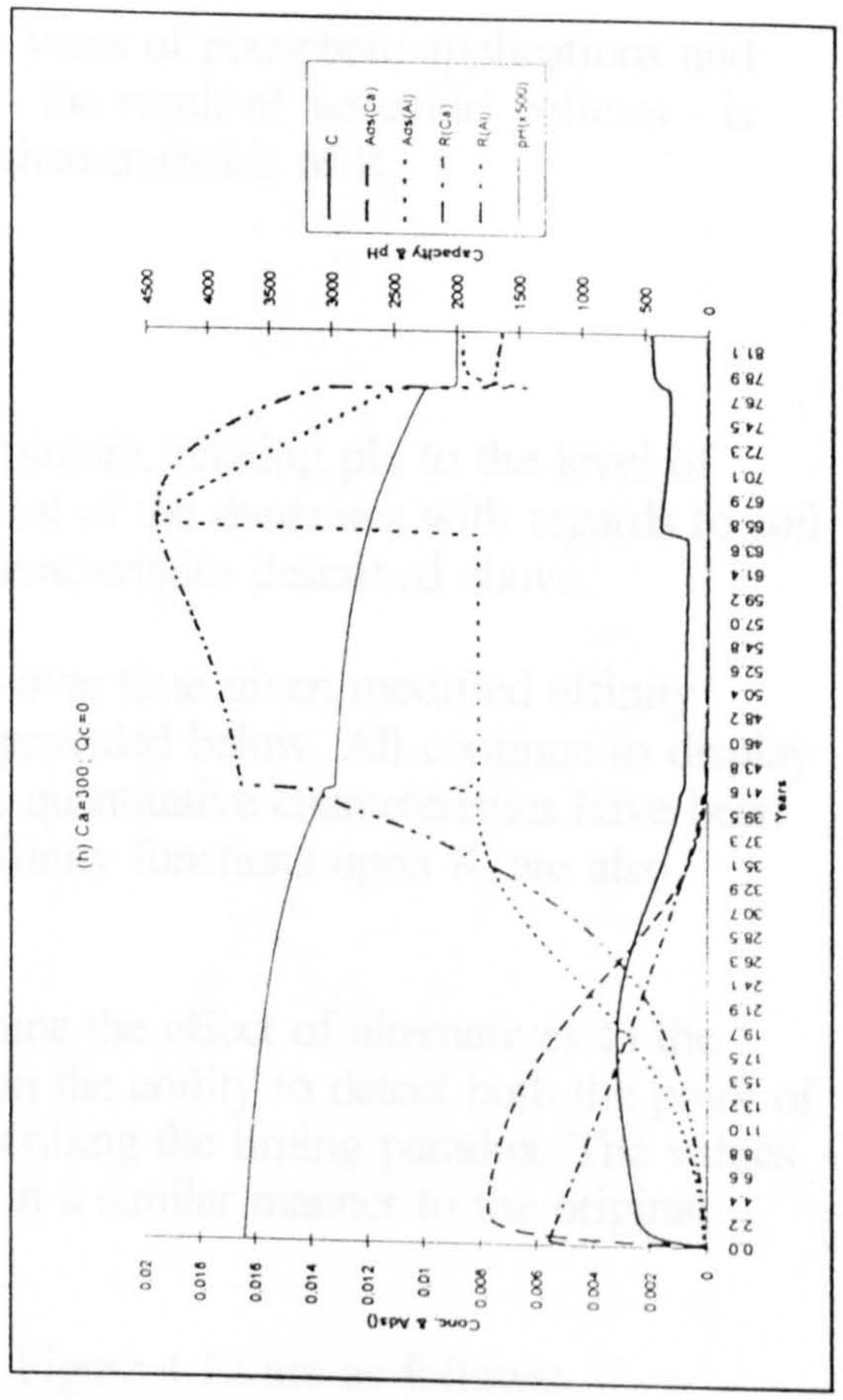

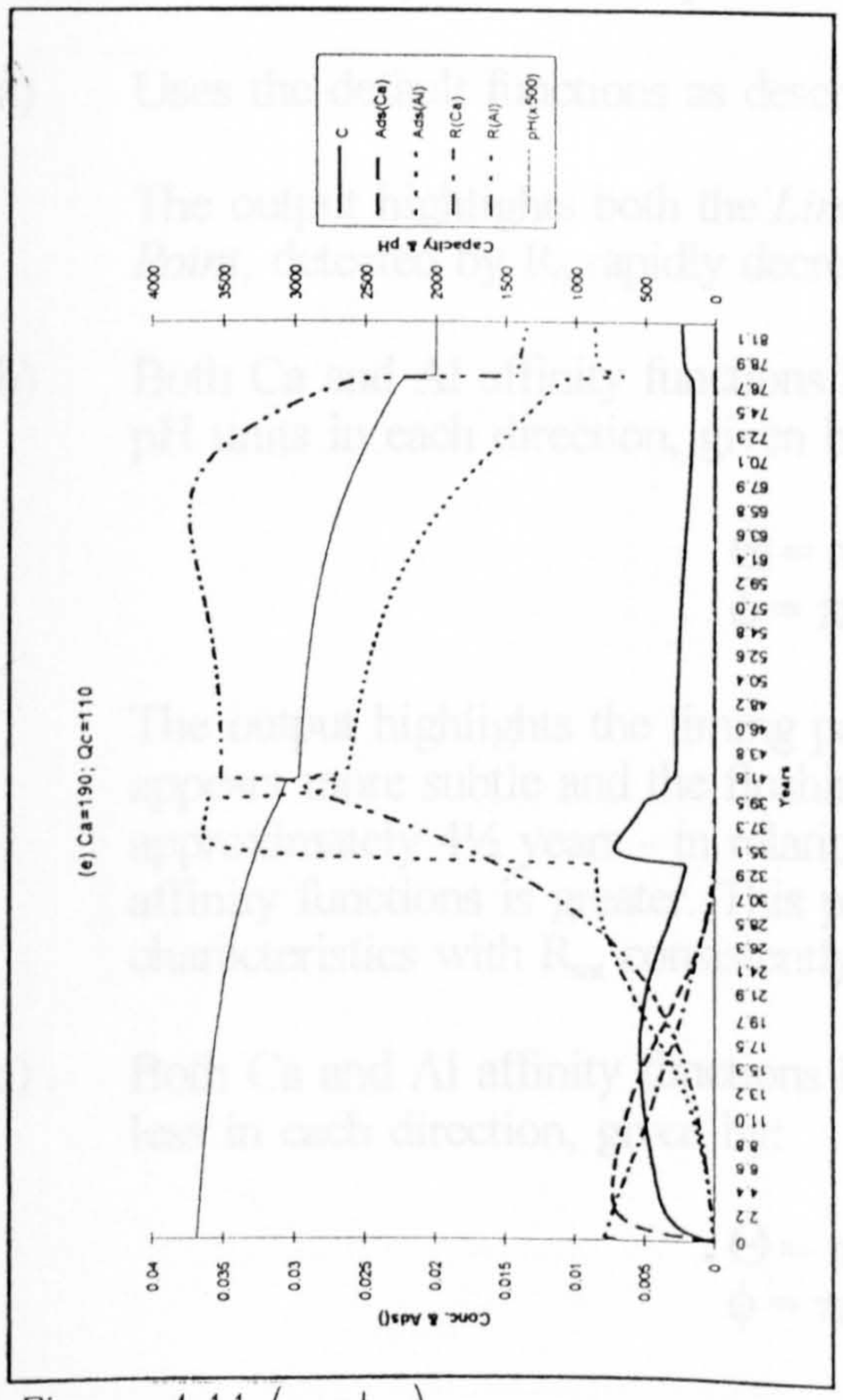

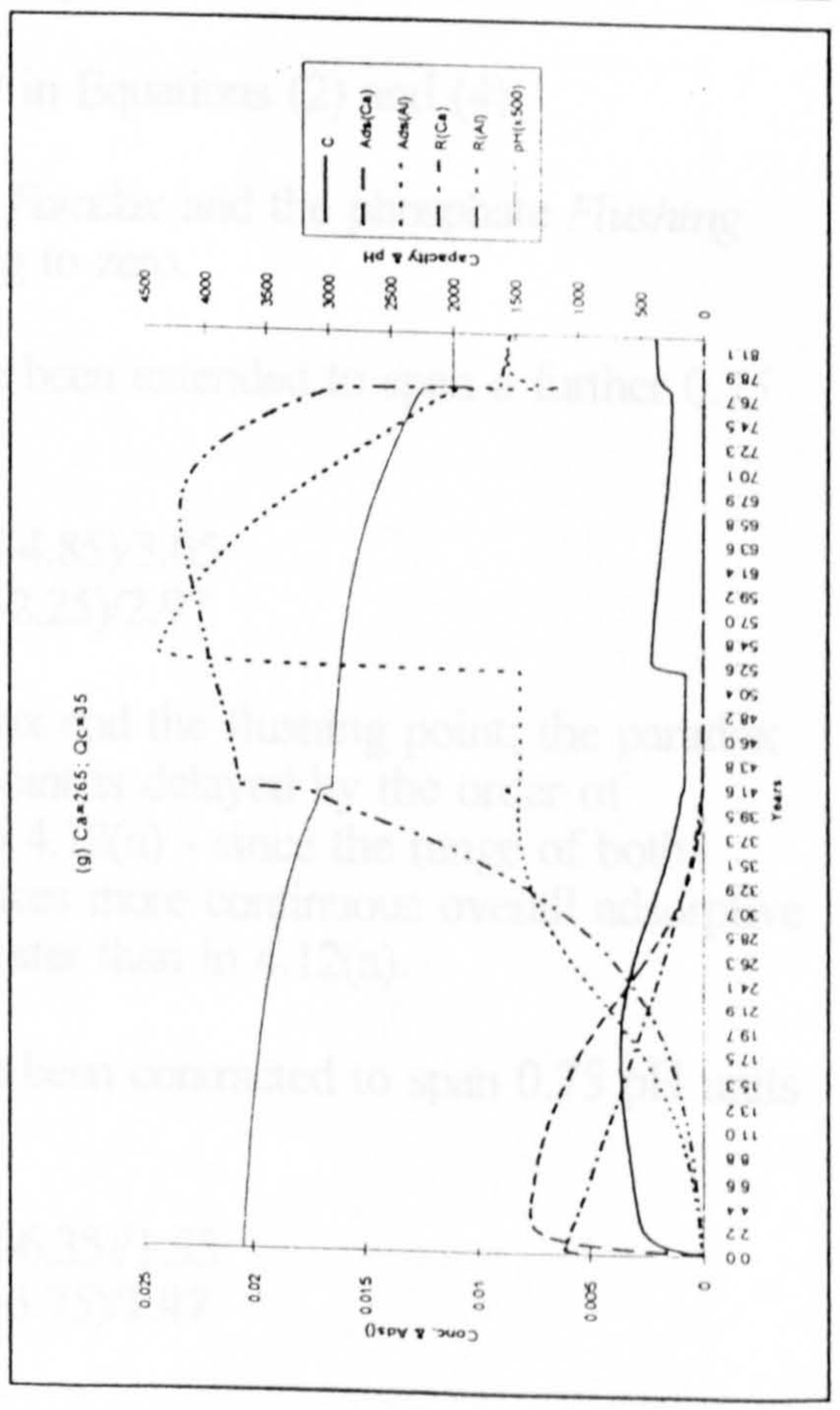

Figure 4.11 (cont...)

halting applications of lime after many years of phosphate applications and thus reduced adsorptive capacity (R_{Ca}) - the result of 'set-aside' policies - is addressed below in the context of the characteristics of R_0.

4.2.1.2 Adsorption Affinity

The affinity terms, for both Calcium and Aluminium, relating pH to the level of phosphate adsorption, provide the overall control of the dynamics with regards to soil pH, but will not affect the existence of the characteristics described above.

Figures 4.12(a) to (g) describe the trajectories over time given modified affinity functions - details of the modifications being provided below. All continue to display similar qualitative characteristics, although the quantitative characteristics have been affected. The effects of such changes to the affinity functions upon R_0 are also described below.

The purpose of these modifications is to examine the effect of alternatives to the functions defined in Equations (2) and (4) upon the ability to detect both the point of flushing and to observe the characteristics describing the liming paradox. The values of Θ and ϕ have been experimentally derived in a similar manner to the original values given in Equations (2) and (4).

The modified affinity functions represented in Figure 4.12 are as follows:

(a) Uses the default functions as described in Equations (2) and (4).

The output highlights both the *Liming Paradox* and the phosphate *Flushing Point*, detected by R_0 rapidly decreasing to zero.

(b) Both Ca and Al affinity functions have been extended to span a further 0.75 pH units in each direction, given by:

$$\Theta = \pi(pH-4.85)/3.05$$
$$\phi = \pi(pH-2.25)/2.97$$

The output highlights the liming paradox and the flushing point; the paradox appears more subtle and the flushing point is delayed by the order of approximately 4½ years - in relation to 4.12(a) - since the range of both affinity functions is greater. This produces more continuous overall adsorptive characteristics with R_{tot} consistently greater than in 4.12(a).

(c) Both Ca and Al affinity functions have been contracted to span 0.75 pH units less in each direction, given by:

$$\Theta = \pi(pH-6.35)/1.55$$
$$\phi = \pi(pH-3.75)/1.47$$

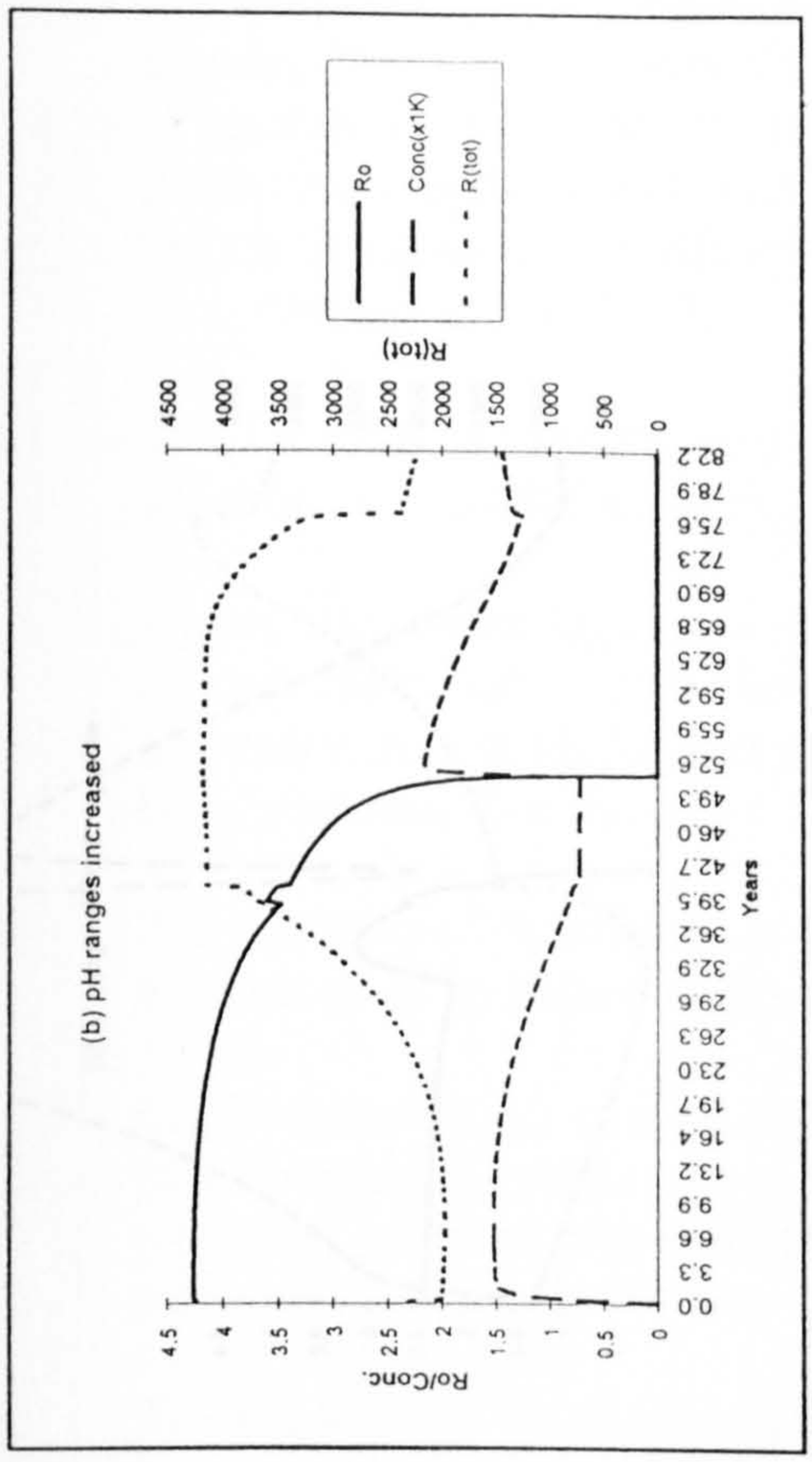

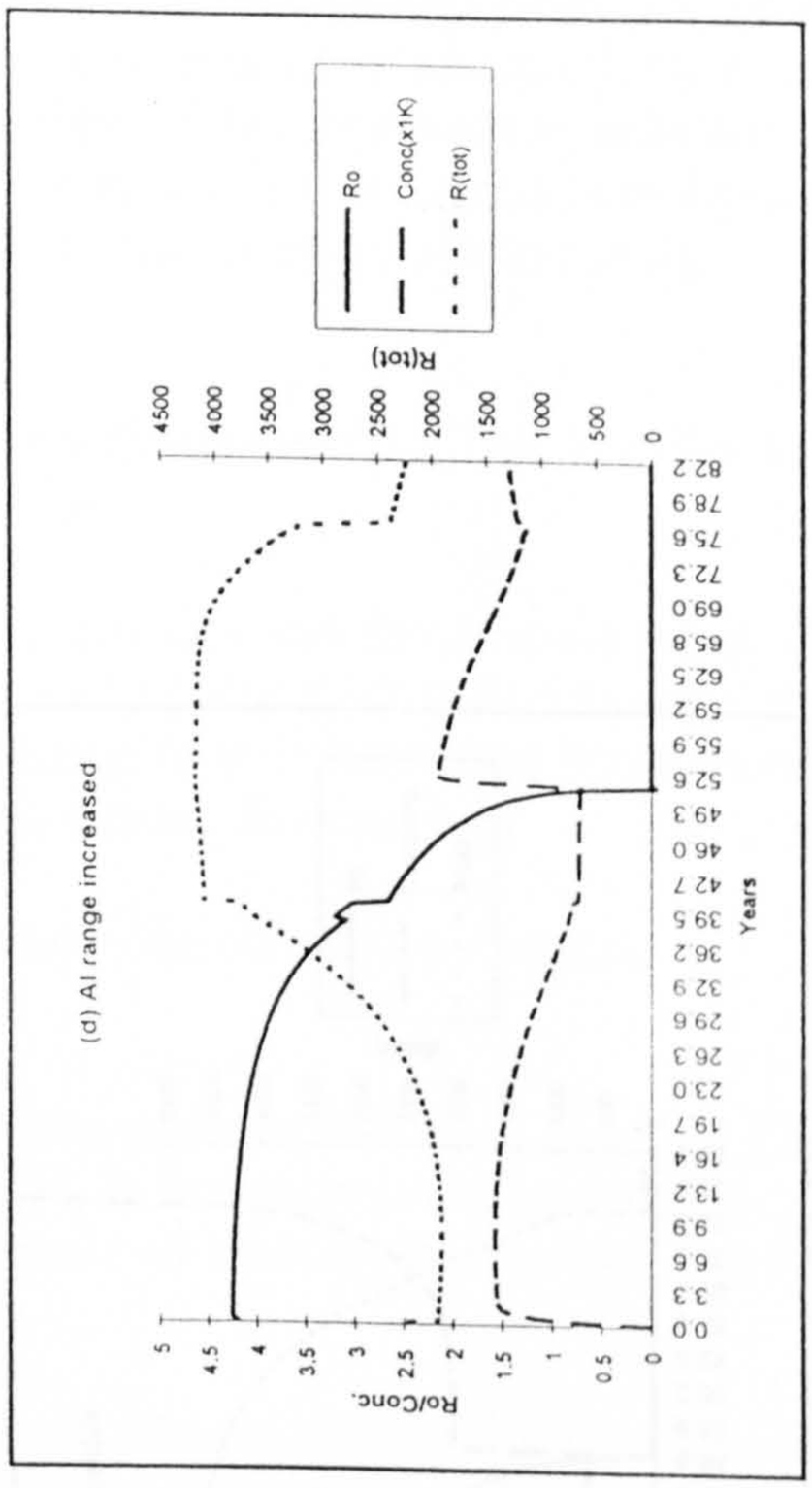

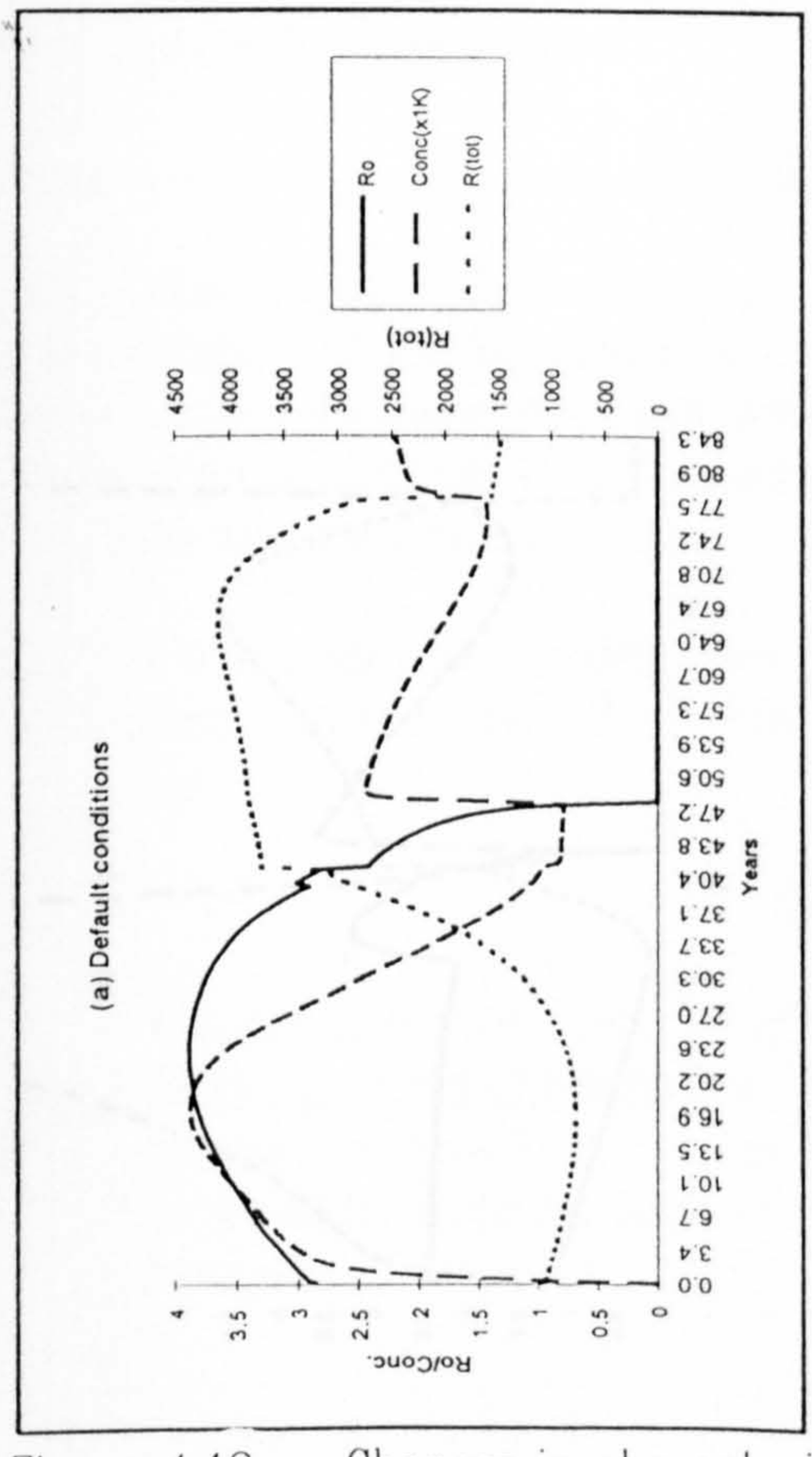

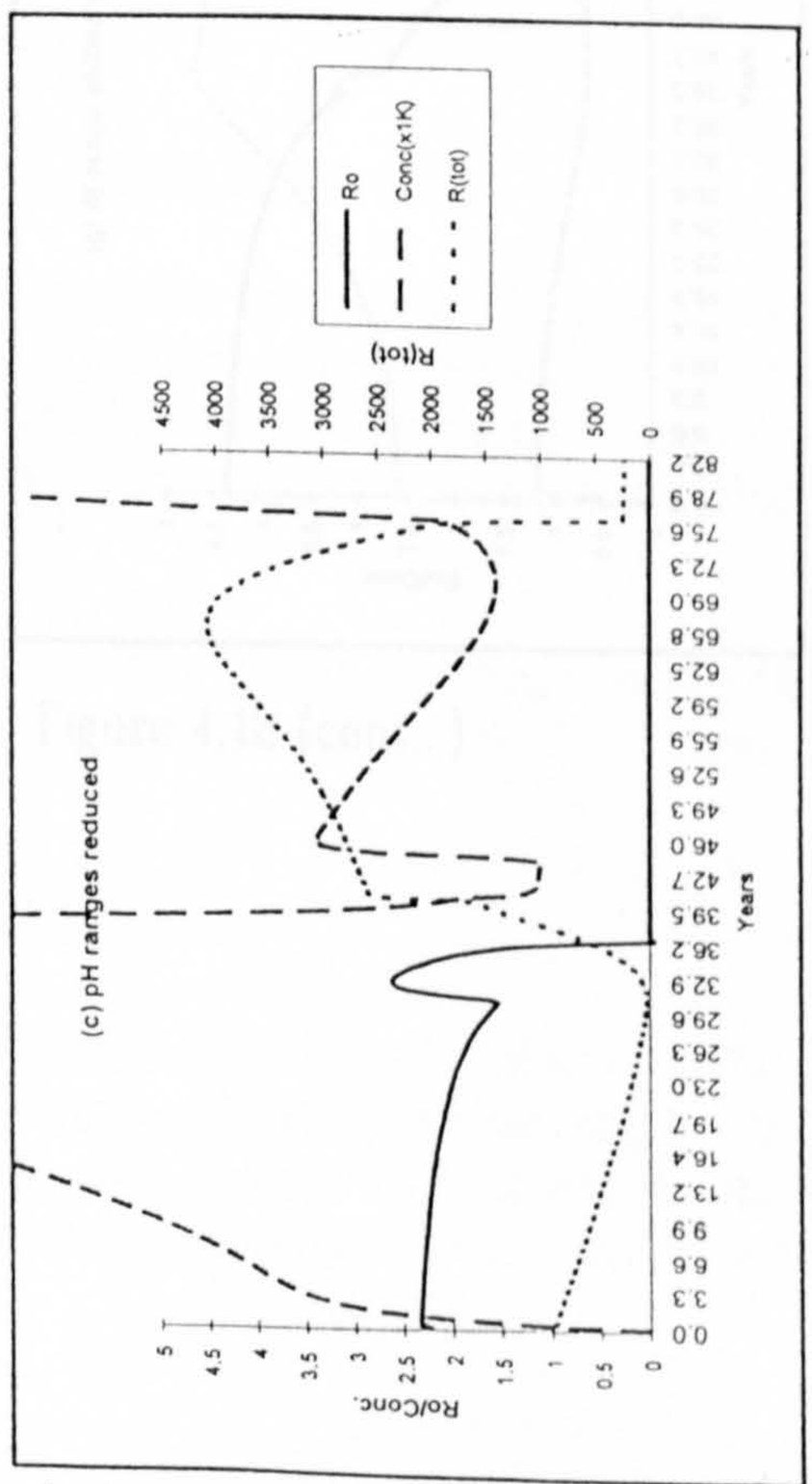

Figure 4.12 – Changes in characteristic trajectories given modified adsorption affinity functions

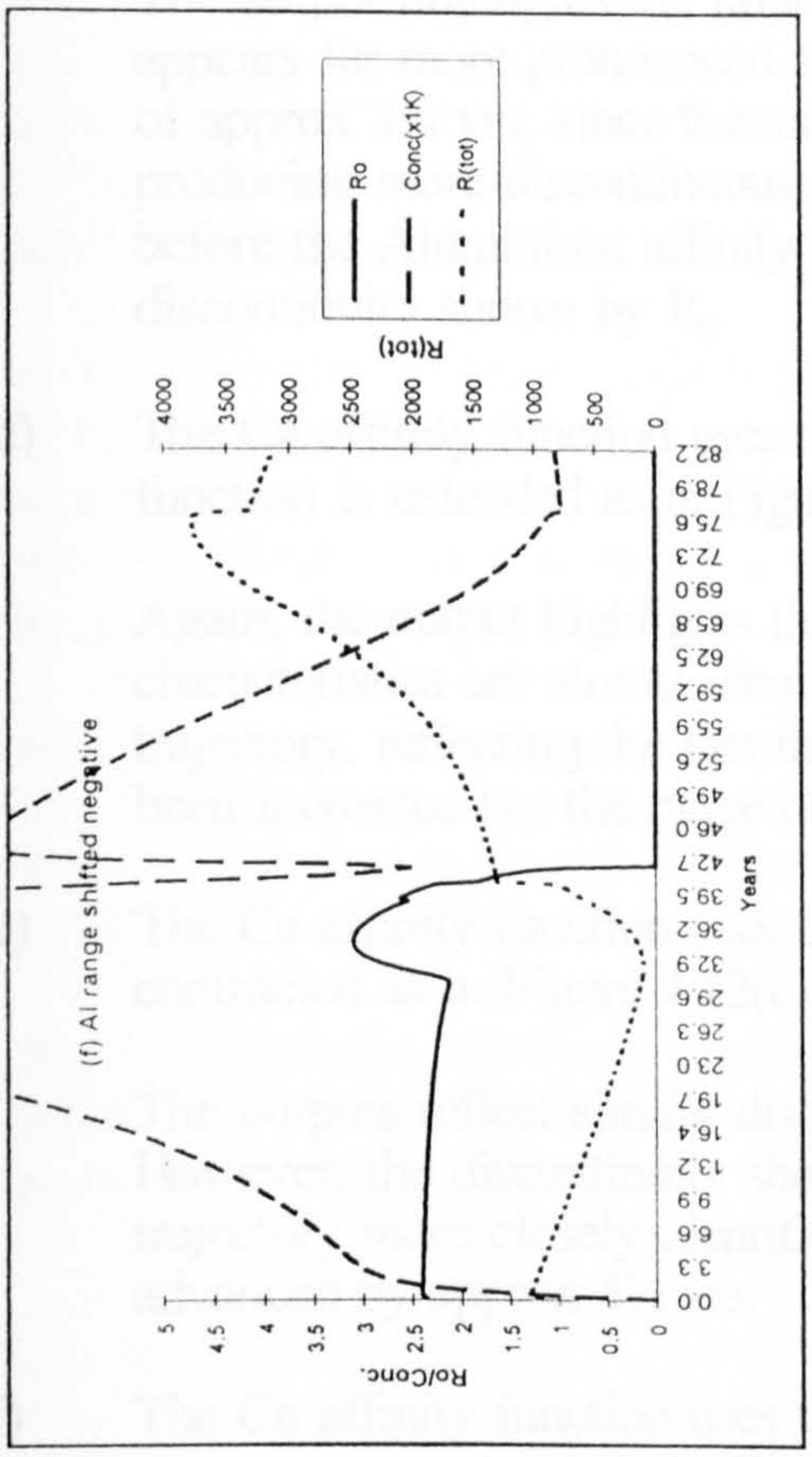

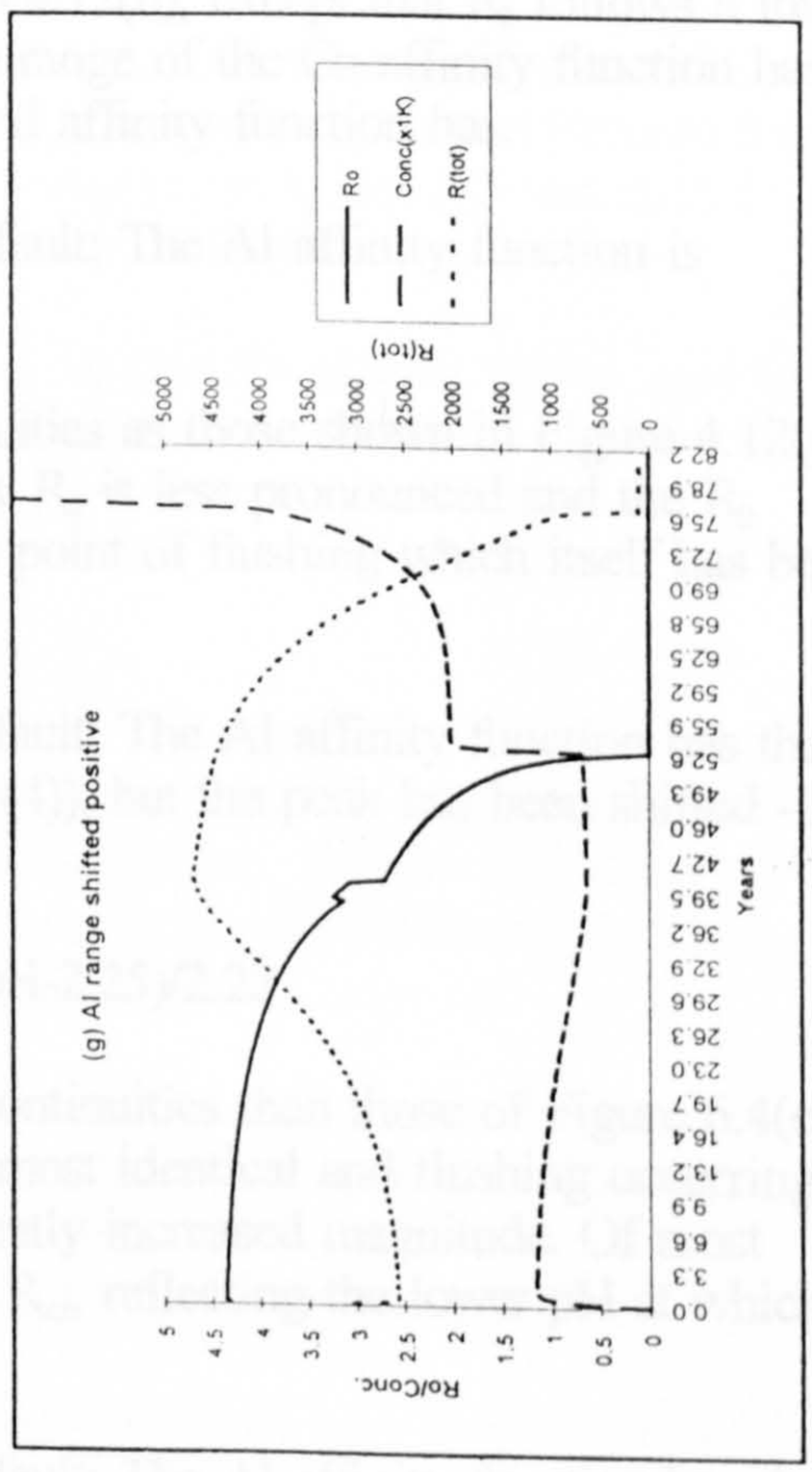

Figure 4.12 (cont...)

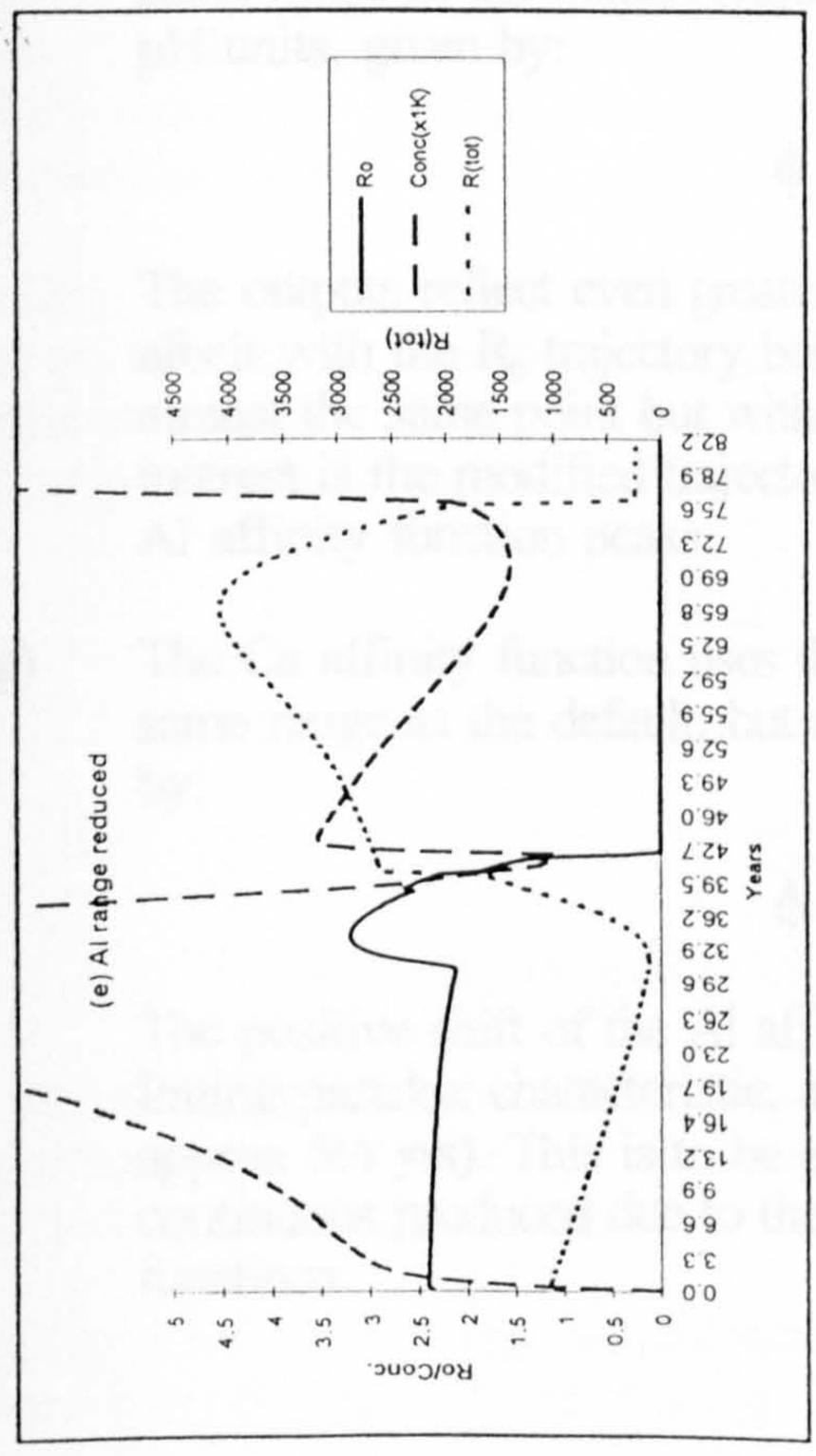

The output highlights the liming paradox and the flushing point; the paradox appears far more pronounced and the flushing point is advanced, by the order of approx 3¼ yrs, since the range of both affinity functions is reduced, producing more discontinuous characteristics where R_{tot} almost reaches zero before the Aluminium affinity increases. This is also reflected in the discontinuity shown by R_0.

(d) The Ca affinity function uses the default (Equation (2)); The Al affinity function is extended as in Figure 4.12(b).

Again, the output highlights the liming paradox and the flushing point; the characteristics are almost identical to 4.12(b), except that R_0 follows a lower trajectory, reflecting the fact that the range of the Ca affinity function has not been increased but the range of the Al affinity function has.

(e) The Ca affinity function uses the default; The Al affinity function is contracted as in Figure 4.12(c).

The outputs reflect similar discontinuities as those shown in Figure 4.12(c). However, the discontinuity shown by R_0 is less pronounced and the R_0 trajectory more closely identifies the point of flushing which itself has been advanced by approx 4½ yrs.

(f) The Ca affinity function uses the default; The Al affinity function has the same range as the default (Equation (4)), but the peak has been shifted -0.75 pH units, given by:

$$\phi = \pi(pH-2.25)/2.22$$

The outputs reflect even greater discontinuities than those of Figure 6.4(e), albeit with the R_0 trajectory being almost identical and flushing occurring at almost the same point but with a greatly increased magnitude. Of most interest is the modified trajectory of R_{tot}, reflecting the lower pH at which the Al affinity function peaks.

(g) The Ca affinity function uses the default; The Al affinity function has the same range as the default, but the peak has been shifted +0.75 pH units, given by:

$$\phi = \pi(pH-3.75)/2.22$$

The positive shift of the Al affinity function has almost totally removed the liming paradox characteristic, and has further delayed the flushing point (by approx 5½ yrs). This is to be expected since the R_{tot} trajectory is the most continuous produced due to the large overlap between the Ca and Al affinity functions.

Since the acid loadings applied to the simulations of Figure 4.12 are identical, where the flushing point has been delayed it is observed that the flushing peak has also reduced, and vice-versa. This reflects the fact that flushing occurs at a lower pH and thus the Al affinity function will be closer to its maximum, therefore able to adsorb greater quantities of phosphate.

The discontinuities in the R_0 trajectories observed in Figures 4.12(a),(b),(d) and (g) may be attributed to a pH value close to the boundary of the Cation Exchange Buffer Range and the Calcium Carbonate Buffer Range; these discontinuities reflect the model switching between alternative calculations of the new pH across a number of temporal iterations.

However, the discontinuities observed in Figures 4.12(c),(e) and (f) reflect the adsorption affinities at a given pH. These discontinuities have arisen because the definition of the affinity functions for either Calcium or Aluminium are such that adsorption is not possible, or is negligible, over a small pH range.

It may be concluded, therefore, from Figure 4.12, that the default values used in Equations (2) and (4) highlight the key characteristics described above more clearly than any of the alternatives.

4.2.2 ACID BUFFERING

As with the phosphate adsorption equations, Figures 4.5(a) to (c) present the change in acid buffering rates, by both Calcium and Aluminium, in terms of the soil pH - which determines the relevant dissolution rates affecting the buffering processes - and the acid loading.

A change in the quantities of Calcium and Aluminium will have a linear effect upon the acid buffering capacity, ignoring the indirect influence upon pH of changing relative quantities of Calcium and Aluminium over time. For example, using Equation (7), buffering due to Calcium reserves may be shown as:

$$BR_{Ca} = 2\, K_{acid}\, k_{Ca}\, CaQ$$

where k_{Ca} is a constant, described earlier, and

$$K_{acid} = Ca_{diss}\, k_t$$

which is independent of the total Calcium reserves, CaQ.

A similar relationship may be found with the Aluminium reserves. Again, these representations in Figure 4.5 are static, requiring examination of the trajectories of the individual variables and rates over time (Figure 4.13).

As suggested by the equations describing these buffering dynamics, it can be observed in Figure 4.13 that at a high pH, buffering is predominately by Calcium

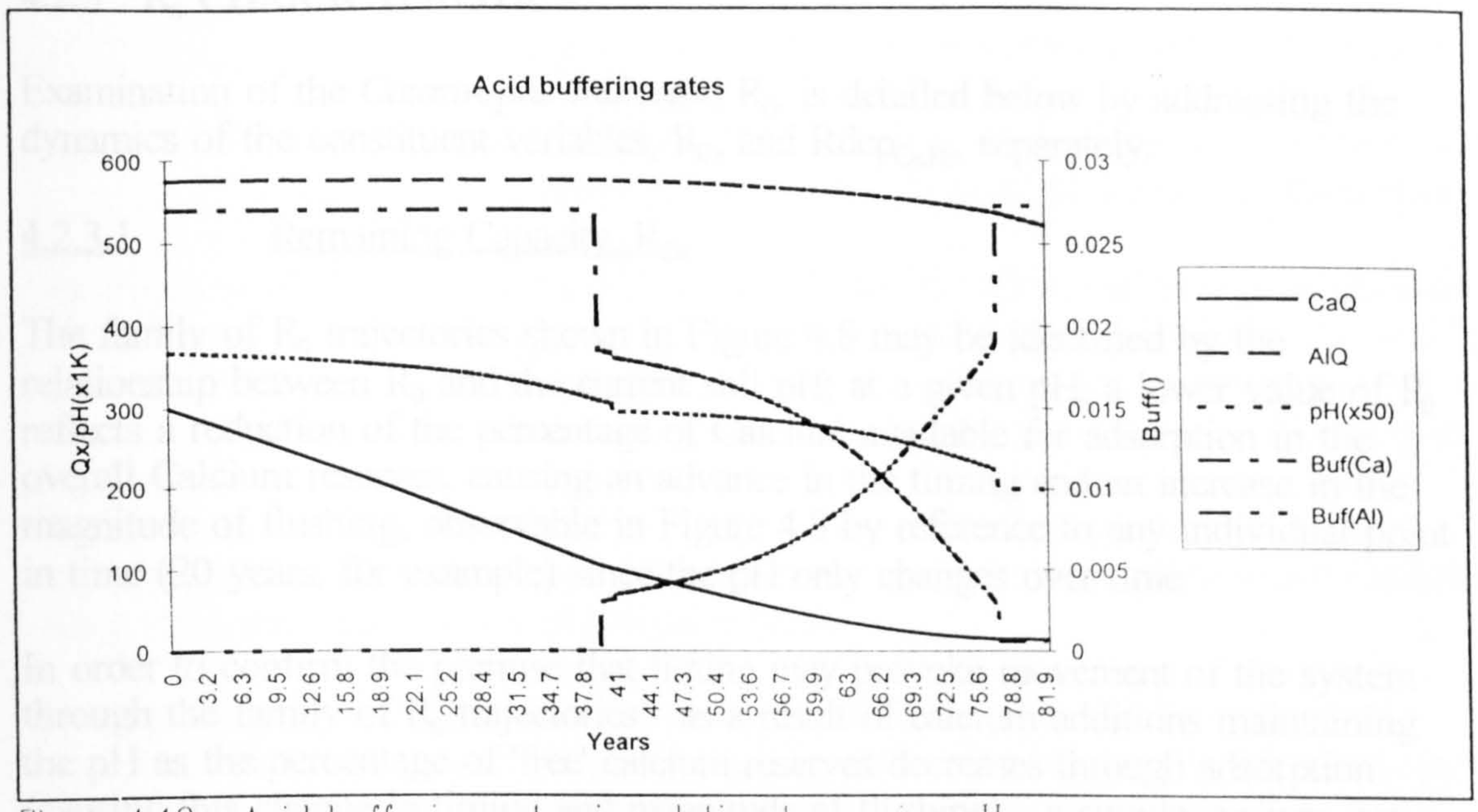

Figure4.13 – Acid buffering rates in relation to varying pH

(Base Cations), and at pH's ranging between approximately 4 and 6, buffering is split between Calcium and Aluminium, with Aluminium accounting for an increasing proportion of buffering as the pH falls. Finally, at a low pH (pH<4), buffering is primarily by Aluminium (Acid Cations) with the base cation reserves severely depleted.

4.2.2.1 Dissolution Rates

The dissolution rates of Calcium and Aluminium are also determined by pH. The dissolution rate defined for Aluminium will remain unaltered since at pH's low enough to result in acid cation buffering alone, the buffer rate has been found to be high enough to buffer very high levels of acid input [Ulrich 1983], above any level addressed by this model.

However, the dissolution rate of Calcium is implemented at two levels, depending upon pH and the ratio of K_1 to K_2 (see Equation (6)). These constants both default, in the model, to 0.5 (ie. 50:50). Simulations were also run with K_1:K_2 ratios of 1:3, 1:2, 1:1, 2:1 and 3:1. The observations suggested that except under extreme levels of acid loading - represented by the concentrations associated with the plateaux described by the static surface in Figure 4.5 - the ratio used has no influence upon both the qualitative and quantitative characteristics of the trajectories; all these simulation outputs were identical for the rates of acid loading used in the model and presented in Figure 4.13. Thus, the default ratio of 50:50 is maintained throughout further simulations.

4.2.3 R_0 CHARACTERISTICS

Examination of the *Catastrophe Indicator*, R_0, is detailed below by addressing the dynamics of the constituent variables, R_{Ca} and $Rdep_{Ca,Po}$, separately.

4.2.3.1 Remaining Capacity, R_{Ca}

The family of R_0 trajectories shown in Figure 4.8 may be identified by the relationship between R_0 and the current soil pH; at a given pH, a lower value of R_0 reflects a reduction of the percentage of Calcium available for adsorption in the overall Calcium reserves, causing an advance in the timing and an increase in the magnitude of flushing, observable in Figure 4.8 by reference to any individual point in time (20 years, for example) since the pH only changes over time.

In order to confirm the premise that liming may provoke movement of the system through the family of R_0 trajectories - as a result of calcium additions maintaining the pH as the percentage of 'free' calcium reserves decreases through adsorption (causing this change in timing and magnitude of flushing) - a simulation was run with controlled lime inputs.

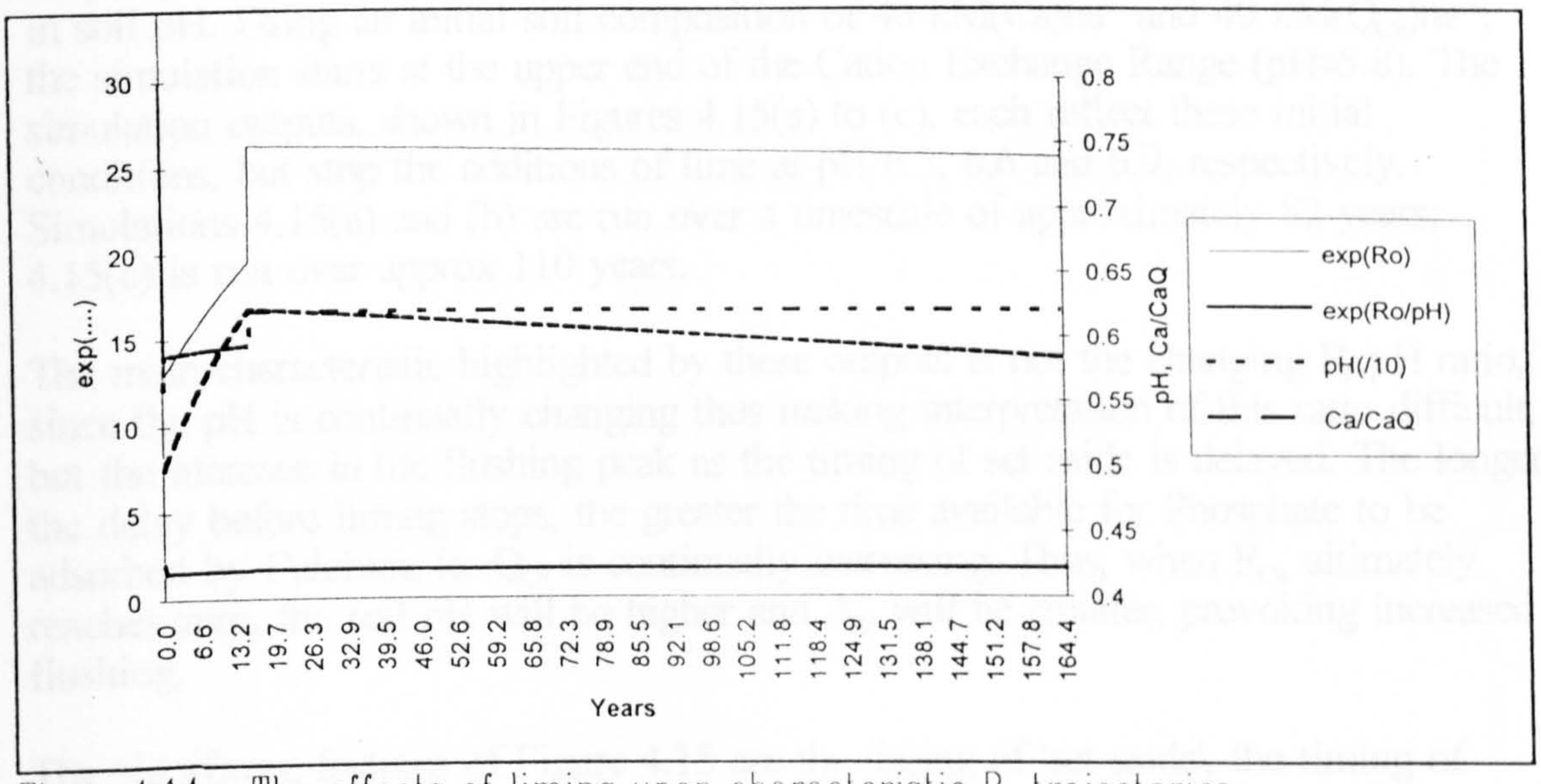

Figure4.14 – The effects of liming upon characteristic R_0 trajectories

The liming rate has been set to equal the acid loading, thus assuring a stabilised pH for conditions within the Carbonate Buffer range, and increasing the pH for conditions in the Cation Exchange range until the pH stabilises at approximately 6.2. In so doing, the following variables have been tracked over time, shown in Figure 4.14:

- Soil pH, remaining stable after approx. 13 years;
- Catastrophe Indicator, R_0, displaying its exponent so that the gradual change may be observed;
- Ca:CaQ ratio, describing the percentage of 'free' calcium reserves; and
- R_0:pH ratio to show the movement through the family of trajectories.

As Figure 4.14 shows, once the pH has stabilized (the additional liming cancelling the effects of the acid loading), it can be observed that both the Ca:CaQ ratio and R_0 gradually decrease over time due solely to the effects of phosphate adsorption. No change in R_0/pH is observable at the given scale, but since the pH is unchanging as R_0 decreases, the change to R_0/pH may be inferred. Thus, over time, the effect of liming would be to slowly shift the 'state' of the system through the family of R_0 trajectories, thus affecting both the timing and magnitude of potential future flushing since R_0 is decreasing as the pH remains static.

Having determined the potential for liming to force the potential for catastrophic phosphate flushing into the nearer future, it is useful also to examine the effect upon the actual timing and magnitude of flushing if these additions of lime are subsequently stopped - referred to below as 'set-aside'.

For these simulations, the liming rate has been set at a slightly greater rate (12 $kEqha^{-1}yr^{-1}$) than the acid loading (10 $kEqha^{-1}yr^{-1}$), thus provoking a gradual increase in soil pH. Using an initial soil composition of 40 $kM(Ca)ha^{-1}$ and 40 $kM(Q_{Ca})ha^{-1}$, the simulation starts at the upper end of the Cation Exchange Range (pH≈5.8). The simulation outputs, shown in Figures 4.15(a) to (c), each reflect these initial conditions, but stop the additions of lime at pH 6.3, 6.6 and 6.9, respectively. Simulations 4.15(a) and (b) are run over a timescale of approximately 82 years; 4.15(c) is run over approx 110 years.

The main characteristic highlighted by these outputs is not the changing R_0:pH ratio, since the pH is continually changing thus making interpretation of this ratio difficult, but the increase in the flushing peak as the timing of set-aside is delayed. The longer the delay before liming stops, the greater the time available for Phosphate to be adsorbed by Calcium; ie. Q_{Ca} is continually increasing. Thus, when R_{Ca} ultimately reaches zero, the soil pH will be higher and A_{Al} will be smaller, provoking increased flushing.

The significant features of Figure 4.15 are the timing of 'set-aside', the timing of catastrophe indicated by R_0, and the subsequent magnitude of the flushing peak. These features are highlighted below:

Figure 4.15:	(a)	(b)	(c)
Timing of 'Set-aside' (yrs)	15	38	72
Delay before catastrophe (yrs)	23	27	30
Timing of catastrophe (yrs)	38	65	102
Magnitude of catastrophe (kM/kl)	0.0018	0.002	0.0023

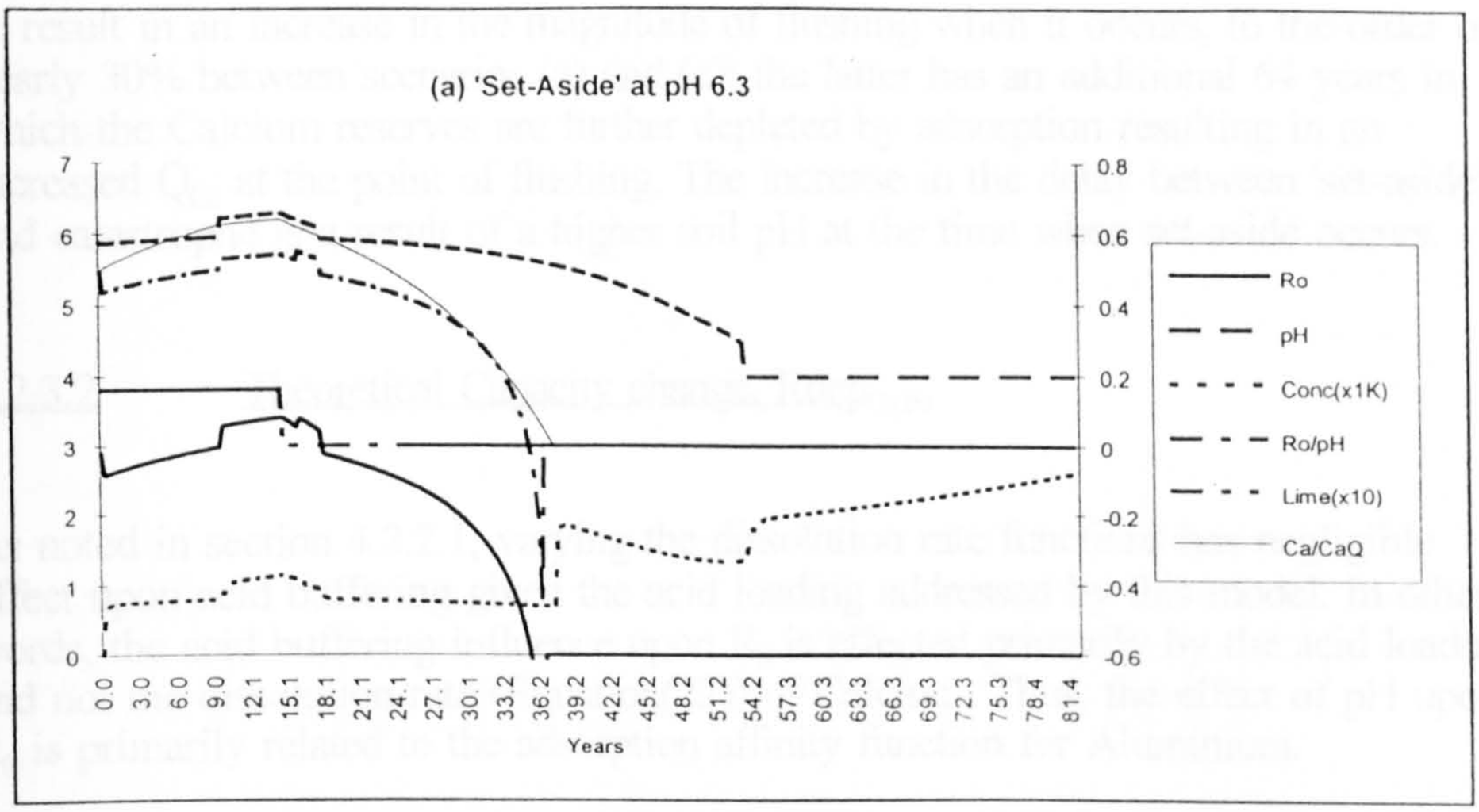

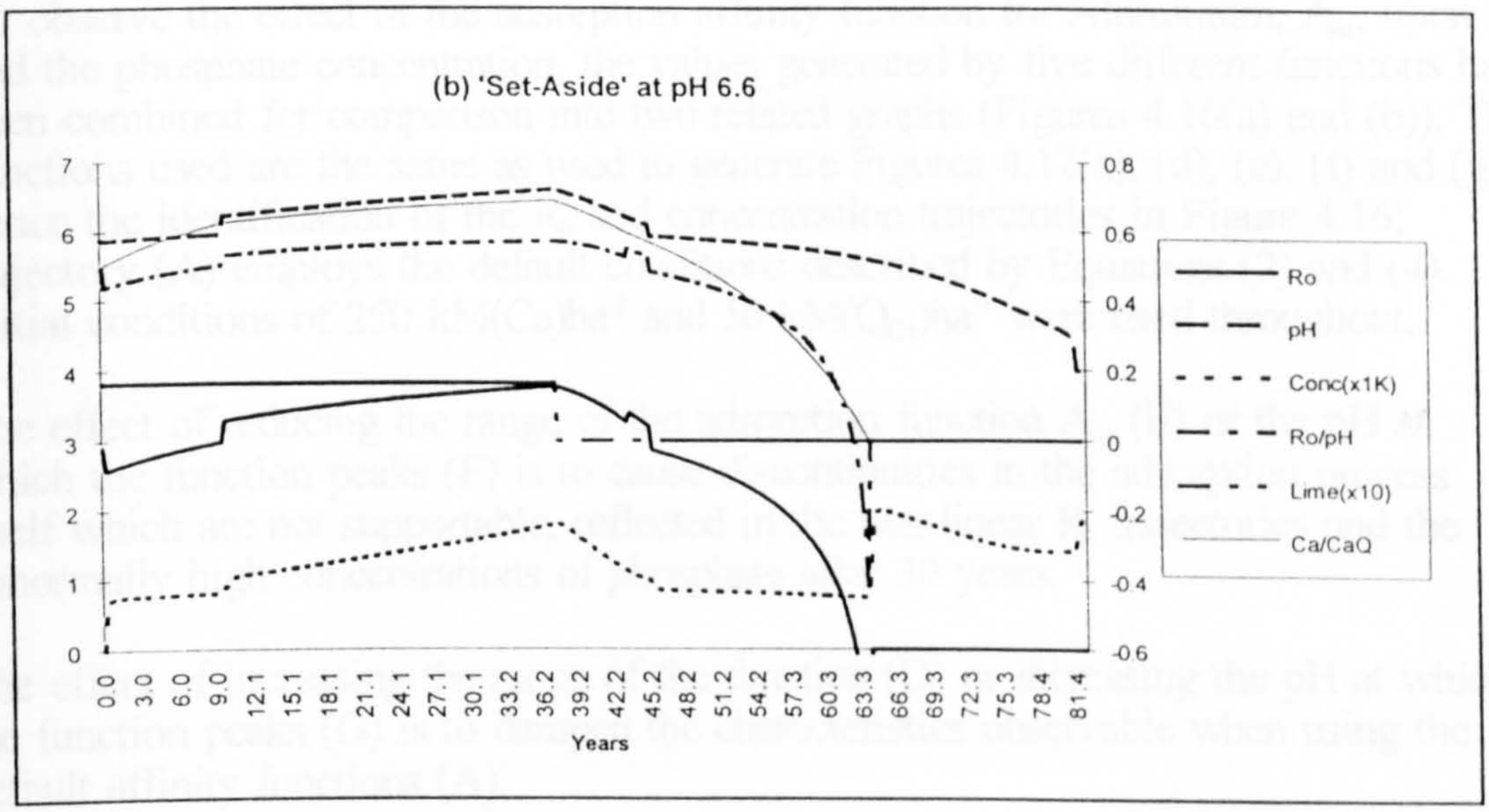

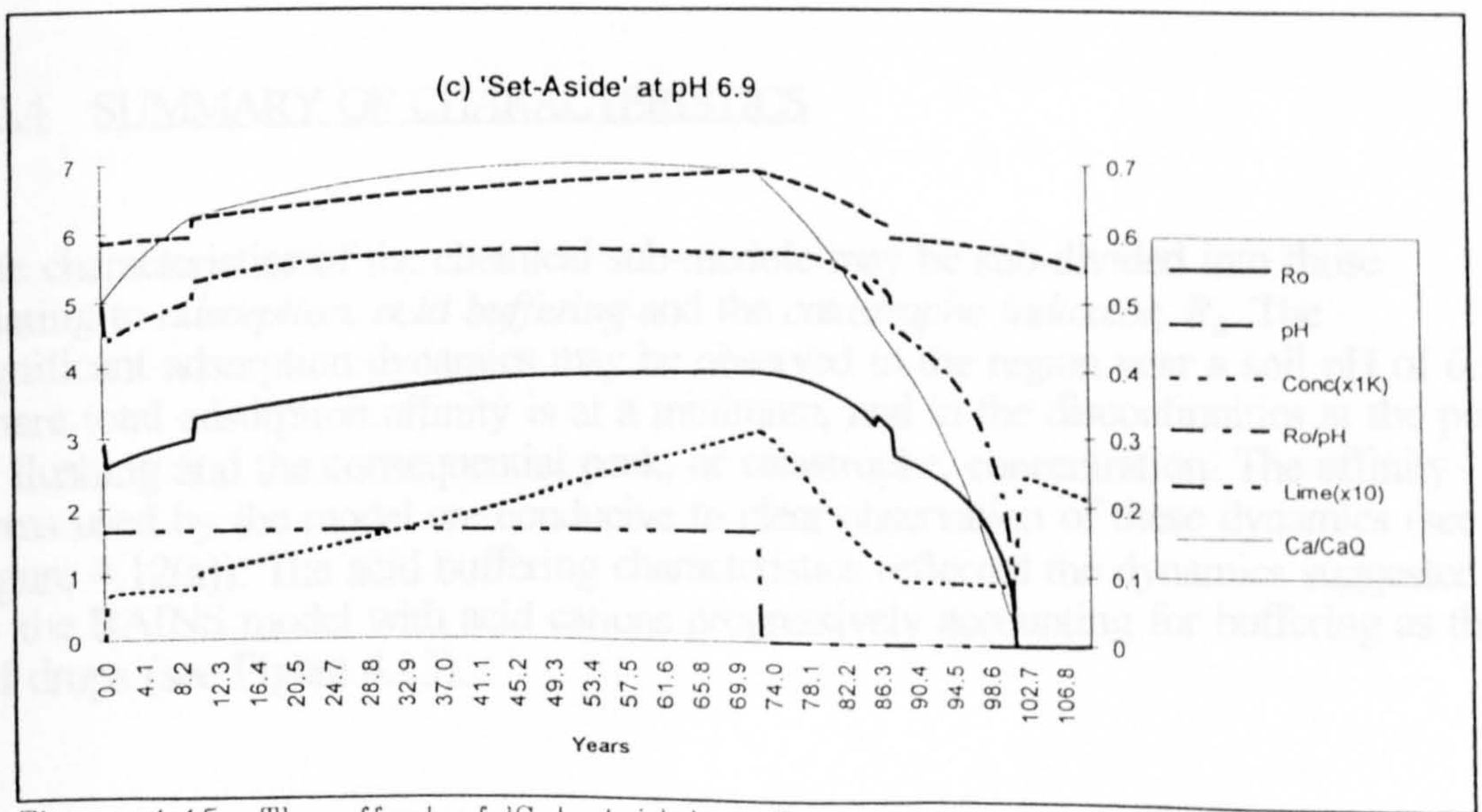

Figure 4.15 The effect of 'Set-Aside' on R_0

Thus, the effect of liming to maintain the soil pH for a number of years can be seen to result in an increase in the magnitude of flushing when it occurs, to the order of nearly 30% between scenarios (a) and (c); the latter has an additional 64 years in which the Calcium reserves are further depleted by adsorption resulting in an increased Q_{Ca} at the point of flushing. The increase in the delay between 'set-aside' and catastrophe is a result of a higher soil pH at the time when set-aside occurs.

4.2.3.2 Theoretical Capacity change, $Rdep_{Ca,Po}$

As noted in section 4.2.2.1, varying the dissolution rate functions has negligible effect upon acid buffering given the acid loading addressed by this model. In other words, the acid buffering influence upon R_0 is effected primarily by the acid loading and not the dissolution rate (Equation(22)) of Calcium. Thus, the effect of pH upon R_0 is primarily related to the adsorption affinity function for Aluminium.

To observe the effect of the adsorption affinity function for Aluminium, A_{Al}, upon R_0 and the phosphate concentration, the values generated by five different functions have been combined for comparison into two related graphs (Figures 4.16(a) and (b)). The functions used are the same as used to generate Figures 4.12(a), (d), (e), (f) and (g), hence the identification of the R_0 and concentration trajectories in Figure 4.16; trajectory (A) employs the default conditions described by Equations (2) and (4). Initial conditions of 250 kM(Ca)ha^{-1} and 50 kM(Q_{Ca})ha^{-1} were used throughout.

The effect of reducing the range of the adsorption function A_{Al} (E) or the pH at which the function peaks (F) is to cause discontinuities in the adsorption process itself which are not supportable, reflected in the non-linear R_0 trajectories and the abnormally high concentrations of phosphate after 30 years.

The effect of increasing the range of the function (D) or increasing the pH at which the function peaks (G) is to dampen the characteristics observable when using the default affinity functions (A).

4.2.4 SUMMARY OF CHARACTERISTICS

The characteristics of the chemical sub-module may be sub-divided into those relating to *adsorption, acid buffering* and the *catastrophe indicator, R_0*. The significant adsorption dynamics may be observed in the region near a soil pH of 6.5 where total adsorption affinity is at a minimum, and in the discontinuities at the point of flushing and the consequential peak, or catastrophe, concentration. The affinity terms used by the model are conducive to clear observation of these dynamics (see Figure 4.12(a)). The acid buffering characteristics reflected the dynamics suggested by the RAINS model with acid cations progressively accounting for buffering as the pH drops (see Figure 4.13).

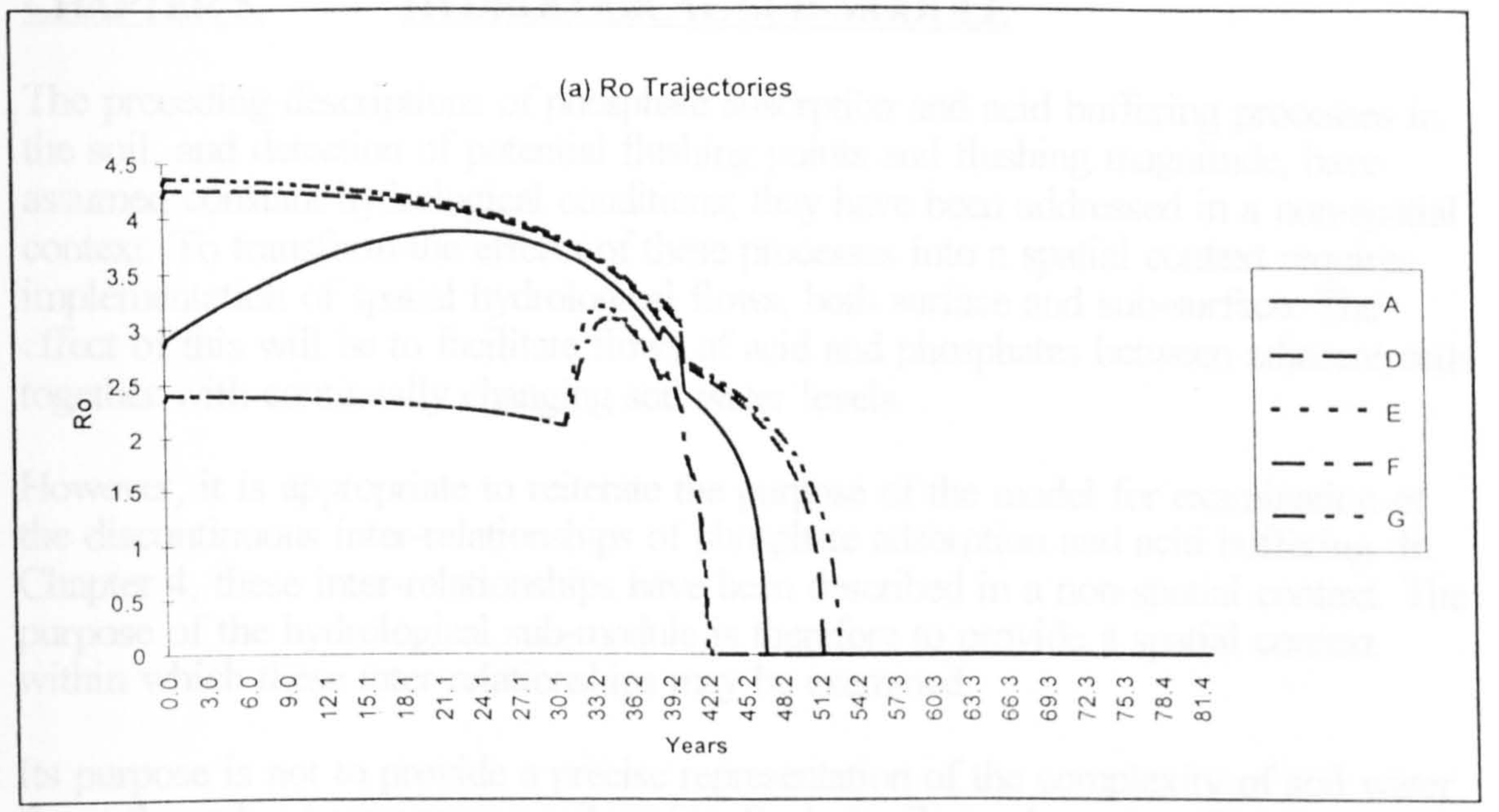

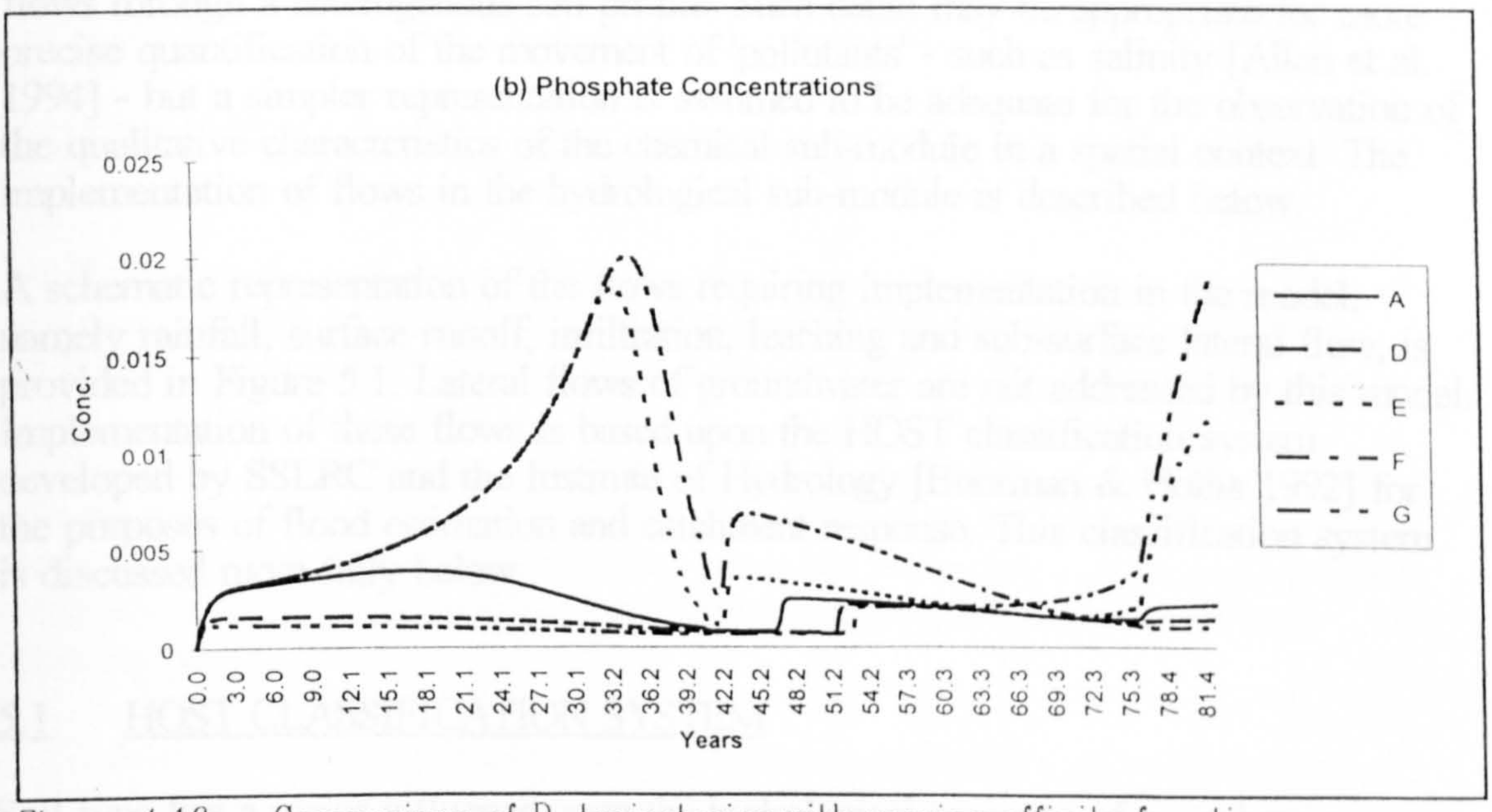

Figure 4.16 Comparison of R_0 trajectories with varying affinity functions

The significant characteristics of the catastrophe indicator, R_0, were displayed by typical temporal trajectories dependent upon the initial soil composition and conditions. These trajectories were shown to be individual trajectories in a continuous family of such trajectories. It was also observed that the effect of liming applications was to shift the actual trajectory within this family, with the result that unexpected delays and changes in the magnitude of catastrophe emerged in the *long-term* (see Figures 4.14 and 4.15).

CHAPTER 5. HYDROLOGICAL SUB-MODULE

The preceding descriptions of phosphate adsorption and acid buffering processes in the soil, and detection of potential flushing points and flushing magnitude, have assumed constant hydrological conditions; they have been addressed in a non-spatial context. To transform the effects of these processes into a spatial context requires implementation of spatial hydrological flows, both surface and sub-surface. The effect of this will be to facilitate flows of acid and phosphates between adjacent cells together with continually changing soil water levels.

However, it is appropriate to reiterate the purpose of the model for examination of the discontinuous inter-relationships of phosphate adsorption and acid buffering. In Chapter 4, these inter-relationships have been described in a non-spatial context. The purpose of the hydrological sub-module is therefore to provide a spatial context within which these inter-relationships may be examined.

Its purpose is not to provide a precise representation of the complexity of soil water flows through a heterogenous soil profile. Such detail may be appropriate for more precise quantification of the movement of 'pollutants' - such as salinity [Allen et al. 1994] - but a simpler representation is assumed to be adequate for the observation of the qualitative characteristics of the chemical sub-module in a spatial context. The implementation of flows in the hydrological sub-module is described below.

A schematic representation of the flows requiring implementation in the model, namely rainfall, surface runoff, infiltration, leaching and sub-surface lateral flow, is provided in Figure 5.1. Lateral flows of groundwater are not addressed by this model. Implementation of these flows is based upon the HOST classification system developed by SSLRC and the Institute of Hydrology [Boorman & Hollis 1992] for the purposes of flood estimation and catchment response. This classification system is discussed more fully below.

5.1 HOST CLASSIFICATION SYSTEM

Soil type has a major influence upon the hydrological response of a catchment [Boorman & Hollis 1992]. Thus, in order to estimate this response, it is useful to classify the soil types and derive aggregations of these influences.

One such classification is the Winter Rainfall Acceptance Potential (WRAP) used in the Flood Studies Report (FSR) [NERC 1975]. Although only five classes are defined and the WRAP system has limited resolution, it has been widely used in flood design studies. Values of Standard Percentage Runoff (SPR) - a daily average - are attached to each WRAP class, in the FSR report varying from 15% to 50%. However, there are potential problems in flood estimation where SPR may vary by a factor of 2 or 3 at the boundaries between classes. Finally, it should be noted that the WRAP system originated from theoretical consideration by hydrologists and soil scientists and not from analysis of hydrological data [Boorman & Hollis 1992].

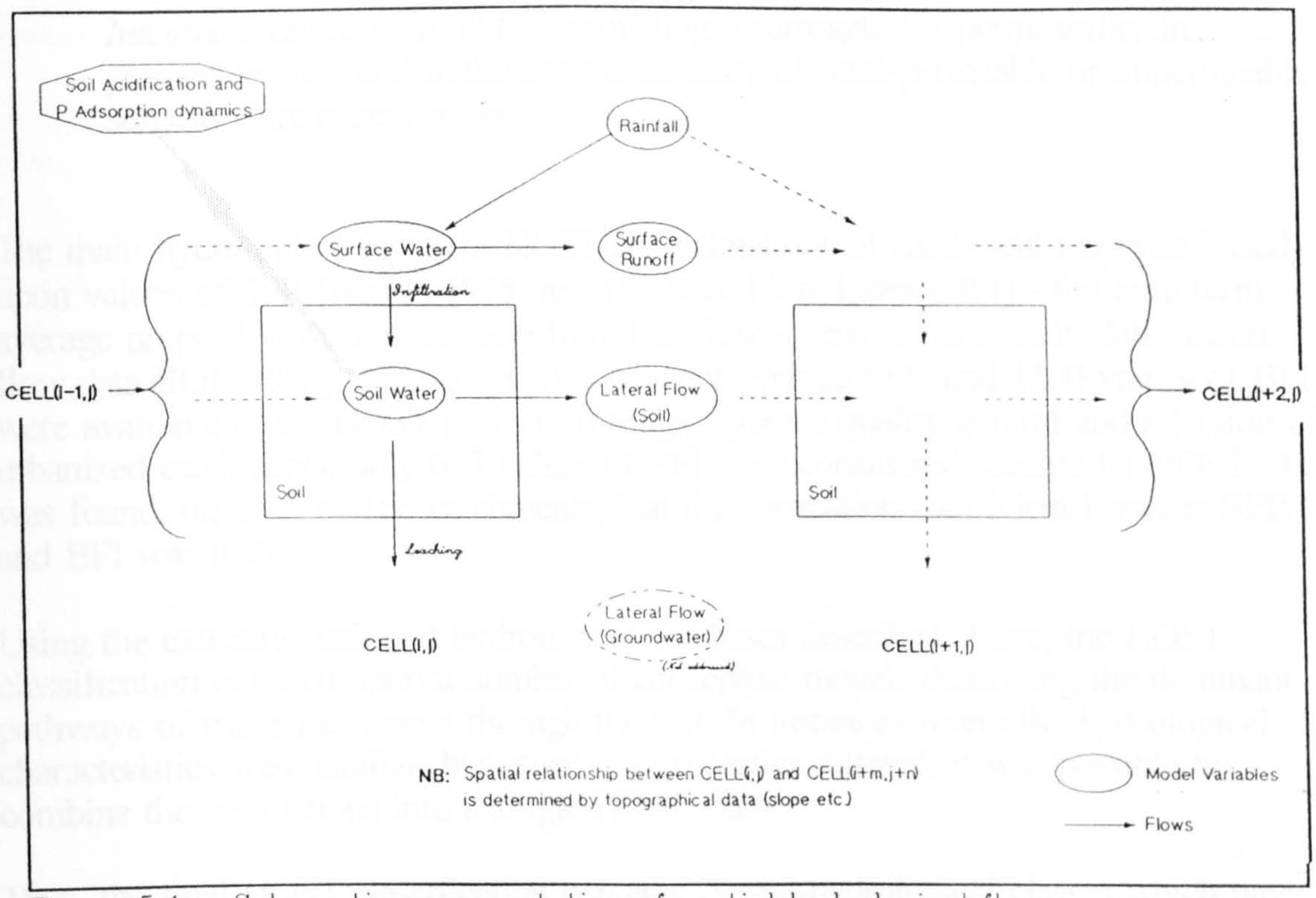

Figure 5.1 – Schematic representation of spatial hydrological flows

The Hydrology Of Soil Types (HOST) classifications overcome these limitations of resolution and lack of analysis against hydrological data through the use of the SSLRC soil maps and the hydrological databases held by the Institute of Hydrology.

The soil maps describe 295 soil associations, each comprising of a number of different soil series out of a total of 417. For each soil series, physical properties were calculated using a database holding measured values from approximately 4000 soil layers and 1000 soil profiles, thus providing aggregate definitions of the following properties:

- *Soil Hydrogeology*, differentiating between mechanisms of vertical water movement, and distinguishing between permeable, semi-permeable and impermeable substrates;

- *Depth to Aquifer/Groundwater*, indicating the time taken for excess water to reach the water table;

- *Presence of peaty topsoil*, potentially limiting infiltration and providing a lateral pathway for rapid response in the topsoils;

- *Depth to semi-permeable layer*, impeding the downward percolation of excess soil water;

- *Depth to gleyed layer*, caused by intermittent waterlogging;

- *Integrated air capacity (IAC)*, providing a surrogate for permeability in permeable soils and indicating the capacity of semi-permeable or impermeable soils to store excess water.

The main hydrological inputs to HOST are estimations of catchment response based upon values of SPR [NERC 1975] and the Base Flow Index (BFI) - the long term average proportion of flow coming from baseflow - derived using only daily mean flow data [IOH 1980]. 174 values of catchment average SPR and 1100 values of BFI were available to the HOST project. Through rigorous quality control and rejection of urbanized catchments, only 633 values of BFI were considered useable by HOST. It was found, on a set of 166 catchments, that the correlation coefficient between SPR and BFI was 0.75.

Using the extensive soil and hydrological databases described above, the HOST classification is based upon a number of conceptual models describing the dominant pathways of water movement through the soil. In instances where the hydrological characteristics were similar, but other soil properties differed, it was possible to combine these situations into a single HOST class.

Thus, the final HOST classification contains 29 soil-hydrological classes which have been found to explain *(sic)* over 80% of observed variations in BFI and 60% of observed variations in SPR. The corresponding figures for the WRAP scheme are 52% and 47%, respectively. These HOST classes are summarized in Table 5.1, reproduced from Boorman & Hollis (1992).

The current research has based the hydrological flows upon the values of SPR and Volumetric Moisture Content (VMC) associated with each HOST class identified in the study region (Rutland Water). Since these data are *preliminary* values, they are not published herein. However, the values derived from the aggregation of HOST classes in each cell in the study region are given in Table 6.1.

Thus, from these classifications, and given data for topography and rainfall, estimates can be made for surface runoff, retention of soil water, lateral flows within the soil and leaching. Surface runoff and sub-surface lateral flow are based upon SPR values associated with the HOST classes, and soil water retention upon VMC reflected by HOST. However, some modification to these values was considered appropriate for the current research, as described below.

5.1.1 MODIFICATIONS TO HOST CLASSIFICATIONS

The HOST classifications are based solely upon the soil type and underlying substrates, and their hydrological inter-relations. They do not account for the effects of surface vegetation, either type or amount or the effects of removal, nor do they account for the physical effects of land management practices such as ploughing.

MINERAL SOILS					PEAT SOILS	
GROUNDWATER OR AQUIFER	SOIL-HYDROGEOLOGY	No impermeable or gley layer with 100cm	Impermeable layer within 100cm but no gleying or Gleyed layer between 40 and 100cm	Depth to gleyed layer <40cm		
>10 m	Weakly consolidated, Microporous, By-pass flow uncommon	1 (6.44)	12 (0.95)	13 (0.61)	14 (9.85)	
	Weakly consolidated Macroporous By-pass flow common	2 (1.56)				
	Strongly consolidated Non or slightly porous By-pass flow common	3 (3.23)				
2 - 10 m	Unconsolidated Macroporous By-pass flow v. uncommon	4 (5.11)				
	Unconsolidated Microporous By-pass flow common	5 (7.28)				
<2 m	Unconsolidated Macroporous By-pass flow v. uncommon	6 (0.78)		Lateral Saturated Hydraulic Conductivity IAC≥12.5% >1m day^{-1}	Drained	Undrained
	Unconsolidated Microporous By-pass flow common	7 (1.51)		IAC<12.5% <1m day^{-1}	9 (2.74) / 8 (3.61)	10 (0.55) / 11 (0.19)
NO GROUNDWATER OR AQUIFER	Permeable	15 (4.64)	Soil water storage capacity IAC >7.5%: 17 (4.88) / IAC ≤7.5%: 20 (4.02)	23 (13.87)	26 (2.52)	
	Slowly permeable	16 (0.86)				
	Impermeable (hard)		18 (2.22) / 21 (1.12)	24 (0.02)	27 (0.87)	
	Impermeable (soft)		19 (0.69) / 22 (1.31)	25 (3.64)		
	Eroded peat				28 (0.59)	
	Raw peat				29 (8.37)	

Numbers outside brackets are HOST classes, numbers inside brackets are percentage of England, Wales and Scotland covered by class.

Table 5.1 – HOST Classifications (reproduced from Boorman & Hollis (1992))

For example, ploughing and harvesting may both have the effect of reducing the water retention ability of the soil; ploughing, through physical destruction of the soil structure, and harvesting indirectly through the removal of organic matter. On the other hand, permanent grassland or livestock pastures may have a positive influence upon the soil structure, thus potentially increasing water retention capability.

The current model will, therefore, modify the HOST classifications appropriately to reflect variations in the slope and the vegetation cover, thus affecting both the SPR values defined by HOST and the infiltration rates respectively.

SPR Modification

The Standard Percentage Runoff identifies the percentage of surface water at any given time which is expected to be 'lost' to adjacent watercourses - defined in the current model by the flow patterns in Figure 3.5 - in a single day; SPR reflects a daily rate of loss from a given cell in the model. However, this loss is the total lost through surface runoff and sub-surface lateral flow, in relation to the current level of surface water.

Since the HOST classification does not directly address the slope, but as a steep hillside would evidently result in a higher runoff potential than a flat valley bottom, although the difference in soil type would be reflected in the HOST classification and the associated SPR, the value of SPR will be modified for the current model to reflect the relative differences in slope found in the study area.

Thus, the model will generate a Modified SPR value, M_{spr}, as follows:

$$M_{spr} = SPR\ (1 + K_{spr})\ ,\ \text{for a relatively steep slope}$$

$$M_{spr} = SPR\ (1 - K_{spr})\ ,\ \text{for a relatively shallow or no slope}$$

$$M_{spr} = SPR\ ,\ \text{for all other slopes.}$$

where: K_{spr} is a constant, arbitrarily set to 0.25

These modifications are thus only relative in the context of the study area, but allow variability of flows dependent upon the topography of the area, whereas the HOST classification may only reflect this difference if the soil type and substrate were to reflect this change.

This modification could be enhanced by linking K_{spr} to detailed variations in the gradient of the slopes. However, for the purposes of this model, where examination of the qualitative nature of the catastrophe indicator is central, it is not necessary to impose this additional complexity on the model.

The units of M_{spr} are equivalent to those of SPR: percentage runoff per day.

Infiltration

As discussed above, infiltration is partially dependent upon the type of surface vegetation cover; for example, livestock pastures will facilitate a greater rate of infiltration than arable land. Similarly, the vegetation will affect the surface runoff potential, thus indirectly affecting the relative rates of surface runoff and sub-surface lateral flow as defined by M_{spr}.

In its present form, the model addresses three general types of surface vegetation cover; woodland and livestock pasture, non-livestock grassland, and arable land. The model deals with urban or water covered (lakes etc.) separately since surface water over such areas is assumed to runoff directly into the watercourses and not into the soil.

In order to distinguish these three types of vegetation, quantification of their effect upon infiltration has been arbitrarily defined so that non-livestock grassland is taken as an average, with arable land reducing infiltration and pasture or woodland increasing infiltration.

For this simple classification of vegetation cover, the percentage infiltration per day, μ, is given by:

$$\mu = 67\% \text{ , for pasture and woodland}$$

$$\mu = 33\% \text{ , for arable land}$$

$$\mu = 50\% \text{ , for non-livestock grassland}$$

This classification could easily be extended to address the type of livestock (cattle, sheep etc.), arable land (wheat, barley etc.) and other variations by calculating μ using a matrix of relationships between vegetation and farming practices, such as rotations of land-use. Again, it is not deemed necessary to impose this additional complexity on the model.

5.2 DESCRIPTION OF SUB-MODULE

The units imposed on the model, with regards the hydrological processes, are all scaled to reflect the spatial and temporal units employed in the adsorption and buffering equations. All state variables, such as soil water levels, are given in kilo-litres per hectare, and all rates are given in $klha^{-1}day^{-1}$. The modifying terms for runoff and infiltration, as described above, reflect unitless percentages per day.

5.2.1 FLOW EQUATIONS

Conceptualizing the flows as shown in Figure 5.1, there are five main flows which need to be addressed; additional inflows affecting surface and soil water must also be noted, but these simply reflect the runoff and lateral flows determined by conditions in an adjacent cell.

Firstly, the rainfall must be accounted for, which provides a direct input to surface water, W_{surf} (see Equation (36)). The rainfall reflects a manipulable input controlled by the catchment module and is derived from rainfall data on a daily basis.

As discussed above, the surface runoff *(Run)* and sub-surface lateral flow *(Lat)* is dependent upon the amount of surface water present. Thus, if there is surface water present, these flows are given by:

$$Run = (1 - \mu)\, M_{spr}\, W_{surf} \qquad ...(28)$$

$$Lat_{surf} = \mu\, M_{spr}\, W_{surf} \qquad ...(29)$$

where: W_{surf} is the amount of surface water present
Lat_{surf} is the lateral flow due to surface water.

Thus, with surface water present, we find that:

$$Run + Lat_{surf} = M_{spr}\, W_{surf}$$

which reflects the SPR characteristics as required by the HOST classifications, modified to account for the relative slope. However, if there is no surface water present, there will still be some sub-surface lateral flow due to the remaining soil water present. This flow can be partially defined by:

$$Lat_{soil} = \Phi\, W_{soil} \qquad ...(30)$$

where: $\Phi = W_{soil}/Cap_{soil} - RMC$

Cap_{soil} depends upon the Volumetric Moisture Content
RMC represents the Residual Moisture Content assumed throughout to be 10% of the total capacity

The term, Φ, is defined so that the rate of lateral flow decreases non-linearly from a maximum in saturated soil towards zero as the volume of soil water converges on its residual moisture content.

Thus, by combining equations (29) and (30), the sub-surface lateral flow, in relation to both surface water and soil water, may be given by:

$$Lat = \mu M_{spr} (W_{surf} + \Phi \varepsilon K_{lat} W_{soil}) \quad ...(31)$$

where: $\varepsilon = k / (k + W_{surf})$, where k is a constant

K_{lat} is a constant

The term, ε, has the effect of inhibiting soil water drainage if there is surface water present; Equation (30) does not apply while there is surface water present. K_{lat} is a constant, the purpose of which is to counteract the influence of μM_{spr} so that a smooth change over is facilitated between the influence of equation (29) and equation (30) upon lateral flow. The values of k (25) and K_{lat} (0.2) were determined experimentally.

Finally, infiltration from the surface *(Inf)* and leaching from the soil water *(Lea)* must be addressed. Infiltration of surface water can be defined by:

$$Inf = \mu W_{surf} \quad ...(32)$$

where: μ is a function of the vegetation cover.

Leaching from the soil water is related to infiltration inasmuch as leaching will not occur in a period of soil moisture deficit, and when it occurs, the soil will be near to saturation and leaching flow will therefore be controlled by the rate of infiltration from the surface. Thus, the rate of leaching may be given by:

$$Lea = \Gamma \mu W_{surf} \quad ...(33)$$

where: $\Gamma = ½ - {}^{1}/_{\pi} \, Tan^{-1}\phi_{\Gamma}$, $\phi_{\Gamma} = 247-(26W_{soil}/VMC)$

The controlling term, Γ, inhibits any leaching until the soil water has reached 95% capacity, above which we find that the leaching rate tends towards the infiltration rate, with these rates equal when the soil reaches saturation. The value of ϕ_{Γ} was derived experimentally to facilitate a smooth but very rapid change in Γ - thus allowing leaching flows - when the soil water reaches 95% capacity.

One further flow needs to be addressed, which is the potential upward flow from the soil water to the surface. This flow may occur when the soil has reached saturation by spatial flows from adjacent regions; with lateral flow and leaching already at their maxima, this excess water must flow somewhere, and the surface is the only option. In this sense, the model will effectively simulate springs or the water table reaching the surface. Since this upward flow is a consequence of soil water (W_{soil}) reaching saturation, it can only be determined in relation to the soil water level itself. Therefore, this upward flow is addressed as a part of the state variable changes below.

Calculation of outflows of phosphates and acid

As discussed above, the spatial flows of phosphates and acid are determined by both the quantities of each in a given cell and the hydrological flows out of that cell. It should be remembered that each individual cell is taken to be internally homogenous. However, given that water may have to flow between 1 and 5 km in 'reality' before entering an adjacent cell, and that the concentration of phosphate or acid across the cell will not be homogenous, an 'inhibition constant', k=0.25, has been included in the following equations in order to account for potentially reduced flows due to variable concentrations. The possibility of modification of k as a means of calibration of these flows against measured data is discussed in later chapters.

These flows may thus be described as follows:

$$\left.\begin{aligned} \text{Lateral Flow (P)} &= k\,(\text{Lat}/W_{soil})\,P = k\,\text{Lat}\,C \\ \text{Leaching Flow (P)} &= k\,(\text{Lea}/W_{soil})\,P = k\,\text{Lea}\,C \end{aligned}\right\} \quad ...(34)$$

Whichever representation of the flow is implemented will result in flows of phosphate in $kMha^{-1}day^{-1}$ to the adjacent model cell. Inflows represent outflows from another adjacent cell.

Similarly, spatial flows of acid may be described by, again in units of $kMha^{-1}day^{-1}$:

$$\left.\begin{aligned} \text{Lateral Flow (H)} &= k\,(\text{Lat}/W_{soil})\,H \\ \text{Leaching Flow (H)} &= k\,(\text{Lea}/W_{soil})\,H \end{aligned}\right\} \quad ...(35)$$

5.2.2 STATE VARIABLE CHANGES

There are two state variables affected by the hydrological flows; the surface water level and the soil water level. The relationships between the flows and these state variables are presented schematically in Figure 5.1. Changes in these state variables may be represented by:

$$W_{surf,t+1} = W_{surf,t} + (\text{SurfIn} + \text{Rain} - \text{Evap} - \text{Run} - \text{Inf} + \text{Upflow})\,dt \quad ...(36)$$

$$W_{soil,t+1} = W_{soil,t} + (\text{SoilIn} + \text{Inf} - \text{Lat} - \text{Lea} - \text{Uptake} - \text{Upflow})\,dt \quad ...(37)$$

where, SoilIn and SurfIn reflect spatial flows from adjacent areas,
and Evap and Uptake represent surface evaporation and plant uptake respectively.

From equation (37) it is possible to determine the upward flow, discussed in the preceding section, in relation to the soil water when the combined rates cause W_{soil} to exceed the capacity, Cap_{soil}. To counteract this, the upward flow, Upflow, is defined as:

$$Upflow = (W_{soil,t} - Cap_{soil})/dt + SoilIn + Inf - Lea - Lat - Uptake \qquad ...(38)$$

Thus, at soil saturation, where W_{soil} is equal to Cap_{soil} and leaching is equal to infiltration we find that, by substituting for Upflow, the following relationship is seen, whereby any variations in the spatial flows, both surface and sub-surface are reflected in the volume of surface water alone:

$$W_{surf,t+1} = W_{surf,t} + \{ \text{External Inputs - External Losses} \} dt \qquad ...(39)$$

Aside from the spatial input flows - representing spatial outflows from adjacent cells - the inputs to the surface water are determined primarily by the rainfall rate, implemented using rainfall measured in mm/day, converted to $klha^{-1}day^{-1}$. At saturation, Upflow (equation (38)) also represents an input to the surface water, W_{surf}. A term for evaporation has been included which would have the effect of reducing the overall volumes of water maintained by the model, but is ignored for the purposes of this model; this term would require implementation of temperature data in the model.

Flows between the surface water and the soil water are defined by the infiltration rates and the potential upward flow described above. Spatial outputs are determined by runoff and sub-surface lateral flow, for horizontal flows, and by leaching for vertical flows. The horizontal flows define spatial inflows for adjacent cells.

Finally, a term has been included for the uptake of water by plants which again would reduce the overall volumes of water present, but it is ignored since it would require detailed knowledge of the water requirements of a wide range of vegetative cover.

5.2.3 LOSSES TO RIVERS

As discussed above, the HOST classification system has been defined to describe the hydrological responses of entire catchments. It accounts for both surface and sub-surface flow and groundwater flow (baseflow). However, since the current model is not directed at the accumulation of river and groundwater flows - whereas the models of Whitehead (1990) and Billen (1992) are (see Chapter 2) - it is based upon the values of SPR associated with the HOST classes. Thus, lateral flows to rivers may be described using SPR, whereas leaching flows represent hydrological 'losses' to groundwater.

Once the lateral flows from the surface water and the soil water reach a river, the model no longer tracks the fate of these flows or the phosphates or acid that are associated with these flows. However, rivers will not be present in every cell in a catchment, meaning that spatial flows may have to cross adjacent cells before entering the river system, thus distorting the effects of SPR. Therefore, the flows described below are defined to account for the presence of, or lack of a river in any given cell in such a fashion that the modelled losses to rivers reflects the intended effect of SPR across the catchment as a whole.

The model addresses these losses by categorizing each cell to represent the type of river, if any, associated with that cell. Three categories are implemented:

1. No river present;
2. Feeders to main catchment rivers present; and
3. Main catchment rivers present.

Using this categorization, a proportion of the sub-surface lateral flow and of the surface runoff flow will remain within the model, the remainder entering the river system, depending upon the categories of the cell providing the source of the flow and of the target cell.

To reiterate the above comments, the SPR is an *average* daily loss to rivers which doesn't account for the distance to an 'available' river. In the real world, flows may enter the river almost instantly where catchment rivers are present, but may take a number of days where rivers are distant. Representation of the losses for each river category reflect this variability of timing. For example, no losses are possible if the target cell does not contain a river (Type 1), whereas the majority of surface water would be expected to be lost if the target cell contains a catchment river (Type 3); the losses occurring at the boundaries between adjacent cells.

Thus, the proportions of surface and soil water remaining within the model (ie. not lost to rivers) are given by:

Soil Water flow

$$\text{Inflow}_{target} = \begin{cases} \text{Outflow}_{source} & \text{(if Target = Type 1)} \\ 0.75\ \text{Outflow}_{source} & \text{(if Target = Type 2)} \\ 0.5\ \text{Outflow}_{source} & \text{(if Target = Type 3)} \end{cases} \quad \ldots(40)$$

Surface Water flow

$$\text{Inflow}_{target} = \begin{cases} \text{Outflow}_{source} & \text{(if Target = Type 1)} \\ 0.5\ \text{Outflow}_{source} & \text{(if Target = Type 2)} \end{cases} \quad \ldots(41)$$

and, for surface flows into a target cell of type 3:

$$\text{Inflow}_{type3} = \begin{cases} 0.5\ \text{Outflow}_{source} & \text{(if Source = Type 1)} \\ 0.25\ \text{Outflow}_{source} & \text{(if Source = Type 2)} \\ \text{Zero} & \text{(if Source = Type 3)} \end{cases} \quad \ldots(42)$$

The constants used in equations (40) to (42) to modify the flows have been derived experimentally so that the effect of reduced losses in category 1 cells and the increased losses in category 3 cells (relative to category 2 cells) combine to reflect the average loss prescribed by the SPR. It is shown in the following section that this is indeed the effect of these constants.

The flows described by equations (40) to (42) are represented schematically in Figure 5.2, below. The percentages shown reflect the percentage retained by the model, not the percentage lost. In most cases, the loss to rivers is controlled solely by the target cell categorization. However, in the case of surface water loss to a catchment river cell (Type 3), it was deemed appropriate to also refer to the categorization of the source cell.

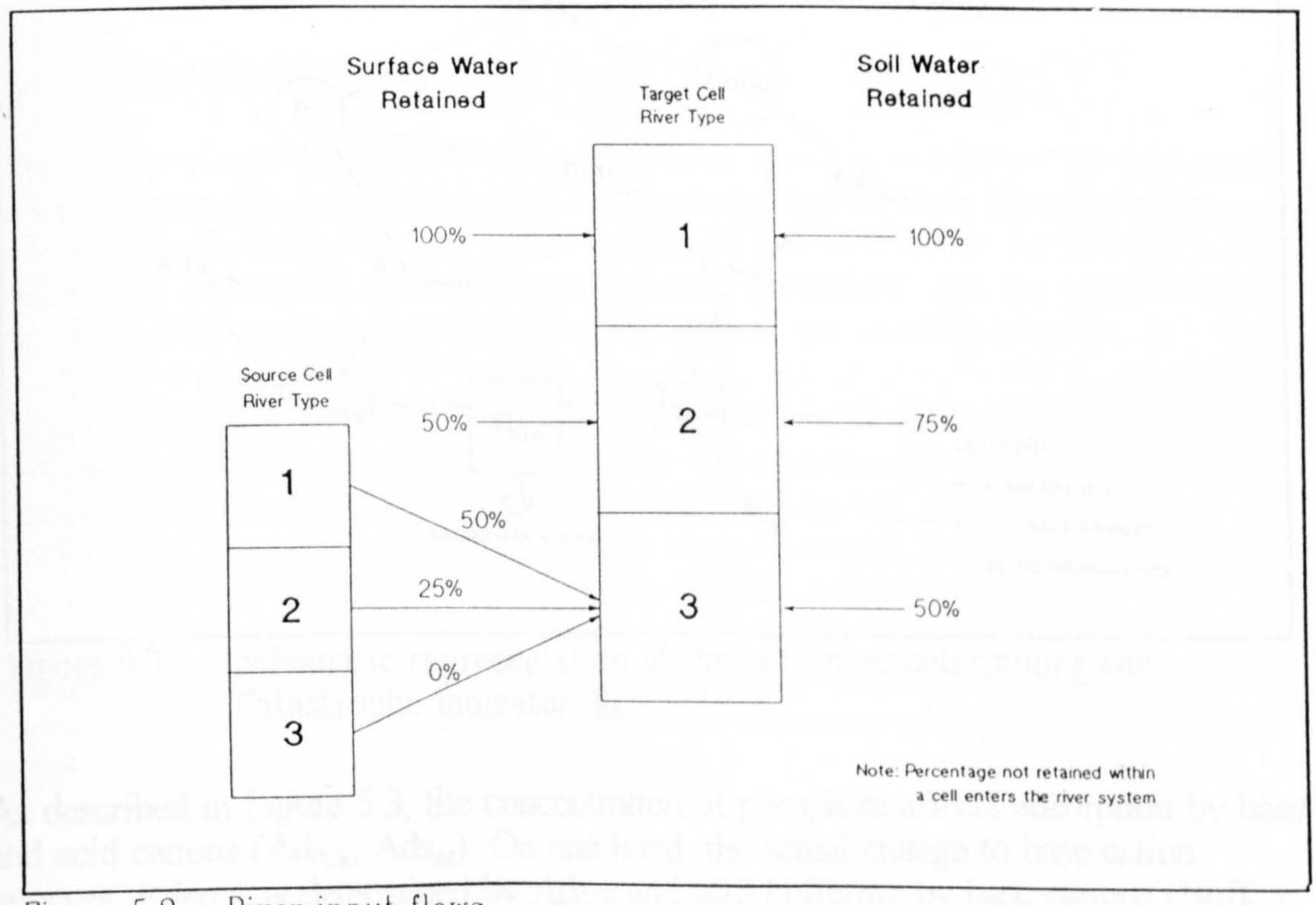

Figure 5.2 - River input flows

As with hydrological flows and phosphate and acid flows from cell to cell, the proportions of flows of phosphate and acid into the river system are determined in a similar fashion to above.

The fate of leaching flows, and associated phosphate and acid are not addressed by the model. Thus the leaching flows will not affect the simulated flows of water, phosphate and acid into the river system; a further groundwater flow model would be required to address these.

5.3 CHARACTERISTICS OF SUB-MODULE

In Chapter 4 a catastrophe indicator has been defined and the characteristic trajectories of this indicator have been examined over time. However, this indicator, R_0, is fundamentally non-spatial, using processual information derived from non-spatial variables and dynamics. The actual and theoretical constituents of R_0 are presented in Figure 5.3; in the non-spatial context, the concentration of Phosphate in solution is unaffected by hydrological flows.

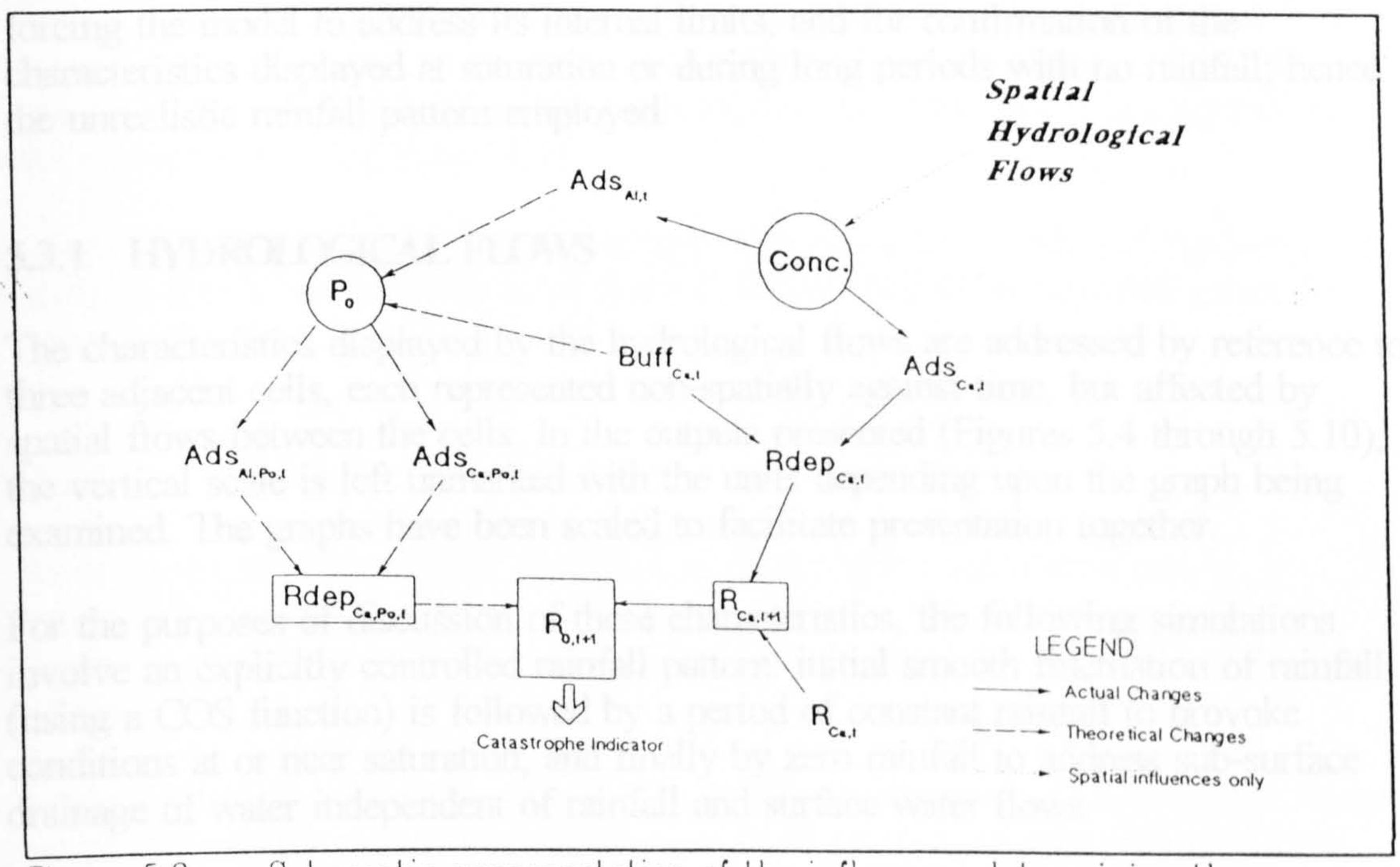

Figure 5.3 – Schematic representation of the influences determining the Catastrophe Indicator, R_0

As described in Figure 5.3, the concentration of phosphate affects adsorption by base and acid cations (Ads_{Ca}, Ads_{Al}). On one hand, the actual change to base cation reserves, $Rdep_{Ca}$, is determined by Ads_{Ca} and acid buffering by base cations ($Buff_{Ca}$); thus $R_{Ca,t+1}$ can be calculated. On the other hand, the catastrophe potential, P_0, is derived from Ads_{Al} and $Buff_{Ca}$. From P_0, theoretical adsorption rates ($Ads_{Ca,Po}$, $Ads_{Al,Po}$) can be determined, providing a definition of the theoretical change in capacity, $Rdep_{Ca,Po}$. Thus a value for $R_{0,t+1}$ emerges.

By introducing a spatial grid, inter-related by spatial hydrological flows and thus flows of acid and phosphates between adjacent cells, R_0 may be perceived as an indicator of relative sensitivity or resilience to catastrophe over the spatial grid. The constituents of R_0 are unchanged, but the concentration of phosphate is influenced by these spatial flows.

Representation of R_0 over such a spatial grid requires conceptualization of a 3-dimensional surface reflecting the grid across two dimensions (X and Y), and R_0 in the third dimension (Z), as discussed in Chapter 3. In this form, the representation becomes static with regard to time; it is the qualitative changes in this surface over time which will suggest the relative resilience and/or sensitivity to catastrophe of any point on the surface. For the purposes of representation in this research, snapshots of this surface at specific time intervals are used to discuss the emergent qualitative characteristics.

However, before such simulations of R_0 in a spatial context are presented - see Chapter 6 - it is necessary to confirm that the implementation of the flows described in the preceding section is consistent with the definition of the equations. Thus, the simulations presented below are for computational purposes with the intention of forcing the model to address its internal limits, and for confirmation of the characteristics displayed at saturation or during long periods with no rainfall; hence the unrealistic rainfall pattern employed.

5.3.1 HYDROLOGICAL FLOWS

The characteristics displayed by the hydrological flows are addressed by reference to three adjacent cells, each represented non-spatially against time, but affected by spatial flows between the cells. In the outputs presented (Figures 5.4 through 5.10), the vertical scale is left unmarked with the units depending upon the graph being examined. The graphs have been scaled to facilitate presentation together.

For the purposes of discussion of these characteristics, the following simulations involve an explicitly controlled rainfall pattern: initial smooth fluctuation of rainfall (using a COS function) is followed by a period of constant rainfall to provoke conditions at or near saturation, and finally by zero rainfall to address sub-surface drainage of water independent of rainfall and surface water flows.

Finally, an equivalent simulation is presented - which uses a real rainfall pattern - for the purposes of completion and to highlight the necessary use of a controlled rainfall pattern to observe the dynamics (Figure 5.10).

5.3.1.1 Baseline Characteristics

Figure 5.4 shows the dynamics of water flows given consistent conditions of Standard Percentage Runoff (SPR) and Volumetric Moisture Content (VMC) across the cells, with no river system present. The direction of the spatial flows are from

cell (a), through cell (b), to cell (c). The output shows the changes to both state variables (Surface Water & Soil Water) and all the flow rates described in Figure 5.1. This simulation provides a baseline against which the subsequent simulations may be compared.

The most apparent characteristic of these outputs is the close relationship of the hydrological dynamics with the rainfall rate; the only input aside from internal lateral flows.

As would be expected from Equations (28), (32) and (36), Figure 5.4(a) shows the surface water, the runoff and the infiltration dynamics qualitatively similar to the rainfall dynamics. However, Figures 5.4(b) and (c) show that with lateral inputs also affecting the dynamics, the dynamics increasing in magnitude by approximately 30% in (b) and a further 5% in (c).

Lateral flow, leaching and the volume of soil water are only partially dependent upon rainfall (Equations (31), (33) and (37)), reflected in the temporal delays in relation to rainfall shown throughout Figure 5.4; the delays in soil water and lateral flow observable in the shift in peaks and troughs, and leaching only evident at saturation. They are also partially dependent upon the volume of soil water itself: lateral flow through independent soil water drainage (Equation (30)) - observable when rainfall stops (0.71 yrs) - and leaching flow requiring soil water saturation in conjunction with surface water (Equation (33)).

Figure 5.4 highlights these temporal delays in response to rainfall and the increased saturation levels and magnitudes of flows in (b) and (c); to be expected given the accumulative effect and direction of flow.

5.3.1.2 Infiltration Rate changes

The effect on the hydrological dynamics of changing the infiltration rate, μ, is presented in Figure 5.5. Figures 5.5(a) to (c) show the effects of decreasing the infiltration percentage to 33%, and Figures (d) to (f) show the effects of an increase to 66%.

A reduction of the infiltration rate is seen to effect a direct increase in surface water present and surface runoff, in comparison with Figure 5.4, of approximately 25%; this may be expected to cause an increase in the leaching rate at soil saturation since the magnitude of leaching is directly affected by the surface water, but this effect is counteracted by the reduced infiltration rate itself. Such a reduction of the infiltration rate also causes a decrease in sub-surface lateral flow. Of most interest is the consequent decrease in the magnitude of the fluctuations - by approx 25% - of soil water levels in relation to the baseline (Figure 5.4), seen in all three cells.

A similar increase of the infiltration rate has precisely the opposite effect; a reduction in surface water and runoff, an increase in lateral flow and soil water fluctuations - all to the order of 25% - and leaching again behaving counterintuitively.

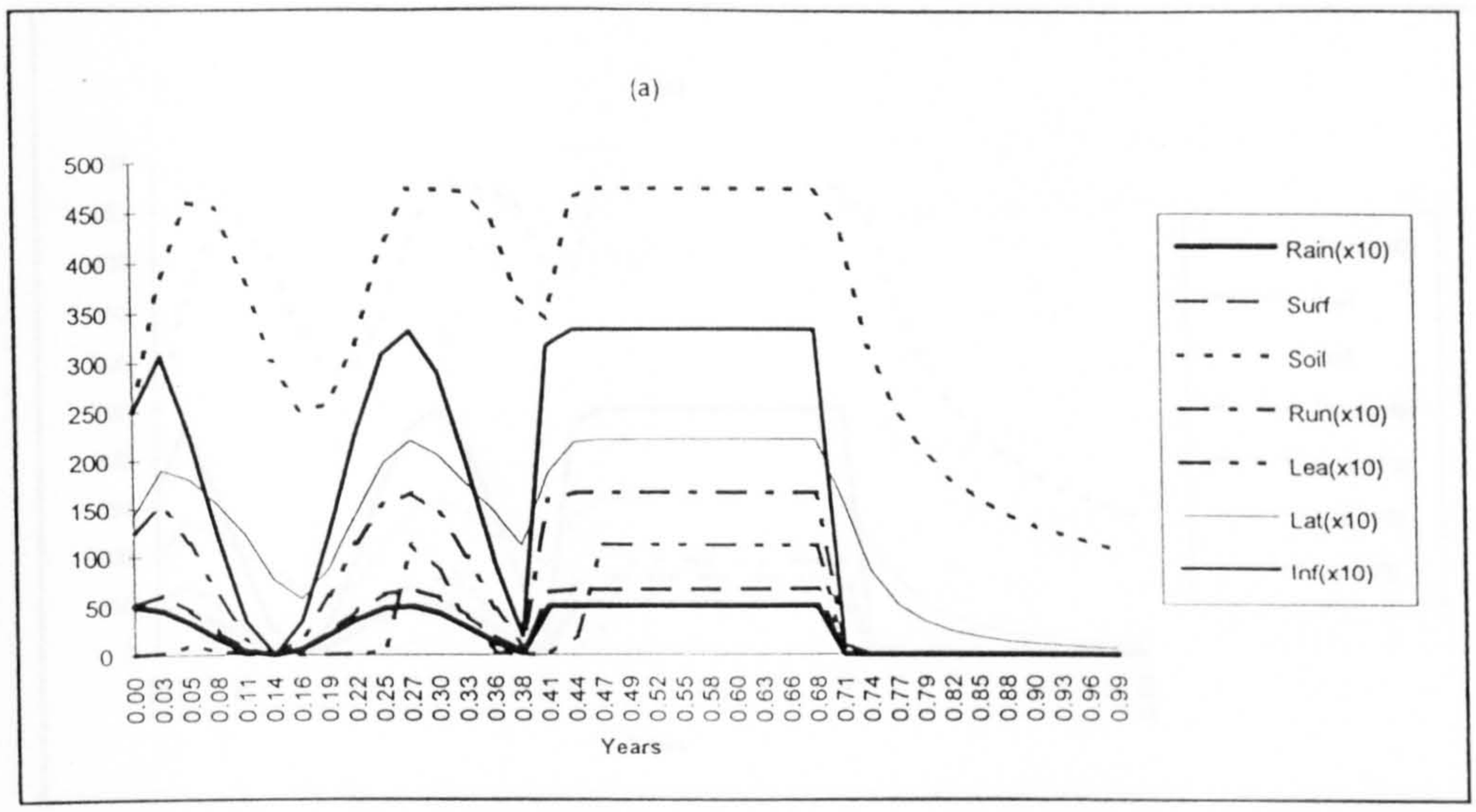

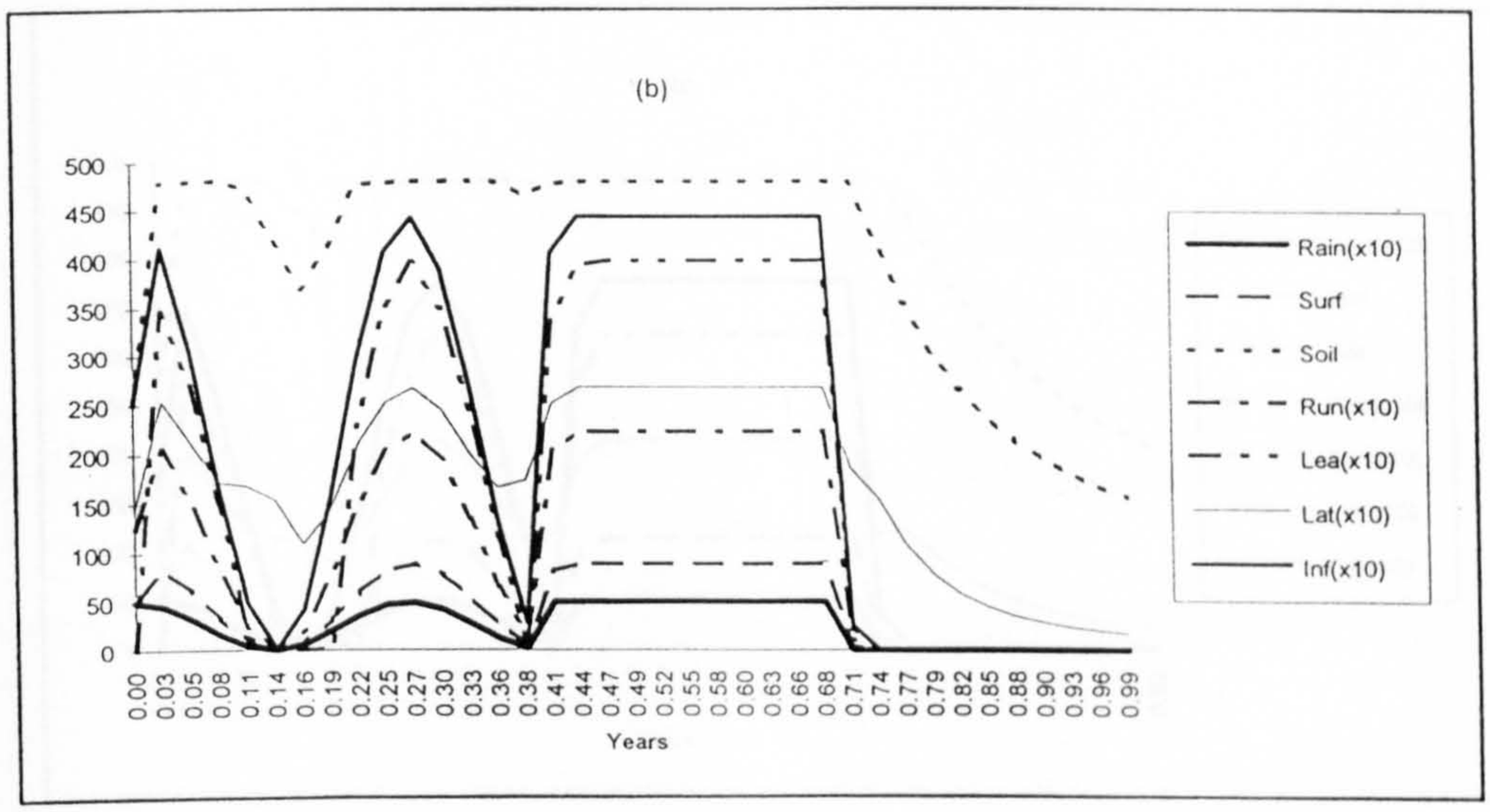

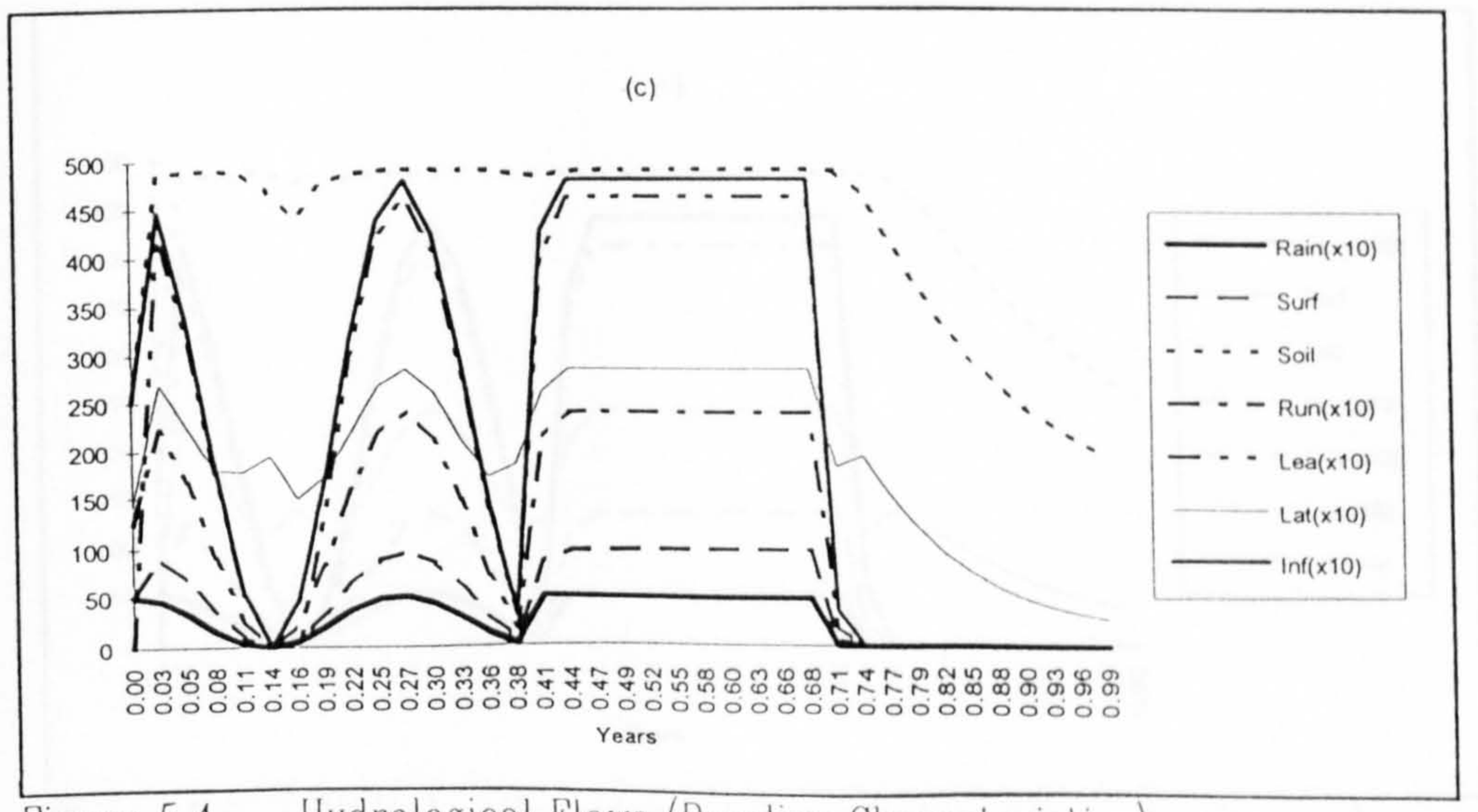

Figure 5.4 - Hydrological Flows (Baseline Characteristics)

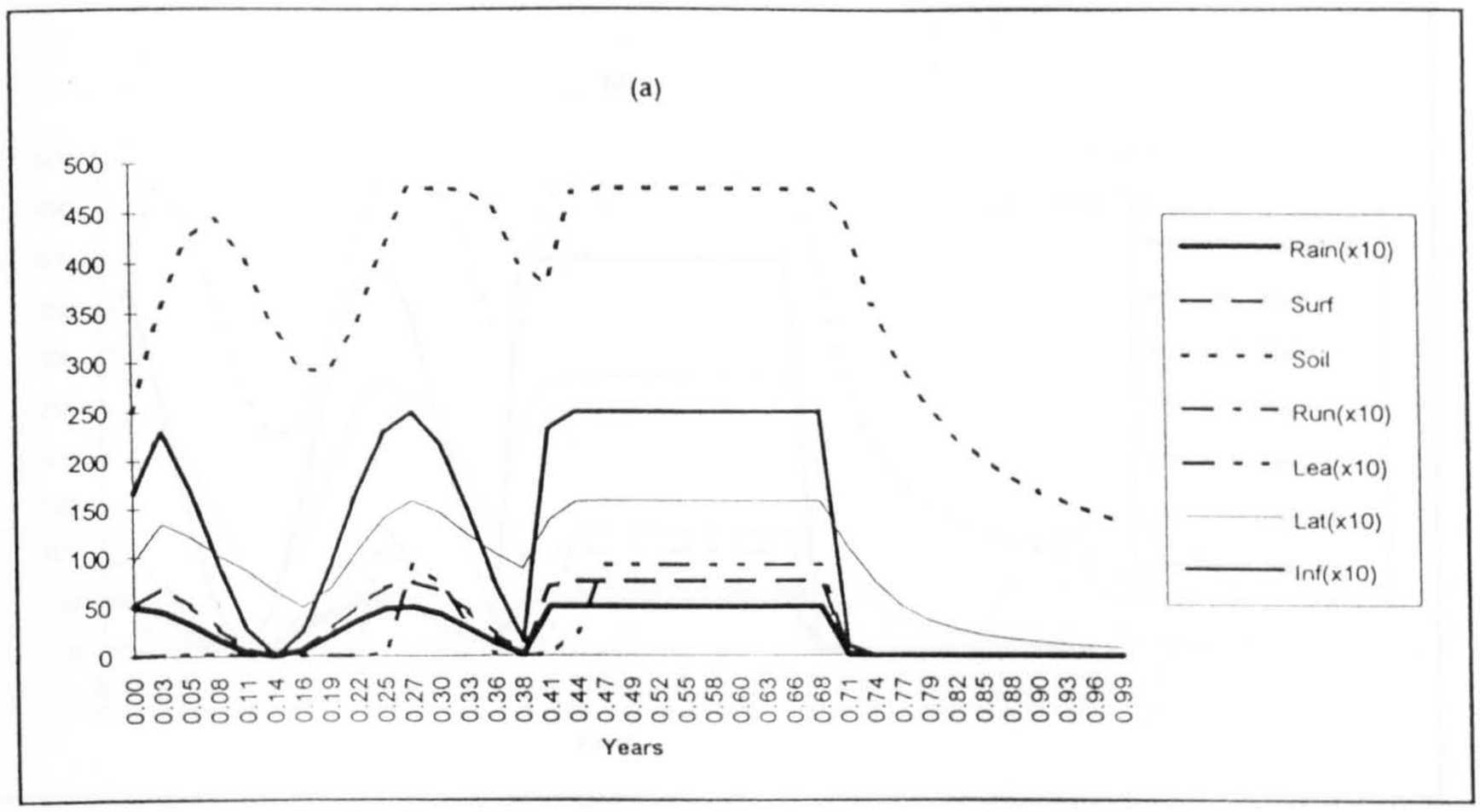

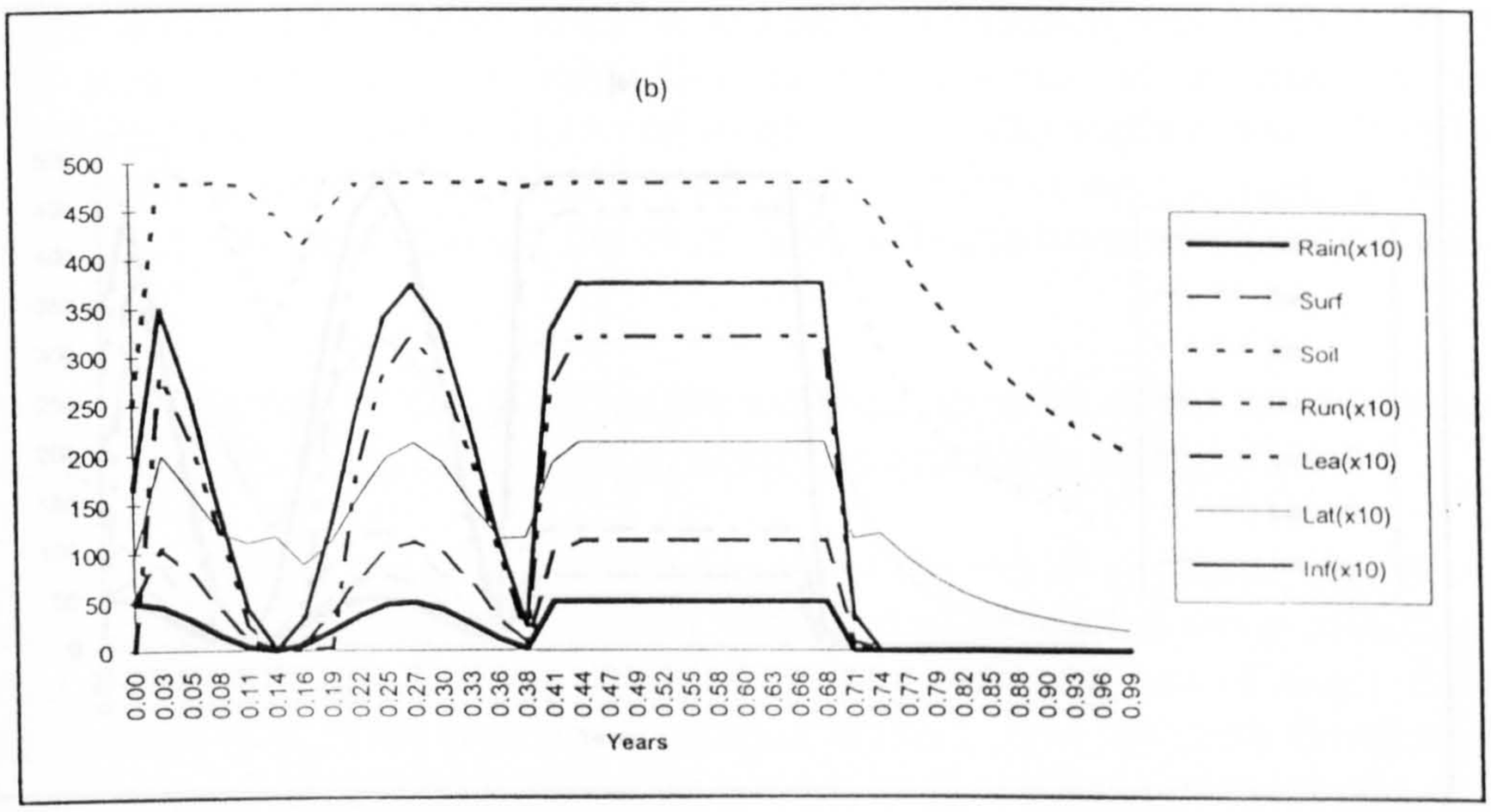

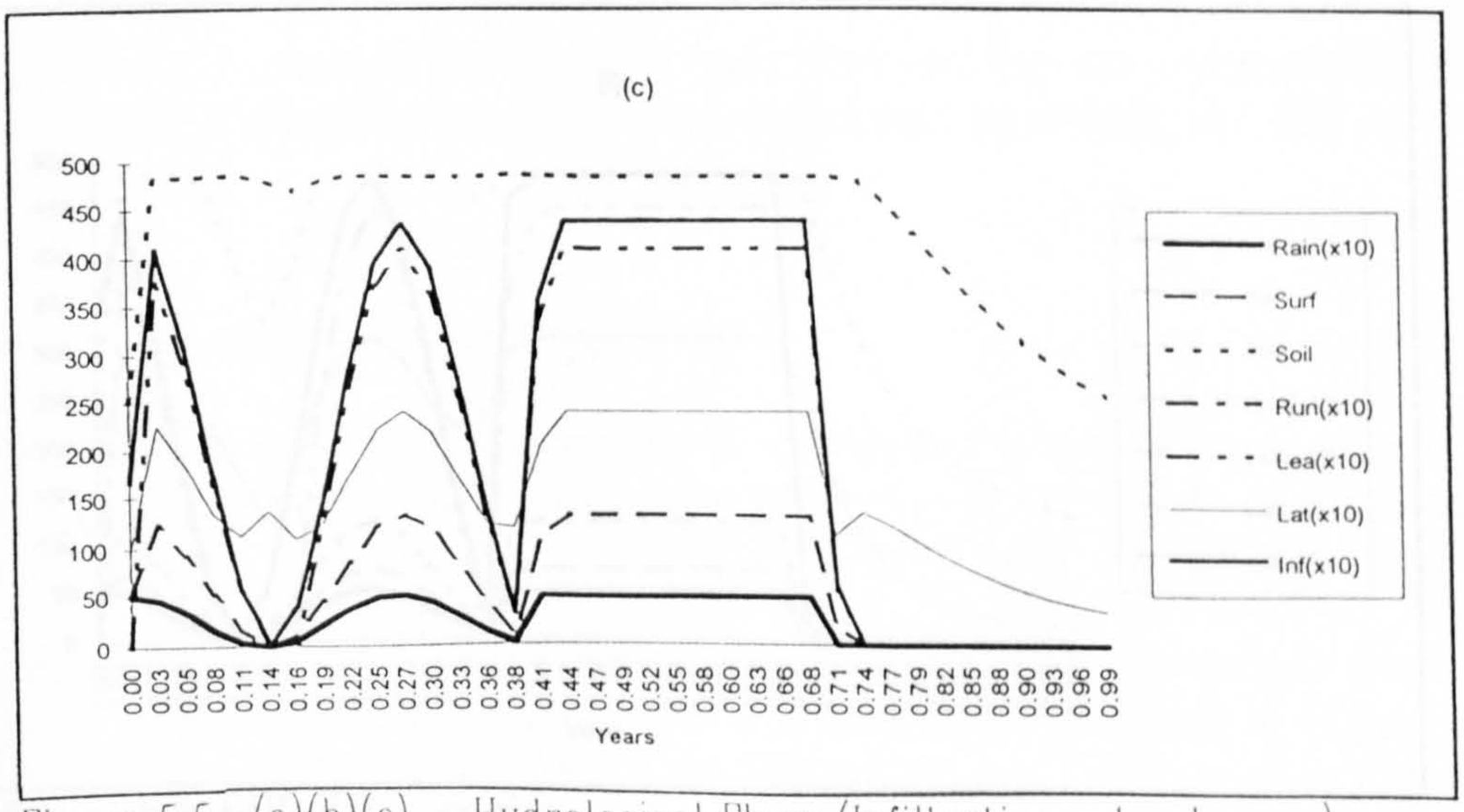

Figure 5.5 (a)(b)(c) – Hydrological Flows (Infiltration rate changes)

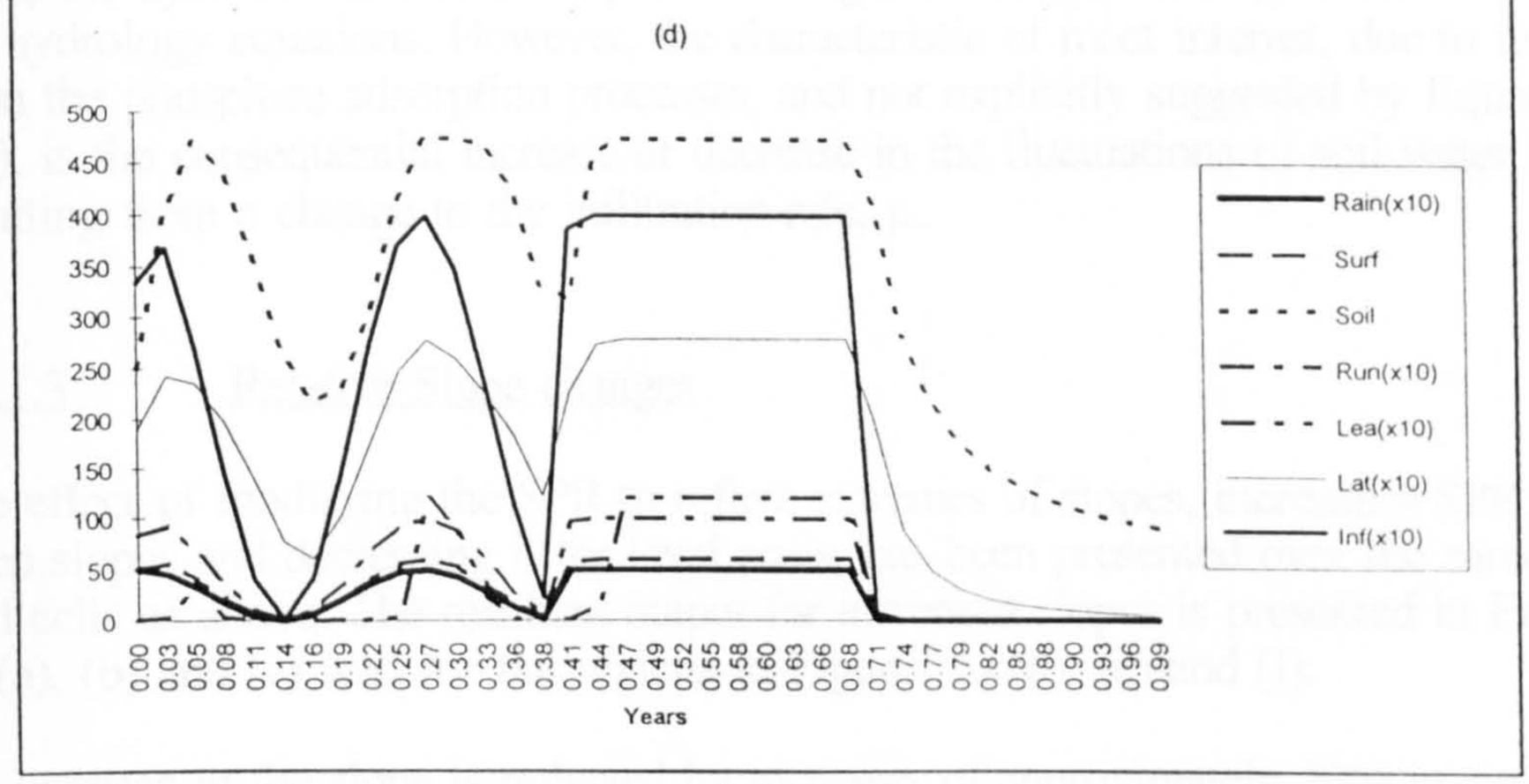

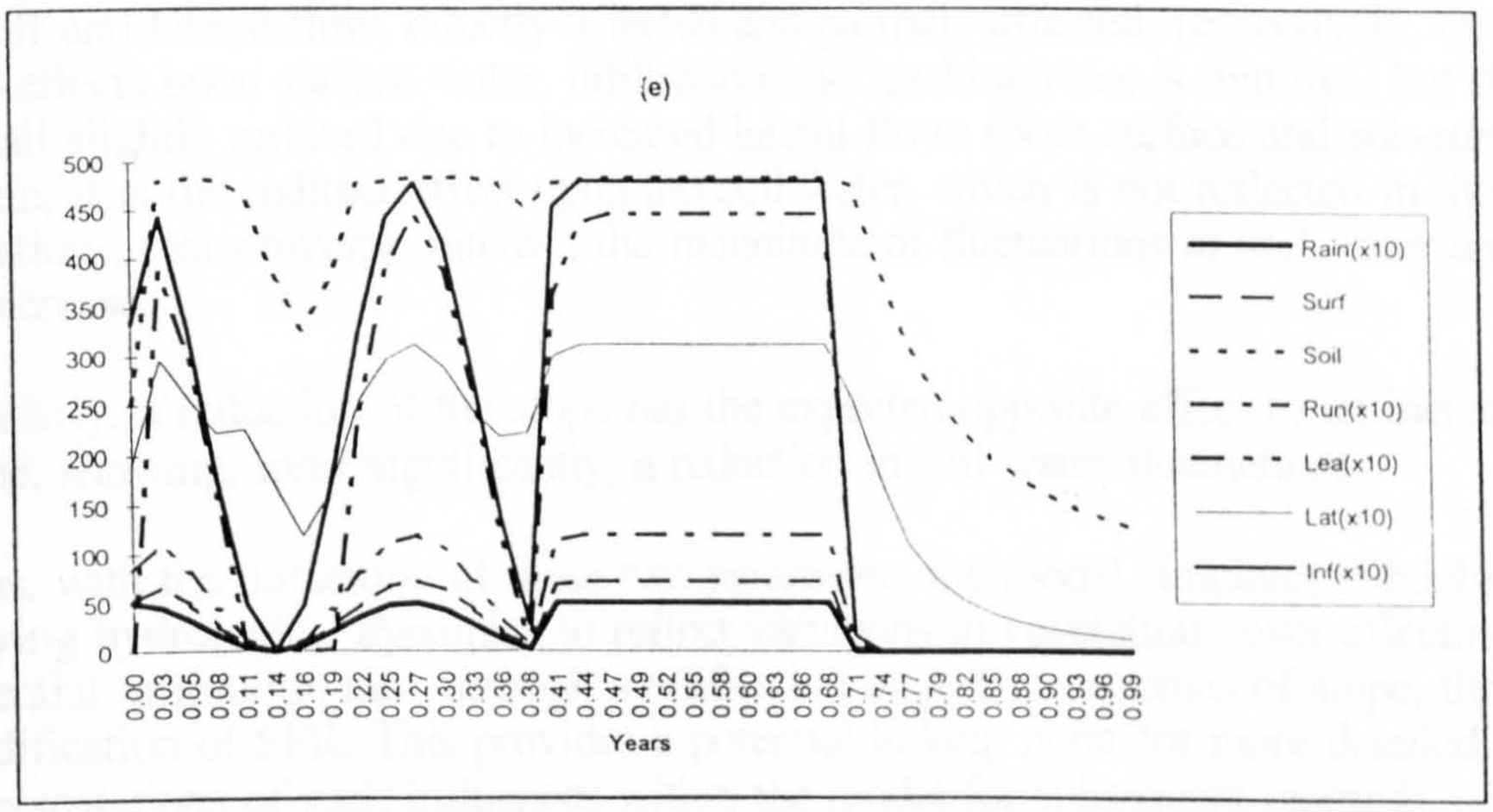

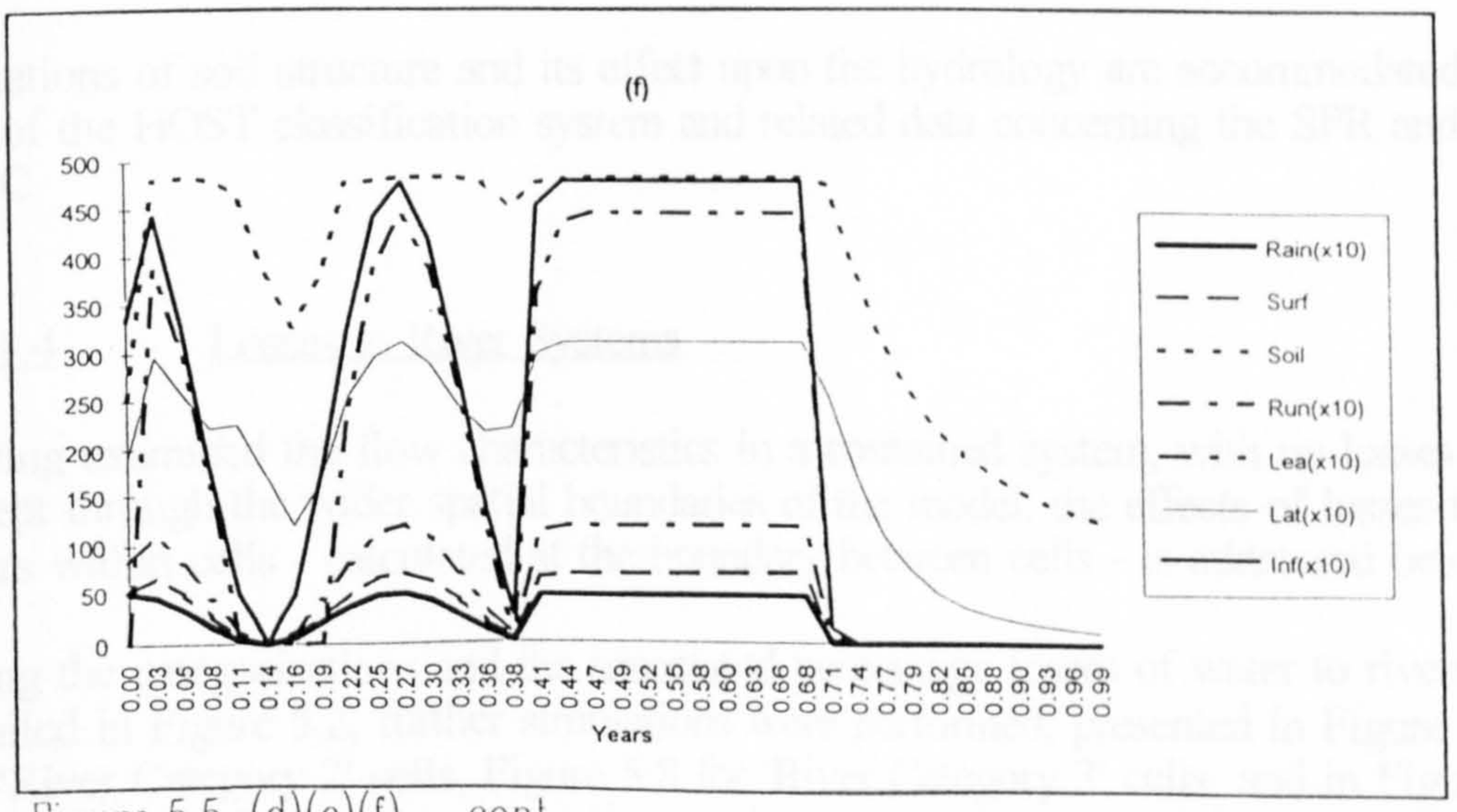

Figure 5.5 (d)(e)(f) ... cont.

Thus, the dynamics reflect the expected changes in the flow rates, as determined by the hydrology equations. However, the characteristic of most interest, due to its effect upon the phosphate adsorption processes, and not explicitly suggested by Equation (37), is the consequential increase or decrease in the fluctuations of soil water levels resulting from a change to the infiltration rate, μ.

5.3.1.3 Relative Slope changes

The effect of modifying the SPR to reflect extremes of slopes, increasing SPR for steep slopes and decreasing it for level areas, has been presented over the same three grid cells as above. The resultant output for increased slopes is presented in Figures 5.6(a), (b) and (c), and for flat regions in Figures 5.6(d), (e) and (f).

An increase in the slope is reflected by increases of approximately 20% in surface runoff and lateral flow, directly affected and partially affected, respectively, by SPR. The effects upon surface water, infiltration and leaching rates is minimal, but they are all slightly reduced due to increased lateral flows (both surface and sub-surface). Again, it is the indirect effect upon the soil water, which is not reflected in the equations, that provokes interest; the magnitude of fluctuations of soil water are seen to increase.

Similarly, a reduction of the slope has the expected opposite effect to an increased slope, showing, most significantly, a reduction in soil water fluctuations

Thus, with the utilization of these two parameters the model simulates subtlely varying hydrological dynamics to reflect variations in vegetation cover affecting the potential infiltration rate, through modification of μ, and extremes of slope, through modification of SPR. This provides a potential linking point for more detailed representations of such influences within the model for subsequent research.

Variations of soil structure and its effect upon the hydrology are accommodated by use of the HOST classification system and related data concerning the SPR and VMC.

5.3.1.4 Losses to River Systems

Having examined the flow characteristics in a contained system, with no losses except through the wider spatial boundaries of the model, the effects of losses to rivers within cells - calculated at the boundary between cells - is addressed below.

Using the categorizations and the associated percentage losses of water to rivers detailed in Figure 5.2, further simulations were performed, presented in Figure 5.7, for 'River Category 2' cells, Figure 5.8 for 'River Category 3' cells, and in Figure 5.9 for a mixture of flows from 'Category 1', through 'Category 2', to 'Category 3'.

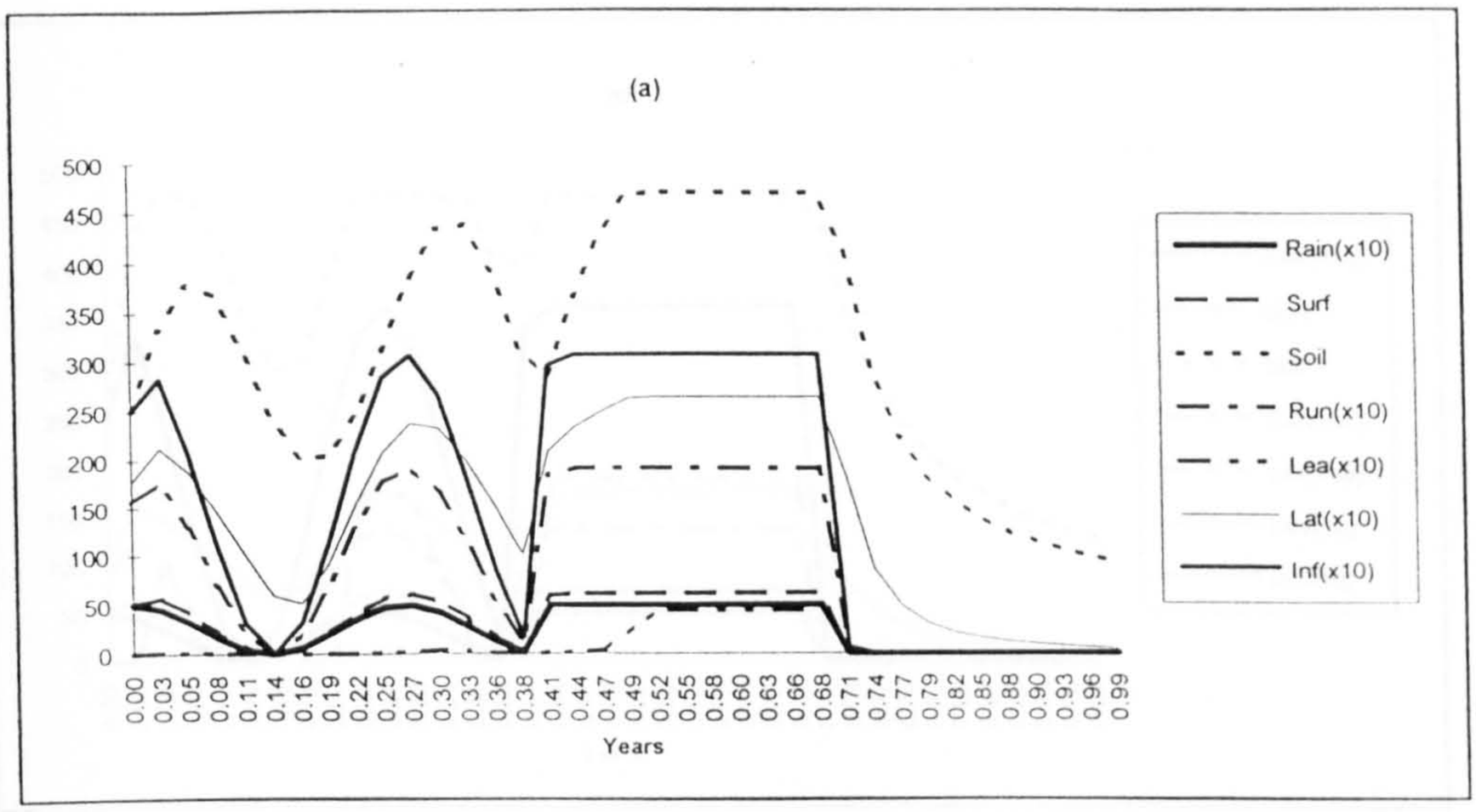

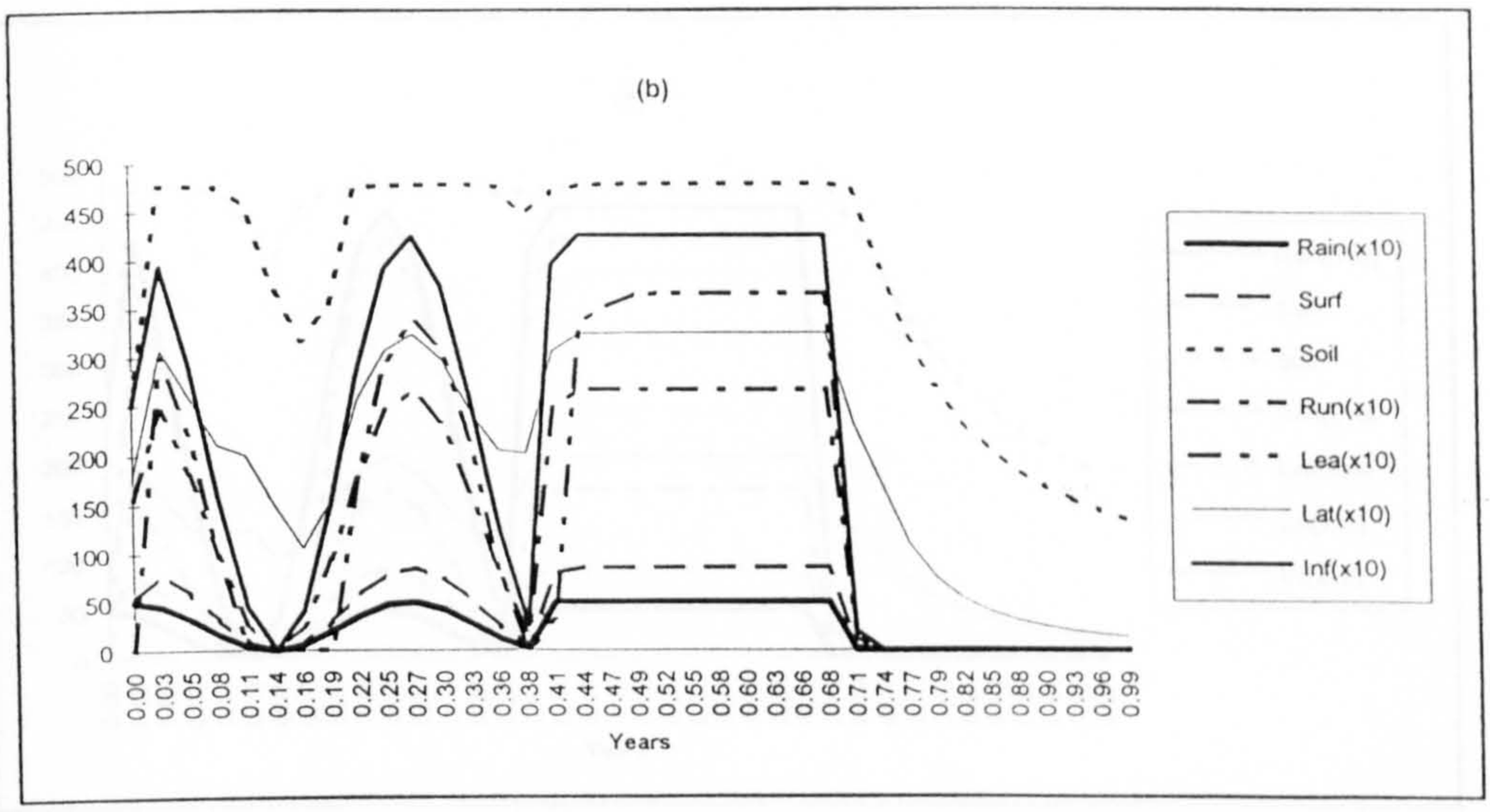

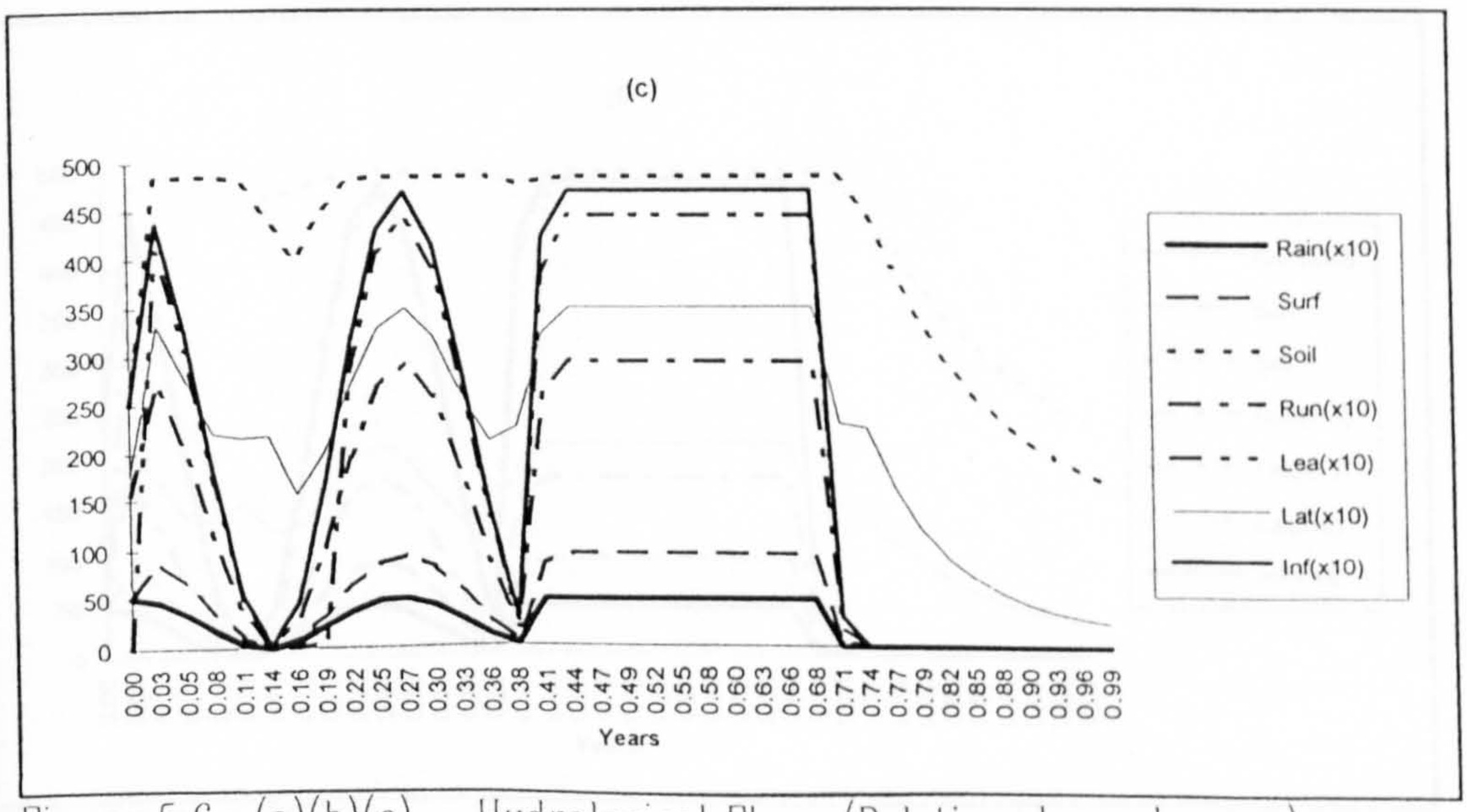

Figure 5.6 (a)(b)(c) – Hydrological Flows (Relative slope changes)

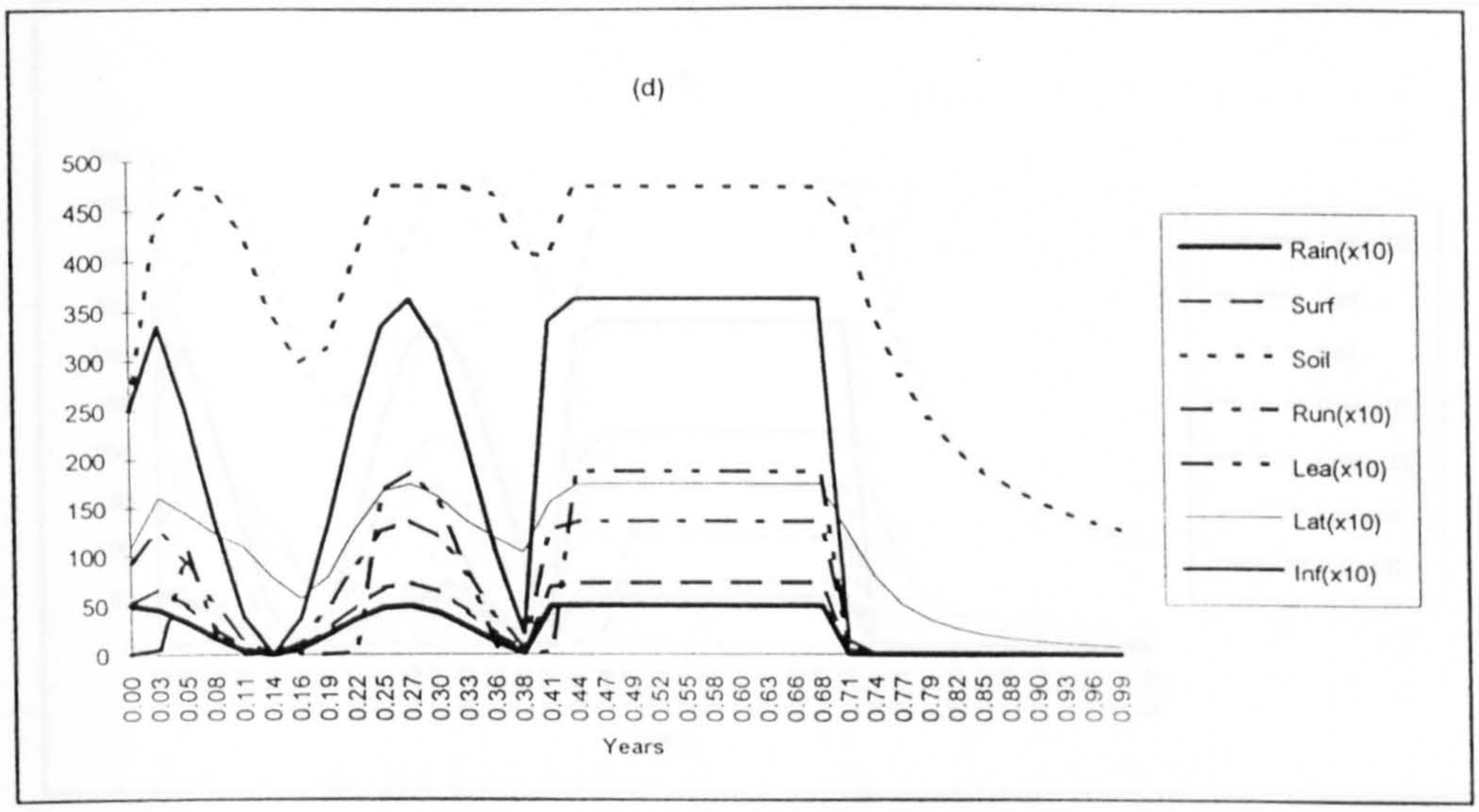

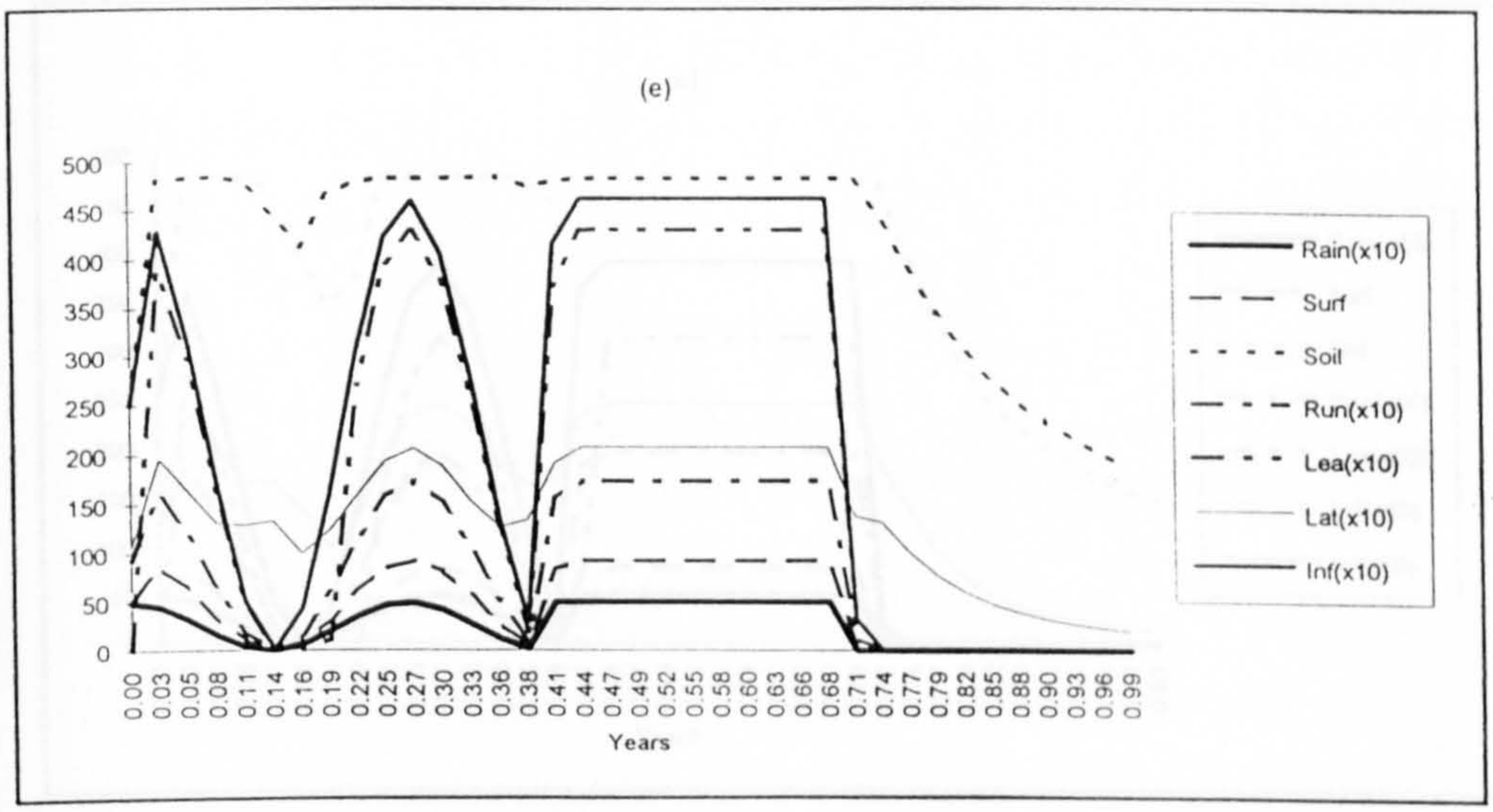

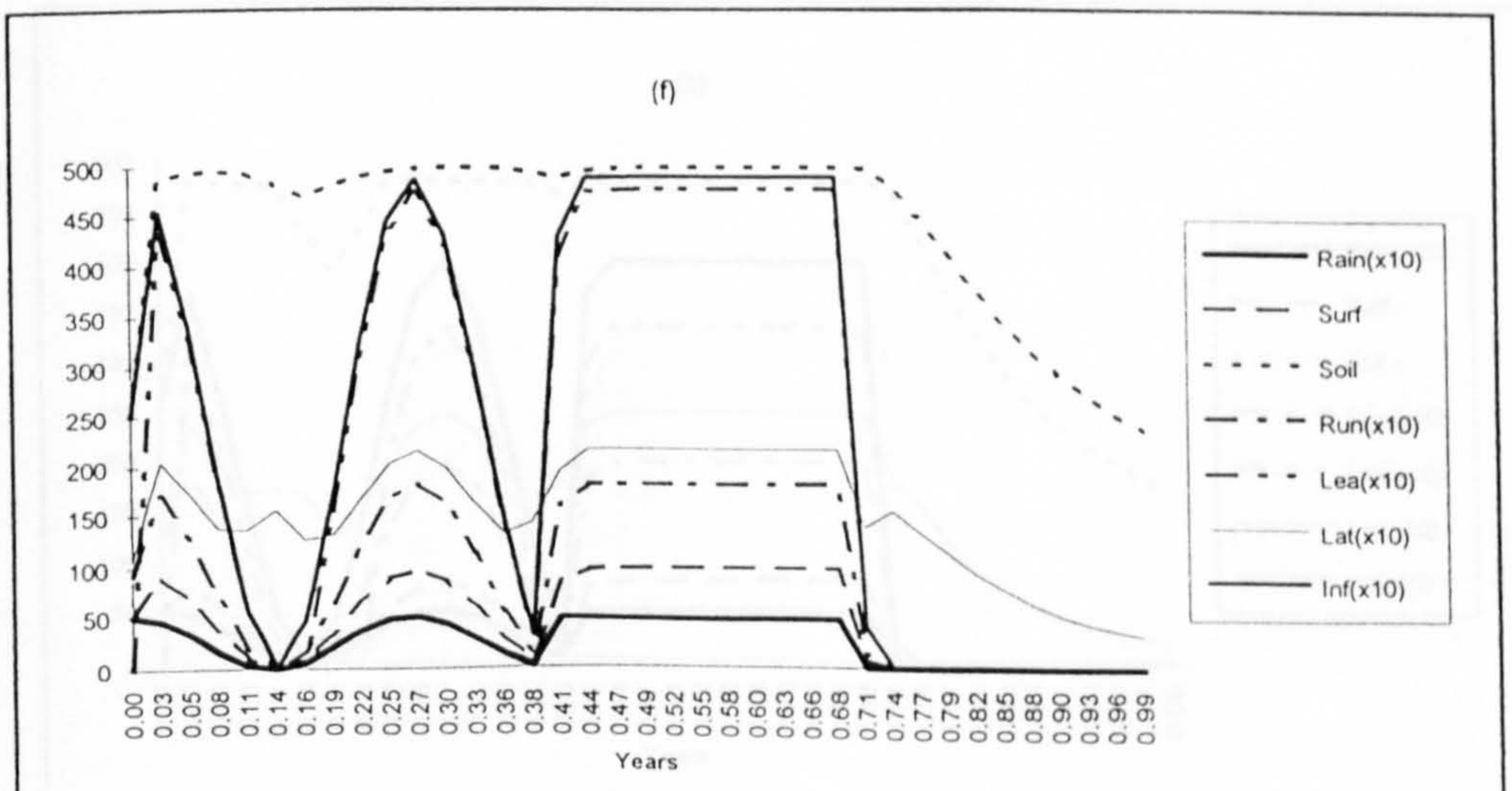

Figure 5.6 : (d)(e)(f) ... cont.

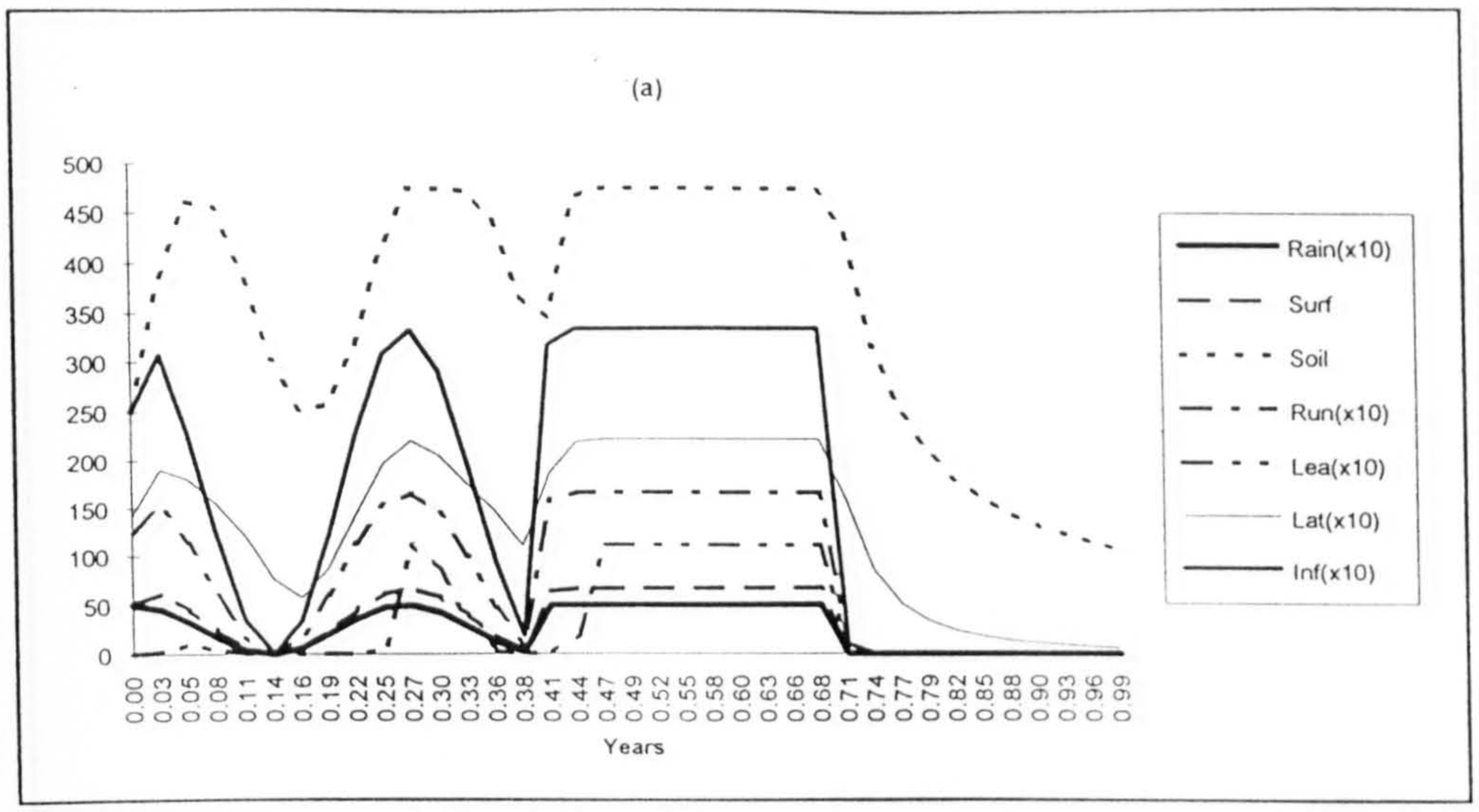

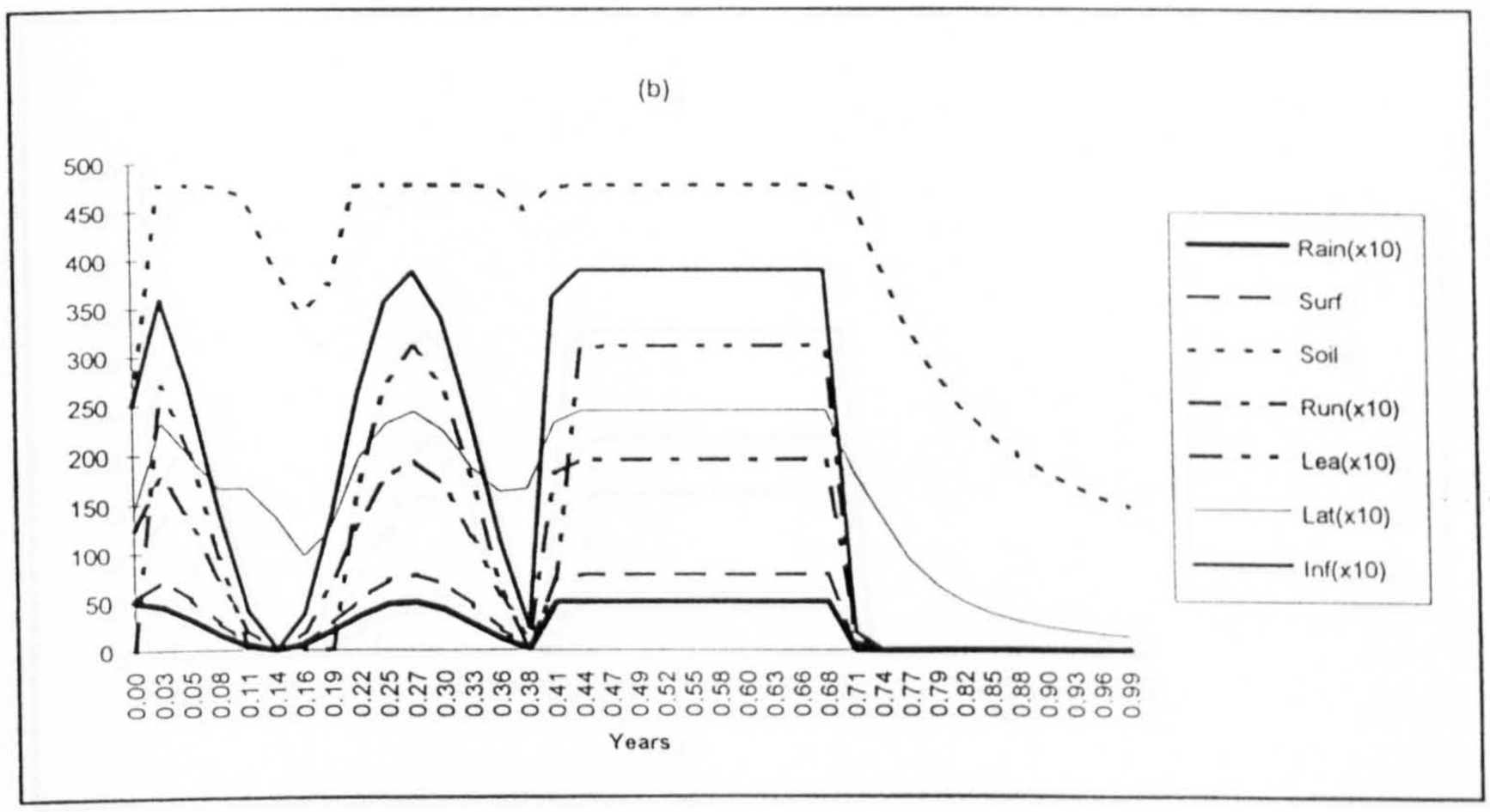

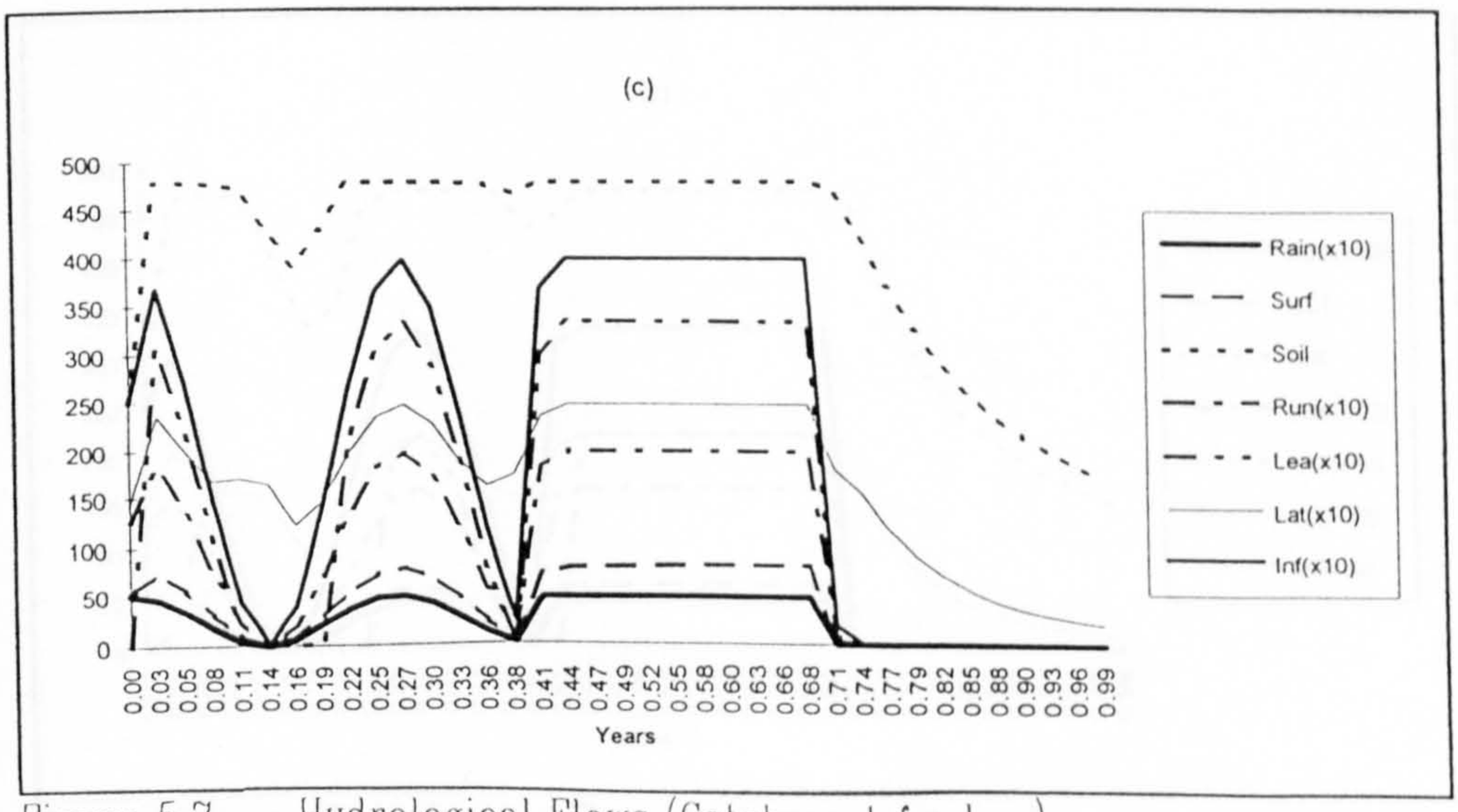

Figure 5.7 - Hydrological Flows (Catchment feeders)

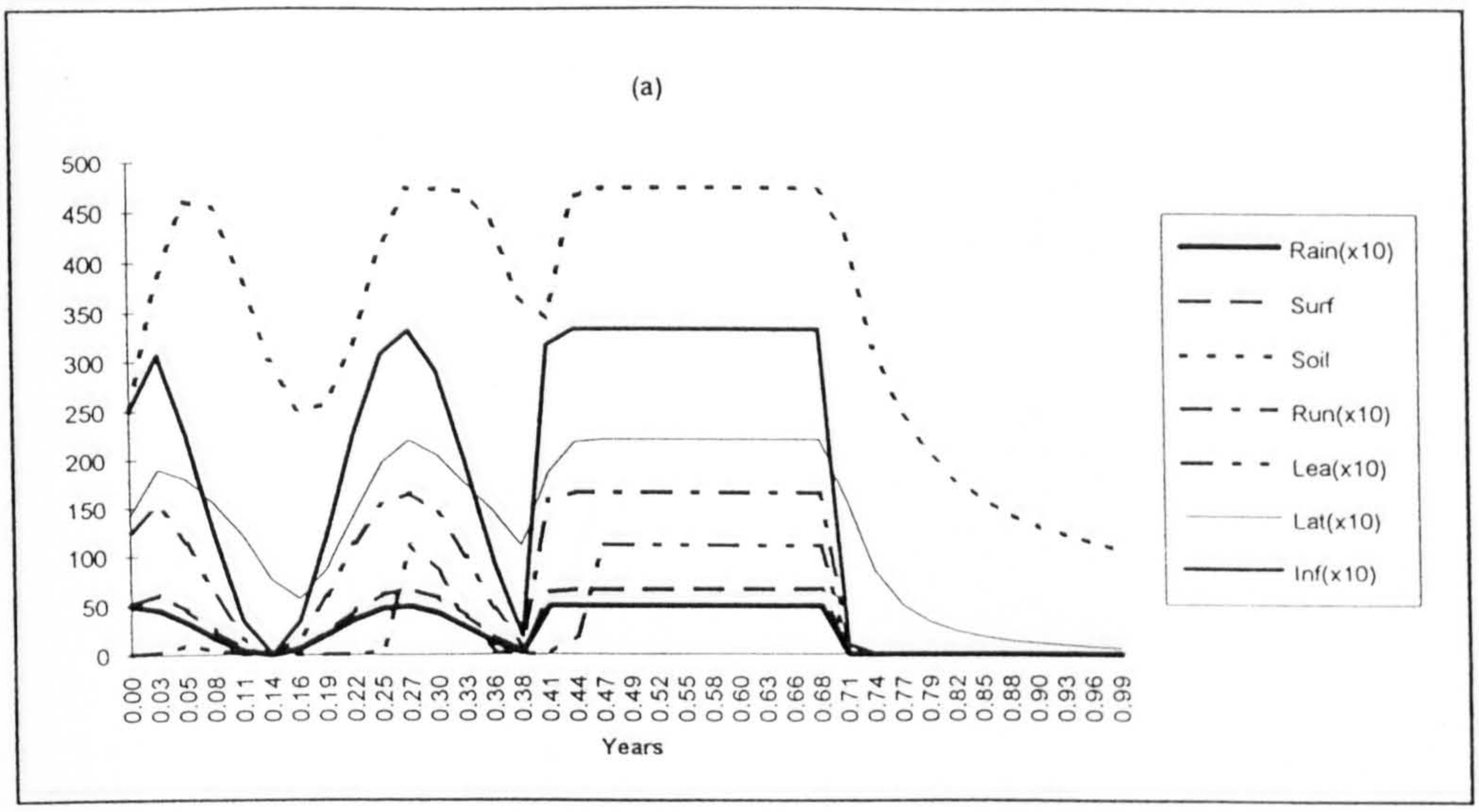

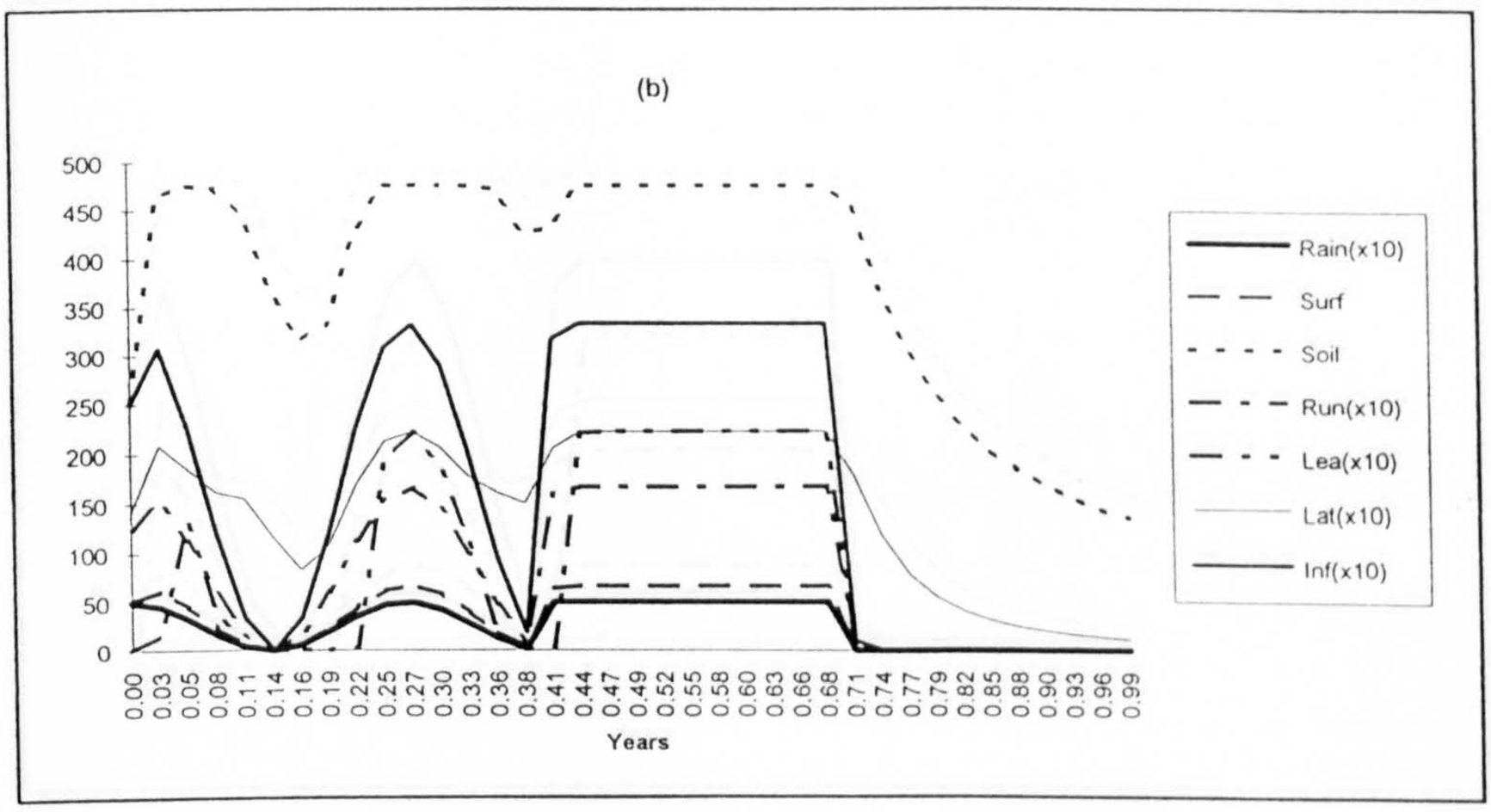

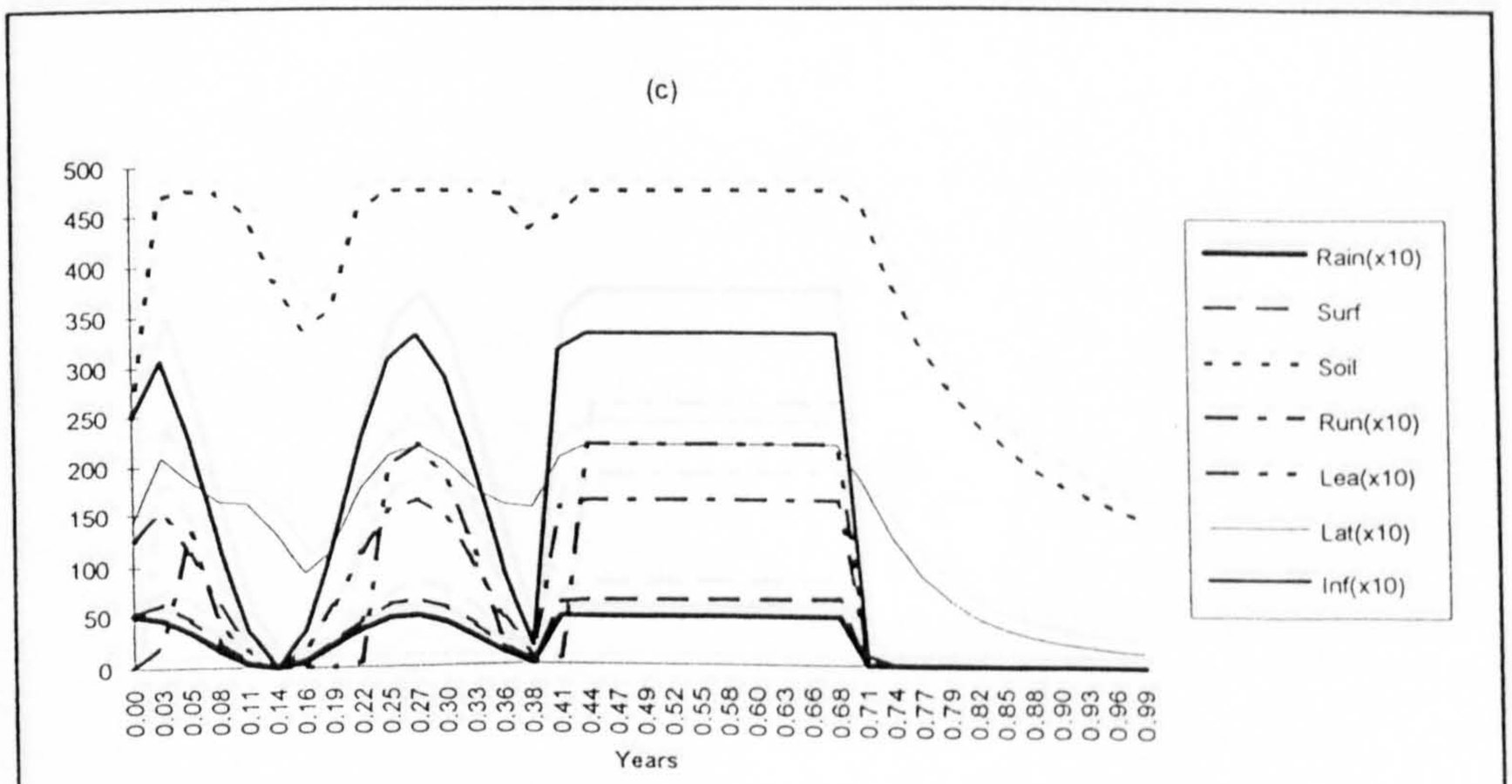

Figure 5.8 - Hydrological Flows (Catchment Rivers)

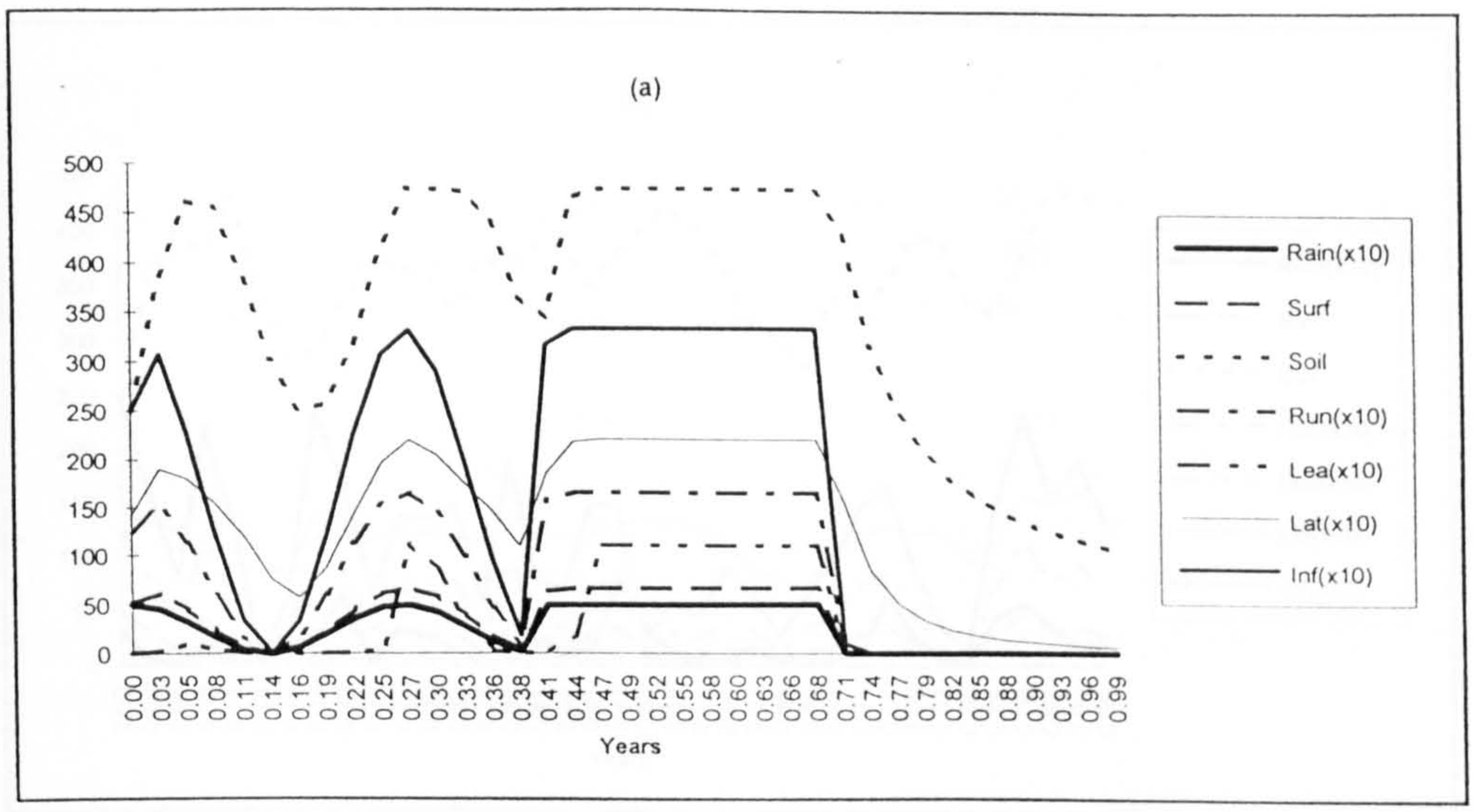

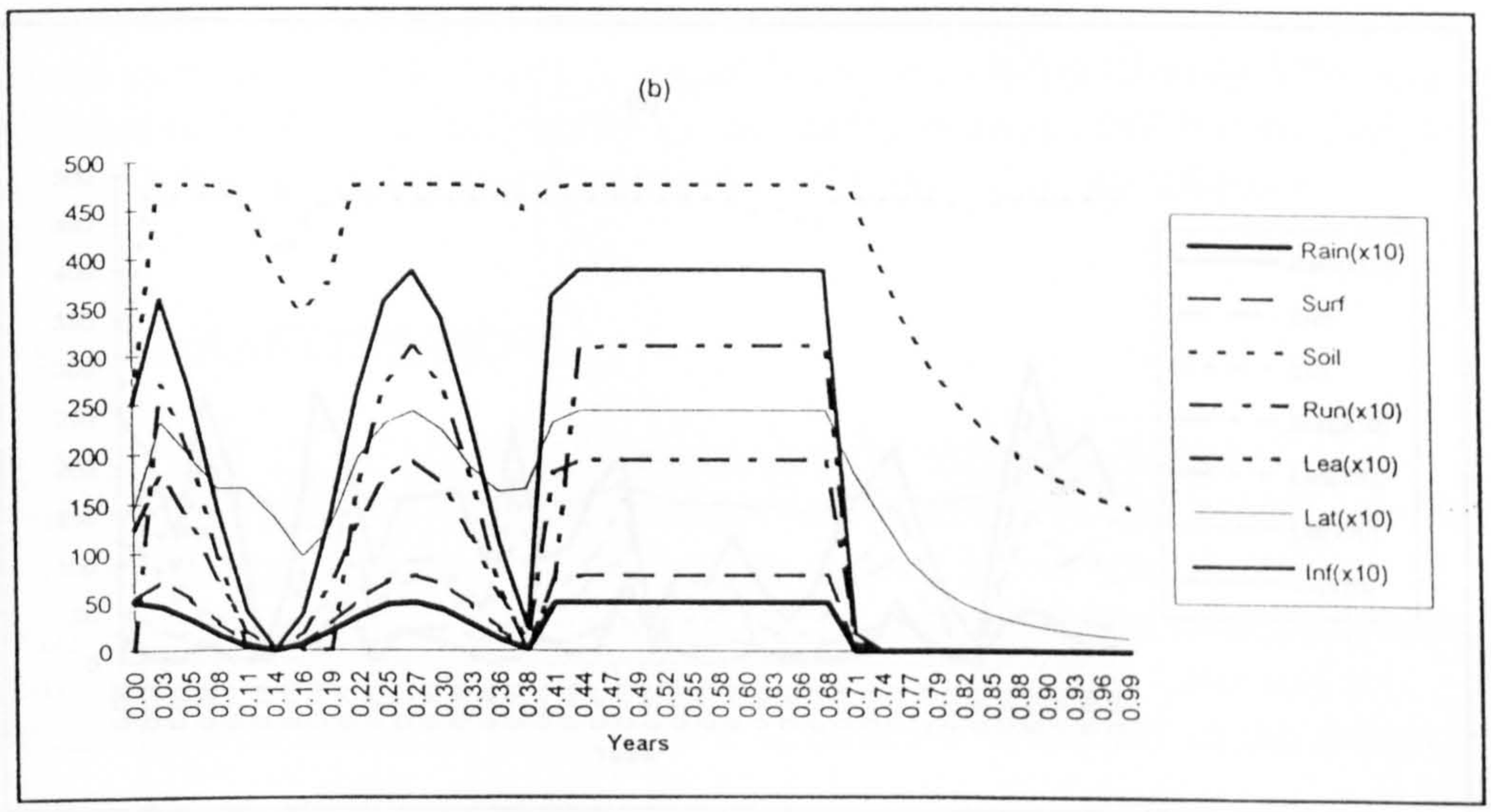

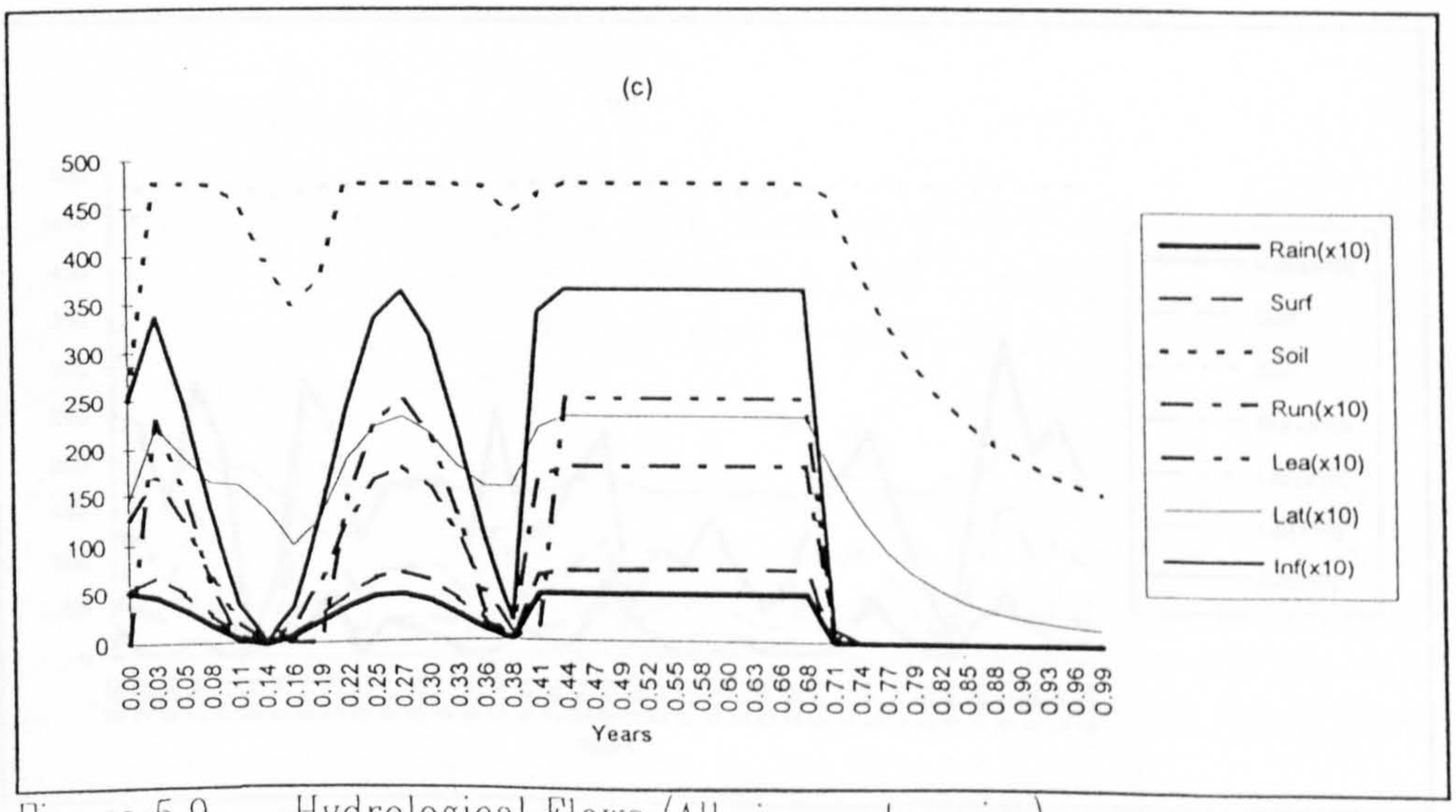

Figure 5.9 – Hydrological Flows (All river categories)

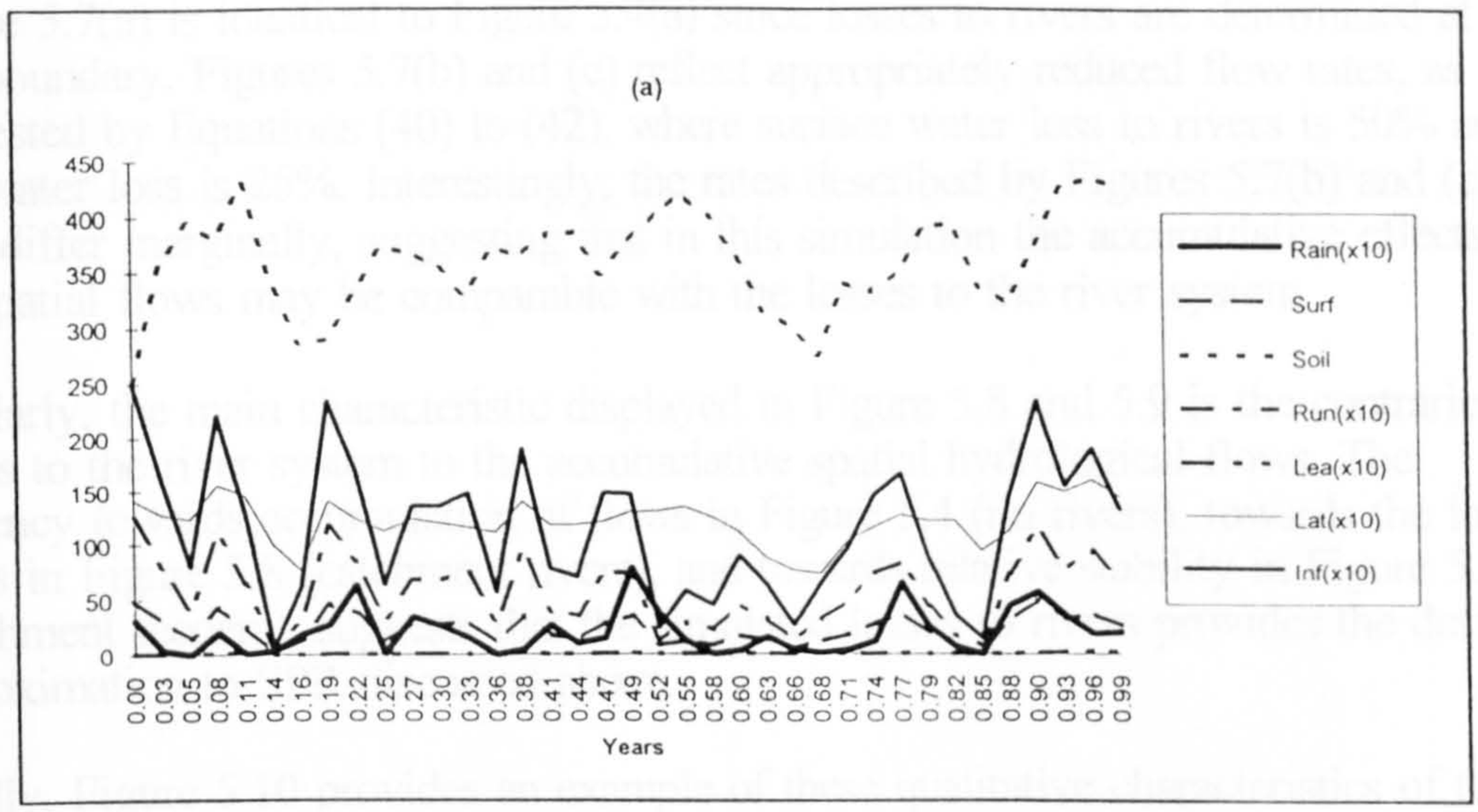

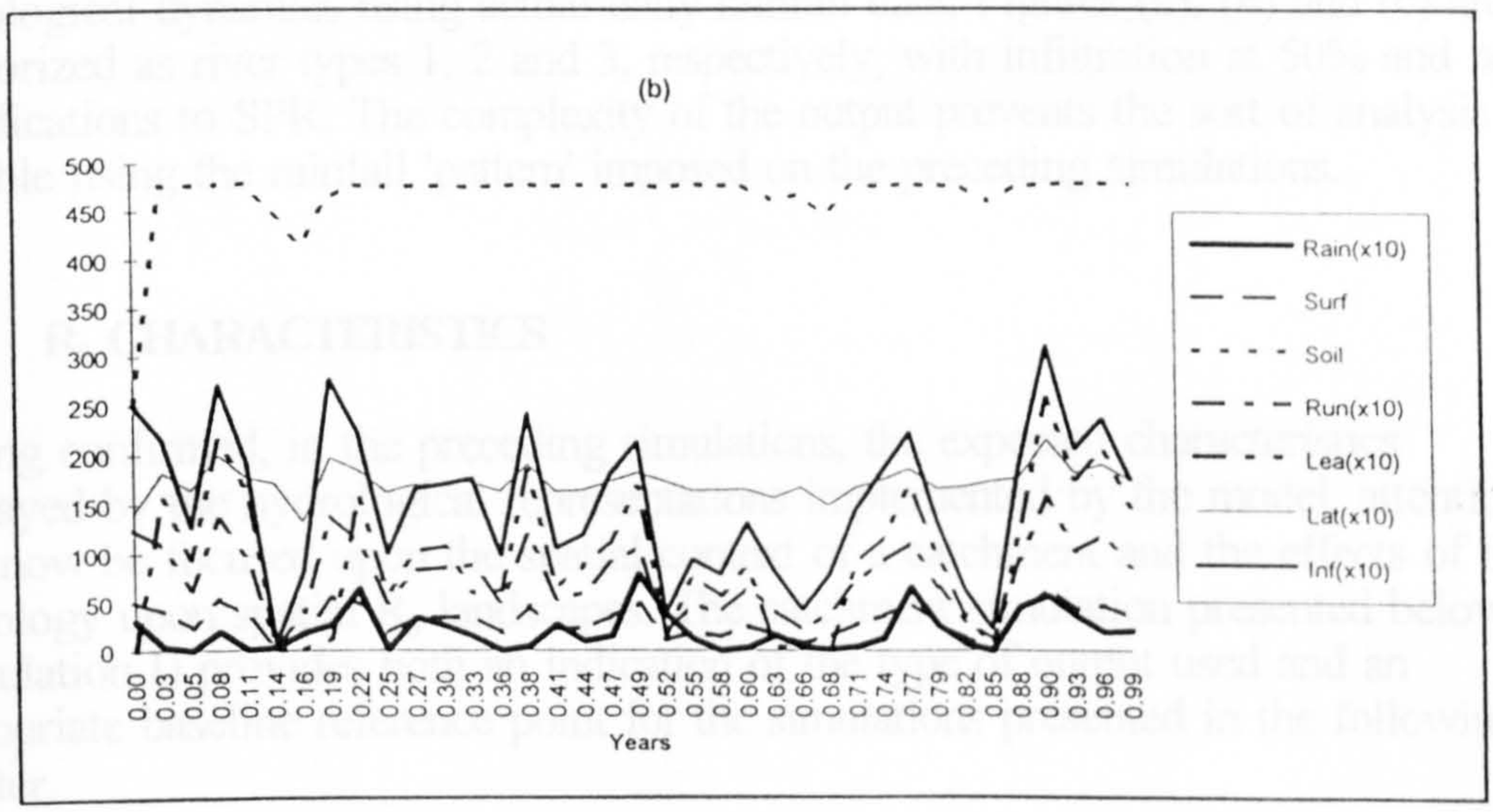

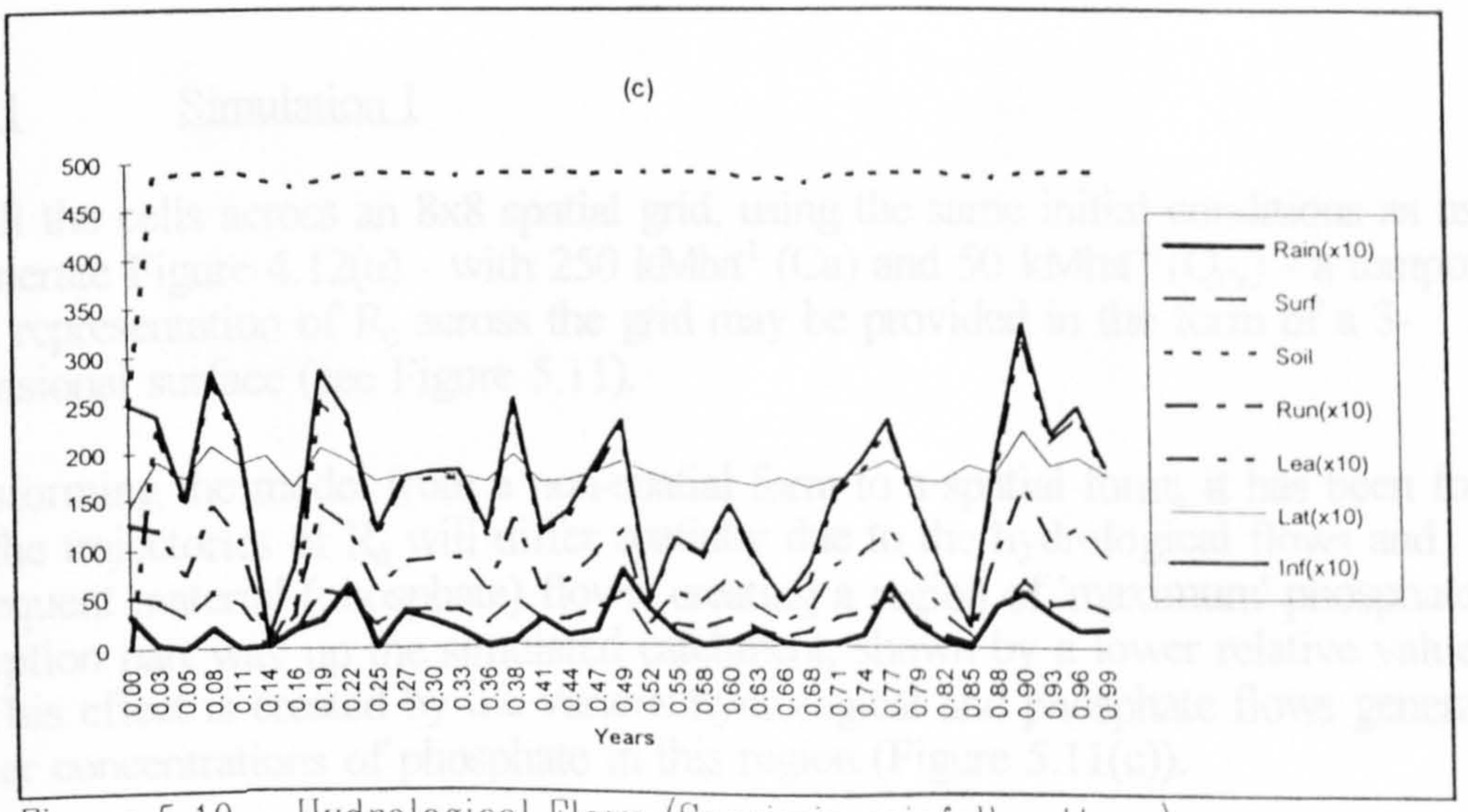

Figure 5.10 – Hydrological Flows (Specimin rainfall pattern)

Figure 5.7(a) is identical to Figure 5.4(a) since losses to rivers are determined at the cell boundary. Figures 5.7(b) and (c) reflect appropriately reduced flow rates, as suggested by Equations (40) to (42), where surface water loss to rivers is 50% and soil water loss is 25%. Interestingly, the rates described by Figures 5.7(b) and (c) only differ marginally, suggesting that in this simulation the accumulative effects of the spatial flows may be comparable with the losses to the river system.

Similarly, the main characteristic displayed in Figure 5.8 and 5.9 is the contrariety of losses to the river system to the accumulative spatial hydrological flows. The tendency towards accumulation of flows in Figure 5.4 (no rivers), towards the loss of flows in Figure 5.8 (catchment rivers), and towards relative stability in Figure 5.7 (catchment feeders), suggests that the simulated losses to rivers provides the desired approximation to SPR discussed above.

Finally, Figure 5.10 provides an example of these qualitative characteristics of the hydrological dynamics using actual daily rainfall data; Figures (a), (b) and (c) are categorized as river types 1, 2 and 3, respectively, with infiltration at 50% and no modifications to SPR. The complexity of the output prevents the sort of analysis possible using the rainfall 'pattern' imposed on the preceding simulations.

5.3.2 R_0 CHARACTERISTICS

Having confirmed, in the preceding simulations, the expected characteristics displayed by the hydrological representations implemented by the model, attention may now be focused upon the spatial context of a catchment and the effects of the hydrology upon spatial R_0 landscapes. The catchment simulation presented below (Simulation I) provides both an indication of the type of output used and an appropriate baseline reference point for the simulations presented in the following chapter.

5.3.2.1 Simulation I

For all the cells across an 8x8 spatial grid, using the same initial conditions as used to generate Figure 4.12(a) - with 250 $kMha^{-1}$ (Ca) and 50 $kMha^{-1}$ (Q_{Ca}) - a temporally static representation of R_0 across the grid may be provided in the form of a 3-dimensional surface (see Figure 5.11).

Transforming the model from a non-spatial form to a spatial form, it has been found that the trajectories of R_0 will differ spatially due to the hydrological flows and consequent material (phosphate) flows, creating a region of 'maximum' phosphate adsorption part way up the simulated catchment, shown by a lower relative value of R_0. This effect is created by the various hydrological and phosphate flows generating greater concentrations of phosphate in this region (Figure 5.11(c)).

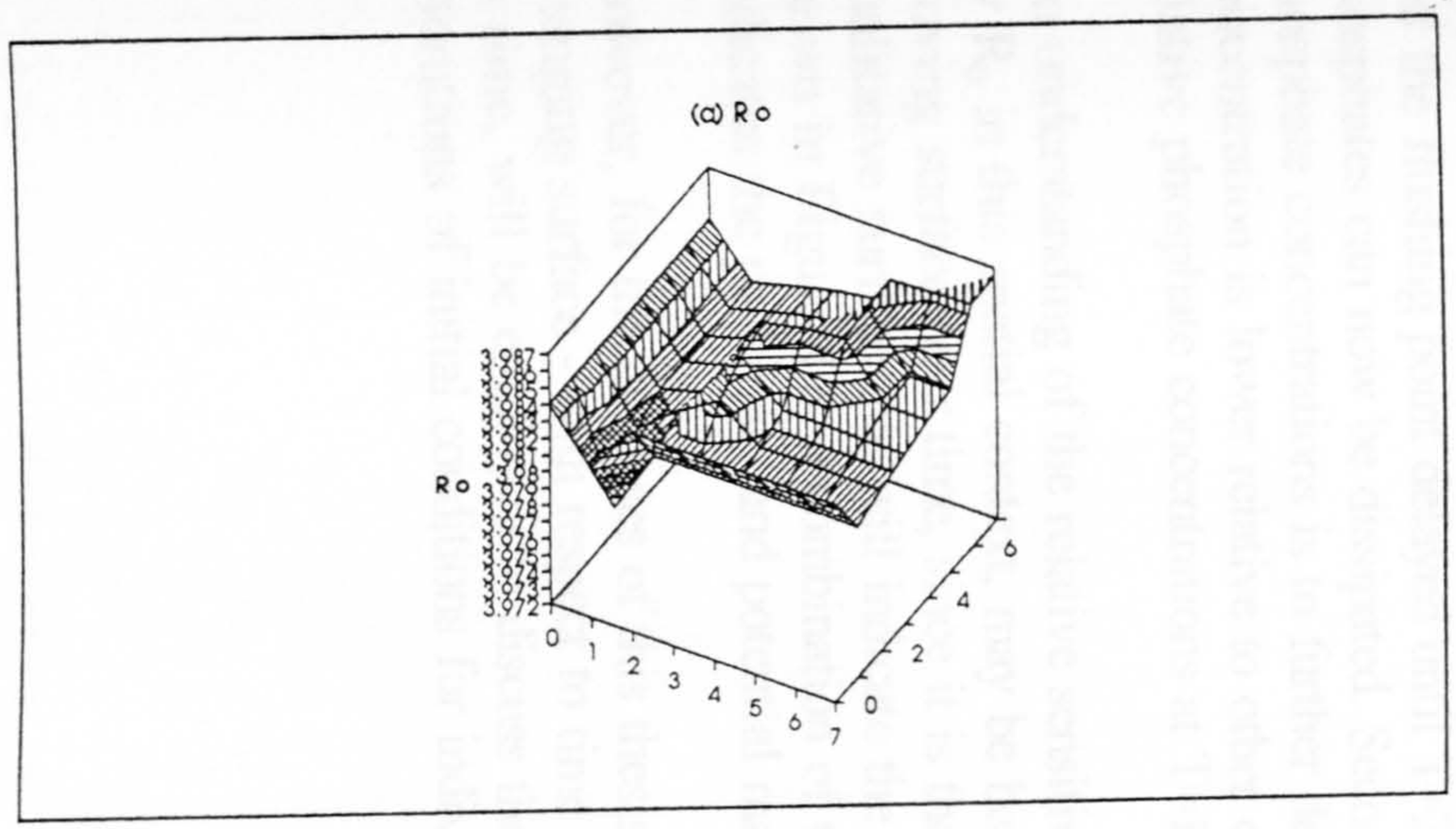

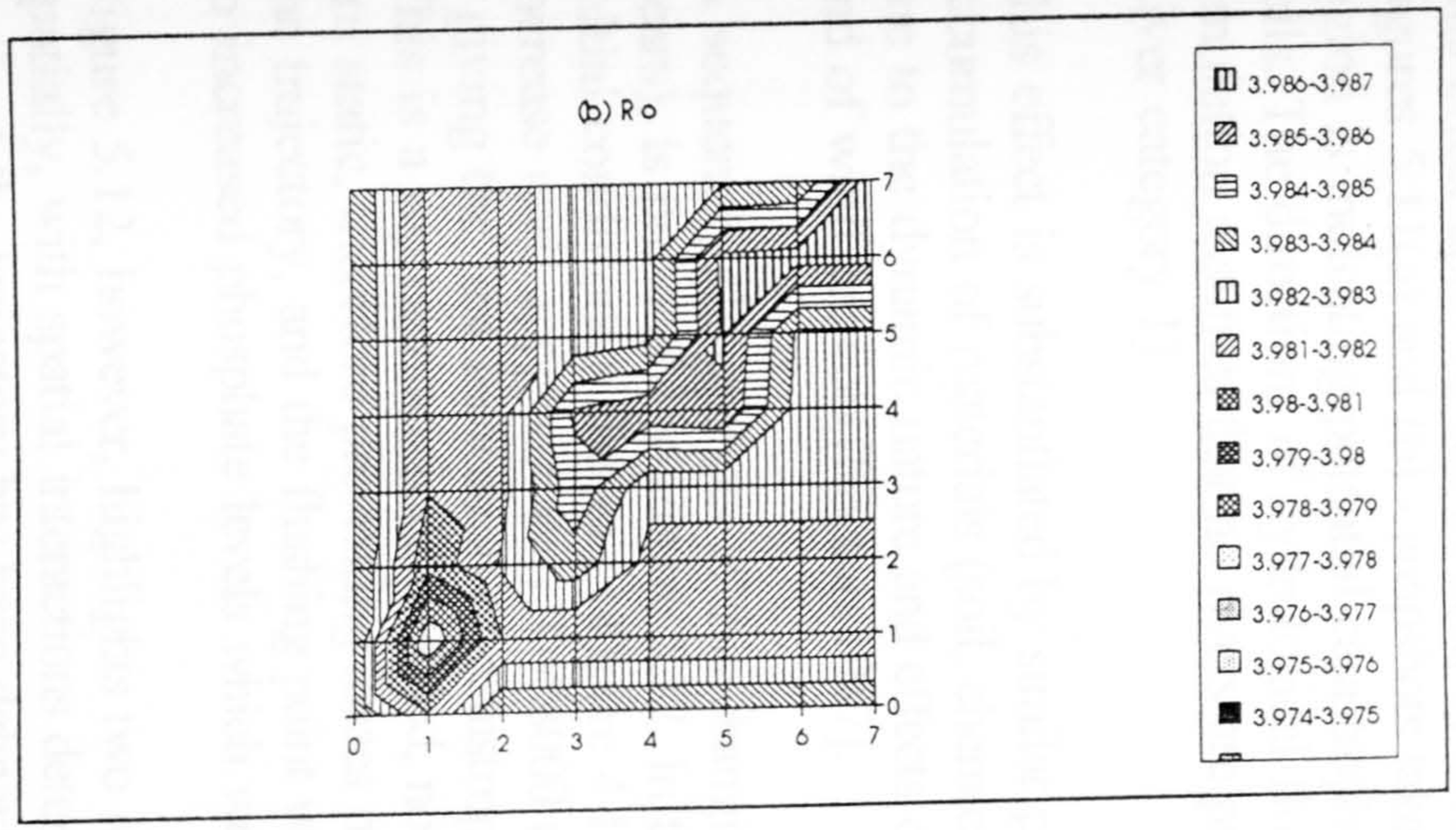

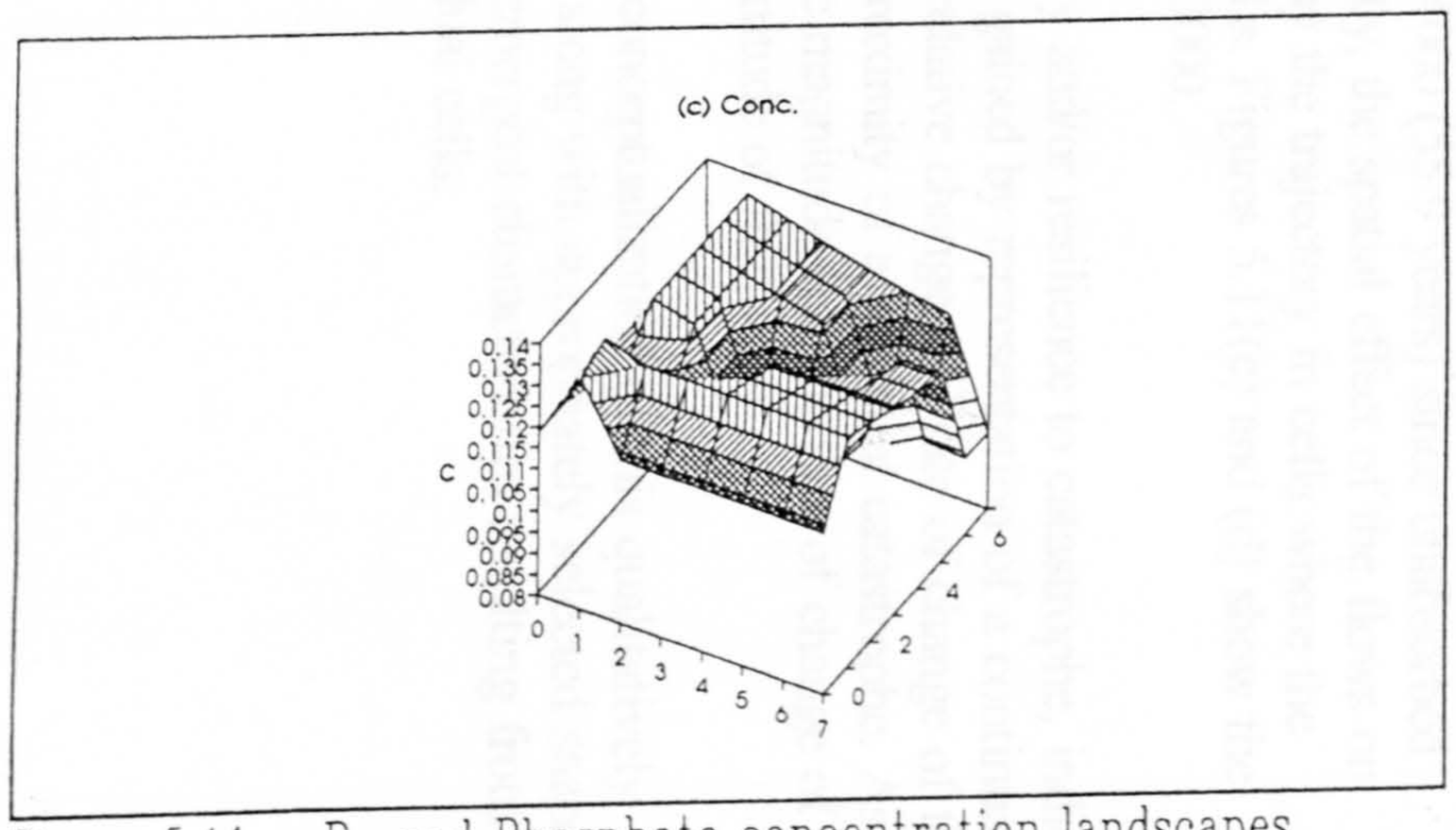

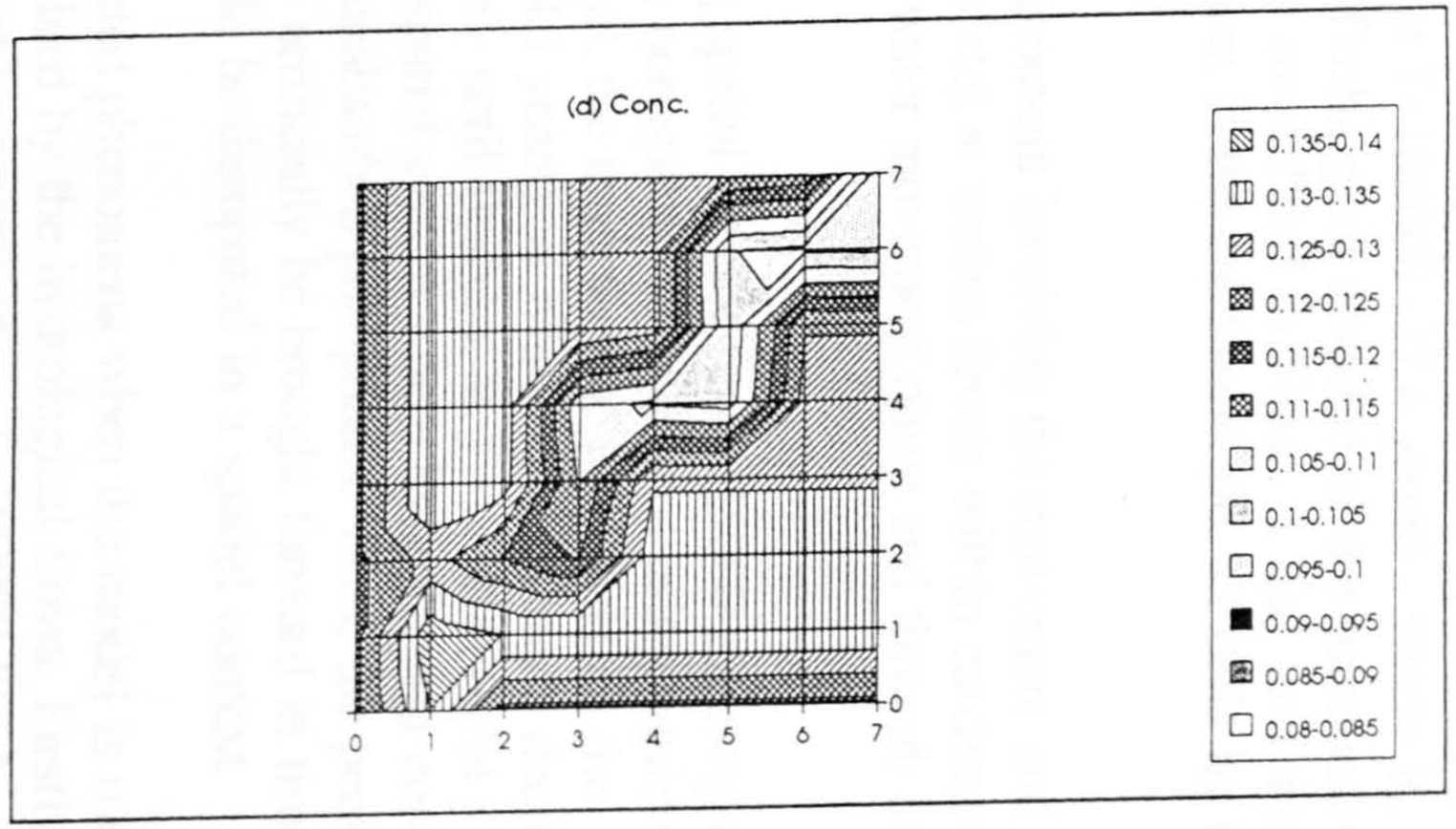

Figure 5.11 - R_0 and Phosphate concentration landscapes

This effect upon R_0 can be seen by reference to the spatial surface presented in Figures 5.11(a) and (b) - snapshots taken at T=100000 (27.4 years) - where R_0 in this region is indicating potential catastrophe (flushing) in advance of the surrounding cells. The directions of hydrological flows are defined in Figure 3.5(a), and this simulation assumes that no rivers are present in the catchment (ie. all cells lie in River category 1).

This effect is substantiated by similar phenomena involving the movement and accumulation of materials (soil, chemicals etc) at certain levels within catchments due to the dynamic nature and effects of water movement down and through slopes, and of wind erosion [Imeson 1987].

A sequence of snapshots of this changing spatial surface, each 25000 timesteps (6.8 years), is presented in Figure 5.12. In the non-spatial simulation - using equivalent initial conditions - shown in Figure 4.12(a), the trajectory of R_0 begins on the increase until approximately T=88000 (24.1 years), at which time it starts decreasing - giving the first indication of catastrophe - until flushing at T=173000 (47.4 years). This is a representation of a closed, non-spatial system where hydrological conditions are static, therefore preventing losses of unabsorbed phosphates. Thus, the peak of the trajectory, and the flushing point will artificially be brought forward in time due to increased phosphate levels which would be dissipated in a spatial context.

Figure 5.12, however, highlights two related phenomena when the model is run spatially, with spatial interactions determined by the hydrological flows. Firstly, the peak of the trajectory has been delayed until approximately T=100000 (27.4 years), and the flushing point delayed until T=204000 (55.9 years) since unabsorbed phosphates can now be dissipated. Secondly, the spatial effect of the flows on phosphate concentrations is to further delay the trajectory in cells where the concentration is lower relative to other cells. Figures 5.11(c) and (d) show the relative phosphate concentrations at T=100000.

An understanding of the relative sensitivity and/or resilience to catastrophe, indicated by R_0 in this spatial context, may be best gained by representation of a continually moving surface over time, since it is the relative change and rate of change of this qualitative surface that will indicate the proximity of a potential catastrophe. As shown in Figure 4.8, a combination of the magnitude and the rate of change of R_0 indicates the proximity and potential magnitude of flushing.

However, for the purposes of this thesis, conceptualization of this qualitatively changing surface - with respect to time - along with appropriately selected snapshots in time, will be employed to discuss the emergent characteristics resulting from alterations of initial conditions for individual cells.

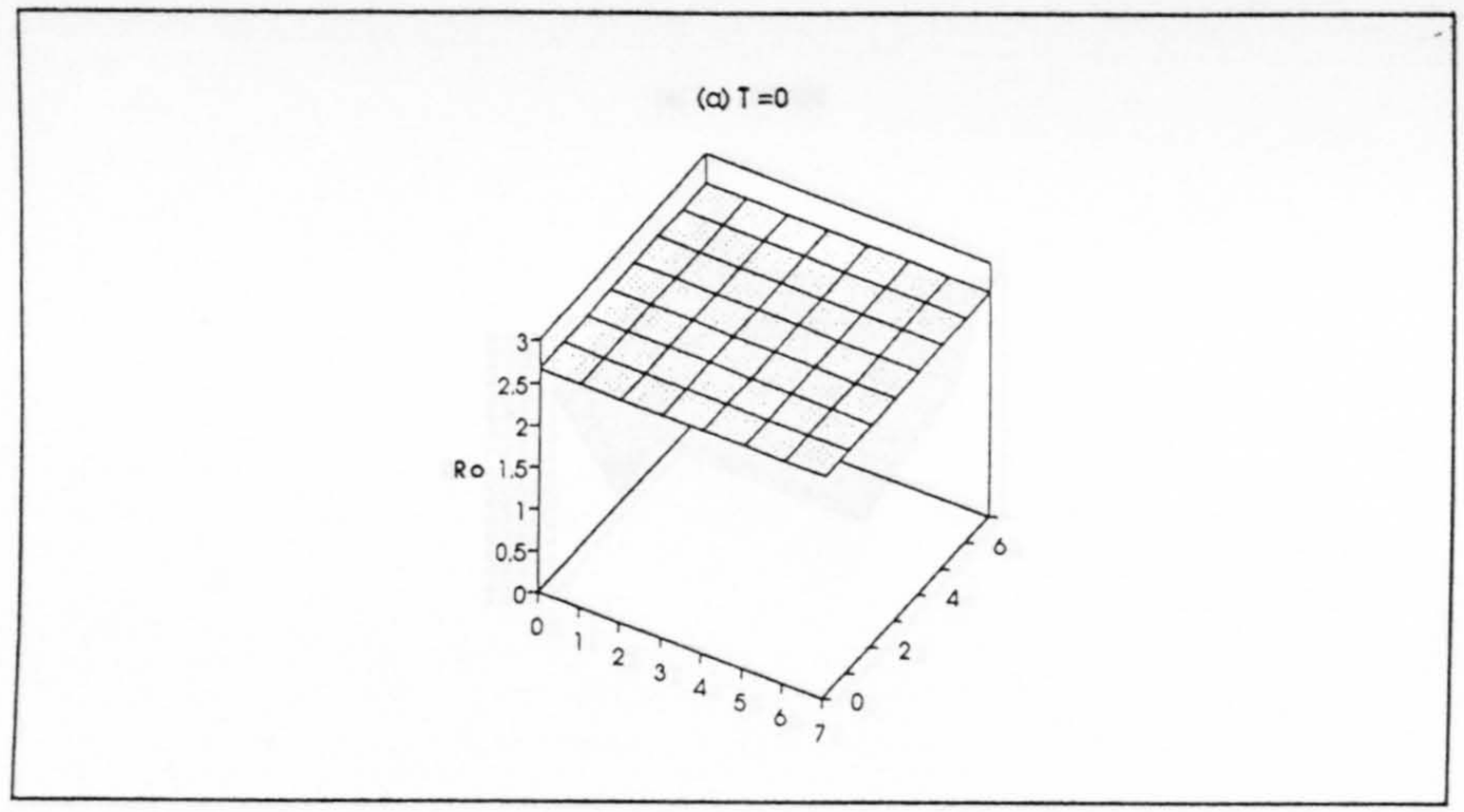

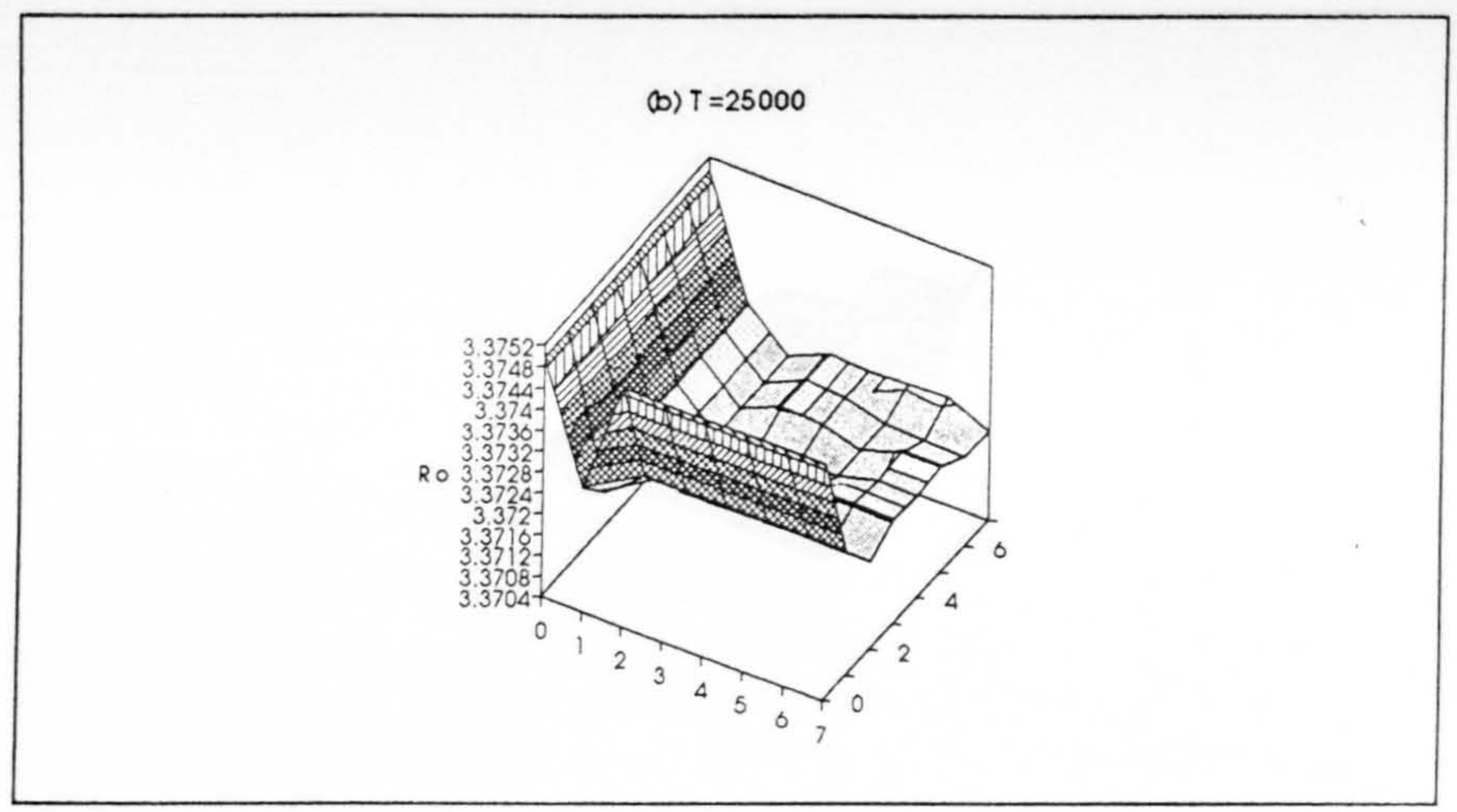

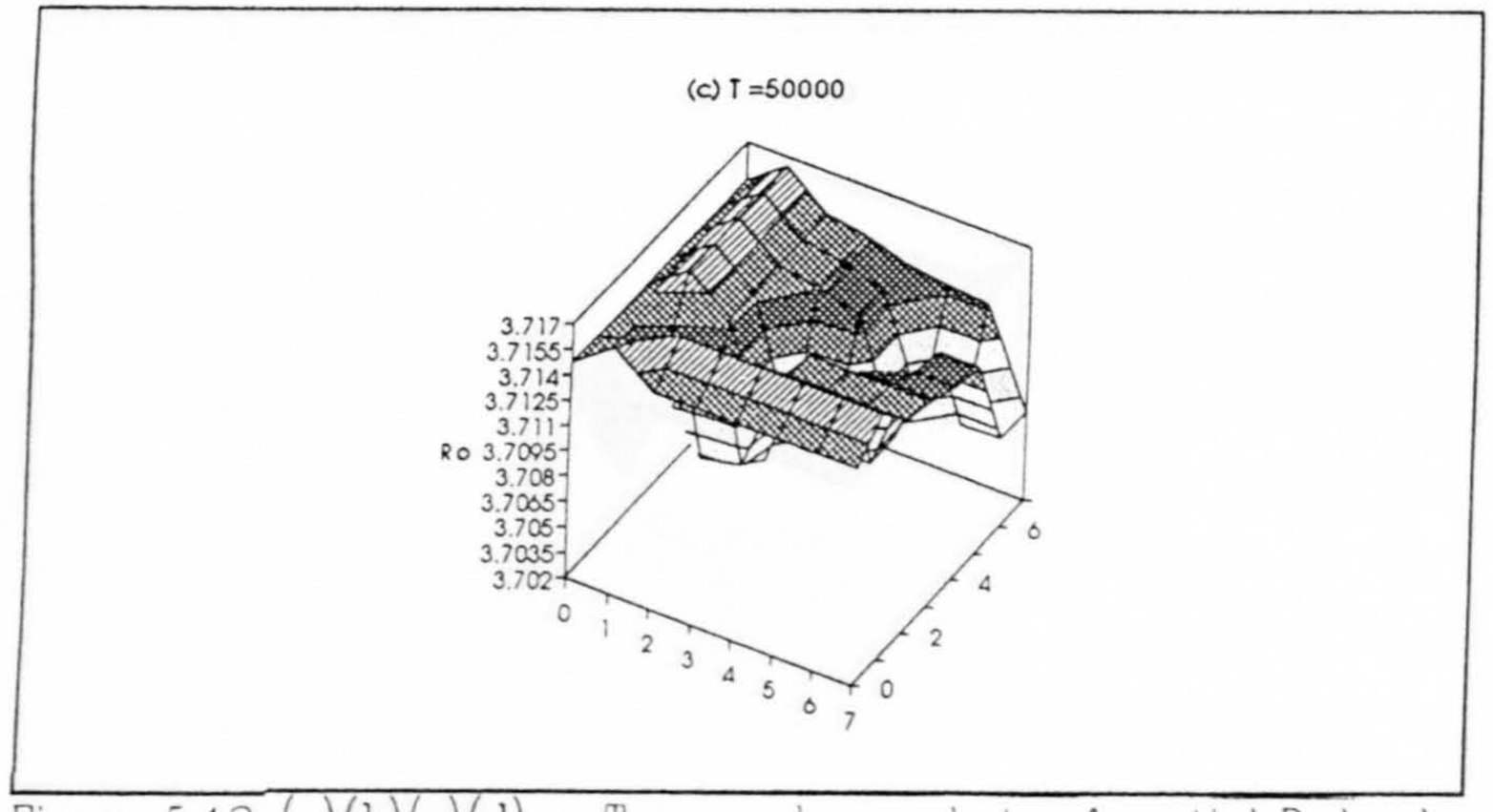

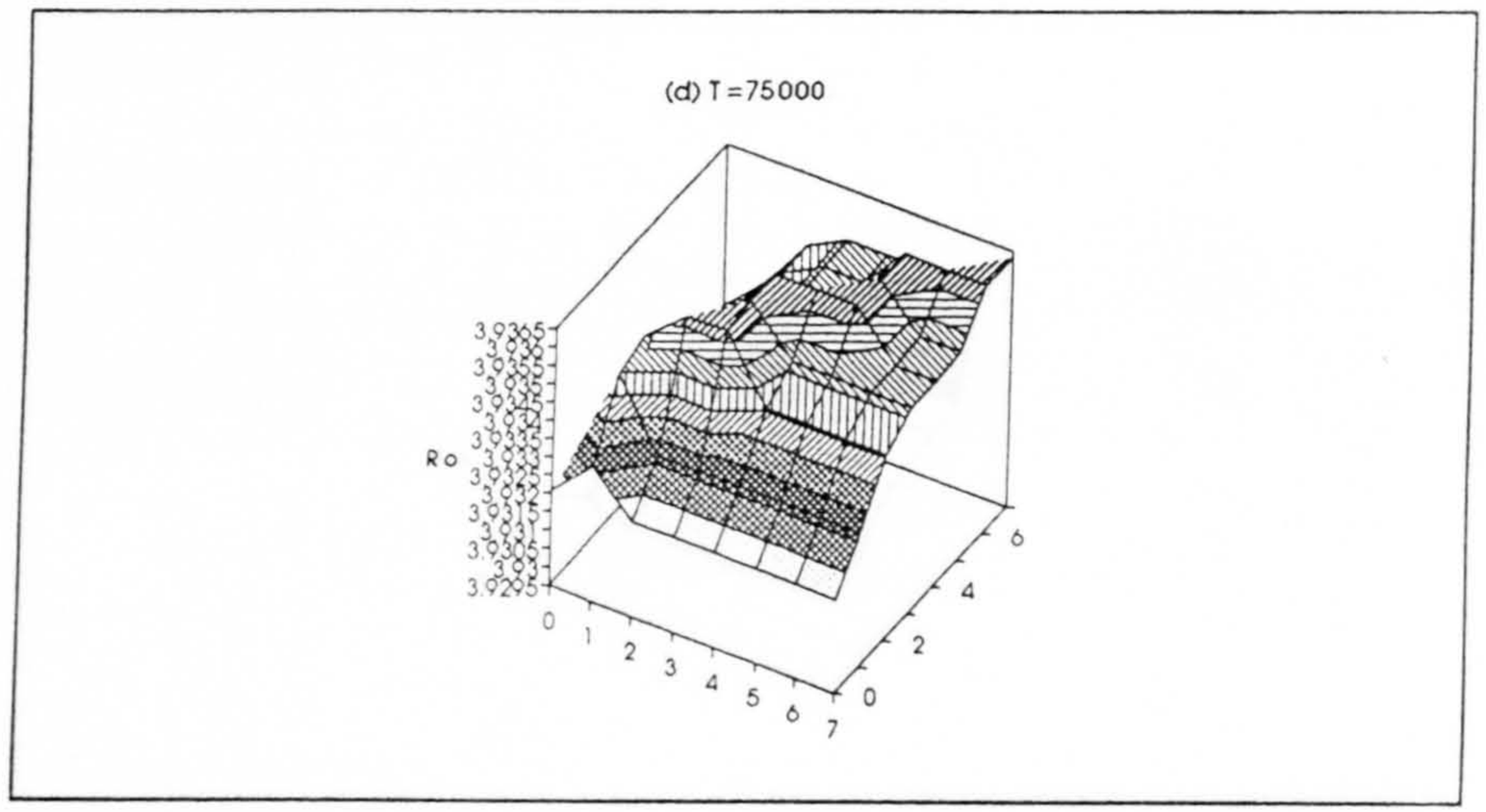

Figure 5.12 (a)(b)(c)(d) – Temporal snapshots of spatial R_0 landscape

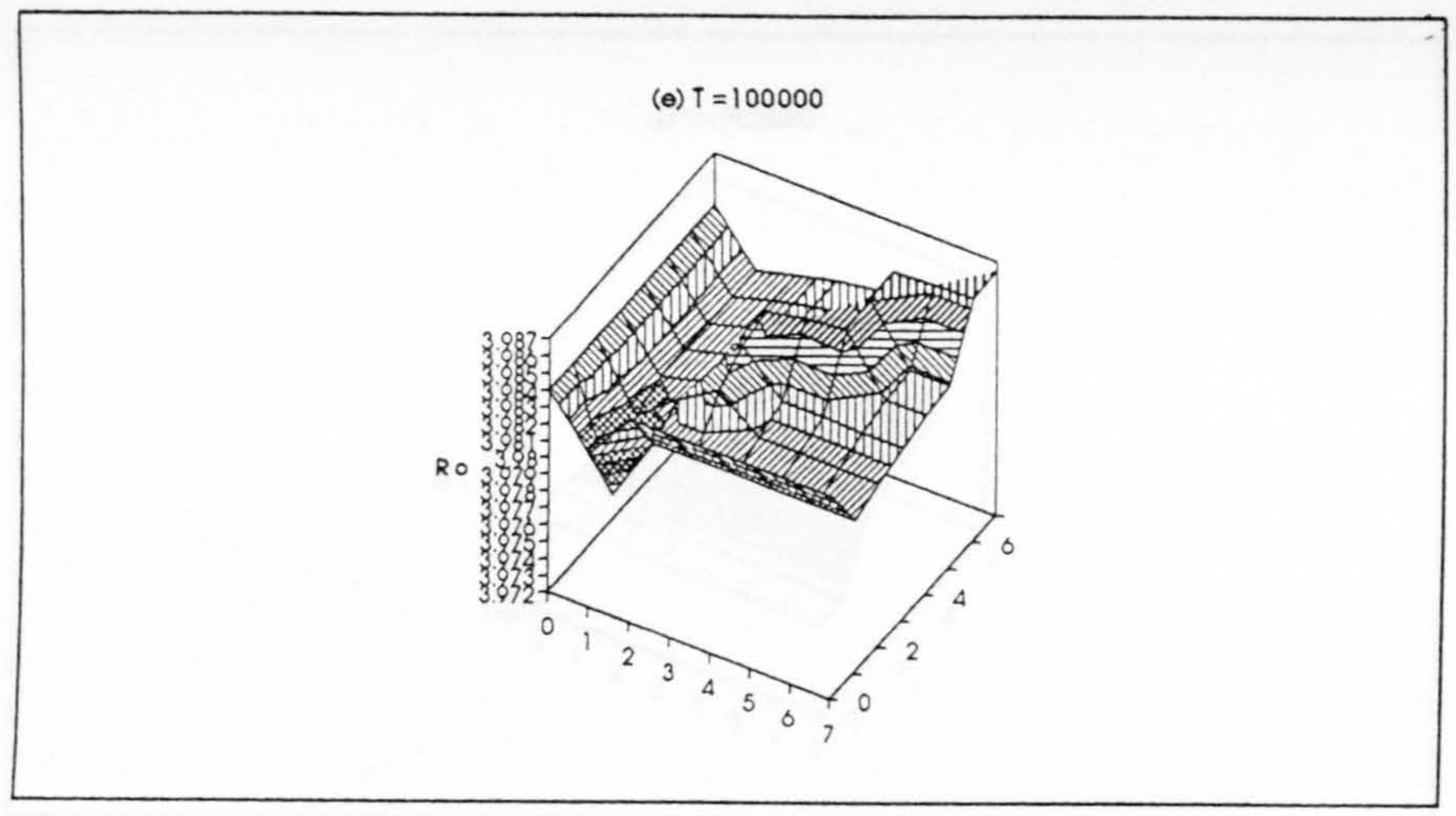

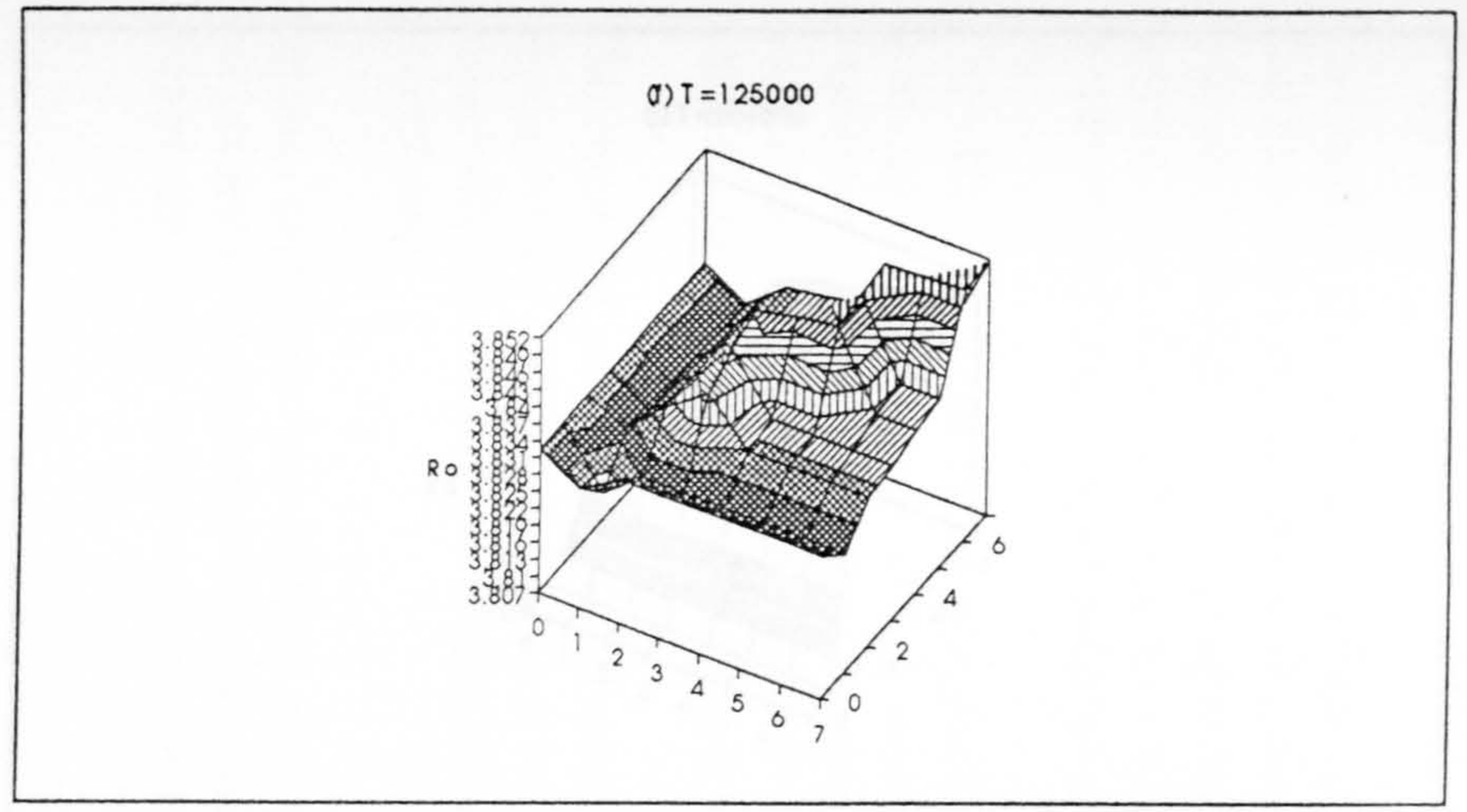

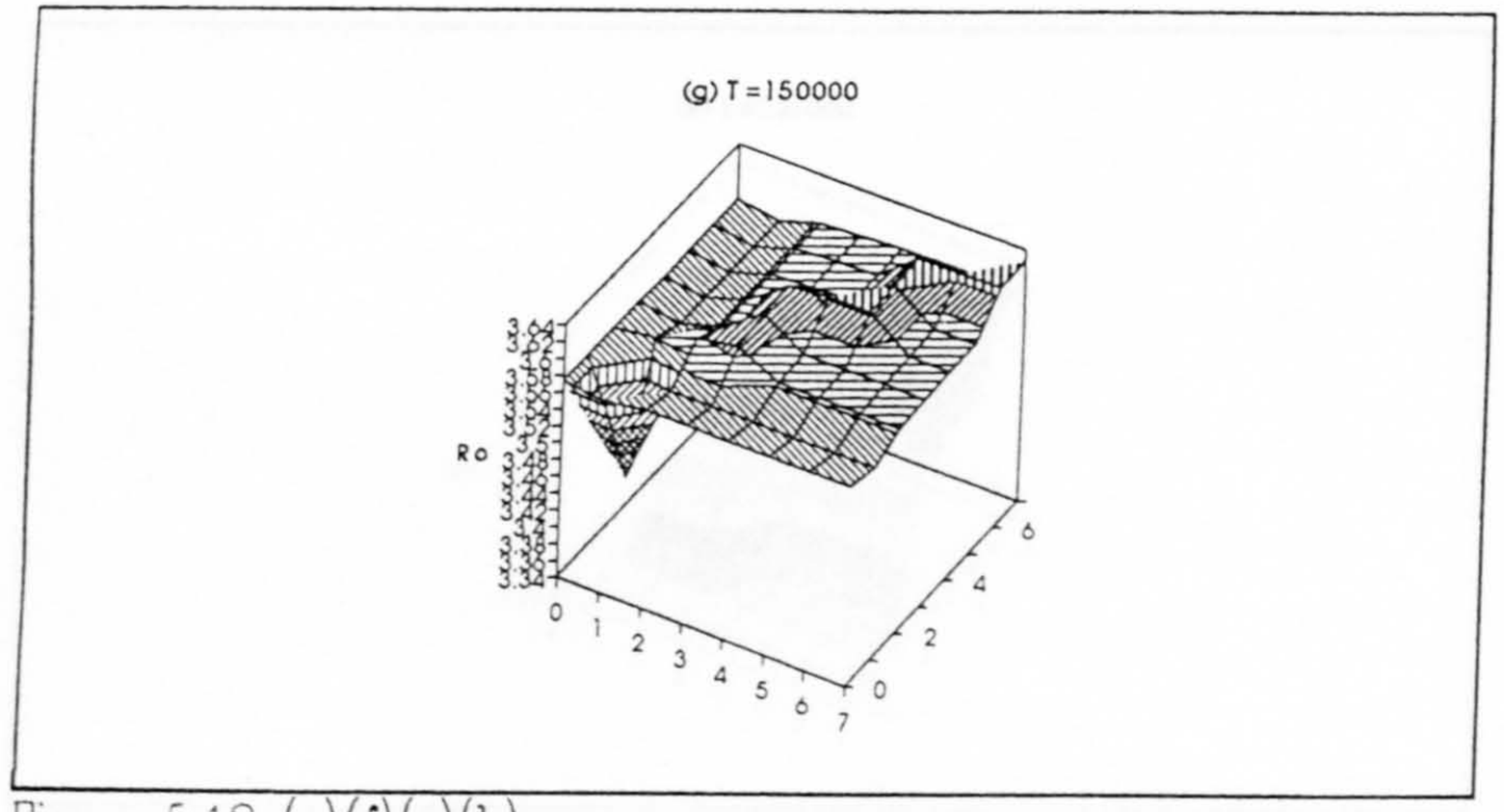

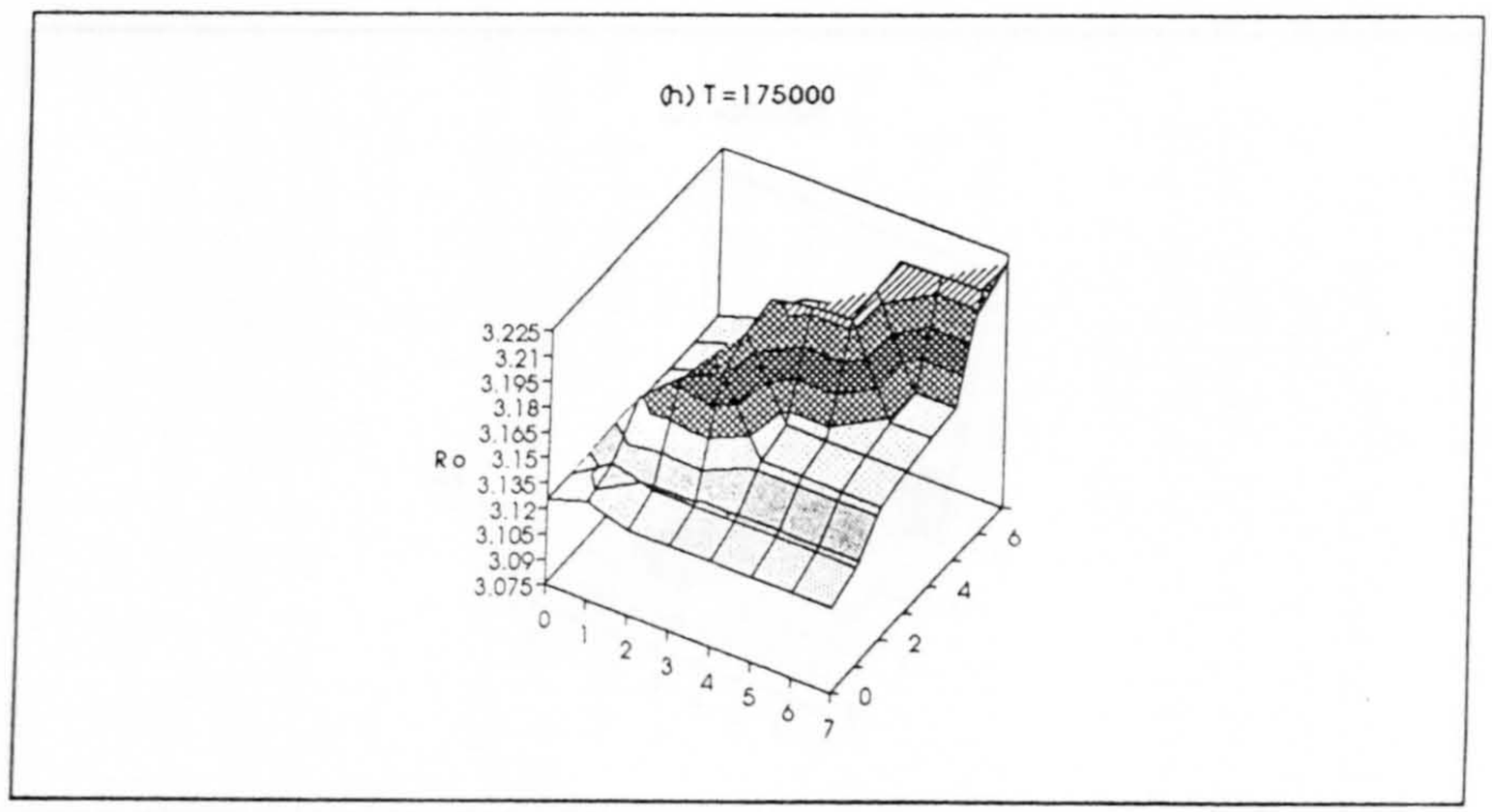

Figure 5.12 (e)(f)(g)(h)

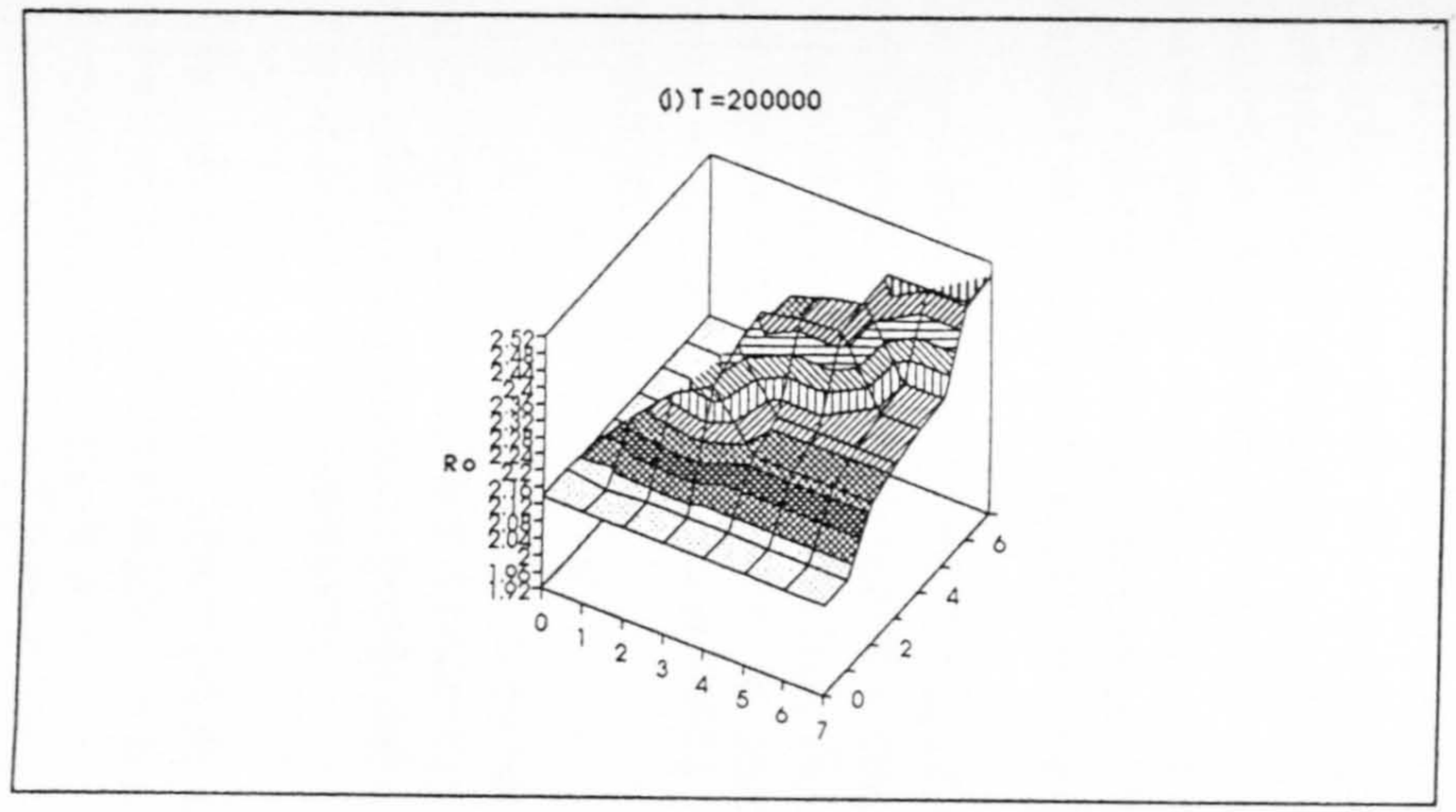

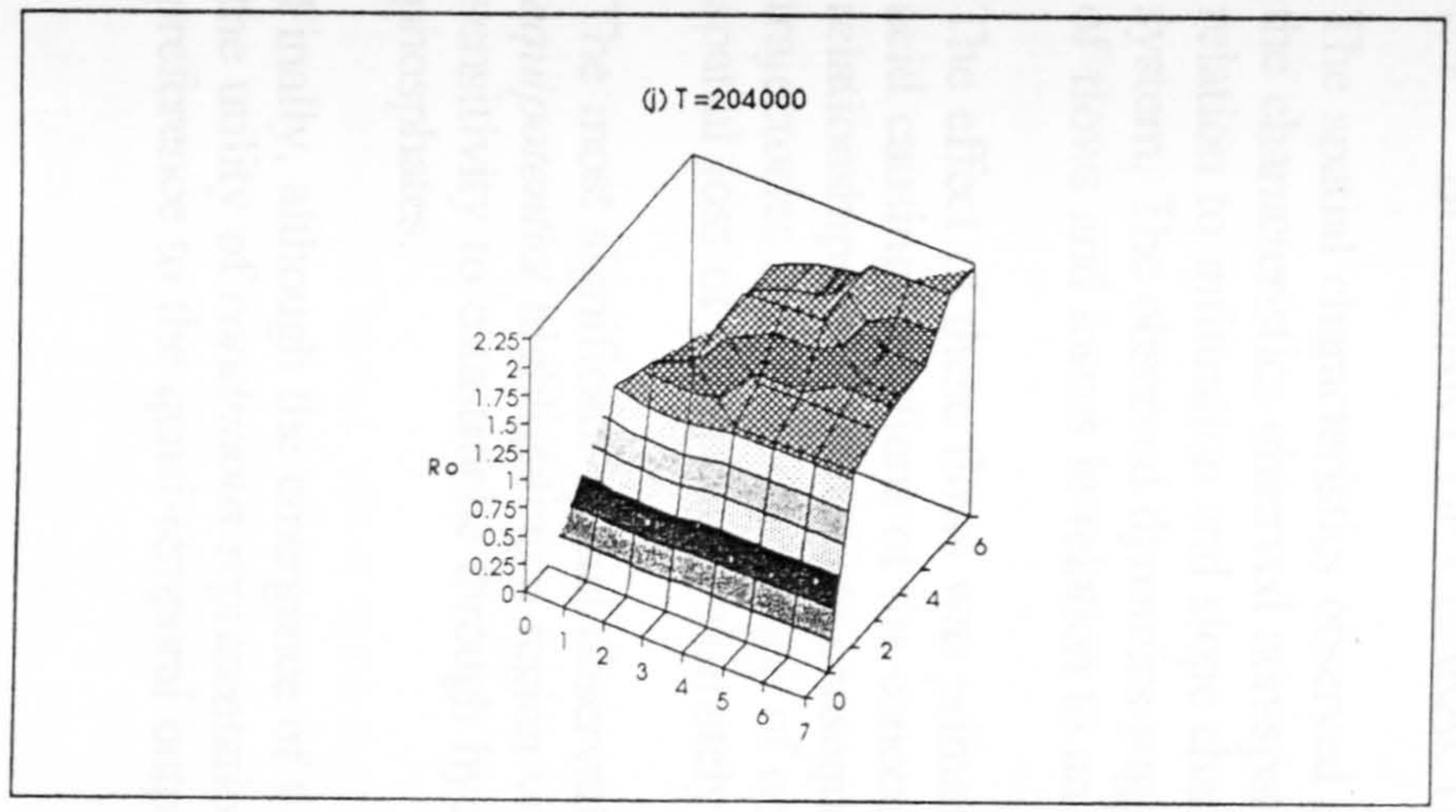

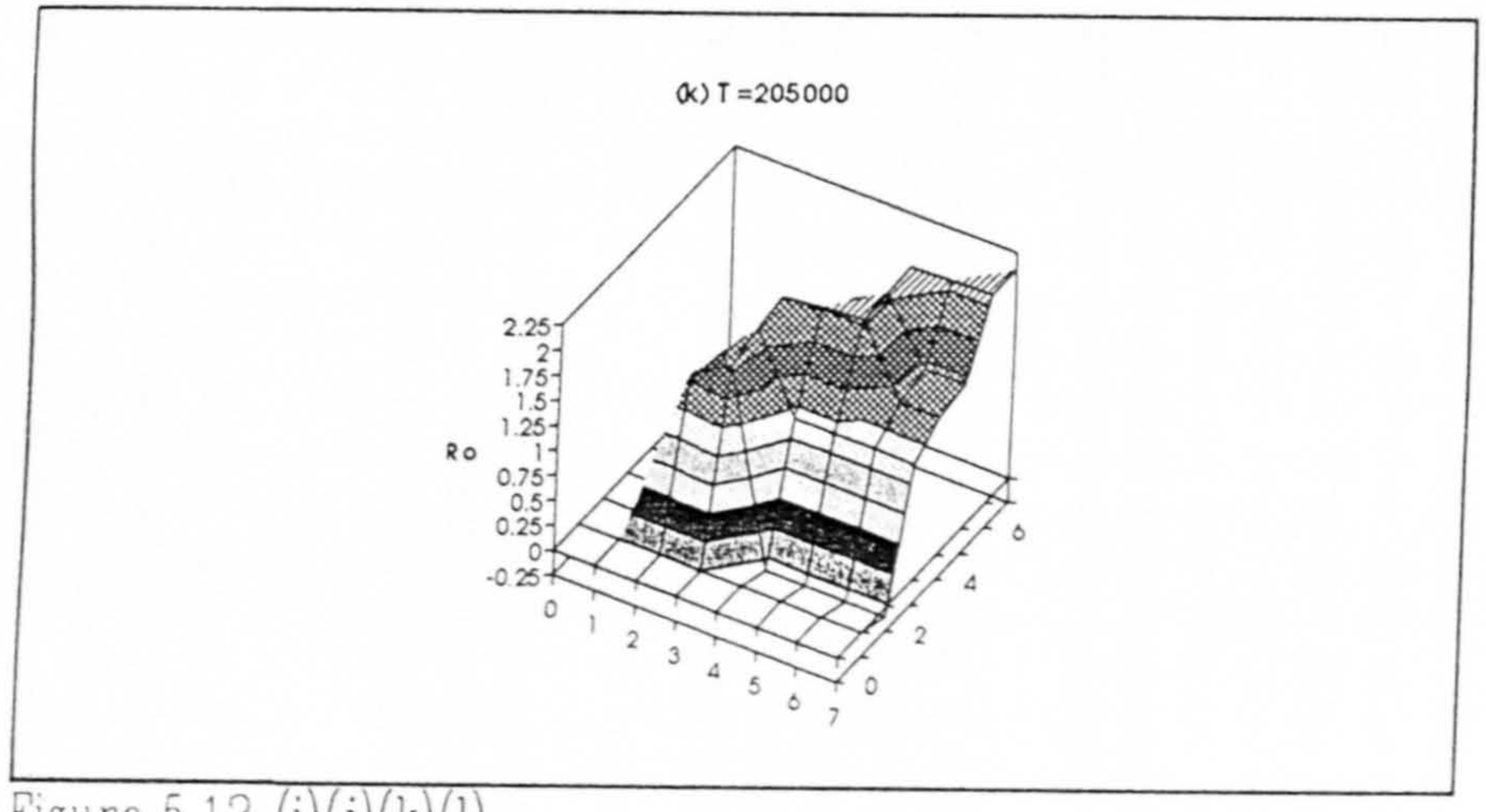

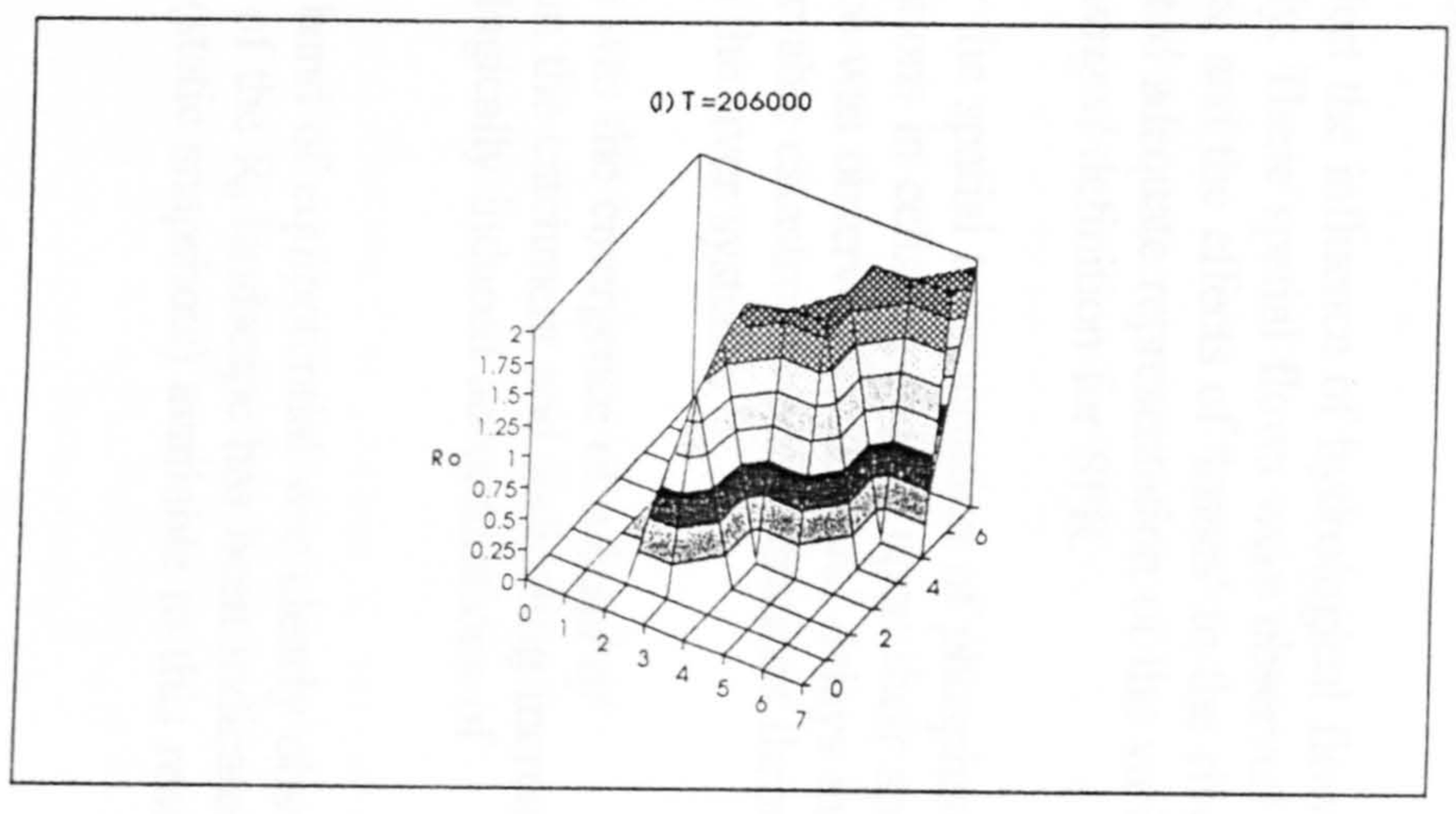

Figure 5.12 (i)(j)(k)(l)

5.4 SUMMARY OF CHARACTERISTICS

The spatial characteristics observed reflect the influence of hydrological flows upon the characteristics observed non-spatially. These spatial flows were observed in relation to infiltration and slope changes, and the effects of 'losses' to the river system. The observed dynamics suggested adequate representation of the variability of flows and losses in relation to an *averaged* definition for SPR.

The effect of these flows was primarily the spatial transportation of phosphates and acid causing variations of the concentrations in cells depending upon their spatial relationships. An immediate consequence was observed in temporal delays in the R_0 trajectories and the suppression of observable catastrophe concentrations through the spatial loss of phosphates, ultimately to the river systems.

The most significant spatial observation was the emergence of a *band of equipotential* highlighting a region within the catchment and indicating increased sensitivity to catastrophe through hydrologically induced accumulations of phosphates.

Finally, although the emergence of this band of equipotential was clearly observable, the utility of *continuous* representations of the R_0 landscape has been indicated, in preference to the quasi-temporal output (static snapshots) available to this research.

CHAPTER 6. CATCHMENT SIMULATIONS

Limitations and lack of availability of appropriate software and hardware to generate a continuous representation of the model output - in the form of moving surfaces - has required that discussion of the model characteristics be in conjunction with snapshots of this dynamic surface. A clear conceptualization of the temporal context, within which these snapshots are taken, must therefore be retained.

With this conceptualization it is possible to observe the emergent characteristics of simulations by examining the spatial differences between the surfaces. Where the initial conditions are spatially homogenous, such differences would be indicating a shift in the timing of potential catastrophe.

Where the simulations are based upon these homogenous initial conditions, snapshots will be taken at T=100000 (27.4 years) so that the emergent characteristics may be compared with the patterns displayed in Simulation I, shown in Figure 5.11.

The effect of spatial flows upon R_0 has been discussed in Chapter 5, and presented in Figures 5.11 and 5.12. The overriding characteristic highlighted by this simulation is the emergence of a band of equipotential around the simulated catchment where an increased accumulation of adsorbed phosphates results in an indication of catastrophe in advance of adjacent regions, and surrounding any troughs indicating particularly high phosphate concentrations, as seen in CELL [1,1] in Simulation I.

As will be shown below, this band of equipotential, highlighting areas of maximum phosphate concentrations and adsorption rates, remains the overriding characteristic irrespective of alterations in initial hydrological conditions. However, these bands cannot be distinguished when the initial chemical conditions (soil composition) are varied spatially, since adjacent cells will no longer reflect equivalent initial values for R_0 or characteristic R_0 trajectories. This latter situation emphasises the potential benefit of continuous output since static comparisons will be less meaningful.

To provide a degree of validation of the emergent patterns generated by the various simulations, it would be useful to have at least two reference points describing the chemical composition of the soil; the major factor determining the remaining absorptive capacity. However, as described in Chapter 3, only a single reference point is available - [Loveland 1990] - which is necessarily used to define the initial conditions for simulations.

This lack of reference points does not invalidate the observed emergent patterns, but more importantly, defines a necessary focus for subsequent monitoring activities. With additional reference points the understanding derived from the simulations may then be reviewed and enhanced.

Although additional reference points may be useful in validating temporal characteristics, and may suggest a need to include additional dynamics or modify existing representations of processes, they will not affect the understanding of the nature of feedbacks and inter-relations in the current model. Since it is an

understanding of the qualitative characteristics of these inter-relationships in the given representation which is central to this thesis, no further reference data has been obtained.

As discussed in Chapter 3, the spatial simulations of catchments presented in the current chapter progress from simple to complex catchments and from hydrologically and chemically homogenous to heterogenous catchments. With such simulations providing a clear understanding of the characteristics of the Rutland Water catchment, the effects of alterations to the overall acid and phosphate loadings are examined. Thus:

- Section 6.1 presents Simulations II to IX - Simulation I presented in Section 5.3.2.1 - addressing the effects of hydrological constraints on chemically homogenous catchments with reference to both simple and complex directional flow patterns defined in Figure 3.5;

- Section 6.2 presents Simulations X to XIII, addressing the effects upon a complex, hydrologically heterogenous catchment of chemical heterogeneity and variations in land use; and

- Section 6.3 presents Simulations XIV to XVII which examine the effects of alterations in acid and phosphate loadings applied to the complex, heterogenous representation of the Rutland Water catchment (Simulation XI).

6.1 HYDROLOGICAL (SPATIAL) CONSTRAINTS

Examination of the effects of the hydrological constraints upon the spatial R_0 landscapes is carried out using chemically homogenous initial conditions throughout. Simulation I (see section 5.3.2) is used as a baseline reference - without rivers - for examination of these constraints upon a simple, hypothetical catchment using a flow pattern defined by Figure 3.5(a). These simulations are presented in section 6.1.1.

Equivalent simulations are performed (see section 6.1.2) using a complex flow pattern representing the Rutland Water catchment (Figure 3.5(b)). The latter simulations (VIII and IX) incorporate a degree of hydrological variability based upon the HOST classifications and the topography of the catchment.

6.1.1 SIMPLE, HOMOGENOUS CATCHMENTS

In order to examine the effects of hydrological losses to rivers, four further simulations were carried out, based upon the same homogenous initial chemical conditions and flow directions as used in Simulation I, altering only the River Type categorization of each cell. Simulation I provides a reference where all cells are of River Category 1 (ie. No rivers are present in the simulation). To summarize the discussions of Chapter 3, the four simulations vary as follows:

II. All cells categorized as Catchment River Feeders (Category 2);

III. All cells categorized as Catchment Rivers (Category 3);

IV. All cells defined as categories 2 or 3 - in Figure 3.5(a) - categorized as Catchment River Feeders (Category 2); and

V. All cells categorized as shown in Figure 3.5(a).

Simulations II and III will provide an understanding of the hydrological effects of catchment river feeders and catchment rivers independently, and can thus be related to the characteristics displayed in Simulation I for category 1 cells. Simulations IV and V will provide an understanding of the effects of the combination of categorizations within a simulated catchment.

6.1.1.1 Simulation II (Catchment River Feeders only)

As can be observed in Figures 6.1(a) and (b), in relation to Simulation I (Figure 5.11) the band of equipotential surrounding the trough at cell [1,1] has been drawn further down the simulated catchment where the main flows from different directions meet. The increase in potential sensitivity (ie. a decrease in R_0) of this central region of the catchment, in relation to Simulation I, is presented in Figure 6.1(c).

Figure 6.2 shows the variation in phosphate concentration across the grid, with the peak concentration emerging at cell [1,1], thereafter falling off as the main line of flow is followed down the catchment. This reduction in concentration emerges as a consequence of the retention of 50% of the surface water flow, containing no phosphate, part of which will infiltrate into the soil further diluting the phosphate.

Thus, an elongation of the pattern generated by Simulation I has occurred since Simulation I involved retention of 100% of the surface water flow, creating a more rapid diluting effect resulting in indication of a potentially less sensitive region further down the valley when no feeder rivers are present.

6.1.1.2 Simulation III (Catchment Rivers only)

Figure 6.3 shows the effects of flows involving major catchment rivers, where all surface water flow enters the river system as opposed to the adjacent cell. Since there is no diluting influence by surface water flows, the band of equipotential appears open-ended, with an initial increase of concentration again emerging in cell [1,1], but in this simulation (III) the concentration subsequently increases rapidly to a maximum, which is maintained along the main flow line (see Figure 6.4) as flows accumulate, whereas Simulation II shows a rapid increase followed by a moderate decrease, and Simulation I, a rapid increase followed by a rapid decrease in concentration down the valley.

The effect of these changes in concentration through the catchment - highlighted by the consequent effect upon R_0 shown in Figure 6.3(d) in the difference between Simulations II and III - is higher concentrations emerging lower down the valley

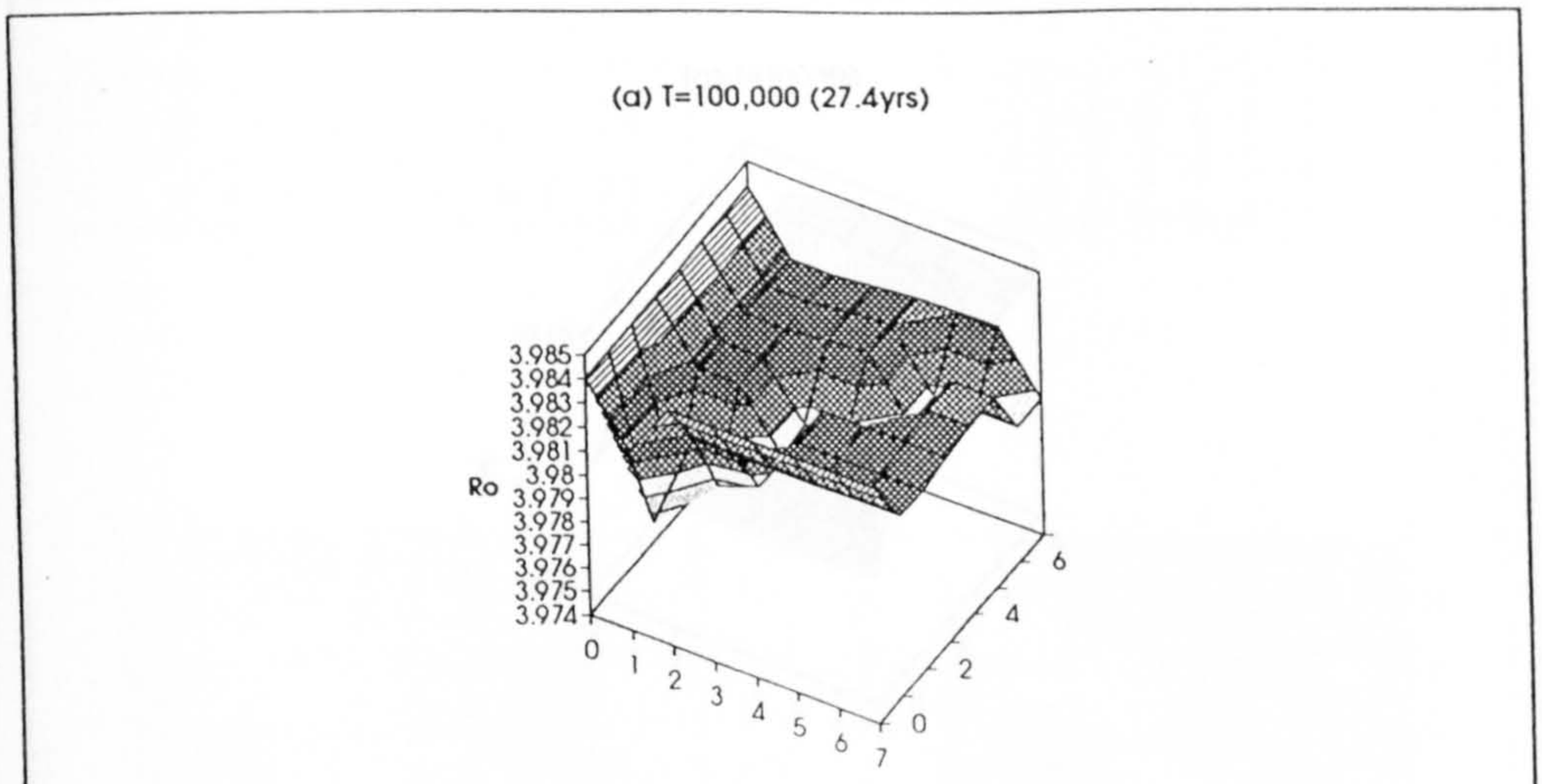

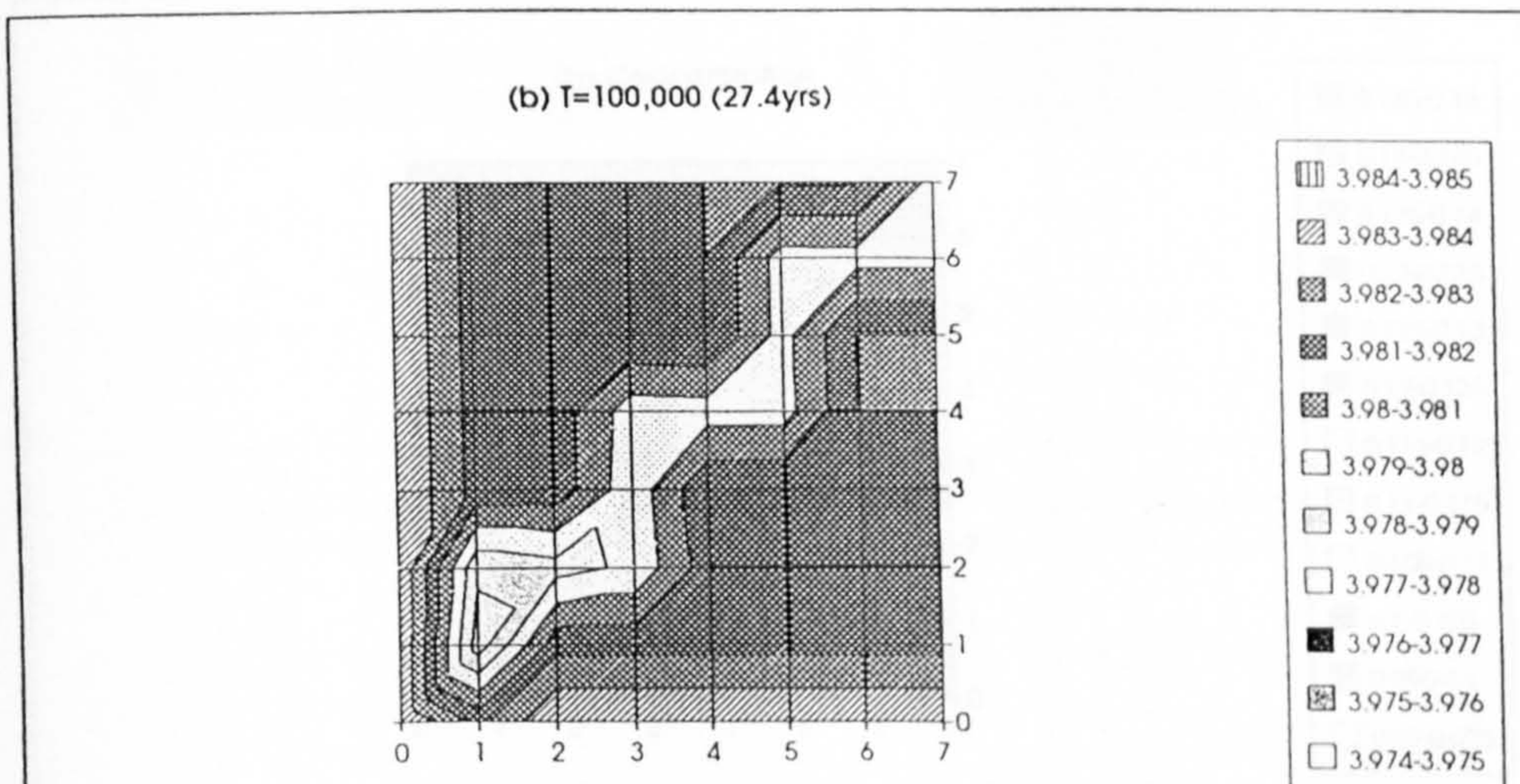

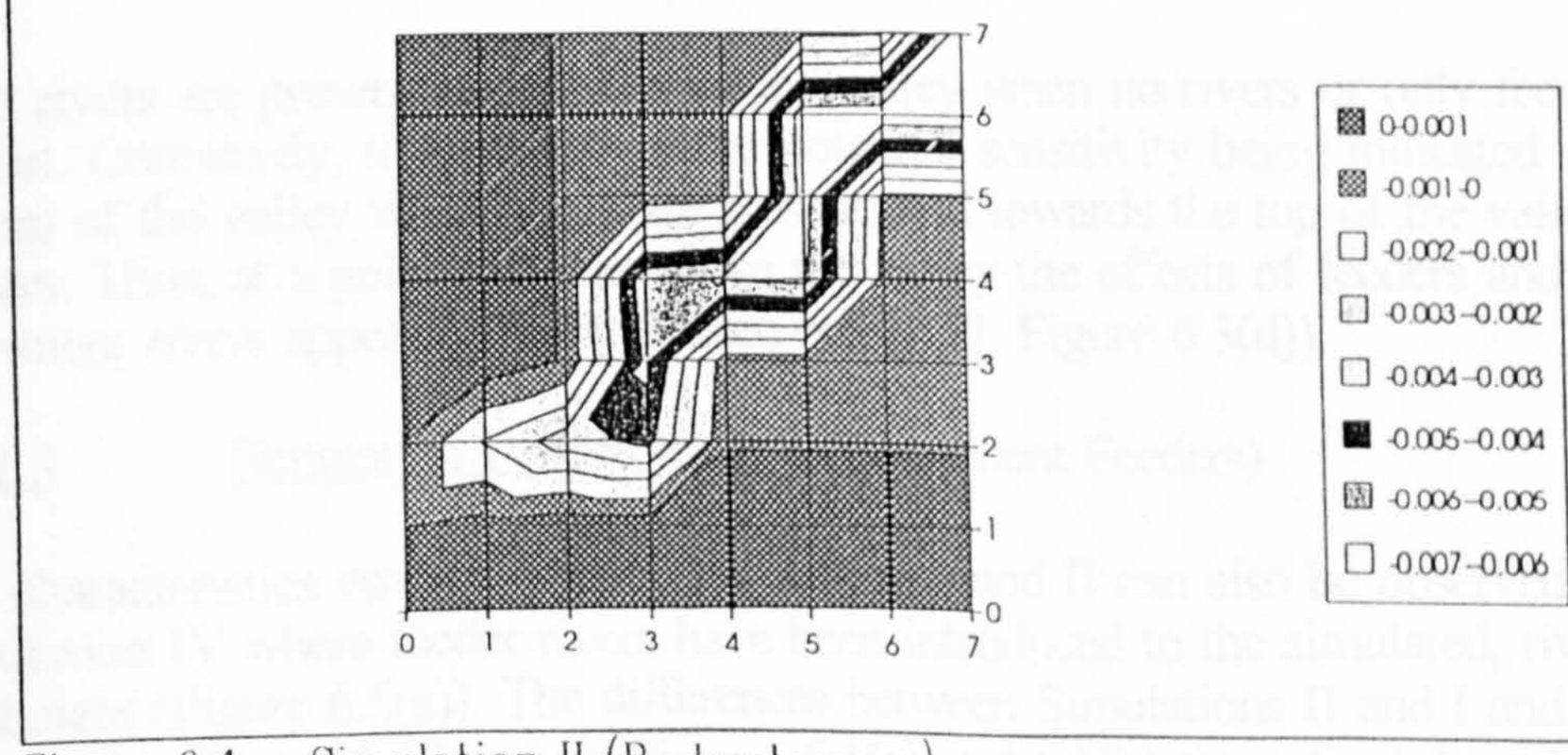

Figure 6.1 - Simulation II (R_0 landscapes)

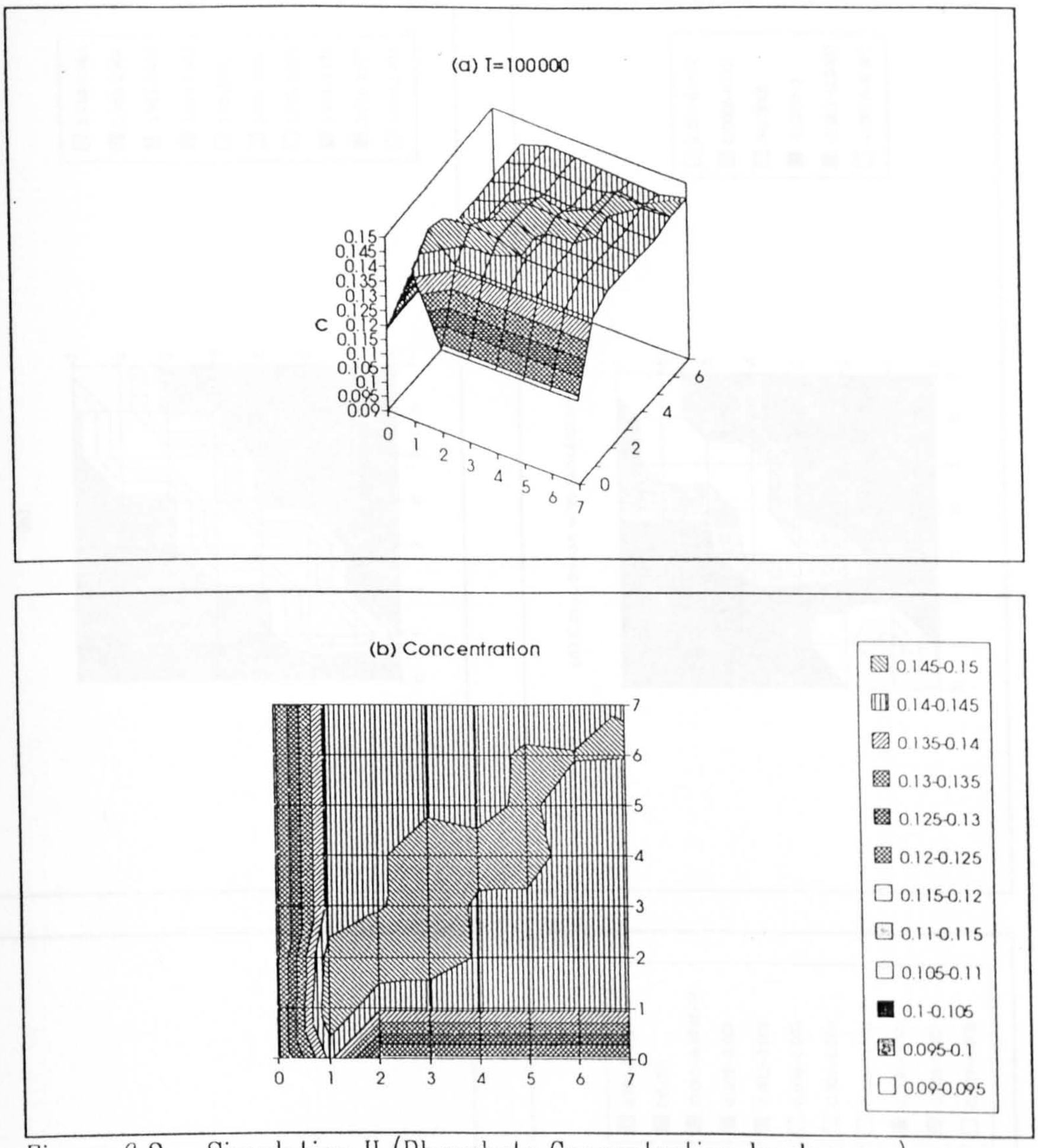

Figure 6.2 - Simulation II (Phosphate Concentration landscapes)

when rivers are present, and higher up the valley when no rivers or only feeders are present. Conversely, this creates greater potential sensitivity being indicated at the bottom of the valley when rivers are present, and towards the top of the valley for feeders. Thus, at a point part way down the valley the effects of feeders and catchment rivers appear to coincide (see cell [2,2], Figure 6.3(d)).

6.1.1.3 Simulation IV (No River & Catchment Feeders)

The characteristics emerging from Simulations I and II can also be observed in Simulation IV where feeder rivers have been introduced to the simulated, river free catchment (Figure 6.5(a)). The differences between Simulations II and I and Simulations IV and I (shown in Figures 6.1(c) and 6.5(b) respectively) are both qualitatively and quantitatively similar.

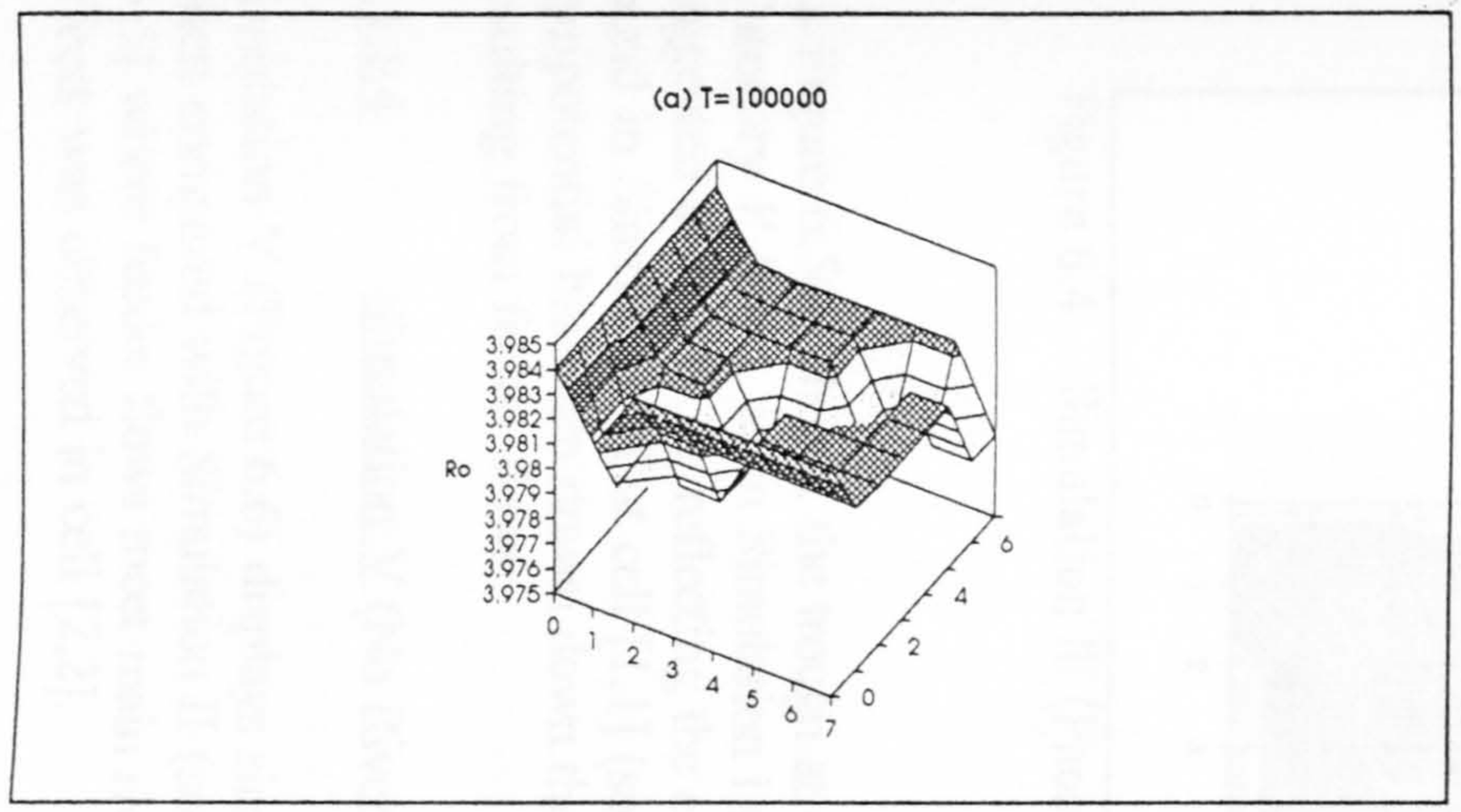

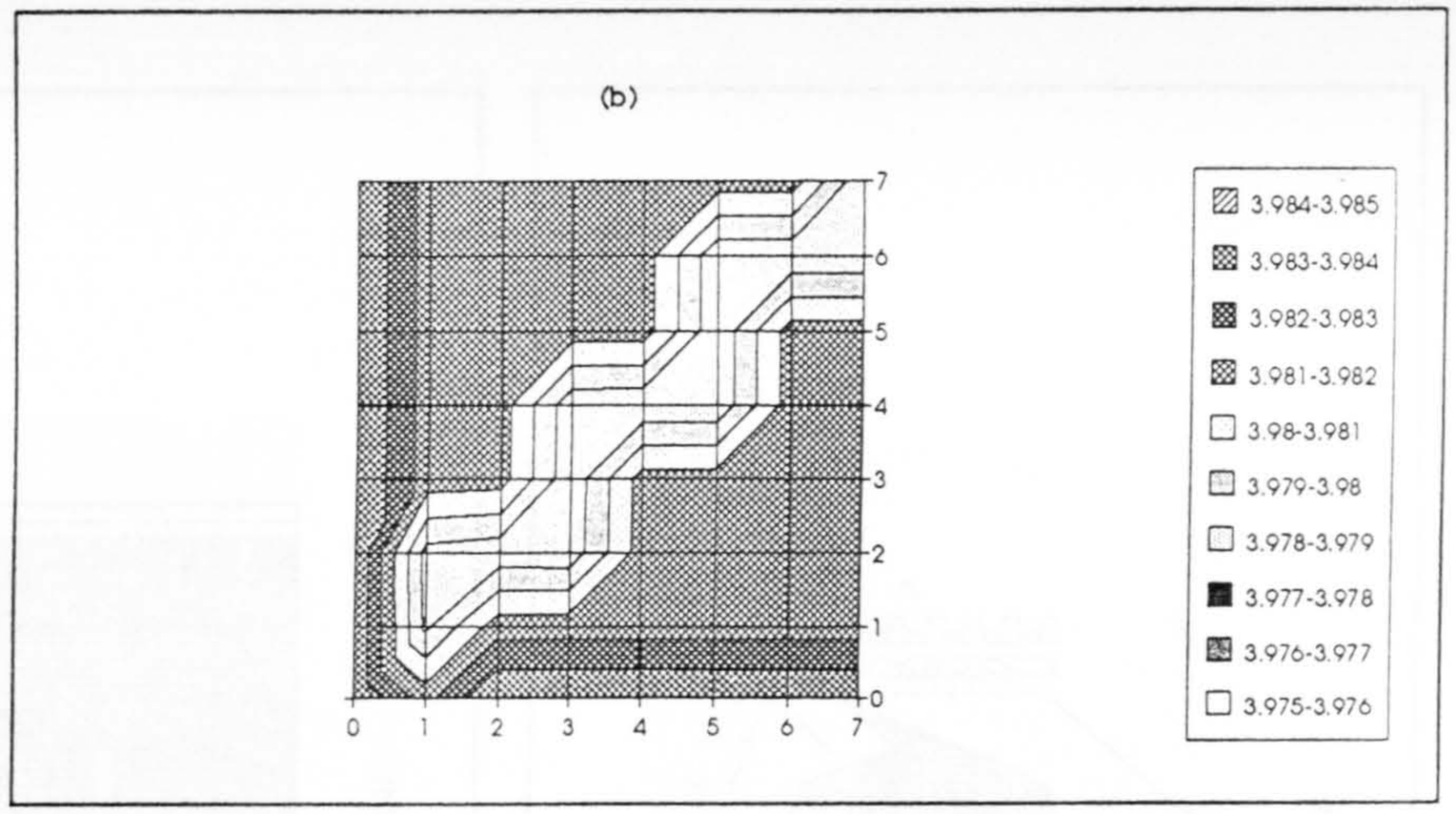

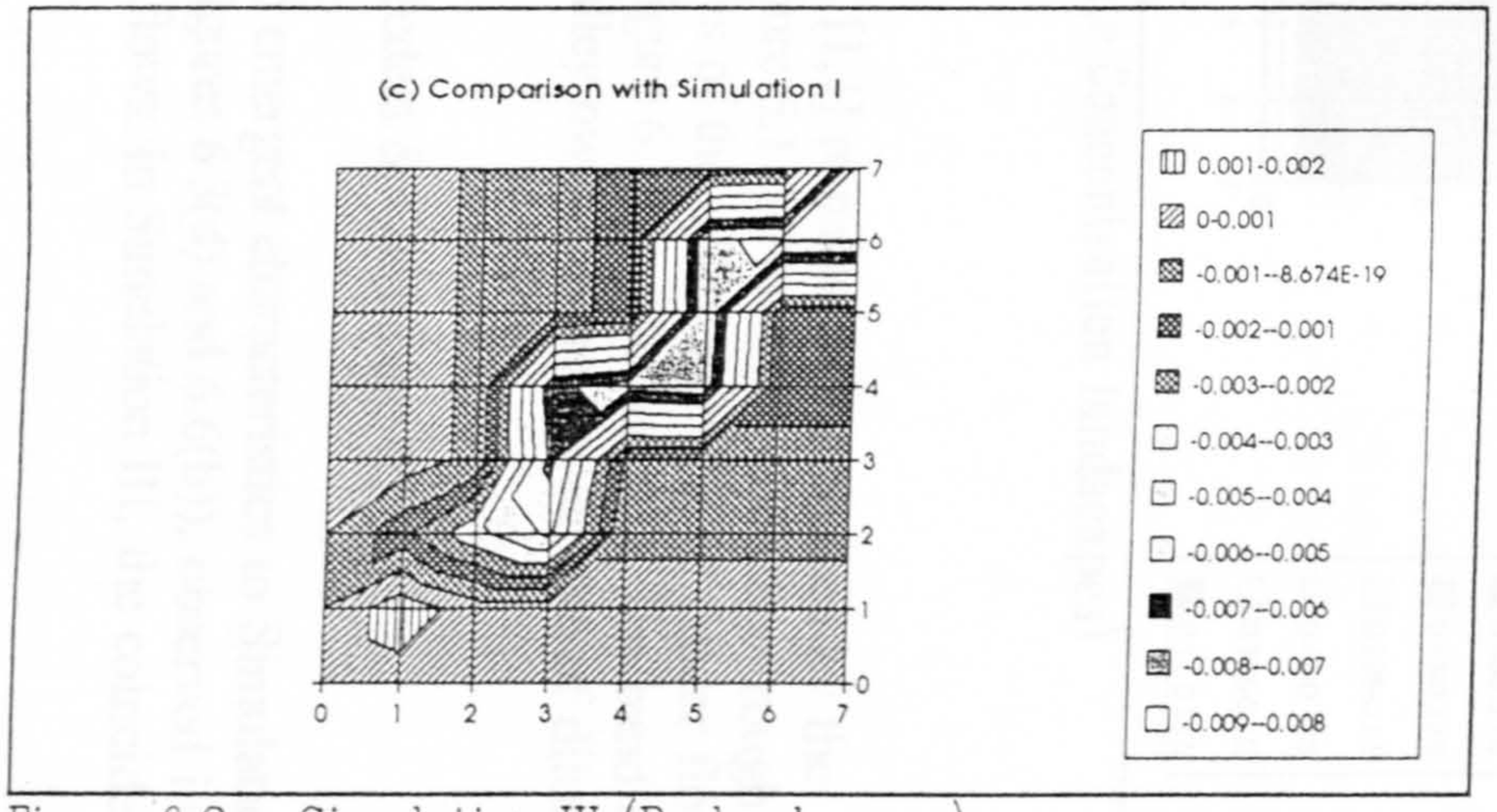

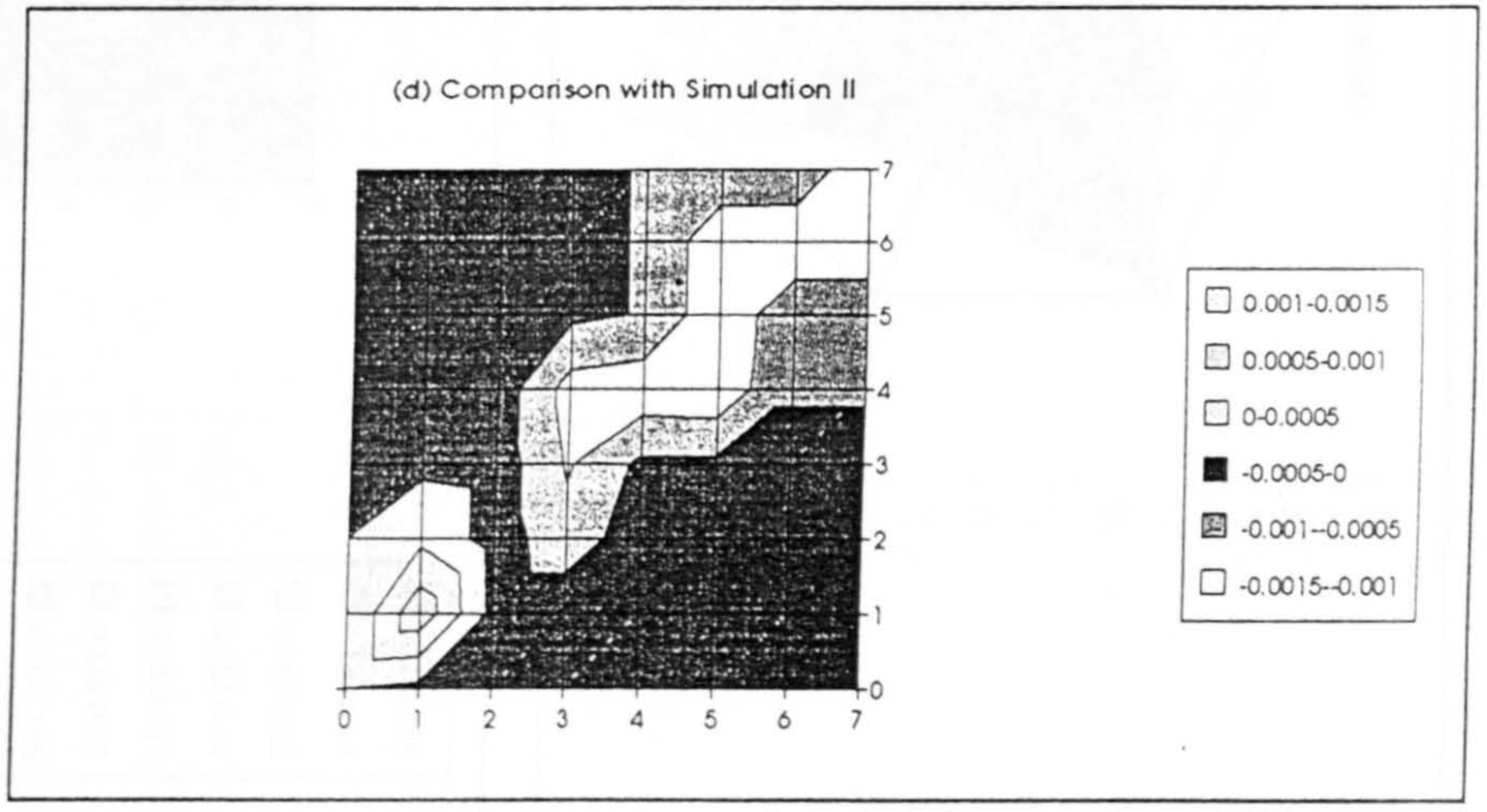

Figure 6.3 - Simulation III (R_0 landscapes)

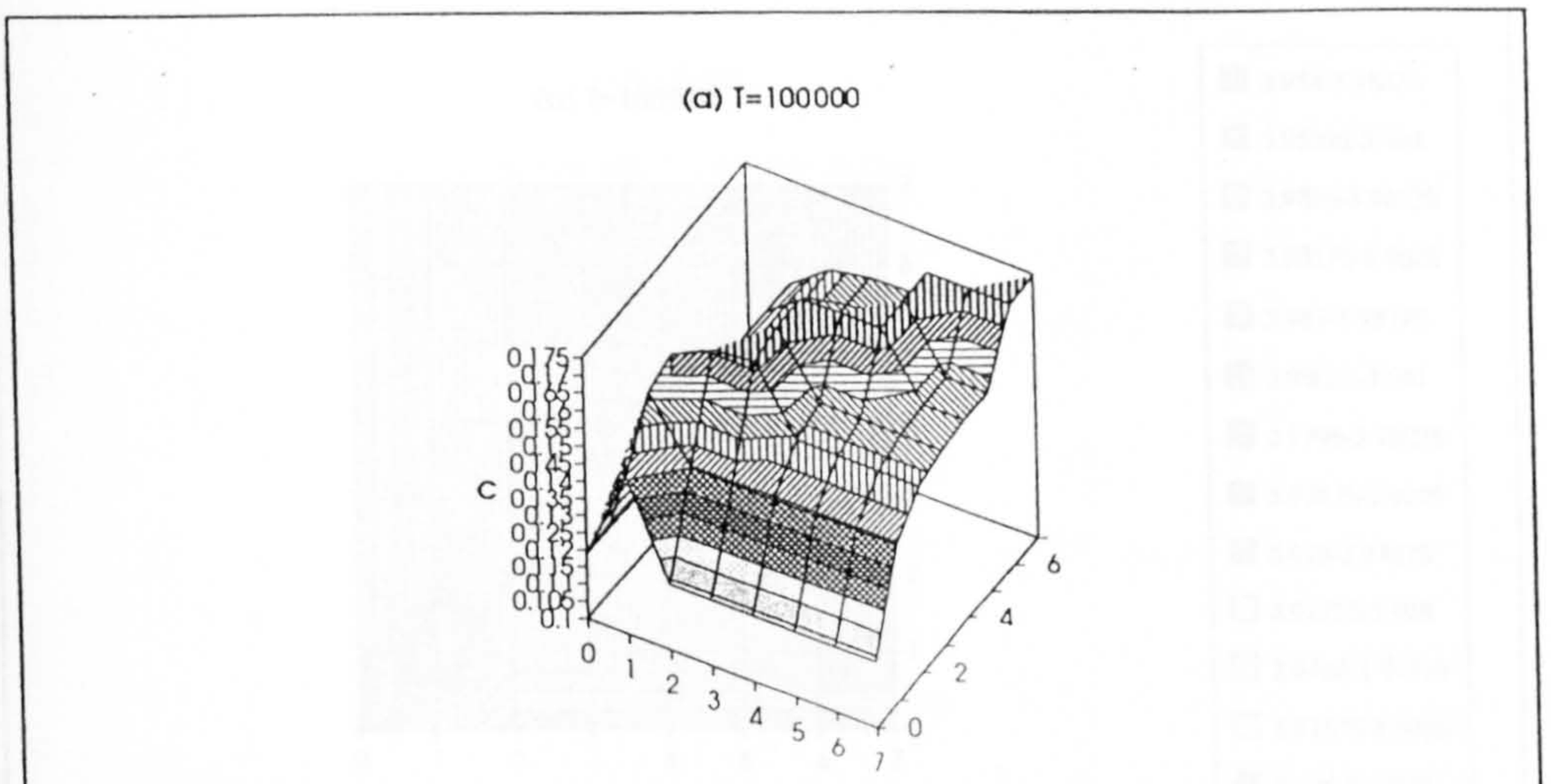

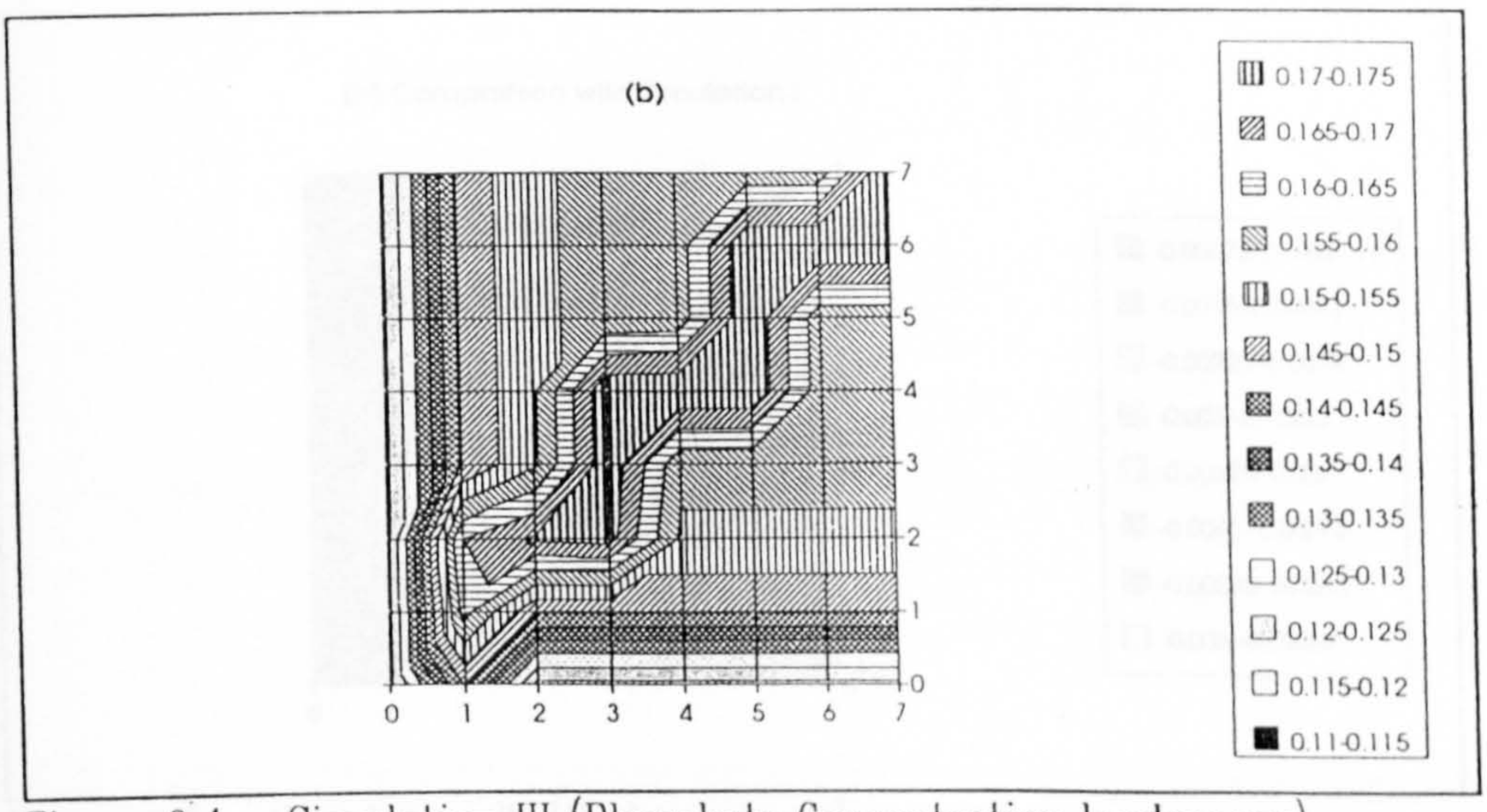

Figure 6.4 - Simulation III (Phosphate Concentration landscapes)

As Figure 6.5(a) shows, the trough at cell [1,1] remains, being created by the 'Category 1' flows, as in Simulation I (Figure 5.11). However, a further trough is suggested at cell [3,2], reflecting the effects of the initial meeting of feeder flows found in Simulation II at cell [1,1] (see Figure 6.1(b)). Furthermore, the band of equipotential has been drawn down the valley owing to the slower rate of dilution resulting from feeder flows.

6.1.1.4 Simulation V (No River, Feeders & Catchment Rivers)

Simulation V (Figure 6.6) displays similar emergent characteristics to Simulation III when compared with Simulation II (see Figures 6.3(d) and 6.6(b)), observed in cell [5,5] where feeder flows meet main river flows. In Simulation III, the coincidence of effects was observed in cell [2,2].

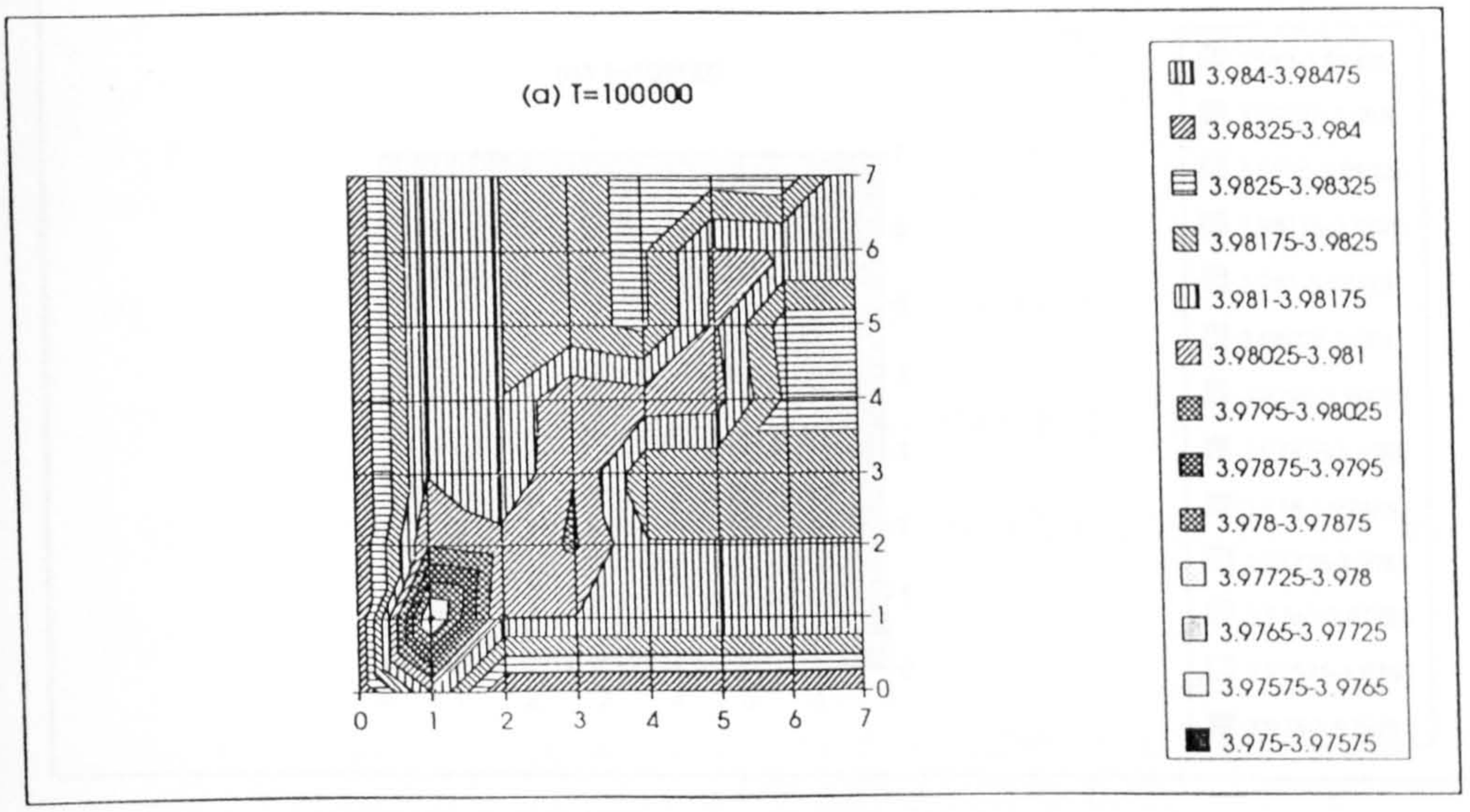

Figure 6.5 – Simulation IV (R_0 landscapes)

In the current simulation (V), this effect is highlighted by an initial drop in concentration, or increase in potential sensitivity, followed by a rapid increase towards a maximum concentration. Thus, a ridge of reduced sensitivity has emerged in cell [5,5] (Figure 6.6(a)), holding the extended band of equipotential surrounding the trough at the point that feeder flows meet river flows, and creating another region of equivalent potential further downstream.

Thus, by varying the percentage losses to rivers - described in Chapter 5 - given the categorizations of cells, the patterns of sensitivity emerging due to hydrological flows may be modified to reflect specific catchment characteristics. Examination of the effects of such individual alterations are not addressed by this work except to identify an area of the model which could be analyzed further.

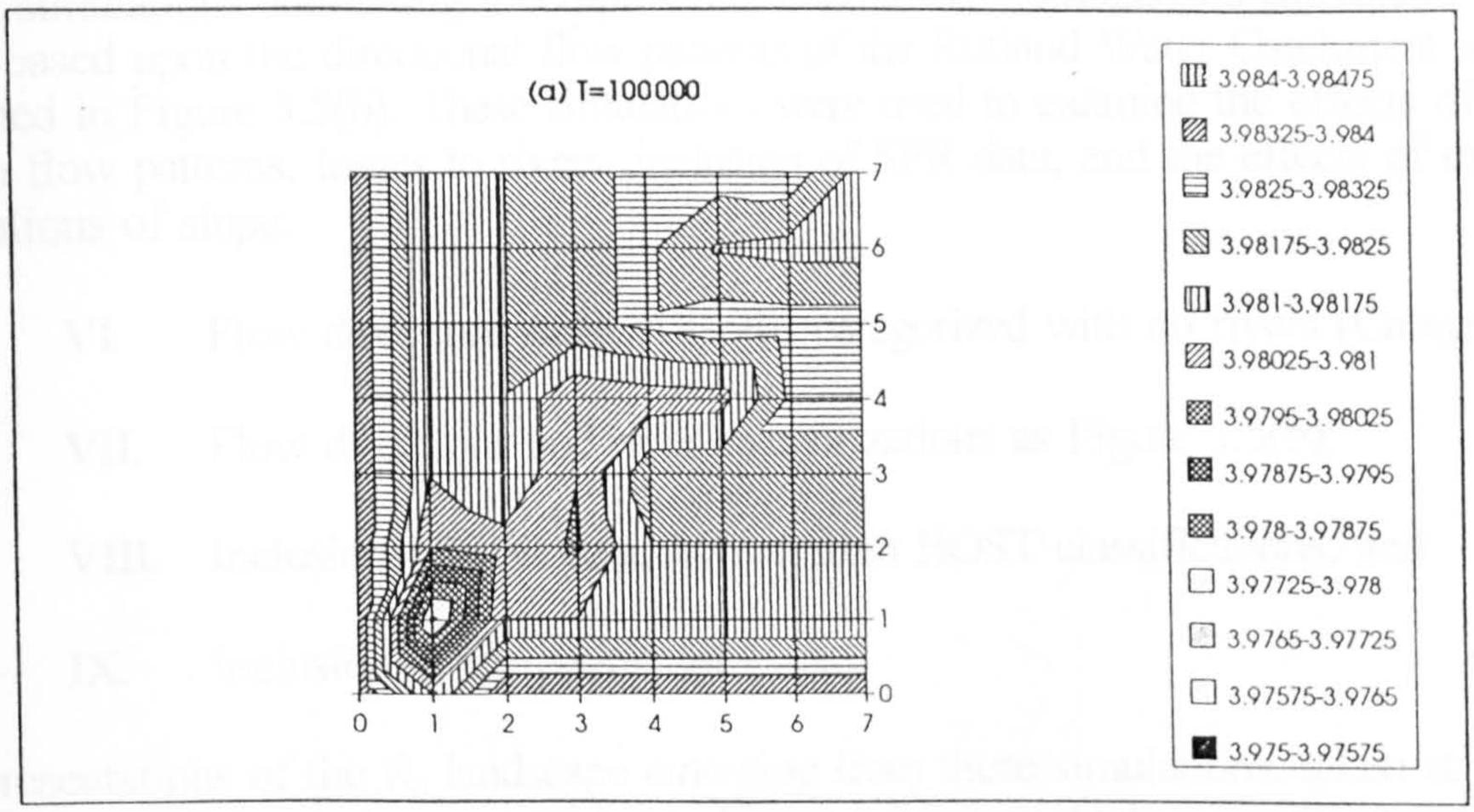

Figure 6.6 - Simulation V (R_0 landscapes)

6.1.2 COMPLEX, HOMOGENOUS CATCHMENTS (RUTLAND)

Observations of the underlying characteristics of R_0, with respect to hydrological flows and losses to rivers have been described above. The direction of flows in Simulations I to V was established with the objective of providing a clear visual representation of the emergent characteristics across the spatial grid. Variations of rates, such as Standard Percentage Runoff (SPR), and capacities, such as Volumetric Moisture Content (VMC), for individual cells were not included.

As may be observed in Simulations VIII and IX, these variations between individual cells represent influences on the internal dynamics of each cell, as opposed to constraints imposed at the catchment level, such as the flow pattern. Such variations may therefore be expected to have a more subtle effect upon the R_0 landscape.

Four simulations addressing a complex, but chemically homogenous catchment were run, based upon the directional flow patterns of the Rutland Water Catchment as defined in Figure 3.5(b). These simulations were used to examine the effects of the main flow patterns, losses to rivers, inclusion of SPR data, and the effects of extreme variations of slope:

VI. Flow directions only; All cells categorized with no rivers (Category 1);

VII. Flow directions and river categorizations as Figure 3.5(b);

VIII. Inclusion of SPR data derived from HOST classifications; and

IX. Inclusion of extremities of slopes.

Representations of the R_0 landscape emerging from these simulations, taken at T=100000 (27.4 years), are provided in Figure 6.7 below. Only a single snapshot is necessary from each simulation in order that the characteristics may be compared with the preceding simulations; although a different flow pattern is employed, the chemical homogeneity ensures that the initial conditions for the simulations remains unaltered.

Representations of the variations between these surfaces, useful for assessing the more subtle effects - relative to the flow pattern - of the additional variability included in each simulation, are provided in Figure 6.8; for example, Figure 6.8(a) - inclusion of rivers - shows a pronounced difference in cells [4,4] and [6,7], and Figure 6.8(b) - inclusion of HOST - shows a pronounced difference in cell [6,7] only, whereas the inclusion of slopes (Figure 6.8(c)) shows minimal change throughout.

6.1.2.1 Simulation VI (No Rivers)

With the same initial conditions for each cell as in Simulation I - but employing a complex flow pattern - regions of equipotential to catastrophe, in relation to the trough highlighted in Figure 5.11(b), may also be observed in Simulation VI. These regions are highlighted in Figure 6.9(a).

The troughs emerging in cells [1,4], [2,3], [4,1], and [6,1] can be related directly to the trough at [1,1] which emerged in Simulation I (Figure 5.11(b)) due to the accumulative effect of the number of cells flowing towards those regions. The peak emerging in cells [4,4] and [4,5], however, reflects similar high levels of saturation, and thus low phosphate concentrations, to those found in Simulation I, cell [7,7].

6.1.2.2 Simulation VII (No River, Feeders & Catchment Rivers)

In Simulation VII, the peak at [4,5] has disappeared as a result of losses of water to the rivers reducing saturation levels and allowing concentrations of phosphate to rise. At the same time, the bands of equipotential have been stretched down both the River Welland and River Nene catchments, following the line of the rivers in both

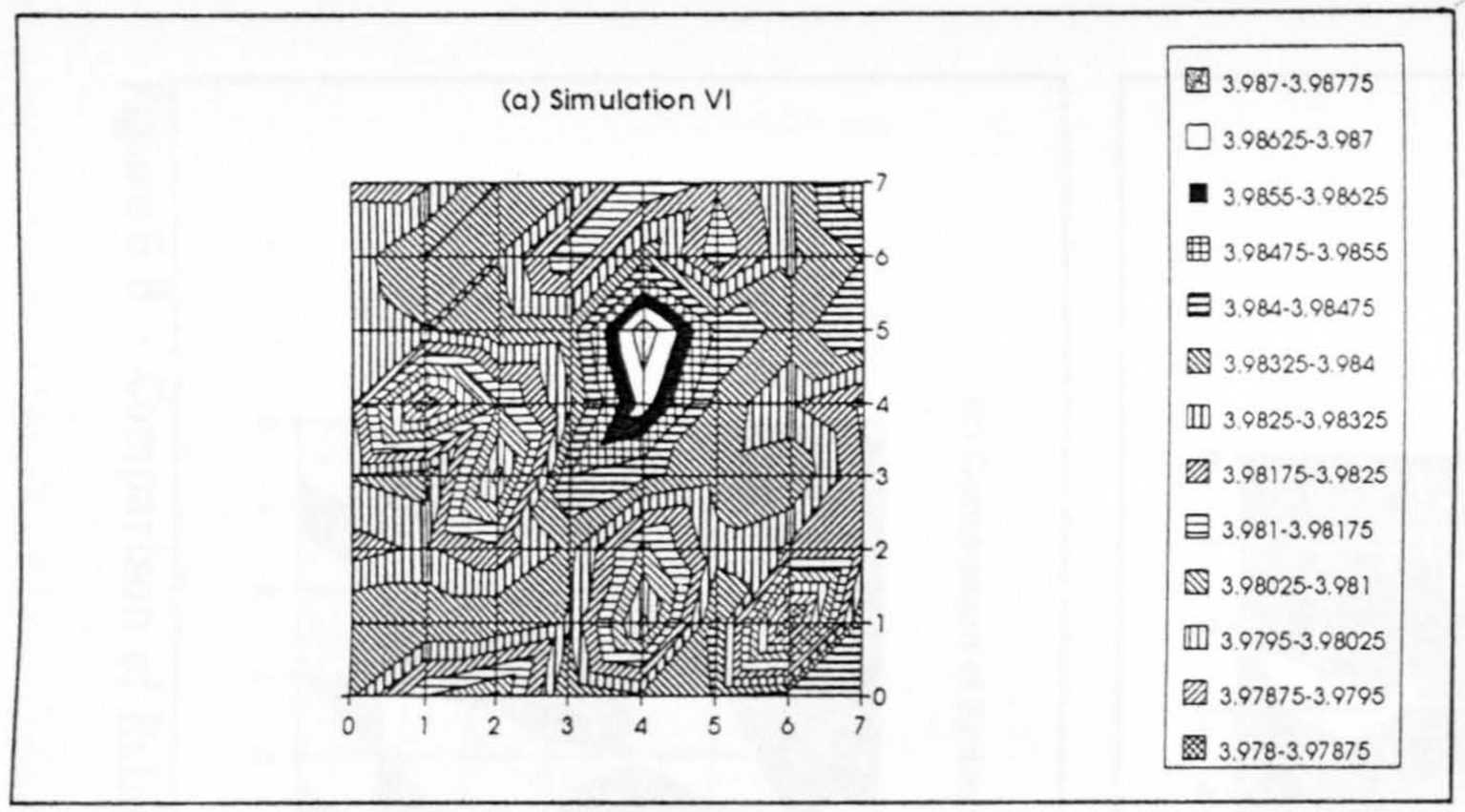

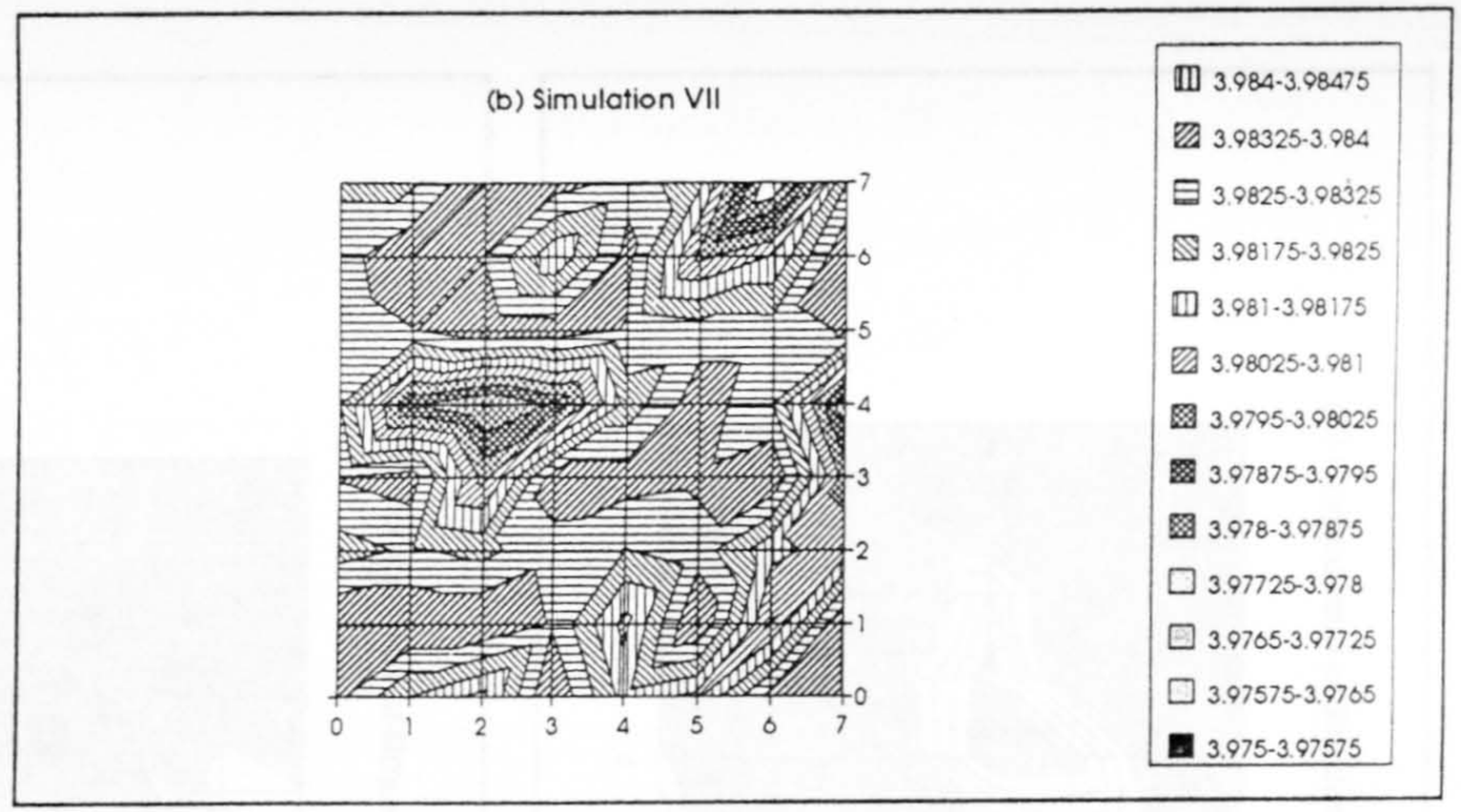

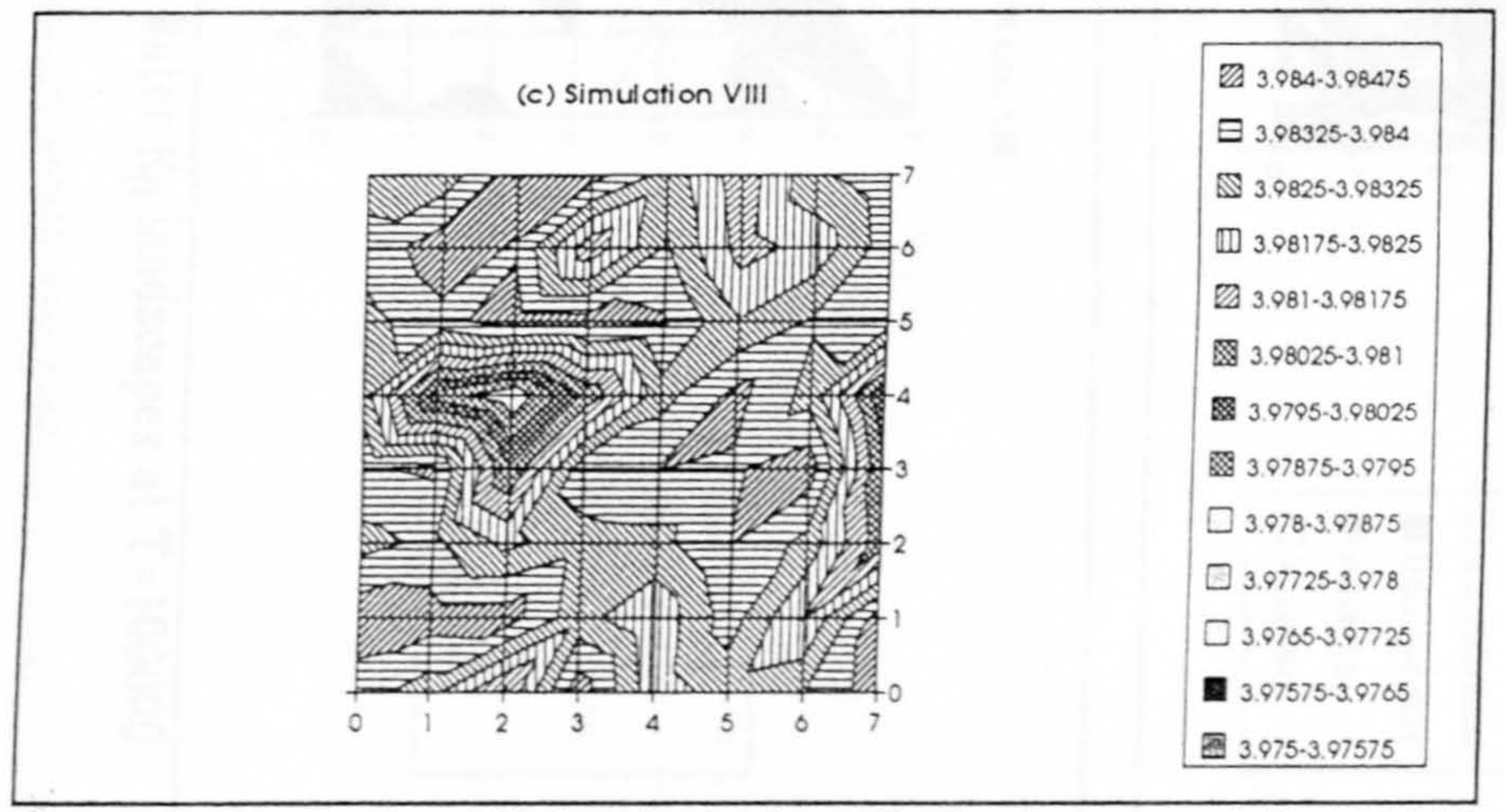

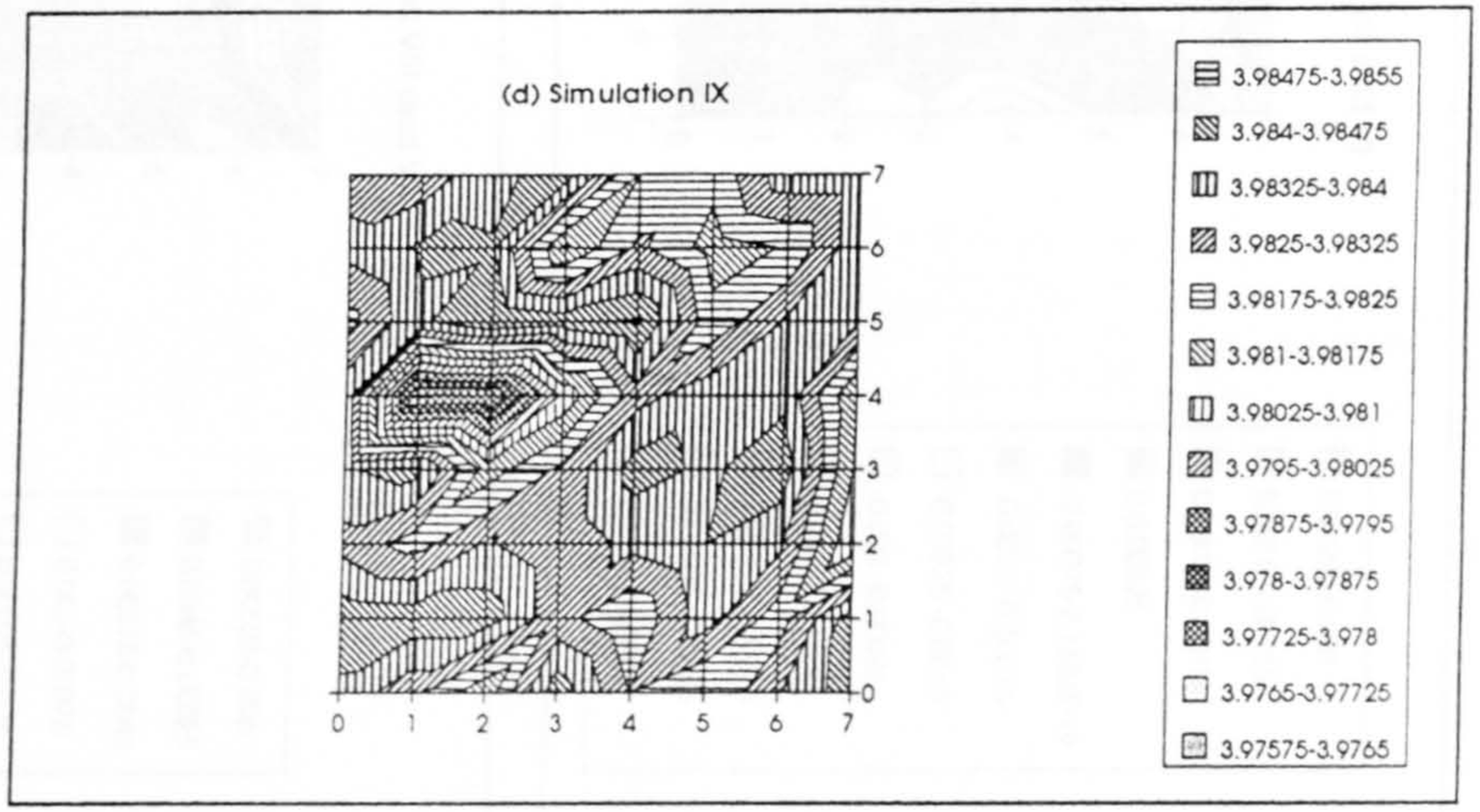

Figure 6.7 – Rutland Water hydrology R_0 landscapes at T=100000

(a) Comparison of Simulations VII and VI

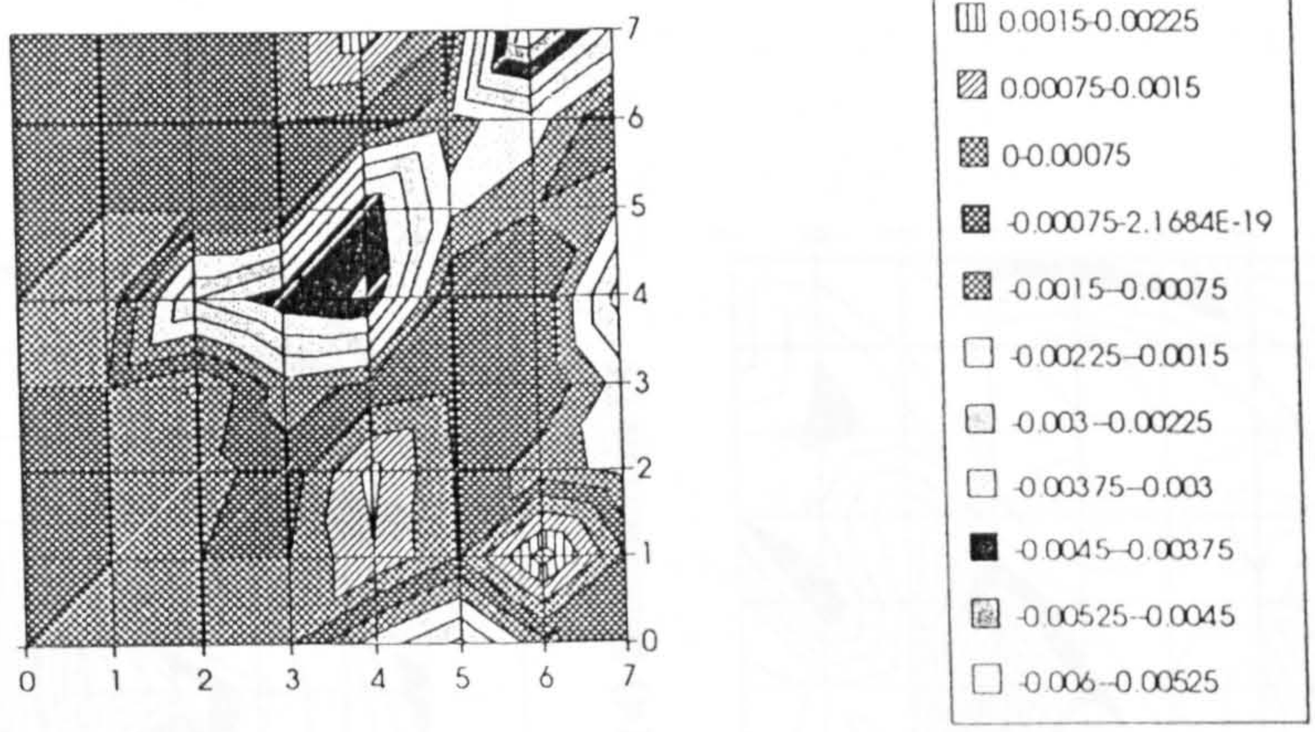

(b) Comparison of Simulations VIII and VII

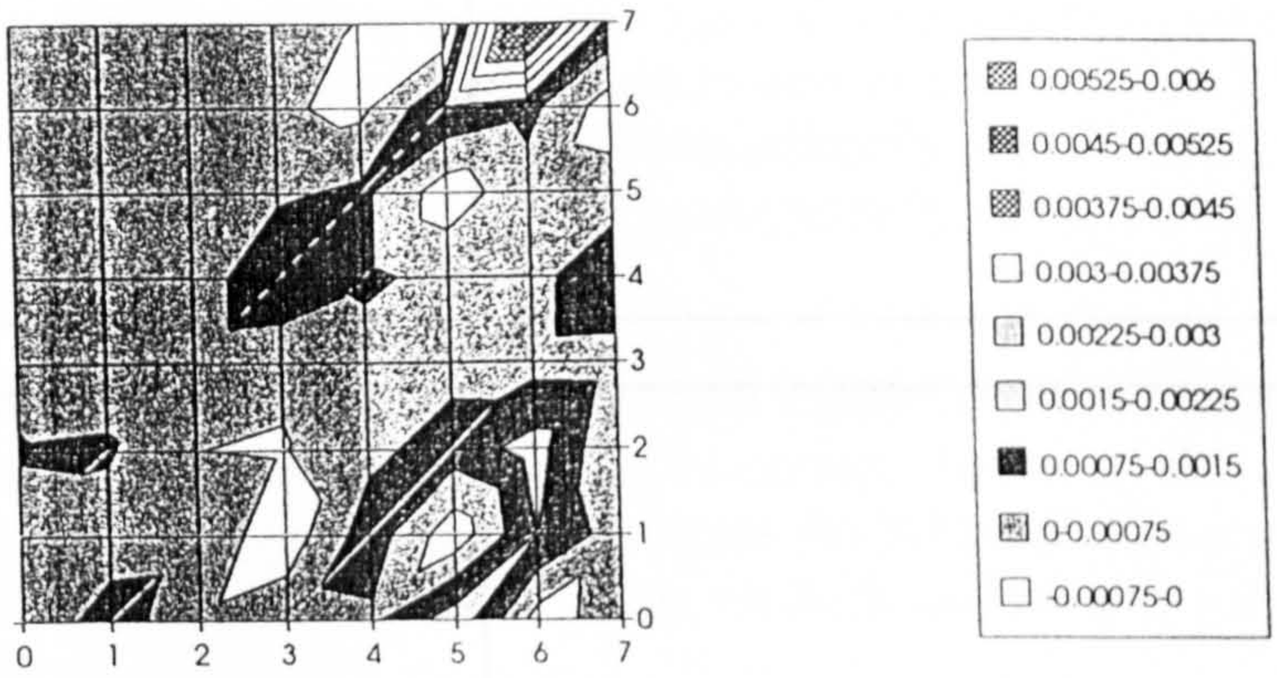

(c) Comparison of Simulations IX and VIII

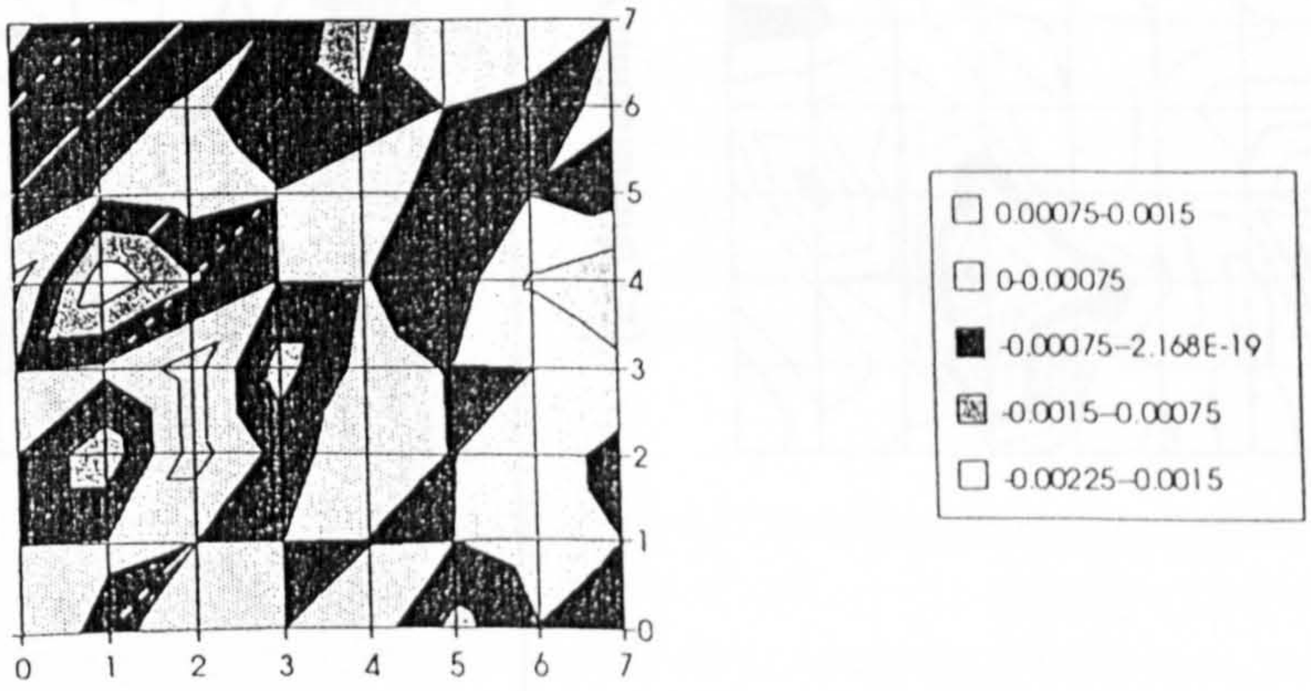

Figure 6.8 – Comparison of Rutland Water R_0 landscapes at T=100000

(a) Simulation VI

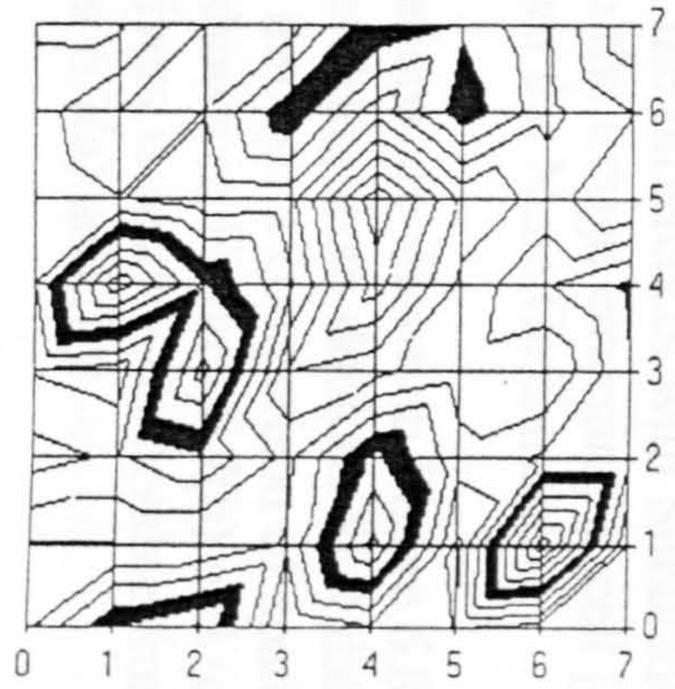

(b) Simulation VII

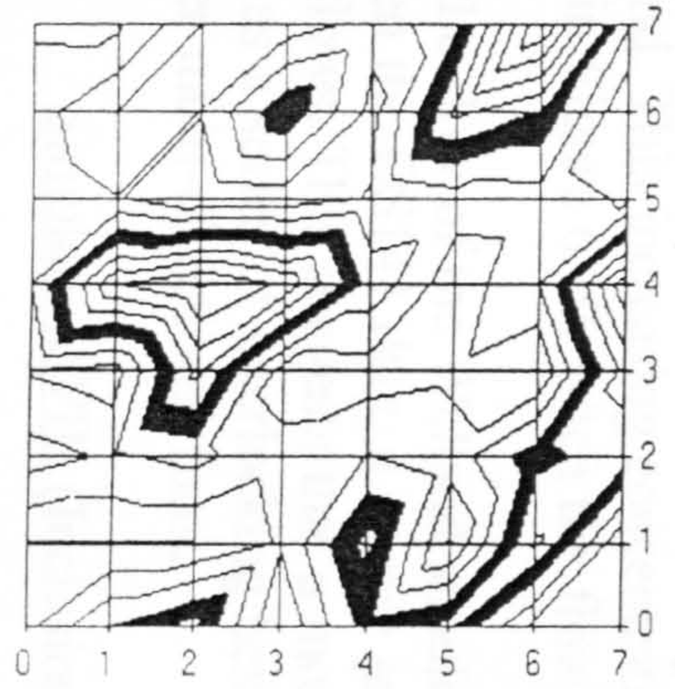

(c) Simulation VIII

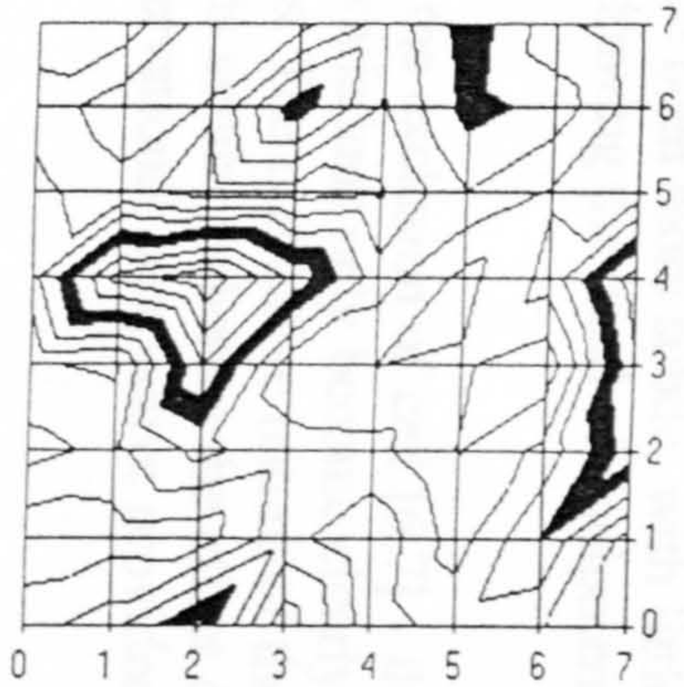

(d) Simulation IX

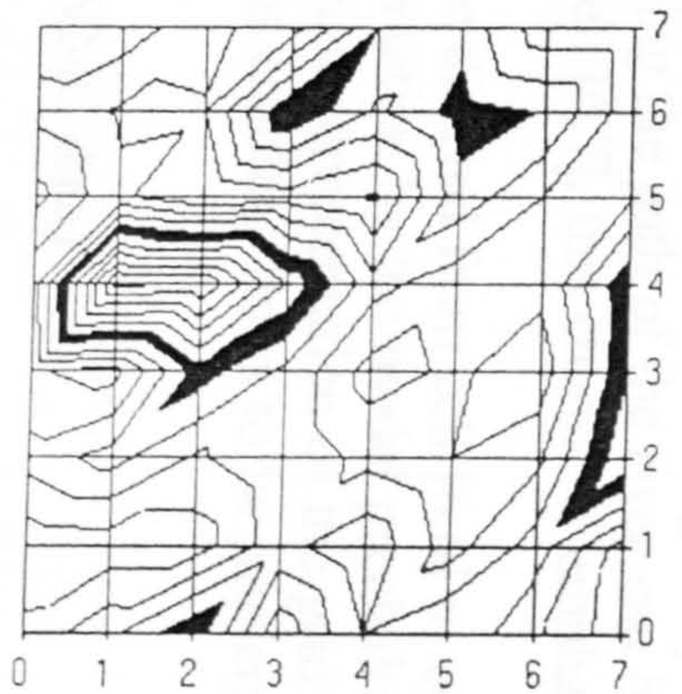

Figure 6.9 – Bands of Equipotential in the Rutland Water Catchment

cases, as shown in Figure 6.9(b). A new trough has emerged as a consequence in cell [7,4] on the River Nene.

An unexpectedly deep trough has also appeared in cell [6,7], which, upon closer examination, is the result of the river in this cell being categorized as a feeder to the Welland, but with the main flow of the Welland directed through this cell, in conjunction with a gradually increasing concentration of phosphate along the path of the Welland. This increasing concentration following the path of the river can be observed in Figure 6.10; when the flow reaches cell [6,7], this change is emphasised. Whereas the flow of the Welland should in fact be directed from cell [6,6] to cell [7,7], given the OS141 data, a square grid representation by the model precludes diagonal flows. This suggests that a more appropriate representation of the grid would be as a series of interlocking hexagons, thus enabling flows to be implemented in a clearer multi-directional form.

6.1.2.3 Simulation VIII (Inclusion of SPR/VMC data)

However, no alterations were made to the model or to the flow directions - to overcome this specific directional flow problem - since this anomalous trough disappears due to changes in SPR and VMC implemented in Simulation VIII (see Figures 6.7(c) and 6.9(c)). This results from an extraordinarily low Standard Percentage Runoff (SPR) suggested by the data, fundamentally affecting the adsorptive processes being modelled.

Already, therefore, an area of lack of knowledge, data and/or understanding has been identified as requiring more detailed examination. In context, however, this cell should already have drawn attention since it represents the initial destination for phosphate rich waters flowing from Rutland Water via both surface and sub-surface flows.

Elsewhere, the differences with Simulation VII have been more subtle, with little effect upon the trough emerging at cell [2,4], but drawing the band of equipotential further down the Nene Catchment.

These variations are shown in Figure 6.8(b). With the exclusion of cell [6,7] - this variation resulting from dubious SPR data - these variations only become clearly observable through a comparison of spatial surfaces. The qualitative nature of the two surfaces - shown in Figures 6.7(b) and (c) - remains similar, whereas the effect of including rivers is readily observable from the observational perspective provided (see Figures 6.7(a) and (b)).

The implication of this is that the river pattern and flow directions represent constraints imposed on the dynamics, the effects of which are clearly observable from a catchment perspective, but the SPR and VMC variations between individual cells represent internal influences on the dynamics which are highlighted only by close examination of variations between outputs of closely related simulation scenarios.

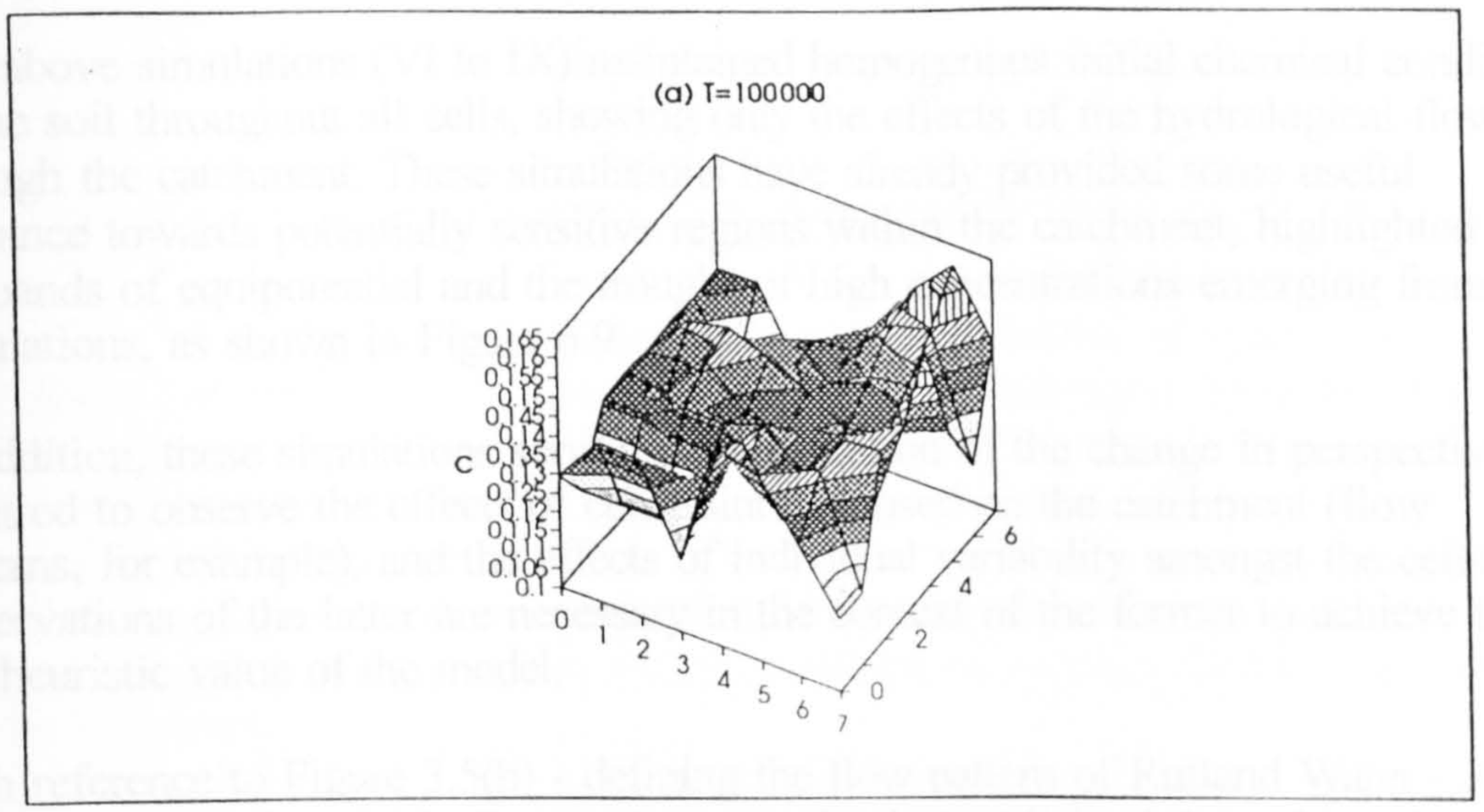

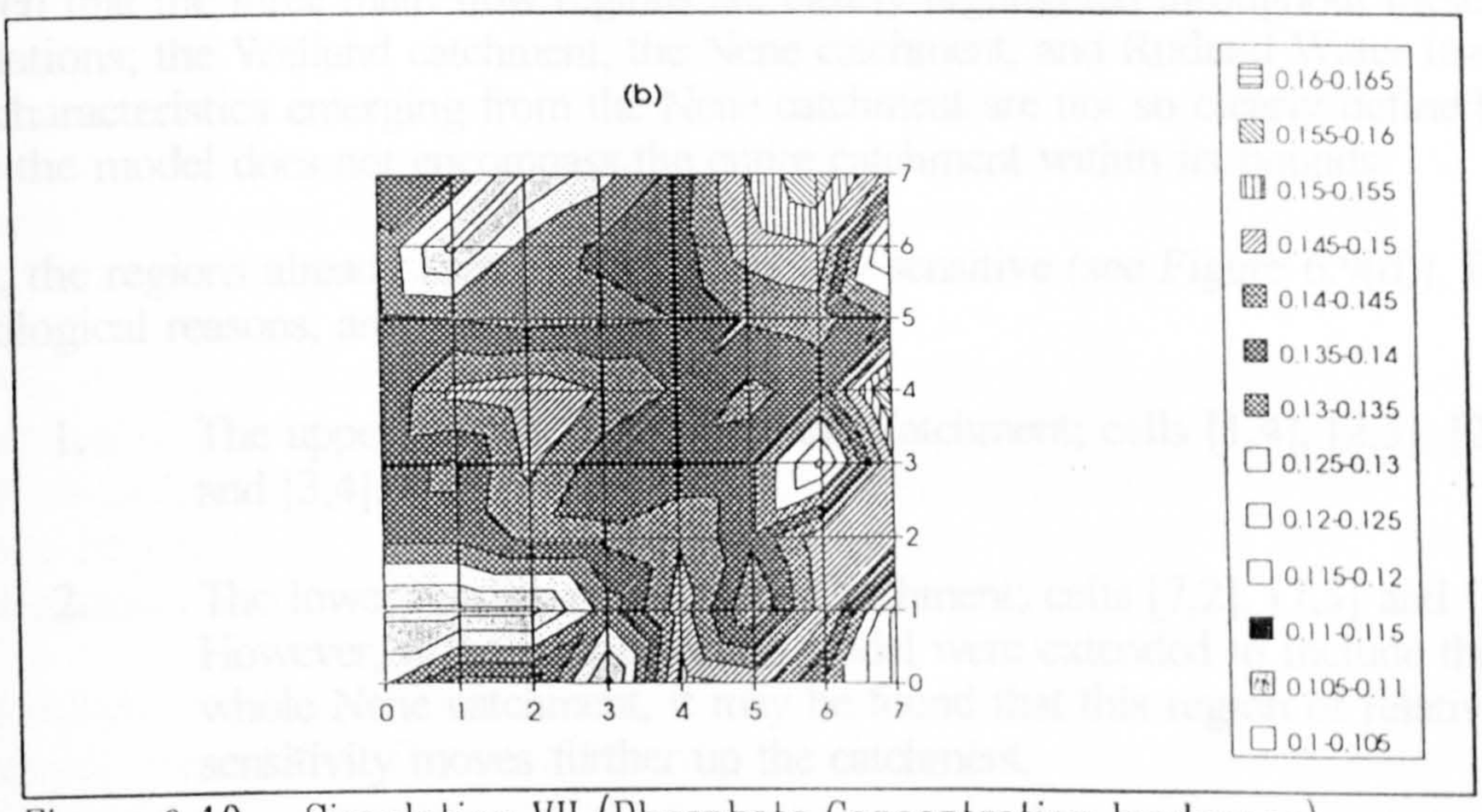

Figure 6.10 – Simulation VII (Phosphate Concentration landscape)

6.1.2.4 Simulation IX (Inclusion of OS141 Slope data)

Simulation IX, incorporating the influence of relative variations of slope across the catchment, has a similarly subtle effect upon the R_0 landscape, as shown in Figure 6.8(d). The effect upon the regions of equipotential has been minimal (see Figure 6.9(d)).

A similar inference can be made, in that the observability of these changes from the catchment perspective is not immediately apparent, suggesting that variations in slope have influence at the cell level and do not represent constraints on the catchment as a whole.

6.1.3 SUMMARY OF HYDROLOGICAL EFFECTS

The above simulations (VI to IX) maintained homogenous initial chemical conditions of the soil throughout all cells, showing only the effects of the hydrological flows through the catchment. These simulations have already provided some useful guidance towards potentially sensitive regions within the catchment, highlighted by the bands of equipotential and the troughs of high concentrations emerging from the simulations, as shown in Figure 6.9.

In addition, these simulations serve as an illustration of the change in perspective required to observe the effects of constraints imposed on the catchment (flow patterns, for example), and the effects of individual variability amongst the cells. Observations of the latter are necessary in the context of the former to achieve the full heuristic value of the model.

With reference to Figure 3.5(b) - defining the flow pattern of Rutland Water - it can be seen that the three main flow regions are clearly highlighted throughout these simulations; the Welland catchment, the Nene catchment, and Rutland Water itself. The characteristics emerging from the Nene catchment are not so clearly defined since the model does not encompass the entire catchment within its bounds.

Thus, the regions already identified as potentially sensitive (see Figure 6.9(d)), for hydrological reasons, are:

1. The upper reaches of the Welland Catchment; cells [1,4], [2,3], [2,4] and [3,4].

2. The lower reaches of the Nene Catchment; cells [7,2], [7,3] and [7,4]. However, if the bounds of the model were extended to include the whole Nene catchment, it may be found that this region of relative sensitivity moves further up the catchment.

3. Rutland Water and the immediately adjacent areas, although this region should have already been identified as potentially sensitive, purely on the basis of the high phosphate concentrations held in Rutland Water, without the need for simulations.

6.2 EFFECTS OF CHEMICAL VARIABILITY

In the preceding section, the effects of constraints imposed on the catchment, and of the hydrological flows between cells, have been observed. Given an understanding of the qualitative effect of these constraints across the catchment, elements of chemical variability amongst individual cells may begin to be included.

Aside from Simulation X - incorporating the initial conditions defined by the chemical variability across the Rutland catchment - the *quantitative* variations effected by this variability may be expected to be subtle since the influences are at

the cell level in a similar sense as found in Simulations VIII and IX. However, it is from the perspective of the catchment that the effects of this variability will be communicated in the form of *qualitative* spatio-temporal landscapes.

6.2.1 COMPLEX, HETEROGENOUS CATCHMENTS (RUTLAND)

Simulations VI to IX, above, have already suggested a number of specific regions in the Rutland Catchment which appear, for hydrological reasons, to be more sensitive to catastrophe (susceptible to flushing) than surrounding regions. In these simulations the variability of soil chemical conditions between individual cells has not been addressed, this diversity fundamentally affecting the remaining adsorptive capacity of the soil at the beginning of the simulations. However, these simulations have provided the spatial context within which the effects of variable chemical conditions may be examined.

The following simulations include these chemical conditions as derived from the NSI data summarized in Table 6.1. From these simulations, therefore, further regions of potential sensitivity are likely to emerge as a consequence of the chemical conditions. Where these regions coincide with hydrologically sensitive regions may provide an indication of the need for a greater degree of resolution in the model to help distinguish between the contributory influences.

The NSI data quantified the soil phosphate content without a distinction between Aluminium or Calcium phosphates. Thus, the derivation of Q_{Ca} and Q_{Al} - discussed below - was achieved in line with the need to calibrate the internal pH calculation with the NSI data; the proportions of Q_{Ca} and Q_{Al} were determined in order that the pH calculation closely reflected the given (measured) pH.

Table 6.1 describes the initial conditions which are gradually incorporated into subsequent simulations. The data described covers the NSI data (units in $kMha^{-1}$), the aggregated HOST data (percentages), the numerical definition of the flow pattern (Figure 3.5(b)) as the proportion of flow in each direction from a given cell, and the data derived from Ordnance Survey information - river types (1, 2 or 3), slope classification (0, 1 or 2), and the percentages of urban and woodland cover.

The NSI data provided details of Aluminium (Al) and Calcium (Ca) content of the soil, phosphates in solution (P), soil pH and 'adsorbed' phosphate. However, given the extent of alternative base cation reserves - such as Sodium (Na) and Potassium (K) - identified by McGrath & Loveland (1992), and the lack of data describing the proportion of phosphates adsorbed by base or acid cation reserves, some modification was required in order to ensure that the model calculated pH values from the chemical data which were comparable with the measured values given in Table 6.1.

Thus, experimentally, the adsorbed phosphates were shared between acid and base cation reserves (defining Q_{Al} and Q_{Ca}), and the alternative Na and K reserves defined as base cations (Ca), until a reasonable correlation between the simulated and measured values of soil pH were observed. This correlation between the calculated and measured pH values is shown in Figure 6.11; no data was available for cell [4,3].

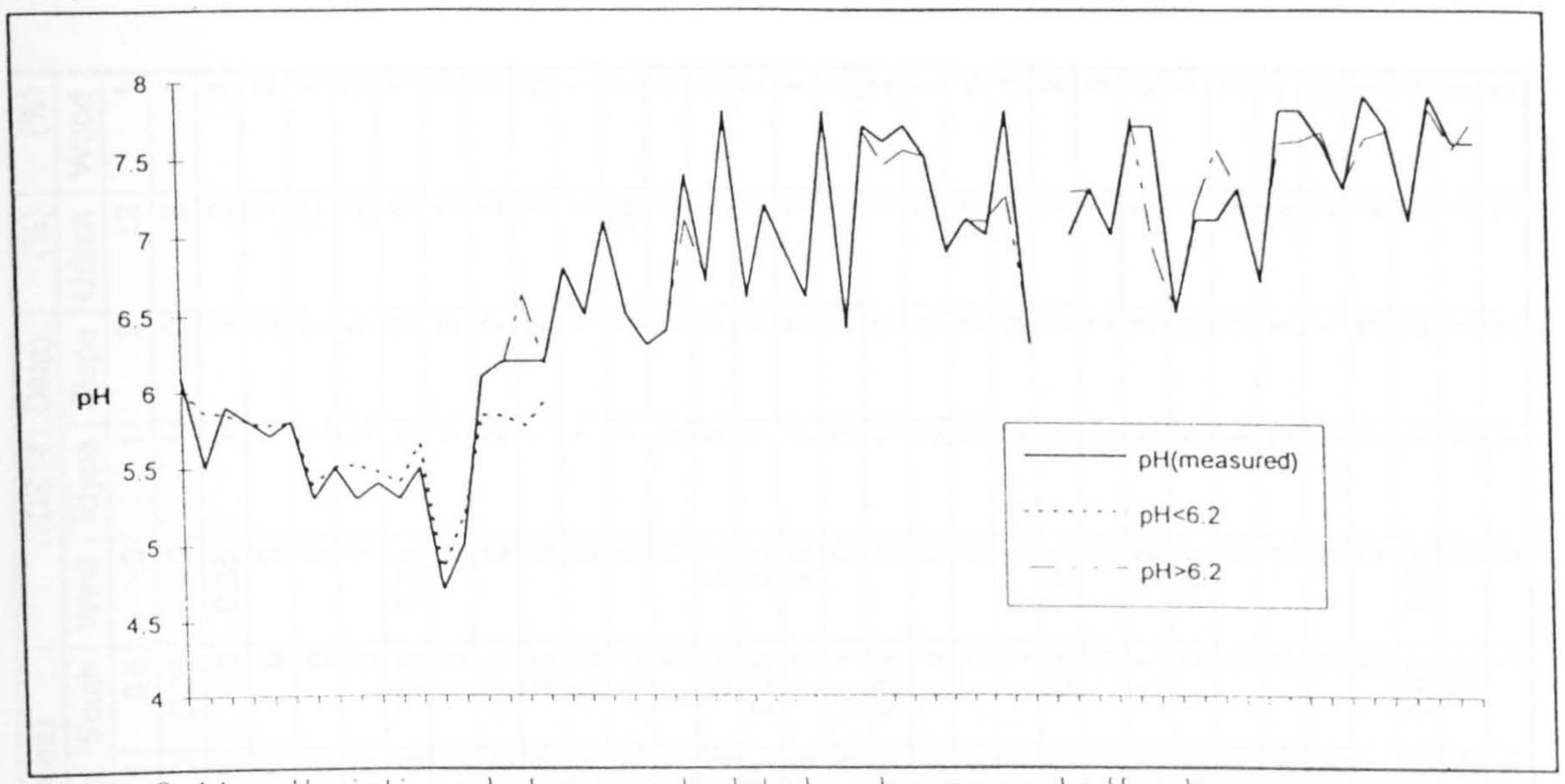

Figure 6.11 – Variations between calculated and measured pH values

A distinction is made in Figure 6.11 between the values below and above pH 6.2 since this represents the boundary between the Carbonate and Cation Exchange buffer ranges, and thus also where the pH calculations switch between Equations (12) and (13), respectively. Note the difference in the calculations in the three cells measured at pH 6.2; an indication of the reason for certain discontinuities observed in R_0 trajectories in Chapter 4 (see Figure 4.8 at 40 years).

6.2.1.1 Simulation X (Inclusion of NSI data)

Simulation X incorporates the initial soil composition conditions derived from the NSI data. Since these diverse conditions imply different temporal positions on the R_0 trajectory and within the family of R_0 trajectories, it is no longer meaningful to examine the emergent patterns with reference to a single snapshot of the spatial surface. These patterns are therefore represented in Figure 6.12 using temporal snapshots each T=25000 (6.8 years), resulting in 12 snapshots spanning the simulation.

In the first snapshot (Figure 6.12(a)), catastrophe is already being indicated - where R_0 has already fallen to zero - in two cells, [5,7] & [7,3], which, when identified in the context of the Rutland Catchment, represent Rutland Water itself and a region just upstream to the Nene take-off point, respectively.

Rutland Water was likely to appear sensitive owing to the acknowledged high accumulations of phosphates in Rutland Water which may enter the surrounding

CELL#	(Modified NSI Data)						(HOST (%))		(Flow Directions)				(OS141 Data)		(%)	(%)
	AI	Qa	Ca	Qc	P	pH	VMC	SPR	North	East	South	West	Rtype	Slope	Urban	Wood
[0,0]	402.56	6.58	86.35	14.81	0.097	6.1	39.40	33.99	0	0.5	0.5	0	1	2	12	1
[0,1]	531.40	3.51	110.40	47.35	0.619	6.8	38.53	47.54	0.75	0	0.25	0	1	0	8	1
[0,2]	1090.62	11.15	180.59	16.72	0.484	5.5	38.73	52.16	0.5	0.15	0	0.35	1	0	2	4
[0,3]	936.11	5.30	93.86	31.77	0.774	6.5	40.73	58.99	0.75	0.25	0	0	1	0	1	2
[0,4]	1061.13	1.80	186.02	24.35	0.310	7.1	39.30	53.73	0.1	0.9	0	0	1	2	10	1
[0,5]	714.49	2.62	110.27	15.72	0.174	6.5	37.51	46.93	0	0	0	1	1	0	4	0
[0,6]	723.00	5.54	92.33	19.39	0.484	6.3	38.51	51.12	0.25	0	0.5	0.25	1	2	6	1
[0,7]	937.98	2.45	102.98	14.70	0.019	6.4	38.41	50.28	0	0	0	1	1	2	1	2
[1,0]	322.51	0.00	157.68	55.42	1.355	7.4	40.59	48.28	0	0	1	0	2	2	8	2
[1,1]	1158.44	2.54	111.39	34.26	0.252	6.7	40.22	41.68	0.5	0	0.5	0	1	2	1	6
[1,2]	969.98	11.60	109.54	17.40	0.271	5.9	40.58	52.26	0.1	0.9	0	0	1	1	1	1
[1,3]	1042.80	0.00	587.63	40.24	0.290	7.8	41.23	55.73	0	1	0	0	1	0	20	0
[1,4]	978.78	2.79	117.77	16.75	0.155	6.6	40.81	55.08	0	1	0	0	2	0	2	0
[1,5]	937.51	0.00	215.94	21.63	0.174	7.2	39.41	51.16	0	0	0.9	0.1	1	2	1	6
[1,6]	495.51	5.85	44.12	13.15	0.135	5.8	39.12	50.94	0	0.25	0.25	0.5	1	2	2	2
[1,7]	1299.44	1.63	149.91	21.97	0.077	6.9	39.11	51.02	0.5	0	0	0.5	1	2	2	1
[2,0]	772.22	3.09	117.49	18.53	0.097	6.6	40.16	37.54	0	0	1	0	2	2	11	2
[2,1]	942.73	29.62	85.05	19.04	0.619	6.2	39.91	47.98	0	0.25	0.75	0	1	0	1	2
[2,2]	446.49	11.11	40.82	11.11	0.368	5.7	40.22	46.14	0.5	0.5	0	0	2	0	5	1
[2,3]	839.53	12.81	78.38	19.22	0.039	5.8	40.43	49.36	0.5	0.5	0	0	2	2	1	4
[2,4]	1577.00	19.35	126.70	12.44	0.116	6.2	41.21	46.00	0	1	0	0	2	0	1	0
[2,5]	1026.53	0.00	646.16	22.82	0.058	7.8	40.05	52.06	0	0	0.8	0.2	1	2	1	2
[2,6]	769.29	14.21	86.88	31.98	1.452	6.4	40.21	56.25	0	1	0	0	1	2	1	8
[2,7]	1116.87	0.00	449.99	121.62	1.277	7.7	39.71	52.69	0	0.2	0.1	0.7	1	2	0	6
[3,0]	612.49	54.81	40.46	0.00	1.413	5.3	39.10	45.50	0.12	0.38	0	0.5	1	0	1	4
[3,1]	803.58	8.50	45.42	8.50	0.135	5.5	39.72	22.76	0.1	0.9	0	0	1	0	9	3
[3,2]	681.40	20.07	52.04	3.34	0.019	5.3	39.49	30.90	0	1	0	0	2	1	12	4
[3,3]	871.82	0.00	323.82	20.55	0.174	7.6	39.10	41.07	0.67	0.33	0	0	1	1	3	10
[3,4]	926.02	0.00	382.93	34.00	0.252	7.7	40.66	44.84	0	1	0	0	2	0	2	1
[3,5]	1061.20	0.00	350.61	30.69	0.135	7.5	39.83	53.93	0	0	0.67	0.33	1	2	2	8
[3,6]	794.13	2.30	138.27	30.99	0.523	6.9	40.39	53.49	0	0.5	0.5	0	1	2	2	3
[3,7]	1174.89	0.00	188.32	20.79	0.039	7.1	39.24	52.39	0	1	0	0	1	2	3	3

Table 6.1 - NSI data used for the definition of initial conditions

CELL#	(Modified NSI Data)						(HOST (%))		(Flow Directions)				(OS141 Data)		(%)	(%)
	Al	Qa	Ca	Qc	P	pH	VMC	SPR	North	East	South	West	Rtype	Slope	Urban	Wood
[4,0]	603.00	9.41	151.66	56.49	0.581	7	40.88	29.76	0	1	0	0	3	2	8	1
[4,1]	625.84	0.00	222.22	34.00	0.116	7.8	41.00	28.63	0	0	1	0	3	0	61	0
[4,2]	1066.20	18.94	86.39	28.41	0.019	6.3	39.96	34.47	0.1	0	0.9	0	3	0	8	12
[4,3]	879.78	12.67	306.82	21.28	0.256	6.8	39.87	38.79	0.5	0.5	0	0	1	0	50	4
[4,4]	620.09	31.72	43.16	0.00	0.232	5.4	40.83	39.12	1	0	0	0	2	0	14	8
[4,5]	1382.44	17.90	75.84	11.51	0.213	5.3	40.26	43.63	0	1	0	0	2	2	8	0
[4,6]	594.33	121.41	262.68	0.00	3.639	7	40.49	38.77	0	1	0	0	2	0	4	0
[4,7]	1001.51	0.00	243.04	24.71	0.194	7.3	40.64	42.89	0	1	0	0	3	1	38	8
[5,0]	574.96	20.77	23.22	31.15	0.600	5.5	39.78	34.22	0	0.25	0.75	0	2	1	8	2
[5,1]	649.11	17.22	43.85	60.26	1.103	6.2	40.45	26.82	0	0.8	0.2	0	1	0	3	4
[5,2]	868.18	1.32	173.10	17.77	0.310	7	39.23	49.76	0	0.6	0.2	0.2	1	0	1	22
[5,3]	961.00	0.00	773.93	36.15	0.600	7.7	39.59	40.52	0.33	0	0.67	0	1	0	16	20
[5,4]	738.89	0.00	157.01	14.17	0.194	7.7	40.19	44.12	0.25	0.75	0	0	1	1	6	14
[5,5]	728.78	4.12	101.24	24.71	0.252	6.5	40.88	34.12	0.5	0.5	0	0	3	0	1	6
[5,6]	783.51	0.00	101.96	131.66	0.968	7.1	40.38	24.29	0	1	0	0	2	0	4	1
[5,7]	1012.31	45.92	35.90	7.65	1.045	4.7	39.35	17.75	0	1	0	0	3	1	34	4
[6,0]	1184.56	0.00	345.48	78.15	2.981	7.1	41.86	23.90	1	0	0	0	3	1	17	0
[6,1]	1187.00	7.31	274.04	10.96	0.019	7.3	41.55	23.62	1	0	0	0	3	1	12	0
[6,2]	1122.56	0.00	253.21	19.97	0.213	7.3	40.33	42.84	0	1	0	0	3	0	2	23
[6,3]	1084.22	39.64	126.86	25.48	2.477	6.7	39.51	47.31	0	1	0	0	1	0	1	12
[6,4]	1025.84	0.00	446.10	18.44	0.271	7.8	40.39	45.30	0.5	0.5	0	0	1	0	1	12
[6,5]	1116.78	0.00	458.85	19.77	0.406	7.8	41.90	41.07	0.67	0.33	0	0	3	0	3	36
[6,6]	1039.38	0.00	535.34	29.73	0.135	7.6	41.04	27.35	1	0	0	0	3	1	4	4
[6,7]	864.09	0.00	255.49	17.80	0.116	7.3	40.54	10.28	0	1	0	0	2	1	4	2
[7,0]	1042.49	0.00	482.51	20.70	0.290	7.9	40.74	49.05	0	0.75	0	0.25	1	0	2	2
[7,1]	934.69	0.00	549.03	21.48	0.271	7.7	40.45	41.77	0.8	0	0	0.2	1	0	4	0
[7,2]	1415.33	0.00	181.14	29.21	0.232	7.1	40.86	33.18	1	0	0	0	3	1	6	4
[7,3]	726.56	7.15	34.02	4.60	0.426	5	40.93	29.80	1	0	0	0	3	1	9	4
[7,4]	1054.04	0.00	1003.76	23.69	0.290	7.9	42.11	39.61	0	1	0	0	3	0	3	19
[7,5]	1322.11	0.00	398.91	27.17	0.852	7.6	42.78	45.15	0	0.1	0.9	0	3	1	3	10
[7,6]	1038.47	0.00	716.40	19.07	0.406	7.6	40.15	6.81	0.5	0.5	0	0	1	1	8	14
[7,7]	1525.67	0.00	134.39	40.21	0.232	6.1	40.40	17.94	0	1	0	0	3	1	25	4

Table 6.1 (cont...)

soils, effectively hastening the R_0 trajectory. However, identification of cell [7,3] as sensitive may suggest that phosphate rich waters from the River Nene may have a high contributory influence upon phosphate accumulation in Rutland Water.

Shown in snapshot T=50000 (Figure 6.12(c)), three further regions of potential sensitivity can be seen emerging from cells [3,0], [5,0], and [4,4]. The spread of these regions can be observed in the subsequent snapshots, but very quickly these regions begin to merge and distort any emergent patterns, aside from the areas of relative resilience which persist throughout.

Two potentially significant observations can be made from this simulation. Firstly, both this simulation and the preceding hydrologically based simulations suggest a degree of sensitivity in similar areas of the River Welland; significantly in an area just downstream of the cell representing Market Harborough - cell [1,3]. Secondly, a persistent band of apparently resilient cells has appeared crossing the Welland from cell [2,5], through cell [3,4], to cell [5,3] (see Figure 6.12(l)). Cell [7,3] on the River Nene has also been identified as sensitive; a further correlation with the previous findings.

The simulation output provided, being temporally static and representing snapshots at approximately 7 yearly intervals, shows regions where sensitivity is apparent, but much information has evidently been obscured or lost through this static representation; regions which have collapsed (R_0=0) are identified but no indication is clear in advance of collapse. This highlights the potential value of a temporally continuous representation of this dynamic spatial surface, facilitating continuous observation and indication of sudden changes which are unobservable using the static representation.

6.2.1.2 Simulation XI (Inclusion of OS141 data)

Whereas Simulation X includes both hydrological and soil composition influences, with further areas of sensitivity are already being suggested, Simulation XI includes aggregated data relating to land use, specifically the percentages of Urban cover and woodland, taken from Ordnance Survey maps [OS 1991] for each 5km cell. These data are presented in Table 6.1.

The effect of urban cover is in the assumption that all rainfall will enter drainage systems and be directed straight into the river system. Hence, expanses of water have also been included in this percentage since the rainfall directly enters the river system. The effect of woodland areas is to modify the infiltration rates as defined in Equation (32). Remaining vegetation cover is assumed to be non-livestock grassland; Simulations XII and XIII will reflect changes in these remaining areas.

The outputs of Simulation XI, shown in Figure 6.13, are snapshots taken at equivalent times to Simulation X. These outputs, at first glance, appear identical to Simulation X, but, on closer examination, there are three cells where differences in the surface are just detectable at this level of resolution, but only when the two outputs are compared. A difference in cell [7,7] is detectable at T=150000 (see

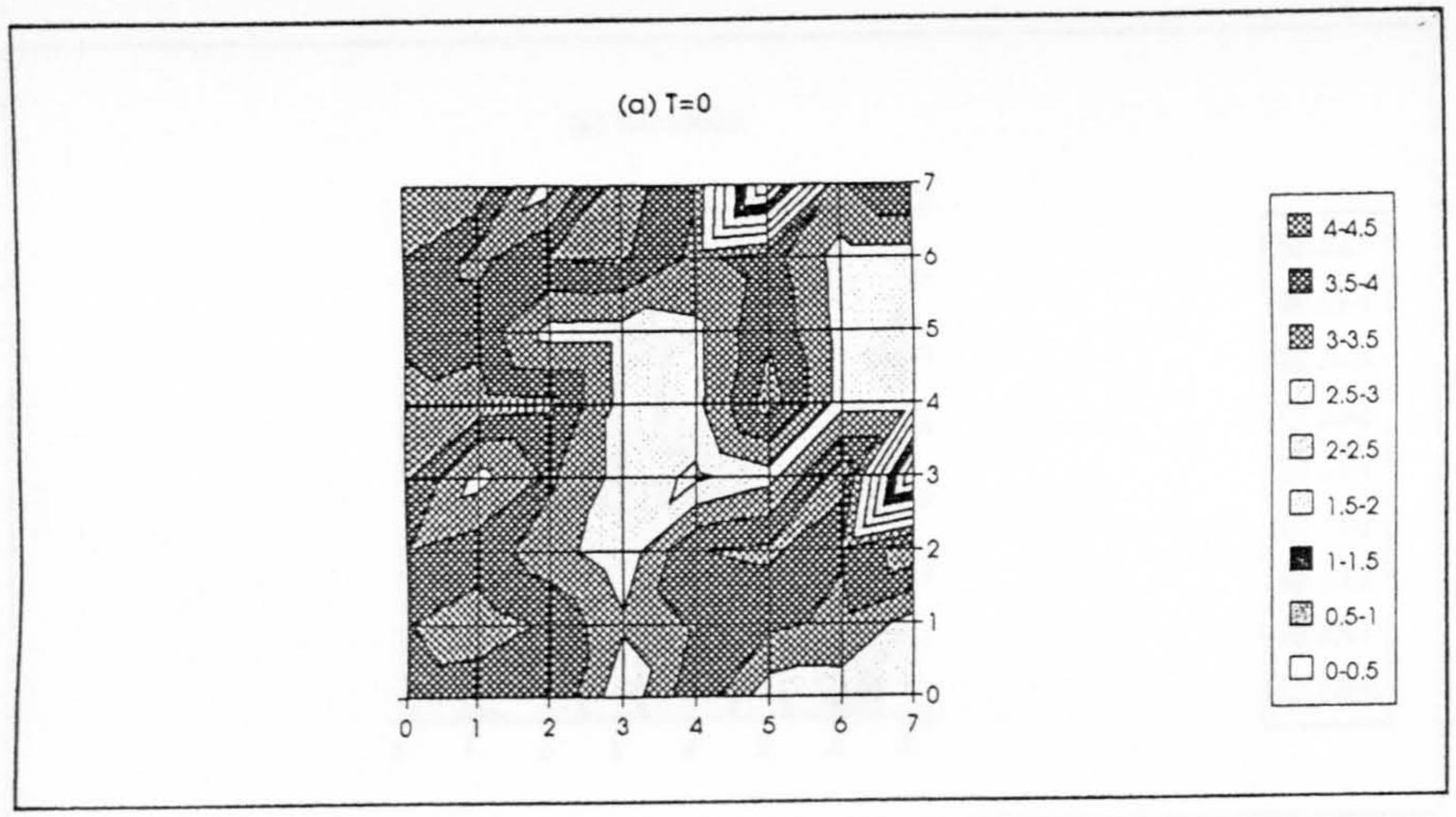

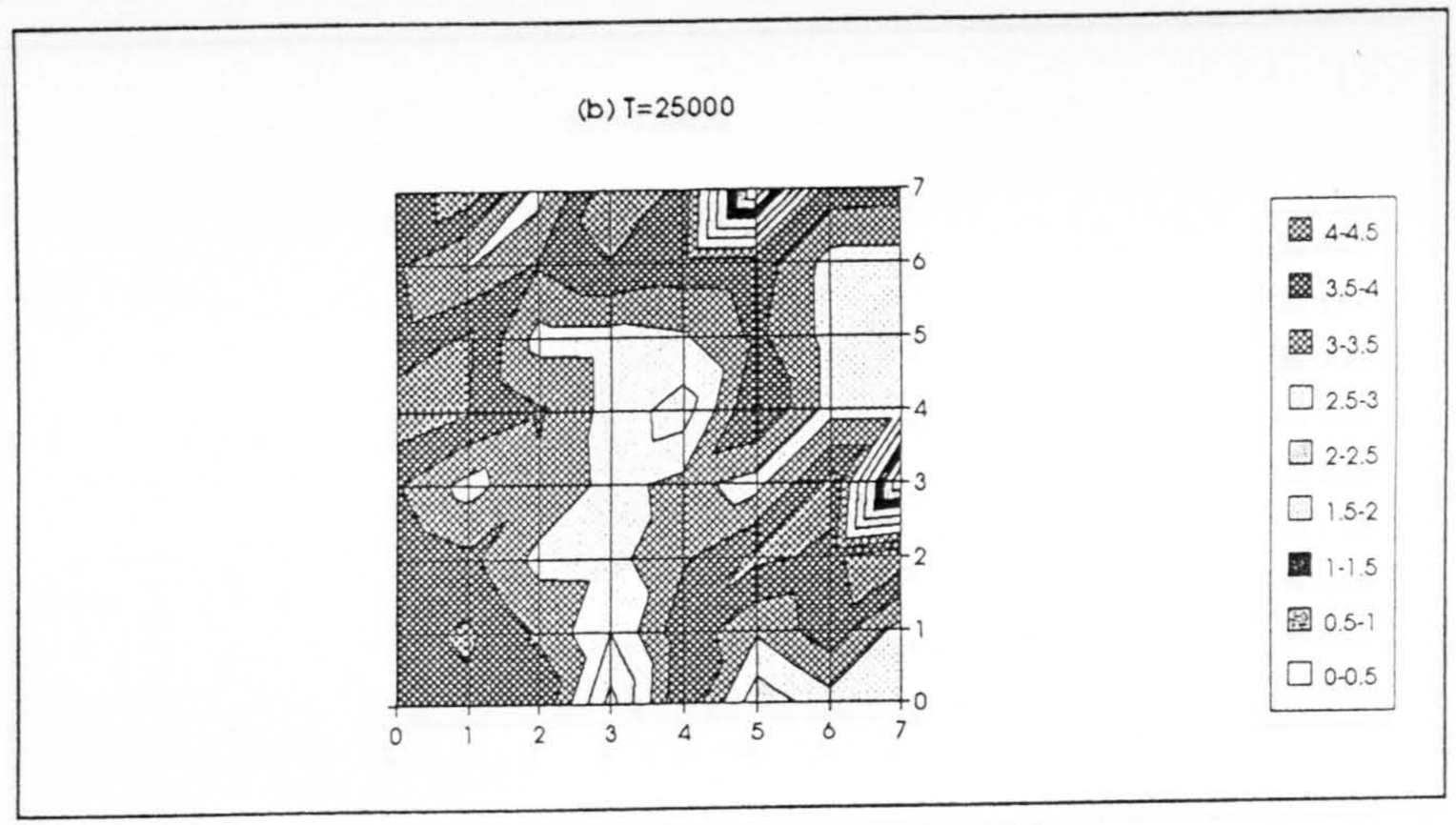

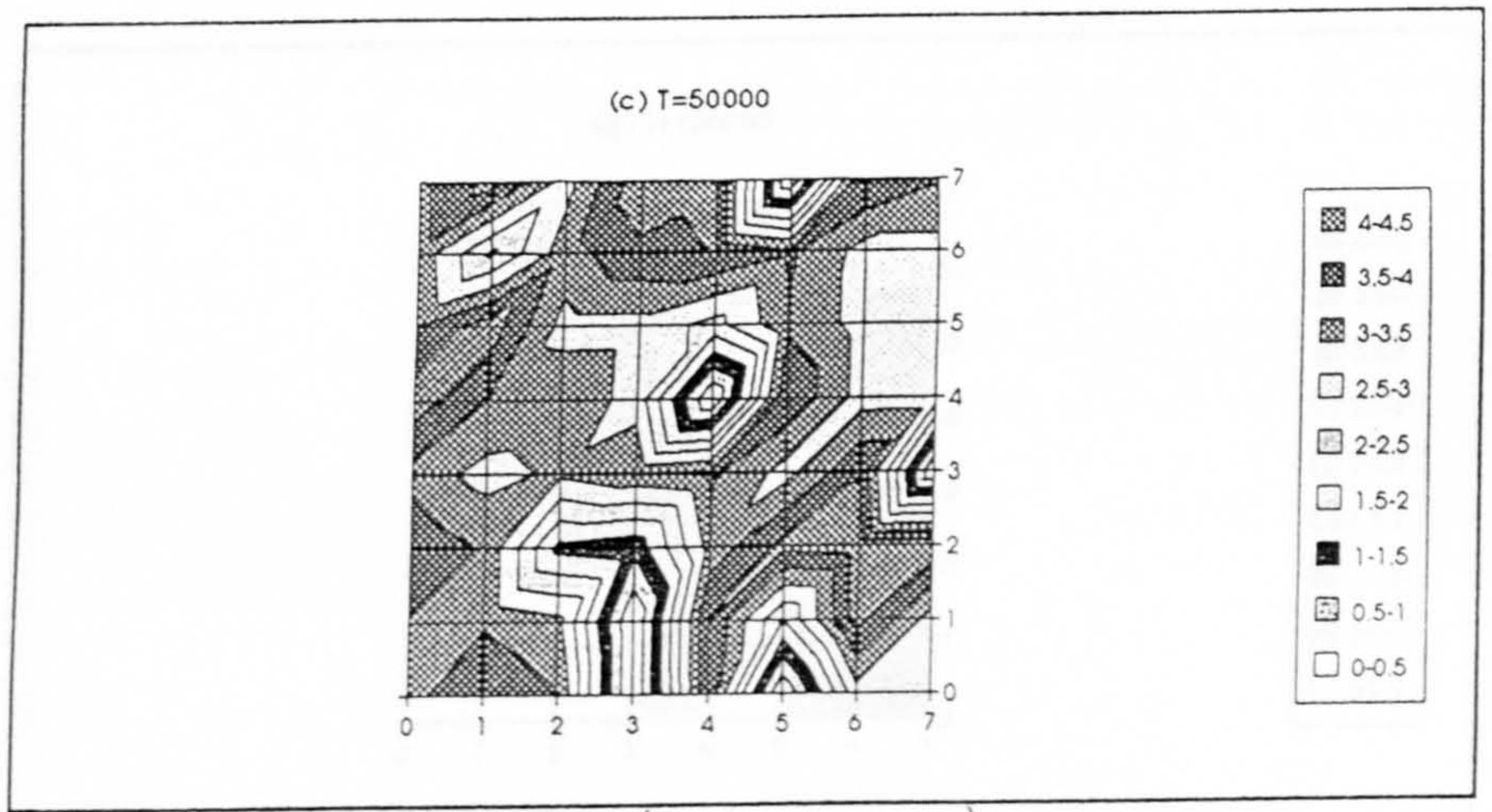

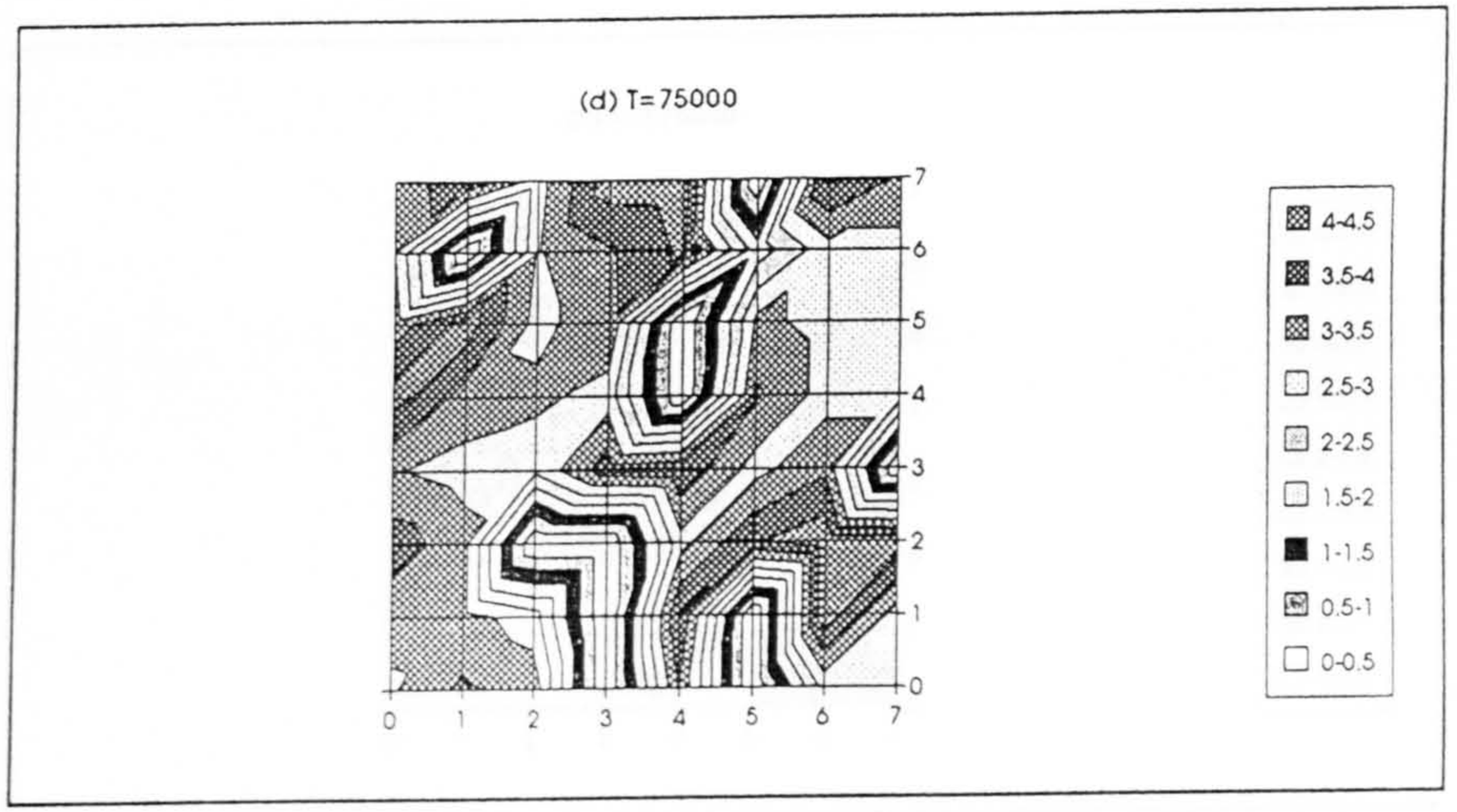

Figure 6.12 – Simulation X (R_0 landscapes)

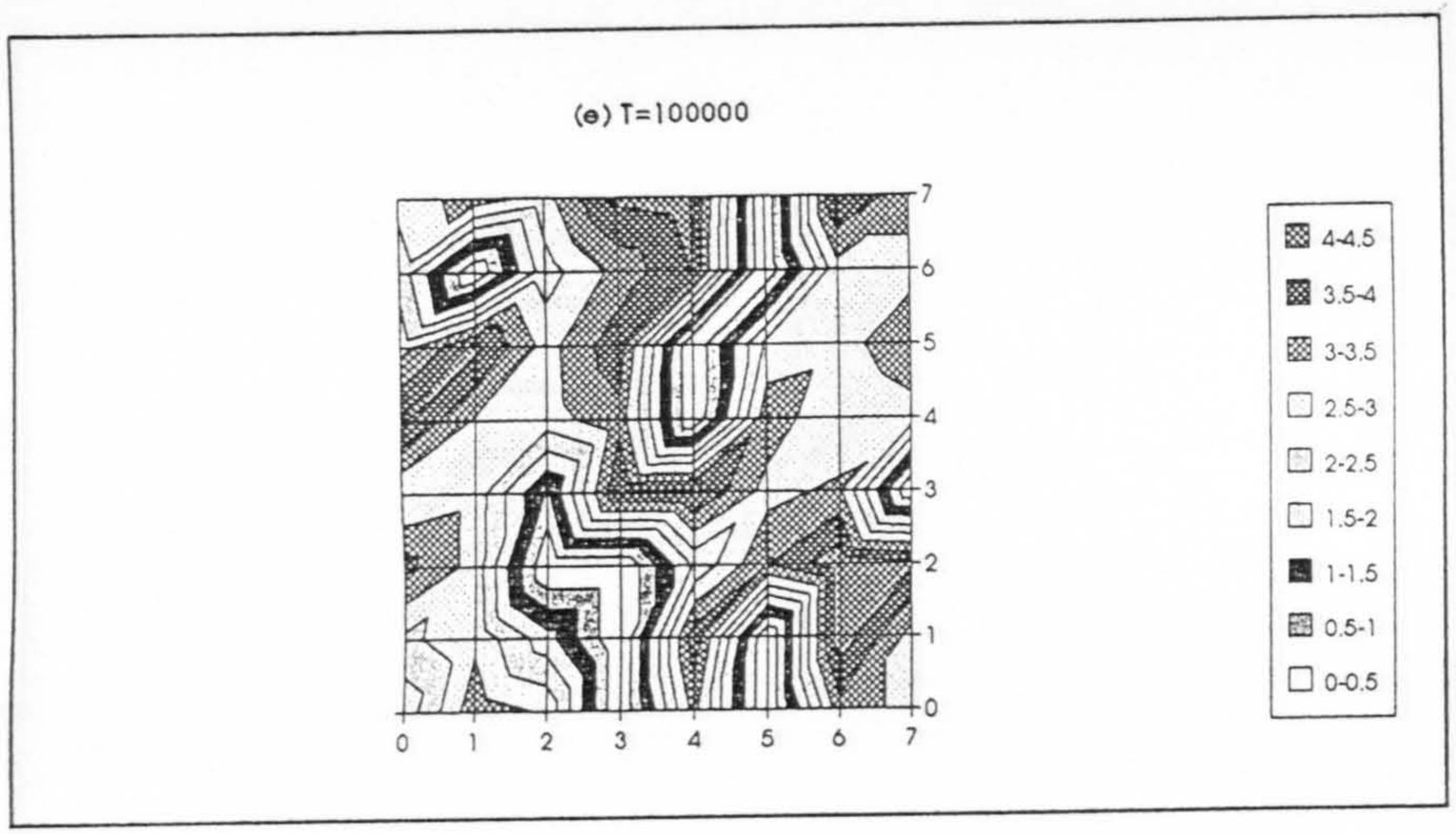

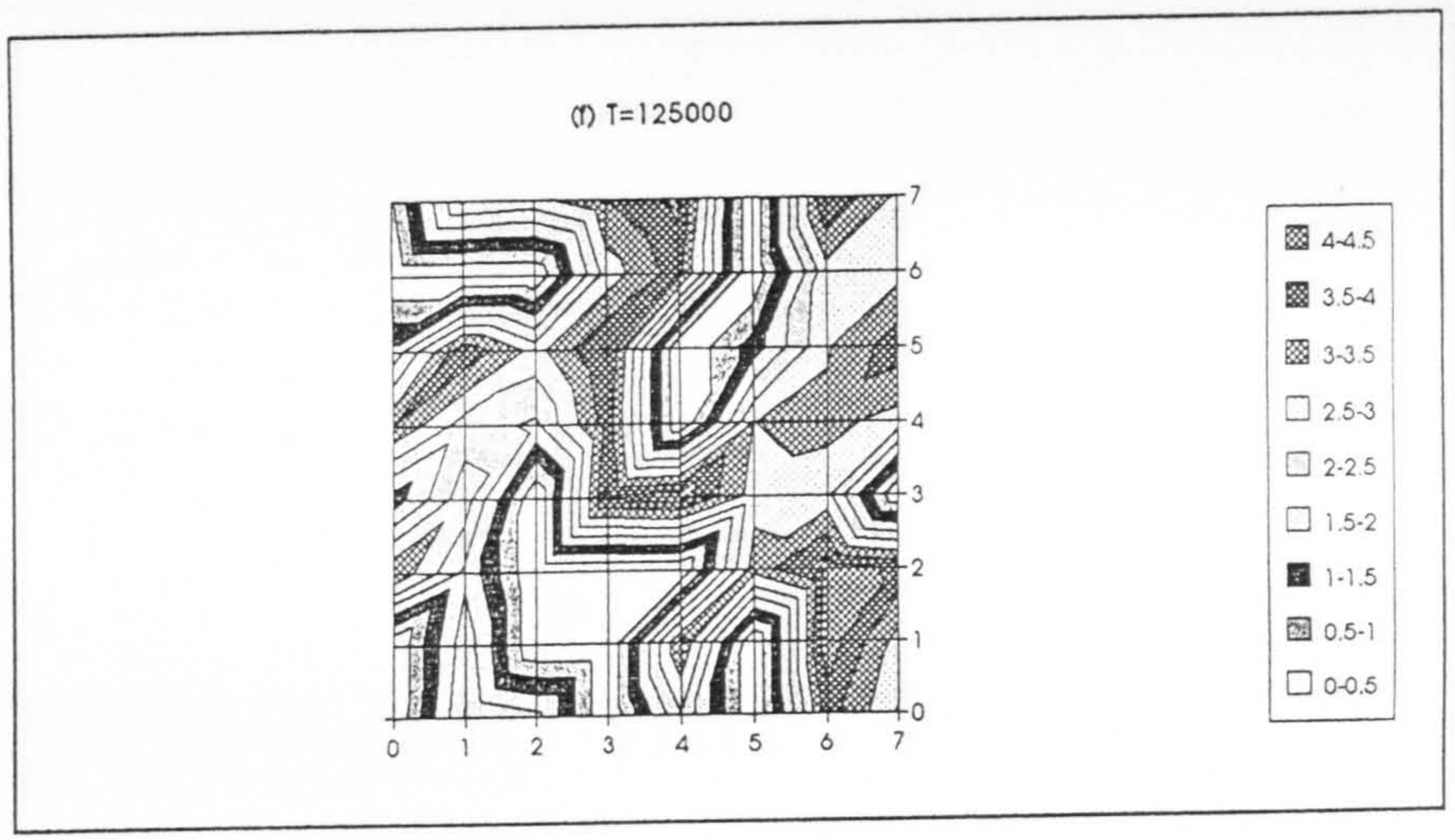

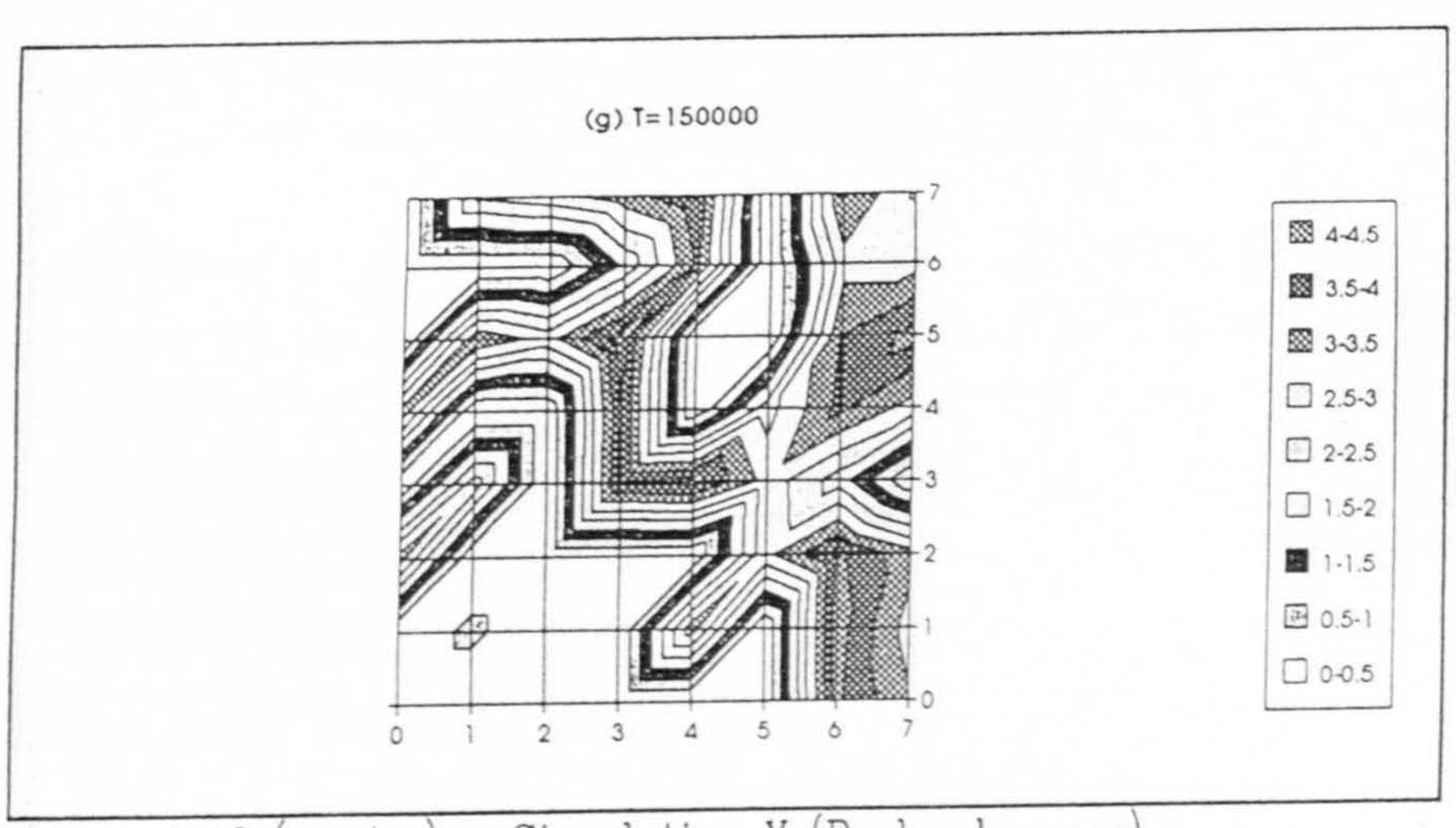

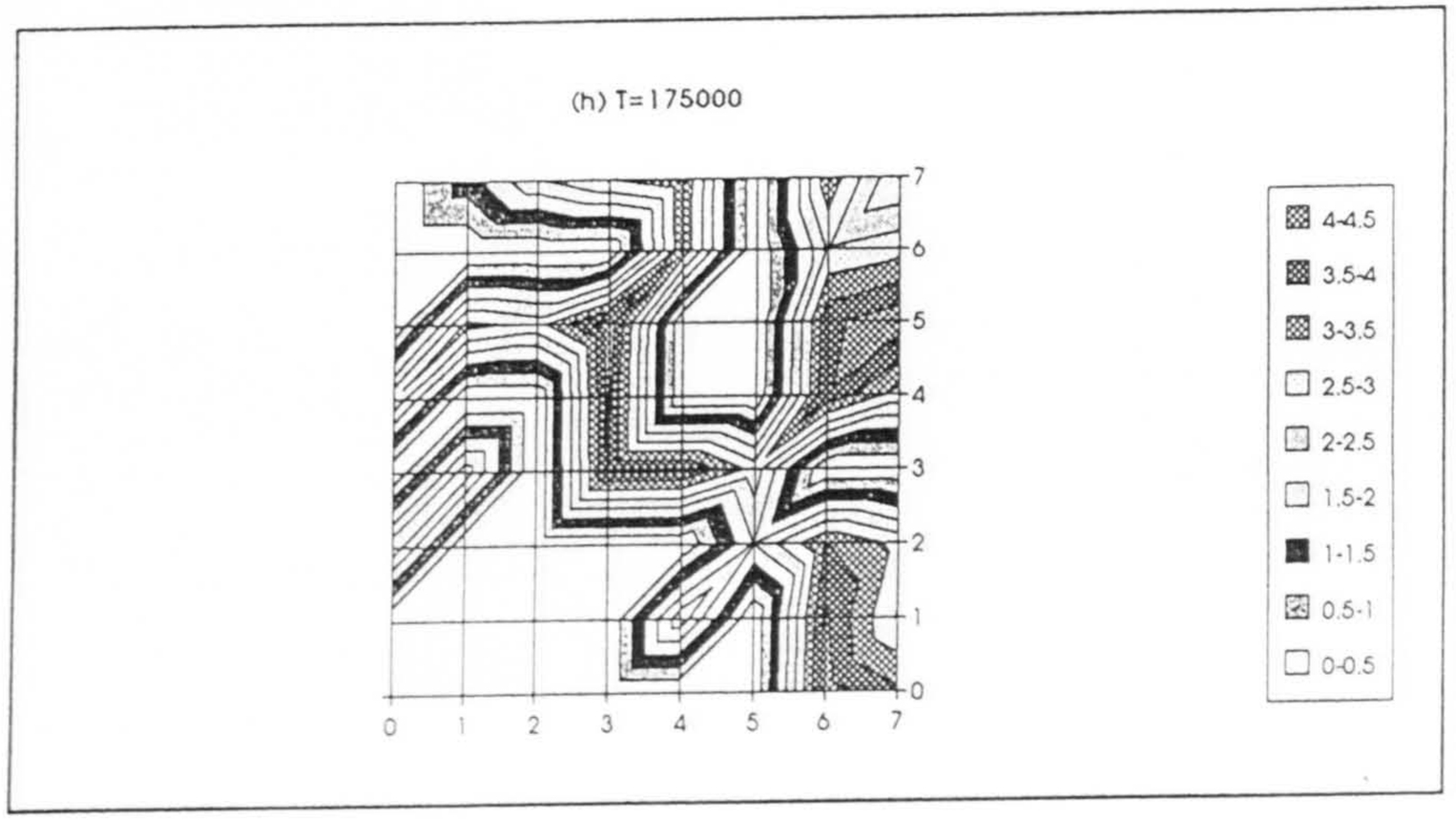

Figure 6.12 (cont...) - Simulation X (R_0 landscapes)

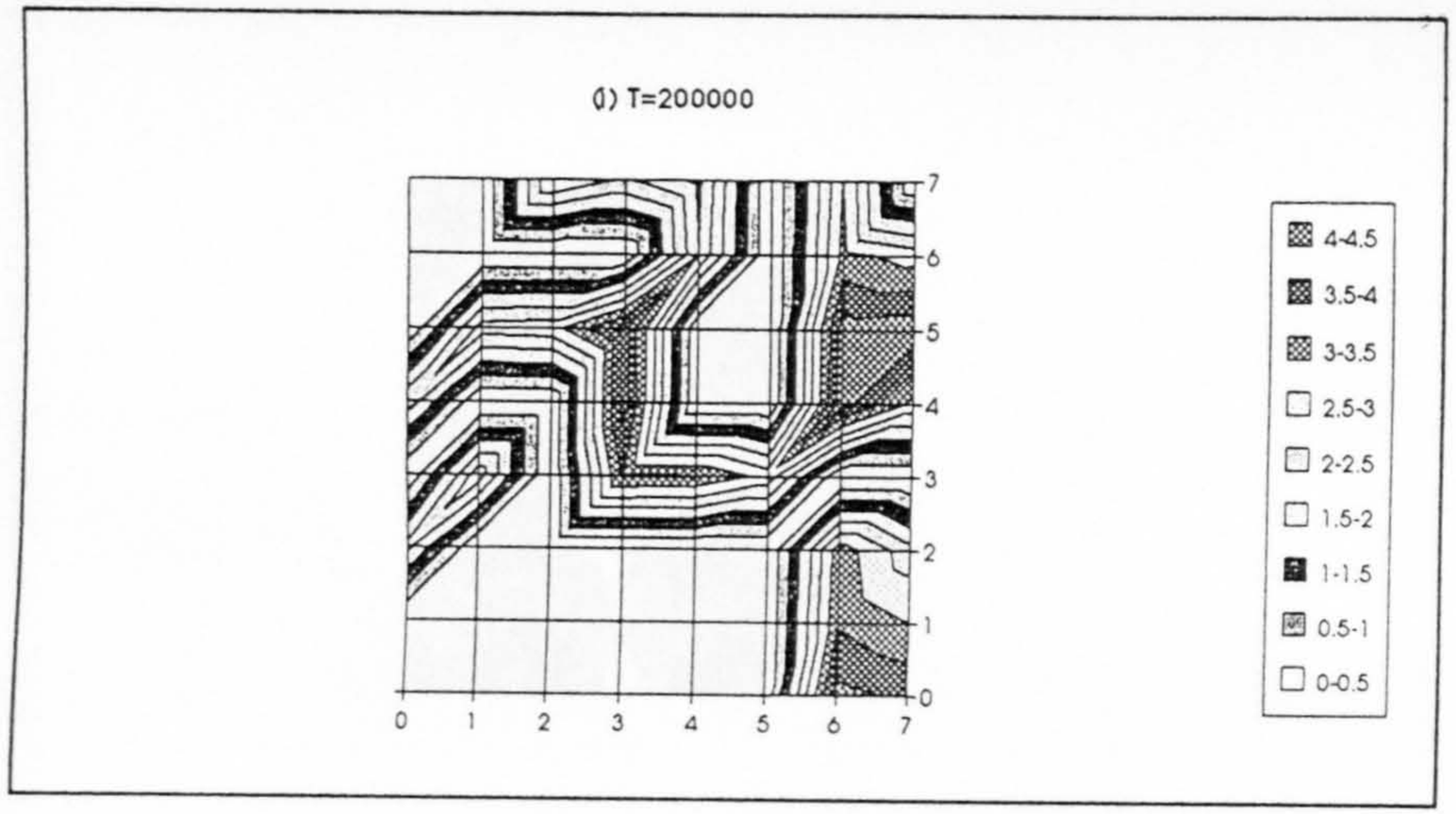

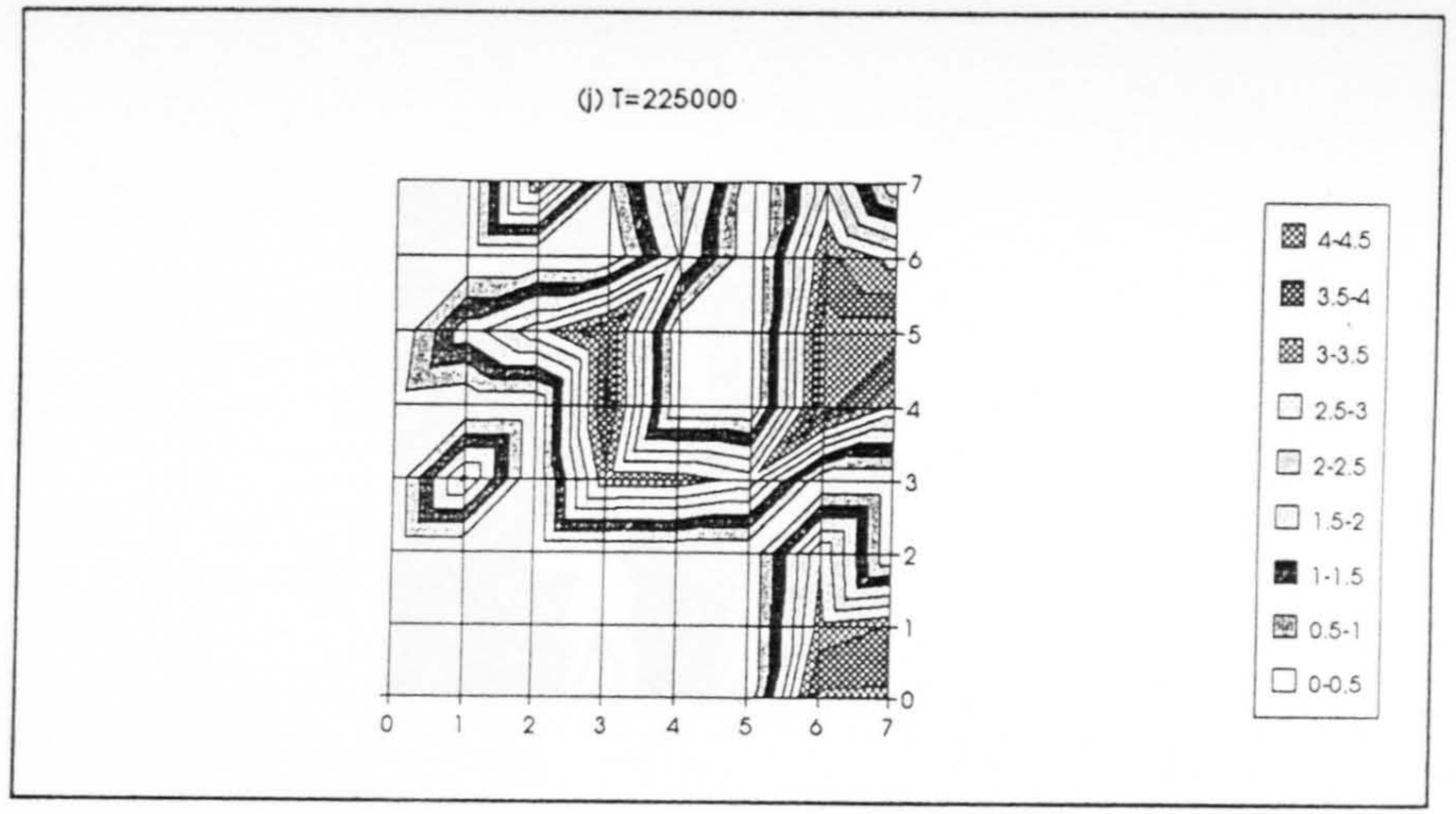

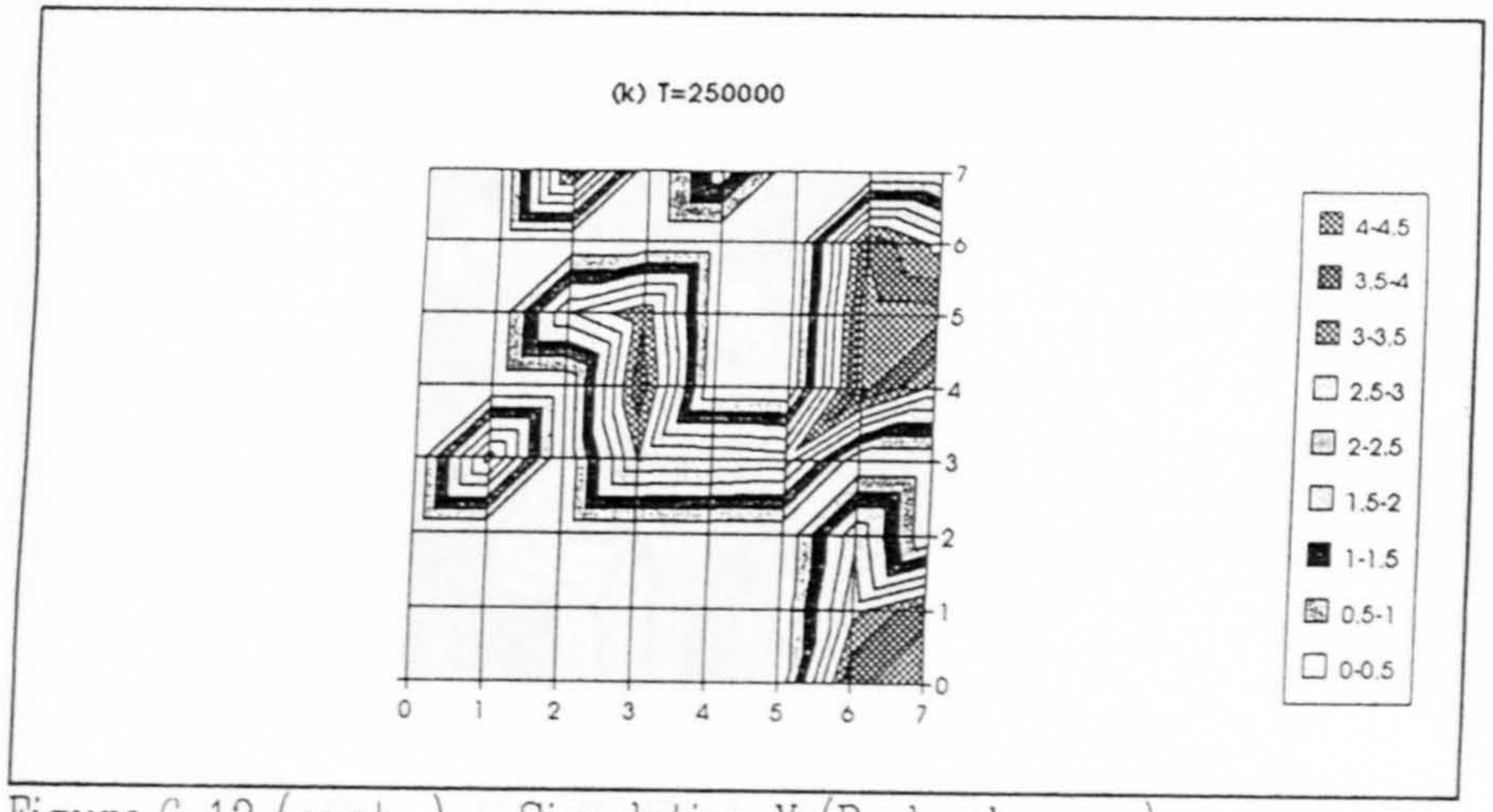

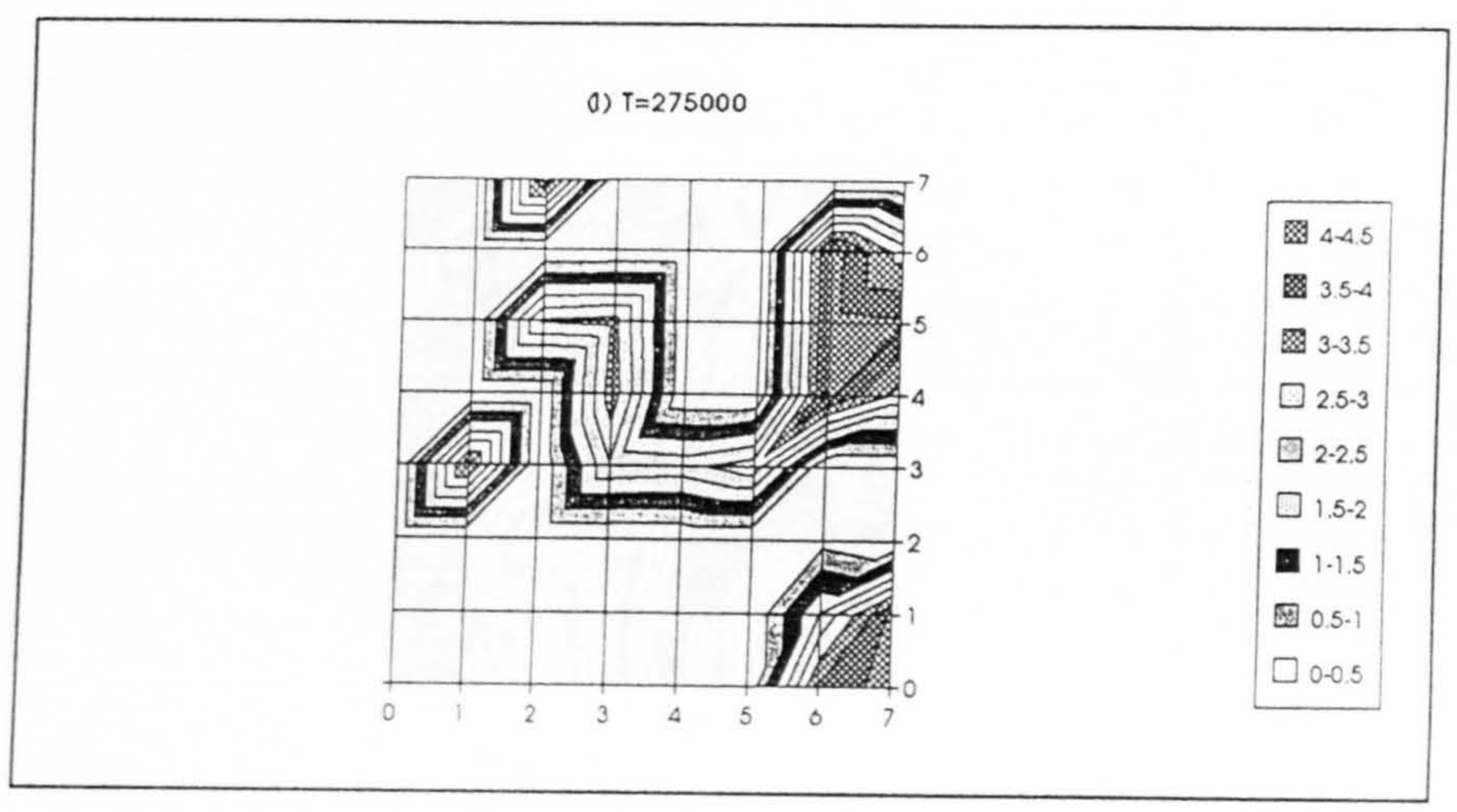

Figure 6.12 (cont...) – Simulation X (R_0 landscapes)

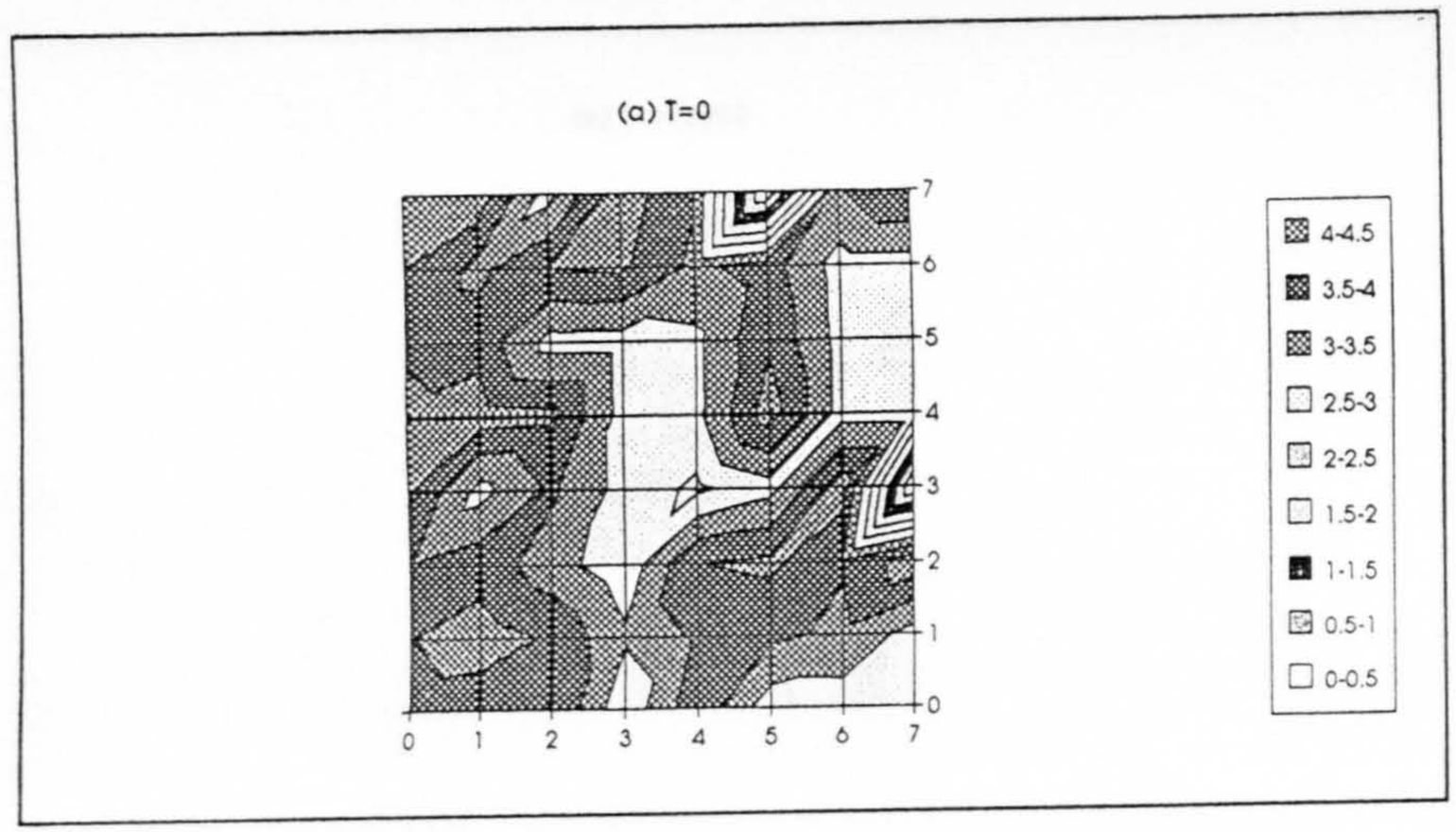

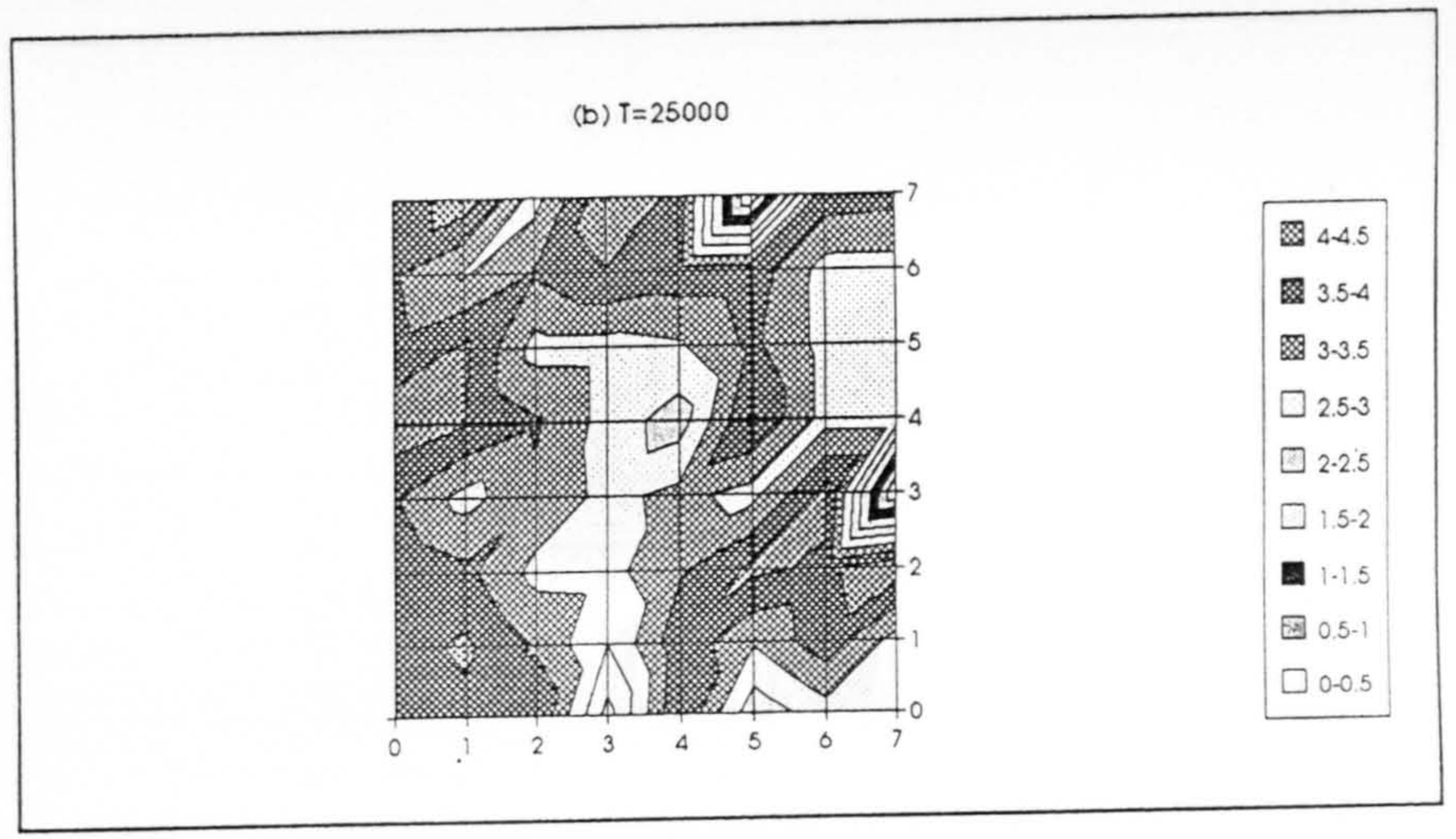

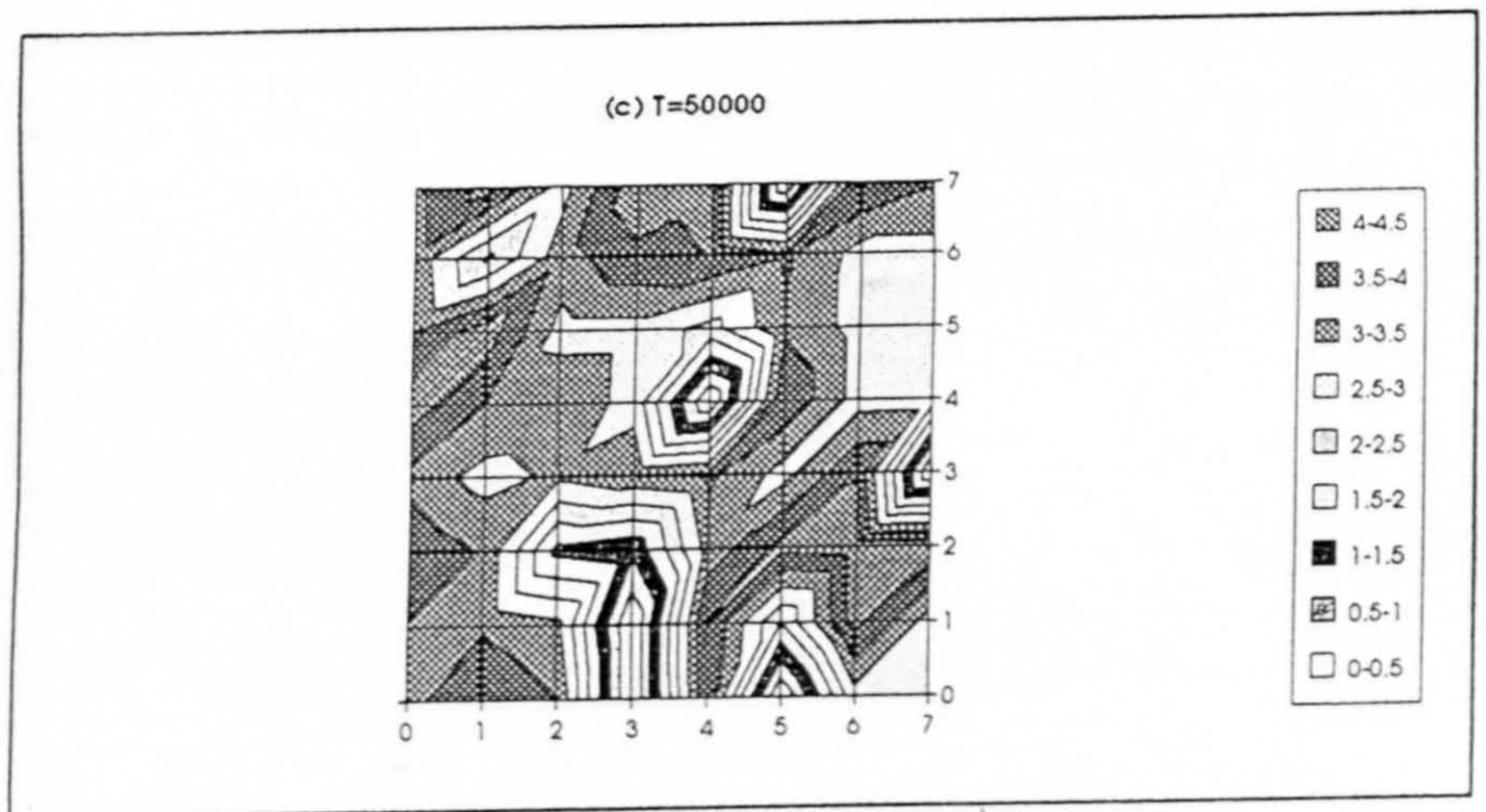

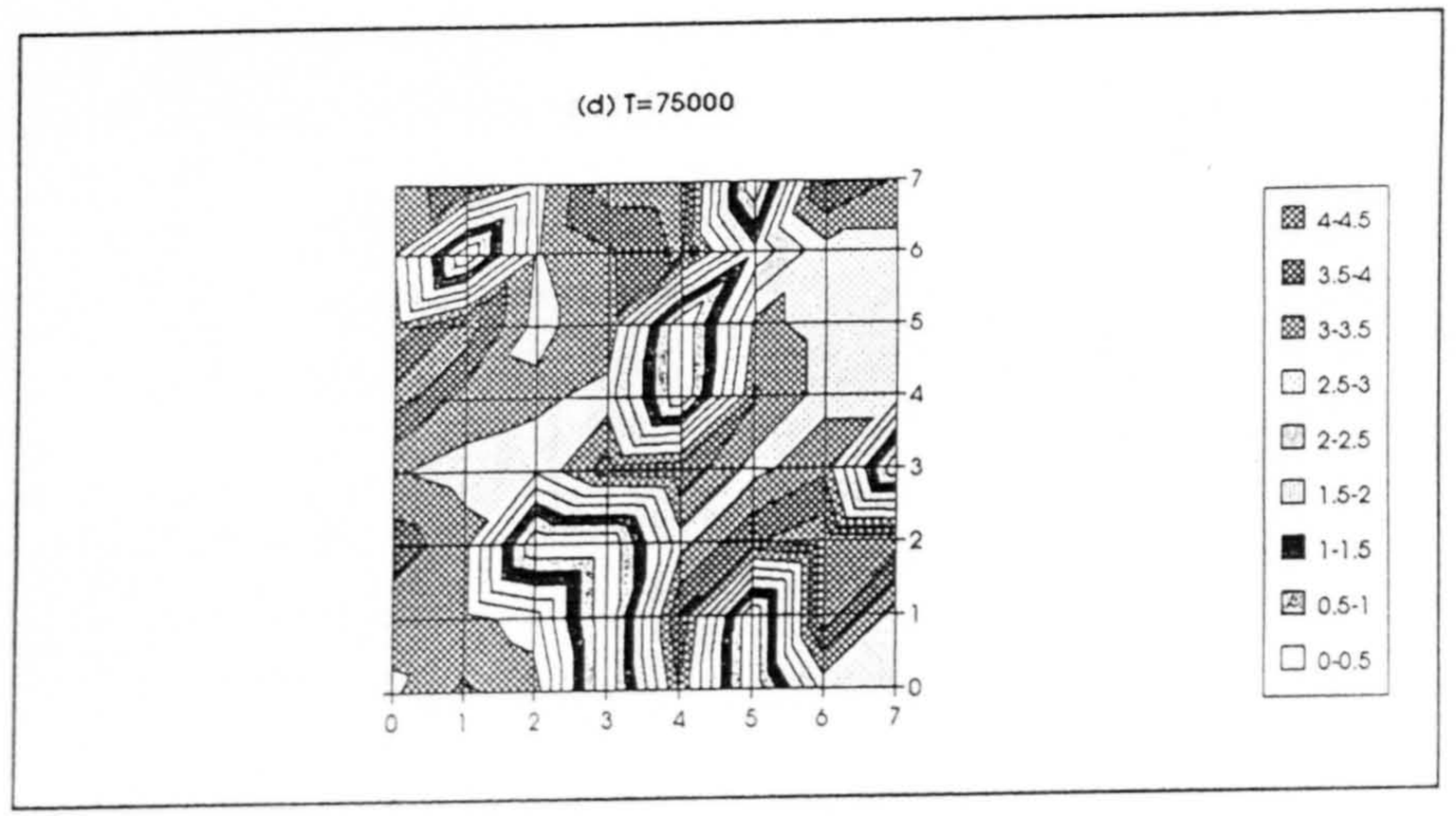

Figure 6.13 – Simulation XI (R_0 landscapes)

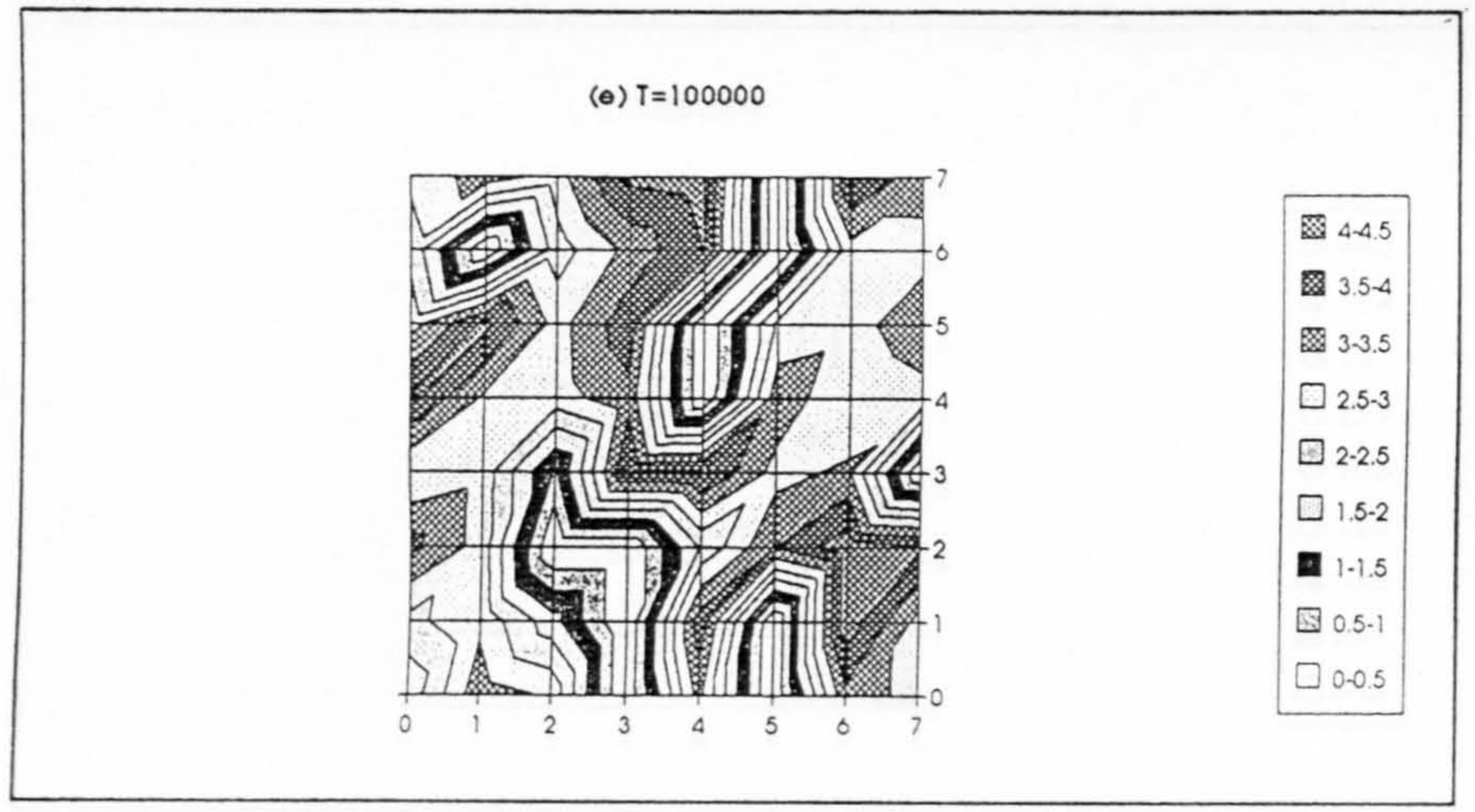

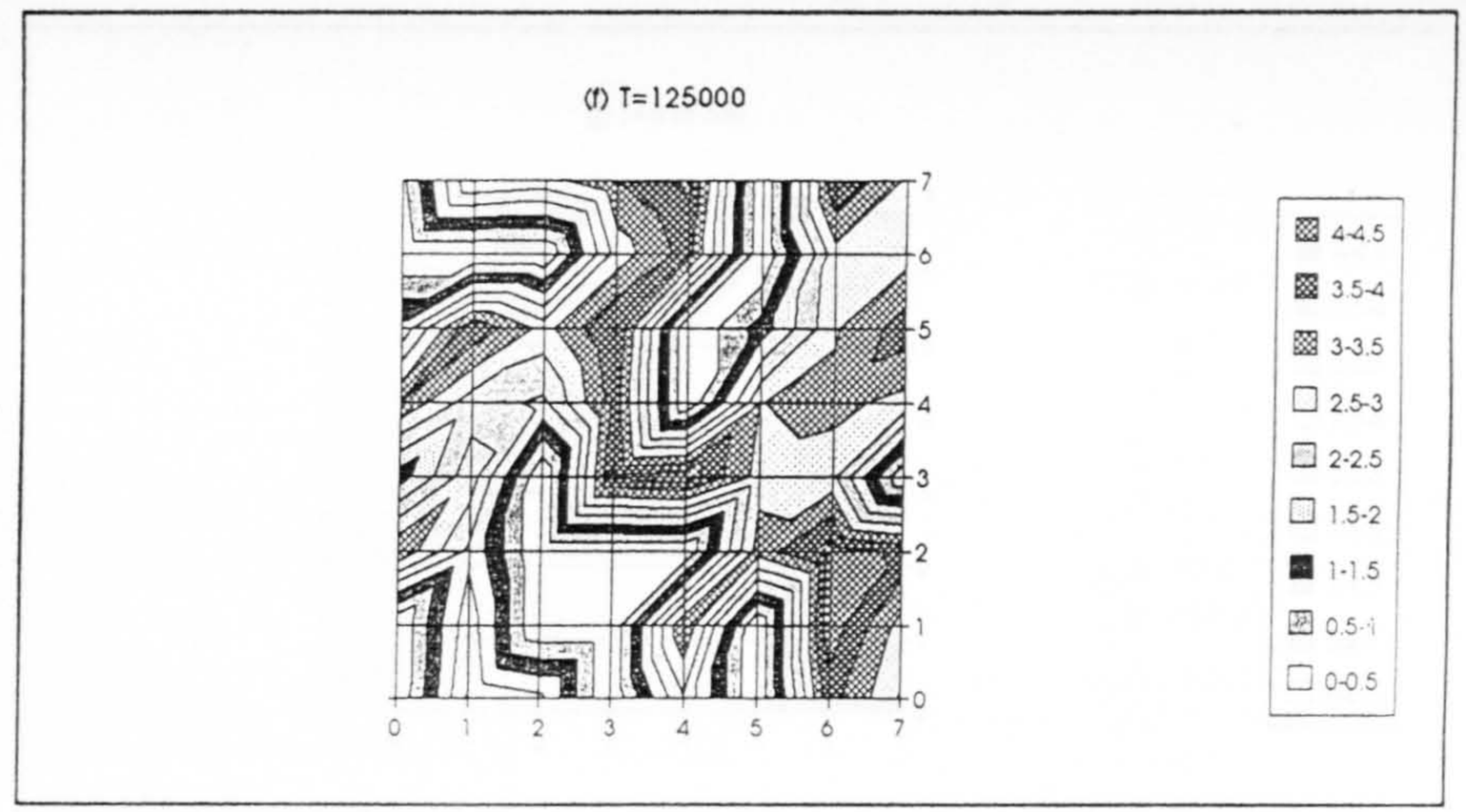

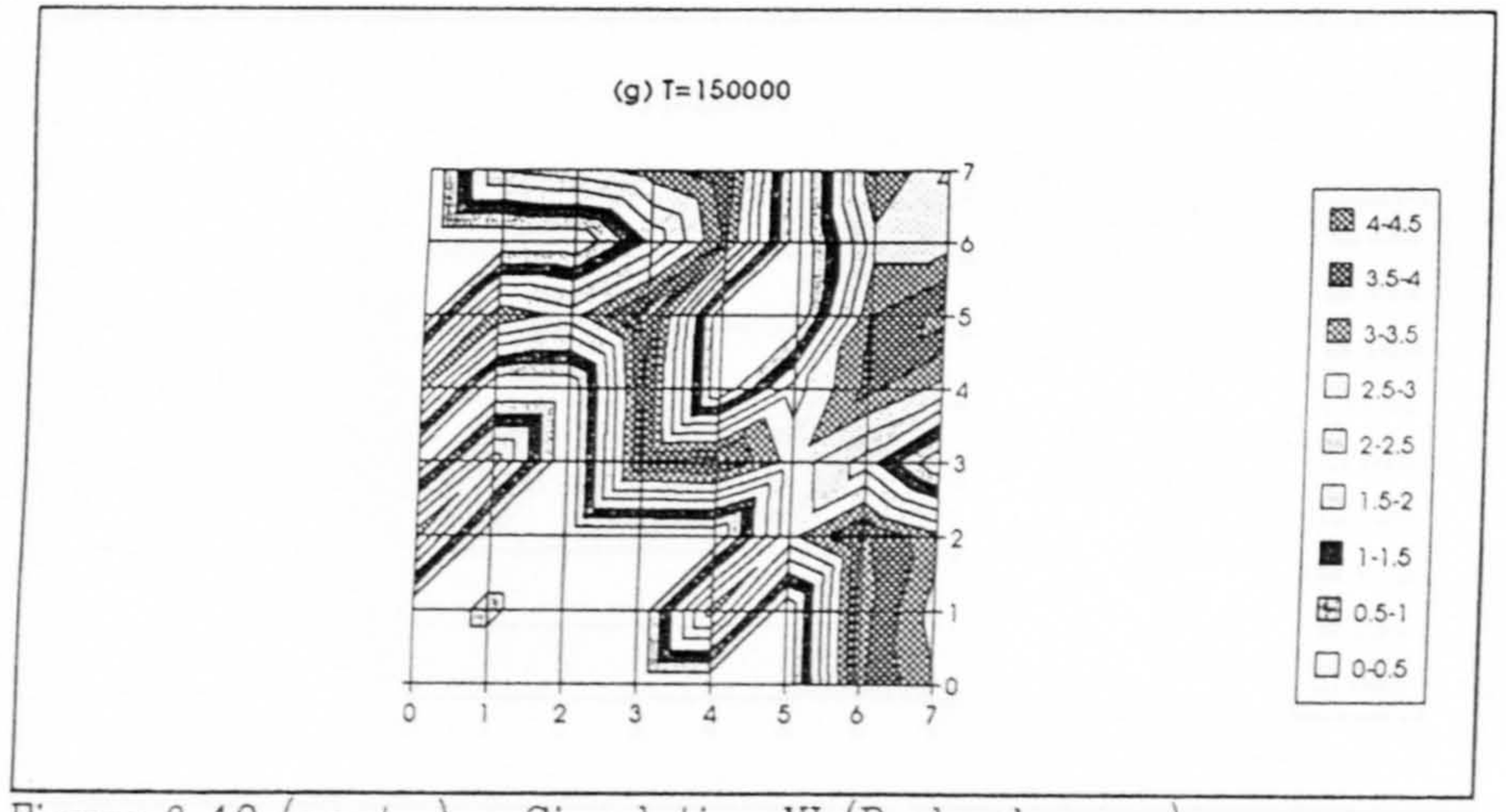

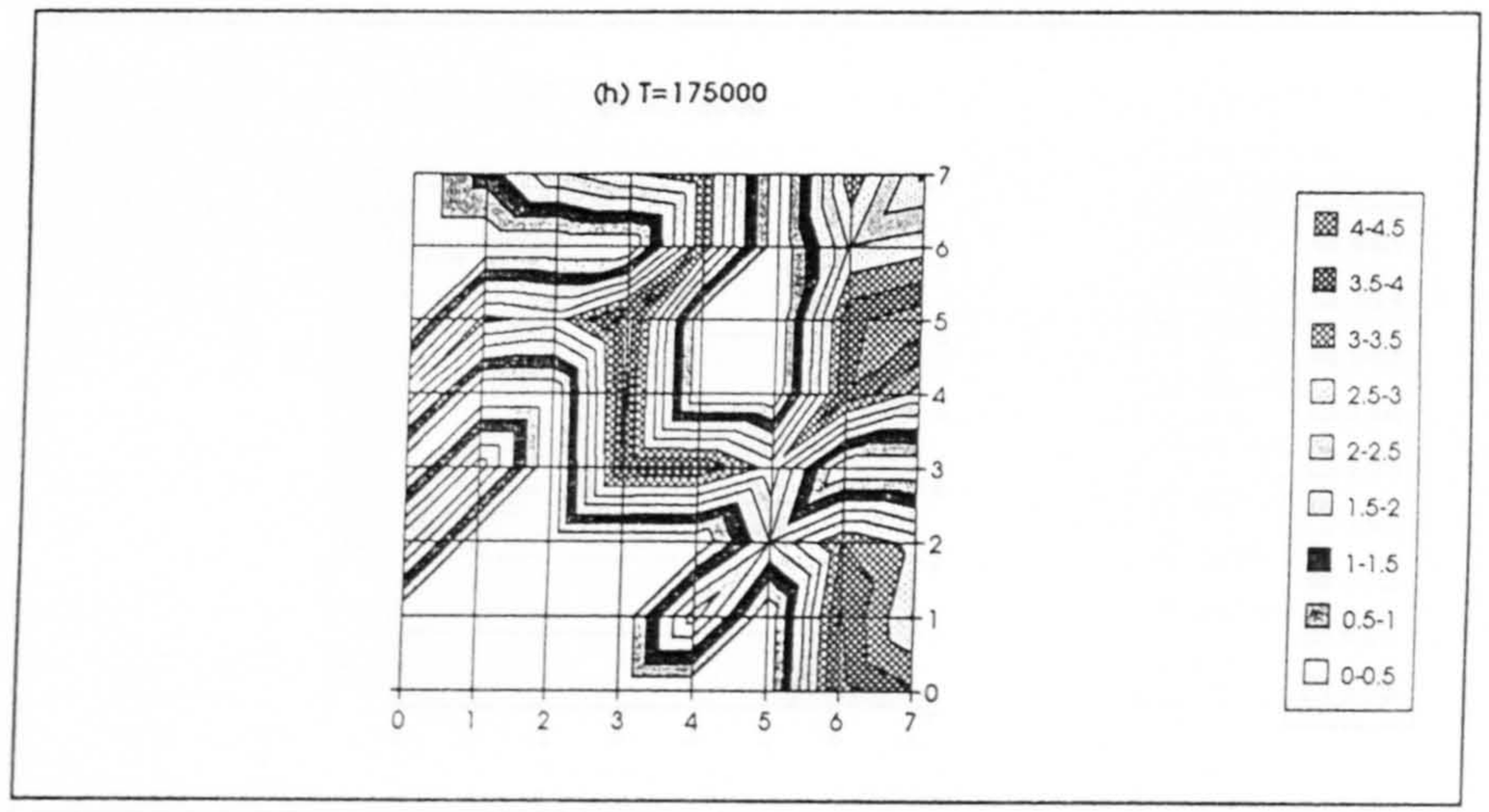

Figure 6.13 (cont...) – Simulation XI (R_0 landscapes)

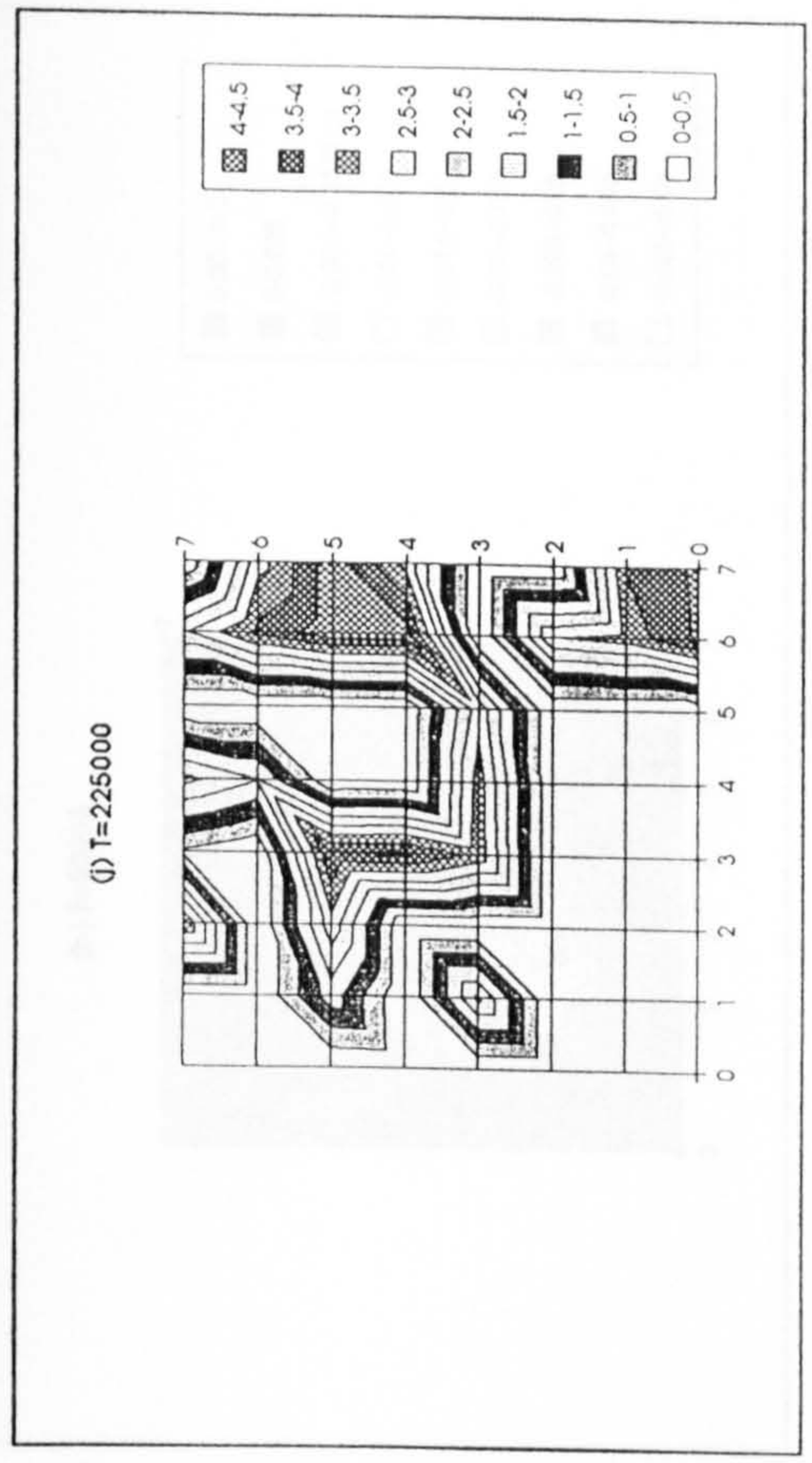

Figure 6.13 (cont...) – Simulation XI (R_0 landscapes)

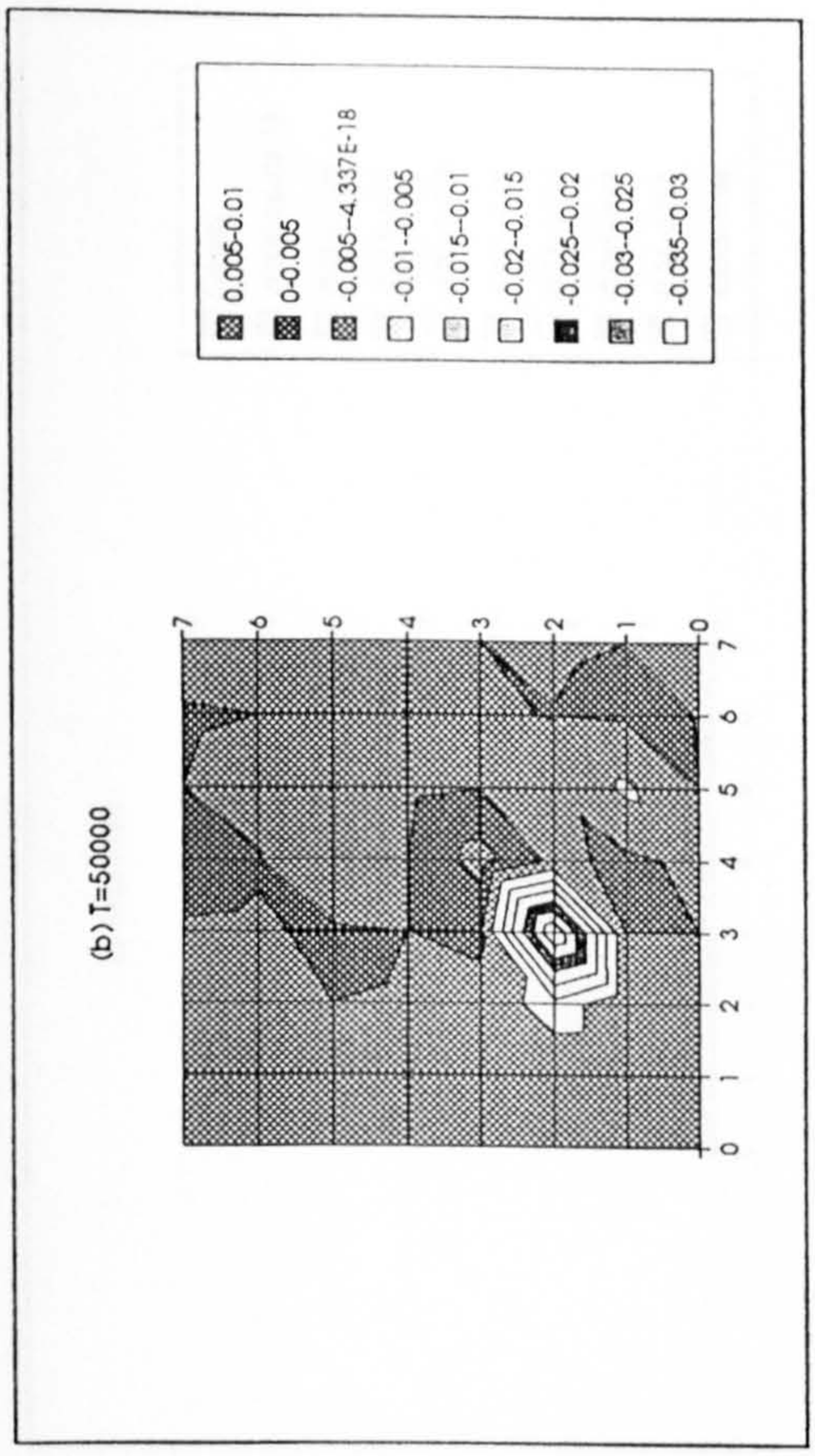

Figure 6.14 – Comparison of Simulations X and XI

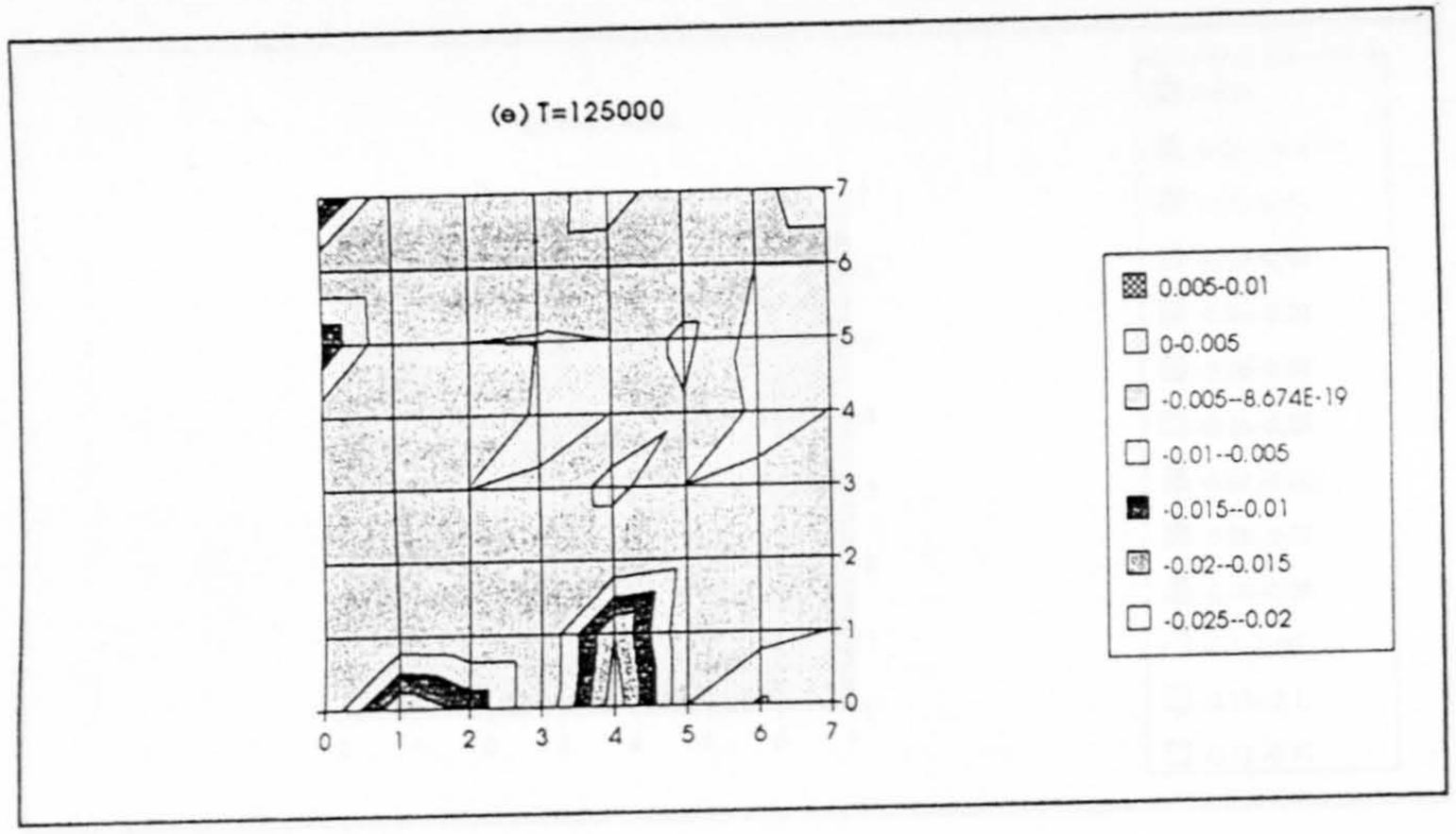

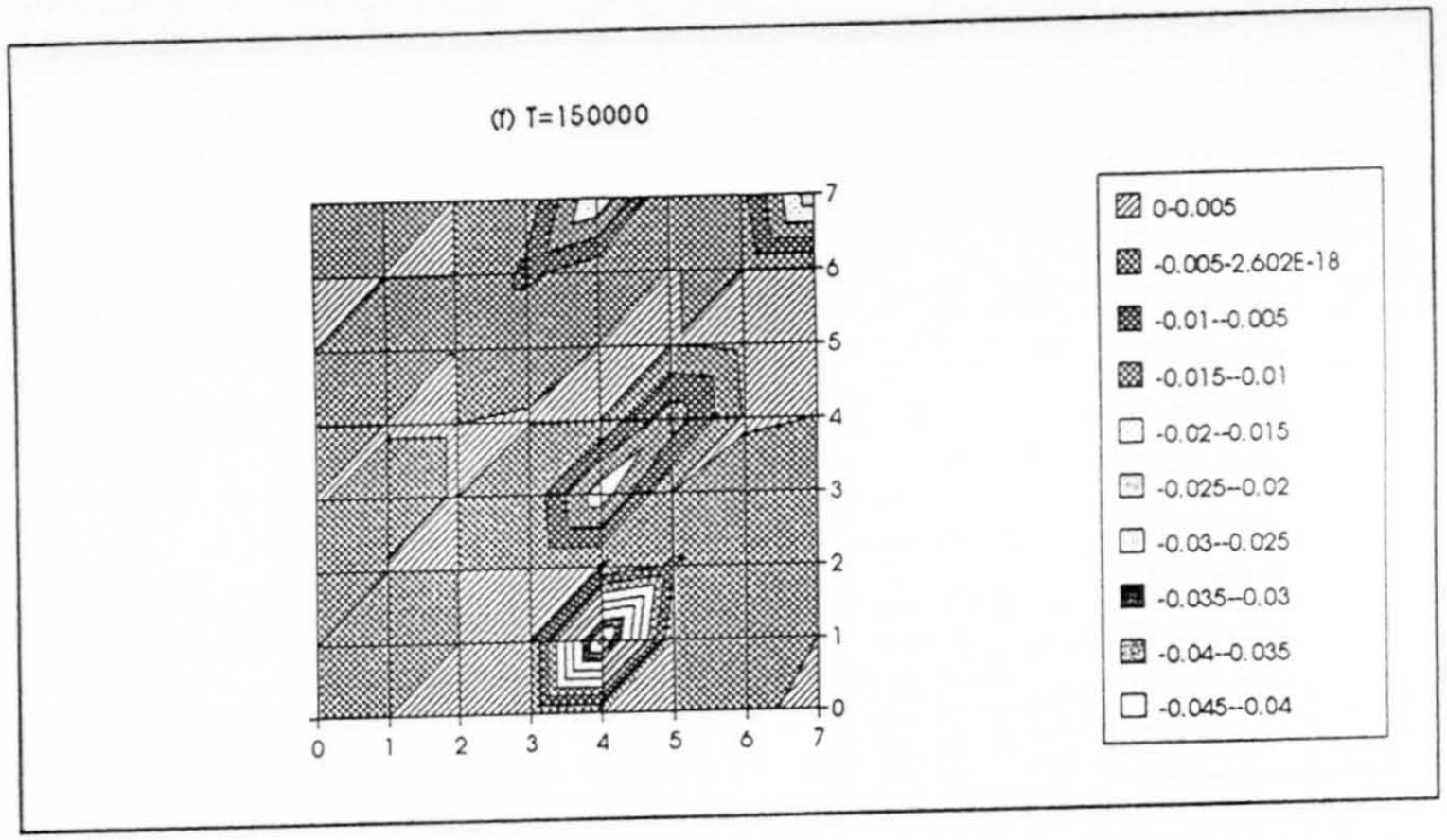

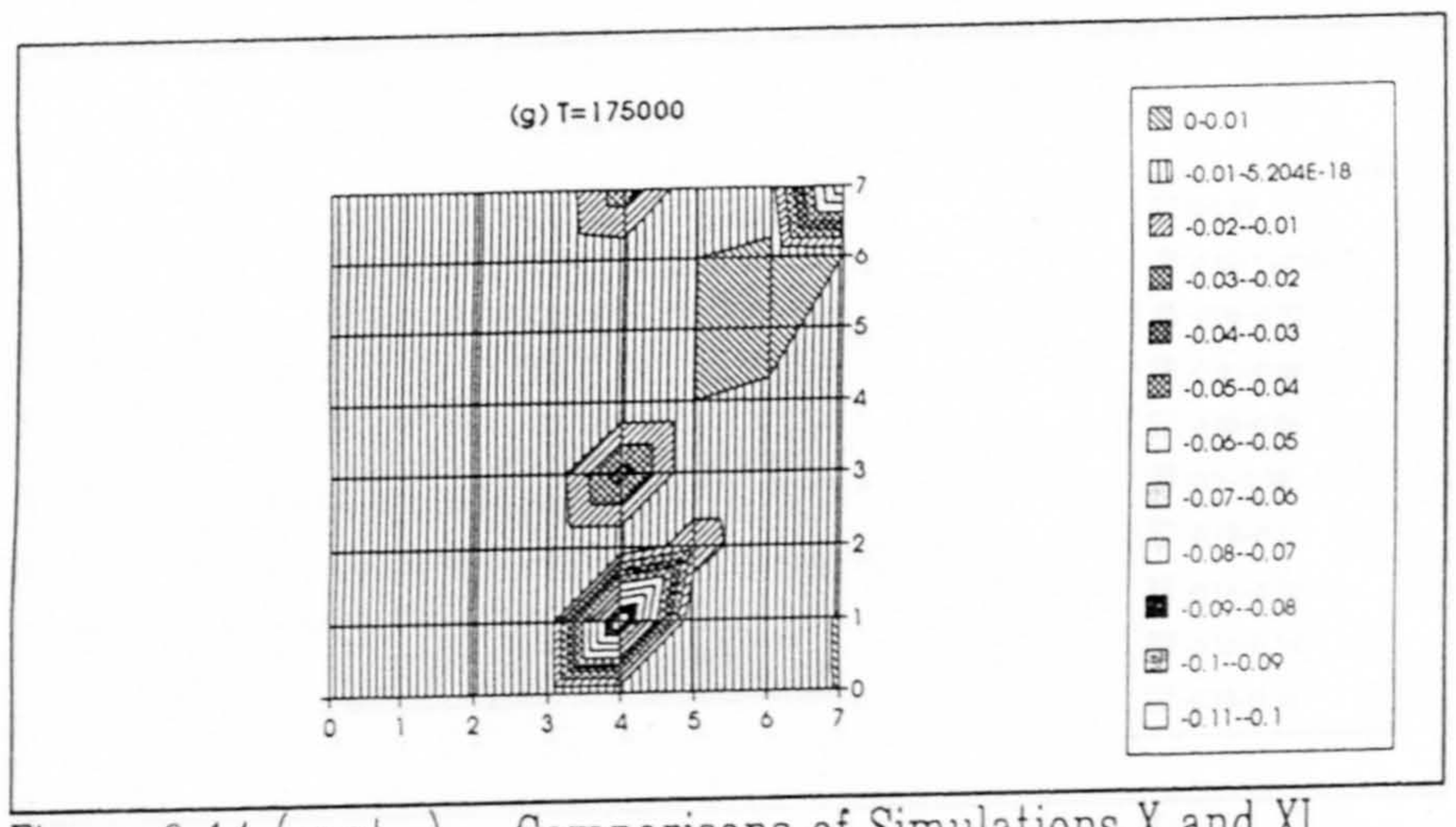

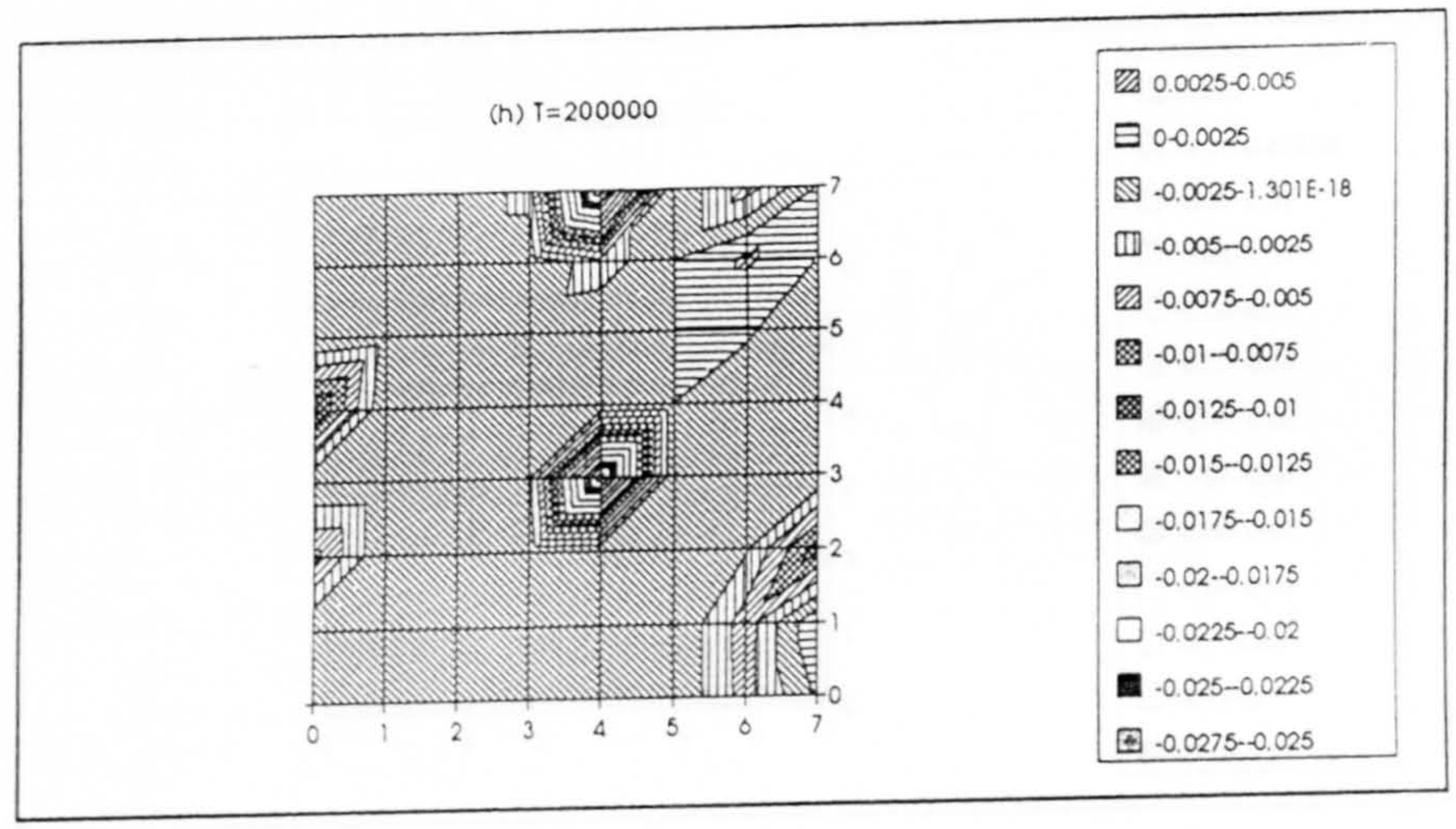

Figure 6.14 (cont...) - Comparisons of Simulations X and XI

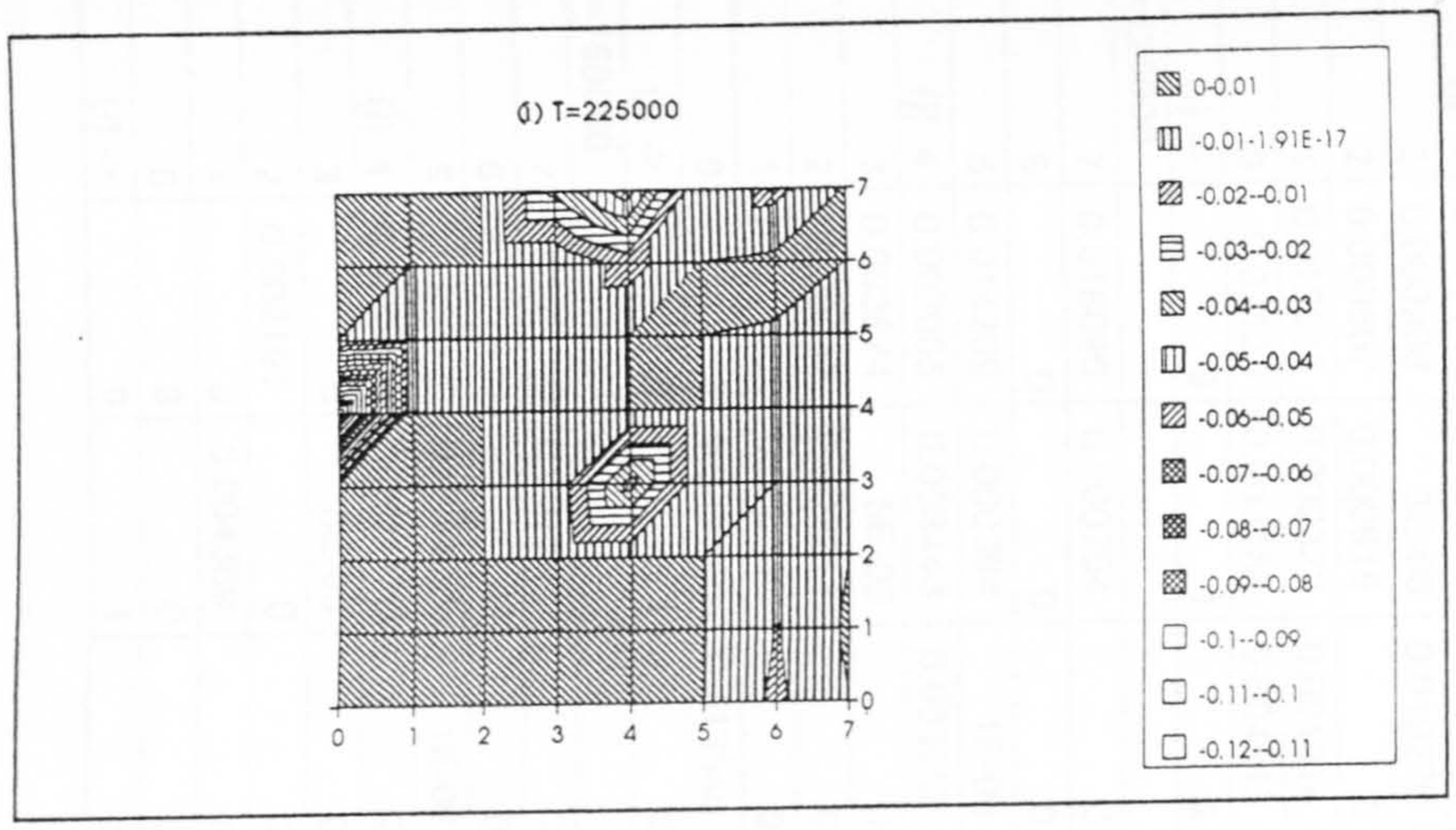

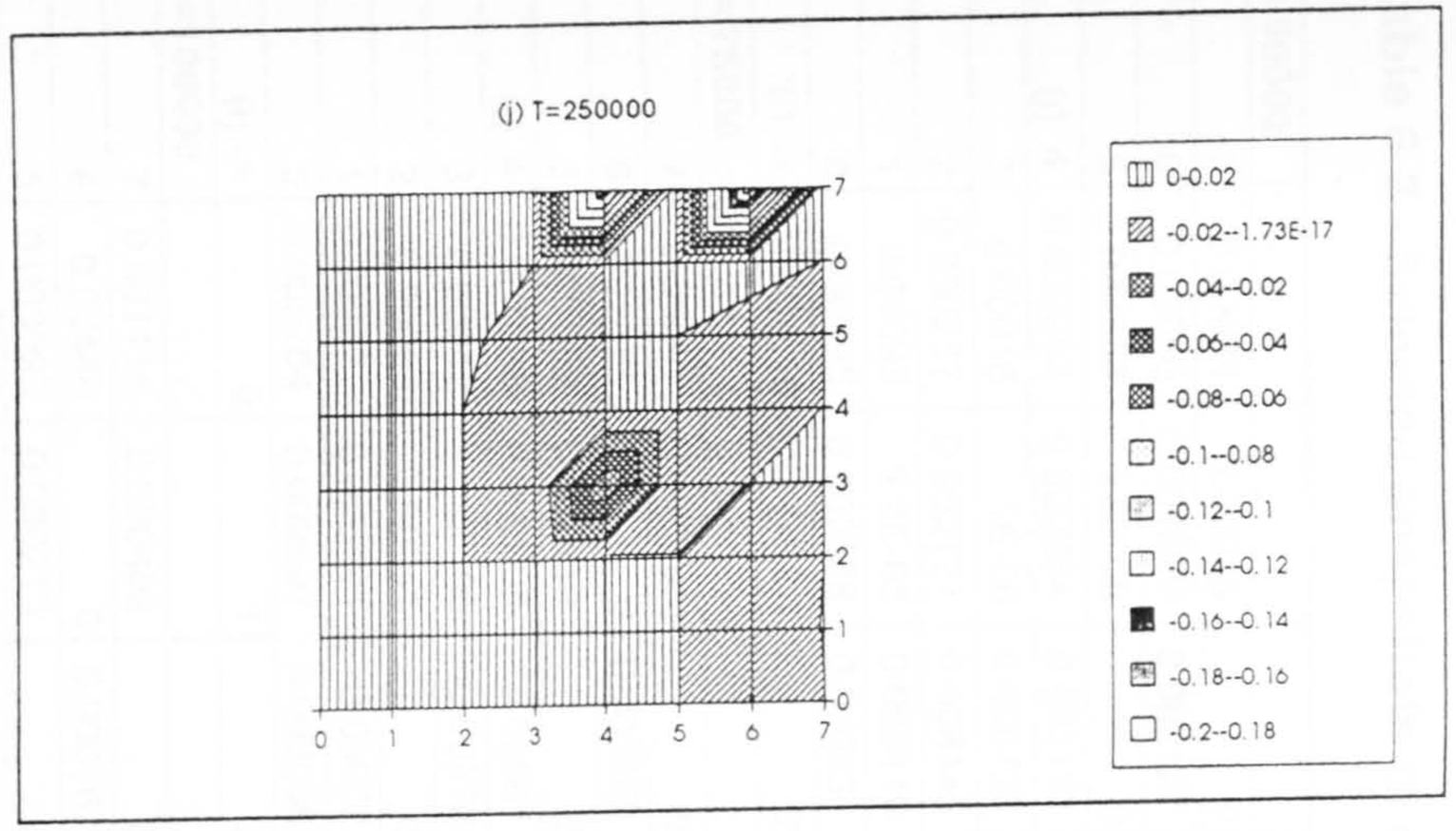

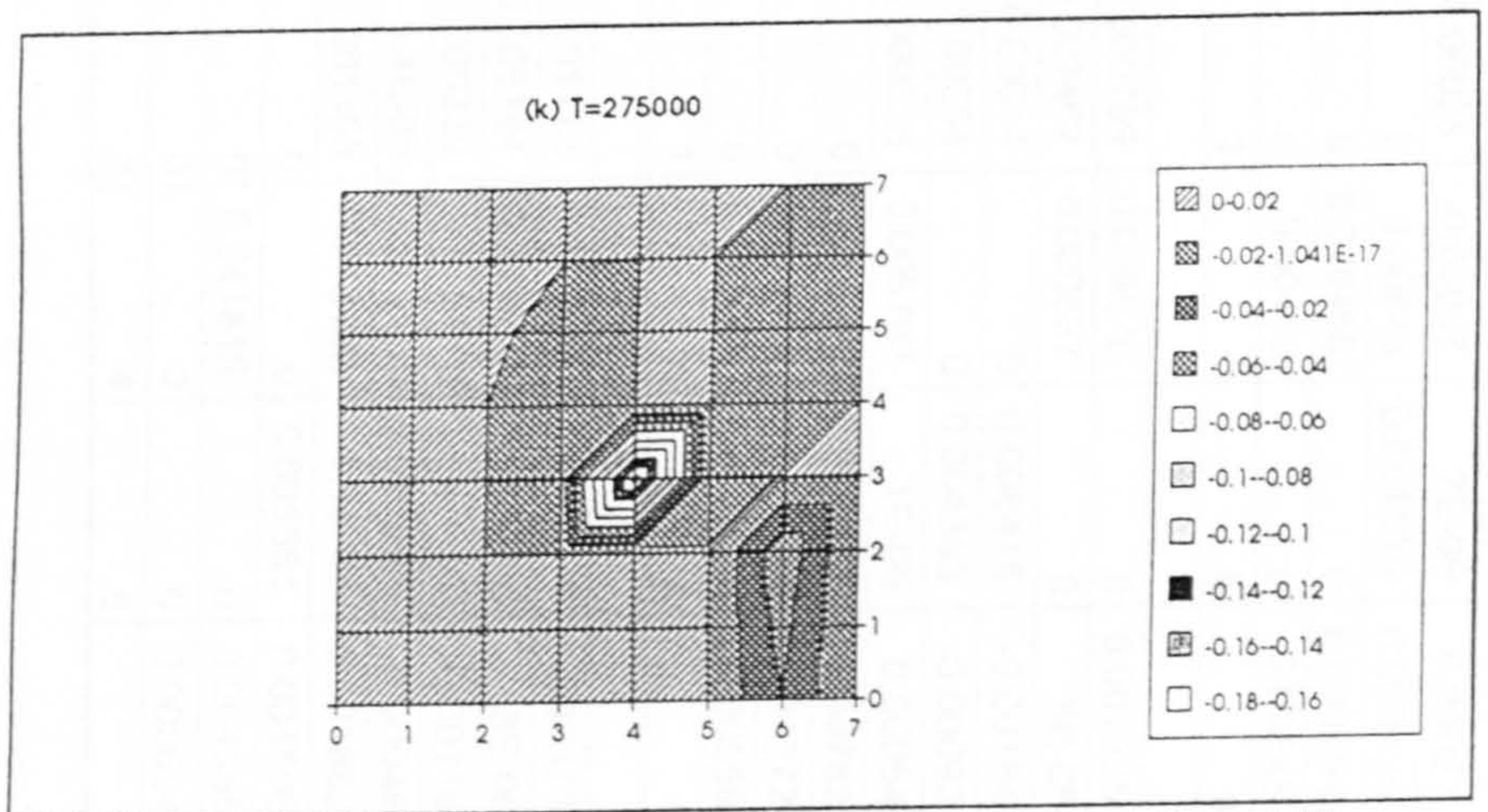

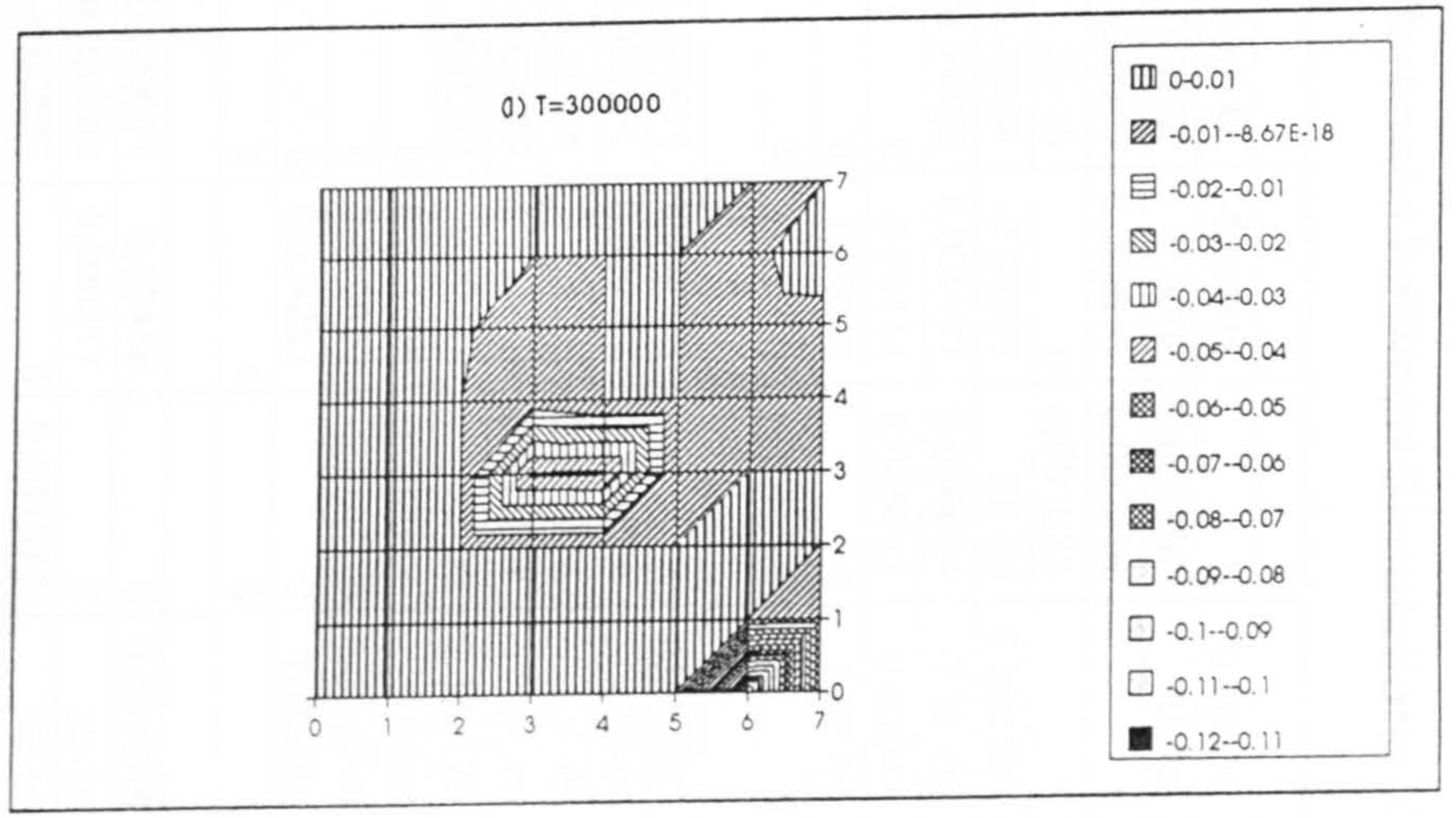

Figure 6.14 (cont...) - Comparisons of Simulations X and XI

Table 6.2 - Selected snapshots of differences between Simulations X and XI

t= 50000								
7	0.00021	0.00016	0	0.000147	-0.00065	0	-0.00031	0.001588
6	0.00066	0.001089	0.000122	0.000262	-0.0002	0.000892	2E-06	0
5	0.000533	5.5E-05	0	-0.0004	0.003645	0.000216	0	0
(j) 4	0.000293	0.000254	0.000153	2E-06	0	0.001033	0	0
3	0.00018	1E-06	0.000733	-0.00054	-0.00705	2E-06	0.000121	0
2	0.000237	0.000121	0.008145	0.03498	0.001167	0.000684	-3.5E-05	0.000211
1	0.00095	9.2E-05	0.000119	0	-0.00114	0.005812	-0.00047	0
0	0.00195	0.000588	0.000931	0	0.00116	0	2.6E-05	1E-06
(i) ->	0	1	2	3	4	5	6	7
t= 75000								
7	0.00067	0.000396	0	0.000454	0.005484	0	0.000902	0.006277
6	0.001675	0	0.000282	0.000561	0.000467	0.094604	2E-06	0
5	0.001888	0.000119	0	-4.2E-05	0	0.000726	2E-06	-0.00072
(j) 4	0.001836	0.000908	0.00067	-0.00056	0	0.002137	2E-06	0
3	0.00042	2E-06	0.00278	-0.0002	-0.00012	3E-06	0.000176	0
2	0.00085	0.00041	0	0	0.003786	0.002047	0.0004	0.001414
1	0.002477	0.000191	0.00032	0	0.010822	0	0.001219	1E-06
0	0.005764	0.002597	0.003008	0	0.004252	0	-0.00863	1E-06
(i) ->	0	1	2	3	4	5	6	7
t=100000								
7	0.001115	0.000402	0	0.000601	0.00468	0	0.001505	0.006084
6	0.00448	0	0.000767	0.000603	0.000817	0	3E-06	1E-06
5	0.003093	0.000213	0	-0.00027	0	0.001379	6E-06	-0.0011
(j) 4	0.001695	0.001257	0.001078	-0.00065	0	0.002269	-0.00075	0
3	0.000908	3E-06	0.019226	-0.00028	-0.00037	7E-06	0.00027	0
2	0.000507	0.000615	0	0	0.00843	0.001535	0.000425	0.001368
1	0.012815	0.000322	0.001314	0	0.020466	0	0.000754	2E-06
0	0.03123	0.003152	0.004313	0	0.00483	0	-0.00848	2E-06
(i) ->	0	1	2	3	4	5	6	7
t=125000								
7	0.018096	0.000704	0	0.000759	0.009076	0	0.002235	0.010376
6	0	0	0	0.001462	0.000837	0	5E-06	0
5	0.014209	0.000394	1E-06	-0.00014	0	0.006415	-0.00184	-0.00083
(j) 4	0.002005	0.003443	0.003652	-0.00054	0	0.004393	-0.00093	0
3	0.003874	5E-06	0	0.000228	0.006792	1E-05	0.00054	0
2	0.000847	0.002211	0	0	0	0.002529	0.000782	0.002517
1	0	0.000736	0	0	0.019845	0	0.001972	3E-06
0	0	0.019345	0.013546	0	0.022667	0	-0.00559	-0.00034
(i) ->	0	1	2	3	4	5	6	7
t=150000								
7	0	0.001591	0	0.001173	0.019594	0	0.003373	0.024183
6	0	0	0	0.006194	0.001613	0	8E-06	2E-06
5	0	0.000443	1E-06	0.000239	0	0	-0.00116	-9.3E-05
(j) 4	0.003915	0	0	-5.4E-05	0	0.012995	-0.00046	0
3	0	8E-06	0	0.001463	0.018198	1.4E-05	0.001682	0
2	0.002101	0	0	0	0	0.005561	0.001506	0.003501
1	0	0.004369	0	0	0.041815	0	0.004555	4E-06
0	0	0	0	0	0	0	0.000694	-0.001
(i) ->	0	1	2	3	4	5	6	7

Figures 6.12(g) and 6.13(g)), and in cells [4,1] and [4,7], detectable at T=175000 (Figures 6.12(h) and 6.13(h)) and T=250000 (Figure 6.12(j) and 6.13(j)) respectively, although the latter two are more difficult to detect since the surrounding areas have already collapsed (ie. R_0=0).

In order to overcome this problem of resolution, the difference between the two simulation outputs (X and XI) has been calculated and presented in an equivalent spatial form (see Figure 6.14). The calculated differences between 5 of the snapshots are detailed in Table 6.2. It can now be clearly observed where the sensitivity has been affected by the OS141 data.

Even with this limited number of snapshots, a surprisingly large number of cells have been identified as being relatively more sensitive to catastrophe. Examining the snapshots from T=50000 (Figure 6.14(b)) to T=150000 (Figure 6.14(f)) - the precise differences given in Table 6.2 - it can be seen that a number of cells have become more sensitive (ie. the R_0 trajectory is falling more rapidly) due to the effects of variations in slope:

Simulation Snapshot		Cells identified
(b)	T=50000	[3,2]
(c)	T=75000	[5,6]
(d)	T=100000	[0,0], [2,3], [4,1]
(e)	T=125000	[0,5], [0,7], [1,0], [2,0], [4,0]
(f)	T=150000	[4,1], [4,3], [4,7], [7,7]

Thus, it has become clear that, at the resolution provided by this model, identification of variations in the R_0 landscapes due to additional variability within individual cells is more readily apparent through examination of the differences between simulated landscapes. However, as can be seen in Figure 6.15 (showing the difference in flushing times of Simulations X and XI of individual cells relative to the actual time to flushing, T), only the cells with a relatively large sensitivity change, or those very close to flushing (eg. cell [0,7] @ T=125000), have been identified.

The ordering of cells in Figure 6.15 reflects the order in which flushing occurred; cell [5,7] was detectable at T=0 (Figure 6.12(a)), whereas cell [6,1] was only becoming detectable at T=300000 (Figure 6.14(l)). Although cell [0,7] was detected in the snapshot at T=125000 (Figure 6.14(e)), and cell [4,1] was detectable from T=100000 through T=175000, Figure 6.15 shows that detection of cell [0,7] was fortunate given the timing of the snapshots; cell [0,7] 'flushed' at T=127169 (a difference of 5.1 days or 0.401%) and cell [4,1] 'flushed' at T=195632 (a difference of 420.1 days or 21.8%). These timings, and those of the other cells, are detailed in Table 6.3.

It has become apparent, therefore, that the resolution addressed by this model appears adequate to observe both the hydrologically and chemically sensitive regions of the Rutland Catchment, highlighted in Simulations IX and X, respectively. However, localized influences of urban cover are only observable through active comparison of

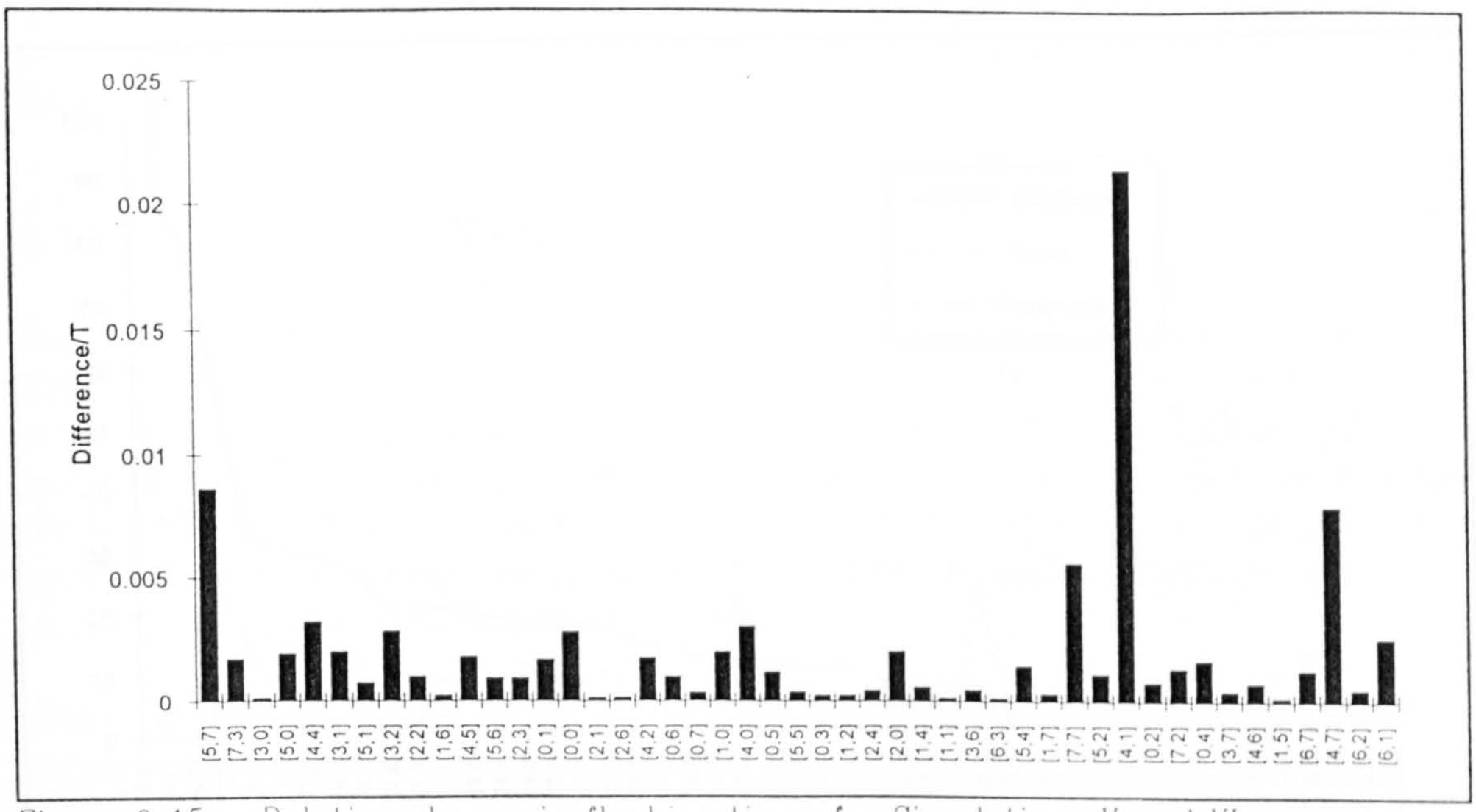

Figure 6.15 – Relative change in flushing times for Simulations X and XI

outputs (such as Figure 6.14), suggesting that increasing the resolution of the model or changing the observational perspective (for example to 1km-square cells), may display more clearly observable changes in the spatial output; an exercise not feasible within this research due to the limits on resolution forced by the resolution of the NSI data (5km).

However, through comparison of Simulations X and XI, a correlation between the urban cover and the relative temporal change in flushing can be seen in Figure 6.16, where the cells have been sorted by the relative change experienced (shown in Figure 6.15). This relative difference in timing (Diff/T) has been scaled up in Figure 6.16 in order that the graphs may be presented together. Woodland and urban areas are percentages as given in Table 6.1. This figure also shows the minimal apparent influence of wooded regions within the catchment. Simulations XII and XIII will determine whether these influences may also become more observable given increased model resolution.

In order to verify the consistent influence of urban cover - as suggested by the correlation displayed in Figure 6.16 - implying increased runoff to rivers, a further simulation, XI(i), was run based upon the homogenous initial conditions for soil composition.

Figure 6.17 (displaying the cells in numerical order) presents the changes shown in Figure 6.15 as percentages (ie. the difference in flushing times between Simulations X and XI as a percentage of the actual flushing time of the given cell). These percentages are detailed in Table 6.3. Similarly, the differences between Simulations XI(i) and IX (chemically homogenous) are also presented as percentages, detailed in Table 6.3. Both Figure 6.17 and Table 6.3 highlight a close correlation with the characteristics emerging from Simulation XI.

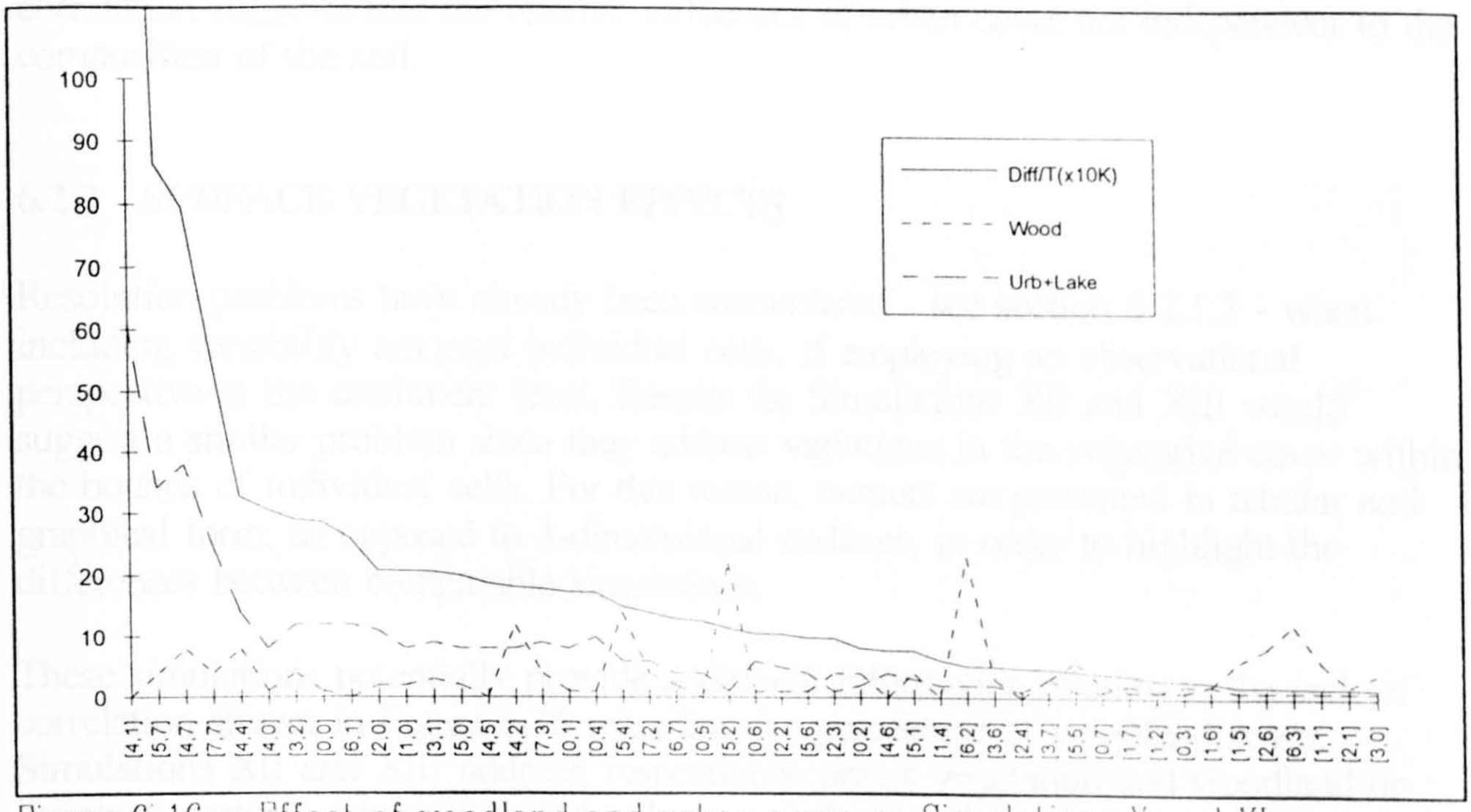

Figure 6.16 – Effect of woodland and urban areas on Simulations X and XI

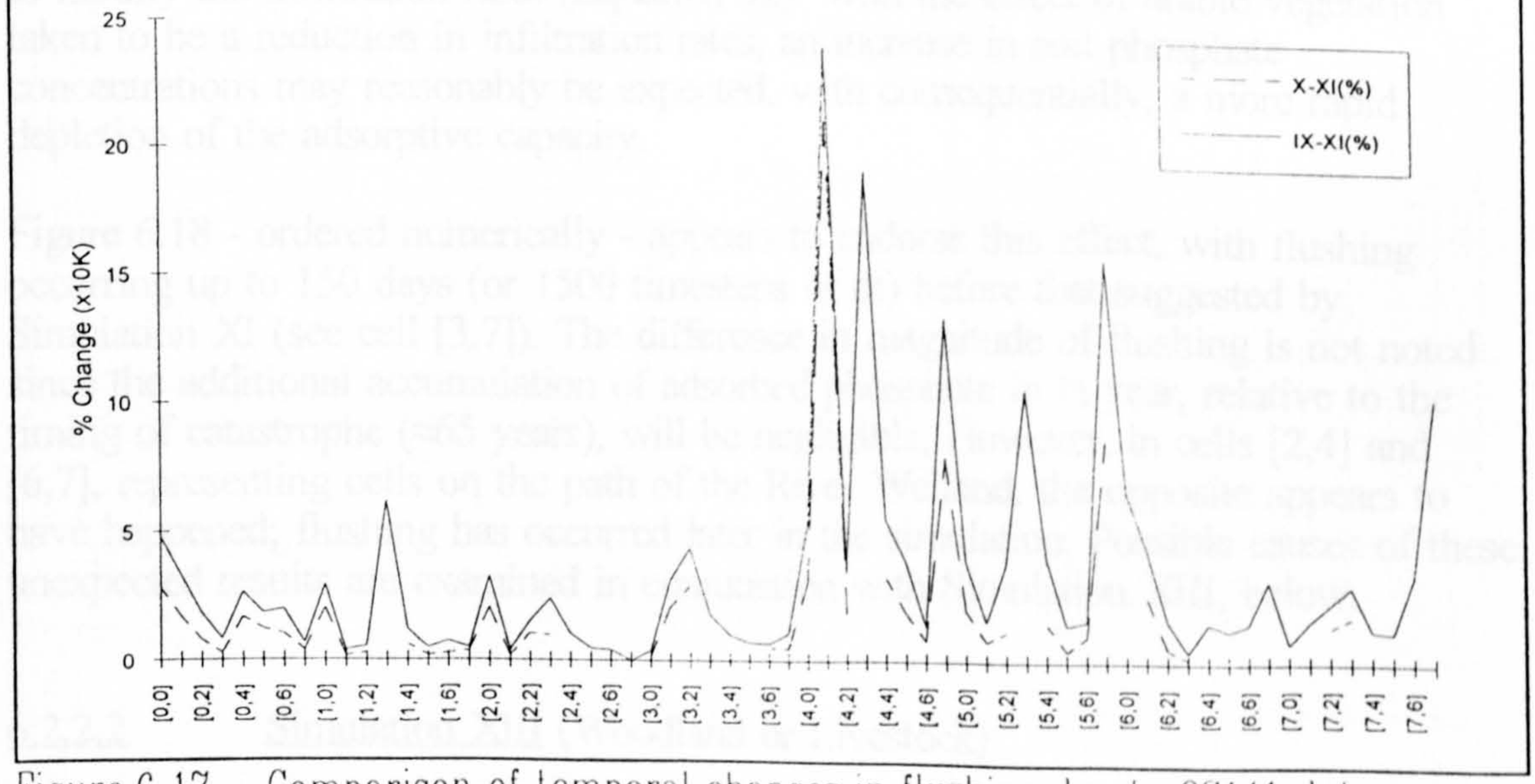

Figure 6.17 – Comparison of temporal changes in flushing due to OS141 data

Although a number (17) of cells did not reach flushing point in Simulation XI, this correlation suggests that the relative influences of urban cover are independent to the composition of the soil.

6.2.2 SURFACE VEGETATION EFFECTS

Resolution problems have already been encountered - see section 6.2.1.2 - when including variability amongst individual cells, if employing an observational perspective at the catchment level. Results for Simulations XII and XIII would suggest a similar problem since they address variations in the vegetative cover within the bounds of individual cells. For this reason, outputs are presented in tabular and graphical form, as opposed to 3-dimensional surfaces, in order to highlight the differences between comparable simulations.

These simulations potentially provide additional information relating to the lack of correlation shown in Figure 6.16 regarding the percentage of woodland cover. Simulations XII and XIII address, respectively, arable vegetation and woodland or livestock pastures where further details are not forthcoming; Simulation XI assumed non-livestock grassland.

6.2.2.1 Simulation XII (Arable vegetation)

Simulation XII assumes that the remainder of vegetation cover, after the inclusion of the Ordinance Survey (OS141) data, is to be taken to be arable. The effect of this is to modify the infiltration rates (Equation 32). With the effect of arable vegetation taken to be a reduction in infiltration rates, an increase in soil phosphate concentrations may reasonably be expected, with consequentially, a more rapid depletion of the adsorptive capacity.

Figure 6.18 - ordered numerically - appears to endorse this effect, with flushing occurring up to 150 days (or 1500 timesteps of dt) before that suggested by Simulation XI (see cell [3,7]). The difference in magnitude of flushing is not noted since the additional accumulation of adsorbed phosphate in ½ year, relative to the timing of catastrophe (≈65 years), will be negligible. However, in cells [2,4] and [6,7], representing cells on the path of the River Welland, the opposite appears to have happened; flushing has occurred later in the simulation. Possible causes of these unexpected results are examined in conjunction with Simulation XIII, below.

6.2.2.2 Simulation XIII (Woodland or Livestock)

Simulation XIII assumes that the remaining vegetation cover is livestock pasture or woodland, the expected effects being a delay in the time to flushing due to an increase in infiltration resulting in a decrease in soil phosphate concentrations.

As with Simulation XII, Figure 6.18 appears to endorse this effect - the maximum delay in the order of 100 days (see cells [1,1] and [6,3]). However, in the current

	Flushing Point (T)				OS141 Data (%)				Flushing Point (T)	
Cell#	Sim XI	Sim X	X-XI(days)	X-XI(%)	Urban	Wood	IX-XI(%)	IX-XI(days	Sim IX	Sim XI(def
[0,0]	108930	109241	31.1	2.847	12	1	4.845	98.6	204490	203504
[0,1]	106258	106441	18.3	1.719	8	1	3.313	67.5	204406	203731
[0,2]	217899	218077	17.8	0.816	2	4	1.856	37.9	204617	204238
[0,3]	136025	136064	3.9	0.287	1	2	0.841	17.2	204616	204444
[0,4]	227169	227559	39	1.714	10	1	2.66	54.4	205044	204500
[0,5]	134407	134575	16.8	1.248	4	0	1.847	37.9	205545	205166
[0,6]	122533	122661	12.8	1.044	6	1	1.997	40.6	203749	203343
[0,7]	127169	127220	5.1	0.401	1	2	0.684	14	204960	204820
[1,0]	130675	130944	26.9	2.054	8	2	2.947	59.9	203832	203233
[1,1]	155477	155503	2.6	0.167	1	6	0.402	8.2	204245	204163
[1,2]	138168	138208	4	0.289	1	1	0.551	11.3	205009	204896
[1,3]	-	-	-	-	20	0	6.178	125.6	204550	203294
[1,4]	144271	144360	8.9	0.617	2	0	1.205	24.5	203595	203350
[1,5]	238882	238926	4.4	0.184	1	6	0.485	9.9	204073	203974
[1,6]	61927	61943	1.6	0.258	2	2	0.749	15.3	204525	204372
[1,7]	182073	182140	6.7	0.368	2	1	0.497	10.1	203402	203301
[2,0]	142905	143200	29.5	2.06	11	2	3.272	66.6	204231	203565
[2,1]	110761	110779	1.8	0.162	1	2	0.397	8.1	204306	204225
[2,2]	55627	55685	5.8	1.042	5	1	1.528	31.3	205154	204841
[2,3]	104488	104590	10.2	0.975	1	4	2.39	48.8	204678	204190
[2,4]	139166	139233	6.7	0.481	1	0	1.05	21.4	204006	203792
[2,5]	-	-	-	-	1	2	0.474	9.7	204683	204586
[2,6]	119725	119747	2.2	0.184	1	8	0.417	8.5	203895	203810
[2,7]	-	-	-	-	0	6	0	0	204587	204587
[3,0]	32401	32406	0.5	0.154	1	4	0.382	7.8	204399	204321
[3,1]	46843	46939	9.6	2.045	9	3	3.091	63.4	205726	205092
[3,2]	53524	53679	15.5	2.888	12	4	4.348	89.1	205831	204940
[3,3]	-	-	-	-	3	10	1.739	36.4	206170	205806
[3,4]	-	-	-	-	2	1	0.985	20.2	205218	205016
[3,5]	-	-	-	-	2	8	0.718	14.7	204918	204771
[3,6]	159751	159834	8.3	0.519	2	3	0.668	13.6	203868	203732
[3,7]	227907	228014	10.7	0.469	3	3	1.064	21.7	204126	203909

Table 6.3 - Comparison of the effects of urban cover in Simulations IX to XI

	Flushing Point (T)				OS141 Data (%)				Flushing Point (T)	
Cell#	Sim XI	Sim X	X-XI(days)	X-XI(%)	Urban	Wood	IX-XI(%)	IX-XI(days	Sim IX	Sim XI(def
[4,0]	132462	132868	40.6	3.056	8	1	5.271	107.4	204815	203741
[4,1]	195632	199833	420.1	21.023	61	0	23.905	479.2	205253	200461
[4,2]	120701	120919	21.8	1.803	8	12	3.404	69.7	205428	204731
[4,3]	299736	-	-	-	50	4	18.975	382.5	205406	201581
[4,4]	37380	37502	12.2	3.253	14	8	5.476	112.2	206027	204905
[4,5]	71909	72043	13.4	1.86	8	0	3.851	78.9	205672	204883
[4,6]	235926	236109	18.3	0.775	4	0	1.318	27	205186	204916
[4,7]	263697	265793	209.6	7.886	38	8	13.259	268.2	204961	202279
[5,0]	34727	34796	6.9	1.983	8	2	3.9	79.9	205652	204853
[5,1]	53016	53057	4.1	0.773	3	4	1.534	31.5	205621	205306
[5,2]	190047	190263	21.6	1.135	1	22	3.758	76.9	205422	204653
[5,3]	-	-	-	-	16	20	10.482	213.1	205434	203303
[5,4]	168585	168837	25.2	1.493	6	14	4.026	82.4	205474	204650
[5,5]	134647	134705	5.8	0.431	1	6	1.405	28.8	205298	205010
[5,6]	75312	75386	7.4	0.982	4	1	1.592	32.7	205688	205361
[5,7]	11241	11338	9.7	8.555	34	4	15.495	313.8	205650	202512
[6,0]	-	-	-	-	17	0	6.554	134	205783	204443
[6,1]	289633	290384	75.1	2.586	12	0	4.413	90.4	205755	204851
[6,2]	277511	277657	14.6	0.526	2	23	1.62	33.2	205214	204882
[6,3]	163817	163845	2.8	0.171	1	12	0.416	8.5	204346	204261
[6,4]	-	-	-	-	1	12	1.555	31.9	205448	205129
[6,5]	-	-	-	-	3	36	1.251	25.6	204883	204627
[6,6]	-	-	-	-	4	4	1.516	31.1	205429	205118
[6,7]	251340	251664	32.4	1.287	4	2	3.185	65.7	206913	206256
[7,0]	-	-	-	-	2	2	0.769	15.7	204236	204079
[7,1]	-	-	-	-	4	0	1.632	33.3	204373	204040
[7,2]	224558	224870	31.2	1.387	6	4	2.305	47.1	204831	204360
[7,3]	25270	25315	4.5	1.778	9	4	2.973	60.8	205148	204540
[7,4]	-	-	-	-	3	19	1.283	26.2	204517	204255
[7,5]	-	-	-	-	3	10	1.2	24.5	204389	204144
[7,6]	-	-	-	-	8	14	3.391	69.8	206507	205809
[7,7]	186923	187969	104.6	5.565	25	4	10.301	210.4	206357	204253

Table 6.3 (cont...)

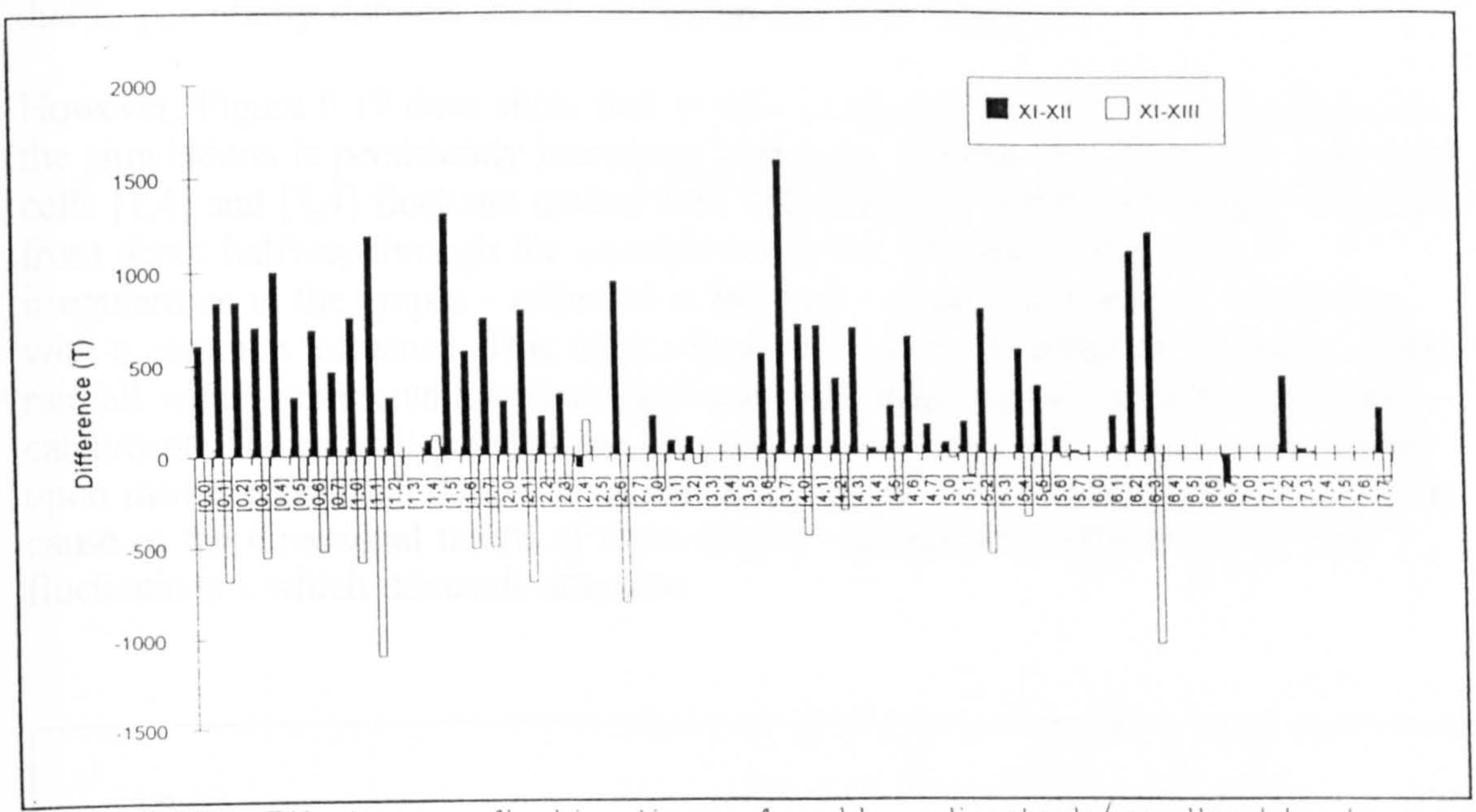

Figure 6.18 – Effects upon flushing times of arable or livestock/woodland land usage

simulation (XIII) there are four cells displaying unexpected results, with more rapid flushing; cells [1,4], [2,4], [4,4] and [7,3]. Again, apart from the latter, these cells all lie on the River Welland.

In the cells displaying the expected results, the quantitative differences between changes observed in the two simulations will be partially the result of different percentages within the cells being predefined as woodland or urban. For example, in Simulation XII, cell [5,2] reflected a vegetation/land-use combination of 1% urban, 22% woodland and 77% arable, but in Simulation XIII it reflected 1% urban, 99% woodland or pasture, and 0% arable (ie. 77% of the land usage has been altered). On the other hand, cell [3,2] reflected (12%;4%;84%) and (12%;88%;0%), respectively; 84% of the land usage being altered. Thus, given this variability in land usage alterations and the difference in percentage of urban cover between the cells, with no other changes, the effects are certain to be variable.

These five unexpected results, highlighted in Table 6.4, suggest the existence of a counteracting dynamic affecting the cells representing the River Welland (and part of the River Nene). It may be reasonable to speculate that this dynamic emerges from the representation used in the model to describe flows into rivers since this will also influence the concentration of soil phosphate. This implied complexity identifies an area where subsequent research may be useful.

No additional, conclusive information is provided when the quantified differences between the two simulations for cells [1,4] and [2,4] are compared with equivalent quantifications for cells [2,6] and [3,6] - cells displaying the expected results in Simulations XII and XIII. Cells [7,3] and [4,4] reached the flushing point too rapidly

to provide useful comparisons, and cell [6,7] has already demanded further attention due to potentially dubious initial conditions and flow directions.

However, Figure 6.19 does show that in cells [2,6] and [3,6] the difference between the simulations is persistently increasing over time, whereas the differences shown in cells [1,4] and [2,4] fluctuate around zero with cell [2,4] going increasingly negative from about halfway through the simulation (approx. 20 years). The general irregularities in the graphs - reflected in them all - suggest a degree of correlation with a common influence. This must necessarily reflect the irregular influence of the rainfall which represents a hydrological constraint affecting all the cells within the catchment. The rainfall pattern (see Chapter 3) is repeated from year to year, based upon measured rainfall data. For an understanding of the unexpected results, it is the cause of the directional trends of these graphs - as opposed to the detail of their fluctuations - which demands attention.

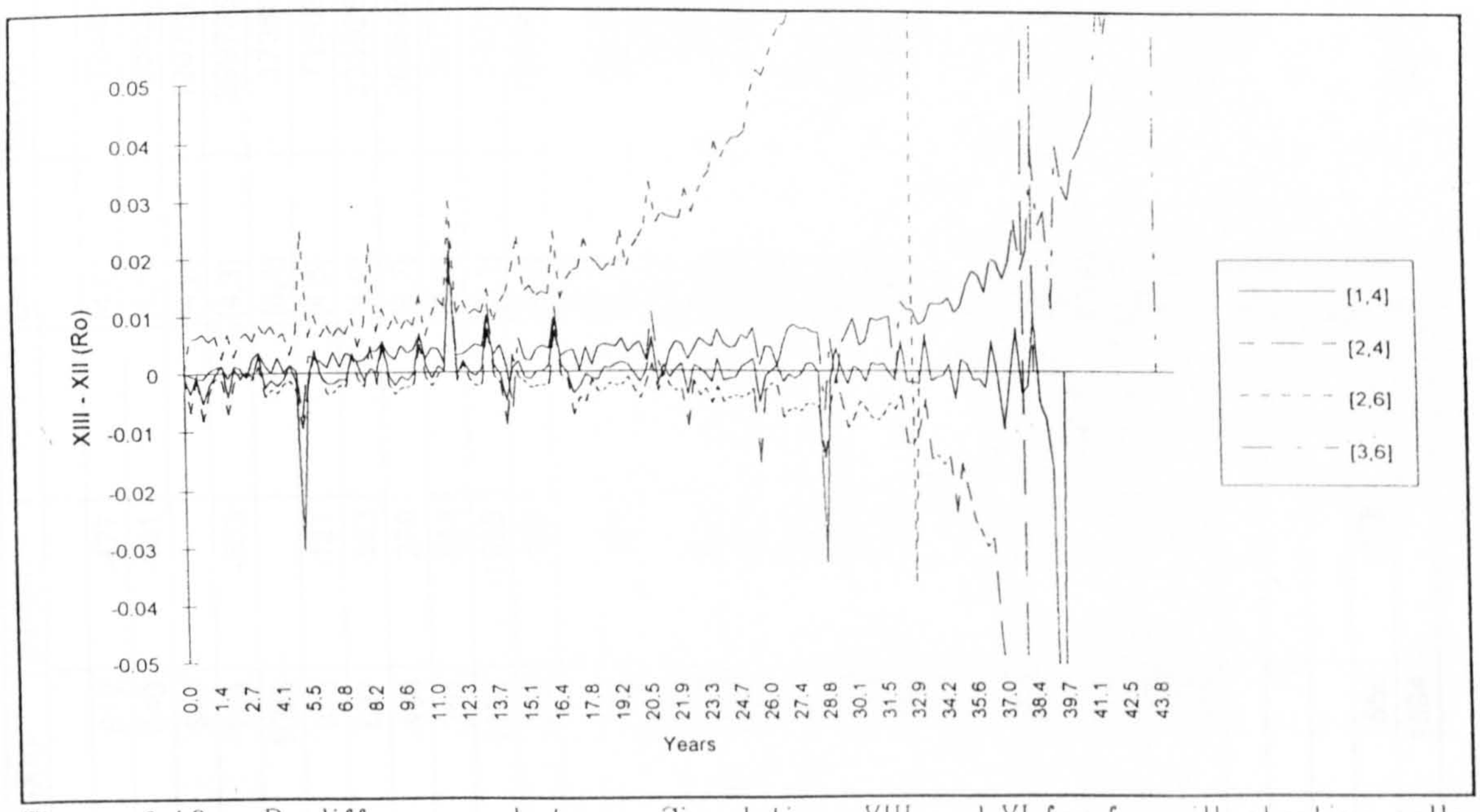

Figure 6.19 – R_0 differences between Simulations XIII and XI for four illustrative cells

6.2.3 SUMMARY OF CHEMICAL EFFECTS

With the inclusion, in Simulation X, of chemical variability amongst individual cells - based upon the NSI data - the preceding homogenous simulations (VI to IX) can no longer be used as reference points against which to examine the outputs. Hence the quasi-temporal outputs provided - using snapshots of R_0 landscapes - so that an impression is provided of the changing qualitative characteristics of the landscapes; as discussed earlier, technical limitations precluded the presentation of continuous outputs.

Cell#	Sim XI	Sim XII	Sim XIII	(XI-XII)	(XI-XIII)		Cell#	Sim XI	Sim XII	Sim XIII	(XI-XII)	(XI-XIII)
[0,0]	108930	108318	109407	612	-477		[4,0]	132462	131755	132912	707	-450
[0,1]	106258	105418	106939	840	-681		[4,1]	195632	194933	-	699	-
[0,2]	217899	217056	-	843	-		[4,2]	120701	120284	121016	417	-315
[0,3]	136025	135321	136578	704	-553		[4,3]	299736	299048	-	688	-
[0,4]	227169	226166	-	1003	-		**[4,4]**	**37380**	**37347**	**37374**	**33**	6
[0,5]	134407	134081	134528	326	-121		[4,5]	71909	71645	72141	264	-232
[0,6]	122533	121846	123056	687	-523		[4,6]	235926	235288	-	638	-
[0,7]	127169	126706	127448	463	-279		[4,7]	263697	263532	-	165	-
[1,0]	130675	129924	131259	751	-584		[5,0]	34727	34663	34748	64	-21
[1,1]	155477	154287	156572	1190	-1095		[5,1]	53016	52836	53133	180	-117
[1,2]	138168	137847	138303	321	-135		[5,2]	190047	189258	190598	789	-551
[1,3]	-	-	-	-	-		[5,3]	-	-	-	-	-
[1,4]	**144271**	**144188**	**144163**	**83**	**108**		[5,4]	168585	168016	168937	569	-352
[1,5]	238882	237571	-	1311	-		[5,5]	134647	134273	134864	374	-217
[1,6]	61927	61352	62438	575	-511		[5,6]	75312	75214	75333	98	-21
[1,7]	182073	181325	182577	748	-504		[5,7]	11241	11223	11248	18	-7
[2,0]	142905	142605	143039	300	-134		[6,0]	-	-	-	-	-
[2,1]	110761	109970	111460	791	-699		[6,1]	289633	289423	-	210	-
[2,2]	55627	55409	55790	218	-163		[6,2]	277511	276416	-	1095	-
[2,3]	104488	104150	104684	338	-196		[6,3]	163817	162625	164858	1192	-1041
[2,4]	**139166**	**139238**	**138975**	**-72**	**191**		[6,4]	-	-	-	-	-
[2,5]	-	-	-	-	-		[6,5]	-	-	-	-	-
[2,6]	119725	118783	120532	942	-807		[6,6]	-	-	-	-	-
[2,7]	-	-	-	-	-		**[6,7]**	**251340**	**251501**	-	**-161**	-
[3,0]	32401	32184	32601	217	-200		[7,0]	-	-	-	-	-
[3,1]	46843	46765	46876	78	-33		[7,1]	-	-	-	-	-
[3,2]	53524	53424	53578	100	-54		[7,2]	224558	224135	-	423	-
[3,3]	-	-	-	-	-		**[7,3]**	**25270**	**25241**	**25259**	**29**	11
[3,4]	-	-	-	-	-		[7,4]	-	-	-	-	-
[3,5]	-	-	-	-	-		[7,5]	-	-	-	-	-
[3,6]	159751	159201	159909	550	-158		[7,6]	-	-	-	-	-
[3,7]	227907	226313	-	1594	-		[7,7]	186923	186670	187079	253	-156

Table 6.4 - Variations in flushing time (T) experienced due to arable (XII) and woodland (XIII) vegetation

However, even with this static presentation, some useful understanding of the catchment has been obtained. Immediate correlation with the previous findings can be seen in the apparent sensitivity observed in cell [7,3], on the River Nene, and cell [5,7], representing Rutland Water itself.

The two potentially most significant characteristics observed may be the apparent sensitivity emerging in the higher reaches of the River Welland when comparisons of later simulations are made with Simulation X - with R_0 falling more rapidly to zero, indicating catastrophe - and the persistent band of apparent resilience - where R_0 remains high throughout - which stretches across the same catchment.

Finally, simulations XI to XIII show that the effects of urban cover or vegetation - varying between individual cells - are significant at that level (see Figure 6.16), but are not clearly observable from a catchment perspective (see Simulation XI, Figure 6.13). However, these individual changes at cell level may represent a catalyst for unexpected or counterintuitive change when their combined influence affects catchment level dynamics as observed in cells [1,4] and [2,4] in Simulations XII and XIII.

6.3 EXTERNAL PERTURBATIONS

Examination of the hydrological constraints upon, and the chemical variability inherent amongst individual cells representing the Rutland catchment, has identified a number of regions demanding further attention. However, these dynamics have been observed under the influence of homogenous rates of acid deposition and phosphate applications across the catchment. In the current model these influences are treated as external perturbations and are not varied between cells.

The following simulations, based upon the initial conditions of Simulation XI, examine variations in the annual acid deposition and average annual rates of phosphate application. In this way the broader effects of changes in these influences may be observed.

In the context of this complex and chemically and hydrologically heterogenous representation of the catchment, simulations XIV to XVII may be used to examine the overall effect of external perturbations, through manipulation of the key inputs - acid loading and phosphate applications. These four simulations are distinguished as:

XIV Acid loading doubled

XV Acid loading trebled

XVI Phosphate applications doubled

XVII Phosphate applications trebled.

6.3.1 VARIATIONS IN ACID DEPOSITION

All the preceding simulations have been carried out assuming a homogenous acid loading of 10 $kMha^{-1}yr^{-1}$ across the catchment; a loading which represents both a reasonable aggregate of acid deposition in a European context, and a level which can be buffered by most soil types [Alcamo et al 1990; Ulrich 1983]. Simulations XIV and XV employ homogenous loadings of 20 and 30 $kMha^{-1}yr^{-1}$, respectively.

By retaining such homogeneity, the effect of a widespread increase in acid deposition may be observed, with any apparent variation in response resulting from the diversity of characteristics inherent in the cells, as opposed to diversity created by variable deposition rates across the catchment.

6.3.1.1 Simulation XIV (Double load)

Employing an acid loading of 20 $kMha^{-1}yr^{-1}$, Simulation XIV may be expected to indicate flushing occurring in approximately half the time shown in Simulation XI since the acid loading has been doubled. The changes in spatial patterns would not be expected to change significantly except in their temporal context since the modification reflected in this simulation does not change the initial variability of conditions, but the external influences imposed upon them.

These temporal effects may be observed in Figure 6.20 where the times to flushing, relative to Simulation XI, are plotted against the time to flushing in Simulation XI (Simulation XIV shown by ■). Individual cells are not identified since the purpose is to display the characteristic effects of increased acidification across the catchment as a whole.

The plot shows that there is a reasonably consistent temporal change across all cells, but flushing occurs more rapidly than suggested above, with flushing occurring in approximately $^4/_9$ (or 0.45) of the time; this may be explained by the effects of acid buffering by silicates - set homogenously at 2 $kMha^{-1}yr^{-1}$ - since silicate buffering is effective in the cation exchange buffer range (see section 4.1.2) and results in an effective change in acid loading from 8 to 18 $kMha^{-1}yr^{-1}$ in the respective simulations (XI and XIV).

A further simulation - XIV(i) - was carried out with the silicate buffer rate set to zero in order to verify this explanation; the effect may be observed in Figure 6.20 (Simulation XIV(i) shown by ○) where the change is in general confirmed as approximately 0.4 (or $^8/_{20}$).

However, there is a distinct variation between individual cells - detailed in Table 6.5 - around this overall temporal change; the five most prominent differences being shown by cells [5,6], [0,1], [1,0], [4,0] and [4,1]. These cells represent areas with two common characteristics - defined by the initial conditions - which may be affecting these variations:

(i) They show a high initial pH (see Table 6.1) which will provoke minor reductions in buffering capacity due to a lack of silicate buffering until the pH has dropped sufficiently to enter the cation exchange buffer range.

(ii) They reflect a high initial adsorbed phosphate content (see Table 6.1, Q_{Ca}), the result of which will be an R_0 trajectory indicating greater proximity to catastrophe (flushing) and therefore the possibility, given the high initial pH, that flushing will occur in the carbonate buffer range.

Thus, depending upon the initial pH and adsorbed phosphate content, silicate buffering may be proportionately less; cell [5,6] reflects a state where no silicate buffering is apparent and flushing occurs within the carbonate range.

The smaller changes observed in the remaining cells reflect generally lower initial pH's and percentages of adsorbed phosphate (Q_{Ca}), varying between cells. The influences of Q_{Ca} and pH on R_0 will thus be less apparent with the variability in relative timings reflecting the variabilities in Q_{Ca} and pH. This variability becomes more pronounced over time because of the cumulative effect of these slight variations. This increasing variability in the relative timing of flushing is reflected by the plots in Figure 6.20.

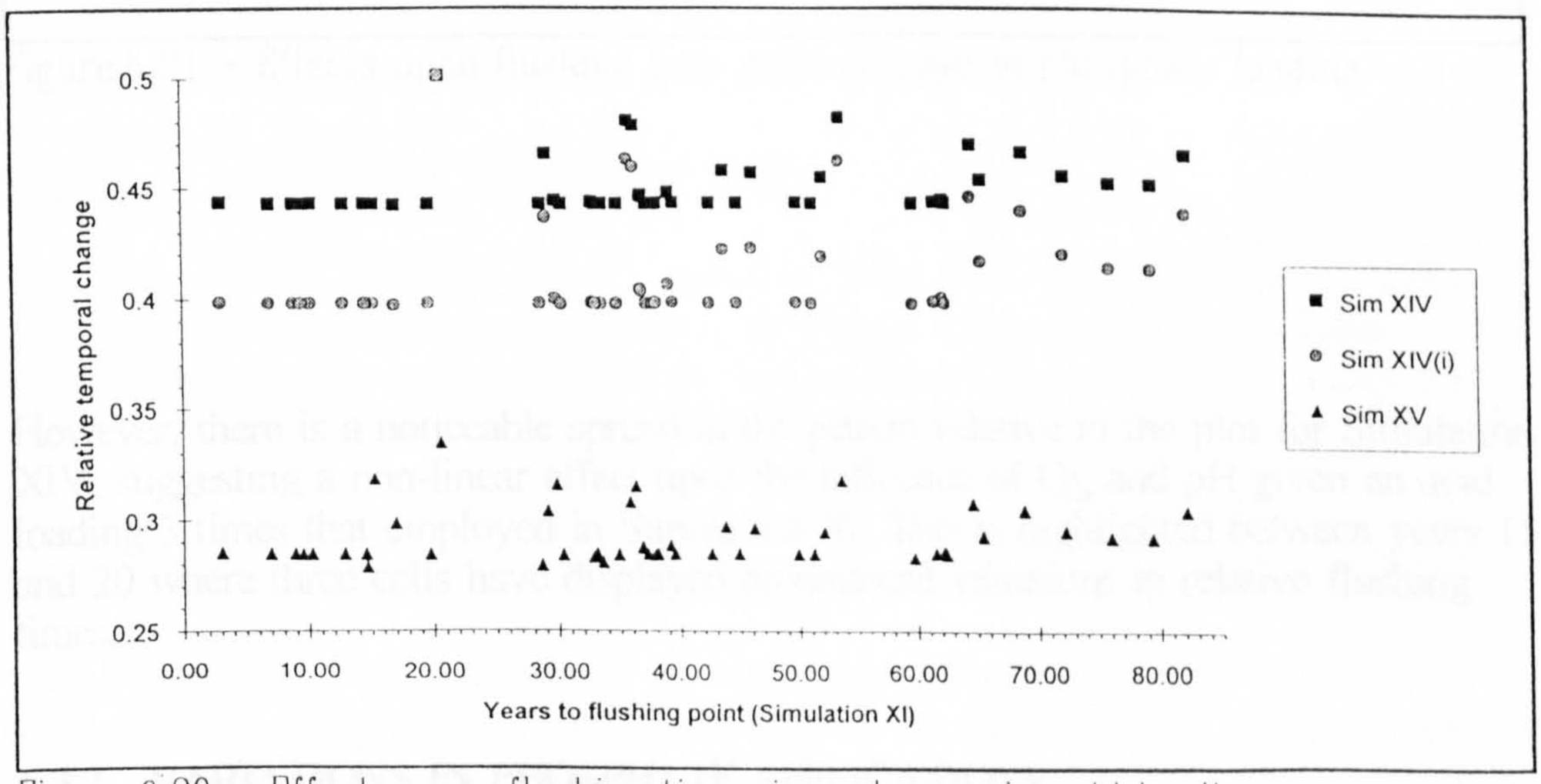

Figure 6.20 – Effects upon flushing time given changes in acid loading

6.3.1.2 Simulation XV (Treble load)

Similarly, Simulation XV - employing an acid loading of 30 $kMha^{-1}yr^{-1}$ - may be expected to indicate flushing generally occurring in a third of the time of Simulation XI; or $^2/_7$ of the time, accounting for the effects of silicate buffering.

The temporal changes resulting from this simulation, shown in Figure 6.20 as ▲, display a similar pattern to those of the preceding simulation. The relative change in flushing time - compared with Simulation XI - is confirmed to be generally between $^2/_7$ and $^1/_3$.

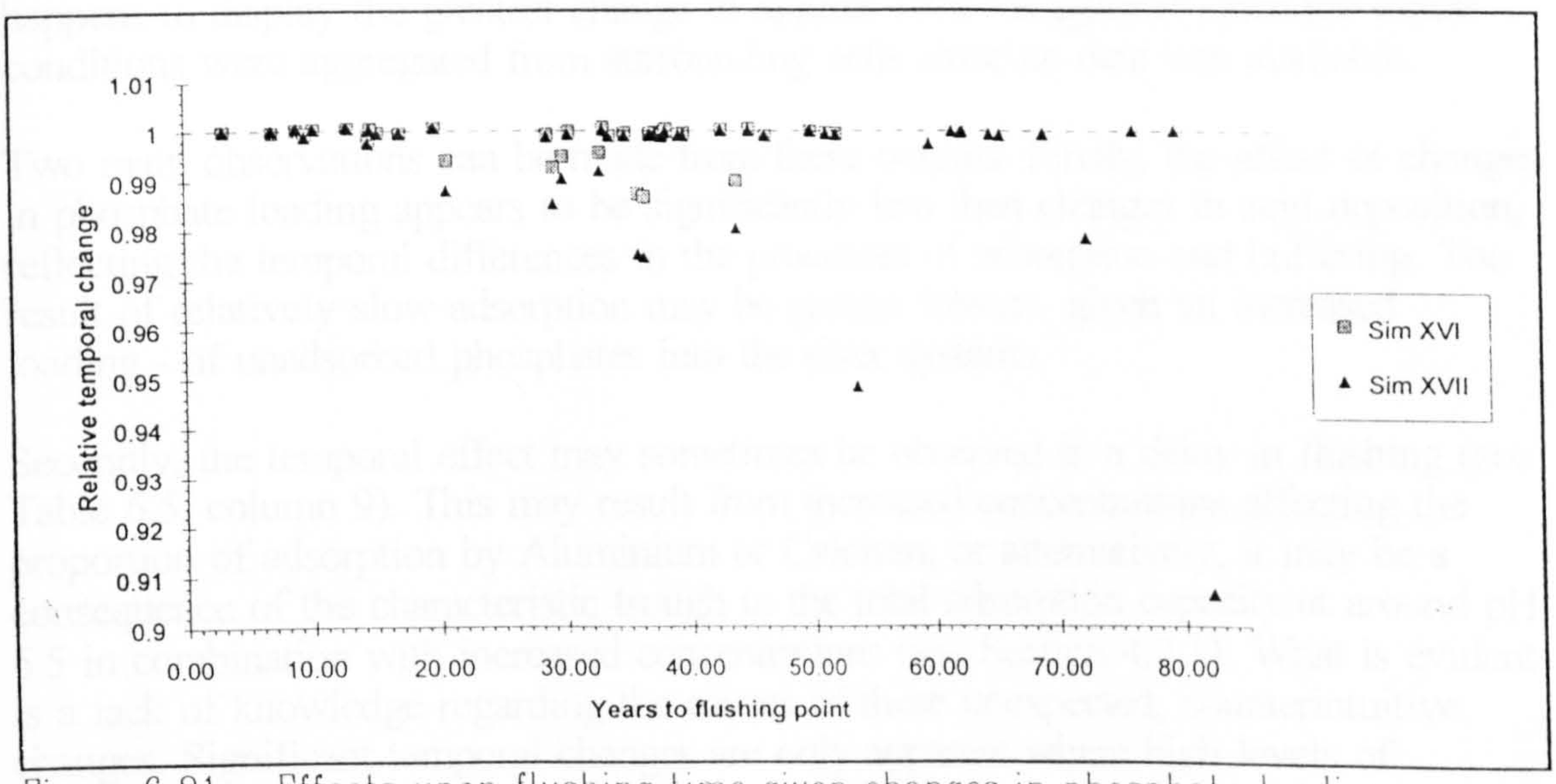

Figure 6.21 - Effects upon flushing time given changes in phosphate loading

However, there is a noticeable spread in the pattern relative to the plot for Simulation XIV, suggesting a non-linear effect upon the influence of Q_{Ca} and pH given an acid loading 3 times that employed in Simulation XI. This is highlighted between years 15 and 20 where three cells have displayed pronounced variations in relative flushing times.

6.3.2 VARIATIONS IN PHOSPHATE APPLICATIONS

As with the acid loading, the phosphate loading also represents a homogenous influence across the catchment. A loading of 31 $kgha^{-1}yr^{-1}$ (1 $kMha^{-1}yr^{-1}$) has been assumed in all the preceding simulations. Although this represents a loading chemically equivalent to 3 $kM(Acid)ha^{-1}yr^{-1}$, the relative temporal effect of changes

in phosphate loadings is shown below to be of a different order of magnitude to that observed with acid deposition levels. Simulations XVI and XVII employ homogenous phosphate loadings of 2 and 3 $kMha^{-1}yr^{-1}$, respectively.

6.3.2.1 Simulation XVI (Double load)

Simulation XVI, employing a doubled level of phosphate applications, suggests a relatively minor influence upon the timing of flushing. Whereas a doubling of acid deposition provoked a proportionate decrease in the timing - or a doubling of the rate of change of the spatial patterns across the catchment - the current simulation shows a maximum variation of roughly 3%, with most cells reflecting changes of +/-0.2%. These relative temporal changes are presented in Figure 6.21 - plotted in a similar fashion to Figure 6.20 - and detailed in Table 6.5. The output for cell [4,3] - which happens to display the greatest change of approx 10% - is ignored since the initial conditions were aggregated from surrounding cells since no data was available.

Two main observations can be made from these outputs. Firstly, the effect of changes in phosphate loading appears to be significantly less than changes in acid deposition, reflecting the temporal differences in the processes of adsorption and buffering. The result of relatively slow adsorption may be greater losses - given an increased loading - of unadsorbed phosphates into the river systems.

Secondly, the temporal effect may sometimes be observed in a delay in flushing (see Table 6.5, column 9). This may result from increased concentrations affecting the proportion of adsorption by Aluminium or Calcium, or alternatively, it may be a consequence of the characteristic trough in the total adsorption capacity at around pH 6.5 in combination with increased concentrations (see Section 4.2.1). What is evident is a lack of knowledge regarding the causes of these unexpected, counterintuitive changes. Significant temporal changes are only apparent where high levels of previously adsorbed phosphates are present in the soil.

6.3.2.2 Simulation XVII (Treble load)

Simulation XVII - $3kM(PO_4)ha^{-1}yr^{-1}$ - provides little additional information, except that the relative changes observed (shown in Figure 6.21 and detailed in Table 6.5) are emphasised. However, the observed changes are still an order of magnitude less than those displayed by changes in acid loading.

6.4 SUMMARY OF OBSERVATIONS

The order in which the simulations are presented in this chapter - and Simulation I in Section 5.3.2.1 - has enabled a picture to be built up, in the context of a catchment, of the dynamic spatial characteristics of the discontinuous inter-relationships between acid buffering and phosphate adsorption in the soil domain.

The logic of the ordering of simulations is described in Chapter 3, progressing from the simple to the complex and from spatial homogeneity to heterogeneity. The summary of findings presented below similarly follows this logical progression.

Cell No.	Yrs(XI)	Sim XI	SimXIV	diff(XIV)	Sim XV	diff(XV)	SimXVI	diff(XVI)	SimXVII	diff(XVII
[0,0]	29.84	108930	48423	0.4445	34415	0.31594	108388	0.995	107891	0.9905
[0,1]	29.11	106258	49483	0.4657	32296	0.30394	105479	0.9927	104713	0.9855
[0,2]	59.70	217899	96505	0.4429	61656	0.28296			217360	0.9975
[0,3]	37.27	136025	60293	0.4432	38727	0.28471	136018	0.9999	135958	0.9995
[0,4]	62.24	227169	100959	0.4444	64907	0.28572			227128	0.9998
[0,5]	36.82	134407	60074	0.447	38684	0.28781	134325	0.9994	134296	0.9992
[0,6]	33.57	122533	54308	0.4432	34444	0.2811	122435	0.9992	122425	0.9991
[0,7]	34.84	127169	56346	0.4431	36182	0.28452	127145	0.9998	127059	0.9991
[1,0]	35.80	130675	62839	0.4809	40255	0.30805	129030	0.9874	127434	0.9752
[1,1]	42.60	155477	68911	0.4432	44260	0.28467	155545	1.0004	155491	1.0001
[1,2]	37.85	138168	61210	0.443	39314	0.28454	138102	0.9995	138022	0.9989
[1,3]					159473					
[1,4]	39.53	144271	63992	0.4436	41098	0.28487	144241	0.9998	144152	0.9992
[1,5]	65.45	238882	108373	0.4537	69922	0.29271			238700	0.9992
[1,6]	16.97	61927	27420	0.4428	18480	0.29842	61902	0.9996	61898	0.9995
[1,7]	49.88	182073	80753	0.4435	51868	0.28487	182083	1.0001	182107	1.0002
[2,0]	39.15	142905	64021	0.448	41266	0.28877	142828	0.9995	142782	0.9991
[2,1]	30.35	110761	49070	0.443	31515	0.28453	110775	1.0001	110692	0.9994
[2,2]	15.24	55627	24654	0.4432	17711	0.31839	55614	0.9998	55601	0.9995
[2,3]	28.63	104488	46308	0.4432	29228	0.27973	104431	0.9995	104377	0.9989
[2,4]	38.13	139166	61704	0.4434	39639	0.28483	139244	1.0006	139153	0.9999
[2,5]					178530					
[2,6]	32.80	119725	53158	0.444	33936	0.28345	119214	0.9957	118762	0.992
[2,7]			175028		116811					
[3,0]	8.88	32401	14362	0.4433	9227	0.28478	32410	1.0003	32421	1.0006
[3,1]	12.83	46843	20763	0.4432	13339	0.28476	46870	1.0006	46879	1.0008
[3,2]	14.66	53524	23727	0.4433	14923	0.27881	53561	1.0007	53544	1.0004
[3,3]			143987		94356				289764	
[3,4]			168642		111396					
[3,5]			164686		107428					
[3,6]	43.77	159751	73143	0.4579	47469	0.29714	158149	0.99	156614	0.9804
[3,7]	62.44	227907	100992	0.4431	64867	0.28462			227920	1.0001
[4,0]	36.29	132462	63418	0.4788	41750	0.31518	130721	0.9869	129084	0.9745
[4,1]	53.60	195632	94334	0.4822	62212	0.31801			185560	0.9485
[4,2]	33.07	120701	53504	0.4433	34373	0.28478	120811	1.0009	120737	1.0003
[4,3]	82.12	299736	139668	0.466	91182	0.30421			271751	0.9066
[4,4]	10.24	37380	16574	0.4434	10648	0.28486	37395	1.0004	37397	1.0005
[4,5]	19.70	71909	31857	0.443	20467	0.28462	71967	1.0008	71970	1.0008
[4,6]	64.64	235926	110796	0.4696	72505	0.30732			235799	0.9995
[4,7]	72.25	263697	120068	0.4553	77828	0.29514			258025	0.9785
[5,0]	9.51	34727	15386	0.4431	9884	0.28462	34710	0.9995	34686	0.9988
[5,1]	14.52	53016	23503	0.4433	15092	0.28467	52927	0.9983	52884	0.9975
[5,2]	52.07	190047	86452	0.4549	56008	0.29471	189949	0.9995	189912	0.9993
[5,3]										
[5,4]	46.19	168585	77014	0.4568	49961	0.29635	168441	0.9991	168440	0.9991
[5,5]	36.89	134647	60114	0.4465	38707	0.28747	134604	0.9997	134553	0.9993
[5,6]	20.63	75312	37769	0.5015	25205	0.33467	74867	0.9941	74419	0.9881
[5,7]	3.08	11241	4991	0.444	3208	0.28538	11241	1	11241	1
[6,0]			147891		97428				284293	
[6,1]	79.35	289633	130868	0.4518	84585	0.29204			289695	1.0002
[6,2]	76.03	277511	125429	0.452	81093	0.29222			277573	1.0002
[6,3]	44.88	163817	72606	0.4432	46632	0.28466	163903	1.0005	163838	1.0001
[6,4]			194984		127605					
[6,5]					131788					
[6,6]					151720					
[6,7]	68.86	251340	117202	0.4663	76532	0.3045			251206	0.9995
[7,0]					137541					
[7,1]					152743					
[7,2]	61.52	224558	99608	0.4436	63996	0.28499			224572	1.0001
[7,3]	6.92	25270	11202	0.4433	7199	0.28488	25263	0.9997	25274	1.0002
[7,4]										
[7,5]			185283		120663					
[7,6]					195266					
[7,7]	51.21	186923	82833	0.4431	53210	0.28466	186864	0.9997	186826	0.9995

Table 6.5 - Difference in flushing times due to changes in acid & phosphate loads (Simulations XIV to XVII)

The simulations of *simple, homogenous catchments* (I to V) - with Simulation I being taken as a baseline reference point, void of rivers - highlighted the significant effects of spatial flows and rivers upon R_0 trajectories observed previously in a non-spatial context (see Chapter 4):

- Simulation I saw the emergence of a *band of equipotential* in the R_0 landscape (see Figure 5.11) spanning a region where an increased accumulation of adsorbed phosphates has resulted in an indication of catastrophe in advance of adjacent regions, and surrounding troughs of particularly high phosphate concentrations (cell[1,1]).

- Simulation II (Section 6.1.1.1) and III (Section 6.1.1.2) indicated that this band of equipotential is shifted in response to the existence of rivers to which both surface and soil water are 'lost', thus affecting the concentrations of phosphates across the catchment.

- Simulations IV (Section 6.1.1.3) and V (Section 6.1.1.4) displayed qualitative variations in the landscape, and thus the band of equipotential, the result of combinations of river types (see Figure 6.6).

The simulations of *complex, homogenous catchments* (VI to IX) - presented in section 6.1.2 - incorporated the first level of definition of the Rutland Water catchment: the directional flow pattern described by Figure 3.5(b) and Table 6.1. The latter simulations (VIII and IX) including also the HOST definitions and topography of the catchment, respectively. The significant findings were:

- The emergence of complex bands of equipotential - those in Simulations VI and VII being relatable to the simple bands shown by Simulations I and V, respectively - which persisted throughout the simulations (see Figure 6.9).

- Unexpected results shown by Simulation VII in cell[6,7] indicated that an alternative hexagonal spatial grid may be more appropriate than a square grid for the representation of spatial flows and river flow patterns.

- Unexpected counteraction in Simulation VIII of the anomalous effect in cell[6,7] (Simulation VII) identified potentially dubious HOST data defining this cell; an abnormally low SPR value was being used.

- Simulations VIII and IX (incorporating heterogenous hydrological conditions) displayed only subtle variations in the R_0 landscape, suggesting that increasing the resolution of the model may make these changes more clearly observable from the catchment perspective.

- Three regions of sensitivity to catastrophe, as a result of the hydrological conditions, were highlighted across the Rutland catchment (see Figure 6.9(d)): the upper reaches of the River Welland, the lower reaches of the River Nene, and Rutland Water itself.

In the simulations of *complex, heterogenous catchments* (X to XIII) - presented in Section 6.2 - it was no longer possible to compare the R_0 landscapes with the preceding simulations since the initial chemical conditions varied between cells, thus also defining unique characteristic R_0 trajectories for each cell. Simulation X (Section 6.2.1.1) thus provides the baseline reference point for all subsequent simulations. Furthermore, it was also, therefore, necessary to utilize sequences of snapshots of the R_0 landscape in examining its characteristics (see Figure 6.12, for example). The main findings were:

- Regions of sensitivity to catastrophe, due to the chemical conditions, were noted (see Simulation X, Figure 6.12), with a region upstream from the Nene extraction point (cell[7,3]) being particularly sensitive. A correlation between these regions and the hydrologically sensitive regions was noted.

- A band of *resilience* to catastrophe emerged across the River Welland - observable in Figure 6.12(l) - indicating a change in the underlying geological conditions across the highlighted region.

- A correlation between the percentage of urban cover and changes to the R_0 landscape were noted (see Figure 6.16) although the potential resolution problems of Simulations VIII and IX were repeated (see Simulation XI, Figures 6.13 and 6.14).

- Simulations XII and XIII (Section 6.2.2) displayed counterintuitive results through unexpected changes in the timing of catastrophe in response to variations in the vegetative cover (see Figure 6.18). These unexpected changes followed the path of the River Welland, and further examinations shed no light on the nature of this apparent complexity.

Finally, the effects of *external perturbations* on the complex, heterogenous catchment were presented in Simulations XIV to XVII (Section 6.3). The significant findings were:

- The difference in magnitude of the effects of varying the acid and phosphate loadings; changes in acid loading having proportionate effects on the timing of catastrophe, whereas the effects of different phosphate loadings is marginal (see Figures 6.20 and 6.21).

- The greater the initial pH and adsorbed phosphate content (Q_{tca}), the greater the variability in timings given changes in acid loading.

- The indication in Simulation XV that a large increase in the acid loading may have a non-linear effect upon the influence of pH and previously adsorbed phosphate on this variability in relative timings (see Figure 6.21, years 15-20).

- Simulations XVI and XVII (Section 6.3.2), showing marginal effects of changes in phosphate loading, provoke concern over the 'fate' of these additional phosphates since, if they are not adsorbed, it is likely that they are flowing rapidly into the water courses.

- Simulations XVI and XVII also display counterintuitive results, again along the path of the River Welland, where the timing of catastrophe is unexpectedly delayed. As with the counterintuitive results of Simulations XII and XIII (vegetation cover), a need to examine further the dynamics emerging along the River Welland is suggested.

CHAPTER 7. INTERPRETATION OF RESULTS

In Chapters 4 and 5 the dynamics displayed by the chemical and hydrological sub-modules, respectively, were examined alongside detailed definitions of the sub-modules. Having provided a clear understanding of the dynamics of the key chemical interactions of acid buffering and phosphate adsorption in a non-spatial context, and the characteristic flow rates determined by the hydrological sub-module, Chapter 6 presents a series of spatial simulations of simple and complex catchments - as described in Section 3.4.5.

The current chapter summarizes the potentially significant observations noted in Chapter 6, and provides an interpretation of their significance in the context of both the Rutland Water catchment and the representation of the catchment by the model.

The focus of the model, an indicator of the propensity of the soil to act as a sink or a source of phosphates, is fundamentally qualitative in nature - it is not directly measurable, but is only determinable from its expanded constituents - and is defined by Equation 27:

$$R_{0,t+1} = LOG_{10}\left\{ \frac{R_{Ca,t+1}}{Rdep_{Ca,Po,t}} \right\}$$

Furthermore, formulation of the constituents of R_0 involves complex interacting processes and theoretical derivations (see Section 4.1.4), making attempts at their direct measurement either complicated or absurd; the dividend representing the remaining adsorptive capacity, and the divisor, the theoretical depletion rate of this capacity required to counteract a catastrophe situation described by P_0, determinable only through measurement of its components and using the appropriate equations as given in Chapter 4.

It has been shown that R_0 may be interpreted as a *Leading Indicator* - its temporal definition inherent - of a perceived qualitative change of state (from sink to source) whereby the *Catastrophe Potential*, P_0, may be exhibited.

Although R_0 has been defined within a specific context for the purposes of this research, its generic form may be interpreted in a broader context. The dividend (R) may be taken to represent a limited resource required by competing phenomena, the loss of which provokes a qualitative change of state in their environment, and the divisor (Rdep) may be taken to represent a theoretical depletion rate of this resource dependent upon the extent of availability of a supplementary resource which is potentially able to mitigate the effects of this change.

This generic interpretation of the indicator of change may add to the clarity of the initial perceived notional indicator of change which focused only on the state of the soil as a sink or source of phosphates. It represents a tangible concept which may be

used to conceptualize potential relationships between the interacting processes. Thus, with the indicator clearly defined, the significance of mechanisms of change and perturbatory influences may be assessed in relation to observable changes in the indicator.

Development of the model proceeded with dynamic simulations being performed at each stage of development. In this way, observation of the dynamics has been possible at every point in the development where the complexity of the implemented dynamics has been increased. The current chapter, therefore, interprets these findings in a similarly logical order, facilitating a progressively enhanced understanding of the dynamics of the model.

The following discussion further separates this interpretation of observations, clearly distinguishing explanations of the inherent characteristics of R_0 and the nature of influences of changes in the modelled environment upon R_0. The former provides an understanding of the indicator of change itself, and the latter, a means of observing the qualitative effects of change within the modelled catchment.

7.1 INHERENT CHARACTERISTICS OF R_0

The catastrophe indicator, R_0, given the definition of its constituent components, may be expected to reflect changes in any one, or more, of the following integral elements:

- *Soil Composition*, specifically 'free' Calcium content;
- *Acid Loading*, provoking depletion of Calcium reserves;
- *Phosphate Adsorption* by Calcium, affecting the 'free' Calcium content;
- *Phosphate Concentration* affecting adsorption rates by both Calcium and Aluminium reserves;
- *Adsorption by Aluminium*, Ads_{Al}, reflecting a supplementary resource utilized upon depletion of 'free' Calcium reserves;
- *Soil pH*, affecting R_{Ca} - in combination with 'free' Calcium reserves - and adsorption rates by both Calcium and Aluminium.

In this definition, and reflected throughout the model, are two major assumptions. Firstly, it is assumed that the composition of the soil is entirely Calcium or Aluminium, and secondly, that the only processes affecting that composition are acid buffering and phosphate adsorption. The latter assumption emerges as a consequence of the perceived phenomena - representing acidification and phosphate retention - under examination, where these two processes represent mechanisms of change utilizing a common resource.

The former assumption assists the modelling of these processes by making the distinction between *base* and *acid* cation reserves required for implementation of acid buffering, but further defining this distinction as Calcium and Aluminium, respectively, to simplify implementation of phosphate adsorption. Thus, omissions have occurred through this simplification which may be summarized as:

- *The effects of alternative base and acid cation reserves*, such as Sodium (Na), Potassium (K), Magnesium (Mg) and Iron (Fe), on the soil composition and the soil pH. Justification for their omission, in the case of the base cations, is the relative abundance of Calcium in most soils in comparison to the others, and in the case of Iron, its influence is relatively benign until very low pH's are evident, in which case soil toxicity may be more significant.

- *The effects of soil organic matter and microbial activity*, on the soil composition and pH. It has been assumed that, given the scaling of the model, their influences are relatively insignificant. However, if the resolution of the model were to be increased, their significance may increase.

- *The effects of Temperature*. No accounting for the effects of temperature fluctuations has been included in the model.

7.1.1 NON-SPATIAL CHARACTERISTICS

The non-spatial characteristics are defined by the specific representations used to implement the adsorption and buffering processes acting to deplete the Calcium reserves in the soil. It is in the identification of the timing and extent of release of previously adsorbed phosphates for which the catastrophe indicator, R_0, has been defined.

Implementation of the processes of acid buffering reflects that used by Alcamo and others (1990) - discussed in Chapter 3 - with calculation of the resultant soil pH being extended over a wider range (Equation (13)). With no appropriate definition forthcoming from complementary texts, a simple linear relationship provides the definition of resultant pH's greater than 6.2 (Equation (12)). However, this quasi-arbitrary calculation reflects the perceived tendency of Calcareous soils to sustain high levels of acid buffering with little effect upon the soil pH.

Implementation of phosphate adsorption utilizes a multi-term derivation of the Langmuir Equation - discussed in Chapter 3 - representing adsorption by Calcium and Aluminium discretely (Equation (1)). Terms describing adsorption affinities of the two resources have been derived to reflect their perceived influence across a range of pH values which suggests minimum combined adsorption at a pH of approximately 6.5 [Stevenson 1986 (see Figure 4.2(a))].

This perceived minimum rate is reflected in agricultural liming practices when used to modify the soil pH prior to phosphate applications, resulting in maximum availability to crops but also maximum potential for loss through spatial solute flows.

With the exclusion of the derived pH calculation, two significant assumptions have been made. Firstly, that the process of acid buffering is almost instantaneous; incomplete buffering apparent only when the buffer capacity - given the related conditions - has been exceeded by the acid loading. Secondly, the representation of phosphate adsorption assumes the existence of only simple phosphate compounds, ignoring complex inorganic, and all organic structures containing phosphates.

Clearly, a number of further potential influences on these dynamics have been omitted from the representation; these in addition to omissions identified in the conceptual activities, but likewise, potentially affecting R_0:

- The effects of natural weathering acting to replenish the cation reserves, counteracting the effects of both buffering and adsorption.
- The effects of organic matter and microbial activity.
- Plant uptake of nutrients.
- Neutralizing deposition.
- Alternative acid sources and their consequent influence.

Given these omissions and assumptions, the underlying characteristics of the representations themselves may be examined. It has been shown that quantitative changes in the resource levels - Calcium and Aluminium - have a linear effect upon adsorption and buffering rates; it is the adsorption affinity and the dissolution rates, both dependent upon the soil pH, which give rise to the observable non-linear dynamics.

Interpretation

For the acid loading imposed on the model throughout most of the simulations (10 $kMha^{-1}yr^{-1}$), it has been found that variation of the dissolution rates has no discernible effects upon buffering (see Section 4.2.2.1). Only when the resource becomes depleted and the pH is reduced accordingly, is there a switch in buffering between base and acid cation reserves. However, unless the acid loading is dramatically increased, the apparent rate of depletion of reserves through buffering is controlled primarily by the pH (see Figure 4.13).

In the case of phosphate adsorption, there is a clearly discernable effect upon the timing and extent of flushing of phosphates which results from variation of the adsorption affinity terms (see Section 4.2.1.2). This effect has been found to be in the order of $^{+}/-$ 8% in relation to the timing of flushing. However, as the implemented affinities are varied, either discontinuities have emerged where the disjunction of affinity terms has inhibited adsorption over small pH ranges (Figure 4.12(c), (e) and (f)), or the paradoxical range of minimum adsorption has shifted or been obscured (Figure 4.12(b), (d) and (g)), suggesting characteristics unsupportable by the literature.

In the light of these omissions and assumptions, and with a clear understanding of the dynamics represented by the model, the implications of changes in the indicator, R_0, become apparent. It was shown in Chapter 4 that a low trajectory of R_0 over time, relative to a high trajectory, suggests that the catastrophe point - complete depletion of 'free' Calcium - will be reached at a higher pH, and that the observable release of adsorbed phosphate from the remaining Calcium reserves - the catastrophe potential - will be greater (Figure 4.8). It was also shown that a rapid fall in the trajectory suggests the imminence of catastrophe.

Implicit in the R_0 trajectories - a subset presented in Figure 4.8 - is the relative abundance of 'free' Calcium and Calcium Phosphates at a given pH. High levels of adsorbed phosphate will result in reduced adsorption affinity and remaining adsorptive capacity. Thus, upon depletion of 'free' Calcium, a greater quantity of phosphates become available for potential release.

Thus, with an indication of the qualitative state - in relation to potential catastrophe - facilitated by R_0, it is no longer necessary to provide detailed quantifications of numerous state variables and processes.

7.1.2 SPATIAL CHARACTERISTICS

Having gained a clear understanding of the meaning of variations in R_0 through observing its inherent dynamics in a non-spatial environment, observation of variations due to spatial interactions - or flows of materials - may be interpreted in this context. These flows are derived from the hydrological dynamics defined in Chapter 5, based upon the HOST classifications applied to individual cells.

Prior to examination of the influence upon R_0 of variations in these hydrological dynamics, the effects of a spatial representation - providing for inflows and outflows of material - irrespective of the hydrological detail, needs to be highlighted. In a non-spatial representation, unadsorbed phosphates remain in solution for later adsorption, and, upon reaching the catastrophe point, the concentration of phosphate will rise to the maximum defined by the catastrophe potential, P_0.

However, in a spatial representation, unadsorbed phosphates in solution will be carried with the hydrological flows to adjacent regions or into water courses; the phosphate concentration will thus fluctuate spatially as a result of these flows and losses. Similarly, following the catastrophe point, released phosphates will be spatially transported with the result that the potential concentration, P_0, will never be observed. The fate of this phosphate loss may be seen in variable dynamics experienced in adjacent regions, or in increased, potentially eutrophic, releases to water courses.

The hydrological characteristics for the final model are base upon the HOST classifications - defining the hydrology by reference to physical soil characteristics and water table levels, as opposed to soil types - and their associated definitions of Standard Percentage Runoff (SPR) and Volumetric Moisture Content (VMC) (see

Chapter 5). The initial analyses assume SPR and VMC to be homogenously 50%. This homogeneity assists observation of the effects of variations in slope and infiltration rates.

In the context of the HOST classification system, SPR and VMC represent aggregated descriptions of significant hydrological characteristics. Although, by reference to detailed maps produced by SSLRC, it would be possible to identify the HOST classification given to any point in England and Wales, the current model has been based upon a 5km square grid to reflect the resolution of the NSI data. The derivation of SPR and VMC for use within the model (see Table 6.1) therefore represents a further aggregation of the original data.

In an attempt to re-introduce some of the variability observable in 'reality', but removed by the use of such aggregations, the model allows modification of the derived SPR through variations of slope and vegetative cover apparent in any given model cell. The former, through gravitational influences, will effect a change in the overall percentage runoff. The latter, through its influence upon infiltration rates, will effect a change in the proportions of SPR observable as surface and sub-surface flows. The Volumetric Moisture Content remains homogenously defined throughout.

SPR reflects the proportion of surface water lost to rivers through both surface and sub-surface flows. This requires that the model should reflect a similar characteristic loss of water in this way. However, in the representation of a 'real' catchment, at a given point there may not be obvious or conveniently proximate rivers for such a loss to be represented. It has been assumed, therefore, that the loss may be delayed through the need to flow a greater distance to a river. The representation of losses to rivers has thus been derived to reflect an aggregate overall loss similar to that suggested by SPR; reflecting also the spatial effect on local flow rates affected by these delayed losses.

With the hydrological dynamics based upon SPR and VMC, implementation of the modifying influences and losses to rivers has been achieved through categorization of the influences of surface vegetation upon infiltration, of variations in slope characteristics, and of river types. The current model assumes that these influences may be adequately represented by the use of three categories in each case. This does not preclude subsequent expansion of the categorizations.

Given this simplified representation of the hydrological dynamics, a number of factors have been omitted, although their potential significance is not readily apparent:

- *Losses due to evaporation, plant uptake and evapotranspiration* have not been addressed since inclusion of this additional complexity would detract from the purpose of the research which is to highlight the heuristic value of this complex systems approach as opposed to providing definitive information about Rutland Water.

- *The effects of soil structuring dynamics* are omitted, although these are perceived to become more significant if the spatial resolution is increased. However, this may also require an alternative hydrological representation since SPR and VMC reflect quantified aggregations of these physical characteristics based upon homogeneity.

- *Variations in water table levels and groundwater flows.* The model addresses leaching flows, but not their subsequent fate or effect.

- No account has been taken of temperature variations, either on the surface or sub-surface.

Interpretation

The effect of these vegetation, slope and river categorizations was examined by tracking the state variables and flow rates for three spatially adjacent cells; the minimum number of contiguous cells which allows examination of the effects of both inflows and outflows simultaneously (see Section 5.3.1). The significant effects of each categorization were observable through the consequent changes in soil saturation levels since it is through the saturation levels that the hydrological dynamics influence the indicator, R_0; changes in soil water content will affect phosphate concentrations, flows and adsorption rates.

The effect of increased infiltration is increased saturation and reduced phosphate concentrations, with less noticeable effects on lateral flows since SPR remains unchanged. Fluctuations continue to reflect the rainfall patterns, but it may be surmised that adsorption rates will remain consistently lower. A reduction in infiltration has, predictably, the opposite effect.

An increase in slope - reflected in an increase in SPR - has a less consistent effect on saturation and thus phosphate concentration levels. However, the magnitude of fluctuations in flow rates is increased in relation to rainfall fluctuations. The effect upon saturation levels is, again, an increase in the magnitude of fluctuations. A decrease in slope has the opposite effect, with reduced fluctuations in saturation levels.

Suggested by these observations is that - indirectly through saturation levels and phosphate concentrations - a shallow slope may result in relatively constant adsorption rates subject only to small changes, whereas a steep slope may result in more extreme variations of adsorption rates.

Finally, in observations of the effects of changes to river categorizations, it was found that the effect of 'Category 2' rivers - catchment feeders - was to compensate for local hydrological variations resulting from spatial flows in an approximation to the Standard Percentage Runoff. The effect of 'Category 3' - main catchment rivers - is an overcompensation of the spatial flows, counteracting the effect of no losses where rivers are not present - 'Category 1'.

This interpretation of the effects of spatial hydrological flows upon the indicator, R_0, has been through implicated indirect effects resulting from changing saturation levels and phosphate concentrations. To observe the qualitative effects, in the context of a catchment, requires examination of spatial R_0 landscapes. It is no longer relevant to examine only quantifications in individual cells because the spatial flows distort the changes observable non-spatially; observations must address the collective influence of changes across the grid. Thus, interpretation of the effects upon R_0 landscapes is provided in the following sections.

7.2 HYDROLOGICAL CONSTRAINTS UPON R_0

In the preceding section the inherent characteristics of R_0 have been interpreted, both non-spatially and spatially, given the representations implemented in the model and the omissions and assumptions necessary to arrive at these representations. It is thus possible to begin examining the relationships between the hydrological constraints, chemical variability - section 7.3 - and external perturbations - section 7.4 - and qualitative spatial changes in the emerging R_0 landscapes.

Ideally, observation of these qualitative changes should be continuous over time, representing both the magnitude and rate of change of R_0 in individual cells as changing spatial surfaces, or landscapes. This would enhance understanding of the relative sensitivity or resilience to change across the grid, and identification of the points of and magnitude of 'catastrophes' as they emerge. Technological limitations have precluded such continuous temporal representations within the constraints of this research, resulting instead in static descriptions of the landscape at specific intervals in time to provide the observable information. However, even using these static representations, a lot of useful information emerged (see Chapter 6).

It is useful first to clarify the effects of the transition in R_0 from the non-spatial to the spatial, and to provide a baseline reference point for examination of the hydrological constraints upon spatial R_0 landscapes. Using homogenous initial conditions throughout - equivalent to those used in the non-spatial simulations - Simulation I (section 5.3.2.1) highlights the effect of spatial flows in delaying the R_0 trajectory relative to those observed in a non-spatial context where there were no spatial phosphate losses.

The predicted temporal delay of the trajectory due to phosphate losses and reduced concentrations - found to be in the region of 15% - was evident in Simulation I. However, there was a variation across the grid in the precise delay, resulting in the emergence of a region of apparently greater sensitivity spreading across the simple, hypothetical catchment. Given the homogenous initial conditions, this region - or band of equipotential - has emerged as a result of the spatial flows alone, and, upon closer examination, it correlates with the directional flow patterns (see Figure 3.5(a)) to represent a region part way up the catchment where phosphate concentrations have remained consistently higher than the surrounding areas.

The emergence of this band of equipotential, representing an accumulation of phosphates, reflects patterns observed as the result of physical erosion in catchments by both wind and water [Imeson 1987]. These latter patterns are observable in the accumulation of hydrologically transported materials such as soil and sediments. The similarity in these phenomena may be helpful in calibration of the flows implemented in this model - to reflect specific catchment characteristics - through variation of the inhibition constant in Equations (34) and (35). This constant will affect the positioning of the band of equipotential in the catchment through the inhibition of hydrologically transported phosphates and acid.

Finally, regarding the transition of R_0 to a spatial context, it has already been highlighted that the 'flushed' phosphates - theoretically represented by P_0 - will also flow spatially. The effects of flushing may become observable as waves of increased concentration moving down the catchment with the hydrological flows. The potential effects of such waves of increased concentration are twofold:

1. A temporary increase - quantitatively dependent upon the magnitude of 'catastrophe' - in concentrations lower down the catchment, provoking increased adsorption and thus depletion of remaining adsorptive capacity, possibly followed by a small consistently increased concentration until the supplementary resource - Aluminium - mitigates the catastrophe in the 'flushed' cell. These effects upon R_0 appear to be marginal since they were not observable from the given observational perspective.

2. Transference of these wave effects directly into the river system.

The implication is that the majority of the 'flushed' phosphates may be lost to the river systems, increasing the eutrophic potential, with minimal amounts retained through adsorption, and little evident effect upon the catastrophe potential in adjacent regions.

An interpretation of these findings may involve perception of a catchment with bands of equipotential - highlighted by the R_0 landscapes - indicating relative sensitivity to catastrophe, and, upon the emergence of catastrophe - when R_0 falls to zero - with the effects spreading spatially in waves until they reach the river system. This interpretation may provide an understanding of relative hydrological sensitivity across the catchment, together with the potential magnitude, duration and fate of catastrophe induced 'waves' of phosphates.

7.2.1 SIMULATIONS OF SIMPLE CATCHMENTS

This emergent band of equipotential is the major observable characteristic of spatial variations in R_0. With no rivers present in Simulation I this band has emerged as a direct consequence of the spatial hydrological flows and the flow inhibition constants. Simulations II to V (Section 6.1.1) examine the effect upon this band of the introduction of rivers and feeders to this simple, hypothetical catchment.

Simulations II and III clearly show these effects for feeders and catchment rivers, respectively. In the former, the band of equipotential has been stretched down the catchment; the effect of 50% surface water flow losses to rivers and consequently reduced potential for the dilution of phosphates in the soil. This effect is further enhanced in the latter, where an open-ended band has emerged due to 100% losses of surface water flows.

From these findings it can be concluded that the band of equipotential persists even when rivers are present, the only influence of the rivers being to change the qualitative shape of the emergent R_0 landscape. Simulations IV and V allow observation of the effects of a combination of river types, moving towards a more realistic representation of the hypothetical catchment.

As may be expected, combinations of river types provokes a spatial shift in this band of equipotential. However, both Simulations IV and V show the emergence of additional troughs and peaks in the landscape. This may be conceptualized as the effect of overlaying the landscapes emergent from Simulations I, II and III, homogenously representing the different river types; in Simulation IV (Figure 6.5), cell [3,2] shows a trough at the point where 'Category-2' flows initially meet, and in Simulation V (Figure 6.6) the trough at cell [3,2] remains, and cell [5,5] shows a peak where the 'Category-2' and 'Category-3' bands of equipotential intersect.

From these simulations it is clear that the model could also be calibrated through modification of flow directions and losses to rivers to reflect specific observations of hydrological characteristics in the catchment represented by the model.

7.2.2 SIMULATIONS OF COMPLEX CATCHMENTS

Given an understanding of these emergent patterns in the R_0 landscape - the result of spatial flows and losses clearly observable in this simple hypothetical catchment - the emergence of similar patterns in a complex catchment may begin to provide useful information about its hydrologically sensitive regions.

Observations of Simulations VI and VII (section 6.1.2) have identified these hydrologically sensitive regions across the Rutland Water Catchment, the former being void of rivers to provide a similar reference point as Simulation I did for examination of the simple catchment.

The troughs and peaks in the emergent landscape described by Simulation VI may be directly related to those emerging in the simple catchment, with the bands of equipotential clearly observable in both the River Welland and River Nene sub-catchments (Figure 6.9). With a single exception - discussed below - the introduction of rivers in Simulation VII has resulted in the expected elongation of the band of equipotential, the loss of certain peaks and appearance of additional troughs.

The exception - cell [6,7] - upon closer examination turned out to be the result of an inconsistent definition of flow directions and river types in the model. This unexpected change, identified because of clear prior understanding of the expected

effects upon the R_0 landscape, suggested that a more appropriate spatial definition of the model may be based upon a hexagonal as opposed to square grid - a spatial representation successfully employed by Allen and McGlade (1987) for modelling fisheries dynamics. Although this change has been suggested, the current representation has retained a square grid in order to remain consistent with the format of available data [Loveland 1990].

Final adjustments to the hydrological flows were included in Simulations VIII and IX (section 6.1.2) to reflect the variability of SPR, VMC and slope across the catchment. However, the subtlety of observable effects upon the bands of equipotential, in both simulations, suggests that these variations are more significant in the context of individual cells within the catchment as opposed to hydrological constraints upon the catchment as a whole, such as flow patterns.

Finally, Simulation VIII, through its negation of the unexpected changes observable in Simulation VII, demanded closer examination of the SPR and VMC representation for cell [6,7]. This identified potentially dubious NSI data, obtained as point measurements but taken to represent the characteristics of a 25km^2 area in the model.

7.2.3 SUMMARY

These nine simulations, showing the effects of hydrological constraints upon R_0, and based upon both simple and complex catchments, have provided useful information relating to both the model itself and its perceived 'reality'. These findings may be summarised as follows:

(i) A clear understanding has been provided, by Simulations I to V, of the spatial characteristics of R_0 and the emergence of bands of equipotential spreading across a catchment. This understanding of R_0 in a simple spatial context - with all the internal non-spatial conditions (both chemically and hydrologically) remaining homogenous - helps to perceive a catchment in terms of the hydrological constraints (resulting from the directional flow patterns) where regions of potential sensitivity emerge, potentially resulting in waves of increased phosphate concentrations moving through the catchment when flushing occurs.

(ii) Means by which the model may be calibrated to reflect specific catchments have been suggested. This calibration may be achieved through modifications to the representations for hydrological losses to rivers and river categorizations (see section 7.2.1), or, with more subtle effects, to the inhibition constant employed to simulate variability in internal phosphate concentrations and thus spatial flows (see Chapter 5, Equation (34)).

(iii) A clear distinction has been made between the hydrological constraints observable from a catchment perspective and those more significant at the individual cell level. The observations clearly show the greater significance of influence upon the spatial R_0 landscape of the hydrological constraints controlled by the catchment module - flow patterns and river definitions - in

comparison with variability in SPR, VMC and slope amongst individual cells (see Simulations VIII and IX). To observe the effects of this internal variability it was necessary to examine the *differences* between subsequent simulations (Figure 6.8).

(iv) It has been possible to identify potentially dubious data and anomalies in the definition of the spatial representation (see Simulations VIII and VII, respectively). Characteristics emerging from cell [6,7] in Simulation VII suggested that a spatial representation based upon a hexagonal grid may be preferable to a square grid. In the same cell it also emerged, because of counterintuitive results in Simulation VIII, that the data being used may be dubious in that specific case, ultimately demanding more detailed scrutiny.

(v) Specific areas of the Rutland Water Catchment have been identified as potentially sensitive to catastrophe for hydrological reasons, namely:

- cells [1,4], [2,3], [2,4] & [3,4] at the top of the Welland catchment;

- cells [7,2], [7,3] & [7,4] at the bottom of the Nene catchment, although this catchment does not fall entirely within the bounds of the current model, so distortions may be expected;

- Rutland Water itself (cells [4,7] & [5,7]).

Finally, it should be noted that the anomalous cell [6,7] represents an area immediately adjacent, and downstream to Rutland Water.

7.3 EFFECTS OF CHEMICAL VARIABILITY UPON R_0

Observations of the effects of the hydrological constraints upon R_0 landscapes were based upon simulations employing homogenous initial chemical conditions. It was possible, therefore, to observe changes through careful selection of a single static snapshot of the landscape. However, upon introduction of chemical variability to the simulations, due to differing initial conditions, the catastrophe potential emergent from each cell will be both following unique R_0 trajectories and reflecting different temporal locations on that trajectory. The potential utility of continuous temporal observations of the changing landscape is therefore more evident, but, in the absence of appropriate outputs and the subtlety of changes in latter simulations, interpretation of the outputs involved a variety of observational perspectives.

A further, related, consequence of the introduction of chemical variability was observed in the immediate disappearance of the band of equipotential discussed above. However, retaining a perception of these previously observed bands of equipotential helps interpretation of observed changes resulting from chemical variability as opposed to the hydrological constraints.

Finally, the necessary data for the definition of the chemical variability, without further measurements and extensive chemical analyses, is represented by only a single snapshot in time. Consequently, only a single reference point is available for implementation of chemical variability; a secondary reference point would have facilitated detailed temporal calibration of the model. Thus, in the circumstances of a single reference point, it should be assumed that temporal quantifications of change may be erroneous. However, *relative* temporal changes will continue to provide useful observational reference points for interpretation of the effects of this chemical variability.

7.3.1 BASELINE REFERENCE POINT

Since the introduction of chemical variability to the simulations conceals the observable effects of the hydrological constraints - with the emergent spatial patterns qualitatively different to those resulting from chemical homogeneity - a new baseline reference point is required for the interpretation of subsequent observations. This reference point is provided by Simulation X (section 6.2.1.1), where the initial chemical conditions are defined by the NSI data (Table 6.1).

Utilizing additional static snapshots of the landscape to extend the output over the entire simulation, and recording the simulated time until catastrophe for each cell, it has been possible to make some useful observations about the emergent landscape, its relationship to Rutland Water, and similarities with landscapes resulting from the hydrological influences.

Two characteristics of the emergent landscape rapidly become apparent. Firstly, the areas represented by cells [5,7] and [7,3] were observed to collapse (R_0=0) almost immediately (see Figure 6.12(a)), suggesting regions of high sensitivity to catastrophe; the scale of catastrophe could not be observed due to the lack of historical data, the rapidity of collapse, and the shortcomings of the static output.

However, when these regions are identified in the context of Rutland Water, a degree of correlation with the perceived eutrophic problems in the catchment becomes apparent; cell [5,7] represents Rutland Water itself, and cell [7,3] represents an area on the River Nene immediately upstream to the extraction point supplying Rutland Water. Rutland Water is already known to be sensitive to eutrophication, but the apparent sensitivity on the River Nene suggests a potential linkage between this unexpectedly sensitive region and the documented eutrophic phenomena [NRA 1990; Matthews 1989; Trow 1990; Phillips 1990].

Secondly, a band of apparently increased *resistance* to catastrophe emerged - identified by consistently high values of R_0 - and persisted throughout the simulation (see Figure 6.12(l)). This band stretched directly across the River Welland, showing no correlation with the hydrological characteristics of the sub-catchment. However, it may suggest a variation in the geochemical characteristics within the catchment reflected in soil types of varying chemical composition; certainly, the Calcium content of the soil remains high in all of the 'resistant' cells.

Finally, a degree of correlation with the hydrological influences is observable in the upper reaches of the Welland catchment, which it may be useful to note, is immediately adjacent to and downstream of an urban area - Market Harborough. Thus, with these observable characteristics of the emergent landscape borne in mind, a reference point has been provided against which observations of changes to the variability between individual cells may be examined.

7.3.2 LAND-USE AND VEGETATION

The preceding simulations have provided representations of the effects of hydrophysical and chemical variability across the catchment. The final aspect of variability perceived to be significant at the resolution provided by this model is the biophysical, encompassing the influences of land-use, specifically urban cover, and variations in surface vegetation.

Aggregated definitions of land-use were described from observations of Ordnance Survey maps and identification of percentages of urban cover, expanses of water and woodland. It was assumed initially that the remaining percentage represented non-livestock grassland, the median category in the modelled representation of surface vegetation. Simulations XII and XIII (Section 6.2.2) vary this remaining percentage to represent arable vegetation and woodland or livestock pastures, respectively, highlighting the influence of such vegetative cover.

Immediately evident in Simulation XI (Section 6.2.1.2) was the difficulty in detecting any variations in the R_0 landscape (Figures 6.13 and 6.14), clear differences only becoming apparent upon observation of the changes in flushing times, or the timing of catastrophe (Figure 6.15). This suggests that the effects of land-use may be more significant at a greater spatial resolution than provided by this model. This apparent resolution problem, similar to that experienced in Simulations VIII and IX whereby the observational perspective of the landscape appears to be inadequate for clear identification of changes, suggests the need for an observational shift to achieve the necessary resolution. In this way apparently sensitive regions may be examined in more detail revealing more clearly the qualitative changes in the landscape.

Observations of the flushing times, however, showed a distinct correlation between the percentages of urban cover and the temporal change in flushing (Figure 6.16). This correlation was also observed in Simulation XI(i), employing homogenous chemical conditions suggesting that the influence of urban cover is independent of the soil composition. Interpretation of these effects may be appropriate in the wider context of hydrological constraints; the effect of losses to rivers was clearly shown in Simulations II to VII, and the effect of urban cover contributes to the percentage loss to rivers through efficient drainage of surface waters.

Observations of Simulation XI were wholly inconclusive with regard to the effect of woodland cover, requiring observation of specific simulations based upon widespread variations in vegetative cover; Simulations XII and XIII addressing arable and woodland cover, respectively.

It has already been shown what the effect is of variations in infiltration rates due to surface vegetation; reduced infiltration provoking consistently increased phosphate concentrations and thus more rapid resource depletion, and vice-versa for increased infiltration. Observation of Simulation XII - arable - would be expected to show more rapid flushing, and conversely, Simulation XIII - woodland and livestock - to show delayed flushing.

The observations generally reflected these expectations, with a degree of variability in the changes reflecting different percentages within individual cells being predefined as woodland by the Ordnance Survey information. However, precisely the opposite effect was observed in a number of cells - [2,4] and [6,7] in Simulation XII, and [1,4], [2,4], [4,4] and [7,3] in Simulation XIII - suggesting the existence of unexpected, and unidentified mitigating influences demanding closer examination (see Figure 6.18).

Discounting the observed changes in cells [6,7] and [7,3], since the former has already been shown to be a dubious representation of its 'reality' and the latter collapses almost immediately, a potentially significant association may be made: all three of the remaining cells lie along the path of the River Welland.

Comparison of the directional trends of R_0, in relation to the trajectories observed in Simulation XI - of these cells and cells displaying expected changes - merely confirms that this unidentified mitigating influence persists over time (Figure 6.19). It is not the purpose of this research to provide conclusive answers about the Rutland Water catchment in such circumstances, but to reveal the utility of information emerging from this form of model. However, insomuch as the cause of these unexpected changes is not immediately apparent - aside from a possible link with the representation of river flows and losses to rivers - these observations have identified an area of lack of knowledge which will need to be addressed if these changes are to be understood.

7.3.3 SUMMARY

These simulations - X to XIII - of the effects of chemical variability upon R_0, based upon measurements within and observations of the Rutland Water catchment, have provided useful additional understanding relating to the significance of changes, appropriate observational perspectives, the 'reality' represented by the model, and potential areas of lack of knowledge. These findings may be summarized as:

(i) It has been found that the effect of urban cover appears to be independent of the soil composition. It may be concluded, therefore, that the extent of urban cover is more significant when viewed in the context of SPR and hydrological losses to rivers through the implicated proportional loss of surface waters through efficient drainage directly to water courses. The observability of changes from the given perspective suggests a scale of influence closer to that of SPR than the definition of river types.

(ii) The observability of changes arising from variations in both urban cover and surface vegetation again suggests that a greater degree of resolution may be required than that provided by this model. A reduction in scale of individual cells, for example to 1km^2, would result in clearer specification of the spatial variability of land-use so that the percentage variation in individual cells may be more representative upon observation of the more detailed R_0 landscape.

(iii) A correlation has been found between the effects of chemical variability and hydrological constraints. Observations of the emergent landscape suggests potential sensitivity of regions representing the upper reaches of the Welland catchment, regions perceived through previous simulations to be on, or within, the bands of equipotential emerging as a result of the hydrological constraints upon R_0.

(iv) A region of apparent resistance to catastrophe has emerged as a result of the chemical composition of the soil. This region is represented by a persistent band of resistance crossing the River Welland, suggesting the possibility of differences in the underlying geochemical conditions, rock and soil types in those regions, reflected in the measured soil composition data.

(v) Observations of unexpected changes have suggested an areas of lack of knowledge as to the causes of these changes. Without further detailed examination it has been found that these changes occurred on the path of the River Welland, with the implication that the representation of rivers provided by the model may be a contributory factor.

(vi) The collapse of cell [7,3] suggests a region of the River Nene catchment which may represent a significant contributory influence upon eutrophic phenomena in Rutland Water itself.

7.4 EXTERNAL PERTURBATIONS

The preceding simulations combine to provide a comprehensive understanding of the effects of both the hydrological constraints and the chemical variability upon the qualitative characteristics of the R_0 landscape. In order to complete this understanding of the model within its wider contextual 'reality', observations are necessary of changes resulting from the key external perturbations, acid and phosphate loading.

With this comprehensive understanding of the influences upon the R_0 landscape, and consequently the relationship of the model with its perceived 'reality', further experimentation with changes to the model is possible within a clearly defined context.

7.4.1 VARIATIONS IN ACID AND PHOSPHATE LOADING

The preceding simulations have provided understanding of the dynamics of the observed catchment. Simulations XIV to XVII (see Section 6.3) give an insight into the effects of changes in the environment containing the catchment - external influences represented by aggregations of acid and phosphate loadings. In the case of acidification, this may be affected by the proximity of acid sources to the catchment, sources such as fossil fuel power stations.

The most significant observation was of the disparity between effects of changing acid loads and phosphates loads; the former showing proportional effects and the latter being minimal. This highlights the temporal disparity between the processes of acidification and adsorption. In the case of acidification, the precise changes varied as a result of silicate buffering, itself affected by the soil pH, and there was an exaggeration of variability through the cumulative effects of the change over time.

The minimal change resulting from substantial variations of phosphate input should be interpreted as a warning signal; if this additional input doesn't affect adsorption levels, then where does it end up? A benefit may therefore be found in the monitoring of river inputs of phosphate since the additional loading may be flowing through the catchment to provoke eutrophic phenomena elsewhere.

The minor spatial variations in response to acid are partially due to variations in the extent of silicate buffering; these variations become more pronounced under very high levels of acid deposition (see Simulation XV, Figure 6.20). However, where variations increased in magnitude there was observed to be high levels of adsorbed phosphate (Q_{Ca}) in an area of relatively high pH. Such conditions will also affect the degree of silicate buffering prior to collapse and thus the overall proportionate change.

Finally, a profoundly unexpected observation was made regarding changes in phosphate inputs; in a number of areas, the timing of flushing was *delayed*. Given the increased input and therefore persistently increased phosphate concentrations flowing through the soil, adsorption would be expected to increase, even if only by a marginal amount. No apparent cause or correlation with watercourses was found, suggesting both evidence of complexity and an area of lack of knowledge.

CHAPTER 8. CONCLUSIONS

With the purpose of modelling and understanding the complex, non-linear and discontinuous inter-relationships of soil acidification and soil phosphate retention - representing the key dynamics of a specific chemical time bomb phenomenon - the preceding chapters define the complex systems model used, and present a series of simulations of these dynamics in the context of a catchment.

The specification of the model is presented in Chapter 3, with the definition and analysis of the chemical and hydrological sub-modules in Chapters 4 and 5, respectively. Chapter 6 presents a series of spatial catchment simulations, commencing with a simple (hypothetical), homogenous catchment and culminating in complex simulations of external perturbations on the Rutland Water catchment. An interpretation of the observations is provided in Chapter 7.

The following discussions begin by summarizing the significant findings of this exercise in complex systems modelling, and considering the detailed observations of simulated change and their interpretation in the context of a catchment. Thus the potential for further experimentation is highlighted, and the potential for expansion of the scope of the model also becomes apparent.

Finally, the full significance of this complex systems approach to modelling environmental catastrophe - resulting from non-linear and discontinuous inter-relationships of apparently disparate phenomena - becomes evident when the findings of the current research are assessed alongside the related models discussed in Chapter 2. Thus, the contributions of the research to modelling and the assessment of environmental catastrophe may be clarified.

8.1 OBSERVATIONS AND INTERPRETATIONS OF CHANGE

The specific findings of the modelling exercise, through observations of simulated change and their interpretation within the context of a complex systems framework, have been detailed and discussed in preceding chapters. This discussion is continued here to comprehend the significance of the findings in a broader context; each of the four areas of observation - the catastrophe indicator R_0, hydrological constraints, chemical variability and external perturbations - provide useful pointers for further analysis or experimentation.

Observations of the internal characteristics of the *Catastrophe Indicator*, R_0 - defined for observation from the catchment perspective - highlighted three areas of importance requiring further analysis. Firstly, details of the omissions and assumptions inherent in the abstract representation, potentially suggesting areas of ignorance or lack of knowledge concerning the nature of the observed change, identify possible areas for experimentation, or linkage points for expansion of the scope of the model. This potential for experimentation and expansion is discussed in following sections.

Secondly, a conceptual understanding of R_0 has been provided, complete with its inherent complexity, through examination of typical temporal trajectories and the nature of these trajectories when observed in a spatial context. This understanding is fundamental to interpretation of subsequent observations since all observations necessarily relate to R_0.

Thirdly, a mechanism by which this representation may be calibrated to reflect specific hydrological characteristics within a catchment has been identified. Through variation of the river categorizations and associated hydrological losses, and of the spatial flow inhibition constants, the model may be calibrated to display characteristics corresponding with observations and measurements of 'reality'. Detailed calibration in this manner was not carried out in this research for lack of appropriate data and in line with the heuristic rather than prescriptive purpose of the research.

Observations of the *Hydrological Constraints* upon the model, besides confirming the utility of continuous temporal representations of change not available to this research, began to provide significant information regarding the resolution of the model and the relative sensitivity of specific regions of Rutland Water. These observations also suggested further areas of ignorance, indicated by dubious data in specific cells, and potential alternative spatial representations of the grid in order to represent the spatial hydrological flows more realistically.

The indication of areas of sensitivity when temporal observations of the R_0 landscape are examined, initially with the emergence of a band of equipotential stretched around a simple theoretical catchment, provides a hint of the inherent complexity of R_0 through observable qualitative variations in an otherwise homogenous spatial environment. The bands of equipotential re-emerged during simulation of a spatially complex, but otherwise homogenous catchment (Rutland Water) providing a significant insight to the potentially hydrologically sensitive regions of the Rutland catchment.

However, it was also clearly shown that only the hydrological constraints imposed by the flow directions and river classifications were easily observable from a catchment perspective. The hydrological effects resulting from soil structural differences (the HOST classifications) were not clearly evident from the catchment perspective, but instead became apparent through observation of changes shown by individual cells. An increase in the resolution of the model may make such changes more clearly observable from the catchment perspective.

Observation of the effects of *Chemical Variability* upon the R_0 landscape similarly required more detailed examination of changes in individual cells, again suggesting a potential benefit in increasing the model resolution. Immediately evident was the loss of the previously observable bands of equipotential, expected as a result of the loss of chemical homogeneity, but also evident was a degree of correlation between areas of apparent sensitivity and those observed to be hydrologically sensitive. In addition, important information emerged both relating to potential monitoring requirements and suggesting evidence of inherent complexity indicated by counterintuitive results.

Whereas many of the characteristics observed throughout the model development represent somewhat predictable changes -, for example in the temporal delay in R_0 trajectories when spatial flows are present - the complexity has been indicated where the observations have departed qualitatively from expectations. Two such unexpected observations emerged from simulations of the chemical variability of the study area:

- A band of resistance to catastrophe appeared, directly crossing the River Welland catchment. In this instance, examination of the soil types and geology of the catchment may indicate reasons for this resilience; certainly, the data available showed a very high Calcium content across this region.

- Along the path of the River Welland the observed changes persistently contradicted expectations when examining the effects of vegetative cover. There was no obvious cause of this apparent complexity, highlighting an area of ignorance which potentially demands closer examination.

Finally, bearing in mind the single data reference point and the broad range of data required for determination of R_0 (see Chapter 4), a number of important monitoring requirements were identified:

- A second reference point detailing the chemical composition in a compatible form with the existing NSI data, to provide a means of finer calibration of internal rates of change.

- A continuation of this monitoring to provide the data necessary for determination of R_0 to enable correlation with simulated changes in R_0.

- Detailed definition of land-use and vegetative cover across the catchment.

- Recording of the flows of phosphates into the rivers for each model cell.

This monitoring may also be focused with reference to apparently sensitive regions and areas of lack of knowledge. The indication of localized monitoring requirements may be in tandem with alterations of the model resolution; where unexpected change has occurred, the model may be suitably refocused.

Observation of the effects of *External Perturbations* begins to highlight the potential utility of the model for assessing the effects of acidification of the environment in relation to potential release of phosphates into the river system. The disproportionately greater influence of changes in acid deposition rates as opposed to phosphate application rates, in terms of the observed potential for catastrophe, raises two issues.

Firstly, it suggests that mitigation measures may be enacted through control of liming practices. However, although liming may counteract short-term acidification, it has been shown that it will also increase the potential magnitude of catastrophe in the long-term. Thus, such mitigation measures may, in combination with continued acidification, effectively magnify the effect of this chemical time bomb.

The second issue emerges as a result of the minimal changes observed following increased phosphate applications. The suggestion is that the slow processes of adsorption allow spatial transportation of phosphates to occur more rapidly, thus provoking proportionately increased phosphate flows into watercourses. The effect may therefore be to directly provoke eutrophication rather that indirectly increasing the potential for eutrophic releases in the future. The subsequent fate of this additional phosphate loading thus becomes highly significant.

Finally, these latter simulations have highlighted a further important area of monitoring to determine the actual loadings of acid and phosphate across the catchment, and the fate of those phosphates. With simulated or measured levels of liming, experimentation with the variability of inputs - being homogenous throughout these simulations - may identify more appropriate mitigation measures in the face of these perturbations.

8.2 POTENTIAL FOR EXPERIMENTATION

Experimentation may be seen as having a dual role, where the focus may either address particular disciplinary areas or concentrate upon areas of observed sensitivity or unexpected change. Potential for experimentation has emerged in the following areas - each discussed below:

- Modification of the spatial representation, the resolution of the model, and the definitions of the internal processes.

- Examination of possibilities for calibration of the hydrological dynamics and the internal rates of change, in conjunction with both experimental data and monitoring programmes.

- Experimentation with external perturbations with the objective of identifying mitigation measures which reflect the spatio-temporal nature the effects of the perturbations.

Potential modifications to the spatial representation of the grid - hexagonal instead of square - were suggested by the earlier simulations of Rutland Water. Observations showed that the square grid, upon which the current model is based, was unable to realistically represent the flow directions. Thus, a hexagonal representation that permits flow definitions across 60° arcs, as opposed to 90° arcs, may provide a clearer spatial correlation with 'reality'. A consequence of this, however, is the need to obtain data which correlates with the hexagonal grid and its spatial resolution; the format of the currently available data necessitated the 5km square representation used in this research.

Modification of the internal processes may further clarify the relationship between 'reality' and the model. The differing effects of alternative adsorption equations, such as the Freundlich equation, may therefore also be observed, but in relation to a necessarily modified form of R_0. Further experimentation with the buffering

processes, in particular the calculations of soil pH, may likewise clarify this relationship. It may also be beneficial to introduce a degree of 'noise', or randomness, to the current model in order to examine the effects of variability within the processes themselves.

Modifications to the categorizations for river flows and their associated hydro-chemical losses, and for vegetation cover, may shed some light on the unexpected changes observed along the path of the River Welland. In the current model there are arbitrarily three categories used to describe river flows, and likewise with vegetation cover. An extension in either or both of these areas, to maybe 5 or 10 categories, would enhance the degree of diversity inherent in the model, potentially also highlighting additional 'surprises'.

Regarding the hydrological characteristics, experimentation with the various means of calibration highlighted by the simulations - river categorizations and flow inhibition constants - may be carried out using imaginary data, thus identifying the sensitivity of the calibration mechanisms and the most appropriate for use given real data.

Calibration of the internal adsorption and buffering processes to reflect the intricacies of the observed catchment is not possible without an additional data reference point to complement the existing NSI data. However, with such data becoming available, this calibration may also highlight more 'unknowns' - in relation to change in the modelled catchment - through examination of the variance with currently observable change simulated by the model.

Experimentation with external perturbations and observations of consequent changes is possibly the most important area for experimentation to provide guidance towards appropriate mitigation measures. This discussion concentrates on the mitigation of acidification through liming in a potentially eutrophic environment. Possible mitigation measures may include:

- Increasing liming applications in sensitive areas, representing localised responses. This may achieve short-term mitigation, but has been shown to be at the expense of long-term qualitative deterioration and increased sensitivity to catastrophe.

- No direct mitigation through liming, but provision for containment or water purification measures in anticipation of releases of phosphates in sensitive areas.

- No mitigation, but instead, utilization of consequential eutrophic phenomena, for example through harvesting of eutrophic blooms to retrieve the phosphates for alternative uses; a possibility suggested by Ball (1990).

The first measure simply shifts the problem from the short-term into the long-term, in much the same way as eutrophic blooms in Rutland Water were precipitated into

the sediments through the addition of iron filings [Trow 1990]. However, mobilization of these sediment phosphates at a later date may provoke eutrophication of a magnitude so far unseen in Rutland Water.

However, responses involving containment, purification or harvesting measures require knowledge of the 'fate' of released phosphates, again tying in to the need for complementary monitoring programmes. Containment and purification may not be practicable in the context of major catchment rivers, and harvesting accepts the inevitability of eutrophication in a confined area such as Rutland Water.

8.3 EXPANSION OF THE SCOPE

Expansion of the scope of the current model is possible both spatially and temporally. Expansion spatially to encompass additional catchments, or temporally to examine more closely the long-term effects of perturbations, would retain the existing definition of the catastrophe indicator, R_0, since the model will not be functionally altered. Spatial expansion to include the entire Nene sub-catchment and temporal expansion to examine the long-term effects of acidification mitigation measures have already been identified as potentially beneficial.

The inclusion of influences such as soil organic matter recycling, physical soil structuring dynamics, water-table fluctuations or groundwater flows would involve a functional expansion of the scope. As a consequence, the definition of R_0 would need to be modified to reflect this additional complexity. However, it may also begin to reduce the degree of abstraction of 'reality' inherent in the model, shifting the balance between generality and realism towards the latter; precision would depend upon the representations used.

An expansion of the scope could also be achieved through integration with a number of the models discussed in Chapter 2. The first, and most obvious, is the RAINS model of acidification across Europe [Alcamo et al 1990]; the emissions, atmospheric transportation and deposition modules would provide more realistic quantifications of the acid loading across the catchment.

There is also the *Escaut* model describing hydro-chemical dynamics within a river system [Billen 1992], which could be of use in determining the 'fate' of phosphates and identifying appropriate mitigation measures. Finally, a socio-economic model such as that of the Belgian provinces [Sanglier & Allen 1989] may be of use in assessing the likelihood of additional future emissions. The latter two of these models have already been integrated to examine the potential implications of socio-economic change on the Scheldt Estuary [Svirejeva 1993].

Owing to the generic nature of the current model - prior to defining the initial conditions - it would be possible to address alternative spatial applications, thus facilitating potential integration with the mentioned models in either the Rutland Water catchment or the Escaut.

8.4 CONTRIBUTION OF CURRENT RESEARCH

The motivation for this research was based upon a recognition of the widespread deterioration of the natural environment, and the continual emergence of sudden catastrophic environmental changes resulting from complex interactions of theretofore apparently disparate phenomena. Further discussions of complexity and chemical time bomb phenomena may be found in Chapter 1.

Thus, perceiving such a relationship between acid rain and eutrophication - specifically through soil acidification and soil phosphate retention - the purpose of this research has been to observe and interpret the interactions and discontinuities emerging from the acid-phosphorus relationships within the soil domain. To this end, a complex systems model has been developed which addresses both chemical interactions and spatial hydrological flows in the context of the Rutland Water catchment.

Owing to the cross-disciplinary nature of this exercise - addressing processes variously encompassed by hydrology, soil science and chemistry, not to mention computer modelling - existing models were found to be limited in scope, inherently unidisciplinary, or incompatible with the multi-disciplinary nature of the CTB phenomenon examined by the current research. These models are discussed in detail in Chapter 2 with the significant limitations summarized below.

Of the three acidification models examined, two were immediately discounted. The MAGIC model [Cosby et al. 1985], used by Whitehead (1990), was limited to a maximum of two soil types, precluding its use in catchments containing many soil types. The SESOIL model [Bonazountas & Wagner 1984] overcame this limitation and was able to address the fate of both acid and phosphate. However, it could not address two 'pollutants' simultaneously, nor their interactions which are central to this research.

The third model, RAINS [Alcamo et al 1990], was limited to the dynamics of acid emissions, transport, deposition and subsequent soil, water or forest acidification, but not the indirect effects of that acidification, except in forests. However, it provided definitions of soil acidification which were not dependent upon soil types.

The current model utilizes the representations described in RAINS, and in conjunction with HOST (see below), overcomes the need to define specific soil types. These were subsequently integrated with the representations of phosphate adsorption in order to examine their inter-relationships.

The phosphate adsorption models examined [Barrow 1978; Enfield et al 1976; Jones et al 1984] were all based upon variations of a limited number of adsorption 'isotherms'. Furthermore, they invariably required large volumes of data, were focused at the micro level, and ignored the spatial context and the possibility of changing environmental conditions such as soil pH.

The current model is based upon a simplification of the 2-term Langmuir isotherm, modified to meet the requirements of the research. Using this modified Langmuir isotherm, it has been possible to link the processes of acidification and adsorption so that the dynamics of their interaction become observable in the context of a catchment and so that the data requirements are minimal.

The soil hydrology models examined [Mein & Larsen 1971; Chen & Waganet 1992; Workman & Skaggs 1990] were found to be unsuitable for the representation of flows across a catchment, operating at the micro level and being excessively data heavy. However, the latter two did recognize that the soil is not a homogenous medium, addressing macropores and preferential flows, respectively.

Attention therefore moved to models of catchment hydrology that addressed nutrient flows and eutrophic phenomena. The model presented by Whitehead (1990) - aside from being antithetical to notions of complexity (see Section 2.1.4) - was location specific, addressed nitrates as opposed to phosphates, and was limited to two soil types.

Billen's (1992) PHISON model, although generic in form and employing the concept of stream orders, addresses the adsorption of phosphate in the context of eutrophication, but only in the aquatic continuum. It does not address adsorption in the soil and indeed takes no account of the ability of the soil to act as both a potential sink and a source of phosphates.

The hydrological processes implemented in the current model are therefore based upon the Hydrology Of Soil Types (HOST) classification system described in Chapter 5. Being based upon the dominant flow pathways through soils classified by physical characteristics in preference to soil types, use of the HOST classification system overcomes the limitations of the micro-level soil hydrology models and accounts for the effects of soil flows omitted from the catchment models.

Finally, through the integration of these chemical and hydrological processes, a catastrophe indicator, R_0, has been defined which provides a dynamic representation of the inherent discontinuities of this CTB phenomenon. This indicator represents a phenomenon specific definition of the discontinuity (CTB trigger) in preference to the theoretical, generic step function described by Stigliani (1991).

The main characteristics of the current model may be summarized as follows:

- It addresses the non-linear inter-relationships of soil acidification and soil phosphate adsorption in the spatial context of a catchment.

- The discontinuities in this relationship - resulting in sudden release of phosphates - are described by a complex, but clearly defined catastrophe indicator, R_0.

- Soil acidification is not dependent upon the soil type, using representations given by Alcamo and others (1990).

- Phosphate adsorption is based upon the 2-term Langmuir isotherm [Barrow 1978], modified to facilitate integration with soil acidification and changing soil pH.

- The hydrological flows are based upon HOST classifications [Boorman & Hollis 1992] which describe the dominant flows in the context of overall catchment response.

- Only minimal data is required to describe soil composition, HOST classifications, topography of a catchment, and river flow patterns.

- The model reflects the notions of complexity and non-linear environmental change discussed in Chapter 1.

It would be incorrect to suggest that the model presented in this thesis is 'better' than any of the models described above and in Chapter 2, but it is different. This is because none of these models span all the phenomena of concern to this research; indeed, in most cases these models display more precise representations of their restricted subject matter.

This complex systems approach extends the scope of these models and shows that, by using simplifications of existing representations, these heretofore apparently disparate phenomena - linking acid rain and eutrophication - may be integrated to create a model which describes their discontinuous inter-relationships in the soil domain using a catastrophe indicator, R_0, which could never have emerged without this integration. However, with this relationship now defined, it would be possible to increase the precision through reintroduction of elements of the original models.

The main contributions of this research may thus be found in the following areas:

* Development of a dynamic complex systems model - transferable to alternative catchments due to the minimal data requirements and its generic representation - which may be used to describe non-point sources of phosphates (within a spatially defined catchment) as part of assessments of potential eutrophication, overcoming such limitations found in existing models [Billen 1992; Svirejeva 1993].

* Definition of a catastrophe indicator (R_0) - which highlights both the proximity and magnitude of catastrophe - describing a specific Chemical Time Bomb phenomenon whereby the soil suddenly changes from being a sink to a source of phosphates; long-term accumulations of phosphate in the soil are released as a consequence of soil acidification in the short-term.

* Presentation of a complex systems approach - hinged upon this concept of a catastrophe indicator - to the representation of non-linearities and discontinuities between heretofore apparently disparate phenomena which are 'competing' for a common resource.

REFERENCES

ADAS (Agricultural Development and Advisory Service) (1982)
"Survey of Fertilizer Practice: Fertilizer use on farm crops in England and Wales" Rothamsted Experimental Station

ALCAMO,J, Shaw,R & Horeijk,L (eds.) (1990)
"The RAINS model of acidification; Science and strategy in Europe" Kluwer Academic Press

ALLEN,P.M (1988)
"Evolution: Why the whole is greater than the sum of its parts." [*in Wolff,W. et al. (eds) "Ecodynamics." Springer Verlag, Berlin*]

ALLEN,P.M (1990)
"Why the future is not what it was. New models of evolution." Futures, July/August 1990, pp 555-570.

ALLEN,P.M, Black,I, Lemon,M, Seaton,R, Blatsou,C & Calamaras,N (1994)
"Agricultural Production and Water Quality in the Argolid Valley, Greece: A policy relevant study in integrated method." IERC, Cranfield, in collaboration with Lab. of Agricultural Hydraulics, Agri. Univ. of Athens; a contribution to the Archæomedes Project [CEC 1993a]

ALLEN,P.M & McGlade,J.M (1987)
"Modelling complex human systems: A fisheries example" Euro. J. of Op. Res., Vol 30, No 2, pp 147-167

ALLEN,P.M, Schieve,W.C & Adams,R.N (eds) (1987)
"Modelling Complex Systems I" Special Issue, Euro. J. of Op. Res., 30(2)

ALLEN,T.F.H & Starr,B (1982)
"Hierarchy. Perspectives for ecological complexity" Univ. of Chicago Press

ARCHER,J. (1988)
"Crop nutrition and fertilizer use" Farming Press Ltd

BALL,K (1990)
"Detergents and blue-green algae: The phosphate link" Rutland & Melton Friends of the Earth, Rutland Green Party

BARROW,N.J (1974)
"The slow reactions between soils and anions 1. Effects of time, temperature and water content of the soil on the decrease in effectiveness of phosphate for plant growth" Soil Sci., 118, 6, pp 380-386

BARROW,N.J (1978)
"The description of phosphate adsorption curves", J. of Soil Sci., 29, 447-462

BARROW,N.J (1980a)
"Differences amongst a wide-ranging collection of soils in the rate of reaction with phosphate", Aust. J. Soil. Res., 18, 215-224

BARROW,N.J (1980b)
"Differences among some North American soils in the rate of reaction with phosphate", J. Env. Qual., Vol. 9, No. 4, 644-648

BARROW,N.J & Shaw,T.C (1975a)
"The slow reactions between soils and anions 2. Effects of time, temperature and water content of the soil on the decrease in phosphate concentration in soil solution" Soil Sci., 119, 2, pp 167-177

BARROW,N.J & Shaw,T.C (1975b)
"The slow reactions between soils and anions 3. Effects of time, temperature and water content of the soil on the decrease in isotopically exchangeable phosphate" Soil Sci., 119, 2, pp 190-197
BEANLANDS,G.E & Duinker.P.N (1983)
"An Ecological Framework for Environmental Impact Assessment in Canada." Institute for Resource and Environmental Studies (IRES)
BILLEN,G, De Becker,E, Servais,P, Lancelot,P & Rousseau,V (1990)
"Modèle mathématique de l'estuaire de l'Escaut. Développement d'un algorithme fournissant les conditions-limites amont (Modèle STRAHLER) au modèle de dégradation de la matière organique dans l'estuaire (Modèle MODESTY)." Int. Rep. Unité de Gestion du Modèle Mathématique de la Mer du Nord et de l'Estuaire de l'Escaut. Réf. BH/88/26
BILLEN,G (1992)
"The Phison River System: a conceptual model of C, N and P transformations in the aquatic continuum from land to sea." [*in NATO ARW on interactions of C, N, P & S biogeochemical cycles*]
BONAZOUNTAS,M (1987)
"Chemical Fate Modelling in Soil Systems: A State-of-the-Art review." *[in Barth.H & L'Hermite.P (eds.) (1987) "Scientific basis for soil protection in the European Community" Elsevier Applied Science]*
BONAZOUNTAS,M & Wagner,J (1984)
"SESOIL: A Seasonal Soil Compartment Model." UESPA/OTS Contract No 68-01-6271. Report by Arthur D Little Inc., Cambridge, MA
BOORMAN,D.B & Hollis,J.M (1992)
"Hydrology Of Soil Types; A hydrologically based classification of the soils of England and Wales" Inst. of Hydrology/SSLRC
BORGGAARD,O.K & Moberg,J.P (1991)
"Estimation of critical phosphate loads in Danish sandy soils." *[in Batjes,N.H & Bridges,E.M (eds.) "Soil Vulnerability to Pollution in Europe" pp 71-75, ISRIC, 1991]*
BOWDEN,J.M, Bolland,M.D.A, Posner,A.M & Quirk,J.P (1973)
"Generalised model for anion and cation adsorption at oxide surfaces." Nature, Lond., Physical Science, 245, pp 81-83
BREEUWSMA,A, Djurhus,D, Jansen,E, Kragt,J, Swerts,M & Thomasson,A (1990)
"Datasets for validation of nitrate simulation models" In: CEC (1991) Final Report of the project: Nitrates in Soils (Chapter 6)
BREEUWSMA,A & Reijerink,J.G.A (1992)
"Phosphate-saturated soils: a 'new' environmental issue" Proceedings of the State of the Art Conference on Chemical Time Bombs, Veldhoven, The Netherlands
CAS (Centre for Agricultural Strategy) (1978)
"Phosphorus: a resource for UK agriculture" CAS Report 2, Feb 1978
CEC (Commission of the European Communities) (1993a)
"ARCHÆOMEDES Project: Understanding natural and anthropogenic causes of soil degradation and desertification in the Mediterranean basin" DG XII Environment (Desertification) Programme EV5V-0021

CEC (Commission of the European Communities) (1993b)
"MEDALUS Project: Mediterranean Desertification and Land Use" DG XII Environment Programme EV5V-0023

CHECKLAND,P (1991)
"Towards the coherent expression of systems ideas" Journal of Applied Systems Analysis, Vol 18, pp 25-28

CHECKLAND,P (1992)
"Systems and Scholarship: The need to do better" J. Opl Res. Soc., Vol. 43, No. 11, pp 1023-1030

CHEN,C & Wagenet,R.J (1992)
"Simulation of water and chemicals in macropore soils. Part 1: Representation of the equivalent macropore influence and its effect upon soilwater flow" Journal of Hydrology, 130, pp 105-126

CLARK,M (1990)
"RAINS: A model for negotiations." Options, Sept 1990, IIASA, p9

CLARK,W.C & Munn,R.E (eds) (1986)
"Sustainable development of the biosphere." IIASA Cambridge Univ. Press

COSBY,B.J, Wright,R.F, Hornberger,G.M & Galloway,J.N (1985)
"Modelling the effects of acid deposition: assessment of a lumped parameter model of soil water and streamwater chemistry." Water Resour. Res., 21, pp 51-63

COSGROVE,D.J (1977)
"Microbial transformations in the phosphorus cycle", Adv. Microb. Ecol., 1, 95-134

COSTANZA,R, Sklar,F.H, White,M.L & Day Jr.,J.W (1988)
"A dynamic spatial simulation model of land loss and marsh succession in Louisiana." *[in Mitsch,W.J, Straskraba,M & Jorgensen,S.E (eds) "Wetland Modelling" Elsevier, Amsterdam, pp 99-114]*

COSTANZA,R, Sklar,F.H & White,M.L (1990)
"Modelling coastal landscape dynamics." BioScience, Vol 40(2)

DALAL,R.C (1975)
"Hydrolysis products of solution and exchangeable aluminium in acidic soils" Soil Science, 119, 2, pp 127-131

DOE (Department of the Environment) (1990)
"Acid deposition in the United Kingdom 1986-1988" Third report of the UK Review Group on Acid Rain, Warren Spring Laboratory

EEC (European Economic Community) (1985)
"Directive on the assessment of the effects of certain public and private projects on the environment (EEC/85/337)" Official Journal of the European Communities, No L 175, pp 40-48

ENFIELD,C.G (1974)
"Rate of phosphorus sorption by five Oklahoma soils." Soil Sci. Soc. Am. Proc., 38, pp 404-407

ENFIELD,C.G, Harlin,C.C & Bledsoe,B.E (1976)
"Comparison of five kinetic models for Orthophosphate reactions in mineral soils" Soil Sci. Soc. Am. J., Vol 40, pp 243-249

GHANI,M.O & Aleem,S.A (1943)
"Fractionation of soil phosphorus II. Chemical nature of the phosphorus fractions." Ind. J. Agri. Sci., Vol 13, pp 142-147
GILLHAM,C.A, Leech,P.K & Eggleston,H.S (1992)
"UK emissions of air pollutants 1970-1990" Warren Spring Laboratory
GLASSTONE,S (1959)
"Textbook of physical chemistry" D Van Nostrand Co. Inc, New Jersey
GUNARY,D (1970)
"A new adsorption isotherm for phosphate in soil" Soil Sci., Vol 21, pp 72-77
HARPER,D (1992)
"Eutrophication of Freshwaters: principles, problems and restoration" Chapman & Hall
HAYWARD,D.O & Trapnell,B.M.W (1964)
"Chemisorption" Butterworth & Co., London
HOLLING,C.S (1987)
"Simplifying the complex: The paradigms of ecological function and structure" Euro. J. of Op. Res., Vol 30, No 2, pp 139-146
HORNSBY,A.G & Davidson,J.M (1973)
"Solution and adsorbed fluometuron concentration distribution in water-saturated soil: experimental and predicted evaluation." Soil Sci. Soc. Am. Proc., 37, pp 823-828
IMESON,A.C (1987)
"Soil erosion and conservation" pp 329-350 in *[Gregory,K.j & Walling,D.E (eds.) "Human activity and environmental processes" J Wiley]*
IOH (Institute of Hydrology) (1980)
Low Flow Studies
JEFFERY,D (1989)
"Yellowstone: the great fires of 1988" National Geographic, Vol 175, No 2, pp 255-273, Feb 1989
JONES,C.A, Cole,C.V, Sharpley,A.N & Williams,J.R (1984)
"A simplified soil and plant phosphorus model: I. Documentation", Soil Sci. Soc. Am. J., 48, pp 800-805
KAMARI,J (1986)
"Linkage between atmospheric inputs and soil and water acidification." [*in Alcamo,J & Bartnicki,J (eds) 1986 "Atmospheric computations for assessment of acidification in Europe", RR-86-5, IIASA*]
KAUPPI.P & Alcamo,J (1990)
"Linkages in the RAINS model", pp 297-317 [*in Alcamo et al. 1990*]
KAUPPI,P, Posch,M, Kauppi,L & Kamari,J (1990)
"Modelling Soil Acidification in Europe" [*in Alcamo et al. 1990*]
KOESTLER,A (1967)
"The Ghost in the Machine" Picador
LAPIDUS,L & Amundson,N.R (1952)
"Mathematics of adsorption in beds. VI. The effects of longitudinal diffusion in ion exchange and chromatographic columns." J. Phys. Chem., 56, 984-988
LEVINS,R (1966)
"The strategy of model building in population biology" American Scientist, 54, 4, pp 421-431

LINKE,W (1958)
"Solubilities: inorganic and metal-organic compounds." 4th ed., American Chemical Society, Washington DC
LOVELAND,P.J (1990)
"The National Soil Inventory of England and Wales" pp 73-80 [*in Lieth,H & Markert,B (eds) 1990 "Element concentration cadasters in ecosystems: Methods of assessment and evaluation" VCH Verlagsgesellschaft, Weinheim*]
MAFF (Ministry of Agriculture, Fisheries and Food) (1983)
"1983-84 Fertilizer Recommendations for agricultural and horticultural crops" HMSO
MANAHAN,S.E (1991)
"Environmental Chemistry" 5th ed., Lewis, Michigan
MANKIN,J.B, O'Neill,R.V, Shugart,H.H & Rust,B.W (1975)
"The importance of validation in ecosystem analysis" [in *New directions in the analysis of ecological systems*, part 1, pp 63-71, Simulation Councils Inc., La Jolla, California]
MANNERMAA,M (1991)
"In search of an evolutionary paradigm for futures research" Futures, May 1991
MATTHEWS,P (1989)
"Algal Bloom at Rutland Water" Anglian Water Services Ltd
McGRATH,S.P & Loveland,P.J (1992)
"The soil geochemical atlas of England and Wales" Blaikie Academic Press
MEIN,R.G & Larsen,C.L (1971)
"Modeling the infiltration component of the rainfall-runoff process" Water Resources Research Centre, Bulletin 4, Minnesota
NERC (Natural Environment Research Council) (1975)
Flood Studies Report
NRA (National Rivers Authority) (1990)
"Toxic Blue-Green Algae" NRA, London
OLSEN,S.R & Watanabe,F.S (1957)
"A method to determine a phosphorus adsorption maximum of soils as measured by the Langmuir Isotherm" Soil Sci. Soc. Proceedings, pp 144-149
OS (Ordnance Survey) (1991)
"Kettering, Corby & surrounding areas" OS Landranger Series 141
PARK,J (1993)
"Towards a sustainable systems framework: The assessment of silvoarable agroforestry as an innovative cropping practice." Unpublished PhD Thesis, INTA/IERC, Cranfield University
PHILLIPS,P (1990)
"Toxic Algae in Rutland Water: a broad ecological view" Environmental Health Officer, Rutland District Council
REUSS,J.O (1983)
"Implications on the Ca-Al exchange system for the effect of acid precipitation on soils." J. Environ. Qual., Vol 12, pp 591-595
ROSE,C (1988)
"Acid Rain: it's happening here", Greenpeace (UK) Ltd

RUSSELL,E.J & Prescott,J.A (1916)
"The reaction between dilute acids and the phosphorus compounds of the soil" J. Agric. Sci., Camb., 8, pp 65-110
SANGLIER,M & Allen,P.M (1989)
"Evolutionary models of urban systems: an application to the Belgian provinces" Environment & Planning A, Vol 21, pp 477-498
SCHEFFER,M (1991)
"Fish and nutrients interplay determines algal biomass: a minimal model" OIKOS, 62, pp 271-282
SIMON,H.A (1962)
"The architecture of complexity" Proc. Amer. Phil. Soc. Vol 106, pp 467-482
SKOPP,J & Warwick,A.W (1974)
"A two-phase model for the miscible displacement of reactive solutes in soil." Soil Sci. Soc. Am. Proc., 36, 545-550
STEVENSON,F.J (1986)
"Cycles of Soil", Wiley
STIGLIANI,W.M (1988)
"Changes in valued 'capacities' of soils and sediments as indicators of nonlinear and time-delayed environmental effects." Environmental Monitoring and Assessment, 10(88), 245-307.
STIGLIANI,W.M (1991)
"Chemical Time Bombs: Definition, Concepts and Examples." Executive Report 16, IIASA
SUSMAN,P, O'Kiefe,P & Wisner,B (1983)
"Global disasters; a radical interpretation." pp 263-283 [*in Hewitt,K (1983) "Interpretations of calamity." Allen & Unwin Inc.*]
SVIREJEVA,A (1993)
"A preliminary integrated framework for exploring policy options concerning eutrophication in river and coastal systems: The Scheldt/Escaut example" Unpublished MPhil Thesis, INTA/IERC, Cranfield
TROW,P (1990)
"Assessing environmental health implications of toxic blue-green algae" Rutland District Council
ULRICH,B (1983)
"Soil Acidity and its relation to Acid Deposition" [*in B Ulrich & J Pankrath (eds.), "Effects of Accumulation of Air Pollutants in Forest Ecosystems", Proceedings Workshop Gottingen, FRG, 1982*]
WHITEHEAD,P.G (1990)
"Modelling nitrate from agriculture into public water supplies" Phil. Trans. R. Soc. Lond. B, Vol 329, pp 403-410
WORKMAN,S.R & Skaggs,R.W (1990)
"PREFLO: A water management model capable of simulating preferential flow" Transactions of the ASAE, Vol 33(6), pp 1939-1948